

University of Southampton Research Repository ePrints Soton

Copyright © and Moral Rights for this thesis are retained by the author and/or other copyright owners. A copy can be downloaded for personal non-commercial research or study, without prior permission or charge. This thesis cannot be reproduced or quoted extensively from without first obtaining permission in writing from the copyright holder/s. The content must not be changed in any way or sold commercially in any format or medium without the formal permission of the copyright holders.

When referring to this work, full bibliographic details including the author, title, awarding institution and date of the thesis must be given e.g.

AUTHOR (year of submission) "Full thesis title", University of Southampton, name of the University School or Department, PhD Thesis, pagination

UNIVERSITY OF SOUTHAMPTON

FACULTY OF ENGINEERING, SCIENCE AND MATHEMATICS

School of Ocean and Earth Science

**Latitudinal gradients in marine invertebrate
shell morphology:
production costs and predation pressure**

By

Sue-Ann Watson B.Sc. (Hons) M.Sc.

Thesis for the degree of Doctor of Philosophy

June 2009

UNIVERSITY OF SOUTHAMPTON
ABSTRACT
FACULTY OF SCIENCE
SCHOOL OF OCEAN AND EARTH SCIENCE
Doctor of Philosophy

LATITUDINAL GRADIENTS IN MARINE INVERTEBRATE SHELL
MORPHOLOGY: PRODUCTION COSTS AND PREDATION PRESSURE
by Sue-Ann Watson

Calcareous marine invertebrates are found in all the world's oceans and extend across latitudes from equatorial to polar seas. Latitudinal gradients in shell morphology may be controlled by the additional cost of producing a shell or the lack of durophagous predators at high latitudes. Representatives from four megabenthic calcareous groups: bivalve and gastropod molluscs, brachiopods, and echinoid echinoderms; were studied across latitudes in both hemispheres. Shell morphology and elemental content, metabolic rate, growth, shell cost and predation pressure were analysed. Total inorganic content, a proxy for skeletal calcium carbonate, decreased with latitude in all four groups. Shell thickness decreased with latitude in buccinid gastropods and echinoids. No difference was found in shell thickness for brachiopods of the genus *Liothyrella*. Within the infaunal bivalve genus *Laternula*, the polar representative had the thickest shell. Shell Ca and minor elements, such as Mg, Sr and Na, were analysed using scanning electron microscope energy dispersive spectroscopy and wavelength dispersive spectroscopy (SEM EDS/WDS). For the taxa studied, Sr:Ca increased with latitude in bivalves and brachiopods, but decreased with latitude in gastropods. Mg:Ca decreased with latitude in molluscs, but there was no trend in brachiopods. Na:Ca increased with latitude in molluscs and brachiopods. The control of substitution of these elements may differ among taxa with latitude. Metabolic rate generally decreased with latitude as a function of temperature in all four taxa. Analysis of Q_{10} values provided no evidence of metabolic cold adaptation. Growth curves determined from shell increments showed polar gastropods and brachiopods were slow growing, but the polar bivalve *Laternula elliptica* had rapid absolute growth compared to tropical and temperate congeners. Growth curves were used in conjunction with metabolic data to estimate the cost of shell production as a percentage of the total energy budget for each species. This proportional cost of shell production was 3-4% in polar molluscs compared to 1.5-2% for temperate molluscs and 0.5-1% for tropical molluscs. Predation pressure, inferred by repaired shell damage and defence architecture decreased with increasing latitude in buccinid gastropods and brachiopods. Although defence morphology decreased with increasing latitude in *Laternula* bivalves, the polar species had more repairs than non-polar congeners. Since these clams are infaunal, shell repair frequency is argued to be a function of their abiotic environment, rather than controlled by predation. For all taxa, relationships of shell repairs with shell thickness suggest an evolutionary control on shell morphology, particularly shell thickness, for the protection of the occupant whether from biotic factors such as predation or abiotic factors such as ice scour. The evolutionary cost of shell failure is high and the ecological need for the shell as protection thus seems to provide a greater control over shell thickness and defence morphology than the energetic cost of producing a shell. However, despite the moderately low cost of shell production in tropical and temperate species, many calcareous forms are vulnerable to climate change, particularly ocean acidification. The additional energetic cost of producing a shell in acidified seawater may be too much to tolerate for larvae of the commercially important edible oyster *Saccostrea glomerata*, which exhibited a marked reduction in survival of 43-72%, reduced growth and retarded development under upper and lower seawater pH predictions for the year 2100. For polar calcareous marine invertebrates, their 1.33-8 times greater proportional shell cost and their adaptation to a low predation environment mean that these polar species are particularly at risk from ocean acidification and climate warming.

List of contents

Chapter 1: Introduction	2
1.1 Rationale	2
1.2 Calcium carbonate shells and skeletons.....	2
1.3 Shell formation.....	3
1.4 Patterns in shell morphology with latitude.....	6
1.5 Competing hypotheses: shell cost versus shell function.....	8
1.6 Aims and hypotheses	11
1.7 Structure of the thesis.....	12
Chapter 2: Sample sites and study species.....	14
2.1 Introduction	14
2.2 Sample sites.....	14
2.3 Study species.....	16
2.4 Collection of animals	20
2.5 Sample site-specific animal collection information.....	21
2.6 Data and statistical analyses.....	32
2.7 Summary	33
Chapter 3: Latitudinal trends in shell morphology	35
3.1 Introduction	35
3.1.1 Aims and hypothesis	36
3.2 Methods.....	37
3.2.1 Sample collection	37
3.2.2 Morphological data collection.....	37
3.2.3 Shell thickness measurements.....	39
3.2.4 Correcting for size differences among species.....	43
3.2.5 Statistical analysis	44
3.3 Results	45
3.3.1 Whole animal morphology (shell and soft tissues).....	45
3.3.2 Shell morphology	57
3.4 Discussion	82
Chapter 4: Shell chemistry - elemental content of calcium carbonate shells and skeletons	89
4.1 Introduction	89
4.1.1 Aims and hypotheses	92

4.2 Methods.....	93
4.2.1 Preparation of sample material.....	93
4.2.2 Determination of shell crystal layer structure	93
4.2.3 Determination of shell elemental composition	93
4.2.4 Precision errors and limits of detection.....	95
4.2.5 Elemental distribution maps.....	96
4.2.6 X-ray diffraction (XRD)	96
4.2.7 Statistical analysis	97
4.3 Results	98
4.3.1 Shell crystal layer structure.....	98
4.3.2 Shell elemental composition	107
4.4 Discussion	135
Chapter 5: Latitudinal gradients in metabolic rate	146
5.1 Introduction	146
5.1.1 Aims and hypothesis	147
5.2 Methods.....	150
5.2.1 Measurements of respiration rate	150
5.2.2 Q ₁₀ calculations	156
5.2.3 Data and statistical analysis	156
5.3 Results	157
5.3.1 Variation in respiration rate with body size	157
5.3.2 Latitudinal variation in respiration rate.....	165
5.4 Discussion	175
Chapter 6: Growth and the cost of shell production	181
6.1 Introduction	181
6.1.1 Aims and Hypothesis	182
6.2 Methods.....	183
6.2.1 Growth bands – age determination and growth models.....	183
6.2.2 Calculating the cost of shell production.....	185
6.2.3 Statistical analysis	195
6.3 Results	197
6.3.1 Bivalvia: genus <i>Laternula</i>	203
6.3.2 Brachiopoda: genus <i>Liothyrella</i>	209
6.3.3 Gastropoda: family Buccinidae.....	213
6.4 Discussion	219
Chapter 7: Predation pressure – latitudinal patterns in shell repair and defence morphology	230
7.1 Introduction	230
7.1.1 Aims	232
7.2 Methods.....	233

7.2.1 Observations of shell repairs on living specimens.....	233
7.2.2 Observations of shell repairs on empty or ‘dead’ shells	234
7.2.3 Shell defence morphology: predator resistance	234
7.2.4 Statistical analysis	235
7.3 Results	236
7.3.1 Observations of shell repairs on living animals	236
7.3.2 Observations of shell repairs on <i>Laternula</i> empty or ‘dead’ shell assemblages.....	247
7.3.3 Shell predator defence morphology	248
7.4 Discussion	255
Chapter 8: The effects of ocean acidification on early larval development of the Sydney rock oyster <i>Saccostrea glomerata</i>.....	263
8.1 Introduction	263
8.2 Methods.....	266
8.2.1 Experimental set-up and pH control	266
8.2.2 Spawning procedure and larval culture.....	267
8.2.3 Processing of larvae	268
8.2.4 Empty shell counts	268
8.2.5 Statistical analysis	269
8.3 Results	270
8.3.1 Larval survival	270
8.3.2 Larval growth and morphology.....	270
8.3.3 Empty shells recovered	271
8.3.4 Shell surface structure	271
8.4 Discussion	274
Chapter 9: Synthesis and conclusions - Latitudinal gradients in shell morphology and the controls of shell cost and predation pressure	279
9.1 Introduction	279
9.1.1 Aims	281
9.1.2 Data and statistical analysis	281
9.2 Key findings in shell morphology, chemistry, cost and predation.....	281
9.2.1 Shell morphology	281
9.2.2 Shell chemistry.....	284
9.2.3 Shell cost	285
9.2.4 Predation pressure: shell damage and defence morphology	289
9.3 Protection or production costs: the controls on shell morphology.....	290
9.3.1 Why cost is not likely to be the primary control.....	291
9.3.2 Why predation is likely to be the primary control	292
9.4 The implications of climate change	304
9.4.1 Global warming.....	304
9.4.2 Ocean acidification.....	306
9.4.3 Summary of the potential effects of climate change	307

9.5 Limitations and suggestions for further work	308
9.6 Summary of the major findings of this study.....	310

List of tables

Table 2.1 Taxonomy for main study species (calcareous megabenthic marine invertebrates).	17
Table 2.2 Study sites from low to high latitudes and species collected at each site.	18
Table 2.3 Species collected from and around Townsville.	23
Table 2.4 Species collected around Melbourne, Australia.	26
Table 2.5 Rothera collection sites (*depths in brackets were where the majority of that species were collected).	31
Table 3.1 Summary data (mean \pm 1 s.d. to 3 d.p.) for key representative species of each animal group at various latitudes.	48
Table 3.2 Regression equations for the morphological relationships plotted on graphs below, where $y = mx + c$. (# Denotes species for which graphs are not plotted. * Denotes slopes that are significantly different from 3.)	50
Table 4.1 Detection limits for elements using EDS and WDS (taken from Goldstein <i>et al.</i> (2003)).	96
Table 4.2 WDS median counting error (%) of X-ray intensities for each group.	96
Table 4.3 Shell crystal layer composition (CaCO ₃ polymorph).	98
Table 4.4 Differences in elemental content among normal shell and light and dark band areas in shells of <i>Liothyrella uva</i> from Rothera, Antarctica.	108
Table 4.5 Shells and skeletons of species analysed with WDS and/or EDS.	110
Table 4.6 WDS data. Pearson product moment correlation statistics for elements for all <i>Laternula</i> clam species combined (<i>L. truncata</i> , <i>L. boschasina</i> , <i>L. valenciennesii</i> , <i>L. recta</i> , <i>L. elliptica</i>). Cell contents are correlation coefficient (r), probability value (p) and number of samples (n). *Denotes p values that are significant at the $p < 0.0125$ level.	112
Table 4.7 WDS data. Pearson product moment correlation statistics for elements for all buccinid gastropod species combined (<i>Cantharus fumosus</i> , <i>Phos senticosus</i> , <i>Cominella lineolata</i> , <i>Buccinum undatum</i> , <i>Neobuccinum eatoni</i> , <i>Buccinum cf. groenlandicum</i> , <i>Buccinum glaciale</i>). Cell contents are correlation coefficient (r), probability value (p) and number of samples (n). *Denotes p values that are significant at the $p < 0.0125$ level.	113
Table 4.8 WDS data. Pearson product moment correlation statistics for elements for all brachiopod species combined (<i>Liothyrella neozelanica</i> , <i>L. uva</i> and <i>Magellania venosa</i>). Cell contents are correlation coefficient (r), probability value (p) and number of samples (n). *Denotes p values that are significant at the $p < 0.0125$ level.	114
Table 4.9 WDS data. Pearson product moment correlation statistics for Ca and minor elements for each <i>Laternula</i> species. Cell contents are correlation coefficient (r), probability value (p) and number of samples (n). *Denotes p values that are significant at the $p < 0.0125$ level.	117
Table 4.10 WDS data. Pearson product moment correlation statistics for Ca and minor elements for each buccinid species. Cell contents are correlation coefficient (r), probability value (p) and number of samples (n). *Denotes p values that are significant at the $p < 0.0125$ level.	118
Table 4.11 WDS data. Pearson product moment correlation statistics for Ca and minor elements for each brachiopod species. Cell contents are correlation coefficient (r),	

probability value (p) and number of samples (n). *Denotes p values that are significant at the $p < 0.0125$ level.	119
Table 4.12 EDS data. Pearson product moment correlation statistics for Ca and minor elements for each species analysed by EDS. Cell contents are correlation coefficient (r), probability value (p) and number of samples (n). *Denotes p values that are significant at the $p < 0.0125$ level.	122
Table 4.13 Ca and minor element content using EDS for species that were not subsequently analysed with WDS.	124
Table 4.14 Statistics on WDS data for differences in mean elemental content (weight %) and elemental ratios among species of <i>Laternula</i>	125
Table 4.15 Statistics on WDS data for differences in mean elemental content (weight %) and elemental ratios among buccinid gastropod species.	126
Table 4.16 Statistics on WDS data for differences in mean elemental content (weight %) and elemental ratios among brachiopod species.	126
Table 4.17 Statistics on EDS data for differences in elemental content among brachiopod species.	127
Table 5.1 Summary of existing data on metabolic rates of key study species of calcareous organisms from scientific literature. Units of $\mu\text{g-at. O.h}^{-1}$ were multiplied by 11.2 to convert to $\mu\text{l O}_2\text{.h}^{-1}$ according to Peck <i>et al.</i> (1986b), and then divided by 1 mole of gas at the appropriate experimental temperature to obtain $\mu\text{mol O}_2\text{.h}^{-1}$	148
Table 5.2 Locations, seawater temperatures and season where respiration experiments were conducted for all <i>Laternula</i> species, buccinids, brachiopods and echinoderms investigated.	153
Table 5.3 Respiration rates for each species in terms of a mean sized animal (calculated using regression equations of $\text{Ln}(\text{AFDM})$ on $\text{Ln}(\text{Length})$ and $\text{Ln}(\text{MO}_2)$ on $\text{Ln}(\text{Length})$) for the species and mass specific respiration calculated for individuals.	158
Table 5.4 Regression equations of $\text{Ln}(\text{MO}_2)$ on $\text{Ln}(\text{length})$ and $\text{Ln}(\text{MO}_2)$ on $\text{Ln}(\text{mass})$ for all species plotted on graphs below, where $y = mx + c$	159
Table 5.5 Respiration rates of standard size animals. A standard size of 223 mg AFDM was used for laternulid clams and buccinid gastropods. The best standard animal size for comparing echinoids was 607 mg AFDM because this was near to the mean size for both species. Data were, however, also calculated for echinoderms of 223 mg AFDM (still within the size ranges studied) for the across phylum comparisons.	168
Table 5.6 Q_{10} values for <i>Laternula</i> species of a standard size of 223 mg AFDM at temperatures for which MO_2 was calculated.	169
Table 5.7 Q_{10} values for standard size buccinid gastropods of 223 mg AFDM.	172
Table 5.8 Q_{10} values for standard size Echinidae echinoids of 607 mg AFDM.	173
Table 6.1 Numerical values of the CaCO_3 solubility products of surface seawater (0 dbar) as a function of temperature and pressure for a salinity of 35 from Sarmiento and Gruber (2006).	186
Table 6.2 Seawater data from Rothera, Antarctica. The table shows total alkalinity (TA), dissolved inorganic carbon (DIC), the saturation state of seawater with respect to calcite (Ω_{cal}) and the saturation state of seawater with respect to aragonite (Ω_{arag}).	187
Table 6.3 Potential cost of shell production when CaCO_3 saturation state is added to data from Palmer (1992).	188

Table 6.4 Scaling factors for converting summer or winter metabolism into annual metabolism.	192
Table 6.5 The rise in metabolic rate following feeding (adapted from Peck (1998)).	193
Table 6.6 Energy content of soft tissues of marine invertebrates.	193
Table 6.7 The percentage of the energy budget accounted for by respiration and growth.	195
Table 6.8 Season, temperature and volume of 1 mole of O ₂ (g) at each location.	197
Table 6.9 VBGF parameters, fitted using $y=a*(1-\exp(-b*x))$. Note t_0 is assumed to be zero (and therefore not present), thus the curve passes through the origin, providing a better fit for small individuals, but still a good fit for larger animals.	200
Table 6.10 Annual SMR expenditure (J.y ⁻¹) for each species based on a mean animal size for each species. Mollusc shell organic content data are taken from Chapter 3. ...	201
Table 6.11 Regressions of shell mass and linear dimensions used in shell cost calculations and for brachiopods regressions for converting known pedicle valve length to brachial valve length for future comparison of data from this study with published data, where $y = mx + c$	202
Table 7.1 Buccinid gastropod shell repair data.	238
Table 7.2 Brachiopod shell repair data.	243
Table 7.3 <i>Laternula</i> shell repair data.	246
Table 8.1 Water chemistry data for treatment tanks (mean \pm 1 s.d.).	270

List of figures

Figure 2.1 Marine regions based on surface seawater temperatures. Figure taken from Castro and Huber (2005).....	15
Figure 2.2 Global sample sites with latitudes.	15
Figure 2.3 Examples of study species by region and taxonomic group.....	20
Figure 2.4 Location of the sample site in Singapore.....	22
Figure 2.5 Location of the sample site in Townsville, Queensland, tropical Australia.	23
Figure 2.6 Location of the sample site in Lucinda, Queensland, tropical Australia.	24
Figure 2.7 Location of the sample sites around Melbourne and Port Philip Bay, Victoria, temperate Australia.	25
Figure 2.8 Location of the sample site in Torquay, Torbay, on the south coast of England.	27
Figure 2.9 Location of the sample site in Southampton Water, Southampton, on the south coast of England.....	28
Figure 2.10 Location of the sample sites around Rothera Research Station, Adelaide Island, Antarctic Peninsula. The northern site is called Hangar Cove.....	30
Figure 2.11 Location of the sample site in Ryder Bay, Adelaide Island, Antarctic Peninsula.	31
Figure 2.12 Location of the sample site in Ny Ålesund, Spitsbergen, Svalbard, in the Arctic Circle.....	32
Figure 3.1 Bivalve shell terminology showing maximum shell length, maximum shell height and shell inflation (\equiv width) (Cox <i>et al.</i> , 1969).	38
Figure 3.2 Bivalve shell terminology used for the burrowing clams of the genus <i>Laternula</i>	39
Figure 3.3 Gastropod shell measurements taken.....	39
Figure 3.4 Bivalve shells were sectioned along the midline of the dorsal-ventral growing axis then the part shown was removed and embedded in resin.....	40
Figure 3.5 Brachiopod shells were sectioned in half along the axis of maximum growth then the part shown was removed and embedded in resin. In brachiopods, length refers to the length of the pedicle (ventral) valve throughout this thesis, unless otherwise stated.....	41
Figure 3.6 For bivalves and brachiopods the mid-section of the shell was measured for thickness. In brachiopods the dorsal valve was always used.	41
Figure 3.7 Shells of coiled gastropods were sectioned perpendicular to the growing lip (i.e. at 90° to aperture whorl end).....	42
Figure 3.8 After sectioning the part indicated was removed and embedded in resin for measurement of shell thickness (and elemental analysis see Chapter 4).	42
Figure 3.9 Echinoids were sectioned in half and the thickness of the mid-section of the test measured with a point micrometer accurate to 0.001 mm.	42
Figure 3.10 SEM photograph to show how measurements were taken across the shell section using CorelDRAW 12. The shell in this photograph is the Antarctic gastropod, <i>Neobuccinum eatoni</i>	43
Figure 3.11 Regressions of height on length for A) <i>Laternula truncata</i> , C) <i>L. boschasina</i> , E), <i>L. recta</i> , G) <i>L. elliptica</i> and regressions of Ln(Mass) on Ln(Length) measurements for B) <i>L. truncata</i> , D) <i>L. boschasina</i> , F) <i>L. recta</i> , H) <i>L. elliptica</i> .	

N.B. Some variation in <i>L. recta</i> AFDM was caused by problems with the muffle furnace at the University of Melbourne.	54
Figure 3.12 Regressions of Ln(Mass) on Ln(Height) for A) <i>Cantharus fumosus</i> , B) <i>Phos senticosus</i> , C) <i>Cominella lineolata</i> , D) <i>Buccinum undatum</i> , E) <i>Neobuccinum eatoni</i> , F) <i>Buccinum</i> cf. <i>groenlandicum</i> and G) <i>Buccinum glaciale</i>	55
Figure 3.13 Regressions of Ln(Mass) on Ln(Length) for A) <i>Liothyrella neozelanica</i> and B) <i>Liothyrella uva</i>	56
Figure 3.14 Regressions of Ln(Mass) on Ln(Test diameter) for <i>Psammechinus miliaris</i> , B) <i>Sterechinus</i> sp. from the Scotia Arc, and C) <i>Sterechinus neumayeri</i>	56
Figure 3.15 Inorganic content of whole gastropods as a percentage of the total animal dry mass by species (left) and by latitude (right). N.B. Negative values of latitude are in the Southern Hemisphere. All species are buccinids except for <i>Thais orbita</i>	58
Figure 3.16 Variation among buccinids in shell dry mass as a percentage of total animal dry mass by species (left) and latitude (right).	59
Figure 3.17 Inorganic content of whole <i>Laternula</i> clams.	60
Figure 3.18 Variation among <i>Laternula</i> species in shell mass as a percentage of total animal dry mass.	60
Figure 3.19 Inorganic content of brachiopods.	61
Figure 3.20 Brachiopod genus <i>Liothyrella</i> A) dry mass, B) ash mass (inorganic mass) and C) AFDM (organic mass).	62
Figure 3.21 Inorganic content of echinoids.	63
Figure 3.22 Echinoid A) dry mass, B) ash mass (inorganic mass) and C) AFDM mass (organic mass).	64
Figure 3.23 Latitudinal variation in whole animal inorganic content (ash as % dry mass). This metric is used because it is a good measure of the amount of skeleton and it is comparable among groups. Standard errors are mostly smaller than the points used to mark the mean.	66
Figure 3.24 Variation in whole animal inorganic content (ash as % dry mass) with temperature. The Arctic buccinids are now included in the buccinid gastropods and are shown as black open circles.	66
Figure 3.25 Organic content of <i>Laternula</i> species shells as a percentage of the total dry mass of the shell.	68
Figure 3.26 Organic content of <i>Laternula</i> species soft tissue as a percentage of the total dry mass of the soft tissue.	68
Figure 3.27 Organic content of buccinid gastropod: A) shell by species, B) soft tissue by species, C) shell by latitude and D) soft tissue by latitude.	69
Figure 3.28 Regressions of Ln(Shell thickness) on Ln(Shell height) in buccinid gastropods on raw (uncorrected) data.	72
Figure 3.29 Uncorrected data for mean shell thickness by buccinid species (left) and by latitude (right). N.B. Negative values of latitude represent the Southern Hemisphere.	72
Figure 3.30 Plot of corrected Ln(Shell thickness) on original Ln(Shell height) data for each buccinid species. Samples were limited to mostly adults from each species and for an approximate maximum size for each species there was a significant negative relationship between height and shell thickness ($F = 11.4899$, $df = 1,5$, $p = 0.0195$, $n = 7$).	73
Figure 3.31 Mean shell thickness for each buccinid species corrected for size.	73

Figure 3.32 Mean shell thickness for each buccinid species corrected for size and plotted by latitude (left) and temperature (right). N.B. Negative values of latitude represent the Southern Hemisphere.	74
Figure 3.33 Regression of Ln(Shell thickness) on Ln(Length) in <i>Laternula</i> clams. <i>L. elliptica</i> has a statistically significant regression equation ($p < 0.0001$).	75
Figure 3.34 Mean shell thickness for each <i>Laternula</i> species (uncorrected).	76
Figure 3.35 Mean shell thickness for each <i>Laternula</i> species corrected for length.	76
Figure 3.36 Mean shell thickness for each <i>Laternula</i> species corrected for length and plotted by latitude (left) and temperature (right). N.B. Negative values of latitude represent the Southern Hemisphere. Temperature axis is reversed.	77
Figure 3.37 Regressions of Ln(Shell thickness) on Ln(Length) in brachiopods.	79
Figure 3.38 Mean shell thickness for each brachiopod species.	79
Figure 3.39 Mean shell thickness for each brachiopod species corrected for length by species (left) and latitude (right).	79
Figure 3.40 Regressions of Ln(Shell thickness) on Ln(Diameter) in echinoids. Shell thickness is test thickness in echinoids.	81
Figure 3.41 Mean shell thickness for each echinoid species (uncorrected data).	81
Figure 3.42 Mean shell thickness for each echinoid species corrected for test diameter. ...	81
Figure 4.1 Resin block with shell sections embedded inside. This block had been polished and was ready for carbon coating.	97
Figure 4.2 Positions of analysis on the shell section (points 1 to 5 were clustered around the mid-section of the shell).	97
Figure 4.3 Shell section of <i>Laternula truncata</i> showing crystal structure. Scale bar is 50 μm	99
Figure 4.4 Shell section of <i>Laternula boschasina</i> showing crystal structure. Scale bar is 10 μm	99
Figure 4.5 Shell section of <i>Laternula valenciennesii</i> showing crystal structure. Scale bar is 50 μm	99
Figure 4.6 Shell section of <i>Laternula recta</i> showing crystal structure. Scale bar is 10 μm	100
Figure 4.7 Shell section of <i>Laternula elliptica</i> showing crystal structure. Scale bar is 500 μm . Problems with gold coating on the <i>L. elliptica</i> sections meant that a clear section was more difficult to photograph compared to the other <i>Laternula</i> species and so this image was taken at 90° to other images. Here it is still possible to make out the shell layers, although not as clearly as on the other species of <i>Laternula</i> shell sections.	100
Figure 4.8 Shell section of <i>Cantharus fumosus</i> showing crystal structure. Scale bar is 100 μm	101
Figure 4.9 Shell section of <i>Phos senticosus</i> showing crystal structure. Scale bar is 500 μm	101
Figure 4.10 Shell section of <i>Cominella lineolata</i> showing crystal structure. Scale bar is 100 μm	101
Figure 4.11 Shell section of <i>Buccinum undatum</i> showing crystal structure. Scale bar is 100 μm	102
Figure 4.12 Shell section of <i>Neobuccinum eatoni</i> showing crystal structure. Scale bar is 100 μm	102
Figure 4.13 Shell section of <i>Buccinum glaciale</i> showing crystal structure. Scale bar is 100 μm	102

Figure 4.14 Shell section of <i>Buccinum</i> cf. <i>groenlandicum</i> showing crystal structure. Scale bar is 50 μm .	103
Figure 4.15 Shell section of <i>Thais orbita</i> showing crystal structure. Scale bar is 100 μm .	103
Figure 4.16 Shell section of the brachiopod <i>Liothyrella neozelanica</i> showing crystal structure. Scale bar is 100 μm .	103
Figure 4.17 Shell section of the brachiopod <i>Liothyrella uva</i> showing crystal structure. Scale bar is 100 μm .	104
Figure 4.18 Shell section of the brachiopod <i>Magellania venosa</i> showing crystal structure. Scale bar is 100 μm .	104
Figure 4.19 Aragonitic sheet nacreous layer of the bivalve <i>Laternula elliptica</i> close up. Scale bar is 5 μm .	105
Figure 4.20 Aragonitic crossed lamellar layer of the gastropod <i>Cantharus fumosus</i> . Scale bar is 10 μm .	105
Figure 4.21 Aragonitic cone complex cross lamellar (CCL) of the gastropod <i>Cominella lineolata</i> . Scale bar is 50 μm .	106
Figure 4.22 Calcite crystals of the brachiopod <i>Liothyrella uva</i> . Scale bar is 10 μm .	106
Figure 4.23 Bivalve <i>Laternula truncata</i> shell showing points of WDS analysis (white dots) on the shell section surface. For this shell all layers were analysed.	108
Figure 4.24 Gastropod <i>Buccinum undatum</i> shell showing points of WDS analysis (white dots) on the shell section surface. For this shell the cross lamellar aragonite and the CCL were analysed.	108
Figure 4.25 Brachiopod <i>Liothyrella uva</i> shell showing points of WDS analysis (white dots) on the shell section surface. For this shell dark and light lines were also analysed. Darker grey lines were analysed for this species (middle row of white dots) and found to be high in Sr.	109
Figure 4.26 Image of the echinoid <i>Sterechinus neumayeri</i> test showing its porosity.	109
Figure 4.27 WDS data showing inter-specific Sr substitution for Ca in species of <i>Laternula</i> . There was a significant negative correlation for all <i>Laternula</i> species pooled (Pearson correlation coefficient $r = -0.215$, $p = 0.00612$, $n = 161$). There were no significant correlations for individual species. Taking mean values of Ca and Sr for each species, there was no significant correlation between Sr and Ca.	115
Figure 4.28 WDS data showing the substitution of Sr or Mg for Ca in the shell of <i>Buccinum undatum</i> . There was a significant negative correlation between Ca and Sr ($r = -0.467$, $p = 0.00314$, $n = 38$) but no significant correlation between Ca and Mg ($r = -0.332$, $p = 0.0630$ NS, $n = 32$).	119
Figure 4.29 WDS data showing Na content is positively correlated with Ca in <i>Buccinum undatum</i> . There is a significant positive correlation between Ca and Na ($r = 0.413$, $p = 0.0100$, $n = 38$).	120
Figure 4.30 EDS data showing intra-specific differences in Mg substitution for Ca in the Antarctic brachiopod <i>Magellania fragilis</i> valves ($F = 74.6665$, $df = 1,36$, $r^2 = 0.6657$, $n = 38$, $p < 0.0001$).	123
Figure 4.31 EDS data showing inter-specific substitution of Mg for Ca into the CaCO_3 valves of brachiopods ($F = 60.5824$, $df = 1,122$, $r^2 = 0.3263$, $n = 124$, $p < 0.0001$).	123
Figure 4.32 WDS data for mean elemental content of major and minor elements (left) and minor element:Ca ratios (right) in shells of <i>Laternula</i> clams.	128

Figure 4.33 WDS data for mean elemental content of major and minor elements (left) and minor element:Ca ratios (right) in shells of buccinid gastropods.	129
Figure 4.34 WDS data for mean elemental content of major and minor elements (left) and minor element:Ca ratios (right) in shells of brachiopods. N.B. Black data points are <i>Liothyrella</i> species and the red data point is <i>Magellania venosa</i> a non-congeneric species.	131
Figure 4.35 EDS data for mean elemental content of major and minor elements (left) and minor element:Ca ratios (right) in shells of brachiopods. N.B. Black data points are <i>Liothyrella</i> spp. and the red data point is <i>Terebratulina retusa</i> and the blue data point is <i>Magellania fragilis</i> , both non-congeneric species.	132
Figure 4.36 Map of Ca content in <i>Phos senticosus</i> (WDS data).	134
Figure 4.37 Map of Sr content in <i>Phos senticosus</i> (WDS data).	134
Figure 4.38 Map of Na content in <i>Phos senticosus</i> (WDS data).	134
Figure 5.1 Respirometers containing <i>Laternula elliptica</i> in the Bonner Laboratory aquarium at Rothera Research Station, Antarctica.	154
Figure 5.2 Fibox-3 system (grey box and fibre optic cable) linked to a computer in the Zoology Department aquarium at Melbourne University, Australia.	154
Figure 5.3 Taking a measurement from a respirometer in the Tropical Marine Science Institute aquarium, National University of Singapore. The end of the fibre optic cable is placed on the glass where the oxygen sensitive foil is glued on the inside.	155
Figure 5.4 Fibox screen display using OxyView PST3-V5.32 program. Graphs of raw data (phase angle) over time are generated in real time by the program allowing the user to determine when the system is producing a stable reading.	155
Figure 5.5 Regression of Ln(MO ₂) on Ln(Mass) for the clams A) <i>Laternula truncata</i> , B) <i>L. boschasina</i> , C) <i>L. recta</i> and D) <i>L. elliptica</i> . Regressions for <i>L. boschasina</i> were not significant because the size range of animal length was too small. Regression statistics and fits are given in Table 5.4.	162
Figure 5.6 Regression of Ln(MO ₂) on Ln(Mass) for the buccinid gastropods A) <i>Cantharus fumosus</i> , B) <i>Phos senticosus</i> , C) <i>Cominella lineolata</i> , D) <i>Buccinum undatum</i> , E) <i>Neobuccinum eatoni</i> , F) <i>Buccinum</i> cf. <i>groenlandicum</i> and G) <i>Buccinum glaciale</i>	163
Figure 5.7 Regression of Ln(MO ₂) on Ln(Mass) for the echinoids A) <i>Psammechinus miliaris</i> and B) <i>Sterechinus neumayeri</i>	164
Figure 5.8 Regression of Ln(MO ₂) on Ln(Mass) for the brachiopod.	164
Figure 5.9 Regressions of Ln(MO ₂) on Ln(AFDM) for <i>Laternula</i> clams. A standard size animal for <i>Laternula</i> species was chosen as -1.5 g Ln(AFDM), which is equivalent to 0.223 g AFDM.	165
Figure 5.10 Regressions of Ln(MO ₂) on Ln(AFDM) for buccinid gastropods. A standard size animal for buccinid gastropods was chosen as -1.5 g Ln(AFDM), which is equivalent to 0.223 g AFDM.	166
Figure 5.11 Regressions of Ln(MO ₂) on Ln(AFDM) for Echinidae echinoids. A standard size animal for echinoids was chosen as -0.5 g Ln(AFDM), which is equivalent to 0.607 g AFDM.	166
Figure 5.12 Standard animal mean respiration rates for <i>Laternula</i> species from tropical, temperate and polar latitudes. Data points beyond the 10 th and 90 th percentiles are displayed as dots.	170

Figure 5.13 Trend in standard animal mean respiration rate for <i>Laternula</i> clams with latitude and temperature. The two tropical species <i>L. truncata</i> and <i>L. boschasina</i> from the same location are slightly offset to aid viewing.	170
Figure 5.14 Buccinid standard animal mean respiration rates for each species.....	171
Figure 5.15 Buccinid gastropod standard animal mean respiration rates plotted with latitude (left) (negative values of latitude are in the Southern Hemisphere) and temperature (right). Tropical species are plotted with open symbols to show their different life habit.....	172
Figure 5.16 Respiration rate for a temperate and polar echinoid for a standard animal of 607 mg AFDM. Data points beyond the 10 th and 90 th percentiles are displayed as dots.	173
Figure 5.17 Summary of trends in standard animal (AFDM = 223 mg for all species) mean respiration rate for each group with temperature, where the mean is the average calculated following the conversion of all individual respiration rates to that for a standard animal.	174
Figure 6.1 The saturation states of calcite and aragonite in the world's oceans today. The difference in the saturation state of seawater from equatorial to polar latitudes is approximately two-fold. Plots were provided by A. Yool from GLODAP data. .	187
Figure 6.2 Annual metabolic rate model schematic showing how the modelled metabolic rate of 6 months winter rate and 6 months summer rate is equal to the idealised actual metabolic rate.	191
Figure 6.3 Estimates of the organic matrix contained within the brachiopod shell. There was a significant difference in the total organic content of brachiopod shells (Welch's F = 23.599, df1 = 2, df2 = 7.082, p < 0.001). Post hoc comparisons using the Games-Howell procedure showed that <i>Liothyrella uva</i> had the highest shell organic content (p < 0.001).	199
Figure 6.4 VBGF curves for A) <i>Laternula truncata</i> , B) <i>L. boschasina</i> , C) <i>L. recta</i> and D) <i>L. elliptica</i>	204
Figure 6.5 Mean shell height measurement for each <i>Laternula</i> species compared. The polar clam, <i>L. elliptica</i> had the fastest growth rate.	205
Figure 6.6 Energy required for shell deposition using VBGF curves and based on CaCO ₃ and organic matrix content of the shell for A) <i>Laternula truncata</i> , B) <i>L. boschasina</i> , C) <i>L. recta</i> and D) <i>L. elliptica</i> . Since Palmer (1992) estimated the cost of shell production to be 1 – 2 J.mg ⁻¹ CaCO ₃ , shell cost at values of 1, 1.5 and 2 J.mg ⁻¹ CaCO ₃ were plotted to demonstrate the range of shell cost values possible. The theoretical cost of producing the shell based on differences in the saturation state of CaCO ₃ in seawater, is shown as blue curves on the graphs. Note that the cost for the temperate species remains the same since Palmer's (1992) cost calculations were done at temperate conditions.....	205
Figure 6.7 Energy required for shell deposition using VBGF curves and based on CaCO ₃ and organic matrix content of the shell for A) all species of <i>Laternula</i> studied and B) scaled for smaller species. The theoretical extra cost of making the shell based on differences in the saturation state of CaCO ₃ in seawater is included in these comparisons.	206
Figure 6.8 Regressions of Ln(MO2) on Ln(Shell height) for A) <i>Laternula truncata</i> (y = 2.1406x - 4.5490, r ² = 0.2625, F = 9.9652, df = 1,28, p = 0.0038), B) <i>L. boschasina</i> (regression not significant), C) <i>L. recta</i> (y = 3.1422x - 8.3019, r ² = 0.8791, F = 145.4885, df = 1,20, p < 0.0001) and D) <i>L. elliptica</i> (y = 2.5067x - 6.0511, r ² =	

0.9247, $F = 368.3433$, $df = 1,30$, $p < 0.0001$). The restricted size range for <i>L. boschasina</i> meant the regression of $\text{Ln}(\text{MO}_2)$ on $\text{Ln}(\text{Shell height})$ was not significant.....	206
Figure 6.9 Variation in the cost of shell deposition with age for A) <i>Laternula truncata</i> , B) <i>L. boschasina</i> , C) <i>L. recta</i> and D) <i>L. elliptica</i> . The theoretical cost of producing the shell based on differences in the saturation state of CaCO_3 in seawater, is shown as blue curves on the graphs. Note that the cost for the temperate species remains the same since Palmer's (1992) cost calculations were done at temperate conditions.	207
Figure 6.10 Variation in the cost of shell deposition as a percentage of the total energy budget (I) with age for all <i>Laternula</i> species studied including differences in CaCO_3 saturation state (left) and excluding differences in CaCO_3 saturation state (right). A mid-value of $1.5 \text{ J.mg}^{-1} \text{ CaCO}_3$ was used.	208
Figure 6.11 Mean lifetime values of shell cost as a percentage of the total energy budget for all <i>Laternula</i> species studied. A mid-value of $1.5 \text{ J.mg}^{-1} \text{ CaCO}_3$ was used.....	208
Figure 6.12 VBGF growth curves for the brachiopods <i>Liothyrella neozelanica</i> (left) and <i>L. uva</i> (right).....	210
Figure 6.13 Average brachial (dorsal) valve length for each <i>Liothyrella</i> species compared using shell increment data. The temperate species <i>L. neozelanica</i> grows nearly twice as fast as the polar species <i>L. uva</i>	210
Figure 6.14 Energy required for shell deposition with and without the shell organic content included for <i>Liothyrella neozelanica</i> (left) and <i>L. uva</i> (right). <i>L. neozelanica</i> is a temperate species, so there was no correction for CaCO_3 saturation state. Note the different key for <i>L. uva</i> (right) as a correction for CaCO_3 saturation state is included.	211
Figure 6.15 Energy required by brachiopods to deposit their shell with and without organic shell matrix at 1 %. Figures shown are based only on the 1.5 J.mg^{-1} value for CaCO_3 deposition costs. The theoretical extra cost of making the shell based on differences in the saturation state of CaCO_3 in seawater is included in these comparisons.	211
Figure 6.16 Regression of $\text{Ln}(\text{Respiration rate})$ on $\text{Ln}(\text{Brachial valve length})$ for <i>Liothyrella uva</i> ($F = 36.2763$, $df = 1,24$, $p < 0.0001$, $r^2 = 0.5852$).	212
Figure 6.17 Variation in the cost of shell deposition with age for <i>Liothyrella uva</i> . The 63 % value for bivalve was used for the percentage of the energy budget accounted for by respiration and growth. Shell organic matrix was assumed to be 1 %. The theoretical extra cost of producing the shell based on differences in the saturation state of CaCO_3 in seawater, is shown as blue curves on the graph.....	212
Figure 6.18 VBGF curves for A) <i>Buccinum undatum</i> , B) <i>Neobuccinum eatoni</i> , C) <i>Buccinum cf. groenlandicum</i> and D) <i>Buccinum glaciale</i>	214
Figure 6.19 Energy required for shell deposition based on VBGF curves and CaCO_3 and organic matrix content of the shell for A) <i>Buccinum undatum</i> , B) <i>Neobuccinum eatoni</i> , C) <i>Buccinum cf. groenlandicum</i> and D) <i>Buccinum glaciale</i> . The theoretical extra cost of producing the shell based on differences in the saturation state of CaCO_3 in seawater, is shown as blue curves on the graphs. Note that the cost for the temperate species remains the same since Palmer's (1992) cost calculations were done at temperate conditions.	215
Figure 6.20 Energy required for shell deposition based on VBGF curves, CaCO_3 and organic matrix content of the shell for buccinid gastropods including differences in	

CaCO ₃ saturation state (left) and excluding differences in CaCO ₃ saturation state (right).	216
Figure 6.21 Variation in respiration rate with size for buccinid gastropods. All regressions were significant: <i>B. undatum</i> ($F = 103.8935$, $df = 1,26$, $p < 0.0001$), <i>N. eatoni</i> ($F = 60.6835$, $df = 1,29$, $p < 0.0001$), <i>B. cf. groenlandicum</i> ($F = 12.6214$, $df = 1,19$, $p = 0.0021$) and <i>B. glaciale</i> ($F = 7.1936$, $df = 1,10$, $p = 0.0230$).	216
Figure 6.22 Variation in the cost of shell deposition with age for <i>Buccinum undatum</i> , <i>Neobuccinum eatoni</i> , <i>Buccinum cf. groenlandicum</i> and <i>Buccinum glaciale</i> .	217
Figure 6.23 Variation in the cost of shell deposition as a percentage of the total energy budget (I) with age for all buccinid gastropods including differences in CaCO ₃ saturation state (left) and excluding differences in CaCO ₃ saturation state (right). The bottom graphs show data only for age ranges sampled.	218
Figure 6.24 The cost of shell as a proportion of the total energy budget was significantly related to temperature for <i>Laternula</i> ($F = 47.4602$, $df = 1,2$, $p = 0.0204$) and for buccinid gastropods ($F = 22.6881$, $df = 1,2$, $p = 0.0414$). The cost of shell was significantly related to latitude in <i>Laternula</i> ($F = 23.7545$, $df = 1,2$, $p = 0.0396$) but not significantly related to latitude in the Buccinidae ($p = 0.0938$ NS). Cost values were taken at age 3 for <i>Laternula</i> and age 5 for buccinids because these ages overlapped measured individuals for most species within the taxa. These costs were based on mid-range data of 1.5 J.mg^{-1} of CaCO ₃ from Palmer (1992).	225
Figure 6.25 The decrease in carbonate ion concentration (Orr <i>et al.</i> , 2005) (left) and corresponding fall in saturation state (plot by T. Tyrrell from GLODAP data) (right) in the world's surface oceans since pre-industrial times.	227
Figure 7.1 Diagram showing position of measurements of shell inflation in <i>Laternula</i> clams. The inflation at gape is the minimum inflation at the gape of the shell.	235
Figure 7.2 Histograms of number of repairs per shell in buccinid gastropods. All shell repairs are shown as black bars and shell repairs characteristic of predation damage are shown as grey bars. There were fewer repairs indicative of predation damage so the histograms for repairs caused by predator attacks are shifted to the left.	237
Figure 7.3 Shell damage data across the Buccinidae by species. N_d is the proportion of individuals with repairs and N_i is the total number of injuries (i.e. the number of repairs per shell).	239
Figure 7.4 Shell repair data across the Buccinidae by latitude (left) and temperature (right). There were no statistically significant trends with latitude or temperature for N_d or N_i .	239
Figure 7.5 Repairs from shell damage likely to have been caused by a predator attack in A) <i>Cantharus fumosus</i> , B) <i>Phos senticosus</i> , C) <i>Cominella lineolata</i> , D) <i>Buccinum undatum</i> , E) <i>Neobuccinum eatoni</i> , F) <i>Buccinum cf. groenlandicum</i> and G) <i>Buccinum glaciale</i> .	240
Figure 7.6 Shell damage characteristic of predation attacks across the Buccinidae by species. P_d is the proportion of individuals damaged by predation, P_i is the total number of injuries from predation, αP_d is the proportion of individuals with damage that was caused by a predator attack, and αP_i is the proportion of all injuries that were caused by a predator attack.	241
Figure 7.7 The proportion of all injuries that were caused by a predator attack (αP_i) across the Buccinidae by latitude (left) and temperature (right). αP_i decreases with increasing latitude in both hemispheres, although there was no statistically significant regression of αP_i on temperature ($p = 0.0961$ NS).	242

Figure 7.8 Examples of brachiopod repaired shell damage in the form of a cleft in A) <i>Liothyrella neozelanica</i> and B) <i>L. uva</i> .	242
Figure 7.9 Repaired shell damage data in brachiopods studied. N_d is the proportion of individuals with repairs and N_i is the total number of injuries (i.e. the number of repairs per shell).	243
Figure 7.10 Echinoid spine length with latitude (left) and temperature (right).	244
Figure 7.11 Echinoid spine length as a percentage of test diameter by latitude (left) and temperature (right). There was a significant regression of spine length as a percentage of test diameter on temperature ($F = 234.7335$, $df = 1,71$, $P < 0.0001$, $r^2 = 0.7645$).	244
Figure 7.12 Shell repair in <i>Laternula recta</i> . The original damage may have been caused by bird predation (E. Harper, pers. comm.).	245
Figure 7.13 Histograms of incidence of shell repairs in species of <i>Laternula</i> from tropical to polar latitudes. Data show numbers of individuals in relation to the number of repairs identified on their shells.	246
Figure 7.14 Graph showing two measures of shell damage repair in <i>Laternula</i> clams: the proportion of damaged individuals (N_d) and total number of injuries (N_i).	247
Figure 7.15 Shell from a dead <i>Laternula elliptica</i> with a drill hole found on the sediment surface whilst diving in Hangar Cove, Rothera, Antarctica (left). Close up of the drill hole in the <i>Laternula elliptica</i> shell from Hangar Cove (right).	248
Figure 7.16 Relationships of shell height and aperture width in gastropods studied.	250
Figure 7.17 Gastropod aperture resistance to predation for each species studied in the form of aperture width as a percentage of shell height. The red point indicates a non-buccinid species.	250
Figure 7.18 Variation in gastropod aperture resistance to predation with A) latitude and temperature, B) latitude regression and C) temperature regression. The red data point on plot B denotes a non-buccinid species and the trendlines are for buccinid species only. There were significant regressions in the ratio of aperture width to shell height with both latitude ($F = 11.7564$, $df = 1,5$, $P = 0.0187$, $r^2 = 0.6419$) and temperature ($F = 26.3014$, $df = 1,5$, $P = 0.0037$, $r^2 = 0.8083$).	251
Figure 7.19 Variation in gastropod aperture narrowness (length/width ratio) by species. The two tropical species have narrow apertures with aperture length:width ≥ 2.5 . The red point indicates a non-buccinid species.	252
Figure 7.20 Variation in gastropod aperture narrowness across latitudes. The red point indicates a non-buccinid species.	252
Figure 7.21 Relationships between <i>Laternula</i> shell inflation at hinge and inflation at gape.	254
Figure 7.22 Variation in <i>Laternula</i> gape with latitude and temperature.	254
Figure 7.23 Data plotted from a table in Harper <i>et al.</i> (submitted) on repaired shell damage data in brachiopods. N_d is the proportion of individuals with repairs and N_i is the number of repairs per shell.	257
Figure 8.1 Set-up of experimental CO ₂ system with 3 pH levels. Treatments labelled pH1, pH2 and pH3 were set to nominal pH values of 8.1, 7.8 and 7.6 respectively.	267
Figure 8.2 Qualitative and quantitative measurements of larval success at different pH: A, Larval survival; B, APM of larvae; C, DVM of larvae; D, Percentage of empty shells remaining from dead larvae; E, Larval dry mass. Error bars are 1 s.e.	272
Figure 8.3 Scanning electron microscope (SEM) images of representative <i>Saccostrea glomerata</i> larvae at 8 days old from pH treatments: A) pH 8.1; B) pH 7.8; C) pH	

7.6. All images were taken at the same magnification. ‘X’ arrows show a growth check and point of change in the surface of the shell to a pitted surface. ‘Y’ denotes areas of new shell growth during exposure to acidified seawater.....	273
Figure 9.1 Flow chart showing how data chapters in this thesis were inter-linked.	280
Figure 9.2 Variation in total animal inorganic content (ash as % dry mass) with latitude (left) and temperature (right). This metric is used because it is a good measure of the amount of skeleton and it is comparable among groups. Standard errors are mostly smaller than the points used to mark the mean. Black open circles denote Arctic buccinids.	283
Figure 9.3 Variation in shell thickness with temperature for standard sized animals. Black open circles denote Arctic buccinids.....	283
Figure 9.4 Latitudinal gradients in Sr:Ca ratios in <i>Laternula</i> , brachiopods and buccinids.	285
Figure 9.5 Summary of trends in standard animal (AFDM = 223 mg) mean respiration rate for each group with temperature.	288
Figure 9.6 The cost of shell as a proportion of the total energy budget was significantly related to temperature for <i>Laternula</i> ($F = 47.4602$, $df = 1,2$, $p = 0.0204$) and for buccinid gastropods ($F = 22.6881$, $df = 1,2$, $p = 0.0414$). The cost of shell was significantly related to latitude in <i>Laternula</i> ($F = 23.7545$, $df = 1,2$, $p = 0.0396$) but not significantly related to latitude in the Buccinidae ($p = 0.0938$ NS). Cost values were taken at age 3 for <i>Laternula</i> and age 5 for buccinids because these ages overlapped measured individuals for most species within the taxa. These costs were based on mid-range data of 1.5 J.mg^{-1} of CaCO_3 from Palmer (1992).	288
Figure 9.7 Shell repairs in relation to temperature.....	290
Figure 9.8 Shell cost and shell thickness for molluscs analysed. Regressions of shell thickness on shell cost were not significant for <i>Laternula</i> bivalves ($p = 0.0821$ NS) or buccinid gastropods ($p = 0.8946$ NS).	292
Figure 9.9 Plots of shell thickness and repaired shell damage in buccinid gastropods for all shell repairs (left) and repaired shell damage from predation (right). There were no significant relationships between shell thickness and the proportion of damaged individuals (N_d) ($p = 0.2728$ NS) and the total number of injuries (N_i) ($p = 0.2552$ NS) or for the proportion of individuals damaged by predation (P_d) ($p = 0.2098$ NS), the total number of injuries from predation (P_i) ($p = 0.2421$ NS), the proportion of individuals with damage that was caused by a predator attack (αP_d) ($p = 0.2140$ NS), and the proportion of all injuries that were caused by predator attack (αP_i) ($p = 0.7502$ NS).	295
Figure 9.10 Buccinid gastropod shell thickness and aperture narrowness metric (aperture length/aperture width).	296
Figure 9.11 There were no significant inter-specific relationships between shell length and thickness ($p = 0.1824$ NS) (left) and shell repairs and thickness ($p = 0.2912$ NS) (right).	297
Figure 9.12 Echinoid spine length with test thickness written above the bar charts. There was a significant difference between test thickness and spine length ($t = -8.207$, $df = 52.256$, $p < 0.001$) and test thickness and spine length as a percentage of test diameter ($t = -12.640$, $df = 57.876$, $p = 0.024$).	298
Figure 9.13 Relationship between shell thickness and repaired shell damage in species of <i>Laternula</i> . Shell thickness was predicted by the proportion of damaged individuals	

(N _d) (F = 20.8045, df = 1,2, p = 0.0449) and the total number of injuries (N _i) (F = 64.2231, df = 1,2, p = 0.0152).....	300
Figure 9.14 Relationship between shell thickness and shell predator defence morphology.	300

List of appendices

Appendix 1 WDS data: Pearson product moment correlation statistics for elements for individual species. Cell contents are correlation coefficient (r), probability value (p) and number of samples (n). *Denotes p values that are significant at the $p < 0.0125$ level.	329
Appendix 2 EDS data: Pearson product moment correlation statistics for elements for individual species. Cell contents are correlation coefficient (r), probability value (p) and number of samples (n). *Denotes p values that are significant at the $p < 0.0125$ level.	338
Appendix 3 An of example of trials showing the constant depletion of oxygen down from 100 to < 70 % saturation. Regression lines are all significant ($p < 0.05$).	341
Appendix 4 Gompertz growth curve parameters, fitted using $y=a*\exp(-\exp(-(x-x_0)/b))$. .	342
Appendix 5 VBGF parameters, fitted using $y=a*(1-\exp(-b*(x-x_0)))$, however infinity is rather high, and values for small individuals are also high (because the curve does not pass close enough to the origin).	342
Appendix 6 Mean shell cost, respiration and tissue energy costs for each species taken from an example mid-valve of $1.5 \text{ J.mg}^{-1} \text{ CaCO}_3$ and including differences in CaCO_3 saturation state.	343
Appendix 7 Watson, S., Southgate, P. C., Tyler, P. A. & Peck, L. S. (in press). Early larval development of the Sydney rock oyster <i>Saccostrea glomerata</i> under near-future predictions of CO_2 -driven ocean acidification. Journal of Shellfish Research. (Proof from publishers. Expected publication date August 2009.).....	344

Declaration of Authorship

I, **Sue-Ann Watson**, declare that the thesis entitled **Latitudinal gradients in marine invertebrate shell morphology: production costs and predation pressure** and the work presented in the thesis are both my own, and have been generated by me as the result of my own original research. I confirm that:

- this work was done wholly or mainly while in candidature for a research degree at this University;
- where any part of this thesis has previously been submitted for a degree or any other qualification at this University or any other institution, this has been clearly stated;
- where I have consulted the published work of others, this is always clearly attributed;
- where I have quoted from the work of others, the source is always given. With the exception of such quotations, this thesis is entirely my own work;
- I have acknowledged all main sources of help;
- where the thesis is based on work done by myself jointly with others, I have made clear exactly what was done by others and what I have contributed myself;
- part of this work has been published as:
Watson, S., Southgate, P. C., Tyler, P. A. & Peck, L. S. (in press). Early larval development of the Sydney rock oyster *Saccostrea glomerata* under near-future predictions of CO₂-driven ocean acidification. Journal of Shellfish Research.

Signed

Date

Graduate School of the
National Oceanography Centre, Southampton

This Ph.D. dissertation by
Sue-Ann Watson
has been produced under the supervision of the following persons

Supervisors

Prof. Paul A. Tyler
University of Southampton
&
Prof. Lloyd S. Peck
British Antarctic Survey

Chair of Advisory Panel

Dr. Martin Sheader
University of Southampton

Member of Advisory Panel

Dr. Lawrence E. Hawkins
University of Southampton

Acknowledgements

This work was funded by a Natural Environment Research Council (NERC) studentship (NER/S/A/2005/13476) from the School of Ocean and Earth Sciences (SOES), University of Southampton, National Oceanography Centre, Southampton (NOCS) and a Co-operative Award in Science and Engineering (CASE) studentship from the British Antarctic Survey (BAS). Antarctic fieldwork at Rothera Research Station was funded by an Antarctic Funding Initiative (AFI) Collaborative Gearing Scheme (CGS) grant (CGS7/24) from BAS.

I would like to thank my supervisors Prof. Paul Tyler (SOES, NOCS) and Prof. Lloyd Peck (BAS) for their supervision and guidance throughout the Ph.D. I would also like to thank Dr. Simon Morley (BAS) for practical help during fieldwork, arranging the collaborative laboratory visits in Melbourne and Singapore and for commenting on drafts of my chapters.

This work would not have been possible without assistance from international collaborators: Prof. Paul Southgate from the James Cook University (JCU), Dr. Tan Koh Siang from the Tropical Marine Science Institute (TMSI) National University of Singapore (NUS) and Dr. Rob Day from the University of Melbourne, and I am particularly grateful for their hospitality and the interest they showed in the research.

I would like to thank Dr. Richard Pearce for support with scanning electron microscope (SEM) energy dispersive spectroscopy (EDS) techniques, and Bob Jones and John Ford for technical assistance in preparing numerous samples for SEM. Thanks to Dr. Elizabeth Harper (University of Cambridge) for showing me how to record repair marks on shells and image crystal structures on the SEM, for conducting X-ray diffraction (XRD) analysis on one species and for commenting on a draft of Chapter 4, which was also improved by comments from Dr. Clive Trueman (NOCS).

I am most grateful to Dr. Simon Morley, Stephanie Martin (volunteer researcher), Prof. Lloyd Peck and Dr. Melody Clark (BAS) for the collection of Arctic samples and respiration data from the NERC research station Ny Ålesund, Svalbard during July 2007. I would like to thank Dr. Katrin Linse (BAS) for the collection of samples from the Scotia

Arc during JCR cruises 144, 145, 146, 147, 149. I would like to thank Jenny Mallinson (NOCS) for the collection of *Buccinum undatum* and the use of the aquarium at NOCS, and Sarah Murty (NOCS) for the collection of *Psammechinus miliaris* from Torquay.

I am grateful for statistical advice from NOC colleagues: Peter Challenor, Dr. Brian Bett and Prof. John Shepherd.

I am exceptionally grateful to my family and friends, especially my parents Barry and Ami Watson, Fraser and Tyler Gibson, and Nina Rothe without whom I would have been homeless.

Fieldwork specific acknowledgements in chronological order:

Temperate Australian fieldwork 2006

Dr. Rob Day kindly hosted our experiments at the Zoology Department, University of Melbourne during July 2006. I would like to thank Dr. Rob Day, Prof. Lloyd Peck, Dr. Simon Morley and Stephanie Martin for their invaluable assistance in the collection of animals around Melbourne. With thanks to the School of Ocean and Earth Science, University of Southampton for a Kristin Bruhn award and the Challenger Society for Marine Science for travel support to help me attend the Scientific Committee on Antarctic Research (SCAR) 2006 conference in Tasmania and subsequent fieldwork in Melbourne.

Antarctic fieldwork 2006-2007

I would like to thank all members of Rothera Research Station during the austral summer season of 2006-2007 for a fantastic field season and for their invaluable support of the science work. In particular, I would like to thank Prof. Andy Clarke (BAS) and all members of the Rothera dive team (2006-2007): Kelvin Murray, Matt Brown, Alison Massey, Helen Rossetti, Dr. Birgit Obermüller, Jim Elliot and Bernard Meehan (also the boatmen), and Dr. Dan Smale for assistance with sample collection.

Tropical Australian fieldwork 2007-2008

I am especially grateful to Prof. Paul Southgate without whom none of the work at the James Cook University (JCU) would have been possible. Thanks for your enthusiasm for shells and shell collecting and the warm welcome at your department. I would like to thank Mark O’Callaghan for arranging my use of the JCU Great Barrier Reef Marine Park Authority (GBRMPA) permits. I would also like to thank Dr. Kevin Blake at the Advanced Analytical Centre (AAC) for guidance and support with SEM imaging and wavelength dispersive spectroscopy (WDS) techniques. Ocean acidification research at JCU was funded by the Australian Institute of Marine Science at JCU (AIMS@JCU) programme. With thanks to John Morrison and Simon Wever at the Marine and Aquaculture Research Facilities Unit (MARFU), Matthew Wassnig and Michael Milione for technical assistance with this part of the study.

Tropical equatorial fieldwork 2008

I would like to thank Dr. Tan Koh Siang and the TMSI NUS for hosting this collaborative research, which is part of a larger project coordinated by Dr. Simon Morley, and for allowing me to use the aquarium facilities at TMSI on St. John’s Island, Singapore. Dr. Simon Morley and Stephanie Martin accompanied the visit and I am grateful to them for arranging the collaboration and their technical assistance during the research. Thanks to Dr. Tan Koh Siang, Lai Chien-Houng (TMSI), Dr. Simon Morley and Stephanie Martin for collecting samples from Singapore for me in 2007 and with me in 2008.

All images copyright Sue-Ann Watson unless the source is otherwise stated.

This thesis is printed on recycled paper and where possible carbon dioxide emissions associated with travel during this work were offset.

For Fraser

Chapter 1: Introduction



Chapter 1: Introduction

1.1 Rationale

Cold-water marine bivalves of the abyssal, Arctic and Antarctic regions tend to be smaller (Nicol, 1964a; 1966; 1970), and have thin chalky shells that lack spines (Nicol, 1955; 1965), colour and ornamentation (Nicol, 1967) compared to those found in warmer waters. Measured as the amount of internal living space per unit shell deposited, marine gastropods decrease in their efficiency of calcium carbonate usage with increasing latitude in the Northern Hemisphere (Graus, 1974). Exactly why these trends occur has been a mystery, although it has been proposed that since in cold waters calcium carbonate (CaCO_3) is more soluble (Revelle & Fairbridge, 1957), the energetic cost of producing a shell will be greater (Clarke, 1983; 1990; 1993). However, some groups with extensive CaCO_3 skeletons and high overall carbonate content are abundant in polar waters (e.g. brachiopods and echinoderms), and some taxa, such as the starfish *Labidiaster radiosus* Lütken, 1871 grow to large size. Data to resolve this problem are scarce and definitive data absent. The purpose of this study is to document latitudinal trends in shell morphology, including shell thickness, for key calcareous marine invertebrates, to determine the cost of shell formation and to determine whether the trends in shells with latitude are controlled by energetic cost, predation or both.

1.2 Calcium carbonate shells and skeletons

Calcium carbonate (CaCO_3), commonly known as limestone, is a hard bioinorganic material and appeared in the fossil record 570 million years ago (mya) (Mann, 2001) during the Cambrian period in the Palaeozoic era. CaCO_3 is well preserved in the fossil record and prior to this period very few fossils are found indicating that before the Cambrian, few biomineralising organisms existed. Various biogenous CaCO_3 skeleton forms appeared during the Cambrian and this diversification of fauna is known as the Cambrian explosion.

CaCO_3 forms have continued to be successful on Earth and today many marine and terrestrial organisms make their shells and skeletons of CaCO_3 . Calcareous animals are

common in marine, freshwater and terrestrial environments. Calcifying marine invertebrates are found from the tropics to the polar seas, from coastal waters to the deep abyssal plains, and in chemosynthetically-supplied ecosystems. In the marine environment, examples of calcifying benthic faunae include molluscs, echinoderms, brachiopods, scleractinian corals, bryozoans and foraminifera. Calcareous flora also exist such as calcareous algae and coccolithophore phytoplankton.

1.3 Shell formation

Seawater is a complex mixture of dissolved salts. The most abundant ions in seawater (chlorine, sodium, calcium, potassium, magnesium and sulphate) are termed conservative ions since they are present in constant concentrations controlled by physical processes. Other ions in seawater are non-conservative because their concentrations are altered by chemical reactions (Libes, 1992). Calcifying organisms produce their skeleton by the precipitation of calcium carbonate from seawater during the process of biomineralisation. The calcium (Ca^{2+}) and carbonate (CO_3^{2-}) ions that marine invertebrates use to build their shells and skeletons are obtained from solution in seawater according to the simplified Equation 1. Ca^{2+} is not limited in the sea, but the solubility of CaCO_3 varies with water temperature and pressure, according to the solubility product (K_{sp}) (Equation 2) of Equation 1. The solubility product $[\text{Ca}^{2+}][\text{CO}_3^{2-}]$ must be exceeded for crystal nucleation and shell deposition to occur (Wilbur & Manyak, 1984).

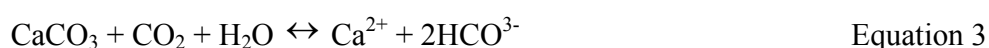


$$K_{\text{sp}} = [\text{Ca}^{2+}][\text{CO}_3^{2-}] \quad \text{Equation 2}$$

The solubility of calcium carbonate is influenced by 1) temperature, 2) pressure and 3) dissolved carbon dioxide (CO_2) concentration. Like most mineral salts, CaCO_3 is more soluble at high pressures but, unlike most substances, it is also more soluble at low temperatures (Revelle & Fairbridge, 1957). However, the increase in solubility of CaCO_3 at low temperatures is only very slight and the main factor affecting the solubility of CaCO_3 is the increase in CO_2 concentration in seawater at low temperatures, driving the

equilibrium reactions to produce less carbonate ions and more bicarbonate ions (HCO_3^-) (Equation 3).

The dissolution of CaCO_3 occurs by:



Calcium (Ca), like magnesium (Mg), strontium (Sr) and barium (Ba), is a Group 2 element in the periodic table of elements. Mg, Sr and Ba can substitute into the carbonate lattice in place of Ca. However, these molecules are of a different size to Ca and their presence in the lattice weakens its mechanical strength. Energy must be expended to exclude these elements during shell and skeleton formation. In environments where more energy is required to take Ca^{2+} ions out of solution and incorporate them into the lattice (such as at cold temperatures), greater substitution of these other Group 2 elements into the shell may be expected. Mg^{2+} ions are readily accommodated in the calcite lattice and biological calcites can contain Mg^{2+} ions up to levels of 30 mol % (Mann, 2001). The Group 2 carbonates tend to become less soluble down the group but barium carbonate is more soluble than strontium carbonate. The trend from most to least soluble is: $\text{MgCO}_3 > \text{CaCO}_3 > \text{BaCO}_3 > \text{SrCO}_3$.

The three calcareous phyla for which controls on shell size are studied in this thesis are the Mollusca, Brachiopoda and Echinodermata. Members of these phyla are highly abundant in many marine communities and are often considered keystone species in ecosystems. Keystone species have a disproportionate effect on their environment relative to their abundance (Paine, 1995). Many species are also important human food sources. Among these three broad taxonomic groups, the structural use of CaCO_3 differs. Gastropod and bivalve molluscs and brachiopods have external shells, or exoskeletons, whereas echinoderms have internal endoskeletons. The rigid test of a living echinoid (sea urchin) is covered by a thin layer of ciliated tissues (Castro & Huber, 2005). Shells and skeletons function to protect the soft tissues of the occupant from abiotic factors such as rock saltation and biotic factors such as predation. They also serve as support for locomotion and provide protection from desiccation in intertidal species.

There are about 93,000 described extant mollusc species, 70,000 extinct species and more living species yet to be described (Brusca & Brusca, 2003). The phylum Mollusca is the second largest phylum of animals after the Arthropoda (Castro & Huber, 2005) and the classes Gastropoda and Bivalvia contain over 98 % of known extant mollusc species (Barnes *et al.*, 1993). Mollusc shell is secreted by shell glands in the mantle (Brusca & Brusca, 2003), which is a thin layer of tissue that covers the body. The shell is usually depicted to form in a series of three compartments: 1) the outer mantle epithelium, 2) the extrapallial space and 3) the inner shell surface (Crenshaw, 1980). CaCO_3 is produced extracellularly (Brusca & Brusca, 2003) and is secreted from extrapallial (EPF) fluid in the extrapallial space (Crenshaw, 1980) during periods of aerobic conditions (Wilbur & Manyak, 1984). Calcium and other cations involved in the formation of shell carbonate are acquired 1) by differential absorption from ambient seawater (the external medium), 2) from metabolic HCO_3^- (Wilbur & Jodrey, 1955), 3) by the solution of previously deposited shell material, or 4) via the diet. Dietary calcium is an important source of calcium for land snails (Ireland, 1991; Stringer *et al.*, 2003; Jubb *et al.*, 2006; Ozgo & Bogucki, 2006) but is of little or, possibly, no importance for marine snails. For example, *Strombus gigas* shows no difference in growth rate with additional dietary calcium (Shawl & Davis, 2006).

In molluscs, CaCO_3 is deposited in two types of layers, an outer chalky prismatic layer and an inner pearly lamellar or nacreous layer. The nacreous layer has been lost in many groups (Brusca & Brusca, 2003). The outer layer of the shell is often covered by the periostracum, or hypostracum, made of conchin (quinone-tanned proteins). Conchin is also incorporated into CaCO_3 layers to help bind crystals together (Brusca & Brusca, 2003). Where the mantle attaches to the shell in bivalves it forms a pallial line.

Brachiopods, bryozoans and crustaceans form shell in a similar way to the molluscan system (Wilbur & Manyak, 1984). Brachiopoda possess bi-valved shells and are divided into two classes: Inarticulata and Articulata. There are about 45 extant species of Inarticulata and just over 290 extant species of Articulata. Inarticulata possess non-hinged valves of an organic composition, whereas Articulata possess valves that are hinged and composed of calcium carbonate and scleroprotein. The inner structural layers of

brachiopod shells are covered with an outer layer of organic periostracum. Brachiopod shell is secreted by the general mantle surface of the mantle lobes and the periostracum is secreted by the mantle edges. Punctate brachiopods bear canals that traverse their shells (punctae) containing tissue extensions of the mantle known as caeca, or mantle papillae (Williams *et al.*, 1997b; Brusca & Brusca, 2003).

There are around 7000 extant and 13000 extinct species of echinoderms. The echinoderm endoskeleton is composed of separate calcareous plates or ossicles arising from the mesodermal tissue with each plate forming from a single calcite crystal (Brusca & Brusca, 2003). There are about 950 extant species of the class Echinoidea (Castro & Huber, 2005) and in this group the skeletal plates of the round, shell-like test are held together by collagen matrix and calcite interdigitations. The moveable spines are also calcified (Brusca & Brusca, 2003).

Natural, or biogenic, CaCO_3 exists chiefly as the polymorphs, or crystal types, calcite, aragonite and vaterite. Of these polymorphs, calcite and aragonite are of widespread biological importance (Clarke, 1983). Calcite and aragonite have the same chemical formula, but different crystal structures: calcite is trigonal whereas aragonite is orthorhombic (Clarke, 1983). The solubility of CaCO_3 varies between CaCO_3 polymorphs; calcite is slightly harder, less dense and 36 % less soluble than aragonite (Vermeij, 1993). Aragonite is used by most bivalves and gastropod molluscs, although some molluscs use both aragonite and calcite (Clarke, 1983). Calcite is formed by some foraminiferans (Clarke, 1983) and adult oysters (Stenzel, 1964; Clarke, 1983). Magnesian calcite is formed by echinoderms (Weber, 1969) in the form of mosaic crystals (Tsipursky & Buseck, 1993).

1.4 Patterns in shell morphology with latitude

Shell size, sculpture, colour and ornamentation

Large-scale biogeographic patterns such as latitudinal trends occur in both the terrestrial and marine environment. In the 1960s and 70s, reports of latitudinal trends in the shell characteristics of marine molluscs began to appear. It was noted that bivalves that live in

the cold waters of abyssal, Arctic and Antarctic regions where temperatures are less than 5 °C tend to be smaller than those found in warmer waters (Nicol, 1964a; 1966; 1970). Cold-water bivalves have shells that are thin and frequently chalky, lack bright coloration and colour patterns, and have growth bands indicative of slow growth (Nicol, 1967). In cold waters, ornamentation, where present, is only slight and calcareous spines are absent among extant bivalves in the polar seas (Nicol, 1955; 1965; 1967). In Arctic and Antarctic waters, there also are no bivalves that cement their shell to the substratum (Nicol, 1955; 1964b)

Among the gastropods, some rocky shore species' spire height decreases towards the equator (Vermeij, 1977). Snails in calcium-poor habitats such as the deep sea, freshwater and terrestrial habitats have thin shells and it is rare for sculpture or a narrow aperture to be found (Vermeij & Covich, 1978).

Shell thickness

Graus (1974) demonstrated a latitudinal cline in various shell properties in over 105 different species of marine prosobranch gastropods along the east coastline of North America. Calcification index (a measure reflecting the efficiency of calcium carbonate utilisation) was calculated by components of shell density, shell thickness index and form index. The gastropods demonstrated an increase in efficiency of calcium carbonate usage with increasing latitude.

As well as these inter-specific latitudinal clines in shell thickness, intra-specific clines also exist in marine gastropods. The cowrie *Cypraea annulus* exhibits greater callus thickness with increasing mean seawater temperature (Irie, 2006). In the Indo-Pacific cowry, *Cypraea caputserpentis*, adult body size increases but shell thickness decreases with increasing latitude (Irie & Iwasa, 2003). Shells of the intertidal gastropod *Littorina obtusata* from the Gulf of Maine weighed less, were thinner and weaker at higher latitudes than lower latitudes, although soft body tissue mass increased with increasing latitude. When transplanted to a different latitude, snails adopted the traits found at the new latitude demonstrating that phenotypic plasticity produces geographic variation within a species (Trussell, 2000).

1.5 Competing hypotheses: shell cost versus shell function

Shell cost: energetics

There are three major costs, and a fourth minor cost, associated with a calcium carbonate skeleton:

- 1) Shell deposition – production of the skeleton from ions in seawater and the organic matrix from metabolising food,
- 2) Locomotion of the skeleton in motile taxa/forms (post-deposition),
- 3) Limited growth rate of the soft tissue depending on the maximum growth rate of the shell,
- 4) Prevention of dissolution (shown to be small in shallow water species) (Palmer, 1981).

Since the planetary temperature gradient of terrestrial and marine surface water habitats is a function of latitude, historically, an energetic hypothesis has been proposed to explain latitudinal trends in marine molluscs. At low temperatures carbon dioxide is more soluble and CaCO_3 has a higher solubility product (Revelle & Fairbridge, 1957). Thus the first cost, that of shell deposition, was hypothesised to control shell size. It was proposed that at lower temperatures shells would be thinner because in cold waters shell-building ions (Ca^{2+} and CO_3^{2-}) are more soluble and hence more energetically expensive to remove from seawater (Graus, 1974; Vermeij, 1978; Clarke, 1983; 1990; 1993). As such, the energetic cost of producing a unit of calcium carbonate skeleton is expected to increase as temperature decreases because the Gibbs free energy of calcification is greater (Clarke, 1983; 1990; 1993).

In addition to the extra cost resulting from increased CaCO_3 solubility at high latitudes, metabolic rates vary with temperature. Metabolic rates of Antarctic marine invertebrates are much lower than species from warmer waters (e.g. Peck, 2002; Harper & Peck, 2003). Since polar organisms are stenothermal with slow metabolic rates and slow growth (e.g. Peck, 2002) that, it has been argued, is limited by resource availability (Clarke, 1991), then at high latitudes this energetic cost may be of particular significance. According to this energetic hypothesis, at high latitudes shells should be 1) thinner or smaller, or 2)

alternative ions such as strontium (Sr) or magnesium (Mg) (Rosenberg, 1980; Dauphin *et al.*, 1990), or organic matrix should be substituted into the skeleton.

Conversely, several groups that dominate faunae at high latitude, including echinoderms, brachiopods and bryozoans, are large and heavily calcified, and would thus appear to be in contrast with the trend for molluscs. However, Arnaud (1974) points out that in Antarctica gigantism is more frequent when animals are not calcareous or have very little calcification. Since those first reports documenting latitudinal trends in the shell characteristics of marine gastropods, with the exception of mathematical studies by Irie & Iwasa (2005) and Irie (2006), few data exist to offer explanations for the latitudinal trends in shell size and form.

Shell function: defence and predation intensity

Shells and exoskeletons provide support for locomotion, a home and protection. In the course of protecting the occupant, shells may become damaged by abiotic factors such as saltating rocks or ice scour, or by biotic factors such as predation, overcrowding or shell boring organisms (e.g. polychaetes, sponges and algae). One of the primary functions of a shell is to protect the occupant from damage by predators. Methods of predation on shelled marine invertebrates include boring (drilling), crushing and smashing.

Durophagous (shell-destroying) molluscivorous predators include teleosts (bony fishes), sharks, rays, crustaceans (Stomatopoda), spiny lobsters, brachyurans (crabs), birds and drilling gastropods (Vermeij, 1977). Asteroids (sea stars), actiniaria (sea anemones) also predate molluscs (Vermeij, 1977) as do birds (e.g. Cadée, 1999) and sea otters. A complete list of molluscivores specialised for breaking shells includes: Phylum Mollusca (Class Gastropoda and Cephalopoda), Subphylum Crustacea (Class Malacostraca), Phylum Chelicerata (Class Xiphosurida and Arachnida), Phylum Chordata (Classes Chondrichthyes, Osteichthyes, Reptilia, Aves and Mammalia) (Vermeij, 1987).

Shelled animals are also attacked by shell-boring, or drilling, predators and in many species of bivalve, a frequent cause of death is attack by boring (drilling) predators (Gabriel, 1981). Drilling predators include molluscan gastropods and cephalopods, beetles (Vermeij, 1987) and turbellarian and nematode worms (Bromley, 1981; Kabat, 1990). The boring attack

may be mechanical, by radula rasping, and chemical by secretory products from the accessory boring organ (ABO) (Gabriel, 1981). It is thought that the chemical dissolution of the shell is achieved by a combination of enzymes, inorganic acid and chelating agents in a hypertonic secretion at around pH 4 (Carriker & Williams, 1978).

Predation pressure is generally considered to decrease towards the poles (Paine, 1966; MacArthur, 1972) and modern durophagous predators are rare or absent in Antarctica (Aronson & Blake, 2001; Clarke *et al.*, 2004; Aronson *et al.*, 2007). Bertness *et al.* (1981) showed empty snail shells glued to rocks were wrenched off by porcupine fish (*Diodon* spp.) more quickly at lower latitudes than higher latitudes studied. Repaired shell injuries in gastropods increase from high to low latitudes in the species *Littorina littorea*, *Terebra dislocata* and *Odostomia impressa*, in the *Hastula cinerea* species complex, and among species of the families Terebridae and Thaididae (Vermeij, 1978; 1980; 1982a; Miller, 1983). Vermeij (1987) knows of no reverse gradient in incidences of repaired shell injuries.

Shell breaking or crushing predators such as brachyuran crabs, stomatopods, lobsters, fishes and shell drilling predators such as muricid and naticid gastropods and octopods (Vermeij, 1978) are limited in, or absent from Antarctica (Aronson & Blake, 2001; Clarke *et al.*, 2004). Reptant decapod crustaceans (reptantia) are poor regulators of magnesium in their haemolymph and are narcotised by the combination of low temperatures and high Mg^{2+} concentration in the haemolymph (Frederich *et al.*, 2000; Frederich *et al.*, 2001). Thus reptant decapods appear unable to inhabit the permanently cold waters in Antarctica and are largely absent in waters south of the Antarctic Convergence (Frederich *et al.*, 2001).

Predator cues induce bigger (Dalziel & Boulding, 2005) and thicker (Trussell & Nicklin, 2002) shells in gastropods, but if predation risk is low or cost of shell production high, the optimal strategy is to not grow shell (i.e. shell-less growth) or to have no shell (Irie & Iwasa, 2005). The conclusion from these factors is that shells could be thinner at high latitudes because of the lack of drilling and crushing predators and latitudinal variation in selection by predation for thicker shells and exoskeletons may be the controlling factor in

skeleton thickness. Understanding the controls on shell thickness in marine invertebrates is important in predicting the effects of climate change on marine calcifiers.

1.6 Aims and hypotheses

Patterns in shell size with latitude may be explained by variations with latitude in 1) the cost of producing a shell and/or 2) variation in predation pressure. The following chapters will investigate changes with latitude in three key groups of calcifying benthic marine animals (molluscs, brachiopods and echinoids) and investigate shell composition, costs and predation pressure associated with shells.

Aims

- 1) To explore the latitudinal variation in shell thickness and skeletal composition in calcareous marine megabenthic invertebrates (molluscs, brachiopods and echinoderms).
- 2) To determine if any variation or trend may be explained by energetic cost.
- 3) To determine if any variation or trend may be explained by predation pressure.

Hypotheses

Hypothesis 1: Shells of marine invertebrates decrease in thickness or size with increasing latitude. Skeletal composition will also vary with latitude.

H₀: There is no difference in the thickness, size or composition of marine invertebrate shells or skeletons with latitude.

Hypothesis 2: Skeletons are more costly to produce at high latitudes and the cost of calcification as a proportion of the total energy budget will increase with increasing latitude.

H₀: Shells and skeletons cost the same amount of energy regardless of the temperature at which they are produced.

Hypothesis 3: Predation pressure decreases with increasing latitude.

H₀: There is no variation in predation pressure with latitude.

1.7 Structure of the thesis

This thesis is arranged into nine chapters. Chapter 2 describes the sample sites and study species investigated. Chapter 3 investigates latitudinal patterns in calcium carbonate skeleton size, thickness and organic content of calcareous megabenthic marine animals. Chapter 4 considers any variation with latitude in skeleton elemental composition. Chapter 5 provides data on the metabolic rates of closely related species with latitude, and Chapter 6 uses growth data to estimate the absolute and proportional cost of producing a skeleton across latitudes. Chapter 7 investigates the alternative hypothesis that latitudinal trends in predation intensity control skeleton size. Chapter 8 presents data on the effects of ocean acidification on the commercially important calcareous bivalve, *Saccostrea glomerata*. Finally, Chapter 9 discusses the results as a whole and summarises the findings from this study.

Chapter 2: Sample sites and study species



Chapter 2: Sample sites and study species

2.1 Introduction

In order to study comprehensively latitudinal variation in calcareous marine invertebrates, sampling sites were chosen in tropical, temperate and polar sites to cover a broad range of latitudes and temperatures. Key megabenthic calcareous taxa were selected for investigation, and these included gastropod snails, bivalve clams, brachiopods (lampshells) and echinoids (sea urchins). For each type of marine invertebrate, species within families (confamilial species) or genera (congeneric species) were chosen to constrain taxonomically the data. Closely related species that occurred over a wide geographic latitudinal range were especially targeted.

In this thesis, a variety of methods were used to investigate latitudinal trends in shell morphology and composition, metabolic costs and predation pressure in calcareous benthic marine invertebrates and details of these methods are described in their respective chapters. This chapter describes the sample sites and study species.

2.2 Sample sites

Based on average water temperatures, marine environments can be categorised into 4 regions: tropical, subtropical (or warm temperate), temperate and polar (Figure 2.1). These regions only refer to surface water since the deep sea is uniformly around 4 °C.

The sample sites chosen for this project were located in tropical, temperate and polar regions and are shown in Figure 2.2. From low to high latitudes, the main sites included: Singapore; Townsville, Queensland, Australia; Melbourne, Victoria, Australia; Doubtful Sound, New Zealand; Torquay and Southampton Water on the south coast of England; Rothera Research Station on the Antarctic Peninsula; and Svalbard in the Arctic Circle. Additional samples from the Southern Ocean, maritime Antarctic and Falkland Islands were also used in this study. Details of the characteristics of the sites sampled are given in Table 2.2.

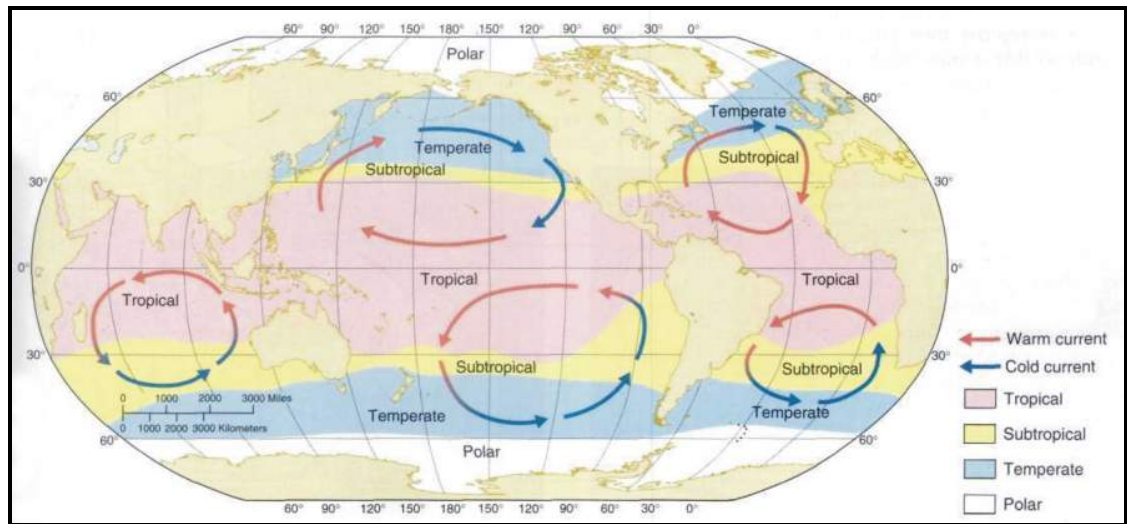


Figure 2.1 Marine regions based on surface seawater temperatures. Figure taken from Castro and Huber (2005).

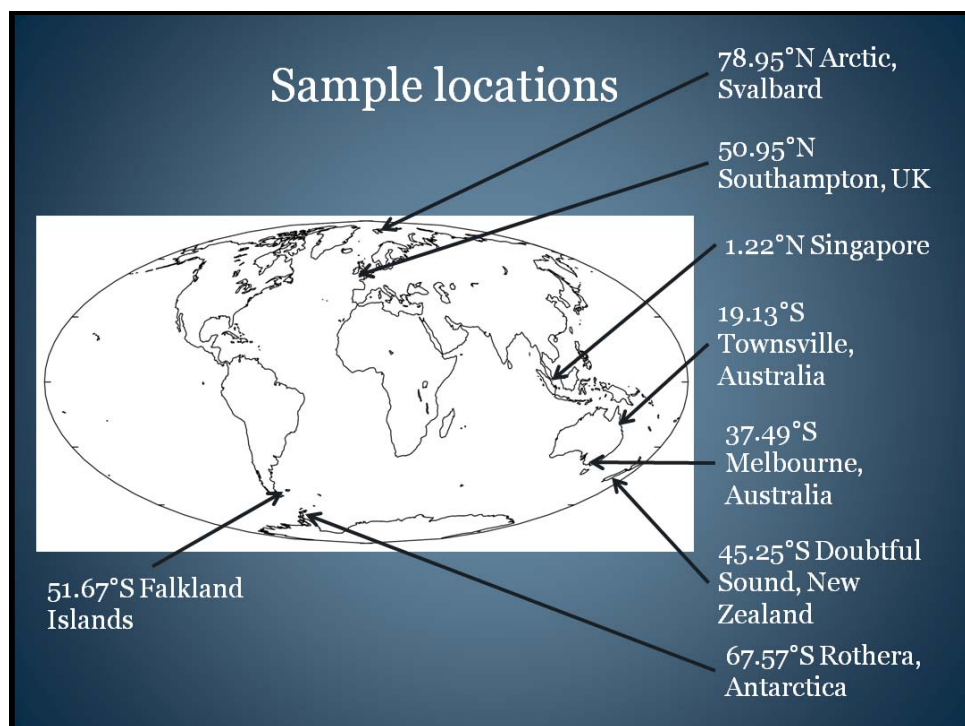


Figure 2.2 Global sample sites with latitudes.

2.3 Study species

Study species were chosen from three key phyla of calcareous (calcium carbonate shell producing) megabenthic (large bottom-dwelling) marine invertebrates: the Mollusca, Brachiopoda and Echinodermata, from the study sites described above. Species were taxonomically-constrained over a wide range of latitudes (Table 2.1). Where it was not possible to collect samples from the same genus (because congeners did not occur over a wide enough latitudinal range), confamilial species were compared instead, thus enabling genera with restricted latitudinal ranges to be included.

The requirement for geographically broad sample locations underpinned choices for study species. The latitudinal variation in four groups of taxonomically-constrained taxa was studied in detail, including bivalves, gastropods, brachiopods, and echinoids (Table 2.2 and Figure 2.3). The bivalve clam genus *Laternula* can be found over a very wide latitudinal range from Antarctica through the Southern Hemisphere and into Singapore and Japan in the Northern Hemisphere. The taxonomic relations of key species studied are given in Table 2.1. In addition, and when time allowed, ‘general species’ unconstrained by their taxonomy were collected on an opportunistic basis and analysed to compare with data from closely related species.

Table 2.1 Taxonomy for main study species (calcareous megabenthic marine invertebrates).

Phylum	Class	Order	Family	Species	Authority	Latitude
Mollusca	Bivalvia	Pholadomyoidea	Laternulidae	<i>Laternula truncata</i>	(Lamarck 1818)	1.22 °N
				<i>Laternula boschasina</i>	(Reeve, 1863)	1.22 °N
				<i>Laternula valenciennesii</i>	(Reeve, 1860)	19.13 °S
				<i>Laternula recta</i>	(Reeve, 1863)	37.49 °S
				<i>Laternula elliptica</i>	(King and Broderip, 1831)	67.57 °S
Mollusca	Gastropoda	Neogastropoda	Buccinidae (Superfamily Buccinoidea)	<i>Cantharus fumosus</i>	Dillwyn, 1817	19.13 °S
				<i>Phos senticosus</i>	(Linnaeus, 1758)	19.13 °S
				<i>Cominella lineolata</i>	(Lamarck, 1809)	37.49 °S
				<i>Buccinum undatum</i>	Linnaeus, 1758	50.95 °N
				<i>Neobuccinum eatoni</i>	(Smith, 1875)	67.57 °S
				<i>Buccinum glaciale</i>	Linnaeus, 1761	78.95 °N
				<i>Buccinum cf. groenlandicum</i>	Hancock, 1846	78.95 °N
Echinodermata	Echinoidea	Echinoidea/ Diadematoidea	Echinidae	<i>Psammechinus miliaris</i>	(Gmelin, 1778)	50.47 °N
				<i>Sterechinus</i> sp.		61.83 °S
				<i>Sterechinus neumayeri</i>	(Meissner, 1900)	67.57 °S
Brachiopoda	Articulata	Terebratulida	Terebratulidae	<i>Liothyrella neozelanica</i>	Thomson, 1916/8	45.25 °S
				<i>Liothyrella uva</i>	(Broderip, 1833)	67.57 °S

Table 2.2 Study sites from low to high latitudes and species collected at each site.

Marine region	Location	Latitude (low to high)	Annual mean temp. (°C)	Temp. range (°C) (min to max)	Source for temp. data	Gastropod species	<i>Laternula</i> species	Brachiopod species	Echinoid species
Tropical	Singapore (lower intertidal)	1.22 °N	28.5*	25.2-31.4*	Morley <i>et al.</i> (unpublished data)		<i>Laternula truncata</i>		
Tropical	Singapore (higher intertidal)	1.22 °N	29.3*	22.3-38.6*	Morley <i>et al.</i> (unpublished data)		<i>Laternula boschasina</i>		
Tropical	Townsville, Australia	19.13 °S	26.0	18.7-32.5	AIMS <i>et al.</i> (2009)	<i>Cantharus fumosus</i> & <i>Phos senticosus</i>	<i>Laternula valenciennesii</i>		
Temperate	Melbourne, Australia	37.49 °S	16.3	12.5-21.5	University of Melbourne	<i>Cominella lineolata</i> & <i>Thais orbita</i>	<i>Laternula recta</i>		<i>Heliocidaris erythrogramma</i>
Temperate	Doubtful Sound, New Zealand	45.25 °S	~14	11-17	Lamare <i>et al.</i> (2009)			<i>Liothyrella neozelanica</i>	
Temperate	Torquay, England	50.47 °N	~13.7	10.3-17	Padin <i>et al.</i> (2007)				<i>Psammechinus miliaris</i>
Temperate	Southampton Water, England	50.95 °N	12.6	7.4-18	BrambleMet	<i>Buccinum undatum</i>			
Temperate	Falkland Islands	51.67 °S	6.0	0.0-13.8	GLOSS			<i>Magellania venosa</i>	
Polar	Signy, Scotia Arc	60.72 °S	~ -0.89	~ -1.86-1.8	GLOSS			<i>Liothyrella uva</i>	

Table 2.2 continued.

Marine region	Location	Latitude (low to high)	Annual mean temp. (°C)	Temp. range (°C) (min to max)	Source for temp. data	Gastropod species	<i>Laternula</i> species	Brachiopod species	Echinoid species
Polar	North of King George Island, Scotia Arc	61.83 °S							<i>Sterechinus</i> sp. (~150 m depth)
Polar	Rothera, Antarctica	67.57 °S	-0.7	-1.8- +1.0	RaTS**	<i>Neobuccinum eatoni</i>	<i>Laternula elliptica</i>	<i>Liothyrella uva</i>	<i>Sterechinus neumayeri</i>
Polar	Ny Ålesund, Svalbard, Arctic Circle	78.95 °N	~2.6	-1.8- +7	Cottier <i>et al.</i> (2005)	<i>Buccinum glaciale</i> & <i>Buccinum</i> cf. <i>groenlandicum</i>			

*Temperature logger data at intertidal collection sites (Morley *et al.*, unpublished)

**Rothera Time Series (RaTS) data courtesy of M. Meredith and A. Clarke (British Antarctic Survey)



Figure 2.3 Examples of study species by region and taxonomic group.

2.4 Collection of animals

Samples were predominantly collected by SCUBA divers or from the low intertidal. Most species in this study were collected from shallow coastal waters from 0 – 30 m in depth. For subtidal species, SCUBA diving was the preferred method of collection as it has a low impact on other benthic fauna and minimised damage to the samples. A few specimens were also collected by dredge or trawl, or acquired from museum and private collections. For each species, animals of a range of sizes were obtained to allow regression of key parameters with animal size. After collection, shells of animals were gently cleaned with a soft toothbrush to remove epibionts such as algae and calcareous worm tubes. Any material attached to the spines of echinoids was removed carefully with forceps. Animals were then transferred to aquaria and allowed to recover from any stress caused during collection.

2.5 Sample site-specific animal collection information

This section provides further details on site-specific animal collection information from low to high latitudes. Samples were mainly collected by the author, the British Antarctic Survey (BAS) or the National Oceanography Centre, Southampton (NOCS), University of Southampton. Where multiple species were collected at one site, they are detailed in table form. Maps of sample sites have been reproduced from Google Maps according to their terms of use.

Singapore, Equatorial Tropics 1.22 °N

Measurements on the metabolic rate of tropical marine clams (genus *Laternula*) were conducted as part of a collaborative project with Dr. Tan Koh Siang and Dr. Simon Morley at the Tropical Marine Science Institute (TMSI), National University of Singapore (NUS) at the research station on St. John's Island, Singapore.

Clams were collected from the intertidal mangroves of the Straits of Johor. Specimens of *Laternula truncata* and *L. boschasina* were collected from around Kranji reservoir (Figure 2.4) (001° 26.428 N, 103° 44.267 E) by digging around mangroves in mud and sand on the mid- to high-intertidal zone on spring tides (0.6 m at low tide). *L. truncata* were generally more abundant around the mid-intertidal, whereas *L. boschasina* were more abundant slightly higher up the beach. Thirty *L. truncata* and 20 *L. boschasina* were collected. The salinity of the water around low tide was 15. Temperature loggers were placed in the sediment by Dr. Simon Morley after collections were finished, and these provided *in situ* environmental measures.



Figure 2.4 Location of the sample site in Singapore.

After collection, the clams were taken to the TMSI aquarium complex on St. John's Island and held in aquaria. Clams were housed in tanks at a salinity of 22. This salinity was recommended by S. Morley (pers. comm.) based on previous experiments on Singapore species of *Laternula* in the aquarium and the salinity of the brackish water around the collection site on high and low tide. Salinity of incoming TMSI aquarium water was 31. Salinity was reduced to the required level by the addition of distilled water.

The TMSI aquarium is only partially enclosed and so exposed to diurnal temperature fluctuations similar to those the clams experience *in situ*. The aquarium roof is comprised largely of glass, exposing the aquarium to illumination of exact natural timing and similar intensity. Dark covers were, however, placed over the *Laternula* tanks to minimise burrowing attempts that are triggered by light, but these were not used for other species.

Townsville and Lucinda, Tropical Australia 19.13 °S

Specimens were collected and experiments run during a collaborative research project with Professor Paul Southgate at the School of Marine and Tropical Biology at the James Cook University (JCU), northern tropical Queensland, Australia, from April to June 2007.

Specimens were collected at low tide from the intertidal (Table 2.3). After specimens were

collected, they were housed in aquaria at the Marine and Aquaculture Research Facilities Unit (MARFU) at JCU.

Cantharus fumosus was collected intertidally at very low tides (< 0.4 m) on the mainly rubble based rocky reef at Kissing Point, to the south end of Rows Bay, Townsville, Qld (Figure 2.5). On low tides when this reef was exposed water temperatures in pools of seawater on the reef reached 28-31 °C. *Phos senticosus* was collected from Lucinda, Qld (Figure 2.6). *P. senticosus* was found at very low tides (< 0.3 m) in the sand on clean sand bars on the incoming tide. Both buccinid species are only exposed at very low tides which occur on average 3 to 4 times a month. They are subtidal for the vast majority of the time.

Table 2.3 Species collected from and around Townsville.

Species	Location	Depth collected
<i>Cantharus fumosus</i>	Rows Bay – rocky rubble reef at very low tides (0.4 m)	Found intertidally at very low tides
<i>Phos senticosus</i>	Lucinda – sand bar at very low tides (0.3 m), popping on the incoming tide	Found intertidally at very low tides

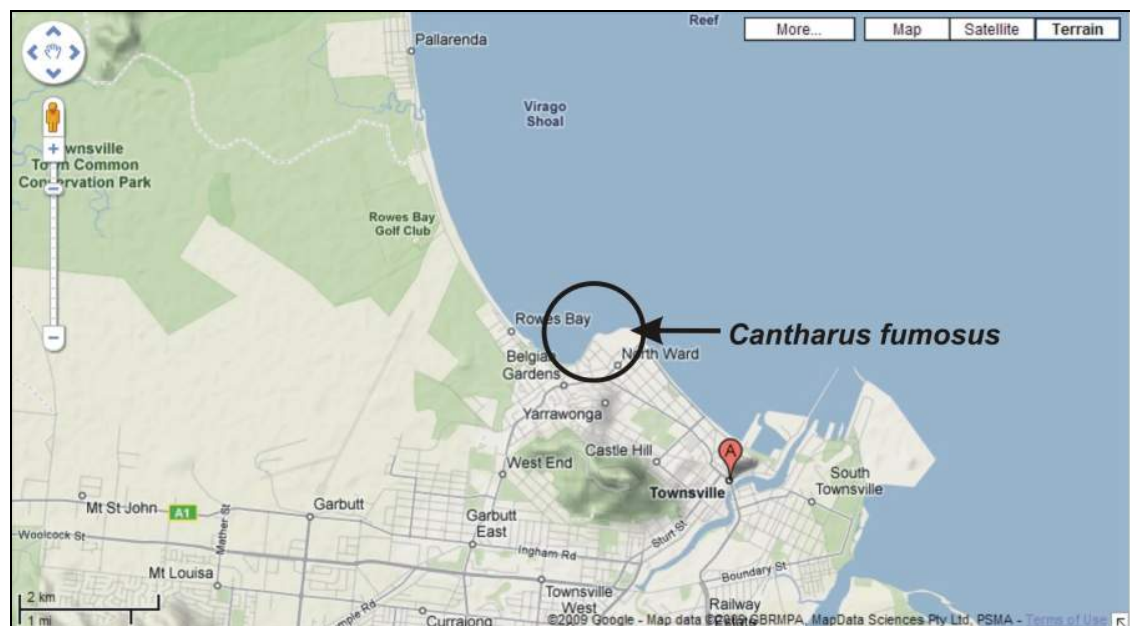


Figure 2.5 Location of the sample site in Townsville, Queensland, tropical Australia.

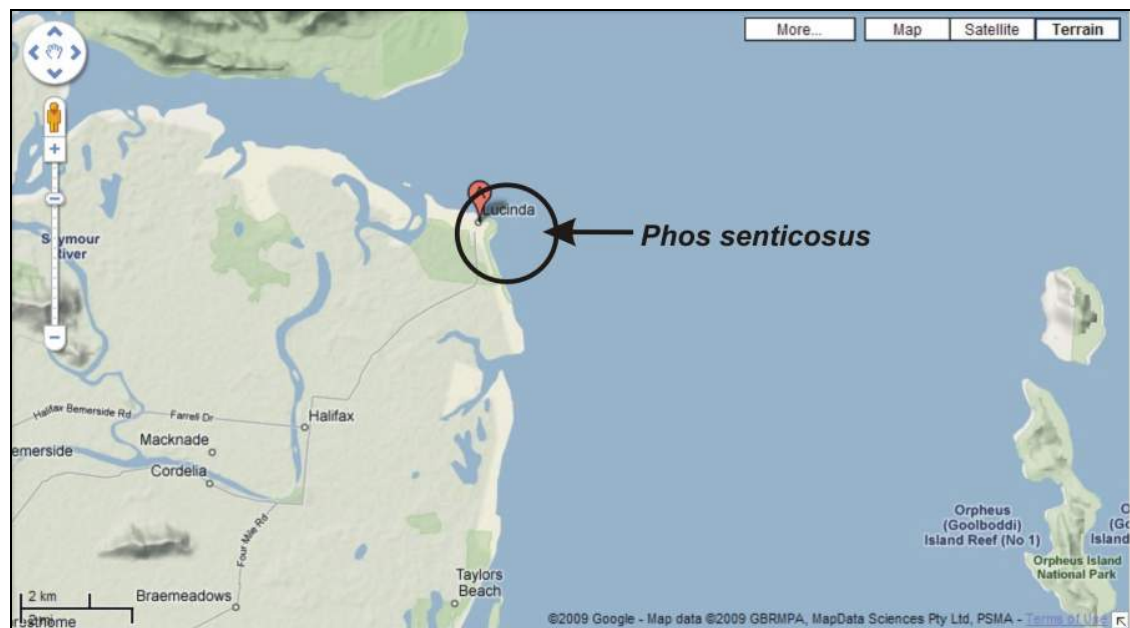


Figure 2.6 Location of the sample site in Lucinda, Queensland, tropical Australia.

Gastropods were held at in aquaria at MARFU. The aquaria for the experiments were run on their own separate seawater system, filtered and UV sterilised to limit micro-organism growth. The temperature in the MARFU aquarium during the experiments was 28.2 – 28.4 °C.

Clams of the genus *Laternula* are reported to occur around Townsville. However, extensive searches in many varied habitats failed to find any live individuals. *Laternula valenciennesii* shells were kindly donated by Prof. Paul Southgate and were collected as ‘dead’ or empty shell on the beach after cyclones. Many of the shells had remains of tissue in them suggesting that they had very recently been uprooted from the substratum. It is likely they live either in shallow murky water just off the coast or, possibly more likely, in estuarine environments. Many of the shells found after cyclones were at the mouths of rivers (P. Southgate, pers. comm.).

A second collaborative research project at JCU was funded by the Australian Institute of Marine Science (AIMS) “AIMS@JCU” programme. This project ran from November

2007 to March 2008 and investigated the effects of ocean acidification on developmental stages of the Sydney rock oyster, *Saccostrea glomerata* (Chapter 8).

Melbourne, Temperate Australia 37.49 °S

During July 2006, invertebrates (Table 2.4) were collected intertidally from around Port Philip Bay, Melbourne, Victoria, Australia. Animals were collected from Geelong and Portsea within Port Phillip Bay and Barwon Heads and Flinders outside of Port Phillip Bay (Figure 2.7). *Laternula recta* were collected from sediments around Geelong, gastropods were collected from the rocky intertidal reefs at Barwon Heads and Flinder's Mushroom Reef and the echinoid *Heliocidaris erythrogramma* was collected from under Portsea Pier.

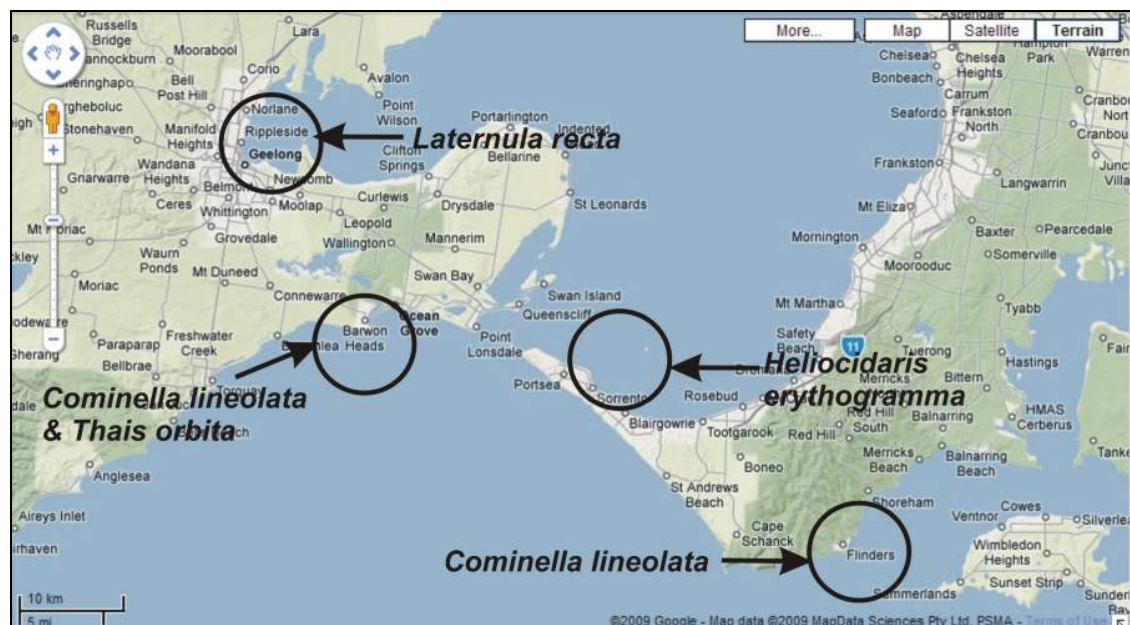


Figure 2.7 Location of the sample sites around Melbourne and Port Philip Bay, Victoria, temperate Australia.

After collection, animals were kept at ambient seawater temperature and transferred to the University of Melbourne aquarium in the Zoology Department. This filtered circulated seawater aquarium is maintained at temperatures close to natural seawater temperatures throughout the year. During July and August 2006, the winter seawater temperatures were 14 °C. Respiration data were collected for *Laternula recta* and *Cominella lineolata* over a 2-week period of experiments.

Table 2.4 Species collected around Melbourne, Australia.

Taxon	Species	Notes	Site	Depth collected
Bivalve	<i>Laternula recta</i> (Reeve, 1860)	Burrowing clam	Geelong (sand and mud)	Intertidal
Gastropod	<i>Cominella lineolata</i> (Lamarck, 1809)	Spotted Cominella, family Buccinidae	Barwon Heads and Flinders Reef (rocky reefs)	Intertidal
Gastropod	<i>Thais orbita</i> (Gmelin, 1791) (= <i>Dicathais textilosa</i>)	whelk, family Muricidae	Barwon Heads (rocky reefs)	Intertidal
Echinoid	<i>Heliocidaris erythrogramma</i> (Valenciennes, 1846)	Purple Sea Urchin, family Strongylocentrotidae	Portsea Pier, Sorrento	1-8 m

Doubtful Sound, New Zealand 45.25 °S

Sample collection was arranged by Prof. Lloyd Peck (BAS) and Dr. Simon Morley (BAS) and carried out by the University of Otago, Dunedin, New Zealand. Samples of the brachiopod *Liothyrella neozelanica* were collected by SCUBA divers from rock walls and overhangs in the fiord at depths of 10-20 m. They were then frozen and transported to the UK for analysis.

Torquay, England 50.47 °N

Specimens of the echinoid *Psammechinus miliaris* were collected from the west end of Torre Abbey Sands, Torquay on rocks at low tide by Sarah Murty (NOCS) (Figure 2.8). Animals were held in the NOCS aquarium at 19 °C (summer aquarium temperatures) and respiration experiments were conducted in May and June 2008.



Figure 2.8 Location of the sample site in Torquay, Torbay, on the south coast of England.

Southampton, England 50.95 °N

Specimens of *Buccinum undatum* were collected by Jenny Mallinson from Southampton Water by dredge from 6-10 m deep (Figure 2.9). Animals were held in the NOCS aquarium at 19 °C (summer aquarium temperatures) and respiration experiments were conducted in May and June 2008.

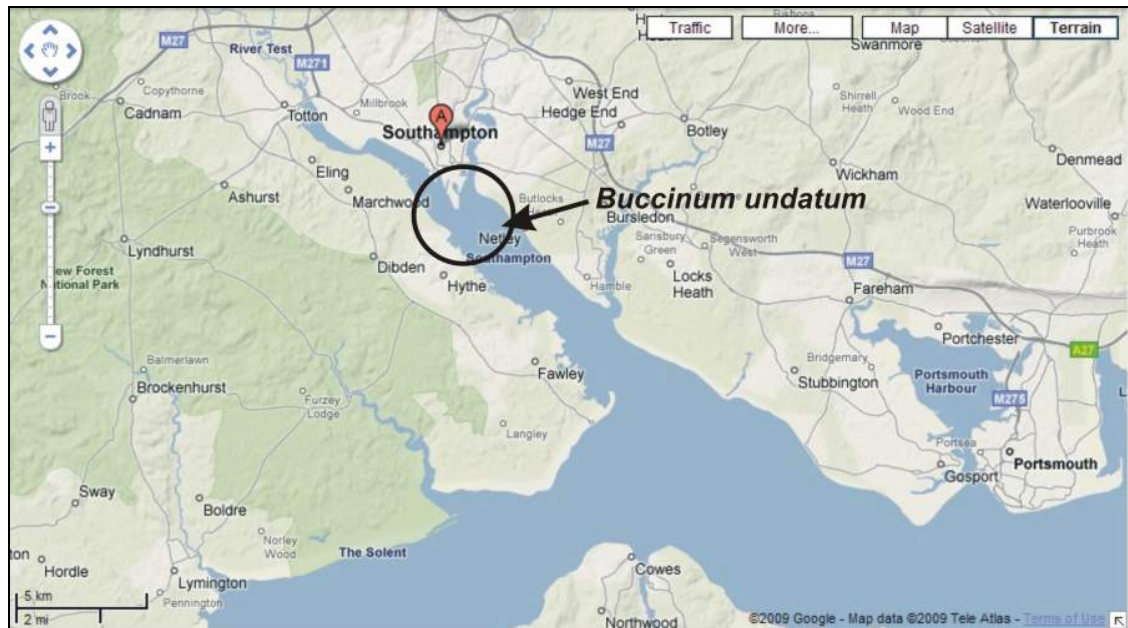


Figure 2.9 Location of the sample site in Southampton Water, Southampton, on the south coast of England.

Falkland Islands 51.67 °S

Brachiopod specimens were collected for L. Peck (BAS) by the Falkland Islands Fisheries Department during the mid-1990s. They were collected as a by-catch from trawling operations in depths of 20-50 m. Samples were frozen for analysis in the UK.

Scotia Arc, Southern Ocean (North of King George Is.) 61.83 °S

Animals were collected by a rough bottom otter trawl from around the sub-Antarctic islands of the Scotia Arc by K. Linse (BAS) on the research cruise JR144 as part of the BAS BIOPEARL project. The samples used in this project were *Sterechinus* sp. samples were collected from North of King George Island (KGI) in the Scotia Arc. Samples were obtained from ~150 m depth on 11/03/2006, sample code BAS KL 06-0304.

Signy Island, maritime Antarctic 60.72 °S

Brachiopod specimens were collected for L. Peck (BAS) from Borge Bay, Signy Island in the maritime Antarctic (60°43'S, 45° 36'W). The collection sites were Polynesia Point (~7

m), Outer Island (at depths of ~11 m, ~27 m, ~36 m), Powell Rock (~18 m). All specimens were collected by SCUBA divers and frozen until analysed in the UK.

Rothera, Antarctic Peninsula 67.57 °S

Samples were collected and experiments run at Rothera Research Station, Graham Land, Adelaide Island, on the Antarctic Peninsula (67°34' S, 68°08' W) during a summer season from December 2006 to March 2007 funded by an Antarctic Funding Initiative (AFI) Collaborative Gearing Scheme (CGS) grant from the British Antarctic Survey. Animals were collected live from around Rothera Point (Figure 2.10 and Figure 2.11) by the Rothera dive team using SCUBA. Animals collected are listed in Table 2.5. Animals were held in the aquarium at the Bonner Laboratory, Rothera. Summer temperatures around Rothera Point range from range from approximately -0.5 to +1 °C. The photoperiod in the aquarium was controlled to replicate natural daylight patterns. Tanks were cleaned regularly to remove any micro-algal build-up.

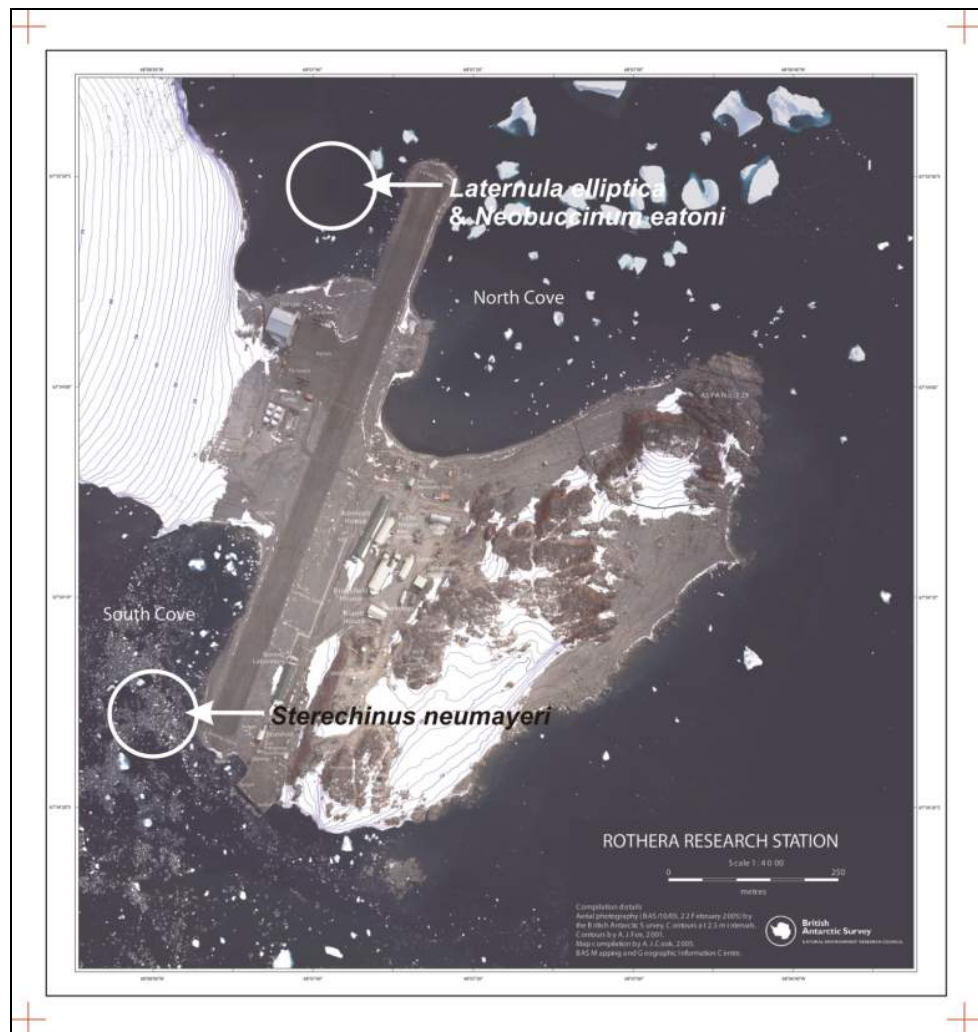


Figure 2.10 Location of the sample sites around Rothera Research Station, Adelaide Island, Antarctic Peninsula. The northern site is called Hangar Cove.

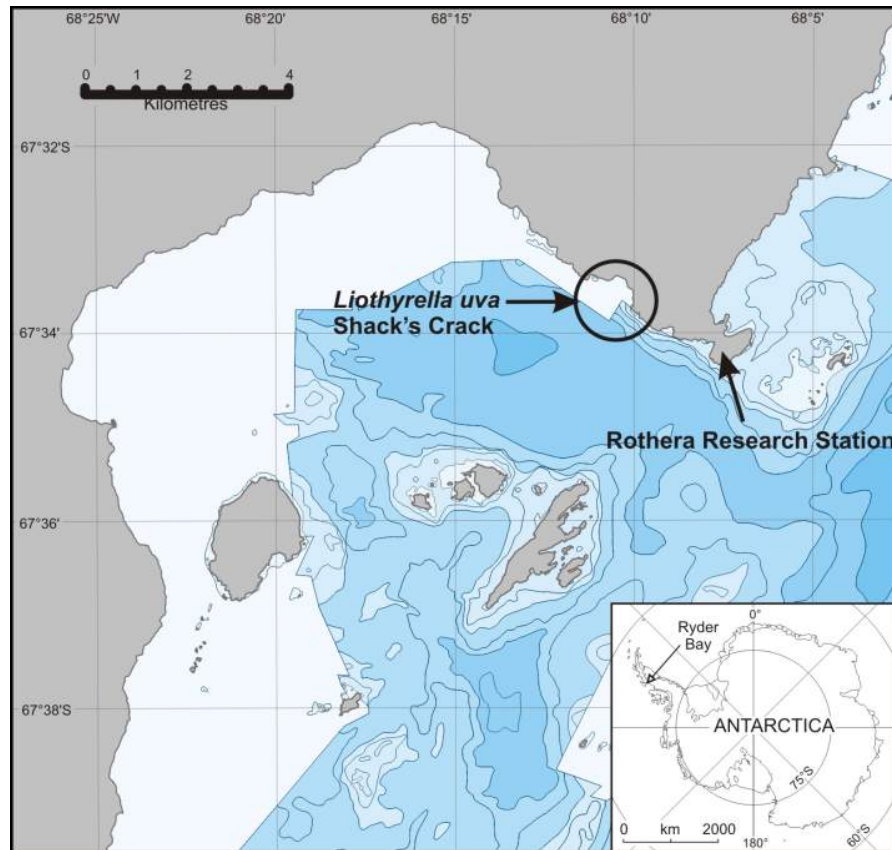


Figure 2.11 Location of the sample site in Ryder Bay, Adelaide Island, Antarctic Peninsula.

Table 2.5 Rothera collection sites (*depths in brackets were where the majority of that species were collected).

Group	Species	Collection site	Depth collected
Bivalve clam	<i>Laternula elliptica</i>	Hangar Cove	13-18 m (15 m)*
Gastropod snail	<i>Neobuccinum eatoni</i>	Hangar Cove	18-25 m (21-25 m)*
Brachiopod	<i>Liothyrella uva</i>	Shack's Crack (Ryder Bay Buttress)	16-25 m
Echinoid	<i>Sterechinus neumayeri</i>	South Cove	6-18 m
Ophiuroid	<i>Ophionotus victoriae</i>	South Cove	14-18 m
Asteroid	<i>Odontaster validus</i>	South Cove	12-18 m
Bivalve	<i>Yoldia eightsi</i>	Hangar Cove (using sediment scoops)	12-18 m

Ny Ålesund, Svalbard, Arctic Circle 78.95 °N

Animal collections and respiration measurements were conducted by Dr. Simon Morley (BAS) and Stephanie Martin (BAS) from Ny Ålesund, Svalbard, Spitsbergen in the Arctic Circle from July to August 2007 (Figure 2.12). The whelks *Buccinum* c.f. *groenlandicum* and *B. glaciale* were collected at New London at 5 m depth off the south coast of Blomstrand halvoya or off the jetty at Ny Ålesund. Respiration data were subsequently processed and analysed by Sue-Ann Watson.

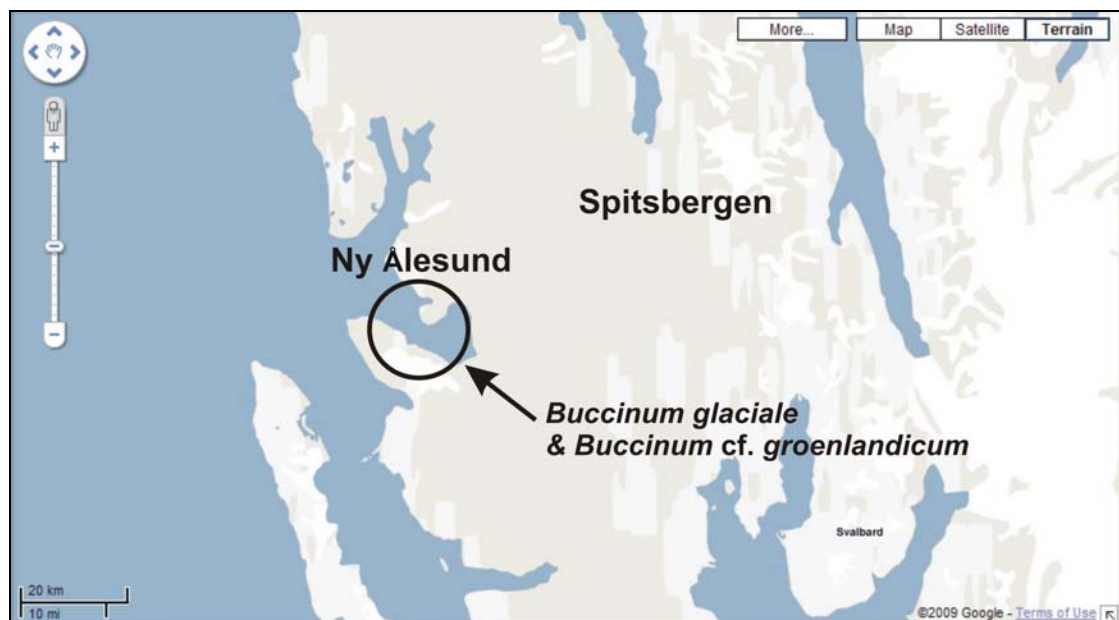


Figure 2.12 Location of the sample site in Ny Ålesund, Spitsbergen, Svalbard, in the Arctic Circle.

2.6 Data and statistical analyses

Data collected during this Ph.D. study were compiled on spreadsheets using MS Excel 2003. Statistical analyses in this thesis were performed in SPSS 16.0, SigmaPlot 10.0 and R 2.7.1. Graphs were produced with SigmaPlot 10.0. N.B. Negative values for degrees of latitude on graphical plots mean data were collected from the Southern Hemisphere. Statistical tests were significant if $p < 0.05$.

For box plots (box-and-whisker plots) throughout this thesis, the ends of the boxes define the 25th and 75th percentiles, with a line at the median (50th percentile) and error bars defining the 10th and 90th percentiles. Data points beyond the 10th and 90th percentiles are displayed as dots. If data are too few for one of these groupings, than that set of points is not shown on the box plot (SigmaPlot).

For regression analysis, a confidence band refers to the “region of uncertainties in the predicted values over a range of values for the independent variable”. A prediction band refers to the “region of uncertainties in predicting the response for a single additional observation at each point within a range of independent variable values” (SigmaPlot). Blue lines denote the 95 % confidence band and red lines denote the 95 % prediction band.

2.7 Summary

A variety of sample sites were chosen across a broad range of tropical, temperate and polar latitudes in both the Northern and Southern Hemispheres. Marine animals sampled were representative of the calcium carbonate depositing groups from four main taxa Bivalvia, Gastropoda, Brachiopoda and Echinoidea. In the following chapters latitudinal trends in their shell morphology and elemental content, metabolic rates, shell cost and predation pressure will be investigated.

Chapter 3: Latitudinal trends in shell morphology



Chapter 3:

Latitudinal trends in shell morphology

3.1 Introduction

Calcareous marine invertebrates first appeared in the Cambrian period and are presently found in all the world's oceans. Differences in shell form in molluscs have been shown across latitudes, but the causes of many of these differences remain to be explained. Cold water bivalve molluscs from polar regions are smaller (Nicol, 1964a; 1966; 1970) with thin, chalky shells that lack colour (Nicol, 1967) and have little or no ornamentation (Nicol, 1955; 1965; 1967). Among species of gastropod mollusc, shell thickness and calcification index decreases with increasing latitude on the east coast of North America with gastropods demonstrating an increase in efficiency of calcium carbonate usage (i.e. more internal living space per unit shell) with increasing latitude (Graus, 1974). Patterns within species have also been demonstrated with thinner, weaker shells but an increase in soft tissue mass at higher latitudes (Trussell, 2000).

One explanation for this pattern was hypothesised to be the increase in energetic cost of producing a calcium carbonate (CaCO_3) skeleton as temperature decreases (Clarke, 1990; 1993) because at lower temperatures CaCO_3 is more soluble and hence its component ions will be more energetically expensive to remove from seawater (Graus, 1974; Vermeij, 1978; Clarke, 1983; 1990; 1993). To compensate for this, shells could have a greater organic content at higher latitudes, although organic shell matrix is expensive to make (Palmer, 1992). Alternatively, shells could be thinner at higher latitudes because there is a reduced level of crushing predation (Aronson & Blake, 2001; Clarke *et al.*, 2004; Aronson *et al.*, 2007) reducing the need for a shell.

Some data on shell morphology and thickness exist for molluscs, but in other groups such as brachiopods and echinoids, shell thickness and shell mass trends with latitude have been little studied, if at all. In order to test the hypotheses of whether, 1) an increase in energetic cost of making a shell or, 2) reduced predation pressure, leads to thinner shells in cold

water, it was first necessary to establish what trends if any there are in shell morphology with latitude across target calcareous groups. This chapter describes latitudinal trends in shell thickness, shell mass, total animal inorganic content, tissue mass:shell mass ratios and organic content of shells. The purpose of this chapter was to collect detailed morphological data for key species since for many target species morphological data are not available in the published literature.

3.1.1 Aims and hypothesis

Aim: To determine any latitudinal variation in calcification of selected megabenthic marine invertebrates including shell thickness.

Hypothesis: Shell calcification varies with latitude and specifically, shell thickness decreases with increasing latitude.

H₀: Shell calcification does not vary along a latitudinal gradient.

3.2 Methods

3.2.1 Sample collection

Samples were collected from the intertidal or by SCUBA divers at a variety of latitudes as described in Chapter 2. Twenty to 60 individuals of a range of sizes from each key group of animals were collected for analysis of whole animal and shell/skeleton morphological features. Any epibionts or sediment adhering to the surface of the shell were removed with a soft brush (as described in Chapter 2) and any predation attack marks were noted (see Chapter 7).

3.2.2 Morphological data collection

Linear dimensions of morphological parameters such as length, width and height were recorded with dial callipers to the nearest 0.1 mm (see Figure 3.1, Figure 3.2 and Figure 3.3 for illustrations of how these measurements were taken). The whole wet weight of the animal (to 0.001 g or 3 s.f.) was measured by blotting excess water from the animal on to paper tissue and then weighing the animal. Whole animal volume, tissue volume and shell/skeleton volume was measured using Archimedes' Principle, i.e. the displacement of water within a beaker on a set of weighing scales. The animal was suspended from a stand in either distilled water or seawater in a beaker on a balance. Brachiopod volumes were measured with the internal cavity both empty and filled with water.

Wet weight, dry weight and ash-free dry mass (AFDM) were measured according to the following method. Containers or "boats" were made from aluminium foil and were pre-ashed in a muffle furnace at 475 °C for 15 min, allowed to cool and weighed. Soft tissue and shell/skeleton were dried separately in foil containers in an oven at 60 °C to constant weight. The dry mass of soft tissue and shell/skeleton in their boats were recorded to 0.0001 g and biomass dry weight calculated by subtraction of boat weight. The organic and inorganic content of soft tissues and shells/skeletons was determined by loss on ignition. After drying, soft tissue and shell material were ignited in their boats in a muffle furnace at 475 °C for 24 hr to remove organic material. Ashed material was placed in a desiccator for

24 hr to cool. Ash mass (inorganic content) was then recorded to 0.0001 g (by subtraction of boat weight) and AFDM (also known as ash-free dry weight (AFDW)) (i.e. organic content) was calculated by subtracting ashed weight from dry weight to give AFDM.

$$\text{AFDM (organic content)} = \text{dry mass} - \text{ash mass}$$

Equation 1

Shell terminology was taken from the Treatise on Invertebrate Paleontology for gastropod (Cox, 1960), bivalve (Cox *et al.*, 1969; Stenzel, 1971) and brachiopod morphology (Williams *et al.*, 1997a). In this thesis, shell length, height and width refer to the maximum shell length, maximum shell height and maximum shell width, respectively.

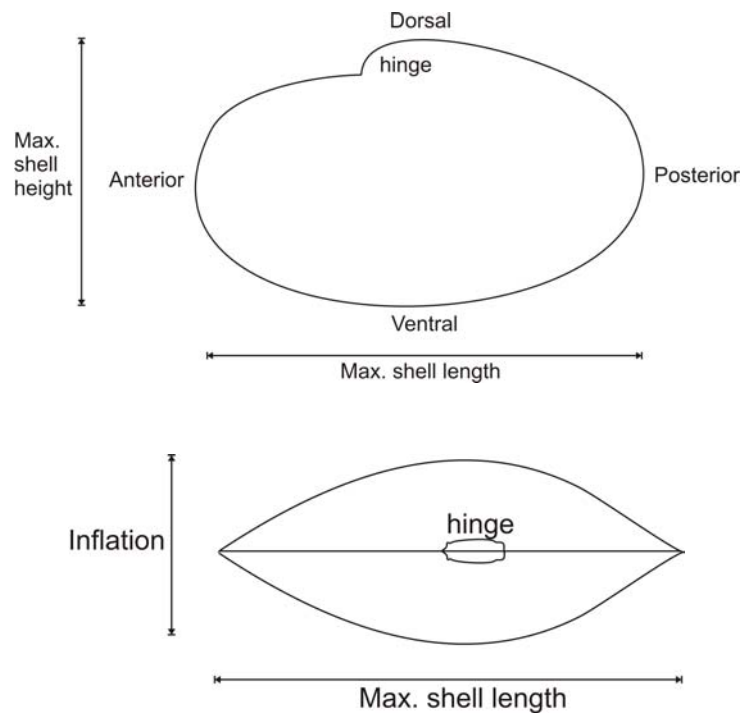


Figure 3.1 Bivalve shell terminology showing maximum shell length, maximum shell height and shell inflation (\equiv width) (Cox *et al.*, 1969).

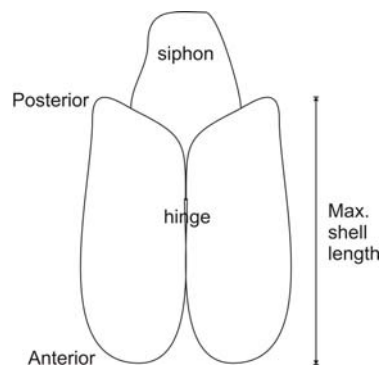


Figure 3.2 Bivalve shell terminology used for the burrowing clams of the genus *Laternula*.

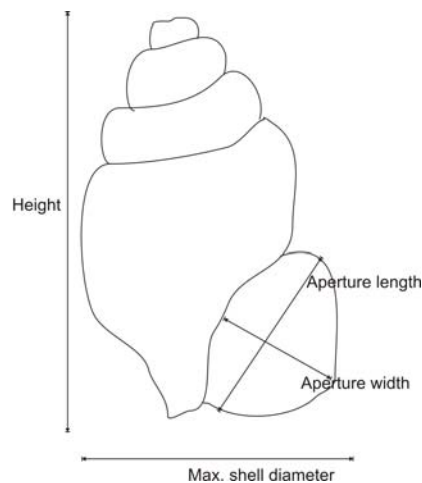


Figure 3.3 Gastropod shell measurements taken.

3.2.3 Shell thickness measurements

Samples of skeletal material (shells, valves and test material) of study species were cleaned and allowed to dry naturally in air at room temperature. Once dry, the skeletal material was sectioned with a thin circular diamond tip saw blade for measurement of skeletal thickness. Bivalve and brachiopod shells were sectioned into two parts along the growth axis (perpendicular to growth bands) (Figure 3.4, Figure 3.5 and Figure 3.6) using a diamond tipped fine (1 mm) circular saw blade on a rotary multi-tool. Gastropods were sectioned along the coil with a diamond grinding wheel perpendicular to the aperture lip (Figure 3.7).

The fine circular saw blade was used to cut the mid-section of shell out of the last whorl (Figure 3.8). Echinoid test was sectioned as shown in Figure 3.9.

Skeleton thickness was measured by 1) capturing images from the scanning electron microscope (SEM) for analysis using the imaging software CorelDRAW 12, or 2) using a micrometer. Both methods produced similar results and both were used. A light microscope can also be used for measuring thickness and Avery & Etter (2006) found no difference between SEM and light microscopy for measuring gastropod shell thickness. Shell thickness was determined by taking an average of 3 thickness measurements across the shell mid-section (Figure 3.10). This mid-section was also the part of the shell where SEM energy dispersive spectroscopy (EDS) and wavelength dispersive spectroscopy (WDS) measurements were taken to measure a range of elemental concentrations (see Chapter 4).

Diagrams of parts of shell used in analyses

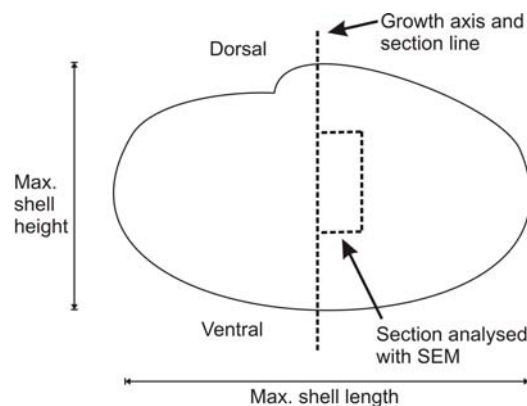


Figure 3.4 Bivalve shells were sectioned along the midline of the dorsal-ventral growing axis then the part shown was removed and embedded in resin.

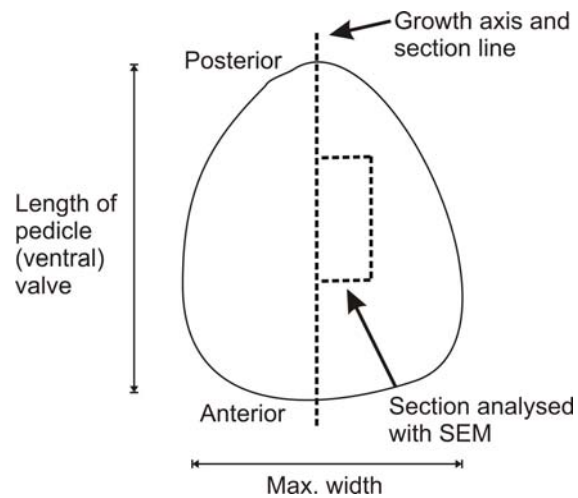


Figure 3.5 Brachiopod shells were sectioned in half along the axis of maximum growth then the part shown was removed and embedded in resin. In brachiopods, length refers to the length of the pedicle (ventral) valve throughout this thesis, unless otherwise stated.

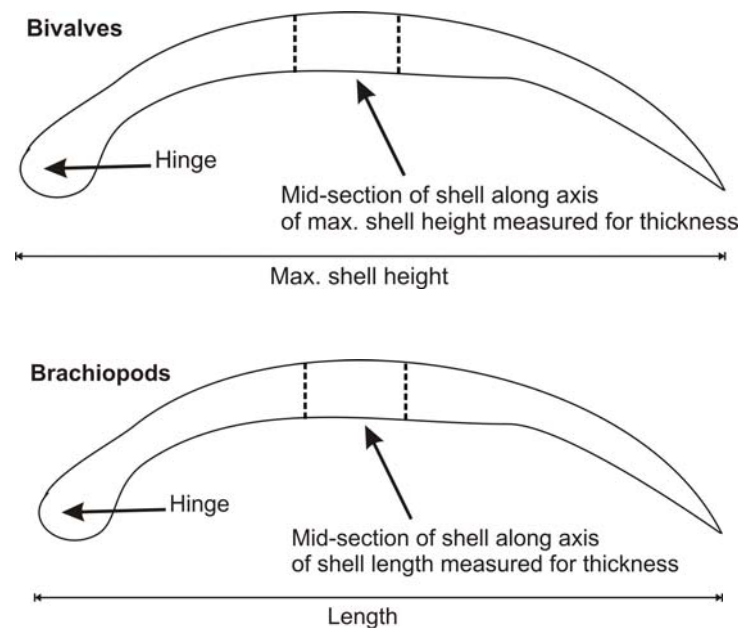


Figure 3.6 For bivalves and brachiopods the mid-section of the shell was measured for thickness. In brachiopods the dorsal valve was always used.

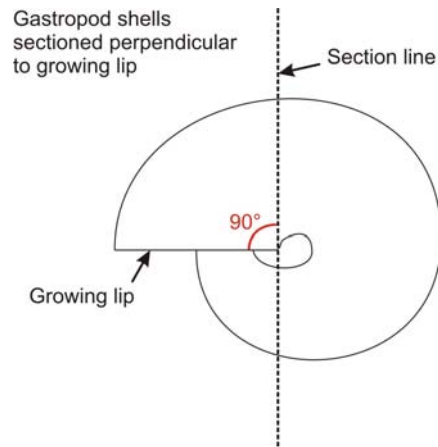


Figure 3.7 Shells of coiled gastropods were sectioned perpendicular to the growing lip (i.e. at 90° to aperture whorl end).

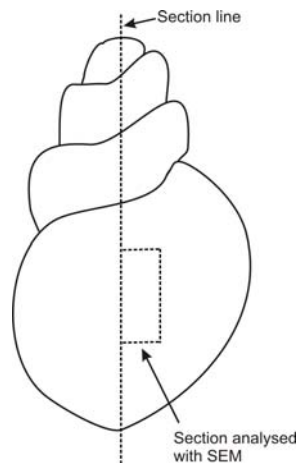


Figure 3.8 After sectioning the part indicated was removed and embedded in resin for measurement of shell thickness (and elemental analysis see Chapter 4).

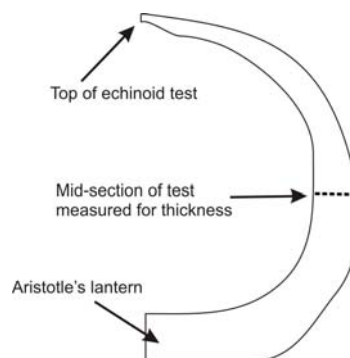


Figure 3.9 Echinoids were sectioned in half and the thickness of the mid-section of the test measured with a point micrometer accurate to 0.001 mm.

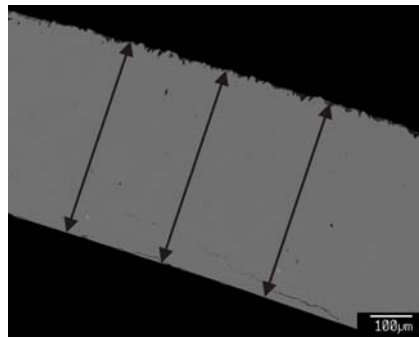


Figure 3.10 SEM photograph to show how measurements were taken across the shell section using CorelDRAW 12. The shell in this photograph is the Antarctic gastropod, *Neobuccinum eatoni*.

3.2.4 Correcting for size differences among species

Correcting for size is useful when comparing species of different mean size, especially where the sample size range is limited. Size corrected data can then be used to compare morphological measurements (such as shell thickness) or physiological measurements (such as metabolic rates). To allow for shell thickness comparisons among different sized species, shell thickness was modelled by regression analysis and then corrected for a standard animal size using a custom algorithm (A. Clarke, pers. comm.). All size differences among species in this thesis were corrected using this method (below).

For a regression equation of a $\text{Ln}[x]$ vs $\text{Ln}[y]$ plot, where $\text{Ln}[y] = a * \text{Ln}[x] + b$, and y is the parameter that needs to be corrected:

$$\text{Ln}[\text{Corrected } y] = (a * (\text{Ln}[x_{\text{std}}])) + (\text{Ln}[y] - (a * \text{Ln}[x])) \quad \text{Equation 2}$$

Where: a is the slope of the regression line
 x_{std} is the standard animal size

Raw data (uncorrected for a standard animal size) were plotted for each species and these $\text{Ln}[x]$ against $\text{Ln}[y]$ regressions were used to correct parameter y for each species to a standard sized animal using Equation 2. The standard animal size was chosen by plotting

the raw data (uncorrected for size) for all species and choosing a mid-point (approximate average) for parameter x. In most cases this mid-point overlapped with the size range of all species compared; however, this was not always possible for very small or very large species.

3.2.5 Statistical analysis

Data were compiled on spreadsheets using MS Excel 2003. Statistical analyses were performed in SPSS 16.0, SigmaPlot 10.0 and R 2.7.1 and included general linear models (e.g. regression analysis, analysis of variance (ANOVA), analysis of covariance (ANCOVA)), post hoc tests and t-tests. Where data did not have equal variances Welch's F test was used (Welch, 1951). Graphs were produced with SigmaPlot 10.0.

For box plots (box-and-whisker plots) throughout this thesis, the ends of the boxes define the 25th and 75th percentiles, with a line at the median (50th percentile) and error bars defining the 10th and 90th percentiles. Data points beyond the 10th and 90th percentiles are displayed as dots. If data are too few for one of these groupings, than that set of points is not shown on the box plot (SigmaPlot).

For regression analysis, a confidence band refers to the “region of uncertainties in the predicted values over a range of values for the independent variable”. A prediction band refers to the “region of uncertainties in predicting the response for a single additional observation at each point within a range of independent variable values” (SigmaPlot).

3.3 Results

3.3.1 Whole animal morphology (shell and soft tissues)

Whole animal morphology data described below incorporate the shell or skeleton and soft tissues of each animal. Linear dimension and mass data were collected during the whole study and data for each species are summarised in Table 3.1. There was large variation in the data, shown by the large standard deviation (s.d.) on mean values for linear and mass measures for many species. This variation is because individuals of a wide range of sizes were used in the study to allow relationships (regression equations) to be determined between size of animal (e.g. length, mass) and parameter under investigation (e.g. shell thickness, metabolic rate). Results of the relationships between linear dimensions and mass are plotted for each species (Figure 3.11, Figure 3.12, Figure 3.13 and Figure 3.14), since for many of the species studied published data for their general morphology are scarce. Table 3.2 details the regression parameters for each relationship plotted on the following morphology graphs.

Since these graphs of natural log (\log_e) transformed relationships (Figure 3.11, Figure 3.12, Figure 3.13 and Figure 3.14) are plotted with a linear measurement on the x-axis (linear measurement is proportional to L^1) and a mass measurement on the y-axis (mass is proportional to the linear measurement cubed (L^3)) then for isometric scaling the slope would be $3/1 = 3$ (untransformed relationships would be curvilinear). The slopes of the regression equations for logarithmic transformed mass to linear dimension morphology relationships are close to 3 (where $y = ax + b$, a is ~ 3) (Table 3.2) suggesting that for each species the shape of the animal does not change over time with growth, and suggesting that these animals exhibit isometric scaling. If the slope $\neq 3$ then the organism changes shape over time with growth and the animal is said to have allometric scaling. In this study, mostly where the size range of animals for a species was not very large, slopes were significantly different from 3. There were 25 slopes significantly different from 3 out of 65 $\ln(\text{mass})$ on $\ln(\text{length})$ slopes analysed (Table 3.2). This does not necessarily imply that the animal does not exhibit isometric scaling, but that sample size is small and if more

individuals of that species were measured, then the slope of the regression trendline may be different.

Bivalvia: *Laternula* spp.

The antero-posterior measurement (APM), the longest linear dimension of the shell, is also termed maximum shell length (Cox *et al.*, 1969) (Figure 3.4). In this thesis, length is used to refer bivalve maximum shell length in accordance with previous research on *Laternula* species that has reported the longest linear dimension of the shell as ‘shell length’ (e.g. Brey & Mackensen, 1997; Ahn *et al.*, 2003). Note Brockington (2001) refers to the longest linear dimension of the shell (shell length) as ‘shell height’. The dorso-ventral measurement (DVM) is referred to in this thesis as maximum shell height measured perpendicular to the maximum shell length (Cox *et al.*, 1969) (Figure 3.4) and graphs comparing shell length with height are useful in understanding differences in the shell morphology of various species. These relationships have been included here with regression equations so that past and future research on species of *Laternula* can be interpreted in terms of both linear dimensions. Relationships between length and mass measurements for clams of the genus *Laternula* are illustrated in the graphs below (Figure 3.11). Relationships for other bivalves are listed in Table 3.2.

Gastropoda: Buccinidae

Relationships between buccinid gastropod shell length and mass measurements are illustrated in the graphs below (Figure 3.12). Relationships for shell length and mass measurements for other gastropods are listed in Table 3.2.

Brachiopoda: *Liothyrella* spp.

Relationships between shell length and mass measurements for brachiopods of the genus *Liothyrella* are illustrated in the graphs below (Figure 3.13). Relationships between shell length and mass measurements for other brachiopods are listed in Table 3.2.

Class Echinoidea: Family Echinidae

Relationships between test diameter and mass measurements for echinoids of the family Echinidae are illustrated in the graphs below (Figure 3.14). Relationships between test diameter and mass measurements for other echinoids are listed in Table 3.2.

Table 3.1 Summary data (mean \pm 1 s.d. to 3 d.p.) for key representative species of each animal group at various latitudes.

Latitude	Species	Longest linear dimension (mm)	Wet weight (g)	Dry weight (g)	AFDM (g)
<i>Laternula</i> clams					
1.22 °N	<i>Laternula truncata</i>	34.229 (\pm 7.094)	5.433 (\pm 2.496)	1.272 (\pm 0.567)	0.237 (\pm 0.091)
1.22 °N	<i>Laternula boschasina</i>	18.168 (\pm 2.578)	0.653 (\pm 0.228)	0.150 (\pm 0.056)	0.029 (\pm 0.009)
37.49 °S	<i>Laternula recta</i>	29.700 (\pm 5.674)	2.125 (\pm 0.974)	0.363 (\pm 0.169)	0.067 (\pm 0.048)
67.57 °S	<i>Laternula elliptica</i>	63.601 (\pm 14.040)	82.577 (\pm 44.967)	21.764 (\pm 13.972)	7.309 (\pm 4.329)
Other bivalves	<i>Bathymodiolus childressi</i>	76.486 (\pm 6.003)	7.669 (\pm 2.818)		
Buccinidae gastropods (Superfamily Buccinoidea)					
19.13 °S	<i>Cantharus fumosus</i>	22.479 (\pm 2.685)	1.605 (\pm 0.466)	1.168 (\pm 0.321)	0.097 (\pm 0.033)
19.13 °S	<i>Phos senticosus</i>	31.420 (\pm 2.414)	3.506 (\pm 0.817)	2.284 (\pm 0.620)	0.209 (\pm 0.081)
37.49 °S	<i>Cominella lineolata</i>	20.136 (\pm 3.329)	1.367 (\pm 0.543)	0.953 (\pm 0.398)	0.072 (\pm 0.034)
50.95 °N	<i>Buccinum undatum</i>	40.717 (\pm 8.946)	9.106 (\pm 5.278)	4.228 (\pm 2.584)	0.935 (\pm 0.676)
67.57 °S	<i>Neobuccinum eatoni</i>	46.983 (\pm 9.299)	17.471 (\pm 7.853)	5.213 (\pm 2.841)	1.879 (\pm 1.003)
78.95 °N	<i>Buccinum glaciale</i>	49.389 (\pm 10.559)	14.858 (\pm 6.326)	6.731 (\pm 3.467)	1.363 (\pm 0.680)
78.95 °N	<i>Buccinum</i> cf. <i>groenlandicum</i>	33.816 (\pm 7.795)	4.322 (\pm 3.027)	1.898 (\pm 1.591)	0.515 (\pm 0.425)
Other gastropods	<i>Nacella concinna</i>	26.162 (\pm 5.312)	1.253 (\pm 0.530)	0.752 (\pm 0.328)	0.201 (\pm 0.088)
	<i>Thais orbita</i> (<i>Dicathais textilosa</i>)	30.788 (\pm 12.185)	7.181 (\pm 6.450)	4.385 (\pm 4.604)	0.374 (\pm 0.424)

Table 3.1 continued.

Latitude	Species	Longest linear dimension (mm)	Wet weight (g)	Dry weight (g)	AFDM (g)
Brachiopods					
45.87 °S	<i>Liothyrella neozelanica</i>	37.178 (± 10.310)	4.078 (± 3.243)	2.824 (± 2.327)	0.074 (± 0.064)
60.72 °S	<i>Liothyrella uva</i> from Signy	41.200 (± 6.833)	5.666 (± 2.089)		
67.57 °S	<i>Liothyrella uva</i> from Rothera	31.072 (± 7.528)	4.271 (± 2.556)	1.956 (± 1.134)	0.203 (± 0.123)
51.67 °S	<i>Magellania venosa</i>	49.757 (± 17.120)	10.668 (± 7.343)	5.847 (± 7.743)	0.148 (± 0.217)
Echinoids					
37.49 °S	<i>Heliocidaris erythrogramma</i>	62.150 (± 16.425)	111.508 (± 61.299)		
50.47 °N	<i>Psammechinus miliaris</i>	25.168 (± 5.550)	8.942 (± 6.907)	3.800 (± 3.121)	0.480 (± 0.451)
61.83 °S	<i>Sterechinus</i> sp. (Scotia Arc)	35.403 (± 8.626)	13.780 (± 11.862)	3.325 (± 2.365)	0.622 (± 0.428)
67.57 °S	<i>Sterechinus neumayeri</i>	28.610 (± 7.728)	10.052 (± 7.483)	1.699 (± 1.435)	0.406 (± 0.348)

Table 3.2 Regression equations for the morphological relationships plotted on graphs below, where $y = mx + c$.

(# Denotes species for which graphs are not plotted. * Denotes slopes that are significantly different from 3.)

Species	Regression of	m	s.e. of m	c	r ²	F	df	p
<i>Laternula</i> clams								
<i>Laternula truncata</i>	Height on Length	0.4606	0.0162	2.6607	0.9129	577.6325	1,54	<0.0001
	Ln(Wet weight) on Ln(Length)	2.3834*	0.1624	-6.8770	0.7256	141.1364	1,52	<0.0001
	Ln(Dry mass) on Ln(Length)	2.7773*	0.0859	-9.6943	0.9291	577.7205	1,43	<0.0001
	Ln(AFDM) on Ln(Length)	2.3892*	0.0919	-9.9704	0.8943	373.1425	1,43	<0.0001
<i>Laternula boschasina</i>	Height on Length	0.4587	0.0263	1.8380	0.8941	288.1145	1,33	<0.0001
	Ln(Wet weight) on Ln(Length)	2.1466*	0.2423	-6.6807	0.6838	74.5230	1,33	<0.0001
	Ln(Dry mass) on Ln(Length)	2.5555*	0.1260	-9.2796	0.9190	330.0285	1,28	<0.0001
	Ln(AFDM) on Ln(Length)	1.9558*	0.1847	-9.1817	0.7541	89.9402	1,28	<0.0001
<i>Laternula recta</i>	Height on Length	0.4270	0.0157	1.3605	0.9385	733.1374	1,47	<0.0001
	Ln(Wet weight) on Ln(Length)	2.9241	0.0889	-9.2543	0.9566	1082.0632	1,48	<0.0001
	Ln(Dry mass) on Ln(Length)	2.5248*	0.1436	-9.6384	0.8890	297.3445	1,36	<0.0001
	Ln(AFDM) on Ln(Length)	3.1718	0.5492	-13.6188	0.4907	27.0127	1,26	<0.0001
<i>Laternula elliptica</i>	Height on Length	0.6566	0.0305	0.7250	0.8906	464.9132	1,56	<0.0001
	Ln(Wet weight) on Ln(Length)	3.0614	0.0968	-8.4270	0.9487	999.7597	1,53	<0.0001
	Ln(Dry mass) on Ln(Length)	3.2017*	0.0966	-10.3611	0.9706	992.2485	1,29	<0.0001
	Ln(AFDM) on Ln(Length)	3.0372	0.1054	-10.7513	0.9614	748.7299	1,29	<0.0001
Other bivalves								
<i>Bathymodiolus childressi</i> [#]	Ln(Wet weight) on Ln(Length)	4.1908	0.8306	-16.1824	0.8030	25.4545	1,5	0.0039
Buccinidae gastropods								
<i>Cantharus fumosus</i>	Ln(Wet weight) on Ln(Length)	2.9180	0.0646	-8.6455	0.9751	2040.5625	1,51	<0.0001
	Ln(Dry mass) on Ln(Length)	2.8619	0.1313	-8.7815	0.9367	474.7363	1,31	<0.0001
	Ln(AFDM) on Ln(Length)	3.4836	0.2917	-13.2067	0.8062	129.9233	1,30	<0.0001

Table 3.2 continued.

Species	Regression of	m	s.e. of m	c	r ²	F	df	p
<i>Phos senticosus</i>	Ln(Wet weight) on Ln(Length)	2.9262	0.1182	-8.8514	0.9272	612.4250	1,47	<0.0001
	Ln(Dry mass) on Ln(Length)	2.8993	0.1859	-9.1496	0.8931	243.2765	1,28	<0.0001
	Ln(AFDM) on Ln(Length)	3.7450	0.4022	-14.4741	0.7471	86.6775	1,28	<0.0001
<i>Cominella lineolata</i>	Ln(Wet weight) on Ln(Length)	2.7841*	0.0660	-8.1101	0.9674	1779.4892	1,59	<0.0001
	Ln(Dry mass) on Ln(Length)	2.7266*	0.0737	-8.2594	0.9624	1228.7755	1,47	<0.0001
	Ln(AFDM) on Ln(Length)	2.7244	0.2160	-10.7667	0.7528	116.7336	1,37	<0.0001
<i>Buccinum undatum</i>	Ln(Wet weight) on Ln(Length)	2.8077*	0.0663	-8.3098	0.9750	1791.4776	1,45	<0.0001
	Ln(Dry mass) on Ln(Length)	2.7208*	0.0568	-8.6326	0.9807	1828.0413	1,35	<0.0001
	Ln(AFDM) on Ln(Length)	3.2227	0.1909	-12.0542	0.8627	227.1273	1,35	<0.0001
<i>Neobuccinum eatoni</i>	Ln(Wet weight) on Ln(Length)	2.7235*	0.0634	-7.7104	0.9720	1842.4497	1,52	<0.0001
	Ln(Dry mass) on Ln(Length)	2.6800*	0.0616	-8.6067	0.9846	1853.8821	1,28	<0.0001
	Ln(AFDM) on Ln(Length)	2.6133*	0.0948	-9.3690	0.9624	743.6135	1,28	<0.0001
<i>Buccinum glaciale</i>	Ln(Wet weight) on Ln(Length)	2.4311*	0.2766	-6.9348	0.8544	77.2695	1,12	<0.0001
	Ln(Dry mass) on Ln(Length)	2.6823	0.1708	-8.6189	0.9485	203.7747	1,10	<0.0001
	Ln(AFDM) on Ln(Length)	2.9018	0.2287	-11.0780	0.9231	133.0981	1,10	<0.0001
<i>Buccinum cf. groenlandicum</i>	Ln(Wet weight) on Ln(Length)	3.0145	0.1135	-9.1719	0.9618	706.0217	1,27	<0.0001
	Ln(Dry mass) on Ln(Length)	3.2640*	0.1196	-10.8690	0.9669	585.4601	1,19	<0.0001
	Ln(AFDM) on Ln(Length)	3.0424	0.1577	-11.3864	0.9358	292.4481	1,19	<0.0001
Other gastropods								
<i>Nacella concinna</i> [#]	Ln(Wet weight) on Ln(Length)	3.4282*	0.1565	-11.0907	0.9756	480.0600	1,11	<0.0001
	Ln(Dry mass) on Ln(Length)	3.1562	0.2383	-10.7075	0.9356	175.4793	1,11	<0.0001
	Ln(AFDM) on Ln(Length)	3.2032	0.2916	-12.1844	0.9089	120.6794	1,11	<0.0001
<i>Thais orbita</i> [#]	Ln(Wet weight) on Ln(Length)	2.9455	0.0368	-8.4893	0.9936	6392.0089	1,40	<0.0001
	Ln(Dry mass) on Ln(Length)	2.9926	0.0466	-8.8888	0.9930	4131.8319	1,28	<0.0001
	Ln(AFDM) on Ln(Length)	3.1282	0.1676	-11.8561	0.9229	348.2183	1,28	<0.0001

Table 3.2 continued.

Species	Regression of	m	s.e. of m	c	r ²	F	df	p
Brachiopods								
<i>Liothyrella neozelanica</i>	Ln(Wet weight) on Ln(Length)	2.8579	0.1158	-9.0919	0.9575	609.3522	1,26	<0.0001
	Ln(Dry mass) on Ln(Length)	2.9812	0.0923	-9.6684	0.9868	1043.9248	1,13	<0.0001
	Ln(AFDM) on Ln(Length)	3.4845*	0.1387	-15.1831	0.9783	631.1104	1,13	<0.0001
<i>Magellania venosa</i> [#]	Ln(Wet weight) on Ln(Length)	2.8054	0.0990	-8.6980	0.9931	720.1735	1,4	<0.0001
	Ln(Dry mass) on Ln(Length)	2.9178	0.1498	-9.2820	0.9947	379.4062	1,1	0.0327
	Ln(AFDM) on Ln(Length)	3.1595	0.5348	-14.0084	0.9443	34.8973	1,1	0.1068
<i>Liothyrella uva</i> (Signy) [#]	Ln(Wet weight) on Ln(Length)	1.4827*	0.5569	-3.8271	0.4035	7.0880	1,8	0.0287
<i>Liothyrella uva</i> (Rothera)	Ln(Wet weight) on Ln(Length)	2.9750	0.0929	-8.9062	0.9597	1024.9055	1,42	<0.0001
	Ln(Dry mass) on Ln(Length)	2.8071	0.1069	-9.0802	0.9486	572.9792	1,30	<0.0001
	Ln(AFDM) on Ln(Length)	3.0228	0.1401	-12.1106	0.9257	386.9469	1,30	<0.0001
Echinoids								
<i>Heliocidaris erythrogramma</i> [#]	Ln(Wet weight) on Ln(Diameter)	2.9800	0.0572	-7.7511	0.9960	2711.5490	1,10	<0.0001
<i>Psammechinus miliaris</i>	Ln(Wet weight) on Ln(Diameter)	3.0490	0.0542	-7.7950	0.9854	3166.4060	1,46	<0.0001
	Ln(Dry mass) on Ln(Diameter)	2.9819	0.0663	-8.4189	0.9815	1701.0681	1,31	<0.0001
	Ln(AFDM) on Ln(Diameter)	3.1440	0.1501	-11.0607	0.9199	368.6012	1,31	<0.0001
<i>Sterechinus</i> sp. (Scotia Arc)	Ln(Wet weight) on Ln(Diameter)	2.9092	0.2559	-7.9280	0.9344	129.2400	1,8	<0.0001
	Ln(Dry mass) on Ln(Diameter)	2.4224*	0.1595	-7.5453	0.9623	230.7007	1,8	<0.0001
	Ln(AFDM) on Ln(Diameter)	2.4913*	0.1787	-9.4703	0.9555	194.4491	1,8	<0.0001
<i>Sterechinus neumayeri</i>	Ln(Wet weight) on Ln(Diameter)	2.8667*	0.0368	-7.4872	0.9907	6073.7858	1,56	<0.0001
	Ln(Dry mass) on Ln(Diameter)	2.7101*	0.0634	-8.5399	0.9854	1755.1426	1,25	<0.0001
	Ln(AFDM) on Ln(Diameter)	2.8000*	0.0997	-10.2846	0.9668	758.3005	1,25	<0.0001

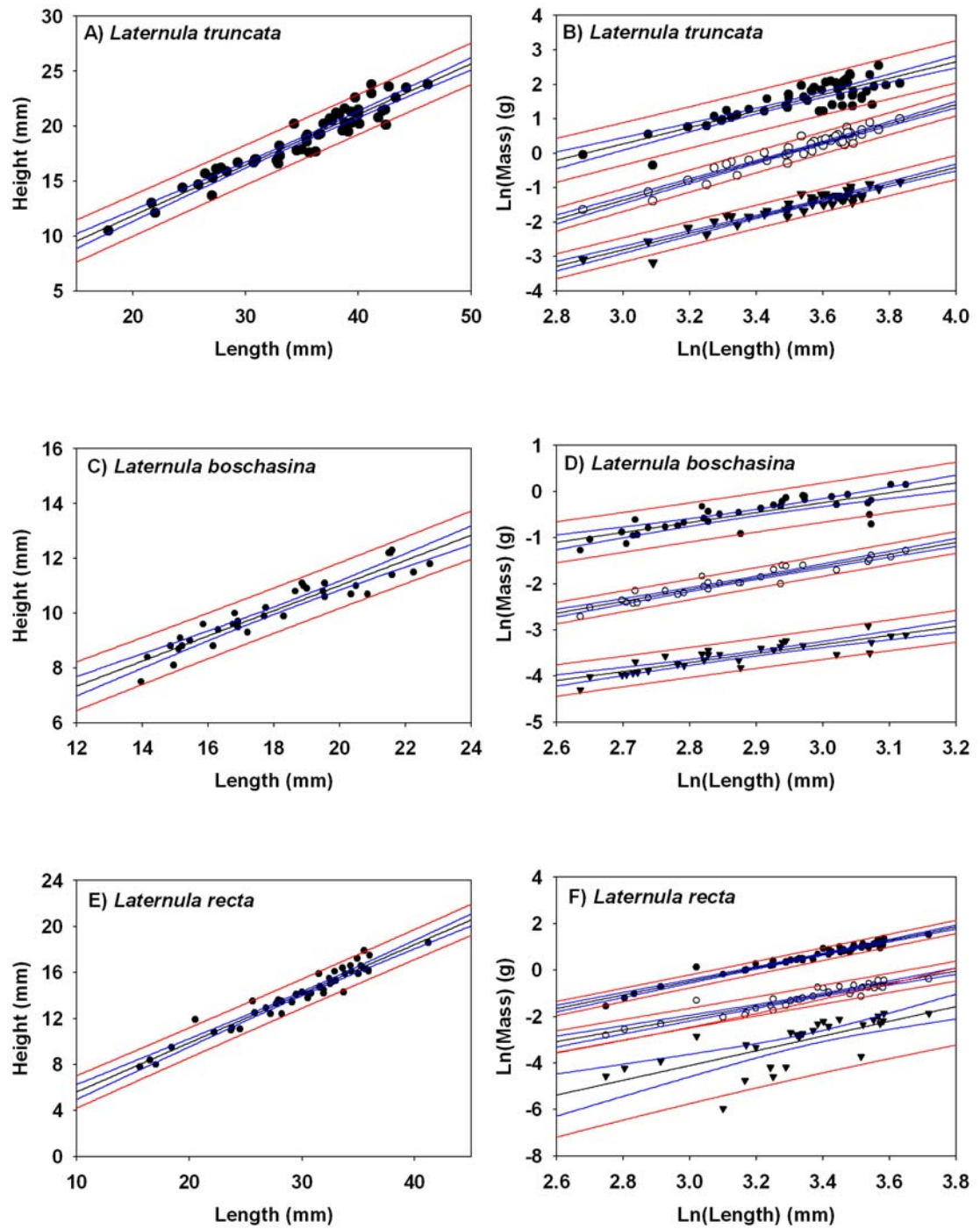


Figure 3.11 continues overleaf.

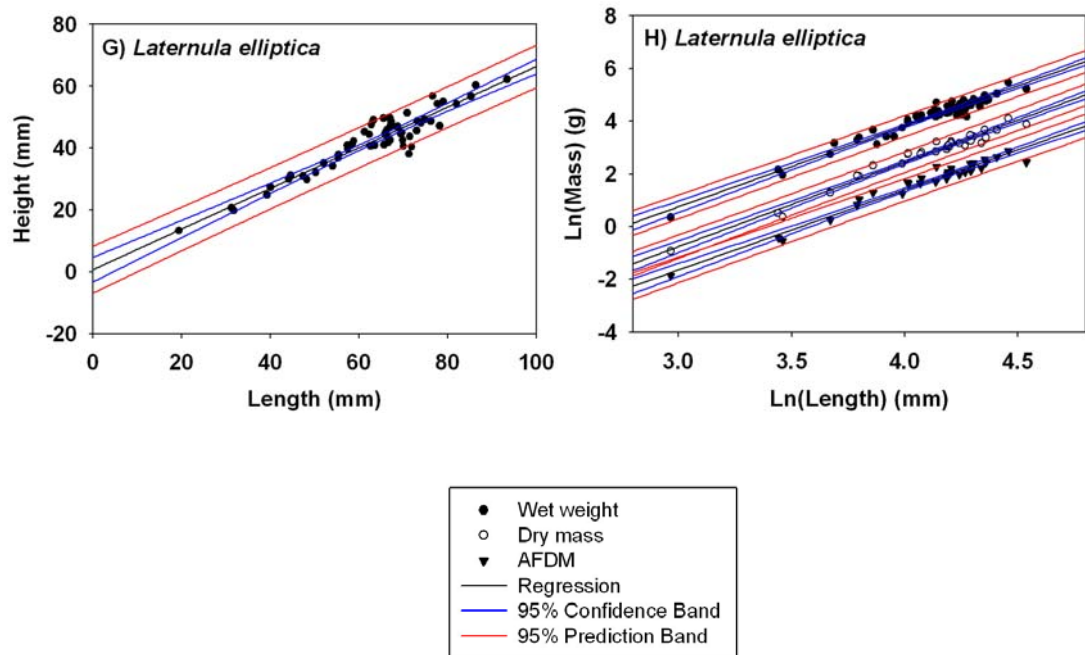


Figure 3.11 Regressions of height on length for A) *Laternula truncata*, C) *L. boschasina*, E), *L. recta*, G) *L. elliptica* and regressions of Ln(Mass) on Ln(Length) measurements for B) *L. truncata*, D) *L. boschasina*, F) *L. recta*, H) *L. elliptica*. N.B. Some variation in *L. recta* AFDM was caused by problems with the muffle furnace at the University of Melbourne.

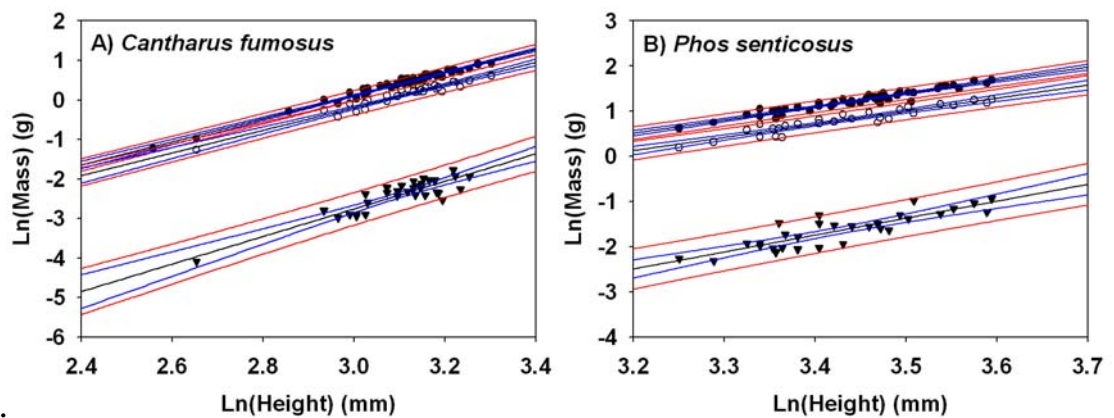


Figure 3.12 continues overleaf.

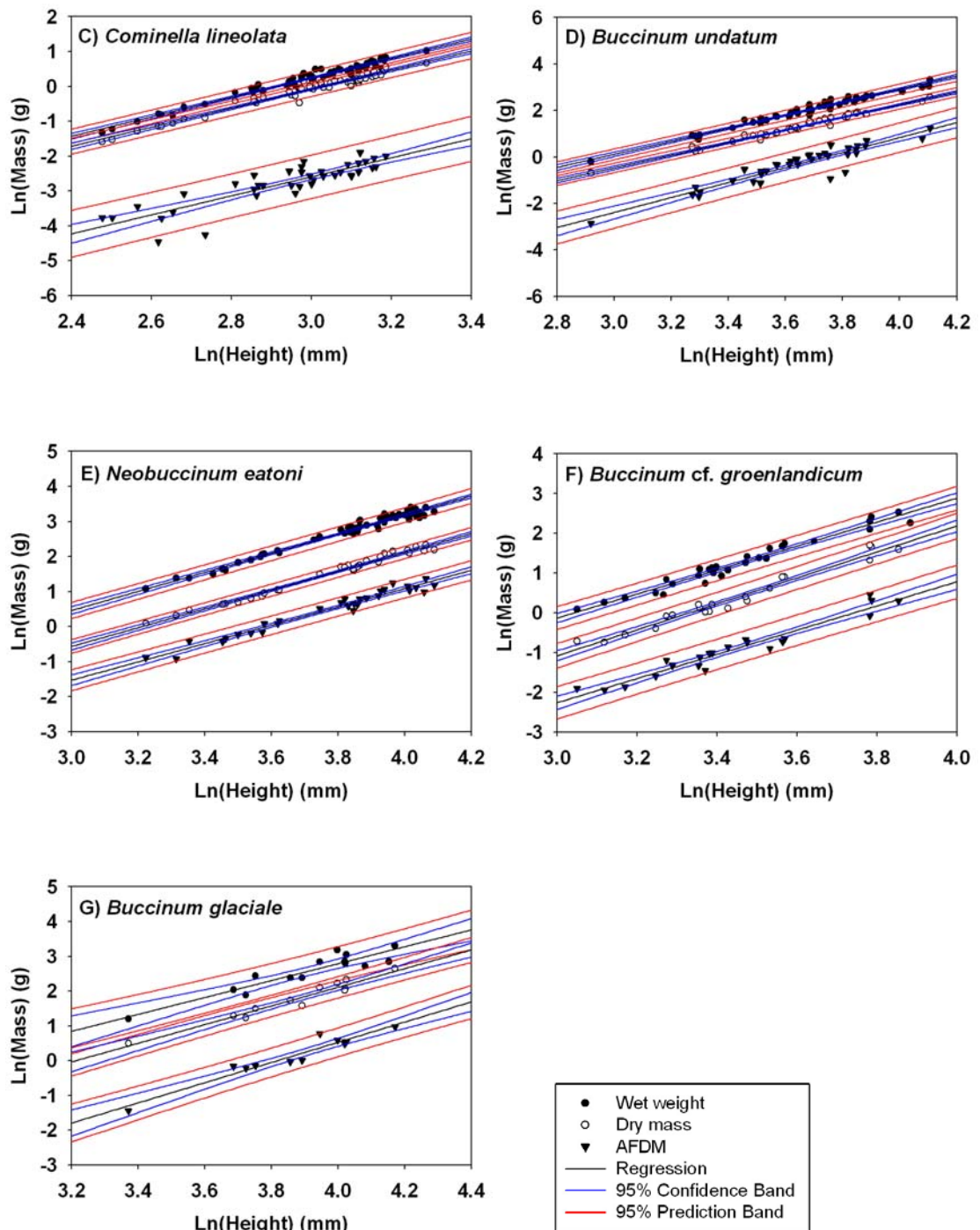


Figure 3.12 Regressions of $\text{Ln}(\text{Mass})$ on $\text{Ln}(\text{Height})$ for A) *Cantharus fumosus*, B) *Phos senticosus*, C) *Cominella lineolata*, D) *Buccinum undatum*, E) *Neobuccinum eatoni*, F) *Buccinum cf. groenlandicum* and G) *Buccinum glaciale*.

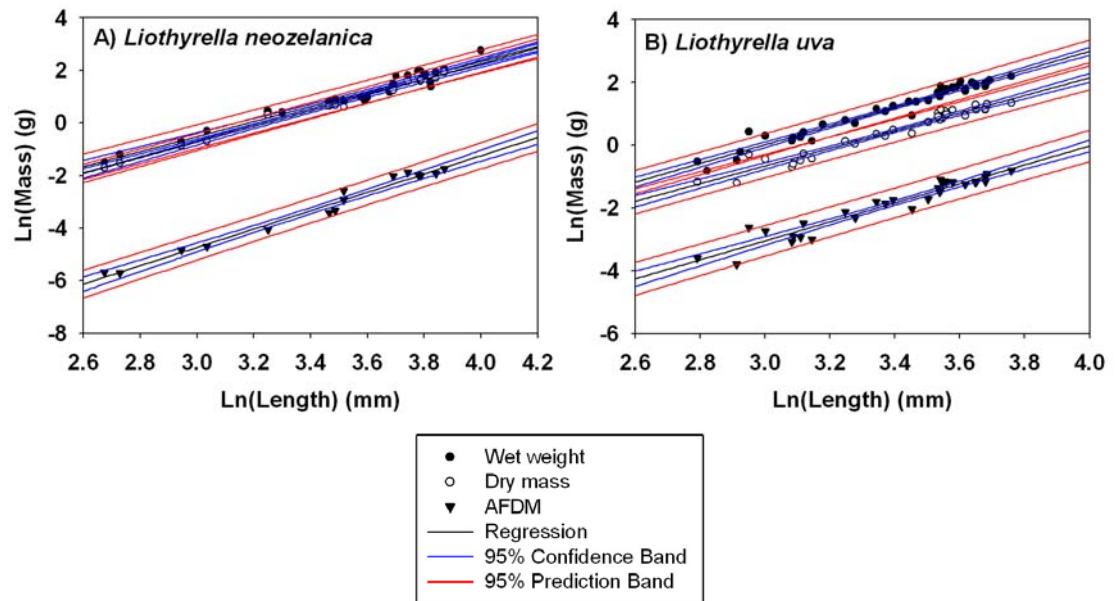


Figure 3.13 Regressions of $\ln(\text{Mass})$ on $\ln(\text{Length})$ for A) *Liothyrella neozelanica* and B) *Liothyrella uva*.

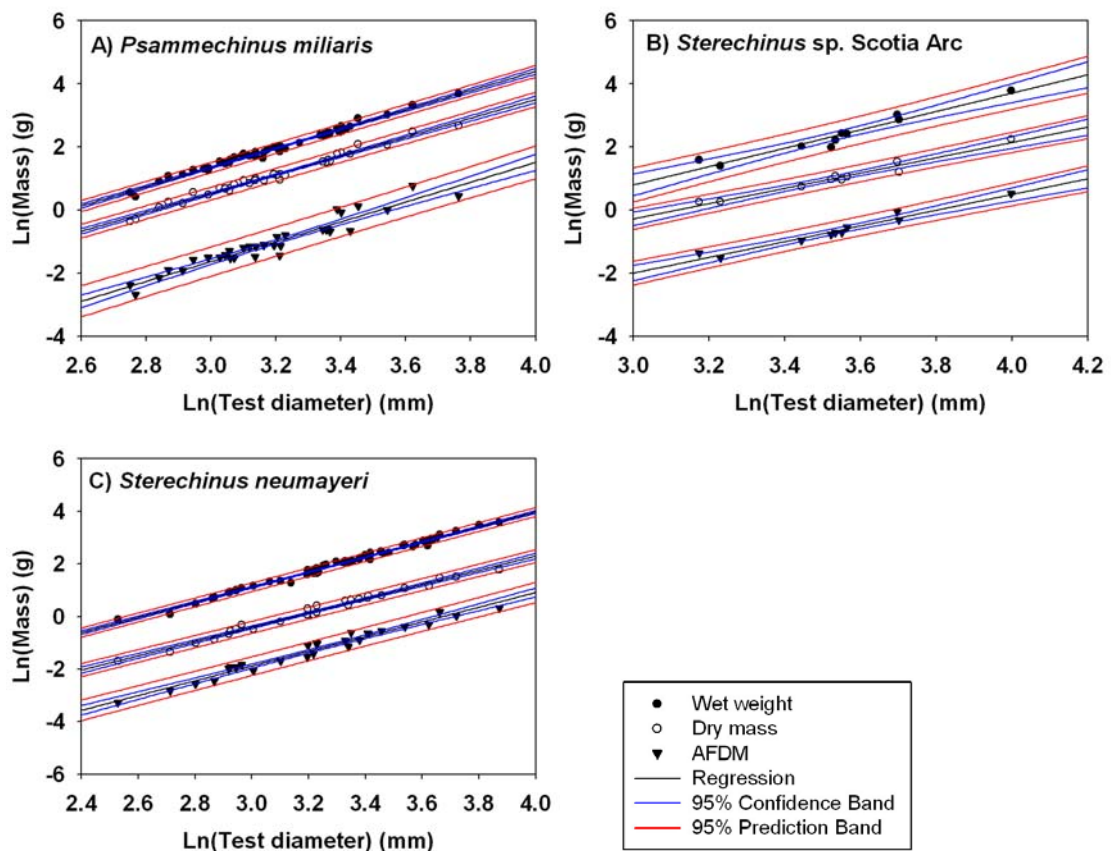


Figure 3.14 Regressions of $\ln(\text{Mass})$ on $\ln(\text{Test diameter})$ for A) *Psammechinus miliaris*, B) *Sterechnus* sp. from the Scotia Arc, and C) *Sterechnus neumayeri*.

3.3.2 Shell morphology

3.3.2.1 Inorganic content and shell mass

This section describes the amount of inorganic material for each species as a percentage of the total animal dry mass (i.e. the sum of the animal inorganic and organic content). This measure of the total amount of inorganic material within an animal can be used as a proxy of the amount of shell or skeleton an animal has. This method assumes the amount of inorganic material in the soft tissues is small compared to the shell/skeleton and does not vary markedly among individuals. Although in some brachiopods spicules in the soft tissues and the lophophore support can amount to over 50 % of the soft tissue dry mass (James *et al.*, 1992; Peck, 1993), this mass was still small compared to the dry mass of the shell. The mean inorganic content (approximate skeletal content) of whole animals (soft tissue and skeleton) is shown across latitudes. For the molluscs, since it is possible to separate shell from soft tissue in bivalves and gastropods, differences in shell mass among latitudes were also calculated.

Gastropoda: inorganic content and shell mass

Data on gastropod inorganic content did not have equal variances so Welch's F test (Welch, 1951) was used instead of the standard one-way ANOVA to test for differences in inorganic content among species. There was a significant difference between the inorganic content of gastropod species studied (Welch's $F = 325.874$, $df1 = 7$, $df2 = 76.433$, $p < 0.001$, $n = 225$) (Figure 3.15). Post hoc comparisons using the Games-Howell procedure (appropriate for groups with unequal variances) showed there were no significant differences among the four Australian gastropod species *Cantharus fumosus*, *Phos senticosus*, *Cominella lineolata* and *Thais orbita* ($p > 0.05$ NS). There was also no significant difference between *Buccinum undatum* and *Buccinum glaciale* ($p > 0.05$ NS). There were significant differences ($p < 0.001$) for inorganic content among all other species. *Neobuccinum eatoni* had the lowest inorganic content ($p < 0.001$).

Tropical and warm temperate species had between 90 and 93 % inorganic content compared to cold temperate and polar species which had between 64 and 80 % inorganic

content. Low latitude species had a high inorganic content and high latitude species had lower inorganic content (Figure 3.15).

Where possible, shell and tissue were separated and dried. Differences in the proportion of shell mass compared to tissue mass can be seen among latitudes and show the same trend as for total inorganic content of gastropods. These trends provide evidence that the total inorganic content of a gastropod is a good indication of the amount of shell it has.

Data on the dry mass of the shell as a percentage of the total dry mass of the animal for buccinid gastropods were distributed normally but had unequal variances. There was a significant difference in the dry mass of the shell as a percentage of the total dry mass of the animal among buccinid gastropods (Welch's $F = 379.607$, $df_1 = 3$, $df_2 = 29.054$, $p = 0.000$, $n = 96$). Post hoc comparisons using the Games-Howell procedure showed each species was significantly different in the dry mass of the shell as a percentage of the total dry mass of the animal ($p \leq 0.003$). In the Antarctic buccinid, the shell accounted for only 35 % of the total dry mass of the animal, whereas in tropical species, shell accounted for 90 % of the total dry mass (Figure 3.16).

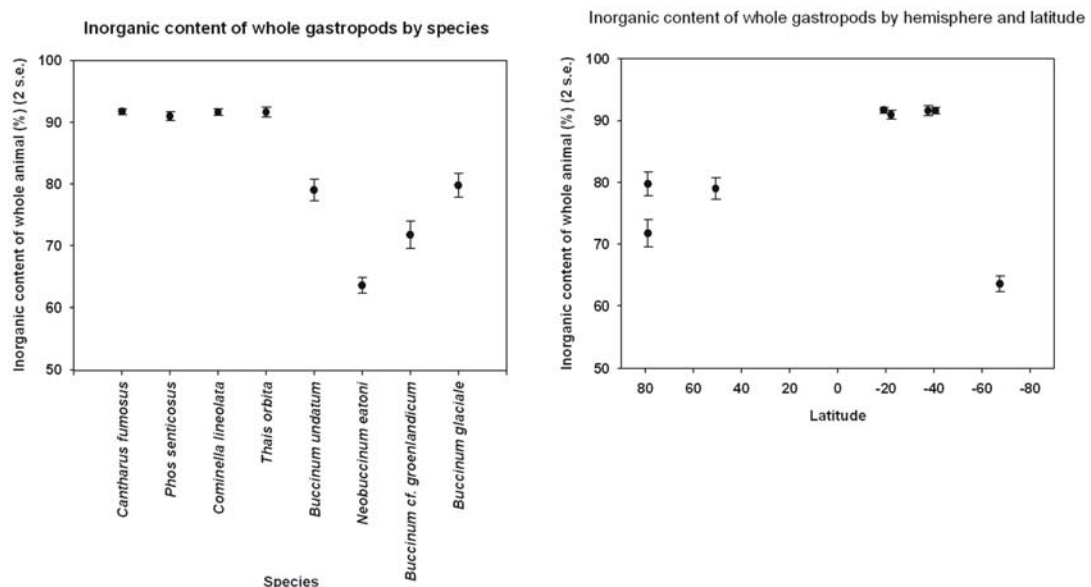


Figure 3.15 Inorganic content of whole gastropods as a percentage of the total animal dry mass by species (left) and by latitude (right). N.B. Negative values of latitude are in the Southern Hemisphere. All species are buccinids except for *Thais orbita*.

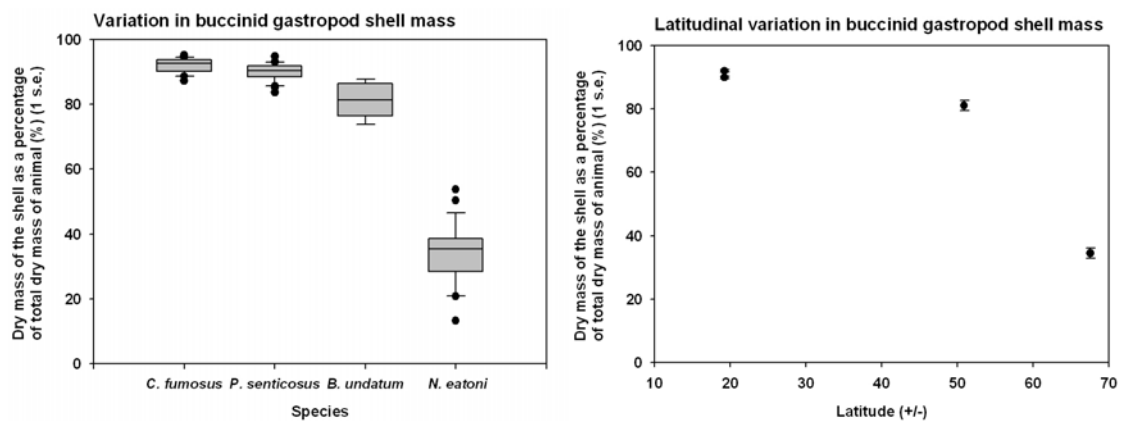


Figure 3.16 Variation among buccinids in shell dry mass as a percentage of total animal dry mass by species (left) and latitude (right).

Bivalvia: *Laternula* - inorganic content and shell mass

Inorganic content data for species of *Laternula* were distributed normally and with equal variances. There was a significant difference between the inorganic content of whole *Laternula* clams ($F = 205.952$, $df = 3,125$, $p = 0.000$, $n = 129$) (Figure 3.17). Post hoc comparisons using Gabriel's procedure (as sample sizes are slightly different) show *L. elliptica* was significantly different in inorganic content to all the other species ($p < 0.001$). *L. truncata* and *L. recta* were significantly different from each other ($p < 0.001$).

Laternula shell dry mass as a percentage of total animal dry mass data are shown in Figure 3.18. *Laternula* shell dry mass as a percentage of total animal dry mass data had equal variances. There was a significant difference in shell dry mass as a percentage of total animal dry mass among *Laternula* clams ($F = 44.143$, $df = 3,87$, $p < 0.001$, $n = 91$). Post hoc comparisons using Gabriel's procedure showed there was no difference in shell dry mass as a percentage of total animal dry mass between *L. elliptica* and *L. truncata* or *L. recta* and *L. boschasina* ($p > 0.05$). There were significant differences among all other species combinations ($p < 0.001$).

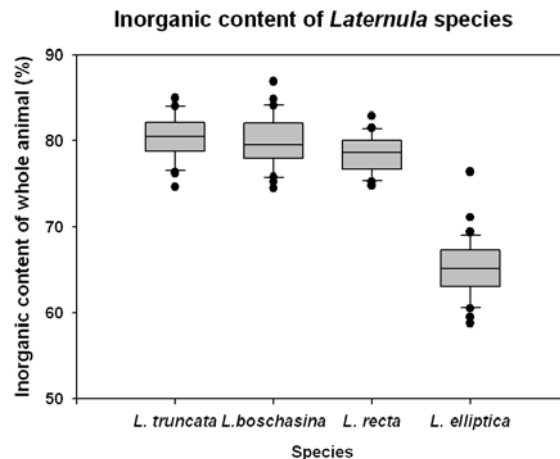


Figure 3.17 Inorganic content of whole *Laternula* clams.

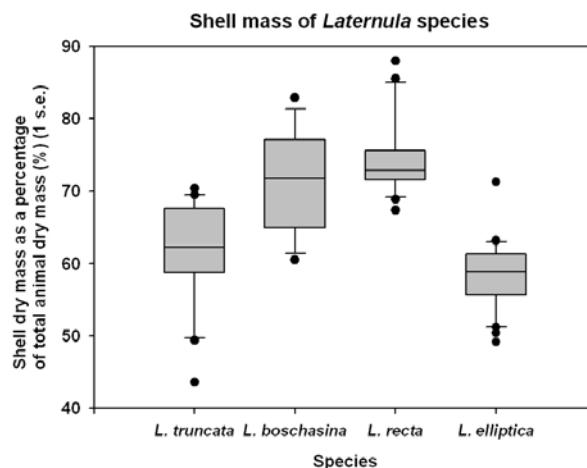


Figure 3.18 Variation among *Laternula* species in shell mass as a percentage of total animal dry mass.

Brachiopoda: inorganic content

Since the soft tissues of punctuate brachiopods extend into their shells it is difficult to compare the amount of brachiopod shell to soft tissue for fresh animals. Brachiopod tissues in caeca of punctuate species have been digested from the shell using hydrochloric acid (HCl) to measure organic and inorganic shell contents in the past, and the results produced were very similar to values obtained by measuring mass loss on ignition (Peck & Edwards, 1996). Articulate brachiopods also often have high inorganic contents of soft tissues due to the lophophore and high spicule content, and these are skeletal elements (Peck, 1993).

Since whole animal data (soft tissue and shell) were generally required for other parts of this study, the inorganic content of the total animal was compared among brachiopods as a proxy for the amount of shell for each brachiopod species.

Data for species of brachiopod were distributed normally with equal variances. There was a significant difference in inorganic content (as whole animal inorganic percentage) among the three brachiopod species ($F = 297.647$, $df = 2,47$, $p < 0.001$, $n = 50$) (Figure 3.19). Post hoc comparisons using Hochberg's GT2 procedure (as sample sizes were very different) showed that *L. uva* was significantly different in inorganic content to *L. neozelanica* and *Magellania venosa* ($p < 0.001$).

Further investigations into inorganic and organic mass of brachiopods revealed that the trends in inorganic content were not that straightforward. Both *Liothyrella uva* and *L. neozelanica* followed the same length to body mass curves for dry mass and ash mass (inorganic mass) on the scale shown (Figure 3.20). However, the inorganic content as a percentage of the total brachiopods was different. This is because the organic content of *L. uva* is much greater than that of *L. neozelanica*. So by not taking a percentage (to control for animal size), *L. uva* and *L. neozelanica* had the same inorganic mass for a given size. Thus in the brachiopods studied, organic mass varied between temperate and polar latitudes; inorganic mass did not vary.

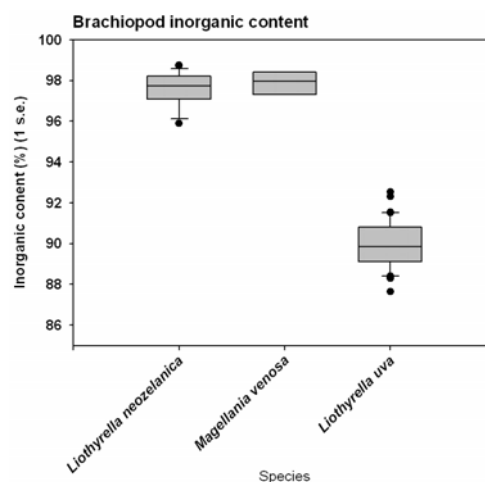


Figure 3.19 Inorganic content of brachiopods.

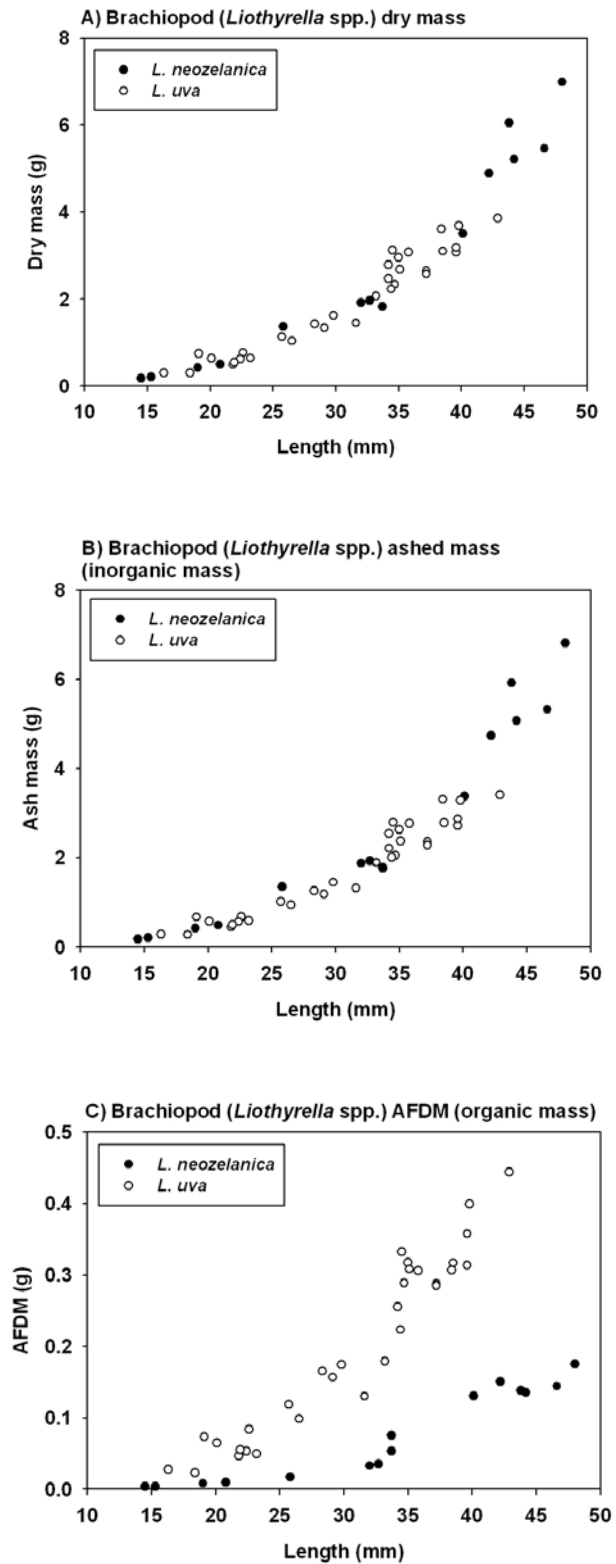


Figure 3.20 Brachiopod genus *Liothyrella* A) dry mass, B) ash mass (inorganic mass) and C) AFDM (organic mass).

Echinoidea: Echinidae - inorganic content

Echinoderms have internal skeletons and since the soft tissues of echinoids are attached to their tests, it is difficult to compare the amount of echinoid test to soft tissue. Instead the inorganic content of the total animal was compared between echinoids as a proxy for the amount of test that each echinoid species had. Echinoid inorganic content data had equal variances. There was a significant difference in inorganic content among the three echinoid species ($F = 174.431$, $df = 2,67$, $p < 0.001$, $n = 70$) (Figure 3.21). Post hoc comparisons using the Gabriel's procedure (as sample sizes are slightly different) show that *P. miliaris* had a higher inorganic content than *Sterechinus* sp. which in turn had a higher inorganic content than *S. neumayeri* ($p < 0.001$).

Similar investigations into inorganic and organic mass of echinoids, to those conducted for the brachiopods, showed that the pattern of inorganic and organic mass partitioning between temperate and polar echinoids was the opposite of that for the brachiopods. *P. miliaris* and *S. neumayeri* followed different test diameter to body mass curves for both dry mass and ash mass (inorganic mass) (Figure 3.22). The temperate echinoid *P. miliaris* had a greater dry mass and ash mass for a given test diameter. However, organic mass was roughly the same in the temperate and polar echinoids for individuals of a test diameter of 15 to 30 mm. So in the echinoids studied, inorganic mass varied between temperate and polar latitudes; organic mass varied little or not at all.

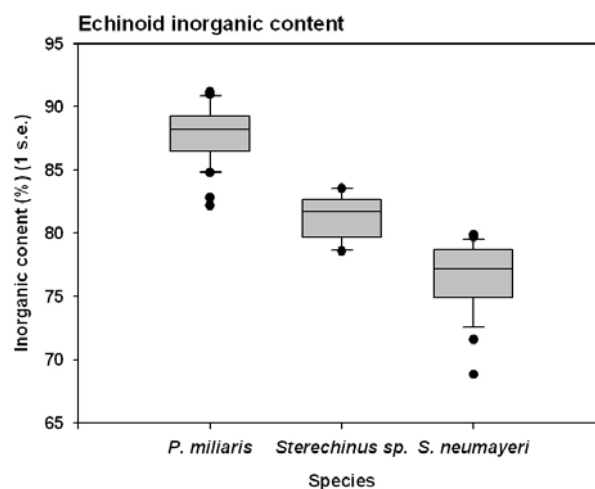


Figure 3.21 Inorganic content of echinoids.

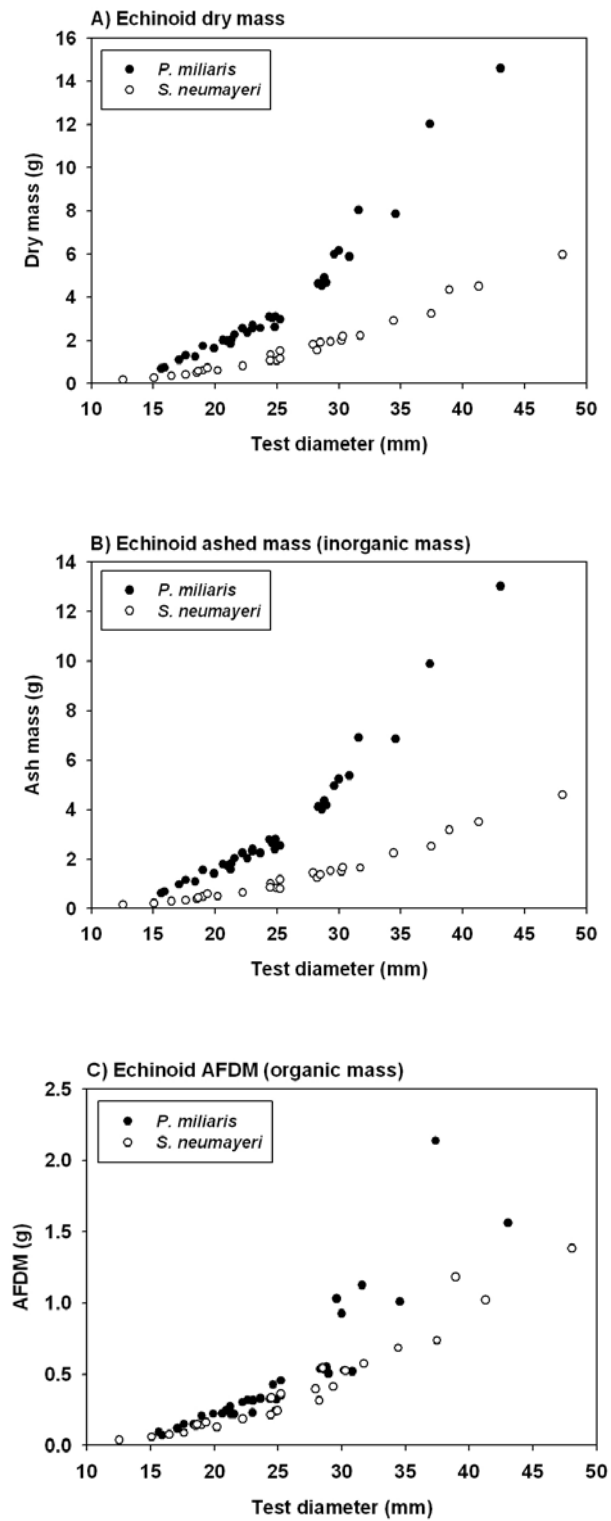


Figure 3.22 Echinoid A) dry mass, B) ash mass (inorganic mass) and C) AFDM mass (organic mass).

Summary trends for inorganic content

Figure 3.23 shows a summary plot of the latitudinal trend in shell mass and inorganic content for all 4 groups of animal studied. Combining all the inorganic content for all groups in one graph shows there is a notable poleward decrease in inorganic content for megabenthic marine invertebrates studied.

However, we now know that in fact the decrease in brachiopod inorganic content as a percentage of the whole animal is due to the increase in organic mass in the polar brachiopod, and actually absolute inorganic mass does not differ between temperate and polar *Liothyrella* species. Changes in the organic content of an organism occur with season, with growth and reproductive state influencing total organic mass.

Arctic buccinid inorganic content is greater than that of the Antarctic gastropod. However, the Arctic buccinids exist in warmer water (sub-Arctic) than may be expected for their latitude and when inorganic content is plotted with temperature (Figure 3.24), inorganic content of all taxa increases as temperature increases.

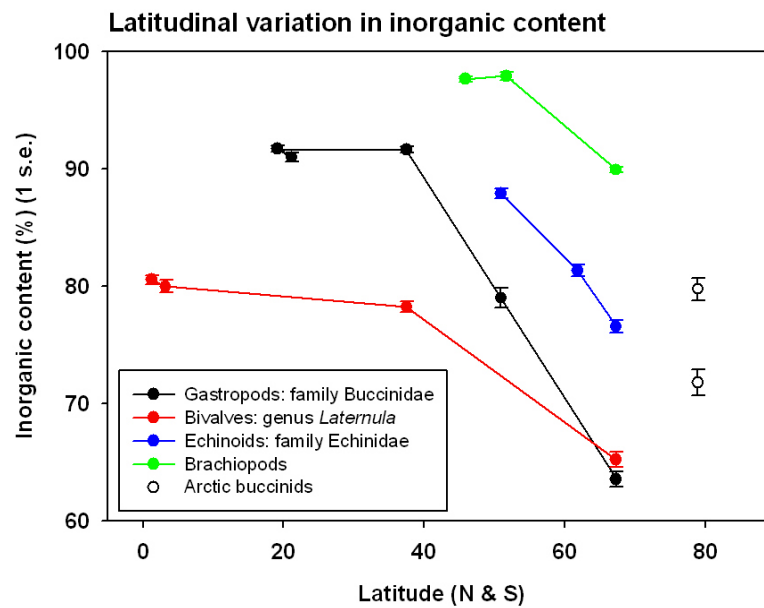


Figure 3.23 Latitudinal variation in whole animal inorganic content (ash as % dry mass). This metric is used because it is a good measure of the amount of skeleton and it is comparable among groups. Standard errors are mostly smaller than the points used to mark the mean.

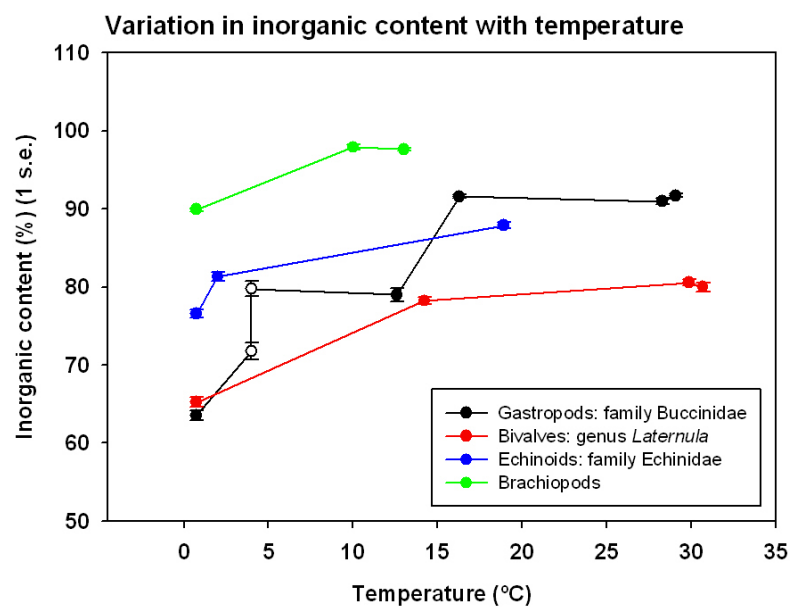


Figure 3.24 Variation in whole animal inorganic content (ash as % dry mass) with temperature. The Arctic buccinids are now included in the buccinid gastropods and are shown as black open circles.

3.3.2.2 Organic content of shells and soft tissue

The organic content of shells and soft tissues were determined for the bivalve and gastropod molluscs for which it was possible to separate the soft tissues of the animal from the shell. Shell organic content data are expressed as a percentage of total shell dry mass. Tissue organic content data are expressed as a percentage of total soft tissue dry mass.

Bivalvia: genus *Laternula*

Laternula clam shell organic content data were distributed normally but did not have equal variances. There was a significant difference between shell organic content (Welch's $F = 6.308$, $df_1 = 3$, $df_2 = 35.040$, $p = 0.002$, $n = 118$) (Figure 3.25). Post hoc comparisons using the Games-Howell procedure showed that *L. elliptica* shell had less organic content in than *L. boschasina* shell ($p = 0.004$) but was not significantly different from *L. truncata* or *L. recta* shell ($p > 0.05$).

Laternula clam soft tissue organic content data were distributed normally but did not have equal variances. There was a significant difference between soft tissue organic content (Welch's $F = 408.695$, $df_1 = 3$, $df_2 = 35.547$, $p < 0.001$, $n = 117$). Post hoc comparisons using the Games-Howell procedure show all species were significantly different from each other in their soft tissue organic content ($p < 0.001$). The soft tissues of *L. elliptica* had the greatest organic content. Soft tissue organic content increased from tropical to temperate to polar species (Figure 3.26).

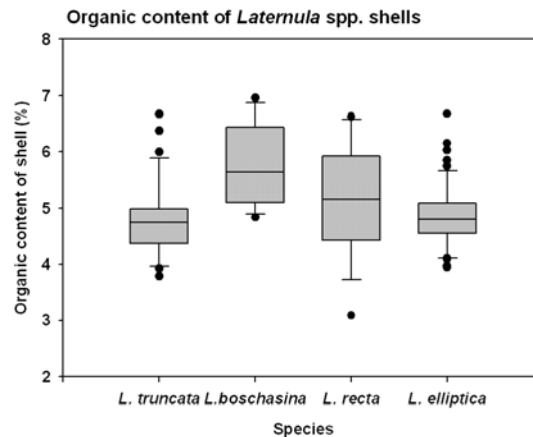


Figure 3.25 Organic content of *Laternula* species shells as a percentage of the total dry mass of the shell.

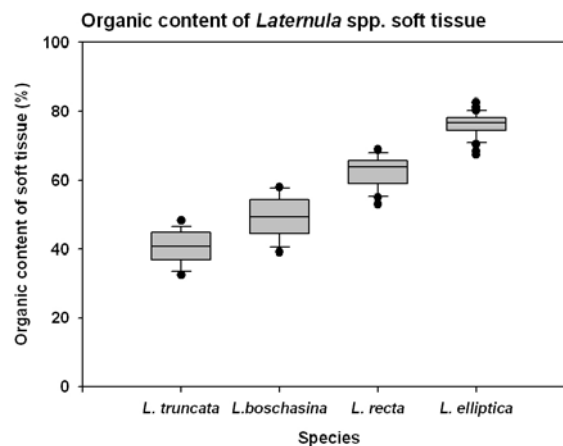


Figure 3.26 Organic content of *Laternula* species soft tissue as a percentage of the total dry mass of the soft tissue.

Gastropoda: family Buccinidae

Buccinid gastropod shell organic content data did not have equal variances. There was a significant difference between gastropod shell organic content (Welch's $F = 36.046$, $df_1 = 5$, $df_2 = 48.556$, $p < 0.001$, $n = 159$) (Figure 3.27). Post hoc comparisons using the Games-Howell procedure showed that *Phos senticosus* had the lowest shell organic content ($p = 0.003$).

Buccinid gastropod soft tissue organic content data did not have equal variances. There was a significant difference between gastropod soft tissue organic content (Welch's $F = 16.415$, $df1 = 5$, $df2 = 49.401$, $p = 0.000$, $n = 155$) (Figure 3.27). Post hoc comparisons using the Games-Howell procedure showed that *Neobuccinum eatoni* had the highest soft tissue organic content ($p = 0.01$). Although there was great variation among species, there was no obvious trend in organic content with latitude for either buccinid shells or soft tissues (Figure 3.27).

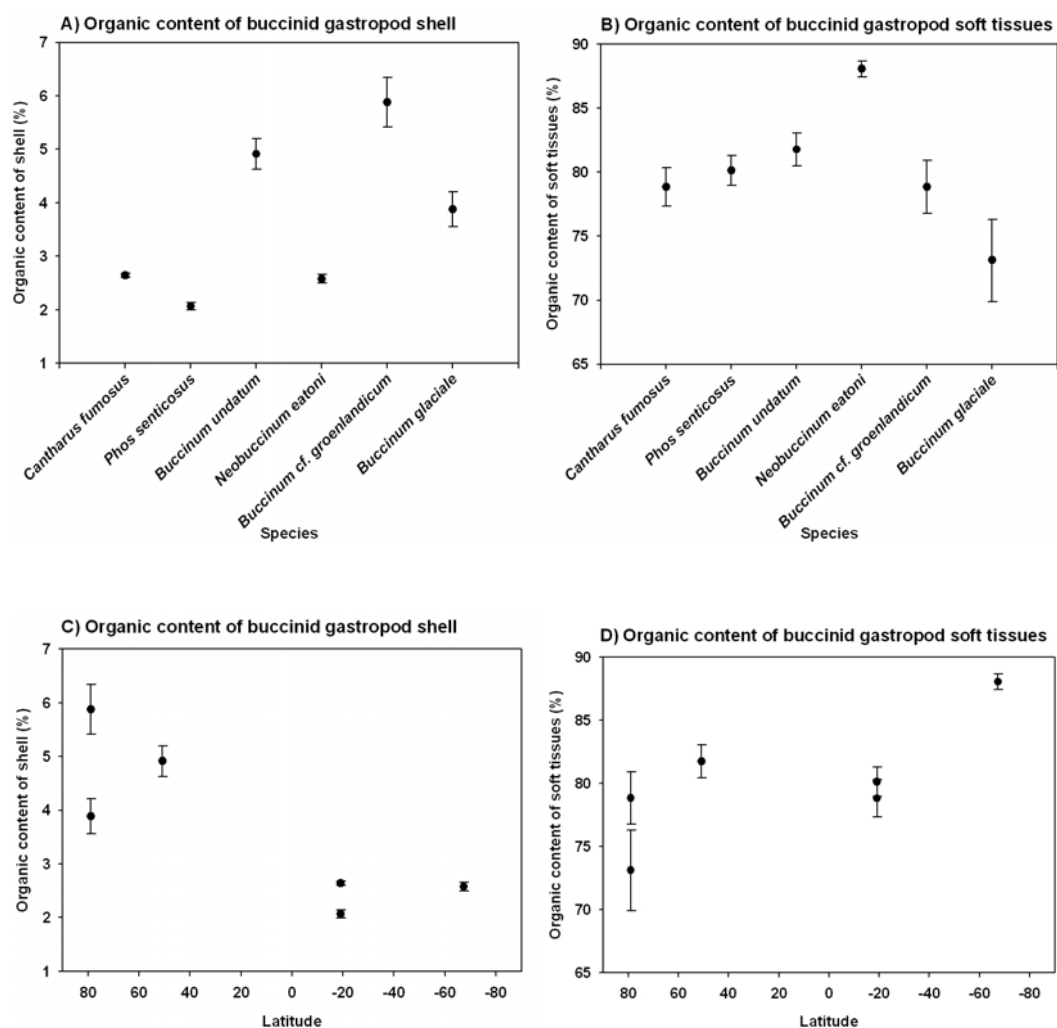


Figure 3.27 Organic content of buccinid gastropod: A) shell by species, B) soft tissue by species, C) shell by latitude and D) soft tissue by latitude.

3.3.2.3 Shell thickness

Shell thickness data are presented as 1) absolute values (raw data) and 2) corrected for animal size using the longest linear dimension, i.e. length in bivalves and brachiopods, height in gastropods and test diameter in echinoids.

Gastropoda: family Buccinidae

1) Absolute values (raw data) uncorrected for size

Regressions

Regression equations of height and shell thickness for each species of buccinid gastropod are shown in Figure 3.28. Individual regressions were plotted for each species from raw (uncorrected) data where significant. For some of the species, the size range of shell height was not large enough to enable significant regressions of shell thickness on shell height. A regression of Ln(Shell thickness) on Ln(Shell height) data for all buccinid species combined showed no significant regression for the uncorrected data for the entire data set ($F = 2.8946$, $df = 1,65$, $p = 0.0937$ NS, $n = 67$). Buccinid raw shell height and shell thickness data were analysed by a general linear model. Akaike's information criterion (AIC) (Akaike, 1974) was used to determine the best model fit to the data. When the 3 models below were tested, model 2 had the lowest AIC value ($AIC = 15.639$). Therefore, the data were best modelled by regression lines of the same slope, but with different intercepts.

Model 1: Shell thickness ~ shell height

Model 2: Shell thickness ~ shell height + species

Model 3: Shell thickness ~ shell height + species + shell height:species

Mean shell thickness

Raw data on buccinid shell thickness did not have equal variances. There was a significant difference between the shell thickness of gastropod species studied (Welch's $F = 40.131$, $df1 = 6$, $df2 = 25.421$, $p < 0.001$, $n = 67$). Raw data show the absolute thickness of the shells and demonstrate that shells are thicker towards the equator even for species that vary markedly in shell length (Figure 3.29).

2) Data corrected for a standard height gastropod

Regressions

Raw data were used to determine the standard-sized animal and a standard animal size of $\text{Ln}(\text{Length (mm)}) = 3.5$, equivalent to length = 33 mm, was chosen as an average sized animal for all buccinid species. Data were corrected for a standard height animal using the mean regression equation slope of significant regressions of $\text{Ln}(\text{Shell thickness})$ on $\text{Ln}(\text{Height})$ (i.e. those for *Buccinum glaciale* and *Buccinum cf. groenlandicum*) (Figure 3.28), which was $a = 1.27$.

Individual regressions for species show shell thickness was generally positively related to shell length, as one would expect when size increases. However, plotting a regression through mean size corrected data for all species gave a significant negative regression for the entire data set¹ (Figure 3.30). Samples of each buccinid species consisted mainly of adults, and adult size decreased from high to low latitudes. Smaller species had thicker shells than the larger species and these reasons are likely to have produced the negative trend in Figure 3.30.

Mean shell thickness

Corrected for a standard height gastropod of 33 mm, the pattern of increasing shell thickness towards the equator is clearer (Figure 3.31 and Figure 3.32). Size corrected data for buccinid shell thickness did not have equal variances. There was a significant difference between the corrected shell thickness of gastropod species studied (Welch's $F = 71.754$, $df_1 = 6$, $df_2 = 24.985$, $p < 0.001$, $n = 67$). Post hoc comparisons using the Games-Howell procedure for corrected data showed *Cominella lineolata* has a significantly thicker shell than all other buccinids ($p < 0.001$) but the other temperate species *Buccinum undatum* and all the polar species (*Neobuccinum eatoni*, *Buccinum glaciale* and *Buccinum cf. groenlandicum*) had a thinner shell than the tropical species and the temperate snail *Cominella lineolata* ($p < 0.001$).

¹ This negative regression equation was not used for the size correction.

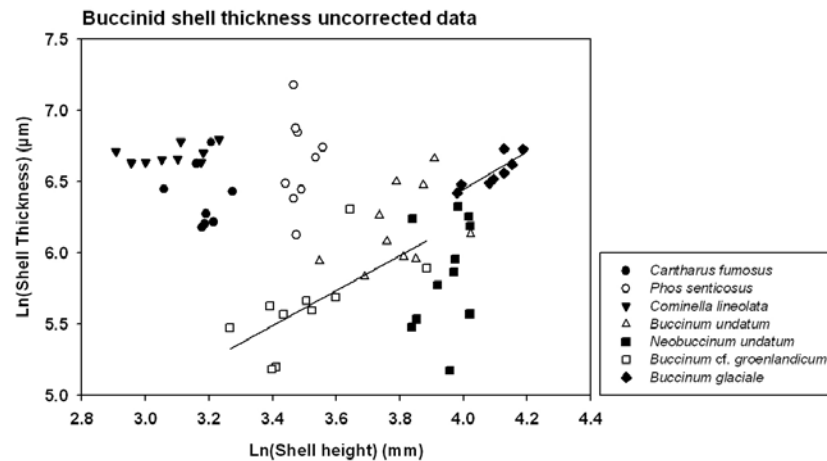


Figure 3.28 Regressions of Ln(Shell thickness) on Ln(Shell height) in buccinid gastropods on raw (uncorrected) data.

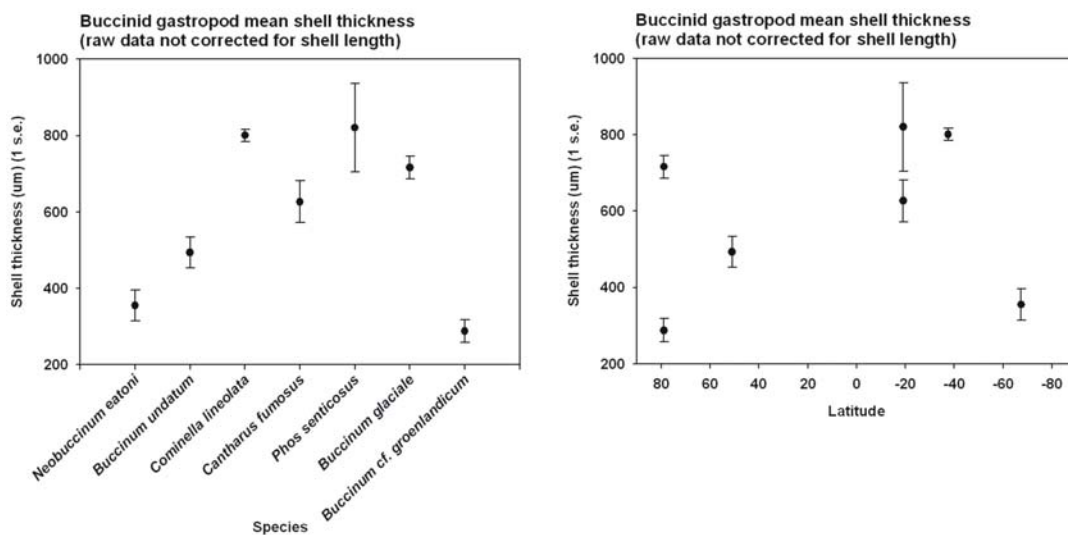


Figure 3.29 Uncorrected data for mean shell thickness by buccinid species (left) and by latitude (right). N.B. Negative values of latitude represent the Southern Hemisphere.

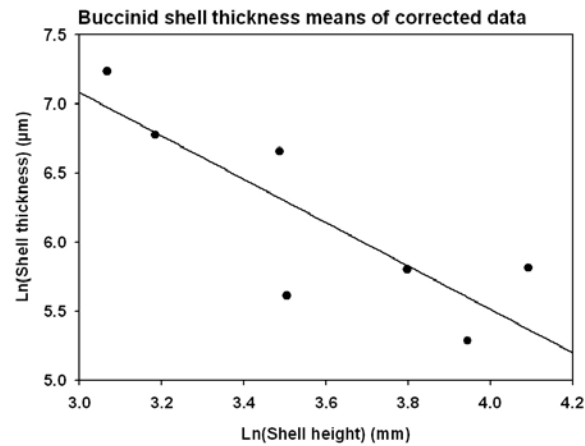


Figure 3.30 Plot of corrected Ln(Shell thickness) on original Ln(Shell height) data for each buccinid species. Samples were limited to mostly adults from each species and for an approximate maximum size for each species there was a significant negative relationship between height and shell thickness ($F = 11.4899$, $df = 1,5$, $p = 0.0195$, $n = 7$).

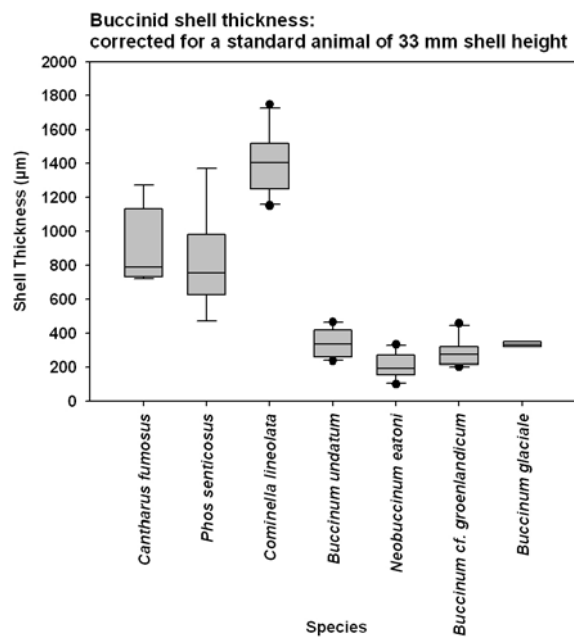


Figure 3.31 Mean shell thickness for each buccinid species corrected for size.

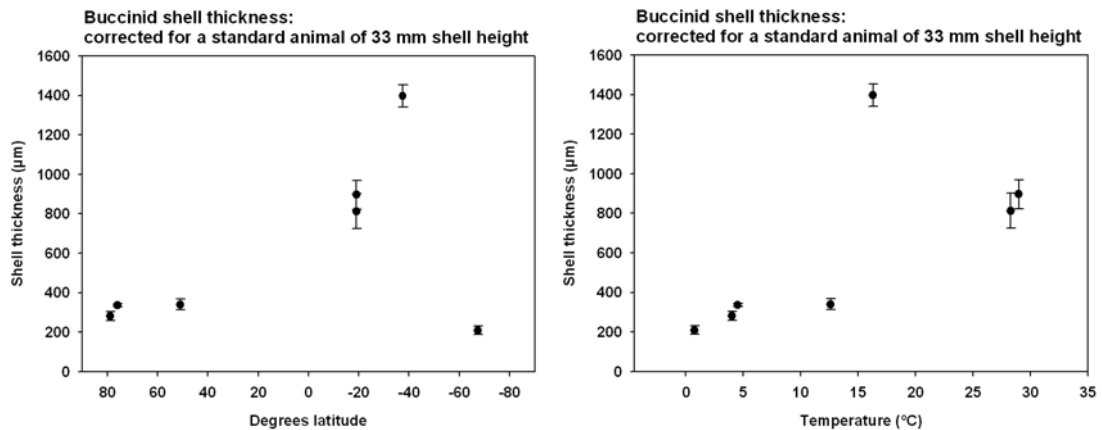


Figure 3.32 Mean shell thickness for each buccinid species corrected for size and plotted by latitude (left) and temperature (right). N.B. Negative values of latitude represent the Southern Hemisphere.

Bivalvia: genus *Laternula*

1) Absolute values (raw data) uncorrected for size

Regressions

Ln(Shell thickness) data were plotted on Ln(Length) data for *Laternula* species (Figure 3.33). There was a significant regression for the uncorrected Ln(Shell thickness) on Ln(Length) data for all *Laternula* species combined ($F = 74.7202$, $df = 1,40$, $p < 0.0001$, $n = 42$, $y = 1.8221x - 1.2336$, $r^2 = 0.6426$).

Mean shell thickness

Raw data for *Laternula* species shell thickness was distributed normally but did not have equal variances. There was a significant difference between the raw shell thickness of 5 species of *Laternula* studied (Welch's $F = 27.232$, $df1 = 4$, $df2 = 10.679$, $p < 0.001$, $n = 45$) (Figure 3.34). Post hoc comparisons using the Games-Howell procedure for corrected data showed that the larger species *L. elliptica* predictably had a significantly thicker shell than any other species ($p = 0.001$).

2) Data corrected for a standard length animal

Shell thickness data were corrected to a standard animal length of $\text{Ln}(\text{Length (mm)}) = 3.5$, equivalent to length = 33 mm. Data were corrected for a standard length animal using the statistically significant regression equation slope of $\text{Ln}(\text{Shell thickness})$ on $\text{Ln}(\text{Length})$ for *Laternula elliptica* (Figure 3.33) ($a = 1.52$) as scaling should be very similar in congeneries. Correcting for size differences among *Laternula* species controlled for differences in species' size. Empty shells from *Laternula valenciennesii* were found, but no live animals, hence this species does not appear in summary Table 3.1 and Table 3.2.

Laternula shell thickness data corrected for length was distributed normally but did not have equal variances. There was a significant difference among the shell thickness of *L. truncata*, *L. boschasina*, *L. valenciennesii*, *L. recta* and *L. elliptica* when corrected for length (Welch's $F = 53.029$, $df_1 = 4$, $df_2 = 16.735$, $p < 0.001$, $n = 45$) (Figure 3.35). Post hoc comparisons using the Games-Howell procedure for length corrected data showed all *Laternula* species had shells of significantly different thickness ($p < 0.05$) to each other. There was no clear latitudinal pattern in shell thickness for *Laternula* clams studied, but the Antarctic species *L. elliptica* clearly had the thickest shell even when corrected for size (Figure 3.36).

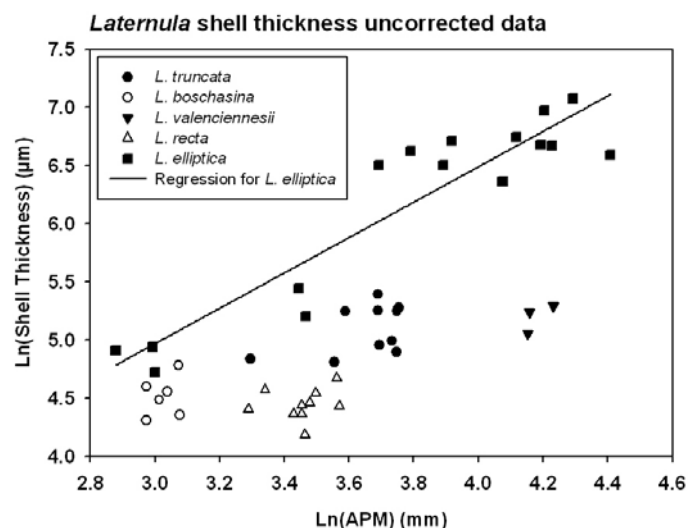


Figure 3.33 Regression of $\text{Ln}(\text{Shell thickness})$ on $\text{Ln}(\text{Length})$ in *Laternula* clams. *L. elliptica* has a statistically significant regression equation ($p < 0.0001$).

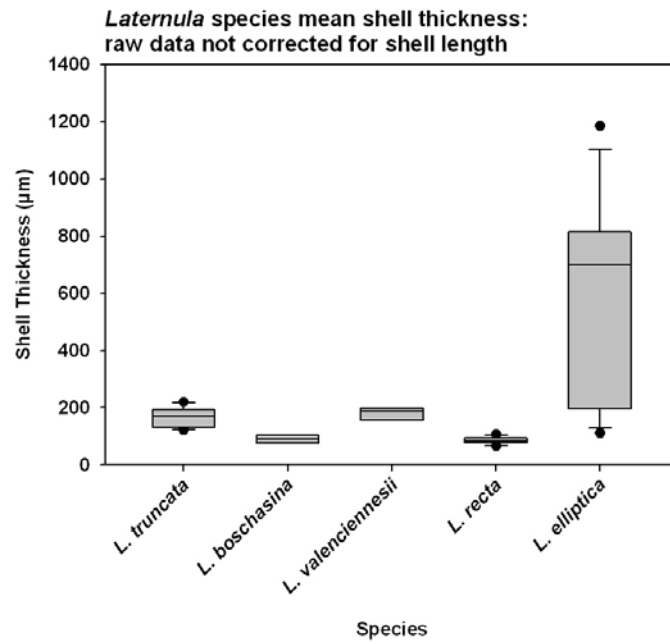


Figure 3.34 Mean shell thickness for each *Laternula* species (uncorrected).

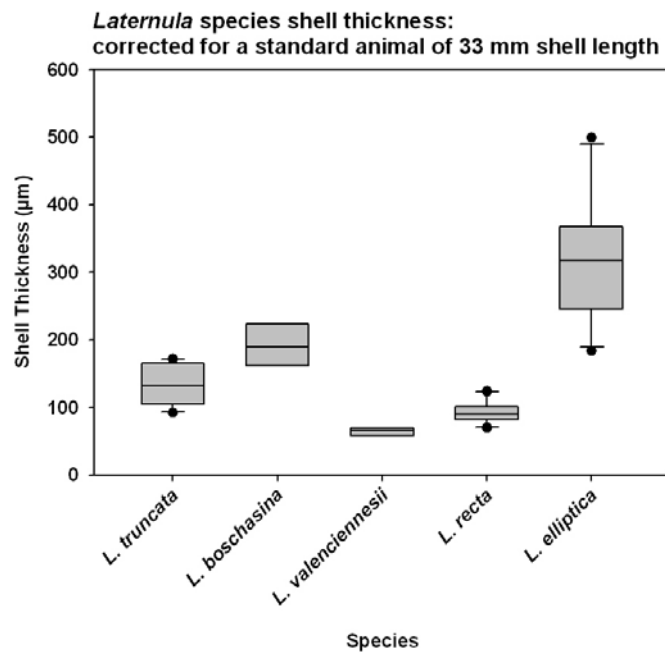


Figure 3.35 Mean shell thickness for each *Laternula* species corrected for length.

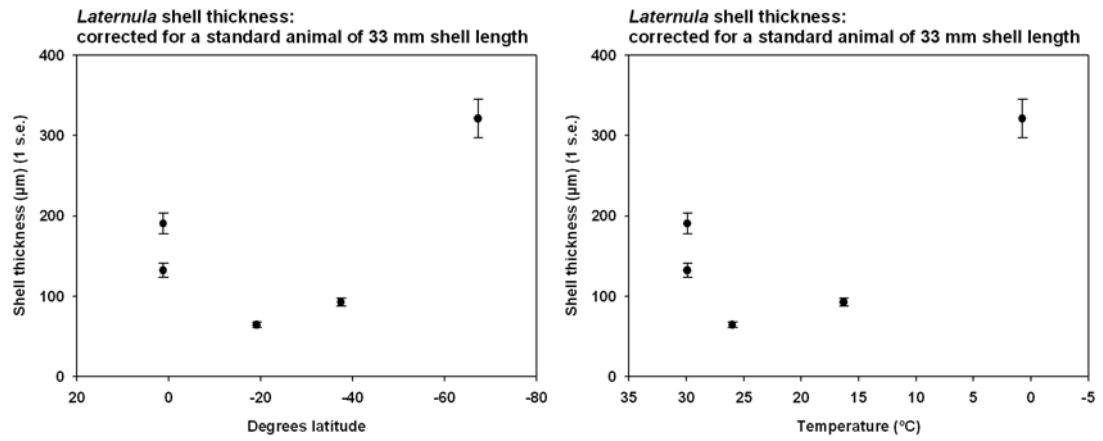


Figure 3.36 Mean shell thickness for each *Laternula* species corrected for length and plotted by latitude (left) and temperature (right). N.B. Negative values of latitude represent the Southern Hemisphere. Temperature axis is reversed.

Brachiopoda

1) Absolute values (raw data) uncorrected for size

Regressions

Brachiopod shell thickness was plotted on length for individual species (Figure 3.37).

There was a significant regression of Ln(Shell thickness) uncorrected data on Ln(Length) data for all brachiopod species combined for the entire data set ($F = 43.9740$, $df = 1,30$, $p < 0.0001$, $n = 32$, $y = 0.6050x + 4.1219$, $r^2 = 0.5945$). Between *Liothyrella neozelanica* and *L. uva* the covariate length was significantly related to shell thickness (ANCOVA: $F = 132.972$, $df = 1,21$, $p < 0.001$). There was no significant effect of species on shell thickness after controlling for the effects of length ($F = 3.592$, $df = 1,21$, $p = 0.72$ NS). Model fitting assessed by AIC showed that the data were best modelled with trend lines of the same slope but with different intercepts (AIC = -21.12).

Mean shell thickness

Brachiopod raw shell thickness data were distributed normally with equal variances. There was no significant difference in shell thickness using raw data among brachiopods ($F = 2.908$, $df = 3,28$, $p = 0.052$ NS, $n = 32$) (Figure 3.38).

2) Data corrected for a standard length animal

Brachiopod shell thickness data were corrected to a standard size animal of Ln(Length (mm)) = 3.5, equivalent to length = 33 mm using the mean slope from statistically significant regressions of Ln(Shell thickness) on Ln(Length), which was $a = 0.757$.

Brachiopod shell thickness data corrected for length were distributed normally but did not have equal variances. There was no significant difference in shell thickness among brachiopod species when corrected for length (Welch's $F = 3.763$, $df1 = 3$, $df2 = 7.219$, $p = 0.066$ NS, $n = 31$) (Figure 3.39).

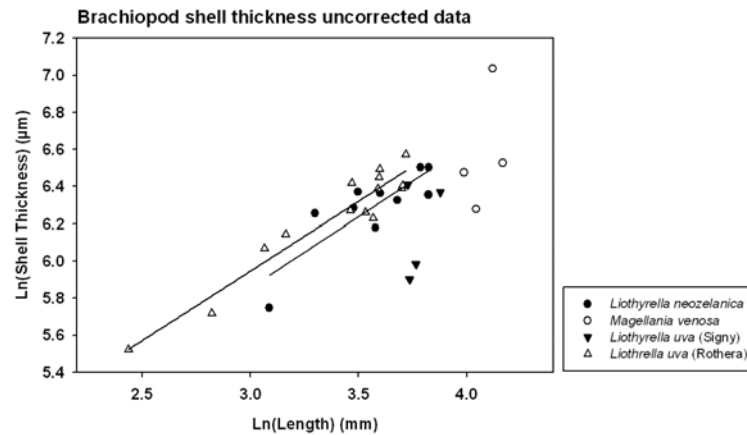


Figure 3.37 Regressions of Ln(Shell thickness) on Ln(Length) in brachiopods.

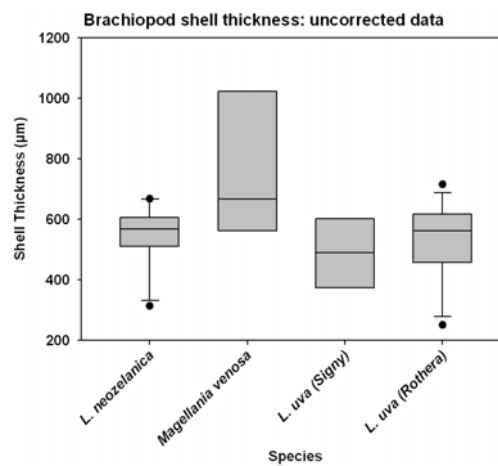


Figure 3.38 Mean shell thickness for each brachiopod species.

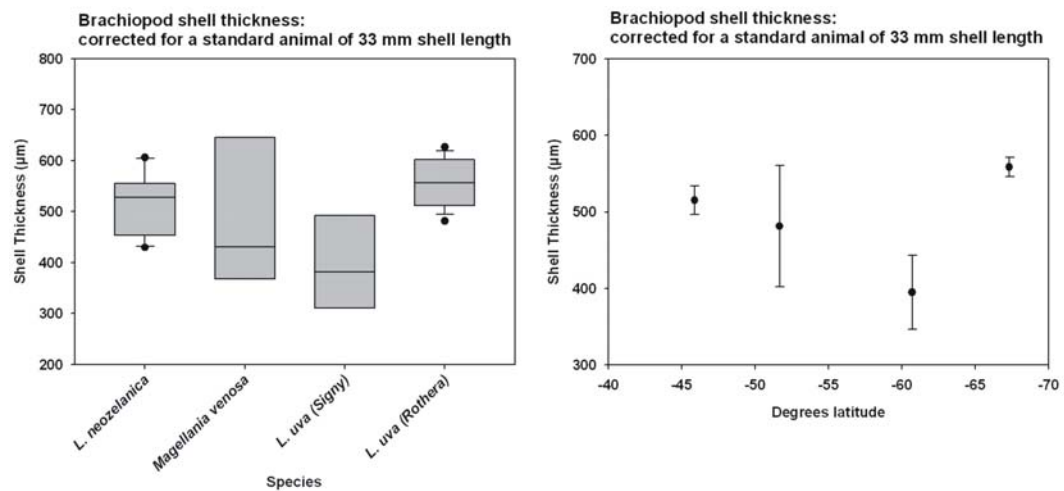


Figure 3.39 Mean shell thickness for each brachiopod species corrected for length by species (left) and latitude (right).

Echinoidea

1) Absolute values (raw data) uncorrected for size

Regressions

Test diameter of regular echinoids was plotted against test thickness for individual species (Figure 3.40). Echinoid test thickness raw data were distributed normally but did not have equal variances. There was a significant difference in test thickness between

Psammechinus miliaris and *Sterechinus neumayeri* ($t = 8.660$, $df = 12.307$, $p < 0.001$, $n = 20$). Mean test thickness was $739.99 \mu\text{m}$ (± 150.46 (1s.d.)) for *P. miliaris* and $290.41 \mu\text{m}$ (± 65.65 (1s.d.)) for *S. neumayeri* (Figure 3.41).

2) Data corrected for a standard echinoid test diameter

Echinoid shell thickness data were corrected to a standard size animal of $\text{Ln}(\text{Diameter (mm)}) = 3.3$, equivalent to diameter = 27 mm. Echinoid shell thickness data were corrected for a standard sized animal using individual regression slopes, which were significant.

Echinoid corrected shell thickness data were distributed normally and with equal variances.

When corrected for a standard size animal, there was a significant difference in test

thickness between *P. miliaris* and *S. neumayeri* ($t = 15.358$, $df = 18$, $p = 0.000$, $n = 20$)

(Figure 3.42). For an echinoid of test diameter = 27 mm, *P. miliaris* has a test thickness of

$768.38 \mu\text{m}$ (± 92.37 (1s.d.)) and *S. neumayeri* has a test thickness of $278.30 \mu\text{m}$ (± 40.63

(1s.d.)). Size-corrected data show *P. miliaris* has a thicker test than *S. neumayeri* (Figure

3.42). The test of *S. neumayeri* is also softer and much more fragile than that of *P. miliaris*.

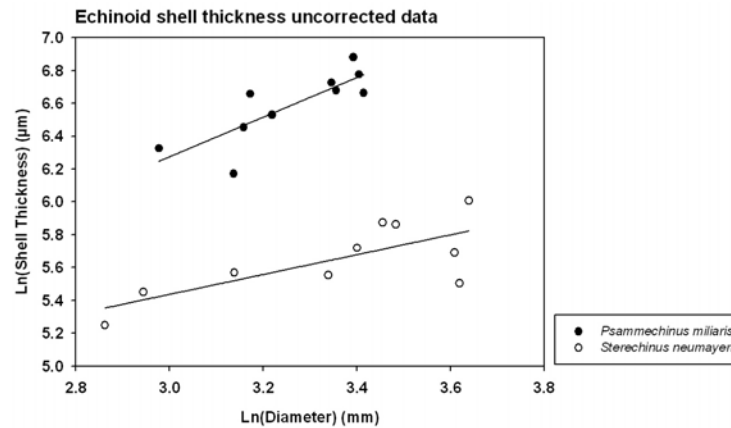


Figure 3.40 Regressions of Ln(Shell thickness) on Ln(Diameter) in echinoids. Shell thickness is test thickness in echinoids.

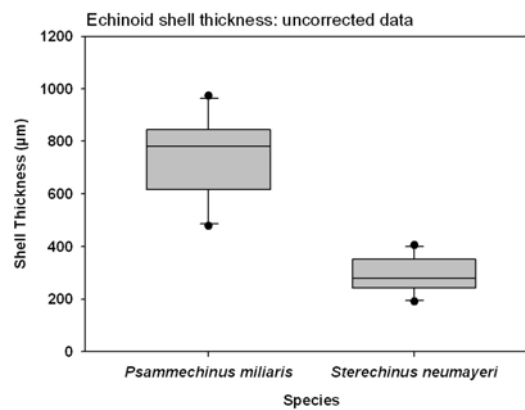


Figure 3.41 Mean shell thickness for each echinoid species (uncorrected data).

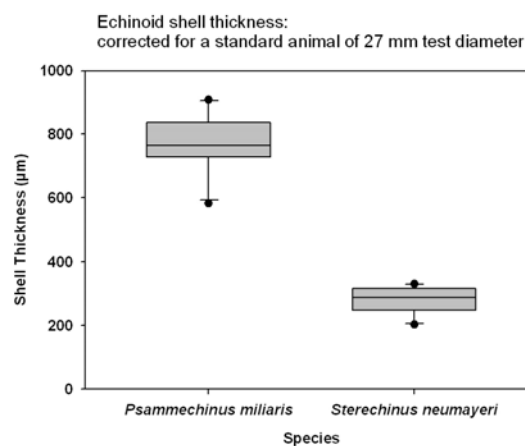


Figure 3.42 Mean shell thickness for each echinoid species corrected for test diameter.

3.4 Discussion

Latitudinal variation in shells and skeletons

In order to test the hypotheses of 1) shell cost versus 2) predation pressure to explain the geographical patterns in shell size and thickness, it was first necessary to determine what patterns in shell morphology existed across latitudes and if these patterns differed among types of calcareous organisms.

Nicol (1964a; 1966; 1967; 1970) reported that polar bivalves are small, thin, lack coloration and have little ornamentation. Graus (1974) described an extensive study into shell thickness and calcification index for gastropods along the east coast of North America, showing a poleward decrease in shell thickness and increase in calcium carbonate efficiency. However, little information is available for other taxa. Arnaud (1974) suggested that although echinoderms are large in Antarctica, gigantism is more frequent when animals have little calcification.

This study has chosen to focus on representatives from four key groups of shallow water megabenthic marine invertebrates that produce calcium carbonate shells or skeletons, consisting of representatives from the classes Bivalvia, Gastropoda and Echinoidea and phylum Brachiopoda. Within each of these classes, a set of closely related species was chosen to constrain phylogenetically the results. This thesis presents data on representatives from Antarctic and temperate latitudes and also, for the molluscs, representatives from tropical and Arctic latitudes. Extending this study to include many more species was outside the scope of this thesis, so results and conclusions presented should be considered in terms of the species studied.

Inorganic content and shell mass

The inorganic content of a whole animal is a proxy for the total amount of shell or skeleton an animal has. Using inorganic content as a measure of shell or skeleton is particularly useful where the shell or skeleton cannot be reliably separated from the soft tissues, such as in brachiopods and echinoderms. Where shell *could* be separated from soft tissues, such as

in the gastropod and bivalve molluscs, the amount of shell compared to soft tissue dry mass was also used. This separate shell and soft tissue mass data from the molluscs supported the use of total animal inorganic content as an indication of the amount of shell or skeleton an animal has since the results from the two approaches were close.

Inorganic content of whole gastropods decreased towards the poles, although it was remarkably constant for tropical and temperate Australian gastropods. The Antarctic gastropod, *Neobuccinum eatoni* had the lowest inorganic content. The mass of shell compared to total body mass also decreased towards the poles for gastropods and was least in *N. eatoni*.

The same pattern was found in *Laternula* clams; whole animal inorganic content decreased towards the poles. Like the Antarctic buccinid, the Antarctic clam, *L. elliptica* had the least whole animal inorganic content. Geographical patterns in shell mass as a percentage of whole body mass in *Laternula* species were less clear and it is proposed that species morphology affected this trend. Additional data collected during this Ph.D. study show *L. elliptica* and *L. truncata* are capable of long extensions of their siphons of $28.8 (\pm 6.5, 1 \text{ s.d.}) \%$ and $22.4 (\pm 7.4, 1 \text{ s.d.}) \%$ of their total body length (shell length plus siphon), respectively. The siphon of *L. boschasina* is relatively only half as long at $10.8 (\pm 4.3, 1 \text{ s.d.}) \%$ of its total body length. Thus the clams capable of long extensions of their siphons have lower shell mass as a proportion of total body mass, presumably because they have comparably more soft tissue.

Harper *et al.* (2009) recently found the highest organic content yet recorded for a mollusc in the shell of the bivalve *Entodesma navicula*. In this bivalve, the granular prismatic microstructure contained 7.4 % organic matrix. This thesis took a “whole shell” approach to organic content since the organic content of the whole shell represented part of the total cost of the shell to the animal. The organic content of whole *Laternula* shells ranged from $4.78 (\pm 0.67, 1 \text{ s.d.})$ to $5.74 (\pm 0.72, 1 \text{ s.d.}) \%$ and the organic content of whole buccinid shells ranged from $2.07 (\pm 0.38, 1 \text{ s.d.})$ to $5.88 (\pm 2.06, 1 \text{ s.d.}) \%$ which was less than that found in the granular prismatic microstructure of the bivalve *Entodesma navicula* by Harper *et al.* (2009). Latitudinal trends in organic content data for mollusc shell and soft

tissue did not show strong overall patterns. *Laternula* data suggest that the organic content of shells decreased, whereas organic content of soft tissues increased, along an increasing latitudinal gradient. Gastropod data showed different patterns for each hemisphere and among buccinids studied shell organic content was low in the Southern Hemisphere species and higher in the Northern Hemisphere species. Palmer (1992) described how organic matrix was more costly to produce than inorganic CaCO_3 . Data from *Laternula* shells support the theory that shells may cost more to make at high latitudes and therefore have less organic content. However, buccinid shell organic content data suggest that cold temperatures do not limit the amount of organic material in the shell.

The temperate brachiopod *Liothyrella neozelanica* had a greater inorganic content (by percent) than its polar counterpart *L. uva*. However, in terms of total inorganic mass, the temperate and polar brachiopods had the same mass of inorganic material; the difference in inorganic content by percent was because the polar brachiopod had a higher organic mass. Some of the difference in organic mass can be explained by season; *L. uva* was collected at the end of summer, whereas *L. neozelanica* was collected in the winter. *L. uva* change their AFDM by 40 – 50 % between summer and winter, with AFDM being highest in summer (Peck, 1989). This would not account for all the difference in organic mass, but would reduce the difference a lot.

The temperate echinoid *Psammechinus miliaris* also had a greater inorganic content (by percent) than its polar counterpart *Sterechinus neumayeri*. The reduction in skeleton in the polar echinoid *S. neumayeri* compared to the temperate echinoid *P. miliaris* supports findings by Arnaud (1974) that Antarctic echinoderm skeletons are often poorly calcified.

In summary, over the four taxa, consisting of representatives from Bivalvia, Gastropoda, Brachiopoda and Echinoidea, there was a general poleward decrease in total animal inorganic content and shell mass, except for the Arctic buccinid gastropods. The Arctic buccinids exist in warmer water than may be expected for their latitude (i.e. sub-Arctic) because the Gulf Stream raises temperatures in the North Atlantic. When total animal inorganic content is plotted with temperature (Figure 3.24) it is possible to see that this

poleward decrease in inorganic content is directly linked to the planetary temperature gradient of shallow water marine habitats rather than latitude *per se*.

Shell thickness

How well an animal's soft tissues are protected from abiotic and biotic factors is often a function of shell thickness. Resistance to breakage generally increases as the square of shell wall thickness (Vermeij, 1993), thus providing a good return in shell strength for each unit of shell wall thickening, as on this criterion resistance to breaking doubles for a 41 % increase in thickness.

In buccinid gastropods, shell thickness decreased towards the poles. This gradient was even more apparent when shell thickness was corrected for animal size. The decrease in shell thickness suggests a corresponding decrease in resistance to breakage. The latitudinal gradient in shell thickness found in this study for buccinids agrees with findings for gastropods by Graus (1974). Samples taken from each species suggest adult size in buccinids increases with increasing latitude. The attainment of a large size can provide a refuge from predation (Vermeij, 1978), although the requirement for a thick shell early on in life may preclude the attainment of large size in the tropical buccinids. However, large size is not impossible to attain in the tropics in gastropods as such, since many other tropical gastropods can grow to large sizes, and indeed the biggest gastropods and bivalves all are tropical.

As expected, regression equations show *Laternula* clams increased in shell thickness with increasing size. The pattern of mean shell thickness with latitude was very different in the *Laternula* clams compared to the gastropods. The Antarctic clam *L. elliptica* is by far the largest of all *Laternula* clams and consequently had the thickest shell; 2 to 3 times thicker than the other *Laternula* clams studied. This contrasts to reports from Nicol (1964a; 1966; 1967; 1970) that cold-water polar bivalves are small with thin shells. The size of the Antarctic *Laternula* compared to its temperate and tropical counterparts showed that attaining a large size in cold polar waters is not impossible for bivalve molluscs, as it is the largest laternulid on record.

When bivalve data were corrected for length, *L. elliptica* still had the thickest shell. It is possible for a clam to have less inorganic content and less shell but still have one of the thickest shells because of the amount of soft tissues that the shell covers; *L. elliptica* has a large siphon relative to its body. There was no clear latitudinal trend in mean shell thickness for size-corrected data and it is suggested that habitat may well be the driving force in shell thickness for these clams. Since they are infaunal, their shells are mostly protected from predation from above such as siphon cropping (nipping) (Chapter 7). Therefore it is unlikely that the non-lethal predation experienced is driving the evolution of shell thickness. Shell thickness could be linked to environmental factors such as substratum type or ice scour in polar regions. *L. elliptica* can be exhumed from the sediment by ice scour but can actively re-bury (Zamorano *et al.*, 1986; Peck *et al.*, 2004). Having a thick shell could provide protection during this process.

As expected, brachiopod raw data showed shell thickness increased with increasing shell length. There was no evidence of a difference in shell thickness between *Liothyrella neozelanica* and *L. uva*. Having a shell of similar thickness for a given size supports the findings that the total inorganic content of these two brachiopods was very similar.

Guidetti and Mori (2005) found differences in test robustness, attachment tenacity and spine length in two species of echinoid from the same location: the Mediterranean. However, test thickness was not significantly different between the two Mediterranean species. This study found differences in test thickness between closely-related echinoids from very different geographical locations. The temperate Echinidae echinoid *Psammechinus miliaris* had a test nearly 3 times as thick as the polar Echinidae echinoid *Sterechinus neumayeri*. Since the echinoids were very similar in size, this trend was true for both uncorrected and corrected data.

Summary

In this chapter, findings for buccinid gastropods agree with findings by Graus (1974) of a decrease in the amount of the calcium carbonate shell towards polar regions. Patterns in Echinidae echinoids also agree with these trends and support observations by Arnaud (1974). Latitudinal trends in inorganic content by percentage for *Liothyrella* brachiopods also agree with the proposed trends; however, brachiopod inorganic mass and shell thickness patterns are not so clear. For the *Laternula* clams, the trends in inorganic content and, to an extent, the trends in shell mass agree with the decrease of shell size towards the poles reported by Nicol (1964a; 1966; 1970). However, the trends in *Laternula* shell thickness show the polar clam has the thickest shell even when corrected for its large size. Clearly the trends in shell morphology vary among these groups of animals and cannot be immediately explained by an obvious single driving factor such as predation or the cost of shell production. The following chapters will explore these driving factors in shell and skeleton size and thickness and consider how the controlling factors for each group may differ and interact with each other.

Hypothesis accepted

There is sufficient evidence to reject the null hypothesis and accept the alternative hypothesis that total animal calcification decreases with increasing latitude for all groups studied, and shell thickness decreases with increasing latitude for Buccinidae gastropods and Echinidae echinoids, but not for *Laternula* clams or *Liothyrella* brachiopods.

Chapter 4: Shell chemistry - elemental content of calcium carbonate shells and skeletons



Chapter 4: Shell chemistry - elemental content of calcium carbonate shells and skeletons

4.1 Introduction

This chapter investigates the shell structure, including shell mineralogy and layering, and the shell chemistry of key species. Shell chemistry here refers to the elemental composition and content of shells.

Shell mineralogy

There are six calcium carbonate (CaCO_3) minerals with the same principal composition but different crystal structure: calcite, aragonite, vaterite, calcium carbonate monohydrate, calcium carbonate hexahydrate and amorphous calcium carbonate. Calcite and aragonite are the two most thermodynamically stable CaCO_3 minerals (crystal polymorphs) and are deposited extensively as biominerals (Mann, 2001). For example, most molluscan shells contain calcite and aragonite, shells of articulated brachiopods are calcite and echinoderm endoskeleton is made from magnesian calcite (high magnesium calcite).

Organic biopolymers such as the insect cuticle are tough but energetically costly, and soft and pliable if squeezed by a predator. In contrast, inorganic minerals are cheap, hard and stiff, but brittle. The solution employed by a vast array of organisms is the biocomposite skeleton, an inorganic-organic hybrid material, made of a lightweight organic frame filled with inorganic CaCO_3 (Mann, 2001). An example of the strength of biocomposite materials is nacre (mother-of-pearl) which, because of its protein-polysaccharide organic matrix, is 3000 times stronger than non-biogenic aragonite (Mann, 2001). Additionally, organic matrix facilitates crystallisation of CaCO_3 by providing a surface to seed (nucleate) crystals, reducing the activation energy of crystallisation, and holding crystals together (Lowenstam & Weiner, 1989; Wheeler & Sikes, 1989).

Many shells, such as those of gastropods are composed of an inner nacreous layer, a middle lamellate layer and an outer prismatic (or palisade) layer (Mann, 2001). A thin organic

periostracum covers the outer prismatic layer (Brusca & Brusca, 2003). During shell formation, the switching between calcium carbonate polymorphs is controlled by the outer epithelium; a layer of closely packed cells (Mann, 2001). The shell microstructure and arrangement of shell layers is under strong genetic control in molluscs and is mostly independent of the environment (Carter, 1980b). However, exceptions to this generalisation exist such as the addition of a calcite layer in the cooler-water representatives of predominantly aragonitic species (Taylor & Reid, 1990) and the dissolution of the shell under long periods of anaerobic respiration (Lutz & Rhoads, 1980).

Shell chemistry

Although shells are composed primarily of CaCO_3 , minor and trace elements are detectable in shells because they either:

- 1) are bound to conchiolin (conchin) or exist in pigments (e.g. S),
- 2) are substituted for Ca or C (e.g. B), or
- 3) have been adsorbed onto the shell surface (e.g. Pb) (Rosenberg, 1980).

Elements can substitute for Ca in the CaCO_3 lattice and this is particularly true for Group 2 elements (e.g. Mg, Sr and Ba) on the periodic table. These substituting elements are present as minor and trace constituents of the shell. Mg is 3 times more abundant by weight in seawater than Ca (Goldberg, 1957) and energy is required to expel Mg^{2+} from the extrapallial fluid (EPF) to prevent incorporation into the shell. The ionic radius of Mg^{2+} is smaller than that of Ca^{2+} and since there is less space in the calcite lattice, Mg^{2+} substitutes for Ca^{2+} more readily in the calcite lattice than in the aragonite lattice (Rosenberg, 1980). Thus biological calcites can contain Mg^{2+} ions up to levels of 30 mol % (Mann, 2001). The ionic radius of Sr^{2+} is larger than that of Ca^{2+} so in biogenic minerals Sr^{2+} should be more abundant in the aragonite lattice than in the calcite lattice. However, Sr concentration in molluscan aragonite and calcite are similar. Unlike Mg, Sr tends not to be controlled by skeletal mineralogy (Rosenberg, 1980). Thus the biological control on Sr may be greater than the control on Mg (Harriss, 1965).

Theoretically, less Sr enters calcite and aragonite lattices with increasing temperature (Lowenstam & Weiner, 1989) because the distribution coefficients (the tendency of an

element to be incorporated into a crystal lattice from solution) for Sr decrease linearly with temperature (Kinsman, 1969; Kinsman & Holland, 1969). Conversely, Mg contents of non-biogeneous calcites increase with increasing temperature (Füchtbauer & Hardie, 1976), although genetically controlled biochemical screening filters the temperature effect in some organisms so that the trend is suppressed or even reversed (Pilkey & Goodell, 1963; Lowenstam, 1964a).

In foraminifera, Mg:Ca ratios increase with increasing temperature (e.g. Nürnberg et al., 1996; Rosenthal et al., 1997). Lea et al. (1999) found that temperature is the primary control of Mg:Ca in the shells of the planktonic foraminifera *Globigerina bulloides* and *Orbulina universa*, but Sr:Ca responds far more weakly to one particular environmental parameter, with high temperature, salinity and pH all appearing to increase shell Sr. In fish otoliths, Ca, Sr and K (Hoff & Fuiman, 1995) and Sr:Ca (Townsend et al., 1995) are correlated with temperature. In otoliths Mg:Ca ratios are not affected by temperature or salinity (Martin & Thorrold, 2005), but Ba (Martin & Thorrold, 2005) and Na (Hoff & Fuiman, 1995) are influenced by salinity. These trends are not true for all fish species.

Research into the effects of temperature on Mg and Sr concentration in mollusc shells has led to uncertain conclusions (Rosenberg, 1980). Clarke and Wheeler (1922) found tendencies for a positive correlation between Mg concentration and temperature, but noted that there were “probable exceptions” to this trend. Dodd (1965) found with increasing temperature, Sr increased in outer calcitic layers of *Mytilus* but decreased in the aragonite nacre layer. Other workers have found Mg:Ca (Gunatilaka, 1975) and Sr:Ca (Thompson & Chow, 1955) in bivalves shells to be independent of temperature. Correlations of Mg and Sr with temperature are likely to be affected by seasonal change rather than temperature change alone (Rosenberg, 1980).

Since Group 2 elements are of a different size to Ca (Mg is smaller and Sr and Ba are larger), their presence in the lattice weakens its mechanical strength. To exclude these elements from the EPF during shell and skeleton formation, energy must be expended. In environments where more energy is required to take $\text{Ca}^{2+}_{(\text{aq})}$ ions out of solution and incorporate them into the lattice (such as at cold temperatures), greater substitution of these

other Group 2 elements could be expected to occur beyond temperature and salinity trends. Lower energy budgets at cold temperatures may make these cost-related substitutions more apparent.

4.1.1 Aims and hypotheses

Aims: To investigate shell mineralogy for key study species and to investigate a potential latitudinal cline in skeletal composition in marine invertebrates.

Hypothesis 1: Substitution of minor elements occurs in shells.

H₀: There is no evidence of substitution.

Hypothesis 2: Substitutions of minor elements vary 1) within species, and/or 2) among species from different geographic locations.

H₀: Substitution occurs evenly.

Hypothesis 3: Shell elemental composition varies with latitude and specifically, the absolute content and/or ratios of elements (Ca or minor) changes among species with latitude.

H₀: There is no change in shell composition with latitude.

4.2 Methods

4.2.1 Preparation of sample material

Study sites and species are described in Chapter 2. Morphological measurements were recorded according to methods described in Chapter 3. Skeletal material (shells, valves and test material) of study species were cleaned and allowed to dry naturally in air at room temperature. Once dry, the skeletal material was either 1) fractured for determination of shell crystal layer structure (shells were snapped by hand), or 2) sectioned with a thin circular diamond tip saw blade for determination of shell elemental composition.

4.2.2 Determination of shell crystal layer structure

Crystal layers within the shell were determined using SEM imaging. Fractured shell material was super-glued onto stainless steel stubs, left to dry and then gold coated 3 times from different angles. Stubs were imaged on a JEOL JSM-5410LV scanning electron microscope (SEM) using secondary electrons. The appearance of crystal structures under the SEM is well documented (e.g. Carter, 1980a). The crystal structure and often the calcium carbonate polymorph can thus be identified by imaging alone without using X-ray diffraction (XRD).

4.2.3 Determination of shell elemental composition

Diagrams showing the areas of shell sectioned for the analysis of elemental content are shown in the methods section of Chapter 3. These were the same parts of the shell measured for thickness. Bivalve and brachiopod shells were sectioned in half along the axis of growth (perpendicular to growth lines). Gastropod shells were sectioned as shown or ground (using a diamond coated grinder wheel) to the axial plane and then sectioned perpendicular to the edge of the last whorl. The skeleton sections were set in epoxy resin (Epofix resin, Struers) with a mix of 3g hardener to 25 g resin, placed in a vacuum at room temperature and then left to harden on a warm plate at *c.* 25 – 35 °C. Once set, the resin

was polished using a series of graded diamond-coated sanding papers, cleaned with ethanol and carbon coated (Figure 4.1).

Skeleton sections were then analysed using a scanning electron microscope (SEM) with X-ray microanalysis to measure any variation in the proportion of calcium and minor elements within and among species. The techniques used were SEM energy dispersive spectrometry (EDS) and wavelength dispersive spectrometry (WDS). EDS and WDS allow the quantitative analysis of elemental content by weight percent in solid materials. These techniques provided both qualitative (elemental composition) and quantitative (elemental content by weight percent) data on shell elemental chemistry. WDS is able to detect elements present at lower concentrations than EDS and so WDS was used predominantly in this study. Skeleton sections then were analysed using a JEOL JXA-8200 superprobe WD/ED combined microanalyzer electron microscope for wavelength dispersive spectrometry (WDS) and a Leo 1450 VP (variable pressure) SEM with a PGT microanalysis energy dispersive system for energy dispersive spectrometry (EDS).

The SEM EDS and WDS were calibrated with standards blocks for each element analysed prior to sample examination. For EDS, area measurements provided less variable results than spot measurements. For WDS a 5 µm probe diameter was used. Initially qualitative analysis was used to determine which elements were present in shells. The elements that were present within the limits of detection of the EDS and WDS then were analysed quantitatively. Elements Ca, Sr, Mg, Na, S, Ba, Al were analysed with EDS on some species. Elements analysed with WDS were Ca, Sr, Mg, Na, S, Si. Fewer elements were analysed with WDS because elements that continually appeared in shells (within detection limits) were chosen and analysed with greater precision. Analysing more elements would have taken more time, or reduced precision, thus reducing the quality or amount of data. Elements such as Ba do substitute for Ca in the CaCO₃ lattice; however, Ba content was below the detection limits of WDS. Ba also is likely to be below the reliable detection limits of EDS, so Ba data should be treated with caution.

For bivalves, the mid-section of the shell had been previously determined as the least variable region in terms of elemental content from a pilot study (Conway & Peck,

unpublished data). Mid-sections of shells were analysed in this study. Any variation found within a shell was less than variation between shells. For each section of shell 3 to 5 points were analysed along the mid-section (Figure 4.2). This was enough to obtain data with low variability for points analysed with a shell. For some trial shells, outer, middle and inner crystal layers also were analysed.

For quantitative analysis of elemental content of shells and skeletons, SEM EDS and WDS requires that the area of shell analysed (a circle of a minimum size of around 5 μm in diameter) is non-porous. A porous structure with air spaces or spaces filled with resin from the block-making process will produce inaccurate readings on the EDS and WDS.

Attempts were made to analyse the elemental content of echinoids. Some data were obtained for *Sterechinus neumayeri* using EDS. However, the echinoid test was generally too porous for WDS (Figure 4.26) as the beam was unable to isolate purely echinoid test without encountering some resin as well.

4.2.4 Precision errors and limits of detection

Detection limits for elements using EDS and WDS are shown in Table 4.1. WDS has a detectability limit approximately an order of magnitude lower than EDS. Table 4.2 shows the precision errors for WDS. Note the errors reported for WDS and EDS were in different forms. Using WDS, the errors associated with Mg and Si for the bivalves and gastropods were high. The error associated with S was quite high.

Precision data were reported for EDS analysis at the $\pm 95\%$ confidence interval for Ca and Na. For Sr, Ba, S, Al and Mg, elemental detection peaks were low, so precision data were not accurately generated by EDS. However, where peaks were present for those elements, the data were included based on the detection limit of each element given in Table 4.1.

Table 4.1 Detection limits for elements using EDS and WDS (taken from Goldstein *et al.* (2003)).

Analysis	Element	Detection limit (CDL) (wt %)
EDS	Na	0.195
	Mg	0.102
	Al	0.069
	Si	0.072
	Ca	0.085
WDS	Na	0.021
	Mg	0.012
	Al	0.008
	Si	0.009
	Ca	0.009

Table 4.2 WDS median counting error (%) of X-ray intensities for each group.

	Na	Ca	Sr	S	Mg	Si
<i>Laternula</i>	3.14	0.26	7.23	16.715	26.43	37.76
Buccinids	3.17	0.26	9.78	16.195	42.845	79.48
Brachiopods	5.155	0.26	10.065	7.855	3.15	3.91

4.2.5 Elemental distribution maps

SEM WDS maps were created by running the WDS overnight. These maps show differences in the elemental content over a shell surface. They can show patterns in the distribution of elements below the detection limits of the WDS, due to the accumulation of large volumes of data. Elemental distribution maps were obtained opportunistically, because of financial constraints.

4.2.6 X-ray diffraction (XRD)

X-ray diffraction (XRD) was conducted by E. Harper at the University of Cambridge on *Neobuccinum eatoni* shell samples using a Bruker 8 diffractometer.

4.2.7 Statistical analysis

Data were compiled on spreadsheets using MS Excel 2003. Statistical analyses were performed in SPSS 16.0, SigmaPlot 10.0 and R 2.7.1 and included general linear models including regression analysis, analysis of variance (ANOVA) and Kruskal-Wallis ANOVA on ranks, and Pearson product moment correlation. Graphs were produced with SigmaPlot 10.0.



Figure 4.1 Resin block with shell sections embedded inside. This block had been polished and was ready for carbon coating.

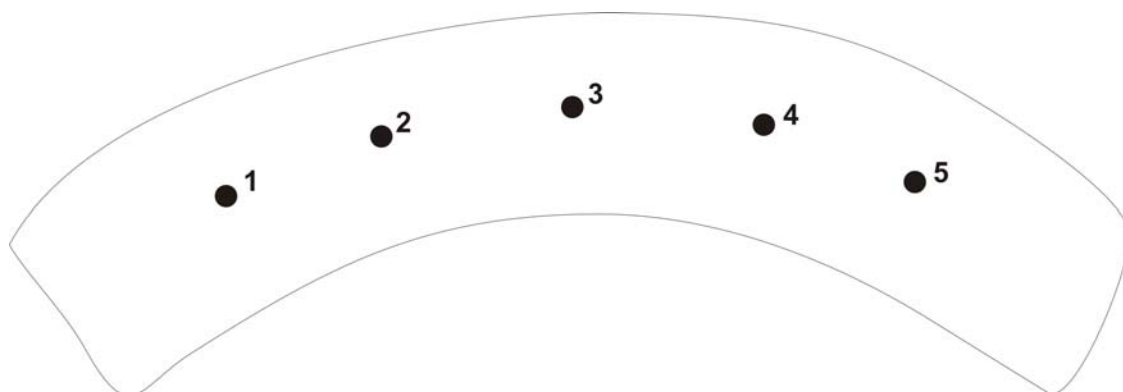


Figure 4.2 Positions of analysis on the shell section (points 1 to 5 were clustered around the mid-section of the shell).

4.3 Results

4.3.1 Shell crystal layer structure

Figure 4.3 to Figure 4.18 show typical shell microstructures for the study species with shell layers labelled. Table 4.3 summarises shell crystal composition.

Table 4.3 Shell crystal layer composition (CaCO₃ polymorph).

Taxa	Shell composition
<i>Laternula</i> clams	Aragonite (nacre and prisms)
Gastropod snails	Predominantly aragonite (cross lamellar and CCL) XRD data show <i>Neobuccinum eatoni</i> is entirely aragonite
Articulated brachiopods	Calcite

The *Laternula* shell is entirely aragonitic (E. Harper, pers. comm.). All species of *Laternula* showed the same pattern of layers within the shell; aragonite prisms were sandwiched between layers of aragonite nacre (Figure 4.3 to Figure 4.7). *Laternula* shells contain a pallial line running through the shell section composed of aragonite prisms. The periostracum is very thin on *Laternula* shells and in most cases could not be seen.

In gastropod shell sections (Figure 4.8 to Figure 4.15), the complex cross lamellar structure is labelled CCL. Gastropods of the family Buccinidae (superfamily Buccinoidea) had a 2 or 3 layer shell composed of complex cross lamellar aragonite and cross lamellar aragonite. XRD on the Antarctic buccinid *Neobuccinum eatoni* showed the shell is composed purely of aragonite with no calcite present. The gastropod *Thais orbita* is not in the family Buccinidae (or the superfamily Buccinoidea) but has a very similar shell layer structure.

Figure 4.16 to Figure 4.18 show shell sections of articulated brachiopods. These brachiopods have a calcite shell and close ups of calcite crystals in the shell of *Liothyrella uva* can be seen in cross section in Figure 4.22. Figure 4.19 to Figure 4.22 show details of close-up shell crystal structure.

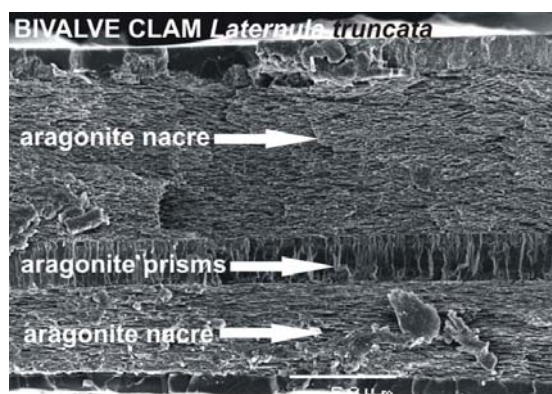


Figure 4.3 Shell section of *Laternula truncata* showing crystal structure.

Scale bar is 50 µm.

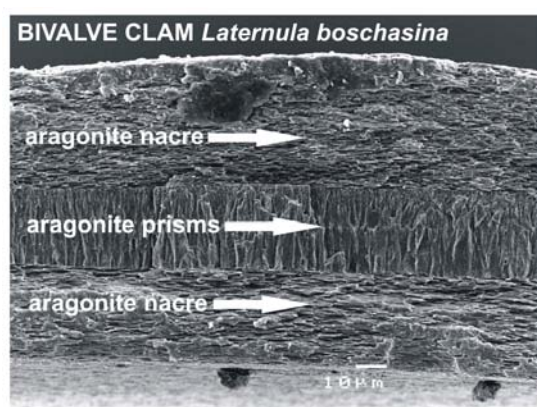


Figure 4.4 Shell section of *Laternula boschasina* showing crystal structure.

Scale bar is 10 µm.

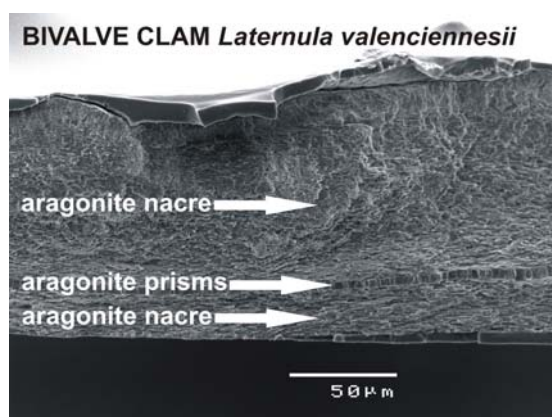


Figure 4.5 Shell section of *Laternula valenciennesii* showing crystal structure.

Scale bar is 50 µm.

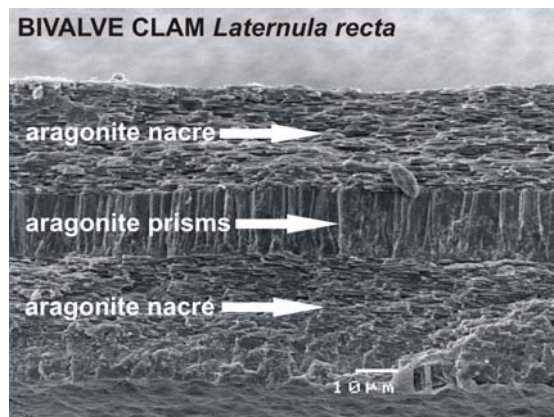


Figure 4.6 Shell section of *Laternula recta* showing crystal structure. Scale bar is 10 μm.

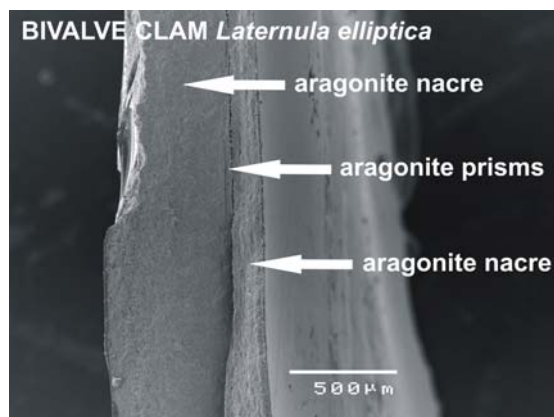


Figure 4.7 Shell section of *Laternula elliptica* showing crystal structure. Scale bar is 500 μm. Problems with gold coating on the *L. elliptica* sections meant that a clear section was more difficult to photograph compared to the other *Laternula* species and so this image was taken at 90° to other images. Here it is still possible to make out the shell layers, although not as clearly as on the other species of *Laternula* shell sections.

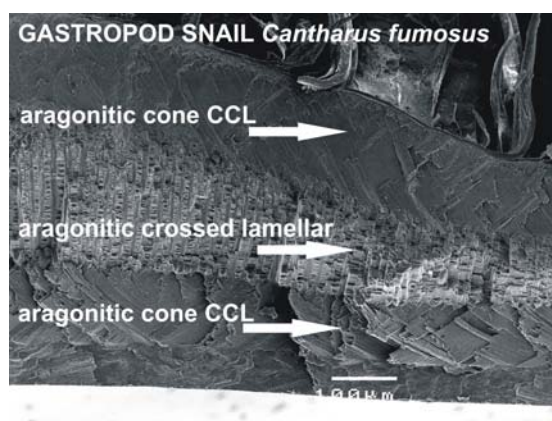


Figure 4.8 Shell section of *Cantharus fumosus* showing crystal structure.
Scale bar is 100 μm.

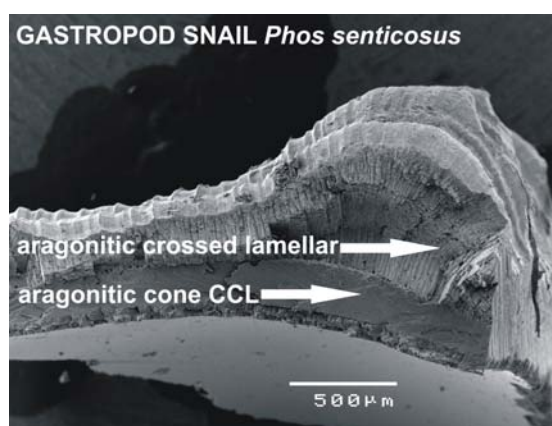


Figure 4.9 Shell section of *Phos senticosus* showing crystal structure.
Scale bar is 500 μm.

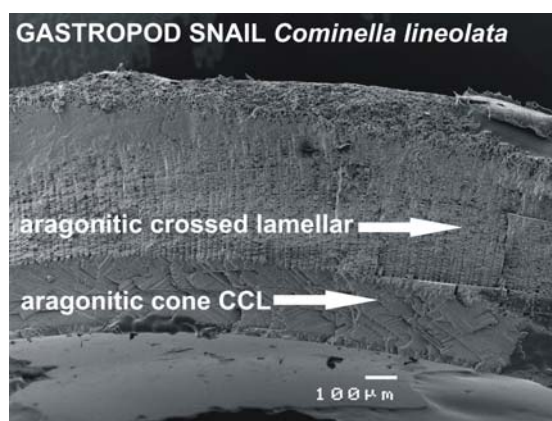


Figure 4.10 Shell section of *Cominella lineolata* showing crystal structure.
Scale bar is 100 μm.

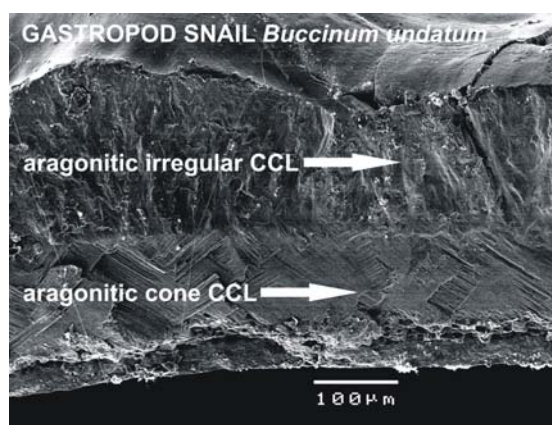


Figure 4.11 Shell section of *Buccinum undatum* showing crystal structure.
Scale bar is 100 μm.

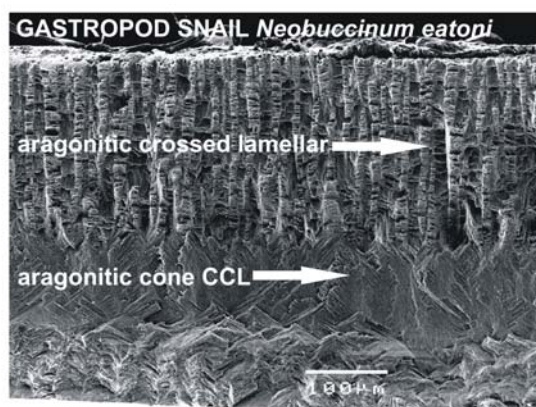


Figure 4.12 Shell section of *Neobuccinum eatoni* showing crystal structure.
Scale bar is 100 μm.

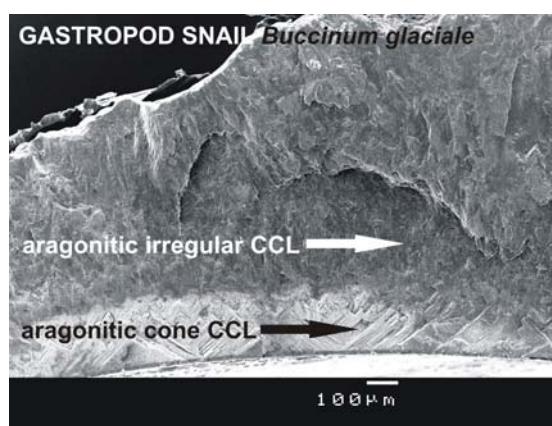


Figure 4.13 Shell section of *Buccinum glaciale* showing crystal structure.
Scale bar is 100 μm.

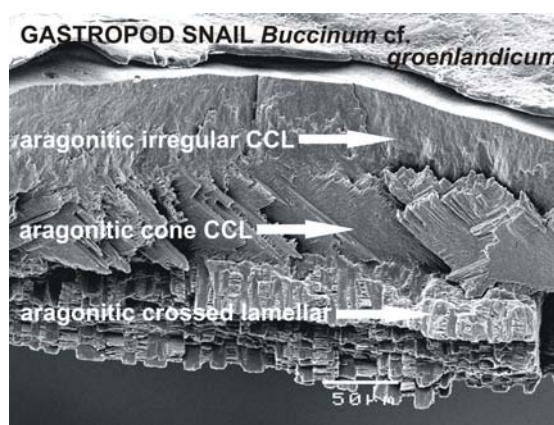


Figure 4.14 Shell section of *Buccinum cf. groenlandicum* showing crystal structure. Scale bar is 50 µm.

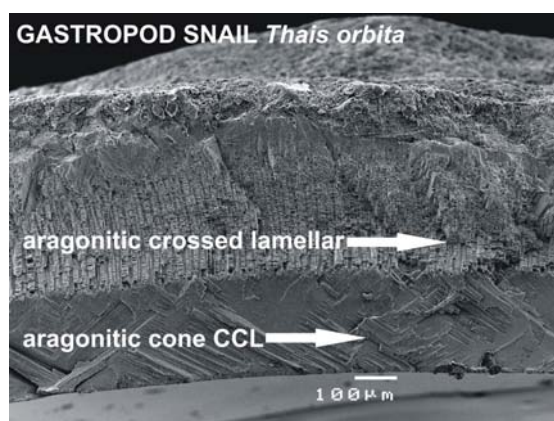


Figure 4.15 Shell section of *Thais orbita* showing crystal structure. Scale bar is 100 µm.

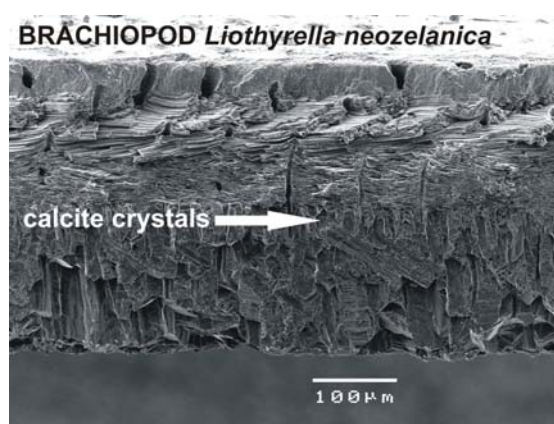


Figure 4.16 Shell section of the brachiopod *Liothyrella neozelanica* showing crystal structure. Scale bar is 100 µm.

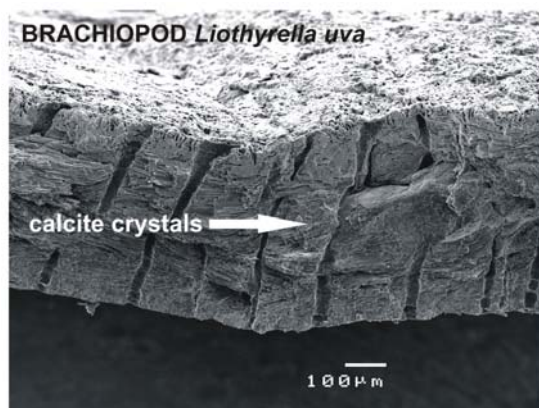


Figure 4.17 Shell section of the brachiopod *Liothyrella uva* showing crystal structure. Scale bar is 100 μm.

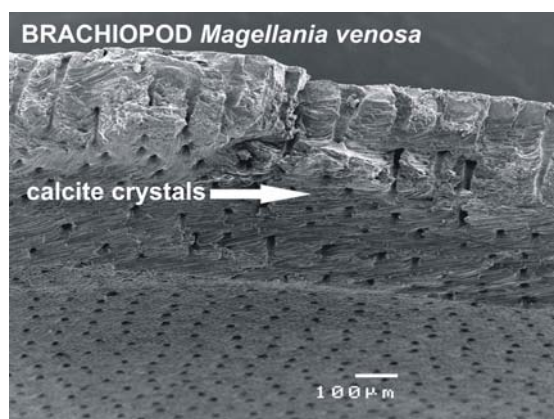


Figure 4.18 Shell section of the brachiopod *Magellania venosa* showing crystal structure. Scale bar is 100 μm.

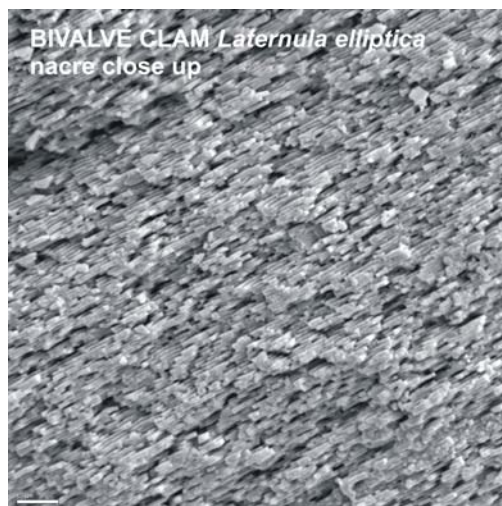
Close up images of crystal structure

Figure 4.19 Aragonitic sheet nacreous layer of the bivalve *Laternula elliptica* close up. Scale bar is 5 μm .

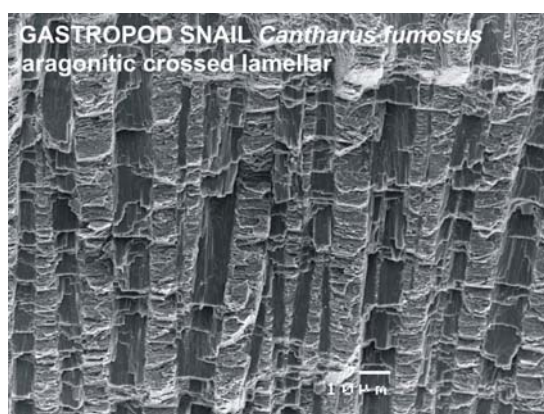


Figure 4.20 Aragonitic crossed lamellar layer of the gastropod *Cantharus fumosus*. Scale bar is 10 μm .

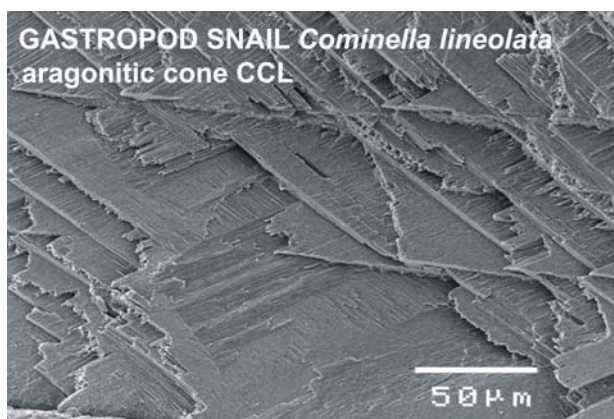


Figure 4.21 Aragonitic cone complex cross lamellar (CCL) of the gastropod *Cominella lineolata*. Scale bar is 50 μm.

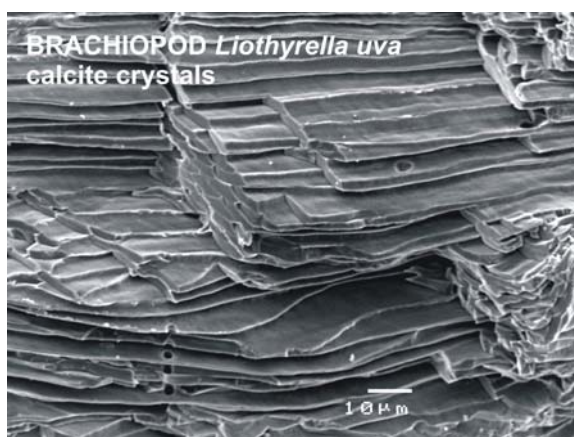


Figure 4.22 Calcite crystals of the brachiopod *Liothyrella uva*. Scale bar is 10 μm.

4.3.2 Shell elemental composition

Data from quantitative analyses of shell elemental content are expressed as mass or weight percent (wt %). That is the weight of the element as a percentage of the weight of all elements in the shell. Photographs taken on the SEM provide examples of where points of analysis during EDS and WDS were located (Figure 4.23 to Figure 4.25).

For *Laternula* clams, SEM EDS and WDS initial analyses evaluated elements in the aragonite nacre layers and the pallial line aragonite prism layer. Elemental content analysed on the pallial line of *Laternula* clams ('pallial data') was different to results from the aragonite nacre layer. These pallial data were few and often drove significant correlations by their different nature. Intra-specific and inter-specific *Laternula* data have been analysed with and without including these pallial data. Comparative analyses among *Laternula* species were conducted using data only from the aragonite nacre layers.

For gastropods, EDS and WDS analyses were made in the aragonitic cone complex cross lamella (CCL) layer as it was less porous and therefore better for EDS and WDS analysis than the other layers.

For brachiopods, EDS and WDS analyses were conducted in the middle of the calcite crystal layer. This area was least porous. Brachiopod valves showed light and dark banding within the cross-section of the shell under backscatter electrons on the SEM, particularly in *Liothyrella uva*. Light and dark areas were analysed. Dark areas were found to contain up to 0.5 – 1.5 wt % more Mg than light areas. Mg substitutes for Ca in the dark areas and since Mg is lighter than Ca, this is why these areas appear dark with backscatter electrons². Darker bands also had a higher Sr content by 0.02 wt % (which was less than the differences in Mg). These dark high Mg and high Sr bands in brachiopods were not included in the main analysis which analysed areas of 'normal shell' of 'mid-grey' tone on the brachiopod shell across all species to standardise the results.

² The greater the density of the substance under backscatter electrons, the more electrons are scattered back and the lighter the area appears.

Table 4.4 Differences in elemental content among normal shell and light and dark band areas in shells of *Liothyrella uva* from Rothera, Antarctica.

	Na	Ca	Sr	S	Mg	Si
Normal shell	0.299	39.975	0.137	0.158	0.495	0.189
Light bands	0.275	40.082	0.121	0.200	0.555	0.304
Dark bands	0.351	38.751	0.164	0.250	1.320	1.207

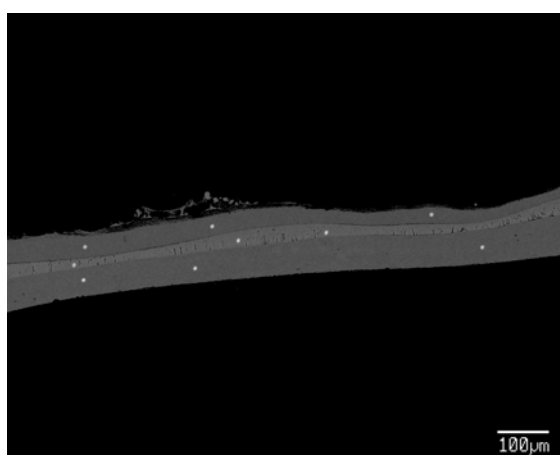


Figure 4.23 Bivalve *Laternula truncata* shell showing points of WDS analysis (white dots) on the shell section surface. For this shell all layers were analysed.

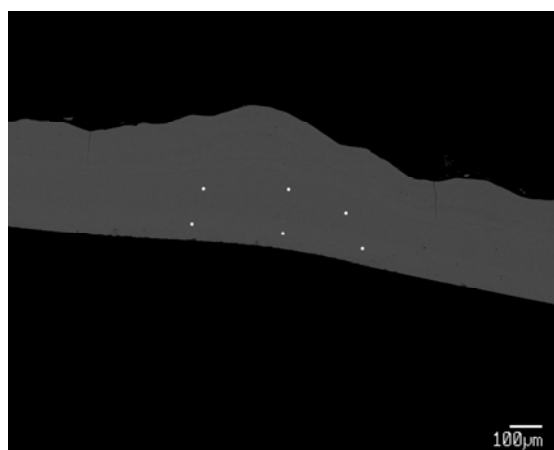


Figure 4.24 Gastropod *Buccinum undatum* shell showing points of WDS analysis (white dots) on the shell section surface. For this shell the cross lamellar aragonite and the CCL were analysed.

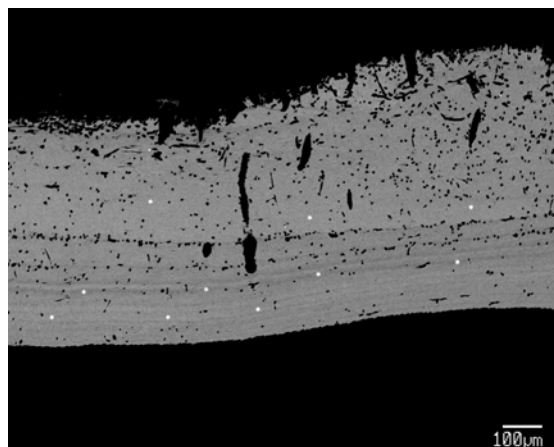


Figure 4.25 Brachiopod *Liothyrella uva* shell showing points of WDS analysis (white dots) on the shell section surface. For this shell dark and light lines were also analysed. Darker grey lines were analysed for this species (middle row of white dots) and found to be high in Sr.

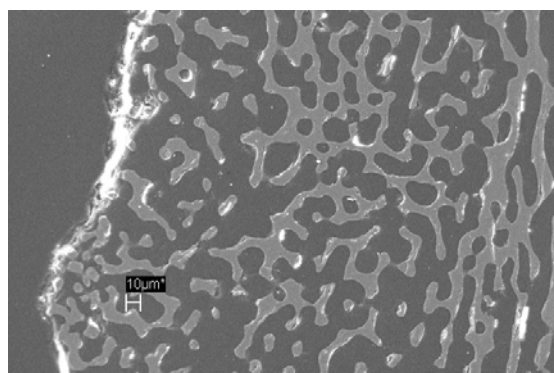


Figure 4.26 Image of the echinoid *Sterechinus neumayeri* test showing its porosity.

4.3.2.1 Substitution of minor elements for Ca in shell

Shells and skeletons were analysed by WDS and/or EDS techniques (Table 4.5).

Quantitative analysis of elemental content allowed the investigation of substitutions of these minor elements (particularly Group 2 elements e.g. Mg and Sr) for Ca by correlation analysis. EDS techniques are slightly different to WDS techniques and equipment for each technique was therefore calibrated with different standards and analysis was conducted at different institutions at different times. Unfortunately this means it is difficult to compare directly EDS and WDS data so results are described separately.

Table 4.5 Shells and skeletons of species analysed with WDS and/or EDS.

Species	EDS (2006)	WDS (2007-2008)
Bivalves		
<i>Laternula truncata</i>	No	Yes
<i>Laternula boschasina</i>	No	Yes
<i>Laternula valenciennesii</i>	No	Yes
<i>Laternula recta</i>	No	Yes
<i>Laternula elliptica</i>	Yes	Yes
<i>Yoldia eightsi</i>	Yes	No
Gastropods		
<i>Cantharus fumosus</i>	No	Yes
<i>Phos senticosus</i>	No	Yes
<i>Cominella lineolata</i>	No	Yes
<i>Buccinum undatum</i>	Yes	Yes
<i>Neobuccinum eatoni</i>	No	Yes
<i>Buccinum glaciale</i>	No	Yes
<i>Buccinum cf. groenlandicum</i>	No	Yes
Brachiopods		
<i>Liothyrella neozelanica</i>	Yes	Yes
<i>Liothyrella uva</i>	Yes	Yes
<i>Magellania venosa</i>	No	Yes
<i>Magellania fragilis</i>	Yes	No
<i>Terebratulina retusa</i>	Yes	No
Echinoid		
<i>Sterechinus neumayeri</i>	Yes	No

4.3.2.1.1 **Inter-specific substitution of minor elements (WDS data)**

WDS data from all species within each broad taxonomic group (i.e. bivalves, gastropods and brachiopods) were pooled. There were significant inter-specific substitutions of elements within shells of bivalves, gastropods and brachiopods (Table 4.6 to Table 4.8). Substitution was assessed by correlation. Negative correlation coefficients suggest the substitution or partitioning of elements. Correlations were conducted for all elements analysed, but the substitutions between Ca and the other, minor, elements are considered most important.

When conducting multiple comparisons Type I (α) errors (i.e. rejecting the null hypothesis (H_0) when H_0 is true) increase. For the 15 multiple comparisons among elements for each broad taxonomic group, with a significance at the 5 % level (i.e. $p < 0.05$) on average there will be $15 \times 0.05 = 0.75$ (i.e. less than 1) Type I errors. The Bonferroni correction can be used to correct these Type I errors and $15/0.05 = 0.00333$, or 0.333 % would be the new significance level. However, this method is controversial because it increases Type II errors (β) (i.e. failing to reject H_0 when H_0 is false) and has other weaknesses (see Perneger, 1998; Garcia, 2004; Nakagawa, 2004; Garamszegi, 2006). Correcting for multiple comparisons should ideally control for both Type I and Type II error rates (Field, 2009). Other post hoc procedures are available and one option when considering the grids of correlation statistics presented here is to correct by 4 so that $0.05/4 = 0.0125$. Thus for these correlation analyses, $p < 0.0125$ denotes a significant test.

In inter-specific analyses, species of *Laternula* substituted Sr for Ca; buccinid gastropods substituted Sr and S for Ca; and brachiopods substituted Mg and Si for Ca. There were also positive and negative correlations among other elements (Table 4.6 to Table 4.8). Figure 4.27 shows inter-specific substitution of Sr for Ca in *Laternula* species. Using a general linear model, Sr and Ca data for *Laternula* species were best modelled by trend lines of the same slope with different intercepts. This model gives the lowest AIC value of -685.77.

Table 4.6 WDS data. Pearson product moment correlation statistics for elements for all *Laternula* clam species combined (*L. truncata*, *L. boschasina*, *L. valenciennesii*, *L. recta*, *L. elliptica*). Cell contents are correlation coefficient (r), probability value (p) and number of samples (n). *Denotes p values that are significant at the $p < 0.0125$ level.

All <i>Laternula</i> species (pallial data not included)						
		Sr	S	Mg	Si	Na
Ca	r	-0.215	-0.136	-0.118	-8.30E-02	-0.182
	p	0.0061*	0.0854	0.25	0.501	0.021
	n	161	161	97	68	161
Sr	r		3.44E-01	0.409	-0.238	-4.40E-01
	p		<0.0001*	<0.0001*	0.0505	<0.0001*
	n		161	97	68	161
S	r			0.105	1.40E-01	4.30E-02
	p			0.307	0.255	0.588
	n			97	68	161
Mg	r				-0.414	-0.377
	p				0.307	0.0001*
	n				8	97
Si	r					-0.102
	p					0.408
	n					68

Table 4.7 WDS data. Pearson product moment correlation statistics for elements for all buccinid gastropod species combined (*Cantharus fumosus*, *Phos senticosus*, *Cominella lineolata*, *Buccinum undatum*, *Neobuccinum eatoni*, *Buccinum* cf. *groenlandicum*, *Buccinum glaciale*). Cell contents are correlation coefficient (r), probability value (p) and number of samples (n). *Denotes p values that are significant at the $p < 0.0125$ level.

All buccinid species (all data)						
		Sr	S	Mg	Si	Na
Ca	r	-0.187	-0.294	-0.07	-0.0613	0.0792
	p	0.0071*	<0.0001*	0.382	0.648	0.257
	n	207	205	158	58	207
Sr	r		-0.202	0.432	0.285	-0.66
	p		0.0037*	<0.0001*	0.0301	<0.0001*
	n		205	158	58	207
S	r			-0.295	-0.0177	0.314
	p			0.0002*	0.895	<0.0001*
	n			156	58	205
Mg	r				-0.118	-0.581
	p				0.499	<0.0001*
	n				35	158
Si	r					-0.243
	p					0.0656
	n					58

Table 4.8 WDS data. Pearson product moment correlation statistics for elements for all brachiopod species combined (*Liothyrella neozelanica*, *L. uva* and *Magellania venosa*). Cell contents are correlation coefficient (r), probability value (p) and number of samples (n). *Denotes p values that are significant at the $p < 0.0125$ level.

All brachiopod species (all data)						
		Sr	S	Mg	Si	Na
Ca	r	-0.108	-0.0443	-0.755	-0.645	-0.0752
	p	0.227	0.619	<0.0001*	<0.0001*	0.399
	n	128	128	29	99	128
Sr	r		0.731	0.787	0.457	0.924
	p		<0.0001*	<0.0001*	<0.0001*	<0.0001*
	n		128	29	99	128
S	r			0.701	0.669	0.758
	p			<0.0001*	<0.0001*	<0.0001*
	n			29	99	128
Mg	r				--	0.675
	p				--	<0.0001*
	n				0	29
Si	r					0.462
	p					<0.0001*
	n					99

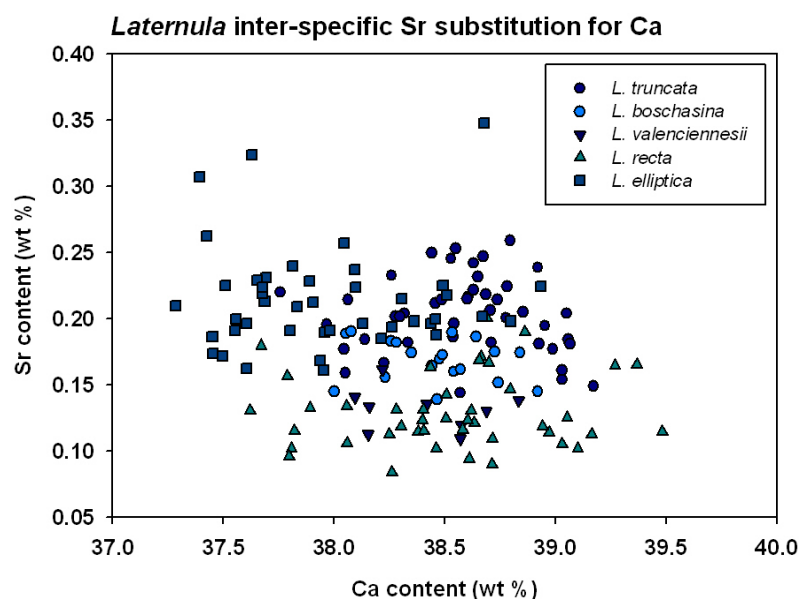


Figure 4.27 WDS data showing inter-specific Sr substitution for Ca in species of *Laternula*. There was a significant negative correlation for all *Laternula* species pooled (Pearson correlation coefficient $r = -0.215$, $p = 0.00612$, $n = 161$). There were no significant correlations for individual species. Taking mean values of Ca and Sr for each species, there was no significant correlation between Sr and Ca.

4.3.2.1.2 Intra-specific substitution of minor elements (WDS and EDS data)

Correlations were tested for minor elements (Sr, Mg, Na, S, Si) to determine if there were any substitutions for Ca within a species (Table 4.9 to Table 4.11). Full tables of all correlation statistics for each species are included in Appendix 1. Summaries of these data are described below.

WDS data

Bivalves: *Laternula* species

Laternula species analysed by WDS were *L. truncata*, *L. boschasina*, *L. valenciennesii*, *L. recta* and *L. elliptica*. Within the aragonite nacre layer (i.e. excluding pallial data) there were no significant correlations between Ca and any element in *Laternula* species analysed (Table 4.9). Since *Laternula* WDS data show for all species combined, *Laternula* clams substituted Sr and S for Ca inter-specifically, this could suggest that among species (and

latitudes) these substitutions are occurring, but substitutions for these elements are not occurring intra-specifically.

Gastropods: family Buccinidae

Buccinid gastropod species analysed by WDS were *Cantharus fumosus*, *Phos senticosus*, *Cominella lineolata*, *Buccinum undatum*, *Neobuccinum eatoni*, *Buccinum* cf. *groenlandicum* and *Buccinum glaciale*. The only buccinid species tested that showed intra-specific substitution was *Buccinum undatum* where Sr substituted for Ca (Table 4.10). *Buccinum undatum* and *Buccinum* cf. *groenlandicum* had positive correlations between Ca and Na. The pattern with Na was in contrast to the inter-specific substitutions (negative correlations) among species (and latitudes) between Ca and Sr and Ca and S. Figure 4.28 demonstrates significant intra-specific substitutions of minor elements in place of Ca in the CaCO_3 lattice. In the gastropod *Buccinum undatum*, Sr substituted for Ca. Mg may also substitute for Ca in shells; however, correlations with Mg were not significant for the buccinid species studied. A larger sample size may be needed to demonstrate any correlations with Mg. Na content was positively correlated with Ca (Figure 4.29).

Brachiopods

Brachiopods analysed by WDS were *Liothyrella neozelanica*, *L. uva* and *Magellania venosa*. *Liothyrella uva* was the only brachiopod that showed intra-specific substitution of minor elements for Ca. *L. uva* from Signy did not have significant minor element substitutions for Ca. *L. uva* from Rothera exhibited negative correlations of Sr and Mg for Ca (Table 4.11) suggesting that individuals of the same species at higher latitudes may exhibit additional substitutions within their shells. Significant negative correlations also were shown between Ca and Si, and Ca and Na in the Rothera population of *L. uva* suggesting substitution for these elements. However, Na and possibly Si are unlikely to substitute into the CaCO_3 lattice in place of Ca, so other factors may be affecting these elements.

Table 4.9 WDS data. Pearson product moment correlation statistics for Ca and minor elements for each *Laternula* species. Cell contents are correlation coefficient (r), probability value (p) and number of samples (n). *Denotes p values that are significant at the $p < 0.0125$ level.

		Sr	S	Mg	Si	Na
Bivalve: <i>Laternula truncata</i> including pallial data						
Ca	r	-0.0066	-0.0027	0.376	0.000	-0.475
	p	0.965	0.985	0.0091*	--	0.0007*
	n	47	47	47	1	47
Bivalve: <i>Laternula truncata</i> excluding pallial data.						
		Sr	S	Mg	Si	Na
Ca	r	-0.109	-0.161	0.0498	0.000	0.0814
	p	0.482	0.297	0.748	--	0.599
	n	44	44	44	1	44
Bivalve: <i>Laternula boschasina</i> (no pallial data were available for comparison)						
Ca	r	-0.223	0.296	--	0.250	-0.0576
	p	0.359	0.219	--	0.303	0.815
	n	19	19	0	19	19
Bivalve: <i>Laternula valenciennesii</i> (empty shells)						
Ca	r	-0.219	0.182	--	-0.463	-0.736
	p	0.572	0.640	--	0.209	0.0237
	n	9	9	0	9	9
Bivalve: <i>Laternula recta</i> including pallial data						
Ca	r	0.385	0.354	0.314	-0.384	-0.571
	p	0.0063*	0.0125	0.0299	0.616	<0.0001*
	n	49	49	48	4	49
Bivalve: <i>Laternula recta</i> excluding pallial data						
Ca	r	0.0843	-0.0065	-0.144	-0.410	-0.0792
	p	0.591	0.967	0.363	0.493	0.614
	n	43	43	42	5	43
Bivalve: <i>Laternula elliptica</i> (trends were no different with or without pallial data)						
Ca	r	-0.0292	-0.0247	-0.630	0.117	0.151
	p	0.847	0.871	0.0378	0.511	0.315
	n	46	46	11	34	46

Table 4.10 WDS data. Pearson product moment correlation statistics for Ca and minor elements for each buccinid species. Cell contents are correlation coefficient (r), probability value (p) and number of samples (n). *Denotes p values that are significant at the $p < 0.0125$ level.

		Sr	S	Mg	Si	Na
Gastropod: <i>Cantharus fumosus</i>						
Ca	r	-0.391	0.107	0.293	0.142	-0.152
	p	0.0588	0.619	0.209	0.909	0.480
	n	24	24	20	3	24
Gastropod: <i>Phos senticosus</i>						
Ca	r	0.353	0.0228	-0.283	--	-0.101
	p	0.0440	0.903	0.110	--	0.577
	n	33	31	33	0	33
Gastropod: <i>Cominella lineolata</i>						
Ca	r	-0.221	-0.0979	0.726	-0.218	-0.0696
	p	0.411	0.718	0.165	0.497	0.798
	n	16	16	5	12	16
Gastropod: <i>Buccinum undatum</i>						
Ca	r	-0.467	0.0760	-0.332	--	0.413
	p	0.0031*	0.650	0.0630	--	0.0100*
	n	38	38	32	0	38
Gastropod: <i>Neobuccium eatoni</i>						
Ca	r	0.0191	-0.233	0.341	0.0330	0.181
	p	0.901	0.123	0.0951	0.928	0.233
	n	45	45	25	10	45
Gastropod: <i>Buccinum cf. groenlandicum</i>						
Ca	r	-0.0998	0.360	0.401	0.568	0.447
	p	0.557	0.0284	0.251	0.0271	0.0055*
	n	37	37	10	15	37
Gastropod: <i>Buccinum glaciale</i>						
Ca	r	0.00866	0.514	--	-0.135	0.481
	p	0.977	0.0599	--	0.691	0.0818
	n	14	14	0	11	14

Table 4.11 WDS data. Pearson product moment correlation statistics for Ca and minor elements for each brachiopod species. Cell contents are correlation coefficient (r), probability value (p) and number of samples (n). *Denotes p values that are significant at the $p < 0.0125$ level.

		Sr	S	Mg	Si	Na
Brachiopod: <i>Liothyrella neozelanica</i>						
Ca	r	0.188	0.0931	--	0.0558	0.222
	p	0.271	0.589	--	0.746	0.193
	n	36	36	0	36	36
Brachiopod: <i>Liothyrella uva</i> from Signy						
Ca	r	-0.626	-0.325	--	-0.0980	-0.125
	p	0.0294	0.303	--	0.762	0.699
	n	12	12	12	12	12
Brachiopod: <i>Liothyrella uva</i> from Rothera						
Ca	r	-0.312	-0.268	-0.774	-0.787	-0.409
	p	0.0102*	0.0286	0.0004*	<0.0001*	0.0006*
	n	67	67	16	51	67
Brachiopod: <i>Magellania venosa</i>						
Ca	r	0.121	0.170	0.0309	--	0.391
	p	0.694	0.578	0.920	--	0.187
	n	13	13	13	0	13

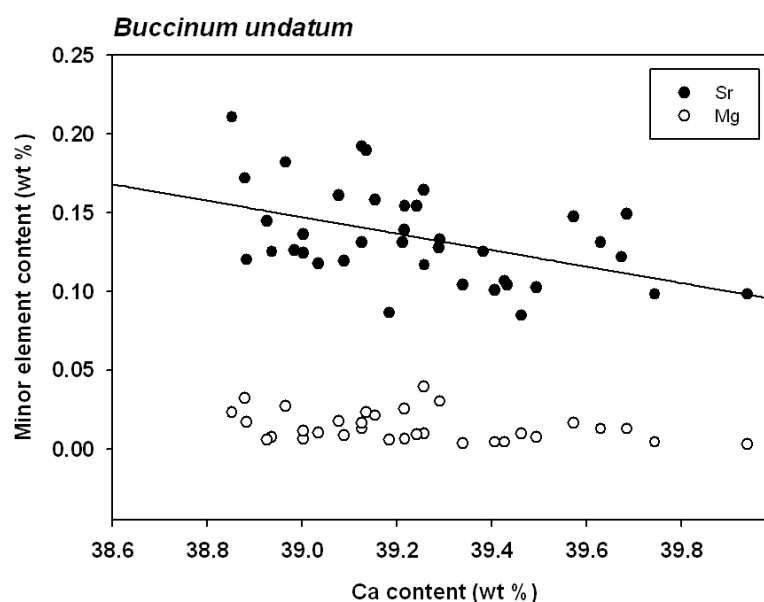


Figure 4.28 WDS data showing the substitution of Sr or Mg for Ca in the shell of *Buccinum undatum*. There was a significant negative correlation between Ca and Sr ($r = -0.467$, $p = 0.00314$, $n = 38$) but no significant correlation between Ca and Mg ($r = -0.332$, $p = 0.0630$ NS, $n = 32$).

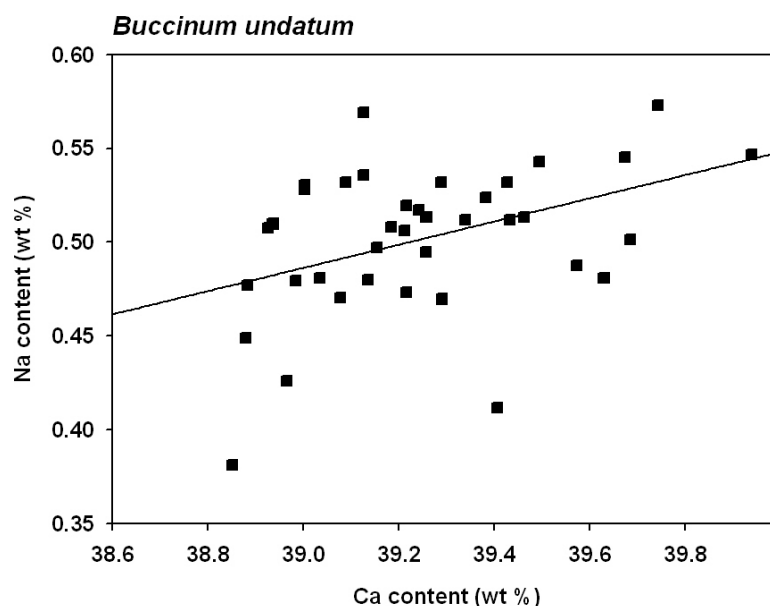


Figure 4.29 WDS data showing Na content is positively correlated with Ca in *Buccinum undatum*. There is a significant positive correlation between Ca and Na ($r = 0.413$, $p = 0.0100$, $n = 38$).

EDS data

All key species were analysed with WDS. In addition, some species were analysed with EDS before the main WDS analysis. Some of these species were not subsequently analysed with WDS. EDS data showed some significant negative correlations among elements (proposed substitutions). Table 4.12 shows the results of correlation analyses between Ca and minor elements. Full correlation statistics tables for every element analysed for each species are displayed in Appendix 2. Summaries of the trends between Ca and minor elements are described below.

Bivalves

Bivalves analysed by EDS were the Antarctic bivalves *Laternula elliptica* and *Yoldia eightsi*. Data show no significant substitutions of any minor elements for Ca in either species (Table 4.12).

Gastropod

The buccinid gastropod *Buccinum undatum* was analysed by EDS. Data show no significant substitutions of any minor elements for Ca for *B. undatum* (Table 4.12); however, these shells were from dead animals and may have experienced some diagenesis.

Brachiopods

Brachiopods analysed by EDS were *Liothyrella neozelanica*, the Antarctic brachiopods *L. uva* and *Magellania fragilis*, and north-west European brachiopod *Terebratulina retusa*. Data show significant intra-specific substitutions of S and Mg for Ca in *Liothyrella neozelanica*, *L. uva* and *Magellania fragilis* (Table 4.12). Na was positively correlated with Ca in *Magellania fragilis*. However, *Terebratulina retusa* showed no significant intra-specific substitutions of minor elements with Ca.

Figure 4.30 demonstrates Mg/Ca substitution in *M. fragilis*. Variation in substitution within an individual was limited, but substitution among individuals was much more noticeable. Plotting data for all *M. fragilis* shells together, the best fitting for this pooled dataset is a linear model which gives an AIC of -75.026. This AIC value is not improved by subsequent models. Brachiopods analysed by EDS showed an inter-specific variation in Mg/Ca substitution (Figure 4.31).

Echinoid

The test of the echinoid *Sterechinus neumayeri* was analysed by EDS. *S. neumayeri* exhibits intra-specific substitution of Mg for Ca (Table 4.12). The echinoid test is composed of magnesian-calcite and *S. neumayeri* had a much higher level of Mg within its test compared to the other groups (bivalves, gastropods and brachiopods) analysed.

Table 4.12 EDS data. Pearson product moment correlation statistics for Ca and minor elements for each species analysed by EDS. Cell contents are correlation coefficient (r), probability value (p) and number of samples (n). *Denotes p values that are significant at the $p < 0.0125$ level.

		S	Mg	Na
Bivalve: <i>Laternula elliptica</i>				
Ca	r	-0.121	0.226	-0.0614
	p	0.563	0.590	0.771
	n	25	8	25
Bivalve: <i>Yolida eightsi</i>				
Ca	r	0.256	0.158	0.0288
	p	0.250	0.685	0.899
	n	22	9	22
Gastropod: <i>Buccinum undatum</i>				
Ca	r	0.0317	0.0073	-0.132
	p	0.861	0.986	0.465
	n	33	8	33
Brachiopod: <i>Liothyrella neozelanica</i>				
Ca	r	-0.619	-0.525	-0.176
	p	0.0013*	0.0085*	0.409
	n	24	24	24
Brachiopod: <i>Liothyrella uva</i>				
Ca	r	-0.467	-0.457	-0.378
	p	0.0092*	0.0111*	0.0396
	n	30	30	30
Brachiopod: <i>Magellania fragilis</i>				
Ca	r	-0.855	-0.821	0.695
	p	<0.0001*	<0.0001*	<0.0001*
	n	42	38	42
Brachiopod: <i>Terebratulina retusa</i>				
Ca	r	-0.274	-0.362	-0.135
	p	0.123	0.0386	0.453
	n	33	33	33
Echinoid: <i>Sterechinus neumayeri</i>				
Ca	r	0.0309	-0.547	-0.447
	p	0.909	0.0282	0.0825
	n	16	16	16

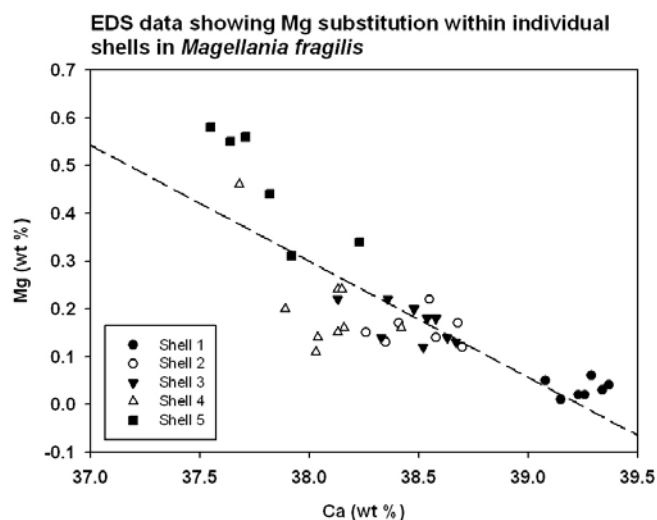


Figure 4.30 EDS data showing intra-specific differences in Mg substitution for Ca in the Antarctic brachiopod *Magellania fragilis* valves ($F = 74.6665$, $df = 1,36$, $r^2 = 0.6657$, $n = 38$, $p < 0.0001$).

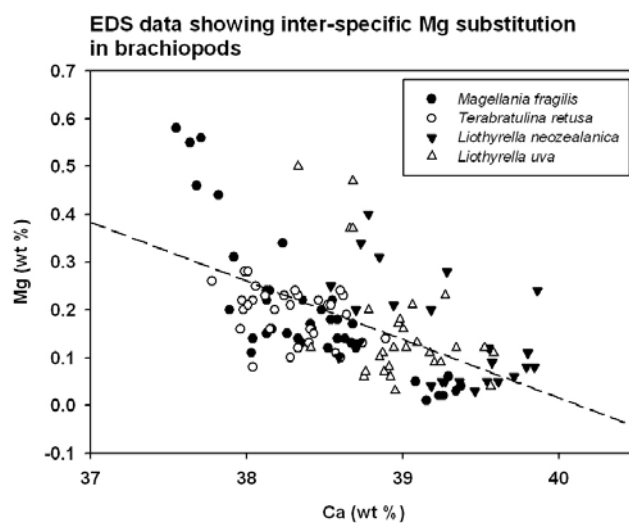


Figure 4.31 EDS data showing inter-specific substitution of Mg for Ca into the CaCO_3 valves of brachiopods ($F = 60.5824$, $df = 1,122$, $r^2 = 0.3263$, $n = 124$, $p < 0.0001$).

4.3.2.2 Inter-specific latitudinal variation and trends:

Shell elemental content and minor element ratios with Ca

WDS data showed both inter-specific and latitudinal variation in mean shell elemental content. Graphs of major (Ca) and minor (Sr, Mg, Na, S, Si) content for key species are shown in Figure 4.32 to Figure 4.35. N.B. In all relevant figures, positive degrees of latitude denote Northern Hemisphere localities and negative degrees of latitude denote Southern Hemisphere sites. Where two species from the same latitude have been analysed and the data points or error bars overlap, the point has been shifted slightly (by 2 degrees latitude) for ease of viewing. Differences in shell chemistry among geographic locations are compared by ANOVA in Table 4.14 to Table 4.17. ANOVAs were conducted on the mean elemental content data for each individual shell.

As mentioned earlier, it is difficult to compare data from EDS and WDS techniques, so data for Ca and minor element content using EDS on species that were not subsequently analysed with WDS are shown in Table 4.13.

Table 4.13 Ca and minor element content using EDS for species that were not subsequently analysed with WDS.

Species		Ca	S	Mg	Na
<i>Yoldia eightsi</i>	mean	38.893	0.097	0.013	0.548
	1 s.d.	0.083	0.006	0.010	0.091
<i>Magellania fragilis</i>	mean	38.423	0.260	0.204	0.395
	1 s.d.	0.548	0.074	0.161	0.100
<i>Terebratulina retusa</i>	mean	38.254	0.231	0.192	0.316
	1 s.d.	0.148	0.023	0.029	0.026
<i>Sterechinus neumayeri</i>	mean	37.264	0.404	1.135	0.615
	1 s.d.	0.513	0.003	0.169	0.030

Skeletal material varies in the amount of inorganic ('bio-inorganic') and organic components. Elemental weight percent of elements may vary depending on whether a shell

region is high in inorganic or organic content. Hence, elemental composition of biological carbonates often is reported as a ratio with another element to control for any potential variation. Ratio data for Sr:Ca show the same patterns as Sr weight percent data (Figure 4.32 to Figure 4.35). For minor elements, practically identical results were obtained for ratios as were obtained from weight percent data implying that analyses were conducted in homogeneous areas of shell and/or that shell inorganic and organic content varied little within a shell. If this is the case, then absolute weight percent data are arguably more useful since they give data on the amount of each element, rather than a ratio.

For mean elemental content significant differences were found among species of *Laternula* for Ca, Sr, Na and S (Figure 4.32). For minor element ratios with Ca significant differences were found among species for Sr, Na, S. Statistics are shown in Table 4.14. Where data were not distributed normally, a non-parametric Kruskal-Wallis one-way analysis of variance (ANOVA) by ranks test was used. Ca content decreased with increasing latitude. Sr decreased with increasing latitude in tropical and temperate species of *Laternula*, but was high in the polar species. Na generally increased with increasing latitude and S generally increased with increasing latitude.

Table 4.14 Statistics on WDS data for differences in mean elemental content (weight %) and elemental ratios among species of *Laternula*.

	Mean elemental content	Minor element:Ca ratios
Ca	p = 0.017 ANOVA	n/a
Sr	p < 0.001 ANOVA	p < 0.001 ANOVA
Mg	Test failed	Test failed
Na	p < 0.001 ANOVA	p < 0.001 ANOVA
S	p = 0.001 ANOVA on ranks	p < 0.001 ANOVA on ranks
Si	p = 0.216 NS ANOVA on ranks	p = 0.286 NS ANOVA on ranks

For mean elemental content significant differences in buccinid gastropods were found among species for Ca, Sr, Na and S (Figure 4.33). For minor element ratios with Ca significant differences were found among species for Sr, Mg, Na and S. Statistics are shown in Table 4.15. Ca decreased with increasing latitude with the exception of the Arctic

species. Sr and Mg decreased with increasing latitude. Mg data for the polar buccinids were below the detection limit; however, Mg data were still consistently low. Na increased with increasing latitude. There was no clear pattern in S with latitude, although tropical buccinids had a lower S content.

Table 4.15 Statistics on WDS data for differences in mean elemental content (weight %) and elemental ratios among buccinid gastropod species.

	Mean elemental content	Minor element:Ca ratios
Ca	p < 0.001 ANOVA	n/a
Sr	p < 0.001 ANOVA	p < 0.001 ANOVA
Mg	Test failed	p = 0.017 ANOVA
Na	p < 0.001 ANOVA on ranks	p < 0.001 ANOVA on ranks
S	p < 0.001 ANOVA	p < 0.001 ANOVA
Si	p = 0.303 NS ANOVA	p = 0.294 NS ANOVA

For mean elemental content in brachiopods using WDS data, significant differences were found among species for Ca, Sr, Na, S and Si (Figure 4.34). For minor element ratios with Ca significant differences were found among species for Sr, Na, S and Si. Statistics are shown in Table 4.16. Sr, Na, S and Si increase with increasing latitude. Mg data were limited.

Table 4.16 Statistics on WDS data for differences in mean elemental content (weight %) and elemental ratios among brachiopod species.

	Mean elemental content	Minor element:Ca ratios
Ca	p = 0.006 ANOVA on ranks	n/a
Sr	p < 0.001 ANOVA	p < 0.001 ANOVA
Mg	Insufficient data	Insufficient data
Na	p < 0.001 ANOVA on ranks	p < 0.001 ANOVA on ranks
S	p < 0.001 ANOVA	p < 0.001 ANOVA
Si	p < 0.001 ANOVA	p < 0.001 ANOVA

For mean elemental content in brachiopods using EDS data, significant differences were found among species for Ca and Na content (Figure 4.35). For minor element ratios with Ca significant differences were found among species for Na:Ca. Statistics are shown in Table 4.17. Ca decreased with increasing latitude. Na increased with increasing latitude. There were no clear patterns with latitude in Mg or S. Sr, Ba and Al were present below EDS detection limits.

Table 4.17 Statistics on EDS data for differences in elemental content among brachiopod species.

	Mean elemental content	Minor element:Ca ratios
Ca	p = 0.009 ANOVA on ranks	n/a
Mg	p = 0.688 NS ANOVA	p = 0.654 NS ANOVA
Na	p = 0.004 ANOVA on ranks	p = 0.004 ANOVA on ranks
S	p = 0.108 NS ANOVA	p = 0.091 NS ANOVA

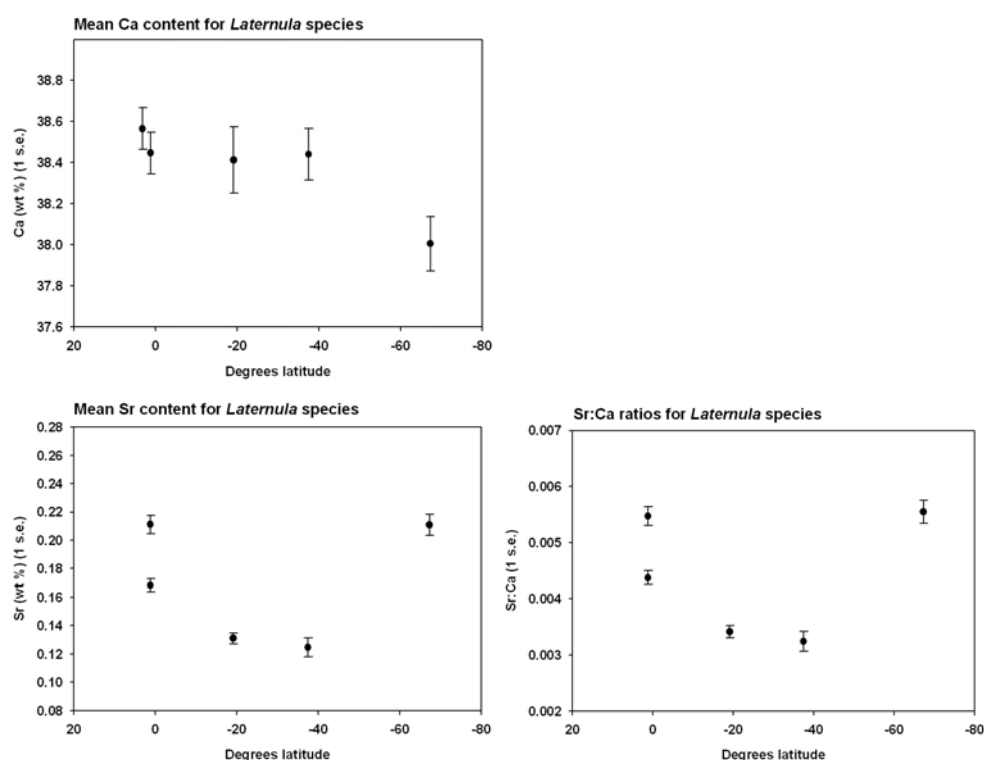


Figure 4.32 continues overleaf.

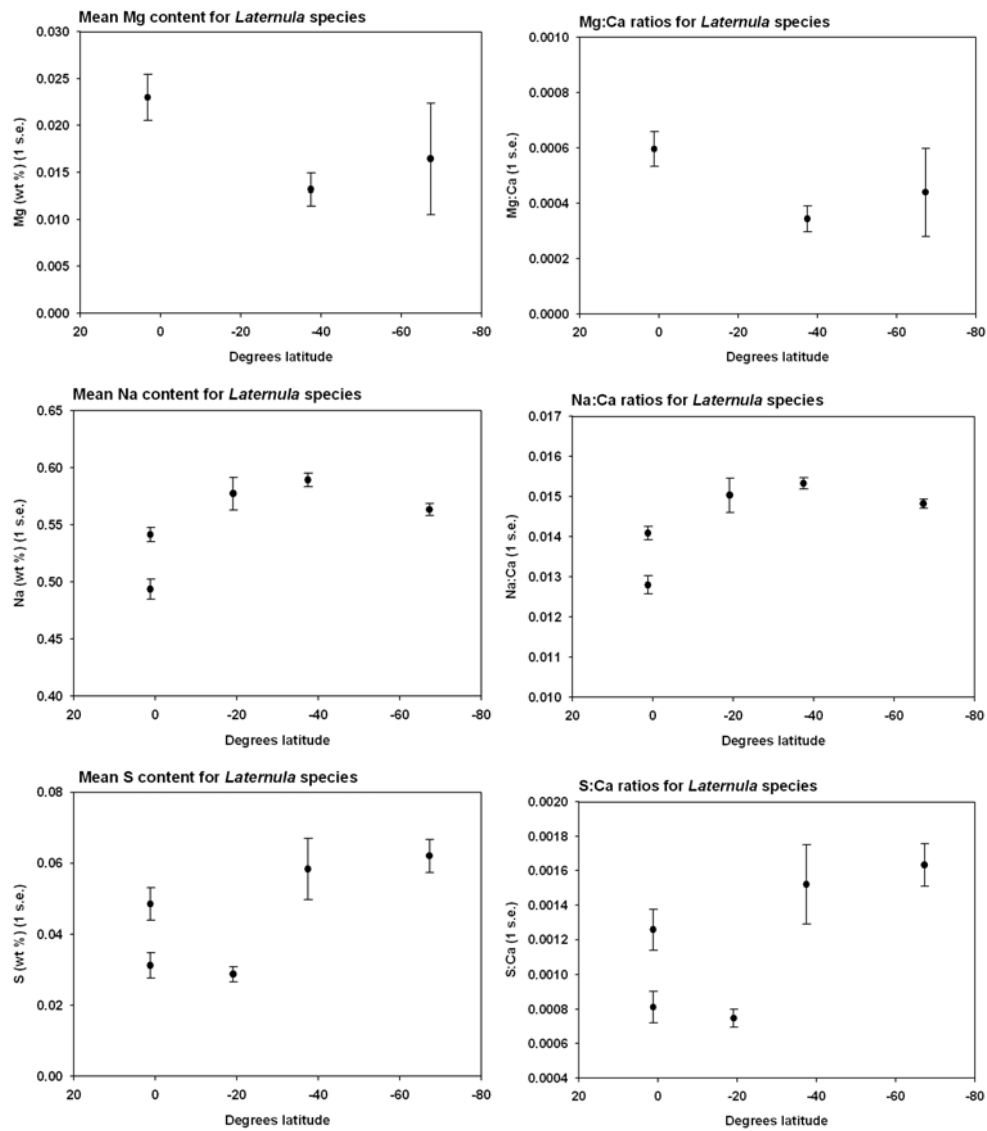


Figure 4.32 WDS data for mean elemental content of major and minor elements (left) and minor element:Ca ratios (right) in shells of *Laternula* clams.

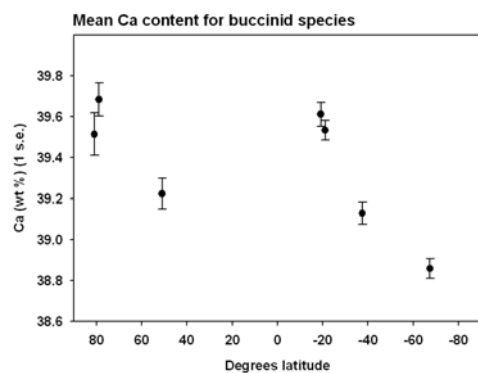


Figure 3.33 continues overleaf.

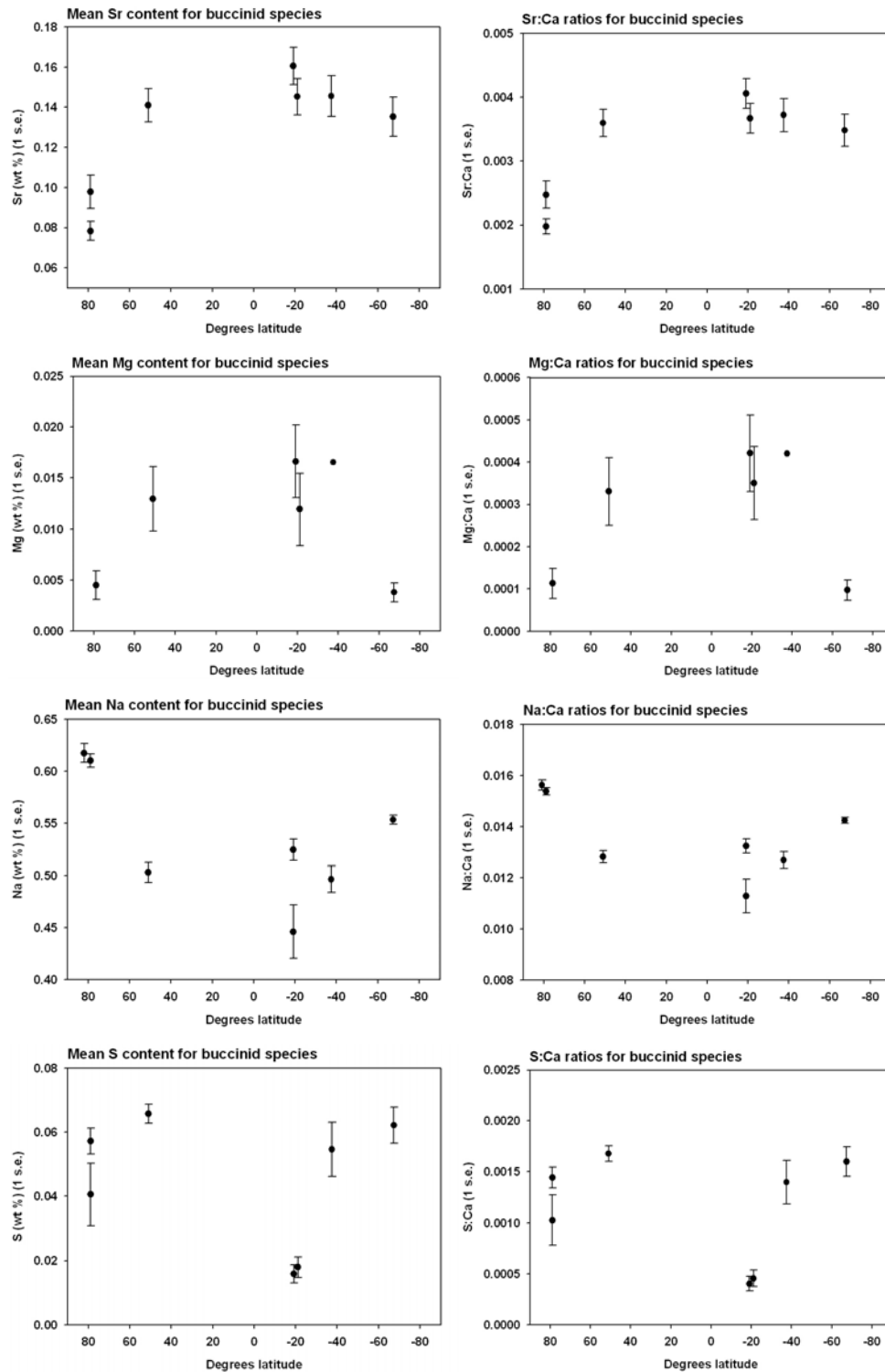


Figure 4.33 WDS data for mean elemental content of major and minor elements (left) and minor element:Ca ratios (right) in shells of buccinid gastropods.

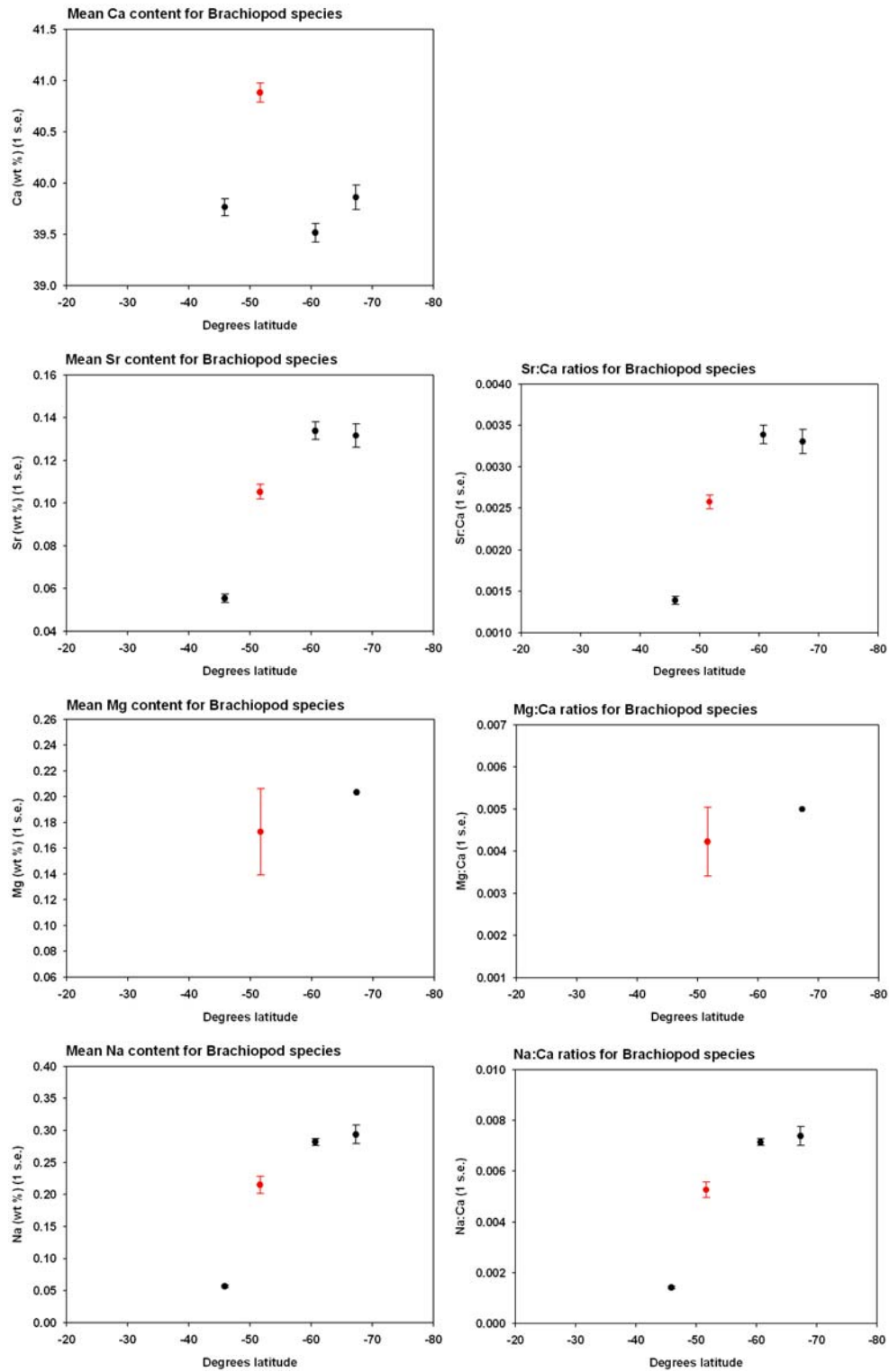


Figure 4.34 continues overleaf.

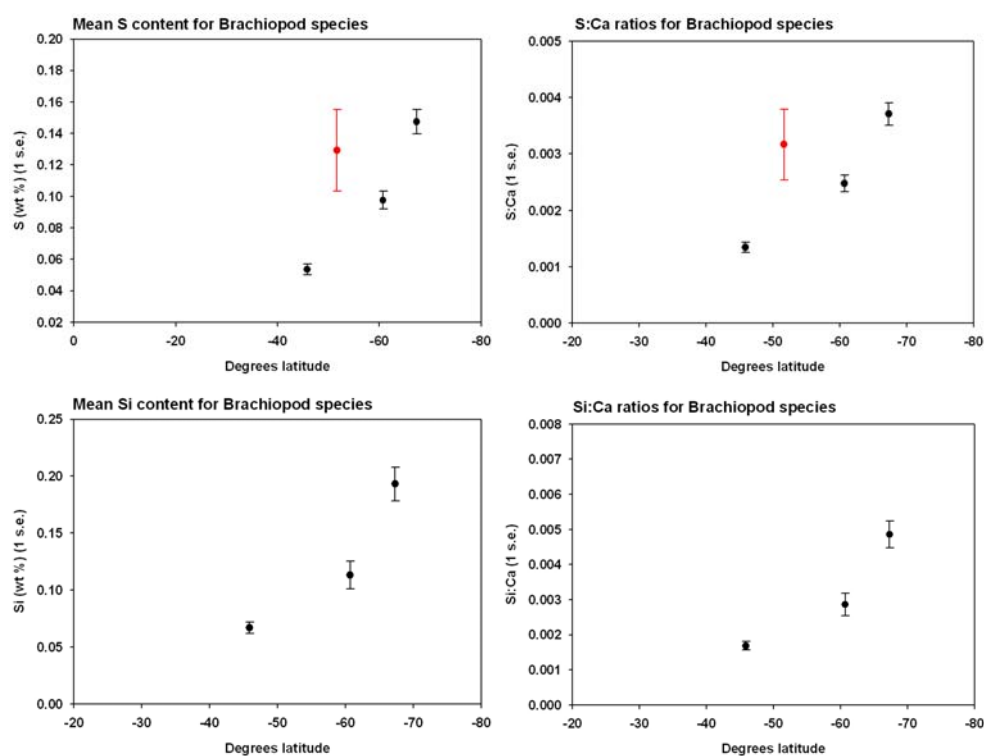


Figure 4.34 WDS data for mean elemental content of major and minor elements (left) and minor element:Ca ratios (right) in shells of brachiopods. N.B. Black data points are *Liothyrella* species and the red data point is *Magellania venosa* a non-congeneric species.

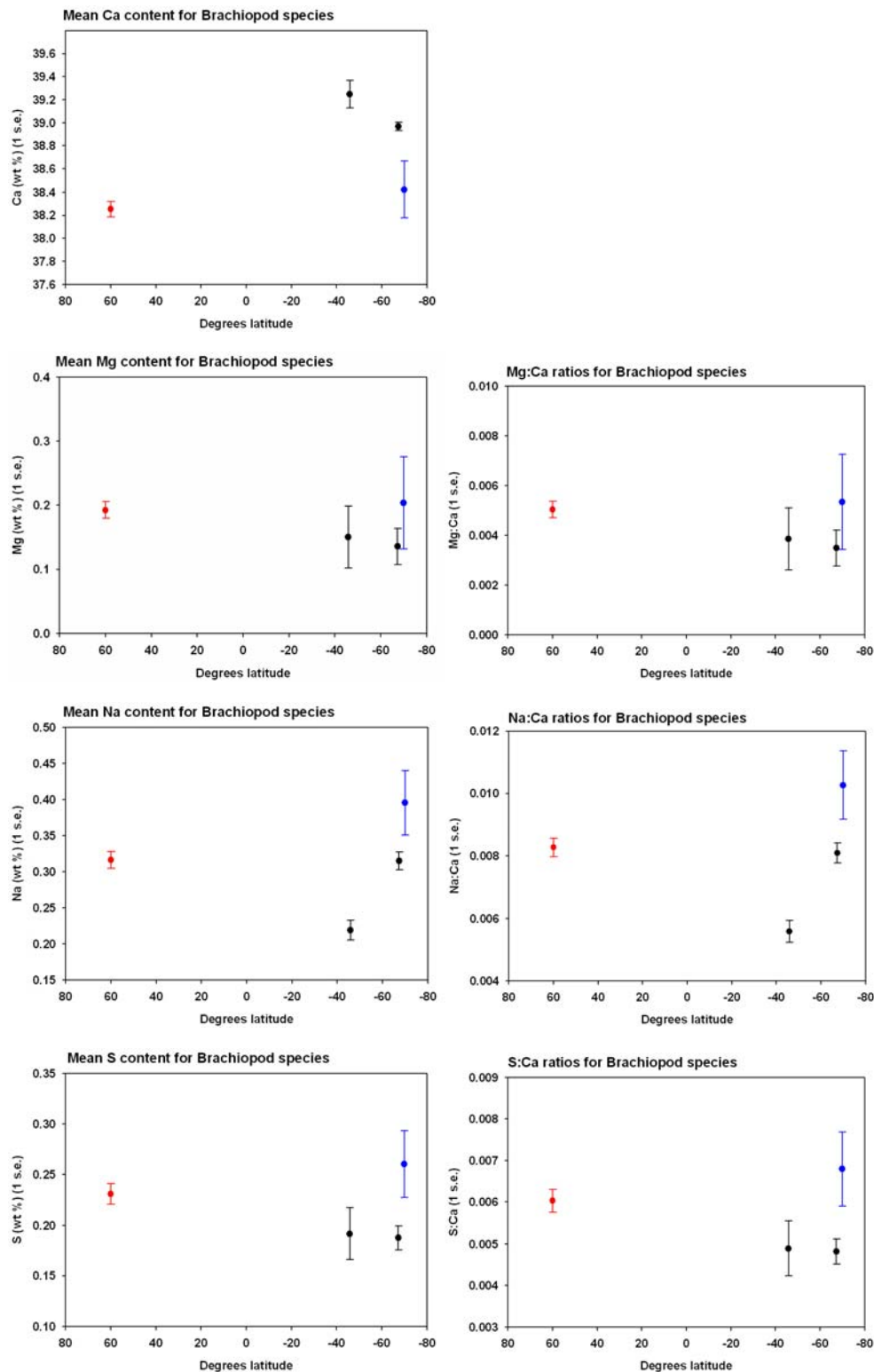


Figure 4.35 EDS data for mean elemental content of major and minor elements (left) and minor element:Ca ratios (right) in shells of brachiopods. N.B. Black data points are *Liothyrella* spp. and the red data point is *Terebratulina retusa* and the blue data point is *Magellania fragilis*, both non-congeneric species.

4.3.2.3 Maps of elemental distribution

The distribution of elements in a section of the gastropod *Phos senticosus* shell was mapped by running the SEM WDS overnight. Figure 4.36 to Figure 4.38 show the distribution of Ca, Na and Sr across the shell section. Ca is very uniform across the shell section. Na and Sr to a lesser extent show layering. Although costly, this technique provides a greater degree of resolution. However, this resolution was not required for the main analysis of elemental composition and so it was not necessary to repeat the technique for other species.

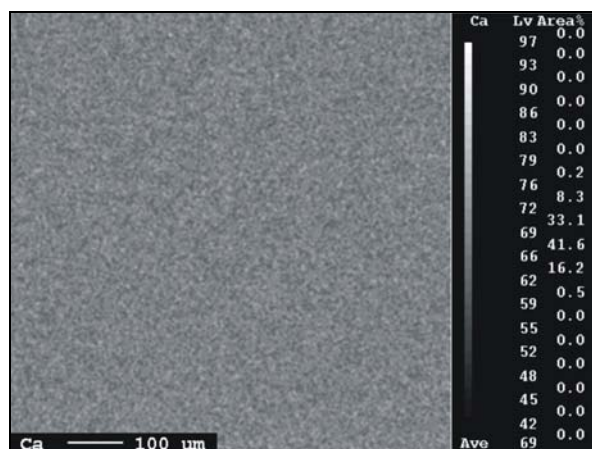


Figure 4.36 Map of Ca content in *Phos senticosus* (WDS data).

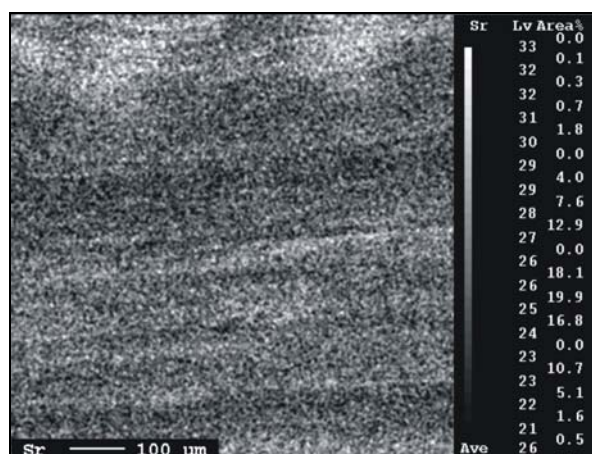


Figure 4.37 Map of Sr content in *Phos senticosus* (WDS data).

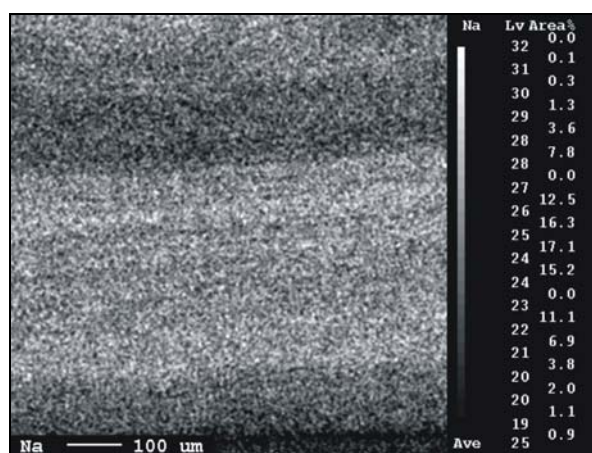


Figure 4.38 Map of Na content in *Phos senticosus* (WDS data).

4.4 Discussion

Shell crystal structure

Shells of species of *Laternula* are composed purely of aragonite (E. Harper, pers. comm.). SEM images of *Laternula* shell sections showed aragonite layers arranged in the same shell structure for all *Laternula* species studied. SEM images of crystal type in buccinid gastropod shell sections showed the shells were composed of aragonite with shell structure again similar for all species. XRD analysis conducted opportunistically on one species showed that the shell of the Antarctic buccinid *Neobuccinum eatoni* was composed purely of aragonite. As XRD was not conducted for the other buccinids, it is not known if these species had exclusively aragonite shells. As expected the brachiopod shells examined were calcite.

A calcite outer layer has been found in cooler water species of littorinid gastropods which may be an adaptation to resist dissolution (Taylor & Reid, 1990) because CaCO_3 is more soluble in cold waters (Revelle & Fairbridge, 1957) and aragonite is more soluble than calcite (Vermeij, 1993). Shells of Antarctic clams and buccinids studied were composed purely of aragonite, and it is likely that shell mineralogy is constrained evolutionarily in the groups studied. Interestingly, crystal size and the proportion of organic matrix in the shell have been shown to be more important than crystal polymorph in determining shell solubility in cold water and so the evolution of outer calcitic layers may not be an adaptation against dissolution (Harper, 2000). In this context it is interesting that the aragonite shells of *N. eatoni* in Antarctica do not appear heavily pitted or to exhibit marked other signs of enhanced dissolution.

Shell elemental composition

- Substitutions

Determination of the shell mineralogy (crystal structure) for each species allowed the subsequent analysis of elemental content within consistent layers. In addition to elements that are generally expected to substitute for Ca in the CaCO_3 lattice (e.g. Mg, Sr), elements such as S, Na and Si that are not expected to substitute for Ca were found to be negatively

correlated with Ca in some species. *Laternula* clams showed inter-specific substitution of Sr for Ca. Buccinid gastropods substituted Sr for Ca; and S was also negatively correlated with Ca. WDS data showed inter-specific substitution of Mg for Ca in brachiopods; and Si was also negatively correlated with Ca. S, Na and Si may either be associated with organic matrix or adsorbed onto the CaCO₃ crystal surface (Lorens & Bender, 1980).

In relation to the hypotheses tested in this chapter, the following conclusions can be drawn:

Hypothesis 1: Substitution of minor elements occurs in shells.

H₀: There is no evidence of substitution.

Conclusion: There were significant correlations between Ca and minor elements with a similar size and valence to Ca, such as Sr and Mg, indicating that substitution did occur.

Hypothesis 2: Substitutions of minor elements vary 1) within species, and/or 2) among species from different geographic locations.

H₀: Substitution occurs evenly.

Conclusion: Substitutions of minor elements varied among shells of the same species in some cases (e.g. brachiopods) and inter-specifically among species from different latitudes, but not intra-specifically in *Laternula* species.

- Patterns in elemental content with latitude (and temperature)

Elements are expected to occur in the same ratios, but not necessarily in the same amounts between organic and inorganic parts (C. Trueman, pers. comm.). Elemental ratios were presented in results to control for differences in the amount of organic material in the shell. Results show that across all species patterns of absolute content (wt %) of minor elements were identical to patterns in ratios of minor elements:Ca. This suggests that areas of shell analysed were highly homogeneous and not subject to fluctuations in Ca content compared to minor element content that might be expected if there were variations in the amount of inorganic and organic material throughout the shell. Variation in absolute content of elements and ratios were thus considered together as absolute content (wt %).

Three factors vary with latitude that may affect minor element content within shells: 1) temperature, 2) growth rate, and 3) metabolic rate.

Temperature is one of the most influential factors and much work has been done to attempt to reconstruct palaeotemperatures using shell composition. For example, Richardson *et al.* (2004) found Mg:Ca and Sr:Ca in shells of the fan mussel *Pinna nobilis* were positively correlated with sea surface temperature (SST). In the Mediterranean fan mussel *Pinna nobilis*, Mg:Ca was correlated to temperature in the early years of life, whereas, Sr:Ca was not correlated with temperature (Freitas *et al.*, 2005). In the king scallop *Pecten maximus*, Freitas *et al.* (2006) found shell Sr:Ca and Mg:Ca were correlated with calcification temperature. However they conclude that Mg:Ca in bivalve shell calcite is not a reliable temperature proxy given taxon- and species-specific variation. In *Mytilus edulis*, the Mg:Ca in shell covaries with temperature, but an interruption after the spring phytoplankton bloom precludes the direct use of Mg calcite as a temperature proxy (Putten *et al.*, 2000). So temperature alone is not the only control and both the environment and physiology of marine organisms affect the composition of the shell.

Minor element incorporation in molluscs varies with growth rate. Sr in shells tends to increase with increased growth rate (Stecher *et al.*, 1996). Growth rate in the form of a daily shell surface area increment can explain 74 % of the variation in Sr:Ca in the calcitic shell of the bivalve *Pecten maximus*, and Sr:Ca may be a potential proxy for calcification rate (Lorrain *et al.*, 2005). Elevated Mg:Ca, Sr:Ca and Mn:Ca ratios were associated with the deposition of elaborate features in *Pecten maximus* and *Mytilus edulis* grown at a constant temperature, although invariant Mg:Ca ratios in the mid- and innermost-regions of *P. maximus* shell were nevertheless found to be suitable for use as a palaeotemperature proxy (Freitas *et al.*, 2009). Carre *et al.* (2006) showed that for the bivalve species *Mesodesma donacium* and *Chione subrugosa*, environmental parameters had little influence, but crystal growth rate did influence Sr:Ca.

The physiology of marine molluscs confounds geochemical records of their shells by the active control of incorporation of trace elements in the skeleton (Schone, 2008). Purton *et al.* (1999) argue that metabolic activity (related to factors such as temperature, salinity, age

and growth rate) was likely to be the primary control in Sr:Ca in fossil aragonitic molluscs and that a single parameter such as growth, calcification rate or temperature cannot be the sole factor controlling Sr incorporation. Klein *et al.* (1996b) found Sr:Ca is primarily controlled by metabolic activity in the mantle and secondarily controlled by salinity in *Mytilus trossulus* (Koehn, 1991, formerly *M. edulis*) shells. As lowered metabolic activity is often linked to ontogenetic age (Schone, 2008) and therefore slower growth within a species, it is difficult to resolve published patterns in shell chemistry caused by either lower metabolic rate or slower growth.

As a result of potential differences in elemental content caused by growth rate, work in this chapter was done not on the micro-scale of growth rate, but instead took average data from the adult shell of each species. This chapter investigated broad scale differences in elemental chemistry – i.e. across populations and latitudes, rather than how the chemistry of a shell varied with seasonal factors such as food supply and growth rate. By analysing species across a wide geographic temperature gradient, it was the intention of this chapter that some large scale temperature effects on shell elemental composition may be determined.

Patterns in calcium (Ca)

Shells with more organic matrix may be expected to have less Ca. In *Laternula* clams, the amount of Ca in the shell was least in the polar clam. In buccinid gastropod shells, Ca content decreased with increasing latitude with the exception of the Arctic buccinids. In shells of *Liothyrella* brachiopods, analysis with WDS showed Ca content remained similar but Sr, Na, S and Si content was higher in the shell of the polar species *L. uva*. This suggests that in Antarctic representatives of the genus *Laternula* and family Buccinidae, shell layers may either be less dense and/or have less Ca relative to minor elements or organic matrix. This suggests that there is some latitudinal effect on shell composition. This approach is different to the analysis of ‘whole shell’ organic content taken in Chapter 3.

Patterns in strontium (Sr) and the potential influence of salinity

Although there are clear exceptions, theoretically there should be less Sr with increasing temperature in calcite and aragonite (Lowenstam & Weiner, 1989). Using latitude as a proxy for temperature, this translates to more Sr with increasing latitude.

The expected temperature trend held for Sr in temperate and polar *Laternula* clams and this could suggest the polar clam *L. elliptica* substituted Sr in place of Ca in its shell. However, the expected trend did not hold for shells of tropical species of *Laternula* because Sr content was high. These species were collected from the Johor Straits between Malaysia and Singapore and inhabit a brackish water environment with a salinity of 22. It is generally expected that the elemental content of shells from brackish waters would reflect the extent to which seawater is diluted (Lowenstam & Weiner, 1989). Growing *Mytilus edulis* in seawater with varying minor element to Ca ratios (Mg:Ca, Sr:Ca and Na:Ca), Lorens and Bender (1980) found Sr:Ca in calcite and aragonite varied linearly in proportion to seawater Sr:Ca. Again exceptions exist and the calcite shells of brachiopods can have higher Sr:Ca in brackish water than open ocean water (Lowenstam & Weiner, 1989). It is possible that minor elemental content in shells is controlled by either temperature, salinity, the local concentrations of the minor elements in seawater, or a combination of these factors (Lowenstam & Weiner, 1989).

Although inhabiting a less saline environment, the tropical species of *Laternula* studied in this chapter had more Sr in their shells. Based on the effects of dilution of elements from seawater in brackish water, it would be expected that these brackish species had less Sr in their shells. Therefore, it appears that temperature and the concentrations of elements in the water were not the primary influence of Sr in the shells of tropical species of *Laternula*. Metabolic rate could have an influence.

Sr concentration in bivalve shell is low relative to other invertebrates (Lowenstam, 1964b; Ueda *et al.*, 1973). However, shells of species of *Laternula* had higher Sr than buccinid gastropods and brachiopods studied. Results for the aragonitic shells of tropical and temperate species of *Laternula*, were in contrast to the findings of Dodd (1965) that with increasing temperature, Sr decreases in aragonite. However, the polar species *L. elliptica*

had a high Sr content compared to temperate species agreeing with Dodd (1965). It may be that a tipping point of excluding Sr from the shell has been reached for this polar species, requiring too much energy to exclude Sr.

Buccinid gastropods showed no evidence of the expected Sr temperature trend. Sr was low in the Arctic buccinids, which could reflect a reversal of the expected temperature trend, or the lower salinity of their environment. The Arctic gastropods were collected from Kongsfjorden fjord where surface water salinity can be less than 28 in the inner basin and 30 in the middle of the fjord (Svendsen *et al.*, 2002). The brackish melt-water extends “several metres” into the water column (Svendsen *et al.*, 2002) and since the Arctic buccinids were collected from 5 m depth, it is likely they are exposed to low salinity waters at certain periods, especially during summer. Sr availability in the environment could affect its incorporation into buccinid shells. Alternatively, salinity could be masking a temperature effect of Sr incorporation into Arctic buccinid shells.

In the calcite shells of brachiopods, there was evidence from WDS that the expected temperature trend for Sr held³. High Sr content in polar brachiopod shells suggests less selection against the Sr^{2+} ion during shell formation. *Liothyrella neozelanica* had much lower Sr concentrations than *L. uva*. However, *L. neozelanica* were collected from 10 – 20 m deep in Doubtful Sound, New Zealand a fjord with a quasi-permanent low-salinity-layer (LSL). The halocline is often < 10 m in depth (Gibbs *et al.*, 2000), so the influence of lowered salinity on *L. neozelanica* is likely to be small. Less Sr availability in the environment could affect its incorporation into *Liothyrella* shells but as mentioned above, brachiopods can have higher Sr:Ca in brackish water than open ocean water (Lowenstam & Weiner, 1989). So temperature and/or salinity could be having an effect on Sr incorporation into brachiopod shells.

The higher Sr content in *Laternula* clams and brachiopods compared to gastropods implies less selection against Sr^{2+} during shell formation. Since the exclusion of Sr^{2+} ions during shell formation requires energy, the presence of high Sr may indicate that the energetic cost of shell production is a significant cost in the bi-valved molluscs and brachiopods studied

³ Sr data from EDS were not available for comparison because they were below detection limits.

here from high latitudes. The cost of shell production or excluding unwanted ions during shell production may be less in buccinid gastropods because of their apparent ability to minimise the amount of Group 2 elements (e.g. Mg and Sr) within the shell even at low temperatures.

Patterns in magnesium (Mg)

Bivalves have low-Mg calcite and aragonite shells compared to other invertebrates (Chave, 1954; Lowenstam, 1963; Dodd, 1967; Wolf *et al.*, 1967; Wyckoff, 1972), but results here from WDS showed that the shells of the genus *Laternula*, buccinids and brachiopods studied had similar Mg content around 0.010 – 0.025 wt % with the exception of the polar buccinids which had Mg contents which fell below detection limits for Mg at c. < 0.005 wt %.

From previous research (Dodd, 1965; 1966) one might expect Mg concentration to be positively correlated with temperature. Generally, one finds more Mg with increasing temperature in calcite (Füchtbauer & Hardie, 1976) following a linear trend (Lorens & Bender, 1980), so there should be less Mg with increasing latitude in calcite. Mg inhibits calcite precipitation at its normal seawater concentration (Berner, 1975) and as a result *Mytilus edulis* controls the Mg concentration in the extrapallial fluid (Lorens & Bender, 1980). Klein *et al.* (1996a) showed that Mg:Ca in *Mytilus trossulus* (Koehn, 1991, formerly *M. edulis*) shells could be used to identify weekly signal of SST. However, in non-biogenic calcite, temperature is not the only first-order factor governing Mg incorporation into crystals (Wasylenki *et al.*, 2005). Less is known about the temperature effect on Mg in biogenic aragonite. Both positive (Dodd, 1965) and negative (Schifano, 1982) correlations of Mg with temperature have been found and Lorens and Bender (1980) found Mg:Ca ratios increased exponentially with temperature in aragonite.

This expected trend for Mg in calcite held for Mg in the aragonite shells of tropical and temperate *Laternula* clams, but Mg content in the polar clam was highly variable. Perhaps another factor such as metabolic rate was also influencing Mg incorporation into the shell of the polar species.

Mg also increased with increasing temperature in the buccinids from polar regions compared to the tropical and temperate snails. Buccinid gastropods in both the Northern and Southern Hemispheres showed an increase in Mg content with increasing temperature compared to polar species. However, Mg content of polar buccinids was below detection limits for Mg, and although data were consistent, indicating reliability in the results, care must be taken with interpretation. Data could suggest the polar buccinids are excluding Mg from their shells as the amount of Mg seemed to be lowest in Arctic and Antarctic species. The proportion of Mg^{2+} in a calcite lattice significantly affects its solubility and calcites with high magnesium contents are more soluble than aragonite (Walter & Morse, 1984; Bischoff *et al.*, 1987). As mentioned above, a calcite outer layer has been found in cooler water species of littorinid gastropods (Taylor & Reid, 1990). If the Arctic buccinid shells were partly composed of calcite, such as a thin outer calcite layer not detectable in the SEM images, and in contrast to shell of the Antarctic buccinid *Neobuccinum eatoni* which is purely aragonite, then this could explain the need to for the Arctic buccinids to exclude Mg from their shells.

For the brachiopods studied, there was no clear trend in Mg and temperature. EDS data showed no evidence of the expected change of Mg in calcite with temperature, and WDS did not provide enough data to test this trend inter-specifically.

Within groups of shelled-animal (e.g. the Bivalvia) the Mg:Ca temperature trend is not clear (Rosenberg, 1980) although similar trends within each taxon would be expected. It should be remembered that the evolutionary response of organisms to physical parameters of the environment occurs at the level of populations and individuals, thus populations can respond differently to similar environmental variables (Rosenberg, 1980). However, this population level variation is expected to be much less than species level variation. Precise determination of controlling factors would require temperature and ion concentration manipulation experiments on individual species.

Patterns in sodium (Na)

Na content was positively correlated with Ca in some species and increased with increasing latitude in buccinids. Na was low in the shells of tropical *Laternula*. WDS and EDS data

showed Na increased in shells of brachiopods from the genus *Liothyrella* with increasing latitude. It is possible to have a large amount of non-lattice bonded Mg and Mn which may explain the presence of some elements one might not expect in the biogenic CaCO_3 lattice (Takesue *et al.*, 2008). For example, a large amount of Na may be adsorbed onto the CaCO_3 crystal surface (Lorens & Bender, 1980). An alternative explanation is that Na^+ , being the perfect size to substitute for Ca^{2+} in the CaCO_3 lattice but the wrong charge, could be coupled with a trivalent ion such as Fe^{3+} . The type of the trivalent ion could vary so that a particular trivalent ion is not found in the same quantity as Na^+ , and this could explain why a trivalent ion such as Fe^{3+} was not detected in shells in this study (C. Trueman, pers. comm.).

Hypothesis 3: Shell elemental composition varies with latitude and specifically, the absolute content and/or ratios of elements (Ca or minor) changes among species with latitude.

H₀: There is no change in shell composition with latitude.

Conclusion: Shell elemental composition varied with latitude and specifically, the absolute content and/or ratios of elements (Ca or minor) changed with latitude. Between two species from very similar latitudes, similar elemental ratios are found. However, minor elements covary with other factors in natural populations and it is difficult to determine precise causal factors of minor element incorporation.

Limitations and further work

Precise determination of the controlling factors of minor element incorporation into shells would require experiments growing individuals of each species in seawater of different temperatures and ion concentration at their respective latitude. This chapter has begun to show potential trends in elemental content within taxa across latitudes and this will prove useful in further work. It has attempted to use phylogenetically controlled comparisons to elucidate latitudinal trends and has shown significant variation among taxa. Future work with more species, and at the population level are needed to identify the details of these trends.

Further work using XRD should be conducted on the shells of all species to determine if mineralogy varies with latitude. Laser ablation inductively coupled plasma mass spectrometry (LA-ICP-MS) would be useful in determining concentrations of elements below the detection limits of WDS.

Maps of elemental distribution showed homogeneous Ca content, thin bands of Sr content and thick bands of Na content. These elements varied in space within the shell but the reasons for these patterns were not clear. Further work mapping elemental distribution may provide more information.

Summary

Patterns of minor element incorporation into the shells of the groups studied varied in some cases with latitude. However, the control on this variation could be due to temperature, growth rate or metabolic rate. Salinity may have had an effect on shell minor element content, but to determine the full controls between temperature and salinity, experimental studies would need to be done. There was no clear evidence that the patterns of elemental substitution could suggest less energy was being used to produce shell in colder waters. Less, not more, Mg was incorporated into shells at lower temperatures, but this is expected given the temperature effect on Mg. For *Laternula* clams and brachiopods more Sr was incorporated into shells, which could suggest higher substitution and less energy use in excluding this elements at high latitudes; however, this trend was also expected because the distribution coefficients for strontium decrease linearly with temperature. In conclusion, there was no consistent pattern for all taxa studied which suggest there was no single factor determining shell composition trends across latitude.

Chapter 5: Latitudinal gradients in metabolic rate



Chapter 5: Latitudinal gradients in metabolic rate

5.1 Introduction

One way to test the importance of the energetic cost hypothesis of differences in shell morphology with latitude is to analyse metabolic rates and energy budgets of calcareous organisms from different latitudes and compare calcification costs with the overall energy budget of the animal. This chapter investigates the first part of this process, latitudinal variation in metabolic rate for key calcareous groups studied.

Routine metabolic rate is one part of the energy budget of an animal and can be estimated from standard metabolic rate (SMR), which is often measured because it is less variable. SMR is the resting and fasting metabolic rate of an animal at a given body temperature (Randall *et al.*, 1997). For ectotherms, also known as poikilotherms or cold-blooded animals, body temperature is usually closely aligned to that of their surroundings (Willmer *et al.*, 2005). The rate of energy metabolism is often estimated by the rate of oxygen consumption (Schmidt-Nielsen, 1990) and SMR can be estimated by measuring the oxygen consumption of an individual or group of individuals under defined conditions. Oxygen consumption is often expressed in a mass-specific way in mass units of $\mu\text{g O}_2\cdot\text{g}^{-1}\cdot\text{h}^{-1}$ or in molar units of $\mu\text{mol O}_2\cdot\text{g}^{-1}\cdot\text{h}^{-1}$ where g is either wet weight, dry weight or ash-free dry mass (AFDM) of the animal. Often the respiration rate for a standard sized animal will be calculated to facilitate and improve comparisons.

On a logarithmic plot, whole animal metabolic rate tends to have a slope of 0.75 when plotted against body mass (Schmidt-Nielsen, 1990). This $\frac{3}{4}$ power scaling relationship between metabolic rate and body mass is exhibited by a wide range of organisms including unicellular organisms, ectotherms and endotherms (Randall *et al.*, 1997; Gillooly *et al.*, 2001; West *et al.*, 2003; Savage *et al.*, 2004; West & Brown, 2005), although differences have been reported (Weibel *et al.*, 2004; Weibel & Hoppeler, 2005), and there is still debate

concerning whether an underlying $\frac{3}{4}$ power scaling relationship exists, and if so what the underlying causes are (Hawkins *et al.*, 2007; del Rio, 2008).

Metabolic rate increases with temperature (Schmidt-Nielsen, 1990) and varies with season (e.g. Brockington, 2001; Brockington & Peck, 2001). The increase in a rate over a 10 °C increase in temperatures is known as the Q_{10} (Schmidt-Nielsen, 1990) and these Q_{10} values can be used as a comparison of metabolic processes at different temperatures.

Metabolic data for only a few of the key species in this thesis have been previously published in the scientific literature and are summarised in Table 5.1. For many species no published data were available. Therefore, metabolic data were collected for key species at each of their latitudes at their respective environmental temperatures. These data were compared between latitudes (this chapter) and also used to estimate the total energy budget to compare the cost of shell production with the total energy budget and determine any variation among latitudes (Chapter 6).

5.1.1 Aims and hypothesis

Aim: To determine SMR of key species to determine how they vary with temperature and latitude. The SMR will then be used to estimate routine metabolic rate for use in calculations of the total energy budget (Chapter 6).

Hypothesis: Respiration rate changes with latitude among closely related species and, specifically respiration rate decreases along an increasing latitudinal gradient in shallow water marine ectotherms.

H₀: There is no change in respiration rate along a latitudinal gradient among closely related species of shallow water marine ectotherms.

Table 5.1 Summary of existing data on metabolic rates of key study species of calcareous organisms from scientific literature.
Units of $\mu\text{g-at. O}_2\cdot\text{h}^{-1}$ were multiplied by 11.2 to convert to $\mu\text{l O}_2\cdot\text{h}^{-1}$ according to Peck *et al.* (1986b), and then divided by 1 mole of gas at the appropriate experimental temperature to obtain $\mu\text{mol O}_2\cdot\text{h}^{-1}$.

Species	Temp. (°C)	Respiration rate	Condition of animal	Standard animal size	Source
<i>Laternula</i> clams					
<i>L. truncata</i>		No metabolic data found			
<i>L. boschasina</i>		No metabolic data found			
<i>L. recta</i>		No metabolic data found			
<i>L. elliptica</i>	0.5	414 $\mu\text{g O}_2\cdot\text{h}^{-1}$ for a 60 mm = 12.9 $\mu\text{mol O}_2\cdot\text{h}^{-1}$	Fasted for 2 days	60 mm shell length	Ahn and Shim (1998)
<i>L. elliptica</i>	0	3000 $\mu\text{l O}_2\cdot\text{h}^{-1}$ = 134 $\mu\text{mol O}_2\cdot\text{h}^{-1}$		12.5 mg	Peck and Conway (2000)
<i>L. elliptica</i>	Not reported	4.3 $\mu\text{mol O}_2\cdot\text{h}^{-1}$ in August (late winter) to 12.9 $\mu\text{mol O}_2\cdot\text{h}^{-1}$ in March (summer)	Held for 4 days in an aquarium	50 mm shell length (reported as 'height')	Brockington (2001)
<i>L. elliptica</i>	-0.4 (lab temp)	19.2 $\mu\text{mol O}_2\cdot\text{h}^{-1}$ in February (summer)	Held for 1 – 5 days in an aquarium	50 mm shell length	Morley <i>et al.</i> (2007a)
Gastropods					
<i>Cantharus fumosus</i>		No metabolic data found			
<i>Phos senticosus</i>		No metabolic data found			
<i>Cominella lineolata</i>		No metabolic data found			
<i>Buccinum undatum</i>	7.5 (March), 10.5 (May), 15 (August)	At 7.5 °C: 0.06-2.80 ml $\text{O}_2\cdot\text{h}^{-1}$ = 2.6-122 $\mu\text{mol O}_2\cdot\text{h}^{-1}$ At 10.5 °C: 0.32-4.44 ml $\text{O}_2\cdot\text{h}^{-1}$ = 14-191 $\mu\text{mol O}_2\cdot\text{h}^{-1}$ At 15 °C: 0.23 to 4.44 ml $\text{O}_2\cdot\text{h}^{-1}$ = 9.7-188 $\mu\text{mol O}_2\cdot\text{h}^{-1}$ Mass specific range for all temperatures: 0.12 to 1.37 ml $\text{O}_2\cdot\text{dry wt}^{-1}\cdot\text{h}^{-1}$ = 5.2-58.9 $\mu\text{mol O}_2\cdot\text{h}^{-1}$	Non-fasted	Over all sizes from 30 to ≥ 90 mm	Kideys (1998)

Table 5.1 continued.

Species	Temp. (°C)	Respiration rate	Condition of animal	Standard animal size	Source
<i>Neobuccinum eatoni</i>		No metabolic data found			
<i>Trophon longstaffi</i> Smith, 1907	0	46.2 $\mu\text{g O}_2 \text{ h}^{-1}$ (=1.44 $\mu\text{mol O}_2 \cdot \text{h}^{-1}$) for a 1.7 g tissue dry mass individual to 18.1 $\mu\text{g O}_2 \text{ h}^{-1}$ (= 0.566 $\mu\text{mol O}_2 \cdot \text{h}^{-1}$) for a 0.98 g tissue dry mass specimen	Fasted for at least 1 month		Harper & Peck (2003)
<i>Buccinum glaciale</i>		No metabolic data found			
<i>Buccinum</i> cf. <i>groenlandicum</i>		No metabolic data found			
Brachiopods					
<i>Liothyrella neozelanica</i>		No metabolic data found			
<i>Liothyrella uva</i>	0	0.48 $\mu\text{g-at. O} \cdot \text{h}^{-1}$ = 0.24 $\mu\text{mol O}_2 \cdot \text{h}^{-1}$	Fasted for 4-6 weeks	35 mm length (210 mg AFDM)	Peck <i>et al.</i> (1986b)
<i>Liothyrella uva notorcadensis</i> (Jackson, 1912)	0	6.11 $\mu\text{l O}_2 \cdot \text{h}^{-1}$ = 0.240 $\mu\text{mol O}_2 \cdot \text{h}^{-1}$	Fasted for 2 weeks	35 mm length (238 mg AFDM)	Peck <i>et al.</i> (1986a)
<i>Liothyrella uva</i>	0	0.205 $\mu\text{g-at. O} \cdot \text{h}^{-1}$ (summer rate) = 0.103 $\mu\text{mol O}_2 \cdot \text{h}^{-1}$	Non-fasted	50 mg AFDM	Peck <i>et al.</i> (1987b)
<i>Liothyrella uva</i>	0	10 – 15 $\mu\text{l O}_2 \cdot \text{h}^{-1}$ (varying with starvation) = 0.45 – 0.67 $\mu\text{mol O}_2 \cdot \text{h}^{-1}$	Fasted for 2 weeks	286 mg AFDM (38.6 mm length)	Peck (1989)
<i>Liothyrella uva</i>	0.76	0.64 $\mu\text{mol O}_2 \cdot \text{h}^{-1}$ (starved for 25 days) 0.97 – 1.06 $\mu\text{mol O}_2 \cdot \text{h}^{-1}$ (after feeding)	All stages	290 mg AFDM	Peck (1996)
<i>Liothyrella uva</i>	0.5	1.35 $\mu\text{g O}_2 \cdot \text{h}^{-1}$ = 0.0422 $\mu\text{mol O}_2 \cdot \text{h}^{-1}$	Fasted for 35 days	50 mg AFDM	Peck <i>et al.</i> (1997a)
Echinoids					
<i>Heliocidaris erythrogramma</i>		No metabolic data found			
<i>Psammechinus miliaris</i>	9, 12, 14	11 $\mu\text{l O}_2 \cdot \text{h}^{-1} \cdot \text{g}^{-1}$ (dry mass) = 0.47 $\mu\text{mol O}_2 \cdot \text{h}^{-1} \cdot \text{g}^{-1}$	Fasted for 2 weeks	n/a – MO2 is mass specific	Otero-Villanueva <i>et al.</i> (2004)
<i>Sterechinus neumayeri</i>	-1.8 to 1.2	0.33–0.65 $\mu\text{mol O}_2 \cdot \text{h}^{-1}$ in winter (between 2 sites) and 1.44–1.62 $\mu\text{mol O}_2 \cdot \text{h}^{-1}$ in summer	Non-fasted	24.4 mm test diameter	Brockington & Peck (2001)

5.2 Methods

5.2.1 Measurements of respiration rate

Calcareous invertebrates were collected according to the methods described in Chapter 2. Once collected, shelled animals were gently cleaned with a soft brush to remove any epibionts or adherent sediment. Any material, such as seaweed or empty mollusc shells, attached to the echinoid test and spines was removed. The epidermis covering the spines was left intact. Animals were then housed in aquaria to recover from the stress of collection and transportation. Invertebrates were held without food (fasted or starved) according to the approximate duration of their post prandial rise in metabolism (SDA) (Peck, 1998) that was expected for each latitude (Table 5.2). Respiration experiments were then conducted to determine the SMR of the organisms.

Respiration rates were measured using closed-system respirometry in Perspex or glass respiration chambers called respirometers (Figure 5.1). Perspex respirometers were similar to those used by Chapelle and Peck (1995). The respirometers ranged in size from 80 to 2000 cm³ as appropriate for the size of the organism and temperature at which the experiment was held, using similar methods to those of Morley *et al.* (2007a). Oxygen concentration in the respirometers was measured using a Fibox-3 optode system (Pre-Sens GmbH, Regensburg, Germany) single-channel temperature compensated oxygen meter (Figure 5.2). Planar oxygen sensors (John *et al.*, 2003) were glued onto a flat surface inside the respirometer using silicon rubber compound, which does not affect the transmission of light. The wall of the respirometer was transparent and non-fluorescent. This method allowed non-invasive and non-destructive measurement of oxygen concentration inside the respirometer (Figure 5.3).

Each oxygen sensor was calibrated with 0 % and 100 % oxygen in seawater. Sodium dithionite (Na₂S₂O₄) at a concentration of 25 mg.ml⁻¹ (a saturated solution of sodium dithionite) was used to remove all oxygen from seawater. Seawater saturated with oxygen was achieved by using an air stone to bubble fine bubbles of air vigorously through 3 l seawater for 30 min. Temperature and atmospheric pressure were recorded at the time of

calibration and during experimental trials. Temperature and pressure affect the fluorescence of the planar sensors and both are needed in the calculation of seawater oxygen concentration. Calibrations were performed before starting the experiments and every 4 to 5 days afterwards whilst the experiments were running. Oxygen sensors were changed every 1 to 2 months or after each major set of experiments at a location, thus ensuring that sensors were changed before the signal strength to the Fibox reduced significantly.

The transfer of animals to the respirometers took place with the animal underwater at all times to minimise stress and avoid the introduction of air bubbles into the system. Before transfer, brachiopods were tapped with a mounted needle and the valve close response noted to ensure they were in good physical condition. Once in the respirometer, animals were left overnight for at least 12 hours to adjust to the conditions in the respirometer and to minimise stress during the experiment. Respirometers were closed the following morning and the measurement of oxygen concentration in the respirometer was subsequently taken throughout the day ensuring that the organism did not suffer from hypoxic stress.

Preliminary respiration trials were conducted prior to the main experiment to determine the best size of respirometer for use and to determine if the organisms studied were oxyregulators, rather than oxyconformers, from 100 % to 70 % oxygen saturation. Respiration experiments were only run over the oxyregulating range for each species.

Individuals across as large a size range as possible for each species were used in respiration experiments. During each experiment 2 to 3 control respirometers (with no animal inside) were used. Having multiple controls provided a backup should a problem arise with a control during the experiment. Respirometers were held in an aquarium tank of stable ambient seawater temperature. The phase angle of the fluorescing chemical surface of the oxygen sensors was measured in respirometers (Figure 5.4) at suitable intervals throughout the experiment depending on the temperature and size of the respirometer. Approximately the same number of readings was taken during each experiment at each latitude.

A custom designed MS Excel spreadsheet program (Paul Giesler, British Antarctic Survey) modified from Christian Huber (Presens) was used to convert raw Fibox phase angle data to oxygen usage expressed as $\mu\text{mol O}_2\cdot\text{h}^{-1}$. This program provided oxygen consumption rates for each animal using regressions generated in MS Excel.

Once oxygen saturation reached 80 %, the experiment was stopped and the animal removed from the respirometer. The respirometers were washed with hot freshwater after every experiment to remove any build-up of bacterial film. Care was taken not to damage or remove the oxygen sensor during washing. The oxygen sensor was inspected and any loose ones were re-glued or replaced. If an oxygen sensor needed re-gluing or replacing, the sensor was re-calibrated.

Once the experiment had finished, the wet weight and volume of each animal was recorded as described in Chapter 3. Additional morphological measurements of individuals were also taken according to the methods in Chapter 3. Shells were dissected from tissues and both shell and tissue were dried at 60 °C to a constant weight then ignited in a muffle furnace at 475 °C for 24 hours, using the same protocol as in Chapter 3.

Respirations rates were calculated from the change in oxygen concentration per unit volume ($\mu\text{mol O}_2\cdot\text{l}^{-1}$) of seawater in the respirometer over the duration of the experiment (h). The volume of the animal was subtracted from the total internal volume of the respirometer to give the volume of seawater in the respirometer during the experiment. Oxygen concentration per litre was then divided by this volume to give oxygen concentration over time ($\mu\text{mol O}_2\cdot\text{h}^{-1}$).

Note that *Liothyrella uva* individuals used in respiration experiments were from Rothera not Signy, where previous measures of oxygen consumption in this species had been made. Also note that experiments were conducted in Melbourne in winter. This means the water temperature of the experiments in Melbourne was cooler than the water temperature for experiments conducted in Southampton in summer even though Southampton is at a higher latitude than Melbourne. Additionally, the water in the National Oceanography Centre,

Southampton aquarium was slightly higher (+ 1°C) than normal summer seawater temperatures in Southampton Water.

Table 5.2 Locations, seawater temperatures and season where respiration experiments were conducted for all *Laternula* species, buccinids, brachiopods and echinoderms investigated.

Location	Latitude	Species	Water temperature (°C) (1 d.p. ± 1 s.d.)	Season	Fasting period (days)
Singapore	1.22 °N	<i>Laternula truncata</i> , <i>Laternula boschasina</i>	29.9 (± 0.5)	Summer	3
Townsville, Australia	19.13 °S	<i>Cantharus fumosus</i> , <i>Phos senticosus</i>	28.3 (± 0.1)	Summer	5
Melbourne, Australia	37.49 °S	<i>Laternula recta</i> , <i>Cominella lineolata</i>	14.2 (± 0.1)	Winter	7
Southampton, UK	50.95 °N	<i>Buccinum undatum</i> , <i>Psammechinus miliaris</i>	18.9 (± 0.4)	Summer	7
Rothera, Antarctica	67.34 °S	<i>Laternula elliptica</i> , <i>Neobuccinum eatoni</i> , <i>Sterechinus neumayeri</i> , <i>Liothyrella uva</i>	0.7 (± 0.2)	Summer	14 (21 days for <i>L. uva</i> *)
Ny Ålesund, Arctic	78.95 °N	<i>Buccinum glaciale</i> , <i>Buccinum</i> cf. <i>groenlandicum</i>	4	Summer	12

**L. uva* needs to be starved for 18-25 days to complete all metabolic processes associated with feeding (Peck, 1996).



Figure 5.1 Respirometers containing *Laternula elliptica* in the Bonner Laboratory aquarium at Rothera Research Station, Antarctica.



Figure 5.2 Fibox-3 system (grey box and fibre optic cable) linked to a computer in the Zoology Department aquarium at Melbourne University, Australia.



Figure 5.3 Taking a measurement from a respirometer in the Tropical Marine Science Institute aquarium, National University of Singapore. The end of the fibre optic cable is placed on the glass where the oxygen sensitive foil is glued on the inside.

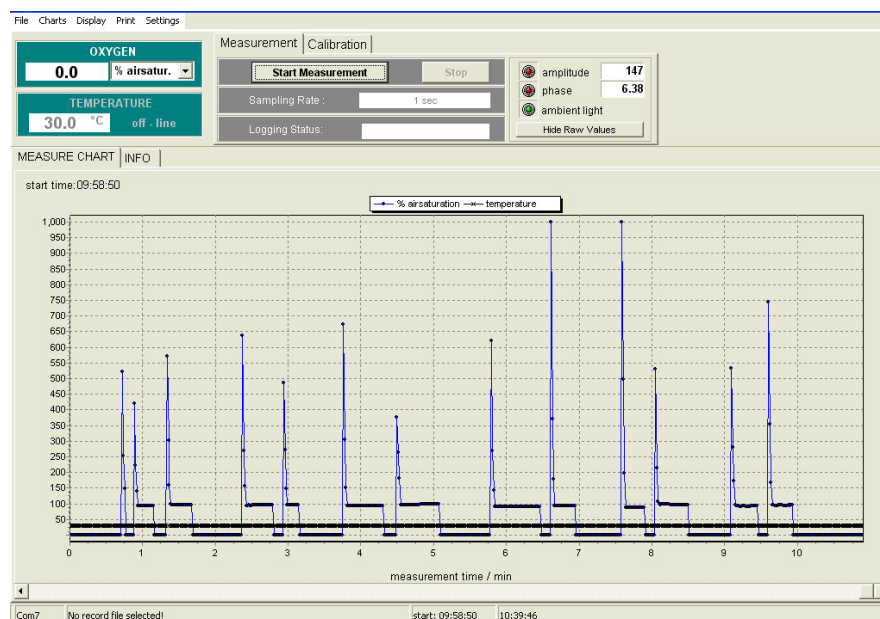


Figure 5.4 Fibox screen display using OxyView PST3-V5.32 program. Graphs of raw data (phase angle) over time are generated in real time by the program allowing the user to determine when the system is producing a stable reading.

5.2.2 Q_{10} calculations

The Q_{10} is the increase in a rate caused by a 10 °C increase in temperature and is defined by Equation 1 (Schmidt-Nielsen, 1990). Q_{10} values were calculated using the MO2 of a standard sized animal at the temperatures recording during the MO2 experiments.

$$Q_{10} = \left(\frac{R_2}{R_1} \right)^{\frac{10}{T_2 - T_1}} \quad \text{Equation 1}$$

Where,

T_1 is the lower temperature

T_2 is the upper temperature

R_1 is the rate at the lower temperature

R_2 is the rate at the upper temperature

5.2.3 Data and statistical analysis

Data were compiled on spreadsheets using MS Excel 2003. Statistical analyses were performed in SPSS 16.0 and SigmaPlot 10.0 and included regression analysis, analysis of variance (ANOVA), post hoc tests and t-tests. Graphs were produced with SigmaPlot 10.0. Regression analyses were used to calculate the amount of oxygen respired with time from decreases in oxygen concentrations in chambers.

For box plots (box-and-whisker plots) the ends of the boxes define the 25th and 75th percentiles, with a line at the median (50th percentile) and error bars defining the 10th and 90th percentiles. Data points beyond the 10th and 90th percentiles are displayed as dots. If data are too few for one of these groupings, than that set of points is not shown on the box plot (SigmaPlot). For regression analysis, a confidence band refers to the “region of uncertainties in the predicted values over a range of values for the independent variable”. A prediction band refers to the “region of uncertainties in predicting the response for a single additional observation at each point within a range of independent variable values” (SigmaPlot). On graphs, blue lines denote the 95 % confidence band and red lines denote the 95 % prediction band.

5.3 Results

In trials all species showed a constant depletion of oxygen down to 70 % oxygen saturation in seawater (Appendix 3). Therefore, all study species are oxyregulators from 100 to 70 % oxygen saturation. There was generally little oxygen depletion in the controls. However, this varied according to the aquarium facility and any change noted in the controls was adjusted for in the calculation of oxygen consumption of the test animals.

5.3.1 Variation in respiration rate with body size

Data for each species studied are presented from low to high latitudes. Table 5.3 shows the respiration rates for each species in terms of a mean-sized animal for the size range of the population sample collected and also as a mass specific respiration rate. Regression equations for all morphological parameters (length, wet weight, dry mass and AFDM) are shown in Table 5.4. *Laternula boschasina* clams were all very similar in size, so regressions of length with respiration data and mass with respiration data are not significant (Figure 5.5 and Figure 5.9). Graphs for each species show the scaling of oxygen consumption with body dimensions: length (or height for gastropods) and mass (wet weight, dry mass and AFDM). Confidence and prediction bands are shown where they do not confuse the graph.

Where a sufficiently large size range was obtained, oxygen consumption regressions with length, wet weight, dry mass and AFDM were all significant (Figure 5.5 to Figure 5.8). This means that experiments to determine respiration rate need not always be lethal since measurements such as length and wet weight predict respiration rate just as well. However, since most literature reports respiration rate in terms of animal dry mass or AFDM (because both mass variables can vary with season), the same protocol was followed in these experiments and respiration rates in terms of AFDM are reported here for ease of comparison with literature values.

Table 5.3 Respiration rates for each species in terms of a mean sized animal (calculated using regression equations of Ln(AFDM) on Ln(Length) and Ln(MO2) on Ln(Length)) for the species and mass specific respiration calculated for individuals.

Latitude	Species	Mean size of animal (max. linear dimension) (mm) (nearest integer)	AFDM (g) of mean size animal (3 s.f.)	MO2 for an animal of mean size ($\mu\text{mol O}_2\cdot\text{h}^{-1}$) (3 s.f.)	Mass specific MO2 ($\mu\text{mol O}_2\cdot\text{h}^{-1}\cdot\text{g}^{-1}$ total animal dry mass) (mean \pm 1 s.d. to 2 d.p.)	Mass specific MO2 ($\mu\text{mol O}_2\cdot\text{h}^{-1}\cdot\text{g}^{-1}$ total animal AFDM) (mean \pm 1 s.d. to 2 d.p.)
Laternula clams		Shell length				
1.22 °N	<i>Laternula truncata</i>	35	0.240	5.75	6.75 (\pm 2.75)	33.09 (\pm 11.99)
1.22 °N	<i>Laternula boschasina</i>	17	0.0278	0.994	14.10 (\pm 5.17)	66.53 (\pm 23.54)
37.49 °S	<i>Laternula recta</i>	29	0.0634	0.949	3.25 (\pm 0.51)	15.37 (\pm 3.05)
67.34 °S	<i>Laternula elliptica</i>	63	6.10	27.4	1.95 (\pm 0.70)	4.77 (\pm 1.32)
Buccinid gastropods		Shell height				
19.13 °S	<i>Cantharus fumosus</i>	22	0.0886	1.14	1.09 (\pm 0.38)	13.20 (\pm 4.87)
19.13 °S	<i>Phos senticosus</i>	31	0.199	1.99	0.92 (\pm 0.25)	10.41 (\pm 3.01)
37.49 °S	<i>Cominella lineolata</i>	19	0.0412	0.756	1.11 (\pm 0.59)	23.37 (\pm 15.54)
50.95 °N	<i>Buccinum undatum</i>	38	0.756	9.66	3.33 (\pm 1.02)	16.35 (\pm 7.54)
67.34 °S	<i>Neobuccinum eatoni</i>	44	1.68	3.27	0.71 (\pm 0.21)	1.96 (\pm 0.54)
78.95 °N	<i>Buccinum</i> cf. <i>groenlandicum</i>	32	0.431	2.55	1.99 (\pm 1.05)	7.24 (\pm 4.27)
78.95 °N	<i>Buccinum glaciale</i>	49	1.24	7.65	1.37 (\pm 0.54)	6.99 (\pm 3.41)
Echinoids		Test diameter				
50.47 °N	<i>Psammechinus miliaris</i>	25	0.390	7.68	2.86 (\pm 0.96)	24.19 (\pm 8.38)
67.34 °S	<i>Sterechinus neumayeri</i>	27	1.14	1.65	1.06 (\pm 0.41)	1.38 (\pm 0.54)
Brachiopods		Shell length				
67.34 °S	<i>Liothyrella uva</i>	30	0.164	0.695	0.49 (\pm 0.31)	4.85 (\pm 2.99)

Table 5.4 Regression equations of Ln(MO2) on Ln(length) and Ln(MO2) on Ln(mass) for all species plotted on graphs below, where $y = mx + c$.

Species	Regression for	m	s.e. of m	c	r ²	F	df	p
<i>Laternula</i> clams								
<i>Laternula truncata</i>	Ln(MO2) v Ln(length)	1.5729 [#]	0.3847	-3.6035	0.3514	16.7145	1,28	0.0003
	Ln(MO2) v Ln(wet weight)	0.6339	0.1228	0.8496	0.4692	26.6364	1,28	<0.0001
	Ln(MO2) v Ln(dry mass)	0.5121	0.1357	1.8872	0.3135	14.2445	1,28	0.0008
	Ln(MO2) v Ln(AFDM)	0.6646	0.1591	2.9374	0.3619	17.4468	1,28	0.0003
<i>Laternula boschasina</i>	Ln(MO2) v Ln(length)	1.2257 [#]	0.8625	-2.9600	0.0536	2.0193	1,17	0.1734 NS
	Ln(MO2) v Ln(wet weight)	0.4546	0.2666	0.7522	0.0958	2.9069	1,17	0.1064 NS
	Ln(MO2) v Ln(dry mass)	0.4567	0.2818	1.4353	0.0829	2.6263	1,17	0.1235 NS
	Ln(MO2) v Ln(AFDM)	0.5614	0.2976	2.5298	0.1244	3.5584	1,17	0.0764 NS
<i>Laternula recta</i>	Ln(MO2) v Ln(length)	2.9148	0.2109	-9.8591	0.8755	148.7126	1,20	<0.0001
	Ln(MO2) v Ln(wet weight)	0.9935*	0.0618	-0.6490	0.9101	213.6643	1,20	<0.0001
	Ln(MO2) v Ln(dry mass)	0.9673*	0.0673	1.1289	0.9129	168.6995	1,15	<0.0001
	Ln(MO2) v Ln(AFDM)	0.8334	0.0673	2.2452	0.9079	119.3220	1,11	<0.0001
<i>Laternula elliptica</i>	Ln(MO2) v Ln(length)	2.5325 [#]	0.1437	-7.1831	0.9090	310.5423	1,30	<0.0001
	Ln(MO2) v Ln(wet weight)	0.8127	0.0367	-0.1741	0.9403	489.6135	1,30	<0.0001
	Ln(MO2) v Ln(dry mass)	0.7946	0.0438	1.1366	0.9135	328.5840	1,30	<0.0001
	Ln(MO2) v Ln(AFDM)	0.8353*	0.0369	1.7813	0.9429	513.1855	1,30	<0.0001
Buccinid gastropods								
<i>Cantharus fumosus</i>	Ln(MO2) v Ln(height)	2.0165 [#]	0.4636	-6.0999	0.3663	18.9186	1,30	0.0001
	Ln(MO2) v Ln(wet weight)	0.6649	0.1569	-0.1157	0.3535	17.9499	1,30	0.0002
	Ln(MO2) v Ln(dry mass)	0.6531	0.1592	0.0897	0.3381	16.8331	1,30	0.0003
	Ln(MO2) v Ln(AFDM)	0.5699	0.1173	1.5129	0.4296	23.5950	1,29	<0.0001
<i>Phos senticosus</i>	Ln(MO2) v Ln(height)	2.2619	0.4871	-7.1086	0.4235	21.5655	1,27	<0.0001
	Ln(MO2) v Ln(wet weight)	0.7798	0.1515	-0.2859	0.4765	26.4892	1,27	<0.0001
	Ln(MO2) v Ln(dry mass)	0.7532	0.1543	0.0498	0.4492	23.8394	1,27	<0.0001
	Ln(MO2) v Ln(AFDM)	0.5792	0.1013	1.5930	0.5308	32.6781	1,27	<0.0001

Table 5.4 continued.

Species	Regression for	m	s.e. of m	c	r ²	F	df	p
<i>Cominella lineolata</i>	Ln(MO2) v Ln(height)	2.0036	0.5509	-6.1794	0.3596	12.2288	1,19	0.0024
	Ln(MO2) v Ln(wet weight)	0.6656	0.1988	-0.3658	0.3194	10.3865	1,19	0.0045
	Ln(MO2) v Ln(dry mass)	0.6525	0.2098	-0.1294	0.2799	8.7734	1,19	0.0080
	Ln(MO2) v Ln(AFDM)	0.3513*	0.1914	0.8440	0.0553	2.1715	1,19	0.1570 NS
<i>Buccinum undatum</i>	Ln(MO2) v Ln(height)	2.2959 [#]	0.2252	-5.9430	0.7921	103.8935	1,26	<0.0001
	Ln(MO2) v Ln(wet weight)	0.7889	0.0687	0.8740	0.8288	131.7522	1,26	<0.0001
	Ln(MO2) v Ln(dry mass)	0.8435	0.0792	1.3489	0.8062	113.3242	1,26	<0.0001
	Ln(MO2) v Ln(AFDM)	0.6650	0.0577	2.5924	0.8298	132.6450	1,26	<0.0001
<i>Neobuccinum eatoni</i>	Ln(MO2) v Ln(height)	2.4196	0.3105	-7.9993	0.6655	60.6835	1,29	<0.0001
	Ln(MO2) v Ln(wet weight)	0.8888	0.1114	-1.1454	0.6761	63.6311	1,29	<0.0001
	Ln(MO2) v Ln(dry mass)	0.9492	0.1047	-0.3184	0.7367	82.1367	1,28	<0.0001
	Ln(MO2) v Ln(AFDM)	0.9527	0.1094	0.6417	0.7206	75.7861	1,28	<0.0001
<i>Buccinum glaciale</i>	Ln(MO2) v Ln(height)	1.6280 [#]	0.6070	-4.3008	0.3602	7.1936	1,10	0.0230
	Ln(MO2) v Ln(wet weight)	0.6499	0.1916	0.3606	0.4884	11.5021	1,10	0.0069
	Ln(MO2) v Ln(dry mass)	0.6584	0.2014	0.8394	0.4682	10.6851	1,10	0.0084
	Ln(MO2) v Ln(AFDM)	0.5860	0.1888	1.9104	0.4397	9.6332	1,10	0.0112
<i>Buccinum cf. groenlandicum</i>	Ln(MO2) v Ln(height)	1.3267 [#]	0.3734	-3.6639	0.3675	12.6214	1,19	0.0021
	Ln(MO2) v Ln(wet weight)	0.4079*	0.1215	0.3965	0.3393	11.2697	1,19	0.0033
	Ln(MO2) v Ln(dry mass)	0.4079*	0.1111	0.7533	0.3843	13.4857	1,19	0.0016
	Ln(MO2) v Ln(AFDM)	0.3809*	0.1261	1.2505	0.2888	9.1216	1,19	0.0070
Brachiopods								
<i>Liothyrella uva</i>	Ln(MO2) v Ln(length)	2.0736 [#]	0.2614	-7.4172	0.6399	57.8762	1,31	<0.0001
	Ln(MO2) v Ln(wet weight)	0.7146	0.0822	-1.2501	0.6823	69.7127	1,31	<0.0001
	Ln(MO2) v Ln(dry mass)	0.8240	0.0923	-0.7513	0.7196	70.3025	1,26	<0.0001
	Ln(MO2) v Ln(AFDM)	0.7574	0.0822	1.0068	0.7353	75.9834	1,26	<0.0001

Table 5.4 continued.

Species	Regression for	m	s.e. of m	c	r ²	F	df	p
Echinoids								
<i>Psammechinus miliaris</i>	Ln(MO2) v Ln(diameter)	2.1792 [#]	0.2044	-4.8674	0.7788	113.6728	1,31	<0.0001
	Ln(MO2) v Ln(wet weight)	0.7081	0.0629	0.7036	0.7974	126.9174	1,31	<0.0001
	Ln(MO2) v Ln(dry mass)	0.7271	0.0669	1.2893	0.7852	118.0080	1,31	<0.0001
	Ln(MO2) v Ln(AFDM)	0.6688	0.0614	2.7737	0.7863	118.7516	1,31	<0.0001
<i>Sterechinus neumayeri</i>	Ln(MO2) v Ln(diameter)	2.6648	0.1696	-8.2802	0.8984	213.2879	1,23	<0.0001
	Ln(MO2) v Ln(wet weight)	0.9407*	0.0601	-1.3511	0.9105	245.2766	1,23	<0.0001
	Ln(MO2) v Ln(dry mass)	1.0034*	0.0587	0.1042	0.9240	292.6485	1,23	<0.0001
	Ln(MO2) v Ln(AFDM)	1.0158*	0.0602	0.3720	0.9221	284.9791	1,23	<0.0001

[#] Ln(MO2) on Ln(length) slope was significantly different from 3.

* Ln(MO2) on Ln(mass) slope was significantly different from 0.75.

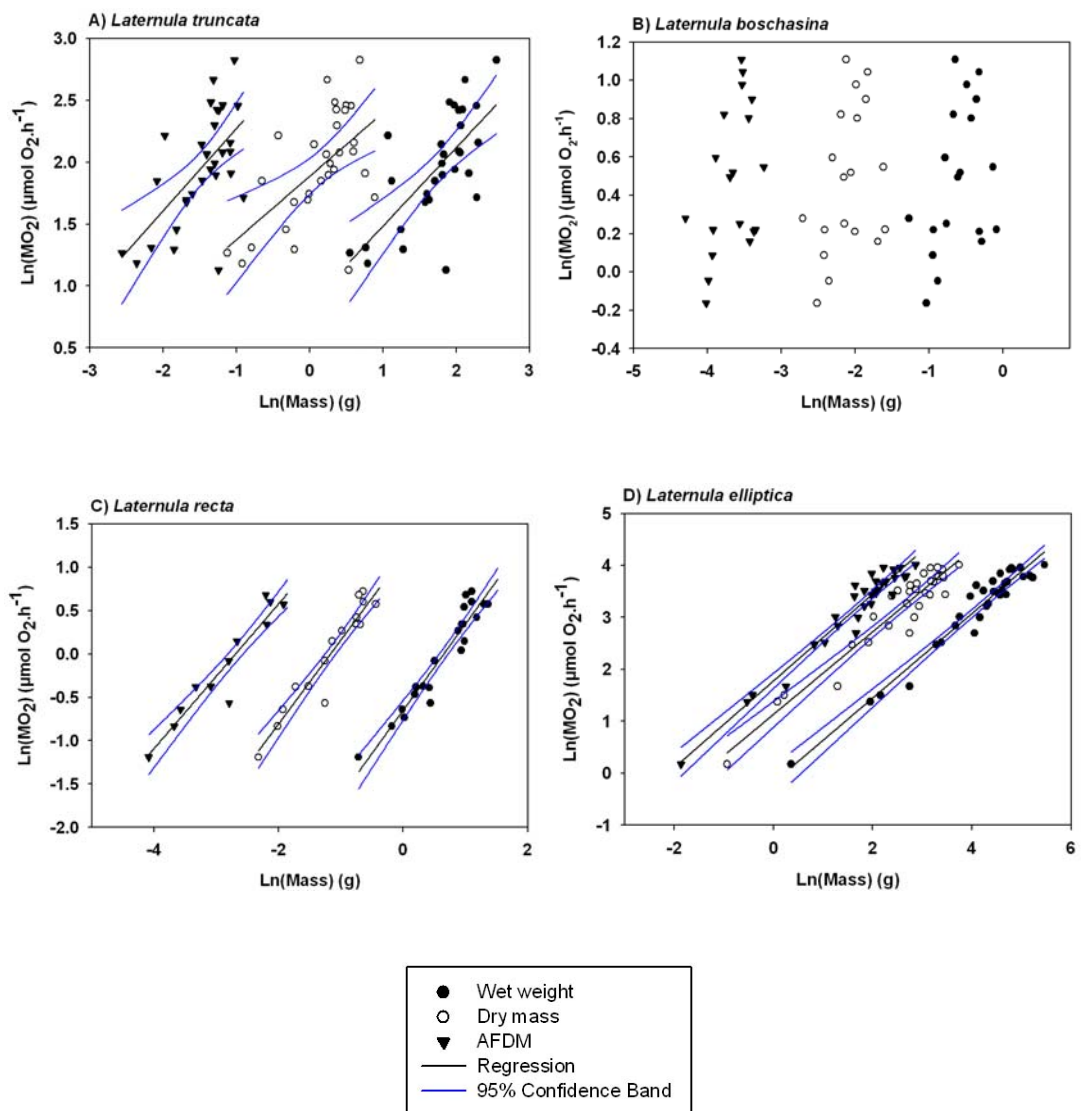


Figure 5.5 Regression of $\text{Ln}(\text{MO}_2)$ on $\text{Ln}(\text{Mass})$ for the clams A) *Laternula truncata*, B) *L. boschasina*, C) *L. recta* and D) *L. elliptica*. Regressions for *L. boschasina* were not significant because the size range of animal length was too small. Regression statistics and fits are given in Table 5.4.

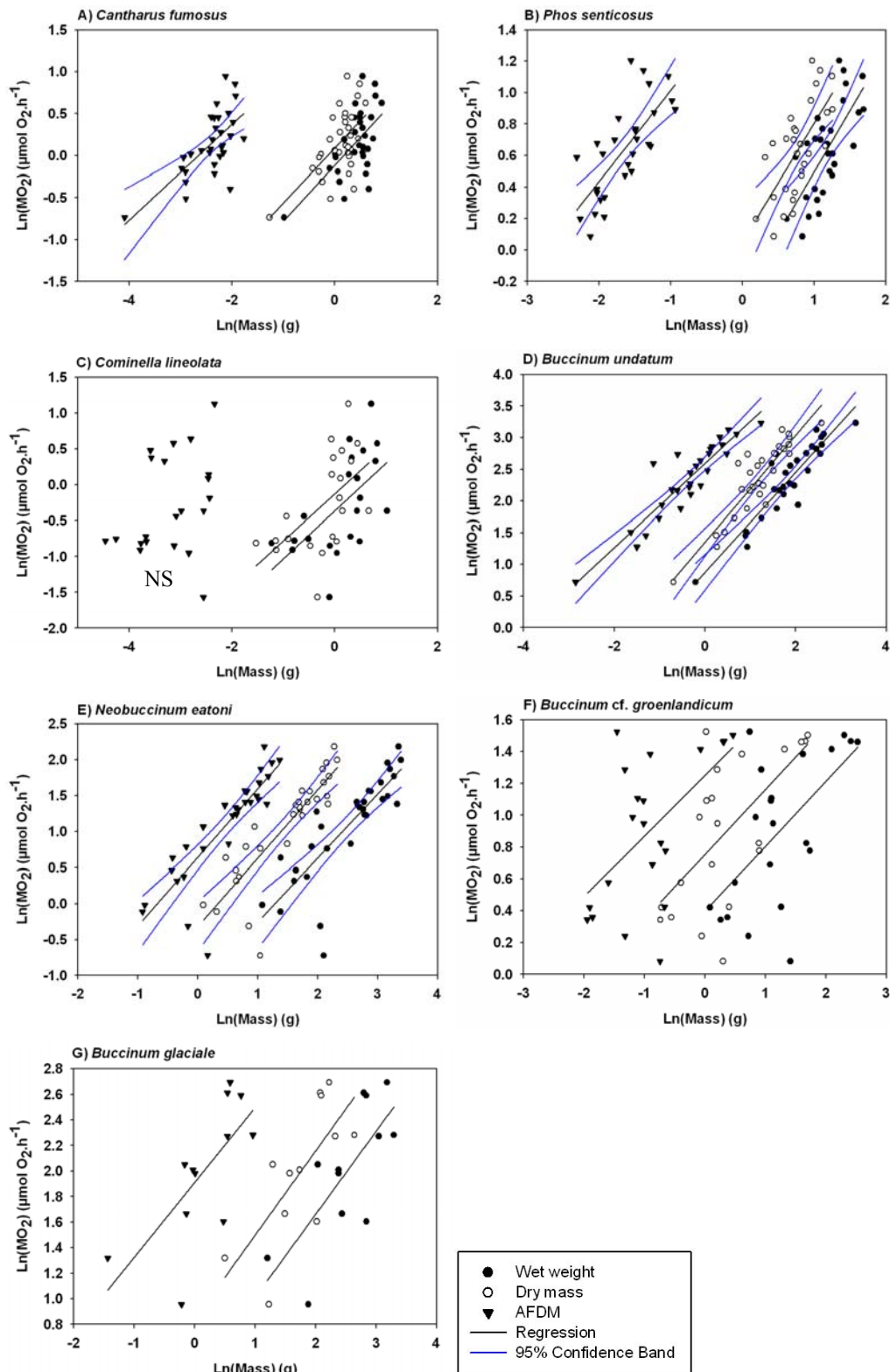


Figure 5.6 Regression of $\text{Ln}(\text{MO}_2)$ on $\text{Ln}(\text{Mass})$ for the buccinid gastropods A) *Cantharus fumosus*, B) *Phos senticosus*, C) *Cominella lineolata*, D) *Buccinum undatum*, E) *Neobuccinum eatoni*, F) *Buccinum cf. groenlandicum* and G) *Buccinum glaciale*.

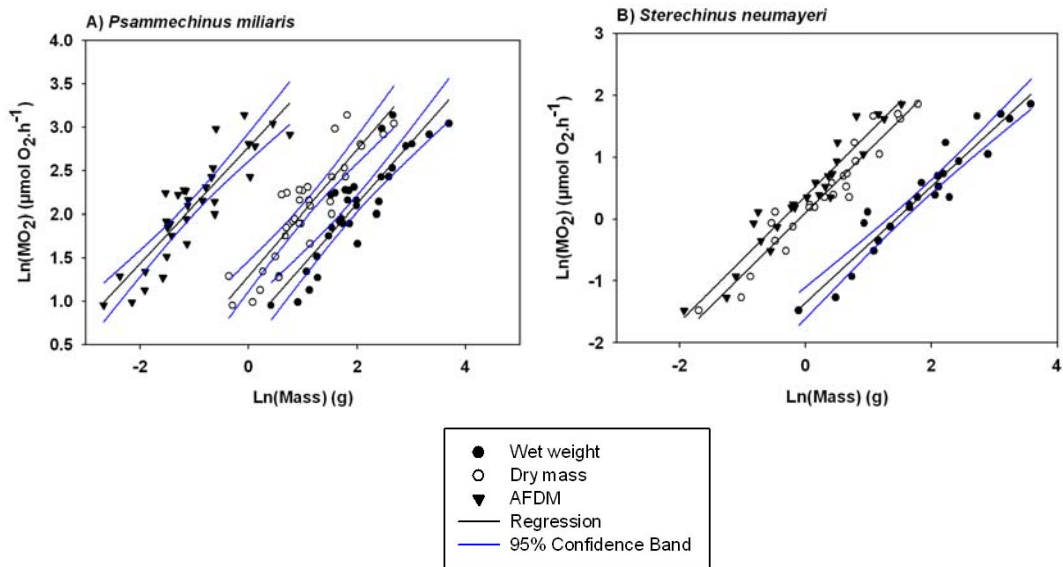


Figure 5.7 Regression of $\ln(\text{MO}_2)$ on $\ln(\text{Mass})$ for the echinoids A) *Psammechinus miliaris* and B) *Sterechnus neumayeri*.

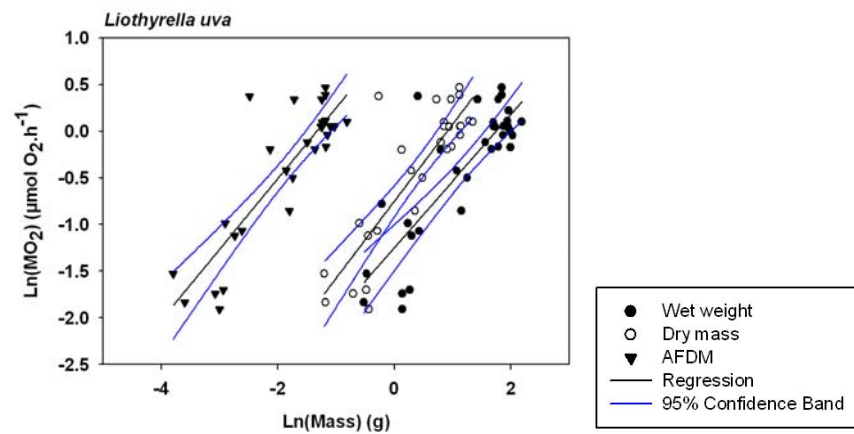


Figure 5.8 Regression of $\ln(\text{MO}_2)$ on $\ln(\text{Mass})$ for the brachiopod *Liothyrella uva*.

5.3.2 Latitudinal variation in respiration rate

5.3.2.1 Raw data (absolute values) uncorrected for size

Figure 5.9 to Figure 5.11 show data for all species studied within each major taxon. Regression line slopes are very similar for *Laternula* clams (Figure 5.9), but have different intercepts on the y axis. The tropical species *L. truncata* is shifted up with a higher intercept than the temperate and polar species. These trends are reflected in the size corrected data of mean respiration rates for *Laternula* clams (Figure 5.12).

Slopes of regression lines are reasonably similar for most buccinid species (Figure 5.10). Slopes are similar for the two echinoids studied with the temperate species clearly shifted above the polar species (Figure 5.11). *Psammechinus miliaris* clearly has a much higher respiration rate than *Sterechinus neumayeri*.

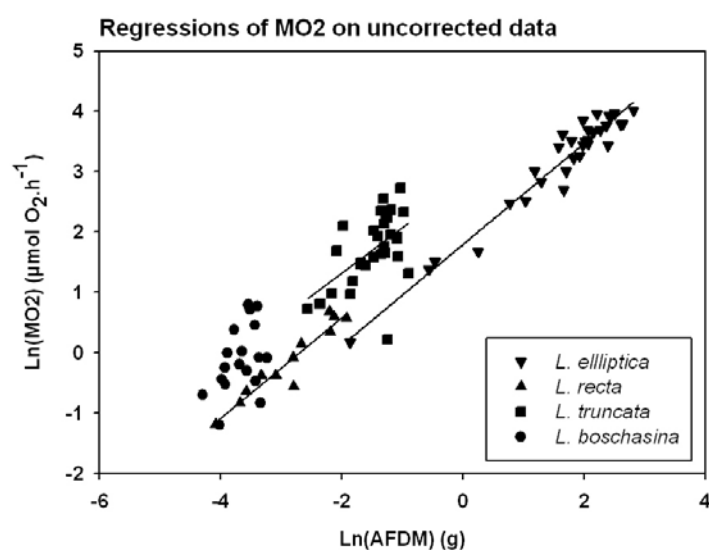


Figure 5.9 Regressions of Ln(MO₂) on Ln(AFDM) for *Laternula* clams. A standard size animal for *Laternula* species was chosen as -1.5 g Ln(AFDM), which is equivalent to 0.223 g AFDM.

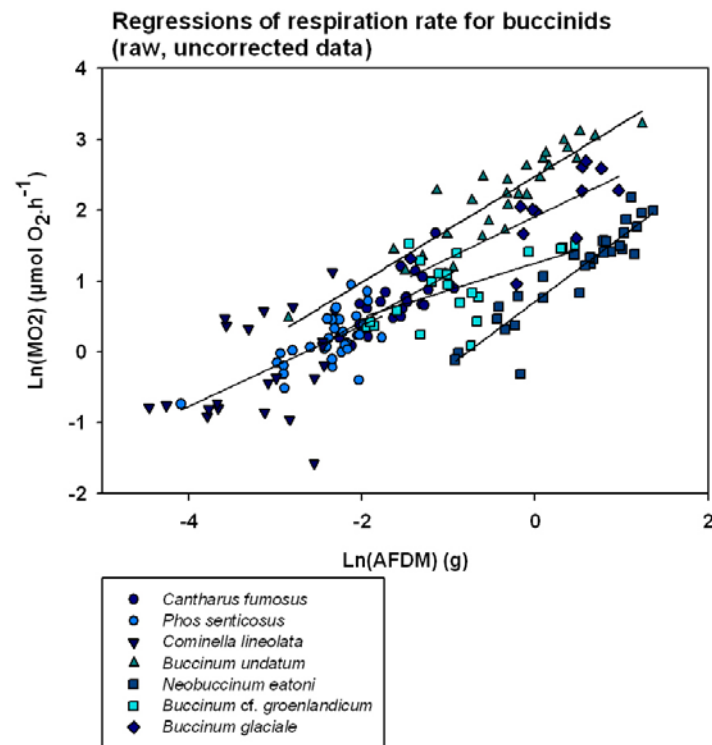


Figure 5.10 Regressions of Ln(MO₂) on Ln(AFDM) for buccinid gastropods. A standard size animal for buccinid gastropods was chosen as -1.5 g Ln(AFDM), which is equivalent to 0.223 g AFDM.

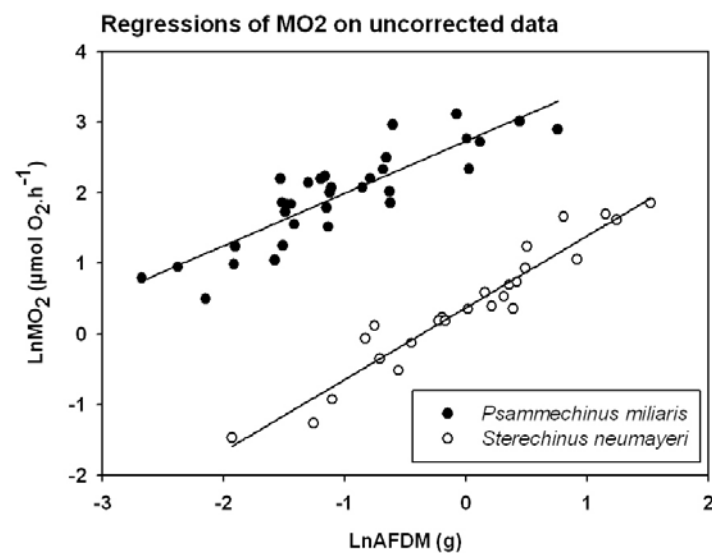


Figure 5.11 Regressions of Ln(MO₂) on Ln(AFDM) for Echinidae echinoids. A standard size animal for echinoids was chosen as -0.5 g Ln(AFDM), which is equivalent to 0.607 g AFDM.

5.3.2.2 Comparing standard sized animals

Standard size animal calculations

To compare respiration rates among species it was necessary to choose a standard sized animal that would be realistic for all species in the group. Methods for the correction of a parameter to that of a standard sized animal are given in Chapter 3. Regressions of $\text{Ln}(\text{MO}_2)$ on $\text{Ln}(\text{AFDM})$ were plotted and a standard animal size chosen; ideally overlapping the size range of all species. However, often a standard animal size had to be chosen which did not encompass the size range of at least one of the species studied. The oxygen consumption for a standard sized animal was then calculated for each group (bivalve clams, gastropod snails and echinoids) using significant individual regression equations for each species (Table 5.5). Note that since the regression for *L. boschasina* $\text{Ln}(\text{MO}_2)$ on $\text{Ln}(\text{AFDM})$ was not statistically significant (due to the restricted size range of individuals available (Table 5.4)), the mean slope of the statistically significant regression equations for the other three species of *Laternula* was used to correct for size in *L. boschasina* (mean slope = 0.808). For *Cominella lineolata*, which did not have a significant regression of $\text{Ln}(\text{MO}_2)$ on $\text{Ln}(\text{AFDM})$ (Table 5.4), the mean slope for all other buccinid gastropods that had significant regressions was used (mean slope = 0.643). Graphs are shown for standard animal oxygen consumption rates with latitude and temperature for both laternulid clams (Figure 5.12 and Figure 5.13) and buccinid gastropods (Figure 5.14 and Figure 5.15).

Table 5.5 Respiration rates of standard size animals. A standard size of 223 mg AFDM was used for laternulid clams and buccinid gastropods. The best standard animal size for comparing echinoids was 607 mg AFDM because this was near to the mean size for both species. Data were, however, also calculated for echinoderms of 223 mg AFDM (still within the size ranges studied) for the across phylum comparisons.

Latitude	Species	LnAFDM (g) of standard size animal	Equivalent size of standard animal (mm)	MO ₂ for an animal of mean length (μmol $\text{O}_2\cdot\text{h}^{-1}$) (2 d.p.)
Laternula clams			Shell length	
1.22 °N	<i>L. truncata</i>	-1.5 (223 mg)	40.0	6.03 (\pm 2.60)
1.22 °N	<i>L. boschasina</i>	-1.5 (223 mg)	33.8	6.05 (\pm 3.00)
37.49 °S	<i>L. recta</i>	-1.5 (223 mg)	41.5	2.74 (\pm 0.45)
67.34 °S	<i>L. elliptica</i>	-1.5 (223 mg)	21.9	1.75 (\pm 0.37)
Buccinid gastropods			Shell height	
19.13 °S	<i>Cantharus fumosus</i>	-1.5 (223 mg)	27.4	2.01 (\pm 0.58)
19.13 °S	<i>Phos senticosus</i>	-1.5 (223 mg)	31.7	2.20 (\pm 0.60)
37.49 °S	<i>Cominella lineolata</i>	-1.5 (223 mg)	25.5	2.73 (\pm 1.70)
50.95 °N	<i>Buccinum undatum</i>	-1.5 (223 mg)	27.3	4.04 (\pm 1.12)
67.34 °S	<i>Neobuccinum eatoni</i>	-1.5 (223 mg)	20.9	0.53 (\pm 0.12)
78.95 °N	<i>Buccinum</i> cf. <i>groenlandicum</i>	-1.5 (223 mg)	26.1	2.12 (\pm 0.84)
78.95 °N	<i>Buccinum glaciale</i>	-1.5 (223 mg)	28.2	2.98 (\pm 0.96)
Echinoids			Test diameter	
50.47 °N	<i>Psammechinus miliaris</i>	-0.5 (607 mg)	28.8	11.16 (\pm 3.66)
67.34 °S	<i>Sterechinus neumayeri</i>	-0.5 (607 mg)	21.3	0.90 (\pm 0.23)
Echinoid data for comparison with other taxa				
50.47 °N	<i>Psammechinus miliaris</i>	-1.5 (223 mg)	20.9	5.32 (\pm 1.75)
67.34 °S	<i>Sterechinus neumayeri</i>	-1.5 (223 mg)	14.6	0.33 (\pm 0.08)

***Laternula* clams**

Data for *Laternula* species standard animal respiration rate did not have equal variances so Welch's F test (Welch, 1951) was used to test for differences in respiration rate among species. There was a significant difference in size corrected respiration rate among *Laternula* species (Welch's $F = 49.873$, $df_1 = 3$, $df_2 = 35.231$, $p < 0.001$, $n = 93$) (Figure 5.12). Post hoc comparisons using the Games-Howell procedure (appropriate for groups with unequal variances) showed the respiration rates of all species were significantly different from each other ($p \leq 0.001$) with the exception of the two Singapore species *L. truncata* and *L. boschasina* ($p > 0.05$ NS). Respiration rates varied with latitude as a function of temperature (Figure 5.13). Q_{10} values for standard size *Laternula* species were calculated from rates taken from Table 5.3 (above) and temperatures used were the *in situ* temperatures measured during the MO₂ experiments. Q_{10} values were 1.40 to 1.66 (Table 5.6) for standard sized animals.

Table 5.6 Q_{10} values for *Laternula* species of a standard size of 223 mg AFDM at temperatures for which MO₂ was calculated.

AFDM	Species at upper temperature	Upper temperature (°C)	Species at lower temperature	Lower temperature (°C)	Q_{10} (2 d.p.)
223 mg	<i>L. truncata</i>	29.9	<i>L. recta</i>	14.2	1.65
223 mg	<i>L. truncata</i>	29.9	<i>L. elliptica</i>	0.74	1.53
223 mg	<i>L. boschasina</i>	29.9	<i>L. recta</i>	14.2	1.66
223 mg	<i>L. boschasina</i>	29.9	<i>L. elliptica</i>	0.74	1.53
223 mg	<i>L. recta</i>	14.2	<i>L. elliptica</i>	0.74	1.40

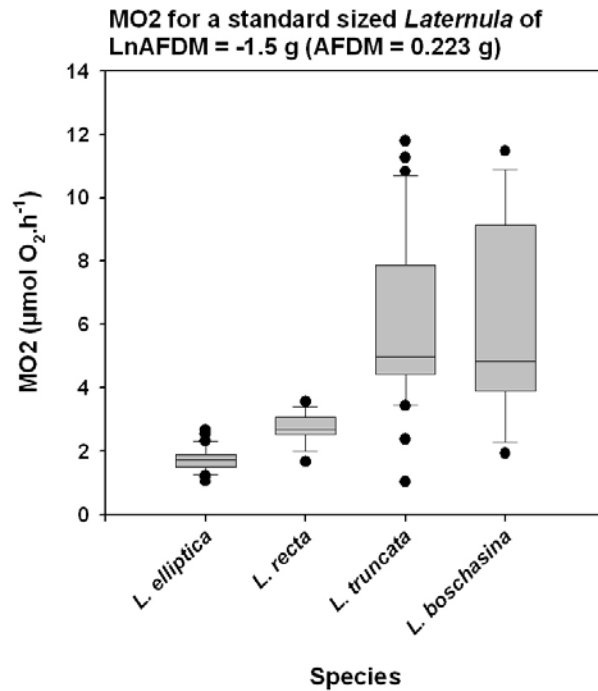


Figure 5.12 Standard animal mean respiration rates for *Laternula* species from tropical, temperate and polar latitudes. Data points beyond the 10th and 90th percentiles are displayed as dots.

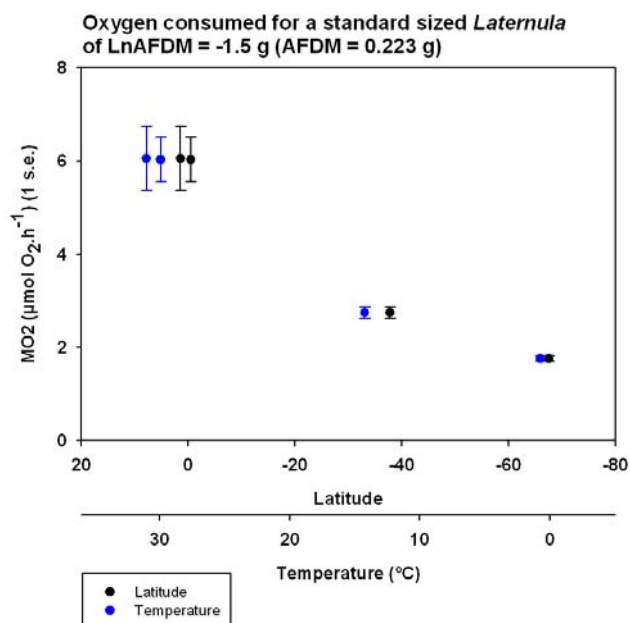


Figure 5.13 Trend in standard animal mean respiration rate for *Laternula* clams with latitude and temperature. The two tropical species *L. truncata* and *L. boschasina* from the same location are slightly offset to aid viewing.

Buccinid gastropods

Data for different buccinid gastropod species standard animal respiration rates did not have equal variances. There was a significant difference in size-corrected respiration rate among buccinid species studied (Welch's $F = 127.814$, $df1 = 6$, $df2 = 55.556$, $p < 0.001$, $n = 172$) (Figure 5.14). Post hoc comparisons using the Games-Howell procedure showed the respiration rate of *Neobuccinum eatoni* was significantly lower than all other species ($p \leq 0.001$). Species from the same locations (i.e. the 2 tropical species and 2 Arctic species) were not significantly different to each other ($p > 0.05$ NS). Q_{10} values for buccinid species studied ranged from 0.48 to 200.01 for standard sized animals (Table 5.7).

Figure 5.15 shows that buccinid gastropod respiration rate decreased from temperate to polar latitudes in both the Northern and Southern Hemispheres. The Arctic species studied here were investigated in Svalbard where shallow-water sea temperatures are significantly warmer (i.e. sub-Arctic) compared to most other sites of similar latitude in the Arctic because of the Gulf Stream. The temperature plot shows how, for a standard buccinid, metabolic rates decreased with decreasing temperature (Figure 5.15). The exceptions to this are the two tropical species, which were the only emerged intertidal species studied⁴.

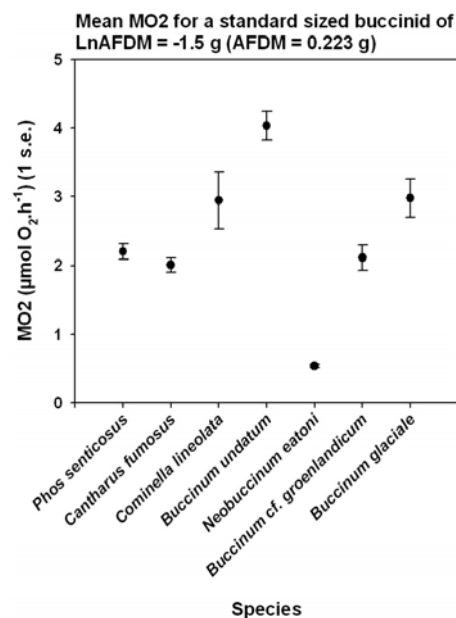


Figure 5.14 Buccinid standard animal mean respiration rates for each species.

⁴ *Cominella lineolata* is intertidal, but inhabits rock pools and is not frequently emerged.

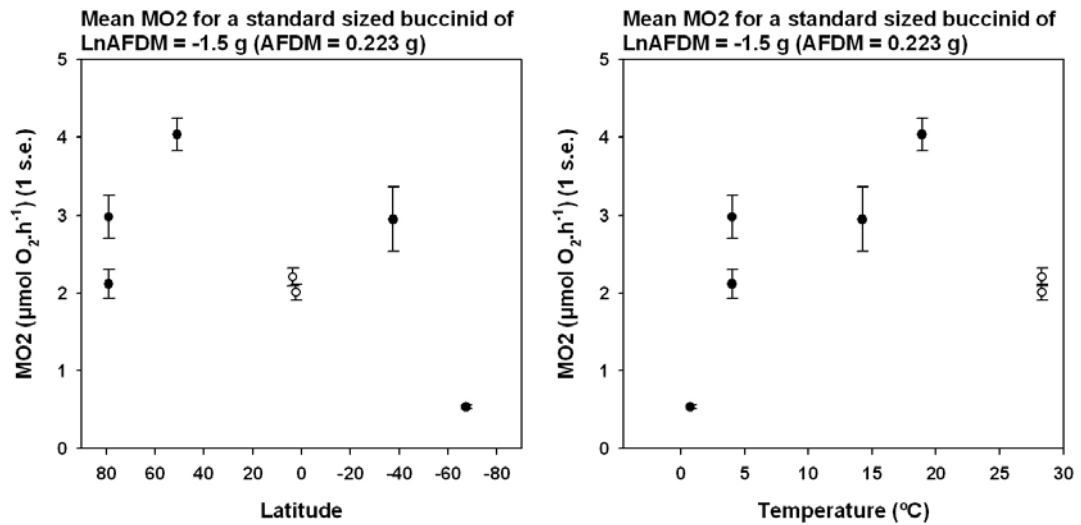


Figure 5.15 Buccinid gastropod standard animal mean respiration rates plotted with latitude (left) (negative values of latitude are in the Southern Hemisphere) and temperature (right). Tropical species are plotted with open symbols to show their different life habit.

Table 5.7 Q10 values for standard size buccinid gastropods of 223 mg AFDM.

AFDM	Species at upper temp.	Upper temp. (°C) (1 d.p.)	Species at lower temp.	Lower temp. (°C) (1 d.p.)	Q ₁₀ (2 d.p.)
223 mg	<i>Cantharus fumosus</i>	28.3	<i>Buccinum undatum</i>	18.9	0.48
223 mg	<i>Cantharus fumosus</i>	28.3	<i>Cominella lineolata</i>	14.2	0.80
223 mg	<i>Cantharus fumosus</i>	28.3	<i>Buccinum cf. groenlandicum</i>	4.0	0.98
223 mg	<i>Cantharus fumosus</i>	28.3	<i>Buccinum glaciale</i>	4.0	0.85
223 mg	<i>Cantharus fumosus</i>	28.3	<i>Neobuccinum eatoni</i>	0.7	1.62
223 mg	<i>Phos senticosus</i>	28.3	<i>Buccinum undatum</i>	18.9	0.53
223 mg	<i>Phos senticosus</i>	28.3	<i>Cominella lineolata</i>	14.2	0.86
223 mg	<i>Phos senticosus</i>	28.3	<i>Buccinum cf. groenlandicum</i>	4.0	1.02
223 mg	<i>Phos senticosus</i>	28.3	<i>Buccinum glaciale</i>	4.0	0.88
223 mg	<i>Phos senticosus</i>	28.3	<i>Neobuccinum eatoni</i>	0.7	1.68
223 mg	<i>Buccinum undatum</i>	18.9	<i>Cominella lineolata</i>	14.2	2.30
223 mg	<i>Buccinum undatum</i>	18.9	<i>Buccinum cf. groenlandicum</i>	4.0	1.54
223 mg	<i>Buccinum undatum</i>	18.9	<i>Buccinum glaciale</i>	4.0	1.23
223 mg	<i>Buccinum undatum</i>	18.9	<i>Neobuccinum eatoni</i>	0.7	3.06
223 mg	<i>Cominella lineolata</i>	14.2	<i>Buccinum cf. groenlandicum</i>	4.0	1.28
223 mg	<i>Cominella lineolata</i>	14.2	<i>Buccinum glaciale</i>	4.0	0.92
223 mg	<i>Cominella lineolata</i>	14.2	<i>Neobuccinum eatoni</i>	0.7	3.37
223 mg	<i>Buccinum cf. groenlandicum</i>	4.0	<i>Neobuccinum eatoni</i>	0.7	70.21
223 mg	<i>Buccinum glaciale</i>	4.0	<i>Neobuccinum eatoni</i>	0.7	200.01

Echinoids: family Echinidae

For standard animal size corrected data, there was a significant difference in respiration rate between the temperate echinoid *Psammechinus miliaris* and the polar echinoid *Sterechinus neumayeri* ($t = 16.041$, $df = 32.429$, $p < 0.001$) (Figure 5.16). The temperate echinoid *P. miliaris* has a mean respiration rate of $11.159 (\pm 3.662 \text{ (1 s.d.)}) \mu\text{mol O}_2\cdot\text{h}^{-1}$. The Antarctic echinoid *S. neumayeri* has a mean respiration rate of $0.900 (\pm 0.245 \text{ (1 s.d.)}) \mu\text{mol O}_2\cdot\text{h}^{-1}$. The temperate echinoid respiration rate was an order of magnitude greater than the Antarctic echinoid respiration rate. Q_{10} values for the two Echinidae species studied were 4.00 (Table 5.8) for standard sized animals

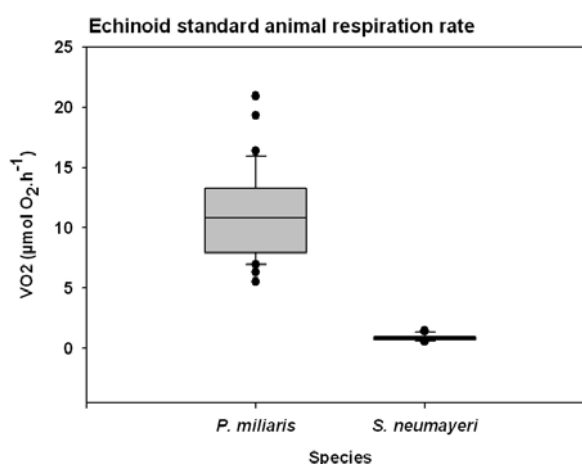


Figure 5.16 Respiration rate for a temperate and polar echinoid for a standard animal of 607 mg AFDM. Data points beyond the 10th and 90th percentiles are displayed as dots.

Table 5.8 Q_{10} values for standard size Echinidae echinoids of 607 mg AFDM.

AFDM	Species at upper temperature	Upper temperature (°C)	Species at lower temperature	Lower temperature (°C)	Q_{10} (2 d.p.)
607 mg	<i>Psammechinus miliaris</i>	18.92	<i>Sterechinus neumayeri</i>	0.74	4.00

Summary respiration data

Trends in standard animal mean respiration rate for *Laternula* bivalves, buccinid gastropods and Echinidae echinoids are shown in Figure 5.17. For these closely related species, respiration rate increased as ambient temperature increased. The exception was the tropical gastropods that had lower respirations rates than may be expected. However, these tropical species were intertidal and having a low respiration rate may be an adaptation to periods of emersion.

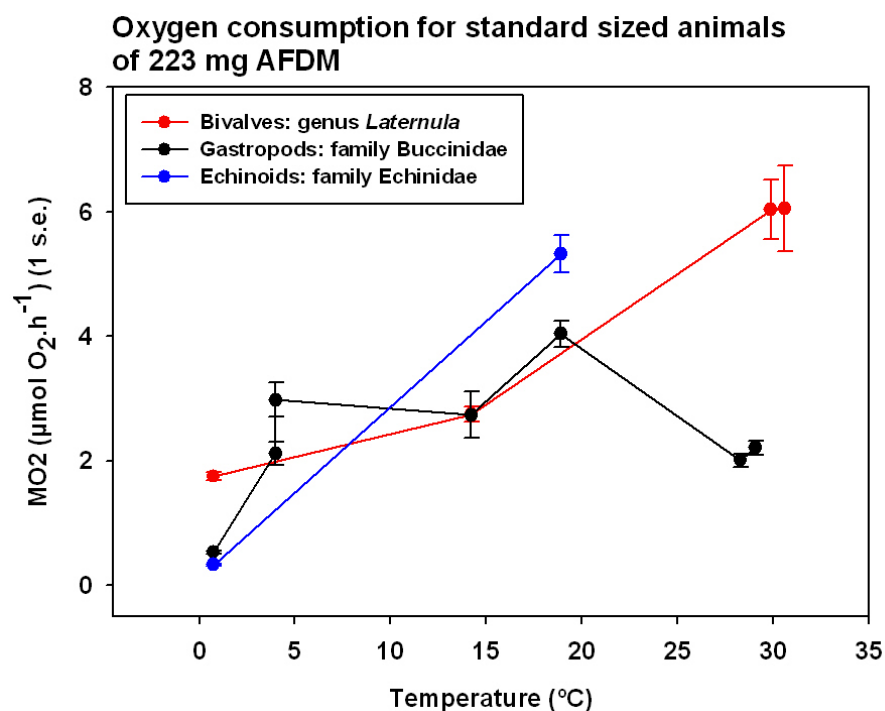


Figure 5.17 Summary of trends in standard animal (AFDM = 223 mg for all species) mean respiration rate for each group with temperature, where the mean is the average calculated following the conversion of all individual respiration rates to that for a standard animal.

5.4 Discussion

Latitudinal gradients in metabolic rates and comparisons

Metabolic rates in marine ectotherms decrease with temperature and since the planetary temperature gradient of marine surface water habitats is generally a function of latitude, it is expected that the metabolic rate of closely related shallow water marine ectotherms would decrease with increasing latitude. The metabolic rates of the majority of species in this study had not previously been measured. Of those that had, the data obtained from this study are also compared to literature values.

Metabolic rate decreased along a gradient of increasing latitude (and decreasing temperature) in species of *Laternula* clam. Polar marine ectotherms have low metabolic rates (Clarke & Johnston, 1999; Peck & Conway, 2000; Peck, 2002) and data from this study show the polar clam had the lowest metabolic rate when corrected for a standard sized animal. The polar summer standard metabolic rate (SMR) for a 50 mm length *L. elliptica* was $15.24 \mu\text{mol O}_2\text{h}^{-1}$. This was similar to the summer respiration rates of $19.2 \mu\text{mol O}_2\text{h}^{-1}$ found for a non-starved (kept in the aquarium for 1 – 5 days) 50 mm shell length *L. elliptica* by Morley *et al.* (2007a). *L. elliptica* respiration rates in this study were higher, however, than the summer rate found by Brockington (2001) of $12.9 \mu\text{mol O}_2\text{h}^{-1}$ for a non-starved (kept in the aquarium for 4 days) 50 mm shell length individual. Individuals in this study were fasted, so it is expected that they would have lower oxygen consumption rates than those that had not been fasted.

Considering confamilial buccinid gastropods from the Northern and Southern Hemispheres separately, metabolic rate decreased with increasing latitude (with the exception of the tropical buccinids). However, Northern Hemisphere buccinids had higher metabolic rates than Southern Hemisphere buccinids for similar latitudes. This was likely to be because all of the Northern Hemisphere buccinids were influenced by the Gulf Stream, which creates warmer water than may be expected for a given latitude in the north Atlantic. Metabolic rates of buccinid gastropods were positively related to temperature (Figure 5.15), with the exception of the tropical gastropods. There are two explanations for the lower metabolic rate of the tropical buccinids: 1) they are intertidal species, and 2) they may have been

starved for too long. These intertidal species have to deal with aerobic respiration stress at very low spring tides (c. 0.3 m) when they are briefly exposed. Intertidal gastropods can exhibit anaerobic respiration (Vermeij, 1973; Sokolova & Pörtner, 2001). If they exhibited a proportion of anaerobic respiration this could be why their aerobic respiration rates were lower than expected, although anaerobic respiration may account for only 1-2 % of ATP turnover (Sokolova & Pörtner, 2001). The temperate intertidal gastropod *Cominella lineolata* does not have a low respiration rate, but this species inhabits rock pools and so is not frequently exposed. Possibly, the more likely explanation for the tropical buccinid low MO_2 is that they were starved for longer than was ideal. The specific dynamic action (SDA) is the rise in metabolism exhibited by animals following feeding (Peck, 1998). The SDA determines how long a feeding event affects metabolic rates, and these are much shorter in warm-water species than cold-water species. As the length of the SDA in the tropical buccinids was not known, they may have been starved to the point where they were in a lower metabolic state than other species from cooler environments (Peck, 1998). Their metabolic rates may be lower than expected because of this increased fasting period.

The Antarctic buccinid *Neobuccinum eatoni* had the lowest respiration rate of the buccinids studied at $0.521 \mu\text{mol O}_2 \cdot \text{h}^{-1}$ for a 0.98 g soft tissue dry mass individual and $0.863 \mu\text{mol O}_2 \cdot \text{h}^{-1}$ for a 1.7 g soft tissue dry mass individual. This is lower than the metabolic rate found for *Trophon longstaffi* of $18.1 \mu\text{g O}_2 \cdot \text{h}^{-1}$ ($= 0.566 \mu\text{mol O}_2 \cdot \text{h}^{-1}$) for a 0.98 g tissue dry mass individual to $46.2 \mu\text{g O}_2 \cdot \text{h}^{-1}$ ($= 1.44 \mu\text{mol O}_2 \cdot \text{h}^{-1}$) for a 1.7 g tissue dry mass individual (Harper & Peck, 2003). The metabolic rate of *N. eatoni* is possibly the lowest so far reported for a gastropod mollusc.

Metabolic rate for the confamilial echinoids was much lower in the polar species than in the temperate species. The respiration rate of *Psammechinus miliaris* in this study was $2.86 (\pm 0.96) \mu\text{mol O}_2 \cdot \text{h}^{-1} \cdot \text{g}^{-1}$ dry mass which was higher than $0.47 \mu\text{mol O}_2 \cdot \text{h}^{-1} \cdot \text{g}^{-1}$ dry mass found by Otero-Villanueva *et al.* (2004). These differences are large, but can be explained in part since the *P. miliaris* in Otero-Villanueva *et al.* (2004) were starved for two weeks, which was twice as long as this study. Their experiments were also run at lower temperatures of 9 to 14 °C compared to the 18.9 °C used here. Data for *Sterechinus neumayeri* from this study are similar to data for *S. neumayeri* summer metabolic rates

from Brockington & Peck (2001) of $1.44 - 1.62 \mu\text{mol O}_2\text{h}^{-1}$ in summer for a non-fasted 24.4 mm test diameter individual. Data from this study show fasted individual of *S. neumayeri* with a test diameter of 24.4 mm consumes slightly less oxygen at $1.26 \mu\text{mol O}_2\text{h}^{-1}$.

Unfortunately there are no comparable data in the literature for the brachiopod *Liothyrella neozelanica*, and it was not possible to measure MO₂ for this species, so latitudinal differences in MO₂ for the genus *Liothyrella* could not be assessed. Oxygen consumption rates from this study for *L. uva* are close to, but at the high end of, values reported in previous work (Peck *et al.*, 1986a; Peck *et al.*, 1986b; Peck *et al.*, 1987b; Peck, 1989; 1996; Peck *et al.*, 1997a). Peck (1996) found a 290 mg AFDM *L. uva* starved for 25 days had a respiration rate of $0.64 \mu\text{mol O}_2\text{h}^{-1}$ and, after feeding, had a rate of $0.97 - 1.06 \mu\text{mol O}_2\text{h}^{-1}$. Data from this chapter found a 290 mg AFDM *L. uva* would be 36.2 mm in length and if starved for 21 days would have consumed $1.06 \mu\text{mol O}_2\text{h}^{-1}$. A possible reason for these differences could be different techniques for measuring oxygen concentration in seawater. Peck *et al.* (1986b; 1987b) used a microwinkler technique and Peck (1989; 1996) and Peck *et al.* (1997a) used coulometric methods based on Peck and Uglow (1990) to measure oxygen usage in *L. uva*. In this study the Fibox-3 was used for the first time to measure respiration rates of *L. uva*. Interestingly, among the Antarctic species measured, *L. uva* had the lowest mass specific MO₂ in terms of total animal dry mass, but the highest mass specific MO₂ in terms of total animal AFDM. As there are seasonal changes in the soft tissue AFDM in *L. uva* (Peck & Holmes, 1989) some of the difference in *L. uva* MO₂ in this study compared to others, could be because of slight variation in time of year (i.e. between different months in summer).

Scaling and Q₁₀ values

On logarithmic plots, metabolic rate scaled with body mass with slopes of 0.35 to 1.0 (2 s.f.) among all animals studied. The average slope was 0.71 (2 s.f.) for all species, which is close to the $\frac{3}{4}$ power scaling relationship between metabolic rate and body mass is exhibited by a wide range of animals (Schmidt-Nielsen, 1990; Randall *et al.*, 1997; Gillooly *et al.*, 2001; West *et al.*, 2003; Savage *et al.*, 2004; West & Brown, 2005). Ten out of 42 slopes were significantly different from 0.75 (Table 5.4), and 16 were

significantly different from 0.66 (the surface area to volume ratio). Therefore, most slopes were closest to the 0.75 power scaling relationship.

The idea behind the theory of metabolic cold adaptation (MCA) (Scholander *et al.*, 1953; Wohlschlag, 1964) was that metabolic rates of cold water ectotherms living near 0 °C should be elevated to compensate for the physiological constraints caused by living at these low temperatures (Krogh, 1916). If metabolic rates are truly elevated at low temperatures, Q_{10} values should progressively decrease with decreasing temperature (Peck & Conway, 2000) as cold compensation would reduce differences between polar and cool temperate species.

Q_{10} values were all very similar among species of *Laternula* ranging from 1.40 – 1.66. These Q_{10} values are low compared to those reported previously for oxygen consumption and temperature comparisons across latitudes (e.g. Peck & Conway, 2000). The usual effect of temperature on biological processes is a doubling to trebling of rate for each 10 °C rise in temperature ($Q_{10} = 2-3$) (Clarke, 1983). These data are, therefore, low compared to expected values. Interestingly, however, the Q_{10} values here are similar too, but slightly higher than the burrowing rate index (BRI) Q_{10} values obtained by Morley *et al.* (2007b) of 1.0 – 1.2 for *Laternula* species. The Morley *et al.* (2007b and unpublished data) values were for burrowing in *Laternula* species from tropical through temperate to polar latitudes. The fact that low Q_{10} values were obtained in both physiological metrics for *Laternula* species across latitudes suggests they may be unusually insensitive to temperature effects compared to other groups. Among the buccinid gastropods Q_{10} values increased at lower temperatures. This same trend was found in bivalves by Peck and Conway (2000) and suggests that metabolic rates of polar ectotherms may be even lower than would be expected than if rates were extrapolated from temperate groups. Metabolic rates of polar ectotherms are now considered not to be elevated (Clarke, 1983) and this study provides no evidence of MCA.

Limitations

Metabolic data were collected in summer in the UK at 18.9 °C and winter in temperate Australia at 14.2 °C. Temperatures in the National Oceanography Centre, Southampton

aquarium were 1 °C higher than maximum summer seawater temperatures for Southampton Water and temperatures in the Zoology Department aquarium at the University of Melbourne were 2 °C higher than minimum winter seawater temperatures for Port Phillip Bay. Average annual seawater temperature for southern England is 12.6 °C and for Melbourne, Australia is 16.3 °C. Therefore, respiration rates found for UK species may be slightly higher than expected based on an annual mean average seawater temperature, and those for southern Australian species may be slightly lower on average.

Summary

Overall data show that among closely related species metabolic rate decreases with increasing latitude, most likely as a direct result of the decreasing planetary temperature gradient. The only exceptions were the tropical intertidal gastropods, which may have different metabolic adaptations for surviving exposure on spring low tides. This decrease in metabolic rate with latitude could have implications for the total energy budget and the amount of energy available to partition into shell growth and the next chapter will analyse differences in shell growth and cost among latitudes.

Chapter 6: Growth and the cost of shell production



Chapter 6:

Growth and the cost of shell production

6.1 Introduction

Growth and age determination

Growth can be defined as the change of body mass with time and can be negative as well as positive, for example, during periods of starvation (Brey, 1999). Hard tissues such as shells and skeletons are often studied to determine age and growth rates of organisms, and this field of research is called sclerochronology. Sclerochronology is defined as “the study of physical and chemical variations in the accretionary hard tissues of organisms, and the temporal context in which they formed” (Jones *et al.*, 2007).

Growth bands, also known as growth checks, growth increments, growth lines or biochecks, are produced in calcareous skeletal structures by the deposition of material of a different density or structure (Dahm & Brey, 1998) and usually mark a period of slower growth in the shell. Growth bands are formed annually in the Antarctic bivalves *Laternula elliptica* (Brey & Mackensen, 1997) and *Yoldia eightsi* (Nolan & Clarke, 1993; Peck & Bullough, 1993). Growth bands are also formed annually in echinoderms including the temperate echinoid *Echinus esculentus* (Gage, 1992) and the Antarctic echinoid *Sterechinus neumayeri* (Brey *et al.*, 1995), and are thought to be formed annually in the deep-sea urchin *Echinus affinis* (Gage & Tyler, 1985). The Antarctic brachiopod *Liothyrella uva* may be unusual in that it was shown to deposit growth bands every 1.84 years (Peck & Brey, 1996); however, this is under debate.

Growth bands are less easy to determine in the shells of coiled gastropods, but can be determined from growth striae (fine rings) on the operculum. Growth striae form annually in *Buccinum undatum* (Santarelli & Gros, 1985), *Buccinum isaotakii* (Ilano *et al.*, 2004) and *Coralliophila violacea* (Chen & Soong, 2002). Statolith rings and Mg:Ca have also been used to age gastropods (Richardson *et al.*, 2005).

Cost of shell production

While many studies have focused on growth of shells and other hard parts, few have attempted to determine the cost of shell production. As shells are predominantly inorganic structures, calculating the cost of their production is difficult because they do not have a calorific content, unlike soft tissues. Palmer (1992) calculated an estimate for the cost of shell production in gastropods by measuring the additional food consumed by thick-shelled individuals among naturally variable populations of two temperate congeners. Palmer (1992) estimated the cost of CaCO_3 deposition to be $1\text{--}2 \text{ J.mg}^{-1}$ of CaCO_3 . This additional piece of information enables calculations of shell cost described in this chapter.

6.1.1 Aims and Hypothesis

This chapter has two main aims. First, it provides data on growth rates for key species and second, using metabolic data from Chapter 5, it provides estimates of the relative (or proportional) cost of shell production as a percentage of the total energy budget for species studied. Annual growth cost was measured in tissue and shell using von Bertalanffy growth function (VBGF) analyses, shell increment analyses and tissue energy content. The theoretical extra cost of shell production at high latitudes caused by the change in solubility of CaCO_3 was calculated.

Hypothesis 1: Warmer water species will have faster growth rates than cooler water species.

H₀: There is no evidence of a latitudinal gradient in growth rate.

Hypothesis 2: Colder water species have lower metabolic rates, so the cost of shell production as a proportion of the annual total energy budget (I) of each species will increase with increasing latitude or decreasing temperature.

H₀: There is no evidence of a latitudinal or temperature gradient in the cost of shell production.

6.2 Methods

6.2.1 Growth bands – age determination and growth models

Morphological measurements of animals were taken following the methods outlined in Chapter 3. To measure growth increments on bivalves and brachiopods, the shell size was measured at each growth band along the growth axis. For species of *Laternula* clams, shell height (along the dorso-ventral axis perpendicular to maximum length (see Chapter 3)) was measured with digital callipers to the nearest 0.01 mm for each growth band.

Growth increments were measured on the brachial (dorsal) valve of brachiopods because the foramen in the pedicle (ventral) valve obscures early growth bands. There is also often significant wear around this part of the shell that removes early growth bands. Brachial valve length from the posterior to the growth increment was measured along the axis of maximum growth with digital callipers to the nearest 0.01 mm for each growth band. Pedicle valve against brachial valve regressions are included in the results to facilitate comparable measurements from the literature (i.e. aging of brachiopods of the same species where pedicle valve length is known but not brachial valve length). Growth bands in the Antarctic brachiopod *Liothyrella uva* were shown to be formed every 1.84 years (Peck & Brey, 1996), however, there is debate on this point and data here are presented as annual bands. Data can be converted to 1.84 year growth increments later if necessary.

Growth bands (striae or furrows) on the operculum are formed annually in the Buccinoidea (Santarelli & Gros, 1985; Ilano *et al.*, 2004). It is thus possible to use the number of operculum striae to determine age. The total number of striae on each operculum was counted and the total length of the shell measured.

Growth curves

Growth equations provide methods for predicting growth from a set of biometric measurements. The shell measurement along the shell growth axis dimension (GAD) (perpendicular to the growth bands) (i.e. shell height in bivalves, length in brachiopods or height in gastropods) was plotted against putative year (growth increment) and a nonlinear

regression model in the form of a sigmoidal growth curve fitted. Commonly used growth curves include the von Bertalanffy growth function (VBGF) and Gompertz curve or Gompertz function. Growth data were fitted to both VBGF (2 and 3 parameter) and Gompertz (3 parameter) growth curves in SigmaPlot 10.0. The best fitting model was assessed by Akaike's information criterion (AIC) with additional due regard to biological meaningfulness. The best fitting model was used in the shell cost calculations.

Equations for growth curves

1) von Bertalanffy growth function (VBGF)

The VBGF predicts the length of an animal as a function of its age,

$$L_t = L_{\infty}[1 - e^{-K(t-t_0)}]$$

Where:

L_t = length at a given time

L_{∞} = maximum length

K = rate of growth (the Brody growth coefficient)

t = time (usually the age of the animal in years)

t_0 = the theoretical time (age) at which $L_t = 0$

2) Gompertz function

$$y(t) = ae^{be^{ct}}$$

Where:

a = the upper asymptote (maximum length)

b = a negative number

c = the growth rate (negative)

t = time

6.2.2 Calculating the cost of shell production

1) Calculate how much new shell is deposited per year

The linear measurement along the GAD was determined from the best fitting growth equation for each species (Table 6.9). Regressions of GAD to shell mass were calculated using data from Chapter 3. Using the GAD against shell dry mass regression, the shell mass at each age and, consequently, the increase in shell mass per year was calculated.

2) Calculate the cost of the shell (CaCO₃ and organic matrix)

Shells are composed of CaCO₃ around an organic matrix. Palmer (1992) calculated that the total cost of production (including metabolic synthesis) of CaCO₃ was 1-2 J.mg⁻¹. Organic matrix in molluscan shells is predominantly protein with a small fraction of amino acids (Lowenstam & Weiner, 1989). Palmer (1992) also calculated that the total cost of protein (the protein matrix in the shell) including the cost of metabolic synthesis is 29 J.mg⁻¹. The total cost of the shell can thus be calculated:

$$\text{Total cost of the shell (J)} = [\text{shell CaCO}_3 \text{ mass (mg)} \times \text{cost of calcification at 1-2 (J.mg}^{-1}\text{)}] + [\text{shell organic mass (mg)} \times \text{cost of protein at 29 (J.mg}^{-1}\text{)}]$$

Using this equation, the cost of shell production in the species studied here was calculated for the increase in shell mass each year. For comparison across the range of Palmer (1992) data, calculations were performed with the cost of CaCO₃ at 1, 1.5 and 2 J.mg⁻¹. Where graphs comparing species are included, a mean value of 1.5 J.mg⁻¹ was used for the cost of CaCO₃.

3) Factor in the change in solubility of calcium carbonate with temperature

The change in CaCO₃ solubility as a function of temperature in seawater with a salinity of 35 is very small over 0 – 30 °C (Table 6.1) and is in fact greater with pressure from 0 – 101 bar (i.e. depth from 0 – 1000 m) than it is over this temperature range. As can be seen from Table 6.1, CaCO₃ solubility in shallow surface seawater changes very little with

temperature. The change in solubility between 0 and 30 °C is only 0.05 % for calcite and 0.3 % for aragonite. These changes of less than 1 % suggest that the increase solubility of CaCO_3 itself at low temperatures has very little effect on the cost of CaCO_3 deposition in shell. A cost of 1.5 J.mg^{-1} for CaCO_3 at these percentages, equates to a difference of 0.0008 and 0.005 J.mg^{-1} of CaCO_3 for calcite and aragonite, respectively, over 0 to 30 °C.

Table 6.1 Numerical values of the CaCO_3 solubility products of surface seawater (0 dbar) as a function of temperature and pressure for a salinity of 35 from Sarmiento and Gruber (2006).

Temp. (°C)	$-\log_{10} K_{\text{sp}} \text{ Calcite } (\text{mol kg}^{-1})^2$	$-\log_{10} K_{\text{sp}} \text{ Aragonite } (\text{mol kg}^{-1})^2$
0	6.368	6.166
10	6.365	6.169
20	6.367	6.180
30	6.374	6.200

The solubility of CO_2 in seawater, however, changes markedly with temperature (see Zeebe & Wolf-Gladrow, 2001). More CO_2 dissolves in seawater at lower temperatures, increasing the bicarbonate ion concentration (H_2CO_3) (Equation 1). This drives Equation 2 to the right, encouraging CaCO_3 to remain in solution. The solubility product $K_{\text{sp}}^{\text{CaCO}_3}$ (Equation 3) is defined by the concentrations of carbonate $[\text{CO}_3^{2-}]_{\text{sat}}$ and dissolved calcium ions $[\text{Ca}^{2+}]_{\text{sat}}$ in equilibrium with the mineral CaCO_3 . The degree of saturation (i.e. the saturation state) Ω is defined in Equation 4 where $[\text{CO}_3^{2-}]$ and $[\text{Ca}^{2+}]$ are the observed calcium ion concentrations (Sarmiento & Gruber, 2006). It is this change in solubility of CO_2 with temperature that is likely to increase the cost of shell production at lower temperatures.



$$K_{sp}^{CaCO_3} = [CO_3^{2-}]_{sat}[Ca^{2+}]_{sat} \quad \text{Equation 3}$$

$$\Omega = \frac{[CO_3^{2-}][Ca^{2+}]}{K_{sp}^{CaCO_3}} \quad \text{Equation 4}$$

Table 6.2 Seawater data from Rothera, Antarctica. The table shows total alkalinity (TA), dissolved inorganic carbon (DIC), the saturation state of seawater with respect to calcite (Ω_{cal}) and the saturation state of seawater with respect to aragonite (Ω_{arag}).

Sample	Salinity	TA	DIC	Ω_{cal}	Ω_{arag}
Rothera 1	32.64	2274.129	2090.64	3.46	2.27
Rothera 2	32.64	2281.391	2101.17	3.42	2.24

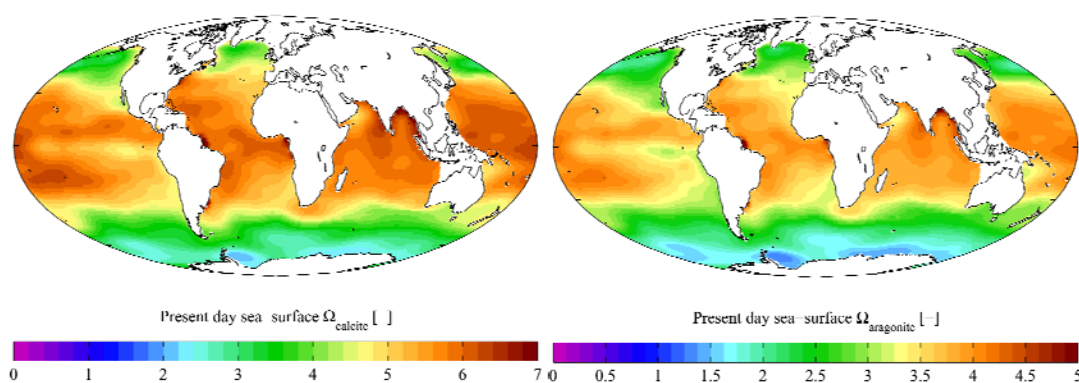


Figure 6.1 The saturation states of calcite and aragonite in the world's oceans today. The difference in the saturation state of seawater from equatorial to polar latitudes is approximately two-fold. Plots were provided by A. Yool from GLODAP data.

The saturation state of seawater with respect to calcite and aragonite was measured in samples taken from the shore at South Cove, Rothera Research Station, Antarctica. Samples were preserved with mercuric chloride and analysed in the UK at the National Oceanography Centre, Southampton (NOCS). Seawater samples were analysed for total alkalinity (TA) and dissolved inorganic carbon (DIC) using a VINDTA (Versatile INstrument for the Determination of Total inorganic carbon and titration Alkalinity). Data for the salinity of seawater were taken from the environmental monitoring programme at Rothera station called the Rothera Time Series (RaTS) programme. Saturation states for

calcite and aragonite (Table 6.2) were calculated using the program CO2SYS (Lewis & Wallace, 1998). Water samples from the nearshore at Rothera match closely with oceanic calcite and aragonite saturation states from global ocean data and models (Figure 6.1).

Seawater with a saturation state of $\Omega > 1$ is supersaturated with respect to CaCO_3 . Seawater with a saturation state of $\Omega < 1$ is undersaturated and CaCO_3 will dissolve in these conditions. However, seawater does not have to fall below $\Omega = 1$ to cause problems for marine animals. Decreases in net calcification have been shown in corals following a reduction in Ω , but with values still well above 1 (Langdon, 1997). So in waters which are still supersaturated with respect to CaCO_3 , the decrease in net calcification suggests calcification is more difficult in conditions of lower Ω .

The difference in Ω for calcite and aragonite from equatorial to polar sea surface waters is approximately two-fold (Figure 6.1). Given that Palmer (1992) based his cost of calcification on temperate marine species, one assumption could be that this cost in the tropics may be 67 % of the cost of temperate species, and in polar regions this cost may be 133 % of the cost of temperate species based on global ocean differences in Ω . Thus the cost shown by Palmer (1992) was adjusted accordingly for Ω in the shell cost calculations (Table 6.3).

Table 6.3 Potential cost of shell production when CaCO_3 saturation state is added to data from Palmer (1992).

Latitude	Range of values for cost (J.mg ⁻¹ of CaCO_3)	Values of cost used in calculations (J.mg ⁻¹ of CaCO_3)
Tropical	0.667-1.333	0.667, 1, 1.333
Temperate	1-2	1, 1.5, 2
Polar	1.333-2.667	1.333, 2, 2.667

4) Convert respiration from $\mu\text{mol O}_2$ to ml O_2

Maintenance metabolic costs for each species were calculated by converting respiration rates from $\mu\text{mol O}_2 \cdot \text{h}^{-1}$ to joules per year ($\text{J} \cdot \text{y}^{-1}$). The first step in this process was to

convert respiration from $\mu\text{mol O}_2$ to ml O_2 . Using the ideal gas law (equation of state for an ideal gas) $\mu\text{mol O}_2$ can be converted to ml (mL) O_2 at different temperatures.

Ideal gas law:

$$pV=nRT$$

Where:

p is pressure in kPa

V is volume of the gas

n is number of moles

R is the gas constant $8.314 \text{ J.K}^{-1}\text{mol}^{-1}$

T is absolute temperature (K)

Standard temperature and pressure (STP) is often defined differently depending on standards organisation, although is usually 0°C and 1 atm. Normal temperature and pressure (NTP) is usually defined as 20°C and 1 atm. In any case,

At 0°C and 1 atm (101.325 kPa)

1 mole (mol) of an ideal gas occupies a volume of 22.414 l

1 mmole gas = 22.414 ml

1 μmol gas = 0.022414 ml

At 25°C and 1 atm (101.325 kPa)

1 mole (mol) of an ideal gas occupies a volume of 24.466 l

1 mmole gas = 24.466 ml

1 μmol gas = 0.024466 ml

Given the linear relationship of gas volume with temperature, the volume of an ideal gas at any temperature can be solved by the equation $y = 0.0821x + 22.414$. This equation was used to adjust for temperature during respiration experiments at each latitude.

5) Convert respiration to energy (J) and calculate annual routine metabolic rate expenditure

Plotting regressions of shell maximum GAD against standard metabolic rate (SMR) data (from Chapter 5) we know the respiration rate of an animal has for a given shell GAD (Table 6.11). We can then calculate the annual SMR available for the animal at any given size.

An oxycalorific coefficient is required to convert oxygen consumption to power expenditure (metabolic energy expenditure). A range of oxycalorific coefficients are available in the literature, but a commonly used one is $4.8 \text{ cal.ml O}_2^{-1}$ at NTP (Elliott & Davison, 1975; Crisp, 1984; Schmidt-Nielsen, 1990).

Calculation of annual SMR expenditure

For an animal 'A', let respiration rate = $A \text{ } \mu\text{mol O}_2.\text{h}^{-1}$

Hours per year = $24 \text{ hr.d}^{-1} \times 365 \text{ d.y}^{-1} = 8760 \text{ hr.y}^{-1}$

Respiration rate = $8760 \text{ hr.y}^{-1} \times A \text{ } \mu\text{mol O}_2.\text{h}^{-1} = 8760A \text{ } \mu\text{mol O}_2.\text{y}^{-1}$

Temperature adjustment: $8760A \text{ } \mu\text{mol O}_2.\text{y}^{-1} \times G_v \text{ ml.} \mu\text{mol O}_2^{-1}$ (where G_v equals the volume of an ideal gas at the temperature of the respiration experiments)

The oxycalorific coefficient used was $4.8 \text{ cal.ml O}_2^{-1}$

$(8760A.G_v \text{ ml O}_2.\text{y}^{-1}) \times 4.8 \text{ cal.ml O}_2^{-1} = 8760A.G_v \times 4.8 \text{ cal.y}^{-1}$

1 thermochemical calorie (cal) = 4.184 joules (J)

$(8760A.G_v \times 4.8) \text{ cal.y}^{-1} \times 4.184 \text{ J.cal}^{-1} = 8760A.G_v \times 4.8 \times 4.184 \text{ J.y}^{-1}$

= **175929 A.G_vJ.y⁻¹**

Seasonal changes in metabolic rate

Seasonal differences in metabolic rate can be accounted for if the difference in summer and winter metabolic rate is known, assuming temperate and polar animals spend 6 months per year at a summer metabolic rate and 6 months at a winter metabolic rate. Thus a step change from summer to winter metabolic rate was used in the calculations, which equates to the idealised actual metabolic rate that varies with season (Figure 6.2). Scaling factors for calculating energy consumption are shown in (Table 6.4). The average metabolic scaling factor used for *Laternula elliptica* was an average of the two published values for the species (i.e. 0.651 for summer and 2.175 for winter).

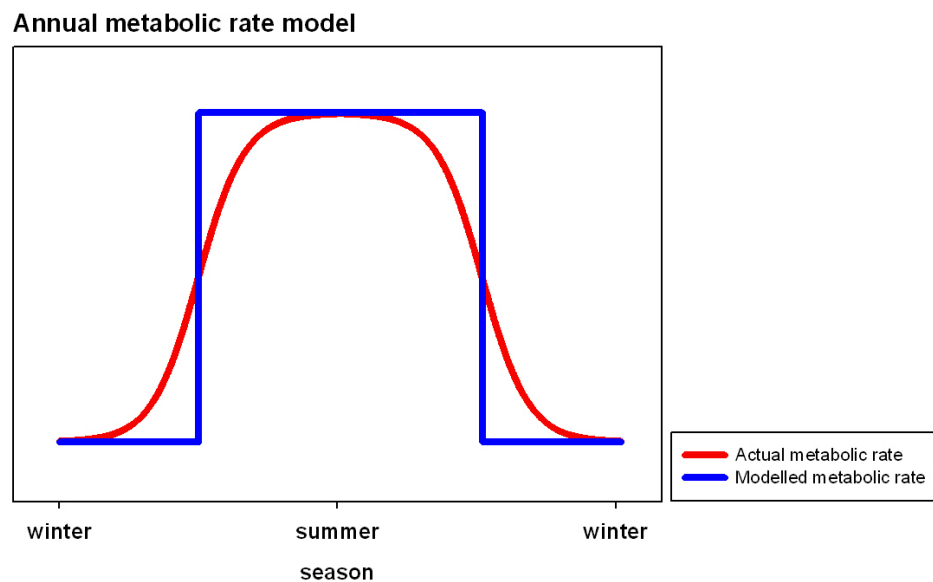


Figure 6.2 Annual metabolic rate model schematic showing how the modelled metabolic rate of 6 months winter rate and 6 months summer rate is equal to the idealised actual metabolic rate.

Table 6.4 Scaling factors for converting summer or winter metabolism into annual metabolism.

Species	Seasonal difference in energy consumption	Reference	Multiplication factor for summer to annual metabolism	Multiplication factor for winter to annual metabolism
Bivalve				
<i>Laternula elliptica</i> (polar)	3.0-fold	Brockington (2001)	0.66667	2
<i>Laternula elliptica</i> (polar)	3.7-fold	Morley <i>et al.</i> (2007a)	0.63514	2.35
<i>Laternula marilina</i> (temperate)	~2-fold*	(Zhuang, 2005)	0.75	1.5
Gastropod				
<i>Buccinum undatum</i> (temperate)	2.3-fold**	Kideys (1998)	0.71739	1.65
Brachiopod				
<i>Liothyrella uva</i> (polar)	1.15 – 1.20-fold	Peck <i>et al.</i> (1986b; 1987b)	0.92553	1.0875

*For clams acclimated for 48 h to temperatures ranging from 10 – 28 °C.

**For whelks from 30 – 59 mm in size from 7.5 – 15 °C temperature change.

Convert SMR to routine metabolic rate

Metabolic rates in this thesis were measured as SMR because SMR is less variable than routine metabolic rate. However, routine metabolic rates were needed to estimate the relative, or proportional, cost of shell production compared to other costs, so a conversion factor was used. SMR values were multiplied by the increase in specific dynamic action (SDA) (i.e. the rise in metabolism exhibited by animals following feeding (Peck, 1998)) from SMR to routine metabolic rate (Table 6.5).

Table 6.5 The rise in metabolic rate following feeding (adapted from Peck (1998)).

Species	Increase from SMR	Reference
Bivalve		
<i>Mytilus edulis</i> (temperate)	2.2	Thompson and Bayne (1972)
Gastropods*		
<i>Nassarius reticulatus</i> (temperate)	2.2-5.2	Crisp <i>et al.</i> (1978)
<i>Buccinum undatum</i> (temperate)	~2	Kideys (1998)
<i>Nacella concinna</i> (polar)	2.3	Peck and Veal (2001)
Brachiopod		
<i>Liothyrella uva</i>	1.6	(Peck, 1996)

*An average of 2.2 was for bivalves and gastropods.

6) Calculate somatic growth

The somatic growth (Pg) increment per year was calculated and added to values of respiration (R) to produce a rough estimate of the energy budget. Using morphology data from Chapter 3, regressions for total animal Ln(AFDM) on Ln(GAD) were determined for each species. Using the growth equation calculated for each species, the annual increase in AFDM was calculated. The energy (caloric) content of soft tissue was calculated by multiplying AFDM by the energy content of tissue appropriate for that taxon (Table 6.6).

Table 6.6 Energy content of soft tissues of marine invertebrates.

Taxon/Species	Energy content of tissue	Reference
Bivalvia	22.79 J.mg ⁻¹ AFDW	Brey <i>et al.</i> (1988)
Gastropoda	23.27 J.mg ⁻¹ AFDW	Brey <i>et al.</i> (1988)
<i>Liothyrella uva</i>	2.91 kcal.g ⁻¹ tissue dry mass = 12.175 J.mg ⁻¹	Peck (1993)

7) Annual energy budget estimate

The energy budget of an organism can be expressed by the energy equation:

$$I = E + P_g + P_r + R + U + M$$

Where I = ingestion, E = egestion, P_g = somatic growth, P_r = reproductive investment, R = respiration, U = excretion, M = mucus production (Peck *et al.*, 1987c).

The percentage of the energy budget accounted for by respiration and growth was sourced from published data on energy budgets of closely related species where available (Table 6.7). These published energy budgets already included mucus production, which can comprise a large proportion of the energy budget in gastropods, and reproduction. Although Kideys (1998) does provide an energy budget for *Buccinum undatum* specifically, there are some discrepancies in the values of R and P_g calculated and it was, therefore, not possible to use his energy budget in this context. Where data were not available for a species or genus a mean value for the taxon was used. The percentage of the energy budget that is partitioned to P_g generally decreases while R and P_r generally increase with age in an animal. For calculations in this chapter, a mid-value was taken for R and P_g . There are no complete energy budgets for any species of brachiopod (Peck *et al.*, 1997b), so the conversion factor for bivalves was used. If energy budgets of brachiopods become available in future, the calculations can be amended.

The total energy budget was calculated by:

$$\text{Total energy budget (J)} = [\text{energy (J) from R} + P_g] * 100 / [(R + P_g)\% \text{ of total energy budget}]$$

Table 6.7 The percentage of the energy budget accounted for by respiration and growth.

Species	R %	P _g %	Sum R + P _g % (mean to nearest %)	Reference
Bivalve: <i>Laternula marilina</i>	42.5-52.1	8.6-23.3*	63	Zhuang (2005)
Gastropod: <i>Haliotis tuberculata</i>	21.6-31.1	12.9-37.5	52	Peck <i>et al.</i> (1987c)
Brachiopods			63 % used	

* Zhuang (2005) did not separate P_g + P_r.

8) Calculate cost of shell as a percentage of the energy budget

Thus for each putative year, we know the shell length, the shell mass deposited, the cost of the shell mass deposited and we have an estimate for the total energy budget for the year. Therefore, the cost of shell as a percentage of the annual energy budget can be calculated:

Cost of shell as a percentage of the energy budget (%) = energy required to build shell mass deposited per year ($J \cdot y^{-1}$) / annual energy budget ($J \cdot y^{-1}$) * 100 %

N.B. This chapter is methodology based. A novel method for estimating the cost of shell production is presented. Any new data from the literature on the energy budgets of a species can be incorporated into the calculations where necessary, and with relative ease.

6.2.3 Statistical analysis

Data were compiled on spreadsheets using MS Excel 2003. Statistical analyses were performed in SPSS 16.0, SigmaPlot 10.0 and R 2.7.1 and included linear regression analysis, non-linear regression analysis for the fitting of growth curves, analysis of variance (ANOVA) and post hoc tests. Where data did not have equal variances Welch's F test was used (Welch, 1951). For regression analysis, a confidence band refers to the "region of uncertainties in the predicted values over a range of values for the independent variable".

A prediction band refers to the “region of uncertainties in predicting the response for a single additional observation at each point within a range of independent variable values” (SigmaPlot).

6.3 Results

Growth curves

von Bertalanffy growth function (VBGF) curves and Gompertz growth curves were calculated for each species. Gompertz growth curves gave slightly higher r^2 values (Appendix 4) than VBGF curves (Table 6.9), however, they did not pass close to the origin. Also Gompertz growth curves did not converge for the Arctic gastropods. VBGF curves were used because they provided more realistic values for small animals. For the majority of the species modelled, the VBGF 2 parameter curves where $t_0=0$ gave the lowest AIC values, can could therefore be considered the best fitting models by this criterion. VBGF 2 parameter curves where $t_0=0$ provided better L_∞ values than VBGF 3 parameter growth curves which gave unrealistic L_∞ values and often unrealistic t_0 values (Appendix 5).

Metabolic rates

Metabolic rates (Chapter 5) for all temperate and polar species in this study were conducted in the summer, with the exception of the bivalve *Laternula recta* and the gastropod *Cominella lineolata* for which metabolic rates were measured in the austral winter (Table 6.8). Metabolic rates collected from temperate and polar latitudes were multiplied by the appropriate factor (Table 6.4) to correct for differences in season in which metabolic rate was measured. The tropical locations studied have little seasonality in temperature so no correction was used for season at tropical locations. N.B. Tropical locations can have seasonal variation in other factors such as the monsoon and variation in productivity from upwelling.

Table 6.8 Season, temperature and volume of 1 mole of O₂ (g) at each location.

Location	Season	Temperature (°C)	Volume of 1 mole of O _{2(g)} (l) (G _v) (3 d.p.)
Singapore	Tropics ('spring')	29.9	24.869
Townsville, Australia	Tropics ('autumn')	28.3	24.737
Melbourne, Australia	Temperate winter	14.2	23.582
Southampton, UK	Temperate summer	18.9	23.967
Rothera, Antarctica	Polar summer	0.7	22.475
Ny Ålesund, Arctic	Polar summer	4	22.742

Organic matrix

Table 6.10 shows differences in annual SMR among key species. Shell organic matrix content data are also included using data from Chapter 3 for bivalves and gastropods. Brachiopod shell organic matrix data were not included in Chapter 3 because of the difficulty in assessing the amount of organic matrix in brachiopod shells versus the soft tissues of the caeca, which extend into the shells. However, it was necessary to determine a figure for brachiopod shell organic matrix for shell cost calculations in this chapter. Estimates for brachiopod shell organic content were obtained by removing the soft tissue from the inner surface of the shell and then drying to a constant weight at 60 °C and igniting the dry shell in a muffle furnace at 475 °C for 24 hours as done for the molluscs (Chapter 3). It must be stressed that data for brachiopod shell organic matrix (Figure 6.3) are thus *estimates* as some caeca (mantle papillae) are likely to have remained within the punctae. The brachiopod shells had a similar construction across the species studied, as they were all terebratulids, and 2 species were congeneric. Therefore, the proportion of tissue remaining in the shell is likely to be very similar.

Peck and Edwards (1996) found shell organic contents (matrix plus caeca) by loss on ignition were 1.87 % for *L. neozelanica* and 3.38 % for *L. uva*, and by HCl digest as 5.54 % for *L. neozelanica* and 3.51 % for *L. uva*. These findings for shell organic content with caeca, using the loss on ignition method, are similar to those found in this study (Figure 6.3). However, the true value of the shell organic matrix could be < 1 % of the shell by weight because of the tissue in caeca (L. Peck, pers. comm.).

These estimated organic content data are needed to adjust the cost of shell production in brachiopods to include the cost of the organic component of the shell. Note that spicules in the soft tissues and the lophophore were not measured for organic content and the organic content of CaCO₃ within the whole brachiopod was assumed to be the same as that of the shell. Endolithic red alga within the shell of *L. uva* (Peck and Porter, unpub. obs. cited in Peck *et al.* (1987a)) could have artificially increased the organic content of some shells. For these reasons, comparisons of brachiopod shell cost between species have included both results with no account for organic matrix and results accounting for organic matrix at

the levels estimated. All mollusc data presented here include the organic content of their shell.

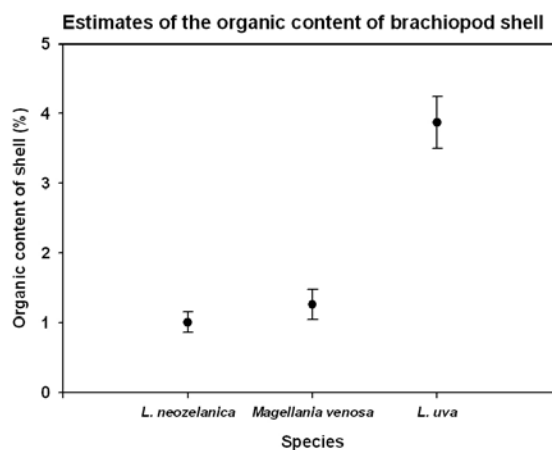


Figure 6.3 Estimates of the organic matrix contained within the brachiopod shell. There was a significant difference in the total organic content of brachiopod shells (Welch's $F = 23.599$, $df1 = 2$, $df2 = 7.082$, $p < 0.001$). Post hoc comparisons using the Games-Howell procedure showed that *Liothyrella uva* had the highest shell organic content ($p < 0.001$).

Table 6.9 VBGF parameters, fitted using $y=a*(1-\exp(-b*x))$. Note t_0 is assumed to be zero (and therefore not present), thus the curve passes through the origin, providing a better fit for small individuals, but still a good fit for larger animals.

Species	L_{∞} (a)	K (b)	r^2	s.e.	F	df	p
<i>Laternula truncata</i>	30.7408	0.1471	0.9552	1.1156	1387.3072	1,64	<0.0001
<i>Laternula boschasina</i>	12.7419	0.3371	0.9430	0.5832	778.6942	1,46	<0.0001
<i>Laternula recta</i>	29.5447	0.0992	0.9593	0.8454	1674.2628	1,70	<0.0001
<i>Laternula elliptica</i>	187.6279	0.0245	0.9530	2.7833	2554.1498	1,125	<0.0001
<i>Liothyrella neozelanica</i>	102.8170	0.0422	0.9684	1.9770	3215.6688	1,104	<0.0001
<i>Liothyrella uva</i>	74.6652	0.0271	0.9712	1.4368	5102.1222	1,150	<0.0001
<i>Buccinum undatum</i>	93.6892	0.1724	0.4769	6.5240	39.2870	1,41	<0.0001
<i>Neobuccinum eatoni</i>	54.8562	0.2225	0.5385	4.4753	26.6747	1,21	<0.0001
<i>Buccinum</i> cf. <i>groenlandicum</i>	42.9443	0.3388	0.6968	2.7999	28.5819	1,11	0.0002
<i>Buccinum glaciale</i>	81.4265	0.1956	0.5997	2.5580	12.9832	1,7	0.0087

Table 6.10 Annual SMR expenditure (J.y^{-1}) for each species based on a mean animal size for each species. Mollusc shell organic content data are taken from Chapter 3.

Species	Mean length		Mean respiration rate ($\mu\text{mol O}_2\cdot\text{h}^{-1}$) (3 s.f.)	Location	Temp ($^{\circ}\text{C}$)	Gas vol. (ml/mol)	Annual SMR expenditure (J.y^{-1})	Mean shell organic content (%)
<i>Laternula</i> clams	Shell length	Shell height						
<i>Laternula truncata</i>	35	18.78	5.75	Singapore	29.9	0.024869	25148	4.78
<i>Laternula boschasina</i>	17	9.64	0.994	Singapore	29.9	0.024869	4349	5.74
<i>Laternula recta</i>	29	13.74	0.949	Melbourne	14.2	0.023582	3937	5.13
<i>Laternula elliptica</i>	63	42.09	27.4	Rothera	0.74	0.022475	108212	4.86
Buccinid gastropods	Shell height							
<i>Cantharus fumosus</i>	22		1.14	Townsville	28.3	0.024737	4963	2.64
<i>Phos senticosus</i>	31		1.99	Townsville	28.3	0.024737	8639	2.07
<i>Cominella lineolata</i>	19		8.14	Melbourne	14.2	0.023582	33786	
<i>Buccinum undatum</i>	38		9.66	Southampton	18.9	0.023967	40732	4.91
<i>Neobuccinum eatoni</i>	44		3.27	Rothera	0.74	0.022475	12933	2.58
<i>Buccinum</i> cf. <i>groenlandicum</i>	32		2.54	Ny Ålesund	4	0.022742	10182	5.88
<i>Buccinum glaciale</i>	49		7.65	Ny Ålesund	4	0.022742	30620	3.88
Echinoids	Test diameter							
<i>Psammechinus miliaris</i>	25		7.68	Southampton	18.9	0.023967	32383	
<i>Sterechinus neumayeri</i>	27		1.65	Rothera	0.74	0.022475	6524	
Brachiopods	Shell length							
<i>Liothyrella neozelanica</i>				New Zealand				1.00
<i>Liothyrella uva</i>	30		0.6949	Rothera	0.74	0.022475	2748	3.87

Table 6.11 Regressions of shell mass and linear dimensions used in shell cost calculations and for brachiopods regressions for converting known pedicle valve length to brachial valve length for future comparison of data from this study with published data, where $y = mx + c$.

Species	Regression for (y variable v x variable)	m	c	r ²	S.E. of estimate	F	df	p
<i>Laternula</i> clams								
<i>Laternula truncata</i>	Ln(Shell wet weight) v Ln(Height)	2.7617	-7.9653	0.8323	0.2578	120.1333	1,23	<0.0001
<i>Laternula truncata</i>	Ln(Shell dry mass) v Ln(Height)	3.4488	-10.4545	0.9548	0.1768	296.5052	1,13	<0.0001
<i>Laternula boschasina</i>	Ln(Shell dry mass) v Ln(Height)	2.7742	-8.6202	0.8417	0.1461	70.1230	1,12	<0.0001
<i>Laternula recta</i>	Ln(Shell wet weight) v Ln(Height)	2.6126	-7.9241	0.8840	0.1694	275.2911	1,35	<0.0001
<i>Laternula recta</i>	Ln(Shell dry mass) v Ln(Height)	2.7503	-8.6862	0.9064	0.1522	233.4327	1,23	<0.0001
<i>Laternula elliptica</i>	Ln(Shell wet weight) v Ln(Height)	3.0047	-8.7110	0.9272	0.2010	675.9781	1,52	<0.0001
<i>Laternula elliptica</i>	Ln(Shell dry mass) v Ln(Height)	3.2620	-9.8112	0.9517	0.2516	591.8478	1,29	<0.0001
Buccinidae gastropods								
<i>Buccinum undatum</i>	Ln (Shell dry mass) v Ln(Height)	2.5703	-8.3188	0.9733	0.1004	1314.6178	1,35	<0.0001
<i>Neobuccinum eatoni</i>	Ln (Shell dry mass) v Ln(Height)	2.7359	-9.3294	0.9703	0.1173	947.8639	1,28	<0.0001
<i>Buccinum</i> cf. <i>groenlandicum</i>	Ln (Shell dry mass) v Ln(Height)	3.4526	-11.9064	0.9254	0.2071	236.5550	1,18	<0.0001
<i>Buccinum glaciale</i>	Ln (Shell dry mass) v Ln(Height)	2.3998	-7.8350	0.9454	0.1322	156.8207	1,8	<0.0001
Brachiopods								
<i>Liothyrella neozelanica</i>	Ln (Brachical valve length) v Ln(Pedicle valve length)	0.9000	-0.3165	0.9972	0.4775	10357.8201	1,28	<0.0001
<i>Liothyrella uva</i> (Rothera)	Ln (Brachical valve length) v Ln(Pedicle valve length)	0.8831	-0.5619	0.9937	0.5296	7248.3184	1,45	<0.0001

6.3.1 Bivalvia: genus *Laternula*

VBGF curves for *Laternula* clams are shown in Figure 6.4. The von Bertalanffy growth coefficient (k) describes the rate at which an average organism reaches its full size. Rate of growth to maximum size from fastest to slowest was *L. boschasina* > *L. truncata* > *L. recta* > *L. elliptica*. The tropical species had higher k values (faster growth to maximum size) than the temperate species, which in turn had higher k values than the polar species (Table 6.9). However, it is not always appropriate to directly compare the k values for very different sized animals such as the *Laternula* clams to determine relative growth rate. Figure 6.5 shows mean shell height measurements with time for each *Laternula* species instead of using the growth curves. The Antarctic clam *L. elliptica* has the fastest growth rate per year in absolute terms.

Figure 6.6 shows the amount of energy needed to deposit shell over time based on the cost of CaCO_3 and organic matrix content within shell. Since Palmer (1992) estimated the cost of shell production to be 1 – 2 J.mg^{-1} of CaCO_3 , shell cost at values of 1, 1.5 and 2 J.mg^{-1} CaCO_3 were plotted to demonstrate the range of shell cost values possible. In addition, the theoretical extra cost of producing the shell based on differences in the saturation state of CaCO_3 in seawater was calculated using values from Table 6.3. The cost for the temperate species remains the same since Palmer's (1992) cost calculations were for temperate conditions. The large size of the *L. elliptica* shell means, unsurprisingly, that it required the most energy to make its shell (Figure 6.7). *L. boschasina* with the smallest shell required the least energy.

Regression equations of $\text{Ln}(\text{MO}_2)$ on $\text{Ln}(\text{Height})$ (Figure 6.8) were used to calculate the portion of the energy budget from respiration available at each growth increment. The regression for *L. boschasina* was not significant ($p > 0.05$) because the size range of individuals of *L. boschasina* was not large enough. Thus the average slope of the significant regression equations for the other *Laternula* clams was used instead for *L. boschasina*. Using this mean slope and *L. boschasina* mean $\text{Ln}(\text{Height})$ and mean $\text{Ln}(\text{MO}_2)$, differences in respiration rate with size were calculated for *L. boschasina*. Mean

shell cost, respiration and tissue energy costs for each species taken from an example mid-valve of $1.5 \text{ J.mg}^{-1} \text{ CaCO}_3$ and including differences in CaCO_3 saturation state are given in Appendix 6.

The cost of shell deposition as a percentage of the total energy budget (I) varied with age in *Laternula* clams (Figure 6.9). The theoretical extra cost of producing the shell based on differences in the saturation state of CaCO_3 in seawater, is both included and excluded so the potential effect of saturation state can be seen. Tropical and temperate clams had the lowest cost of producing a shell at approximately 0.5 – 1 % of their total energy budget (I) (Figure 6.10 and Figure 6.11). *L. elliptica* had the highest cost of producing a shell as a proportion of its energy budget at approximately 3 – 3.5 % as an average lifetime value.

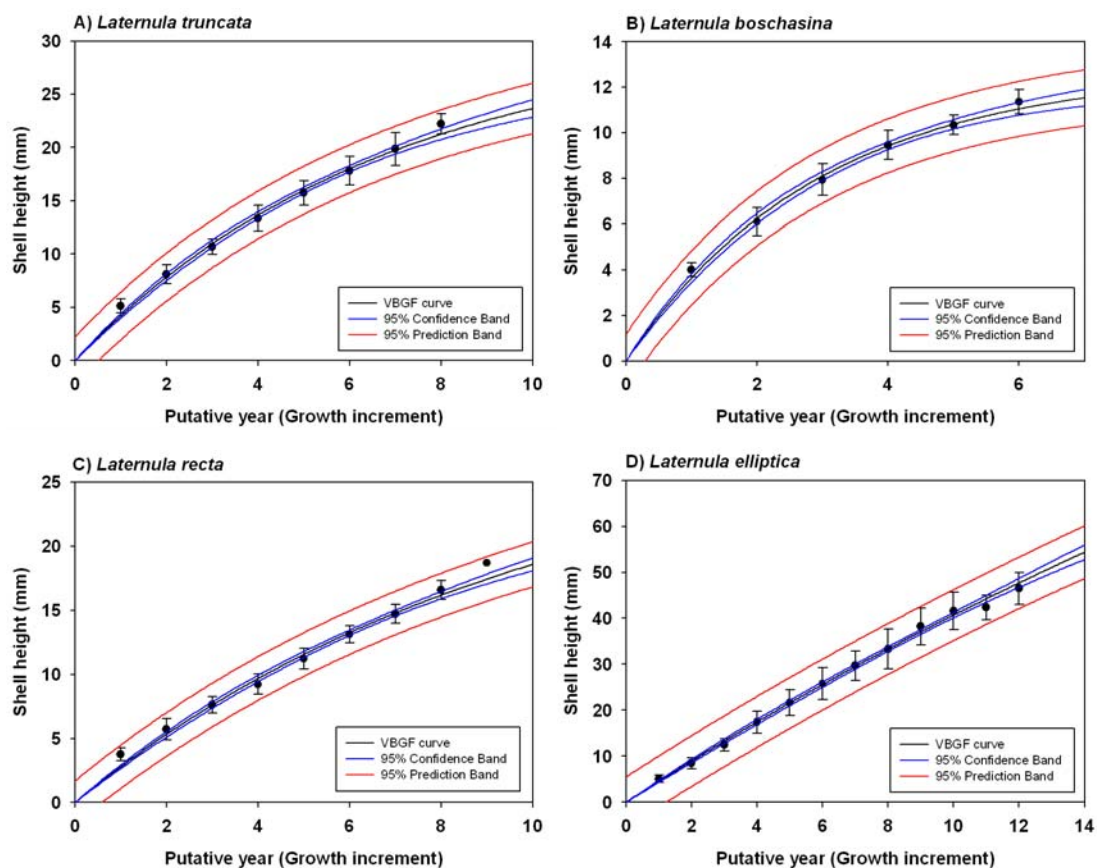


Figure 6.4 VBGF curves for A) *Laternula truncata*, B) *L. boschasina*, C) *L. recta* and D) *L. elliptica*.

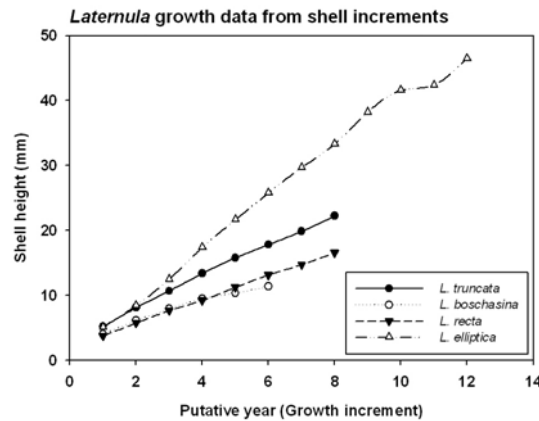


Figure 6.5 Mean shell height measurement for each *Laternula* species compared. The polar clam, *L. elliptica* had the fastest growth rate.

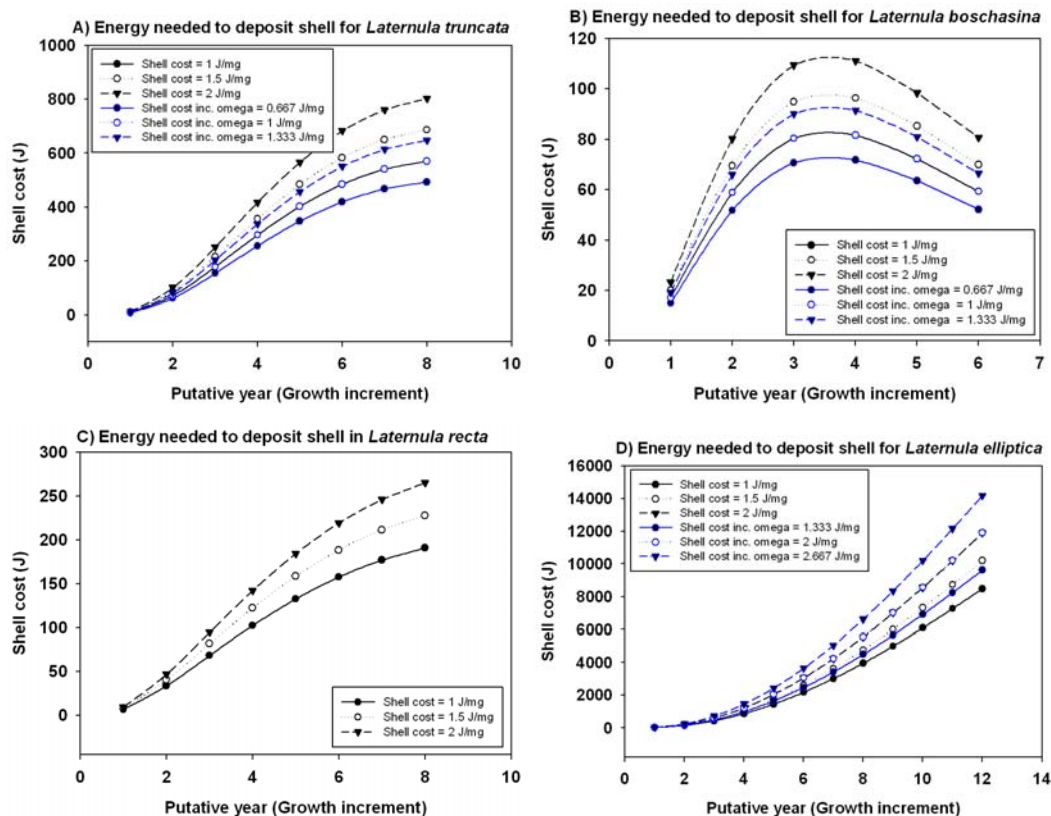


Figure 6.6 Energy required for shell deposition using VBGF curves and based on CaCO_3 and organic matrix content of the shell for A) *Laternula truncata*, B) *L. boschasina*, C) *L. recta* and D) *L. elliptica*. Since Palmer (1992) estimated the cost of shell production to be $1 - 2 \text{ J.mg}^{-1} \text{ CaCO}_3$, shell cost at values of 1, 1.5 and $2 \text{ J.mg}^{-1} \text{ CaCO}_3$ were plotted to demonstrate the range of shell cost values possible. The theoretical cost of producing the shell based on differences in the saturation state of CaCO_3 in seawater, is shown as blue curves on the graphs. Note that the cost for the temperate species remains the same since Palmer's (1992) cost calculations were done at temperate conditions.

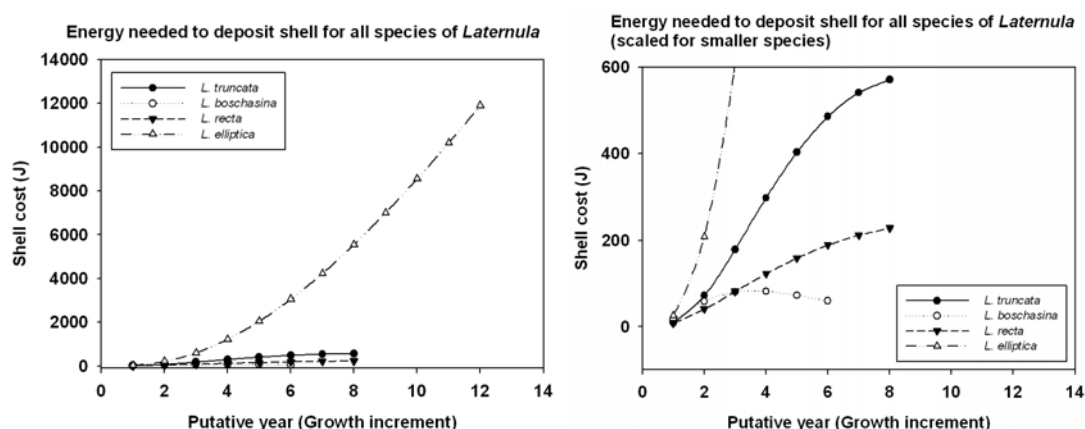


Figure 6.7 Energy required for shell deposition using VBGF curves and based on CaCO_3 and organic matrix content of the shell for A) all species of *Laternula* studied and B) scaled for smaller species. The theoretical extra cost of making the shell based on differences in the saturation state of CaCO_3 in seawater is included in these comparisons.

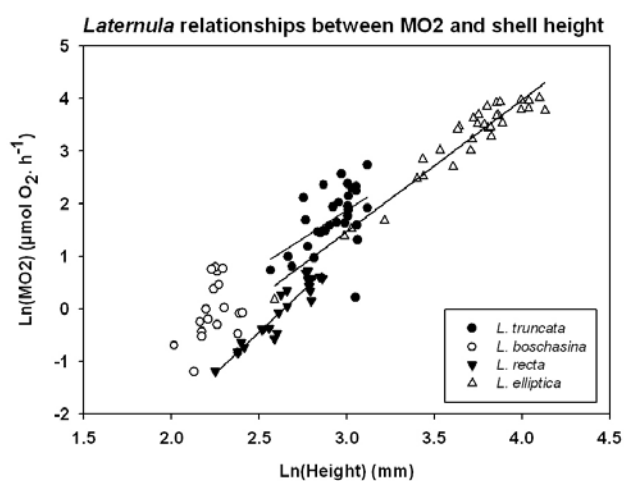


Figure 6.8 Regressions of $\text{Ln}(\text{MO}_2)$ on $\text{Ln}(\text{Shell height})$ for A) *Laternula truncata* ($y = 2.1406x - 4.5490$, $r^2 = 0.2625$, $F = 9.9652$, $df = 1,28$, $p = 0.0038$), B) *L. boschasina* (regression not significant), C) *L. recta* ($y = 3.1422x - 8.3019$, $r^2 = 0.8791$, $F = 145.4885$, $df = 1,20$, $p < 0.0001$) and D) *L. elliptica* ($y = 2.5067x - 6.0511$, $r^2 = 0.9247$, $F = 368.3433$, $df = 1,30$, $p < 0.0001$). The restricted size range for *L. boschasina* meant the regression of $\text{Ln}(\text{MO}_2)$ on $\text{Ln}(\text{Shell height})$ was not significant.

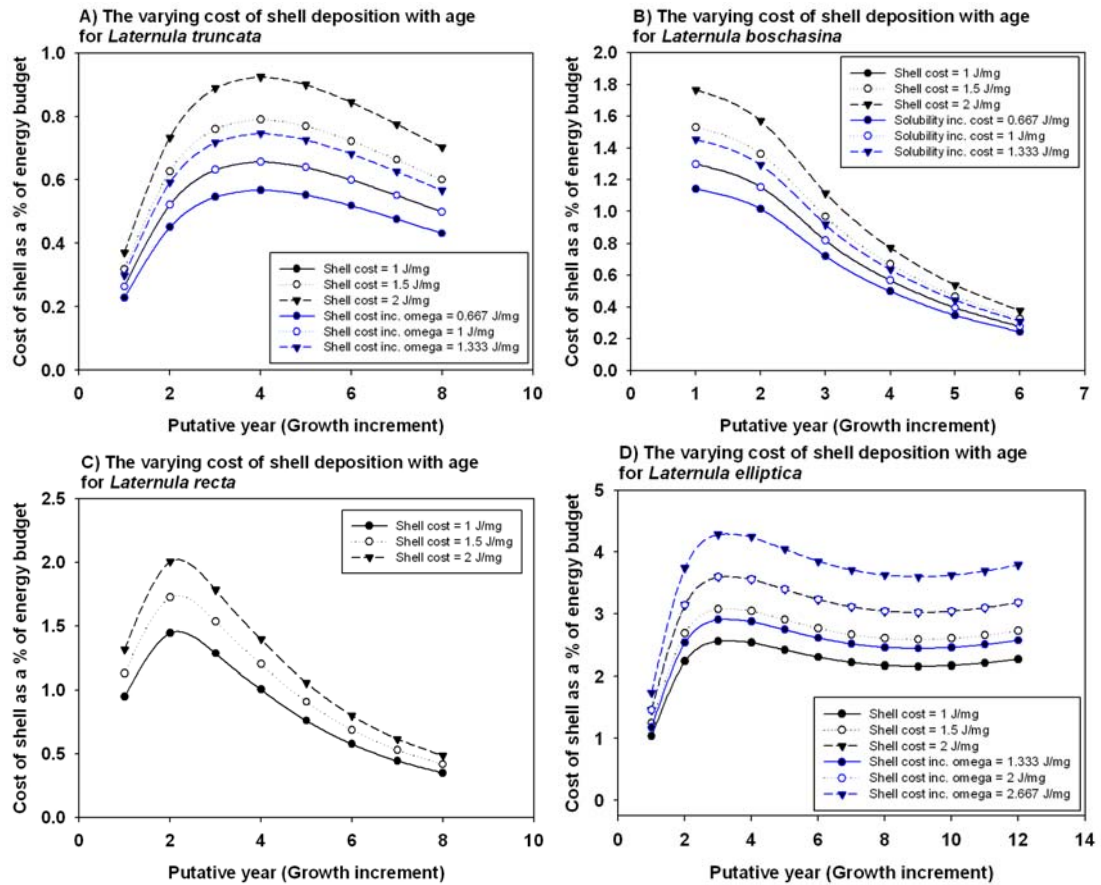


Figure 6.9 Variation in the cost of shell deposition with age for A) *Laternula truncata*, B) *L. boschasina*, C) *L. recta* and D) *L. elliptica*. The theoretical cost of producing the shell based on differences in the saturation state of CaCO_3 in seawater, is shown as blue curves on the graphs. Note that the cost for the temperate species remains the same since Palmer's (1992) cost calculations were done at temperate conditions.

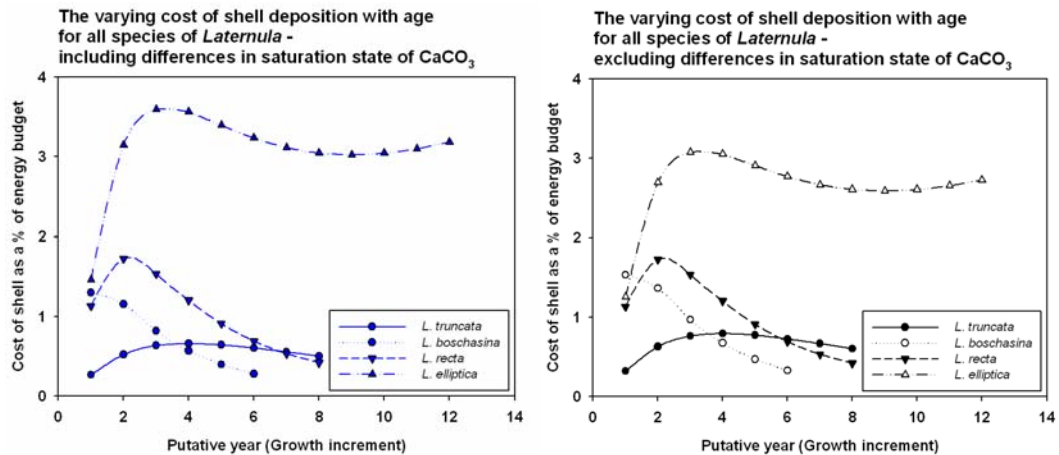


Figure 6.10 Variation in the cost of shell deposition as a percentage of the total energy budget (I) with age for all *Laternula* species studied including differences in CaCO_3 saturation state (left) and excluding differences in CaCO_3 saturation state (right). A mid-value of $1.5 \text{ J.mg}^{-1} \text{ CaCO}_3$ was used.

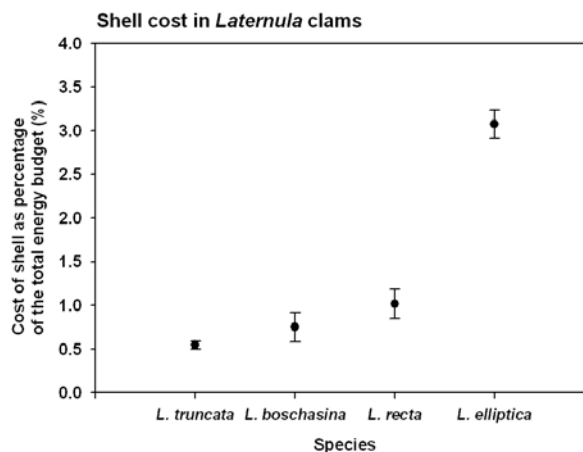


Figure 6.11 Mean lifetime values of shell cost as a percentage of the total energy budget for all *Laternula* species studied. A mid-value of $1.5 \text{ J.mg}^{-1} \text{ CaCO}_3$ was used. The theoretical cost of making the shell based on differences in the saturation state of CaCO_3 in seawater is included in these comparisons. There was a significant difference in the cost of shell as a percentage of the total energy budget among species over all life stages ($F = 72.859$, $df = 3,30$, $p < 0.001$). Post hoc comparisons showed *L. elliptica* had a significantly higher proportional shell cost than other species ($p < 0.001$).

6.3.2 Brachiopoda: genus *Liothyrella*

VBGF curves for brachiopods from the genus *Liothyrella* are shown in Figure 6.12. Figure 6.13 shows mean brachial valve length with time for each *Liothyrella* species instead of using the growth curves. The temperate brachiopod *Liothyrella neozelanica* grows approximately twice as fast as the Antarctic brachiopod *Liothyrella uva*. *Liothyrella neozelanica* had a higher k value (Table 6.9) and absolute growth (Figure 6.13) than *Liothyrella uva*.

Since the data for the organic matrix content of brachiopod shells are estimates (see Methods), comparisons of brachiopod shell cost between species included both results with and without accounting for shell organic content at the levels estimated (Figure 6.14). This is to demonstrate the size of the effect of accounting for shell organic content and the range of values of likely shell cost. Since animals need organic matrix to seed crystals during shell formation, the cost excluding organic matrix is likely to underestimate the absolute cost required to deposit the shell.

As a result of a faster growth rate, the amount of skeleton deposited per year is much greater in *L. neozelanica* than in *L. uva*. *L. neozelanica* thus incurs a much higher absolute cost of shell production than does *L. uva* both with organic matrix included and excluded (Figure 6.15). The organic content of *L. neozelanica* shell was estimated at around 1 % and Figure 6.14 shows that including the cost of the organic component makes little difference to the total cost of the shell in J. The organic content of *L. uva* shell was estimated at around 3.87 %, which is high and may have been affected by the presence of endoliths in the shell (Peck and Porter, unpub. obs. cited in Peck *et al.* (1987a)). Including the cost of the organic component makes more of a difference to the total cost of the shell in J for *L. uva*. However, if the true organic content of the shell is more like 1 %, shell cost will be much closer to the cost without organic matrix included as in *L. neozelanica*.

Using the relationship between *L. uva* shell size and respiration rate (Figure 6.16), the cost of the shell as a percentage of the total energy budget (I) was calculated (Figure 6.17).

Without including the potential effects of CaCO_3 saturation state in Antarctic waters, the cost of shell production was approximately 3 – 10 % of the energy budget. Including the effects of CaCO_3 saturation state, the cost of shell production increased to 4 – 14 %. Unfortunately, no respiration data were available for *L. neozelanica*, so proportional shell cost in terms of the total energy budget could not be calculated for the temperate congeneric.

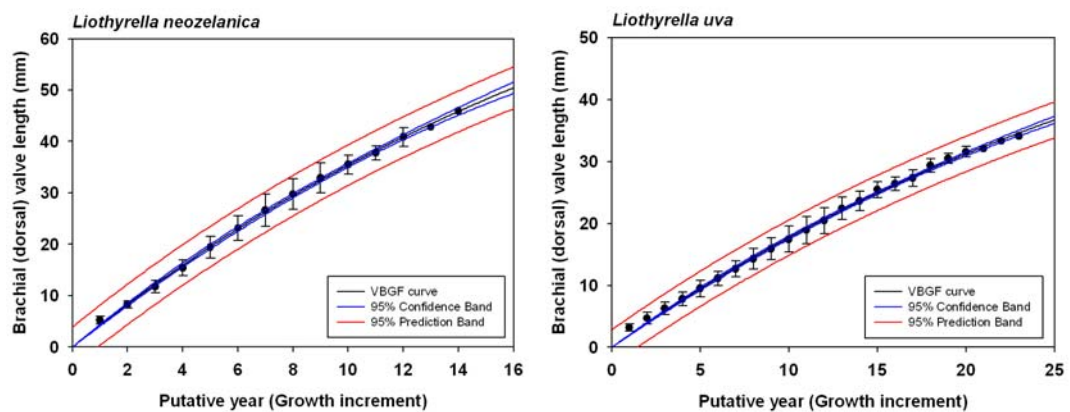


Figure 6.12 VBGF growth curves for the brachiopods *Liothyrella neozelanica* (left) and *L. uva* (right).

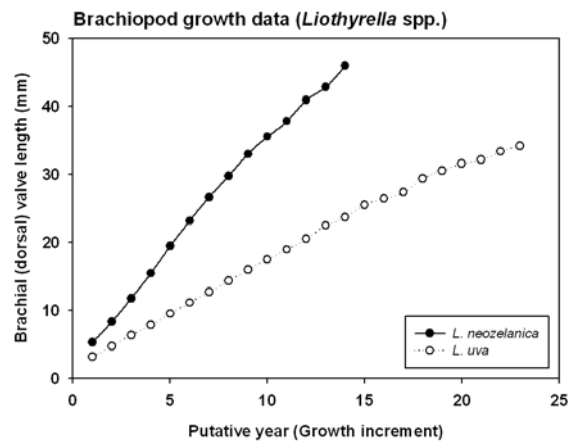


Figure 6.13 Average brachial (dorsal) valve length for each *Liothyrella* species compared using shell increment data. The temperate species *L. neozelanica* grows nearly twice as fast as the polar species *L. uva*.

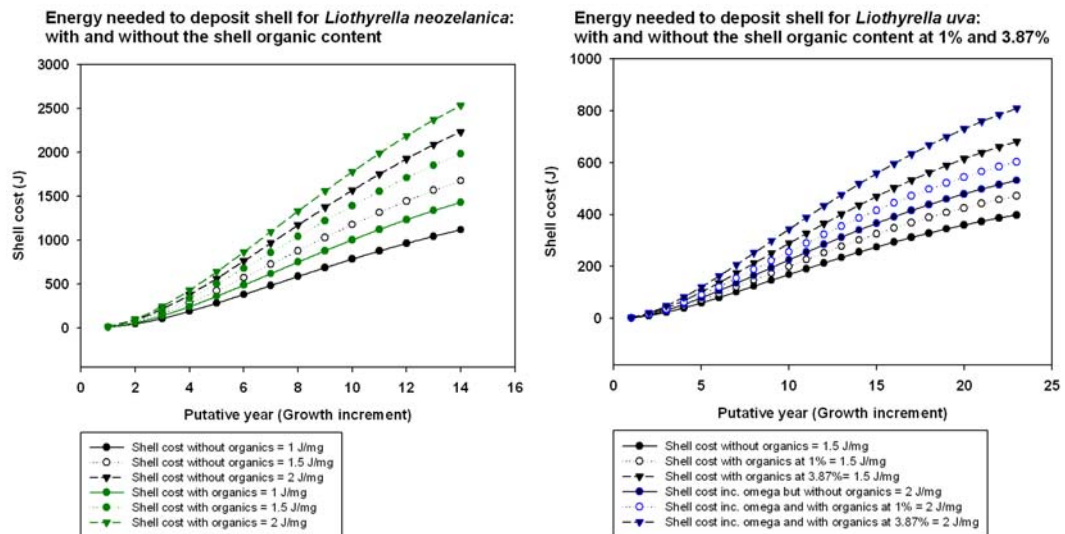


Figure 6.14 Energy required for shell deposition with and without the shell organic content included for *Liothyrella neozelanica* (left) and *L. uva* (right). *L. neozelanica* is a temperate species, so there was no correction for CaCO_3 saturation state. Note the different key for *L. uva* (right) as a correction for CaCO_3 saturation state is included.

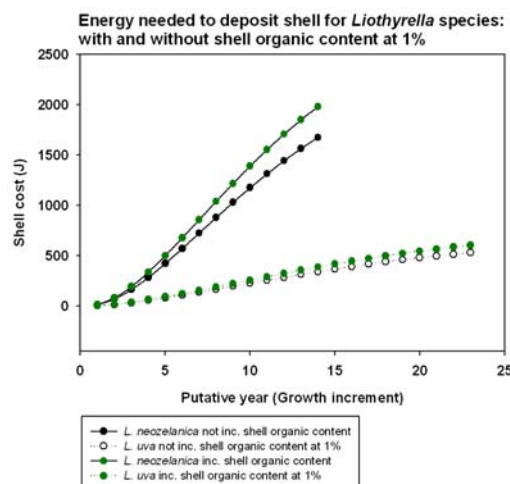


Figure 6.15 Energy required by brachiopods to deposit their shell with and without organic shell matrix at 1 %. Figures shown are based only on the 1.5 J.mg^{-1} value for CaCO_3 deposition costs. The theoretical extra cost of making the shell based on differences in the saturation state of CaCO_3 in seawater is included in these comparisons.

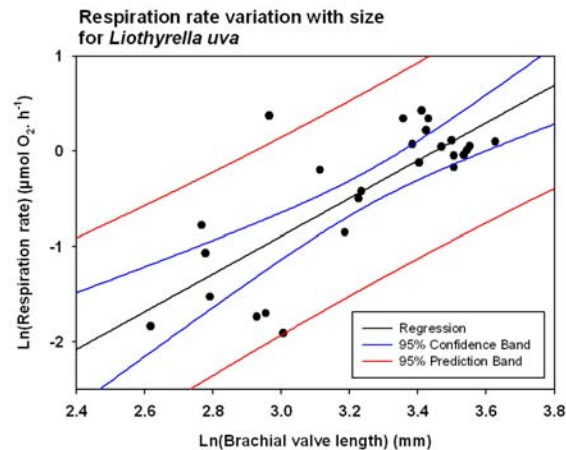


Figure 6.16 Regression of Ln(Respiration rate) on Ln(Brachial valve length) for *Liothyrella uva* ($F = 36.2763$, $df = 1,24$, $p < 0.0001$, $r^2 = 0.5852$).

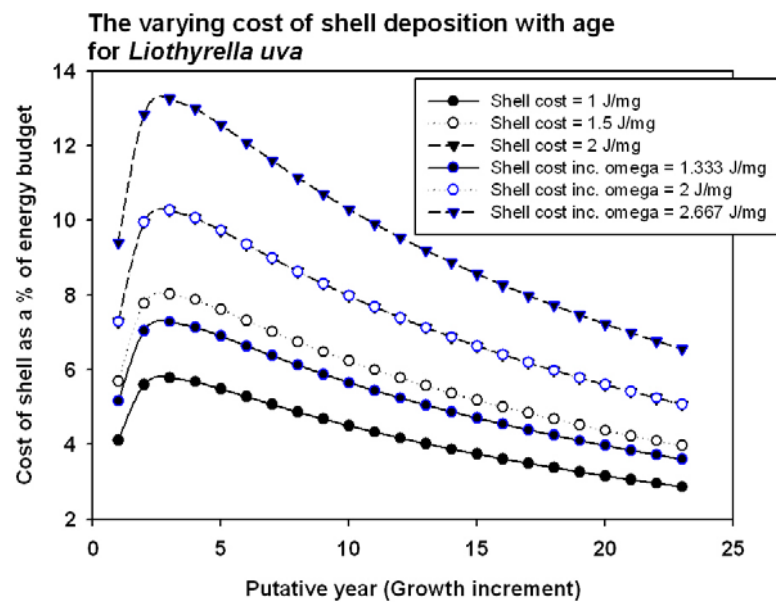


Figure 6.17 Variation in the cost of shell deposition with age for *Liothyrella uva*. The 63 % value for bivalve was used for the percentage of the energy budget accounted for by respiration and growth. Shell organic matrix was assumed to be 1 %. The theoretical extra cost of producing the shell based on differences in the saturation state of CaCO_3 in seawater, is shown as blue curves on the graph.

6.3.3 Gastropoda: family Buccinidae

VBGF curves for buccinid gastropods are shown in Figure 6.18. The smaller species *Buccinum* cf. *groenlandicum* and *Neobuccinum eatoni* had the fastest rates of growth to their maximum size according to the k values (Table 6.9). For some species, n values for growth curves are small because opercula had become detached from the snails and could not be matched to their rightful owner. The operculum had to remain attached to each snail to allow shell measurements to be compared with number of striae on the operculum.

Figure 6.19 shows the amount of energy needed to deposit shell over time based on the cost of CaCO_3 and organic matrix content within shell. In addition, the theoretical extra cost of producing the shell based on differences in the saturation state of CaCO_3 in seawater was calculated using values from Table 6.3. The physical cost of the shell is a function of the size of the shell and its organic content. *Buccinum undatum* had the greatest shell mass as well as a high organic content and so had the greatest cost associated with producing its shell (Figure 6.20). Absolute cost of the shell was lowest in the thin-shelled species: *N. eatoni* and *Buccinum* cf. *groenlandicum*.

Respiration rate varied with height of gastropod according to the regressions in Figure 6.21. At $\text{Ln}(\text{height}) = 3.6$ mm, the warmest water species (temperate *B. undatum*) had the highest respiration rate with the highest regression trendline and the coldest water species (Antarctic *N. eatoni*) had the lowest respiration rate with the lowest regression trendline. The regression equations were used to calculate the portion of the energy budget from respiration available at each growth increment.

The cost of shell deposition as a percentage of the total energy budget (I) varied with age of buccinid as shown in Figure 6.22. The cost of shell as a percentage of the total energy budget (I) decreased with age in all buccinid species after around 2 or 3 years. Not including the theoretical extra cost of producing the shell based on differences in the saturation state of CaCO_3 in seawater, the cost of the shell as a percentage of the total energy budget is fairly similar for all buccinids studied ranging from 0.5 – 6 % (Figure

6.23). Including the theoretical extra cost of producing the shell based on differences in the saturation state of CaCO_3 in seawater, the cost of shell was higher in *B. glaciale* and *N. eatoni* peaking at around 5 - 6 %, and lowest in *B. undatum*.

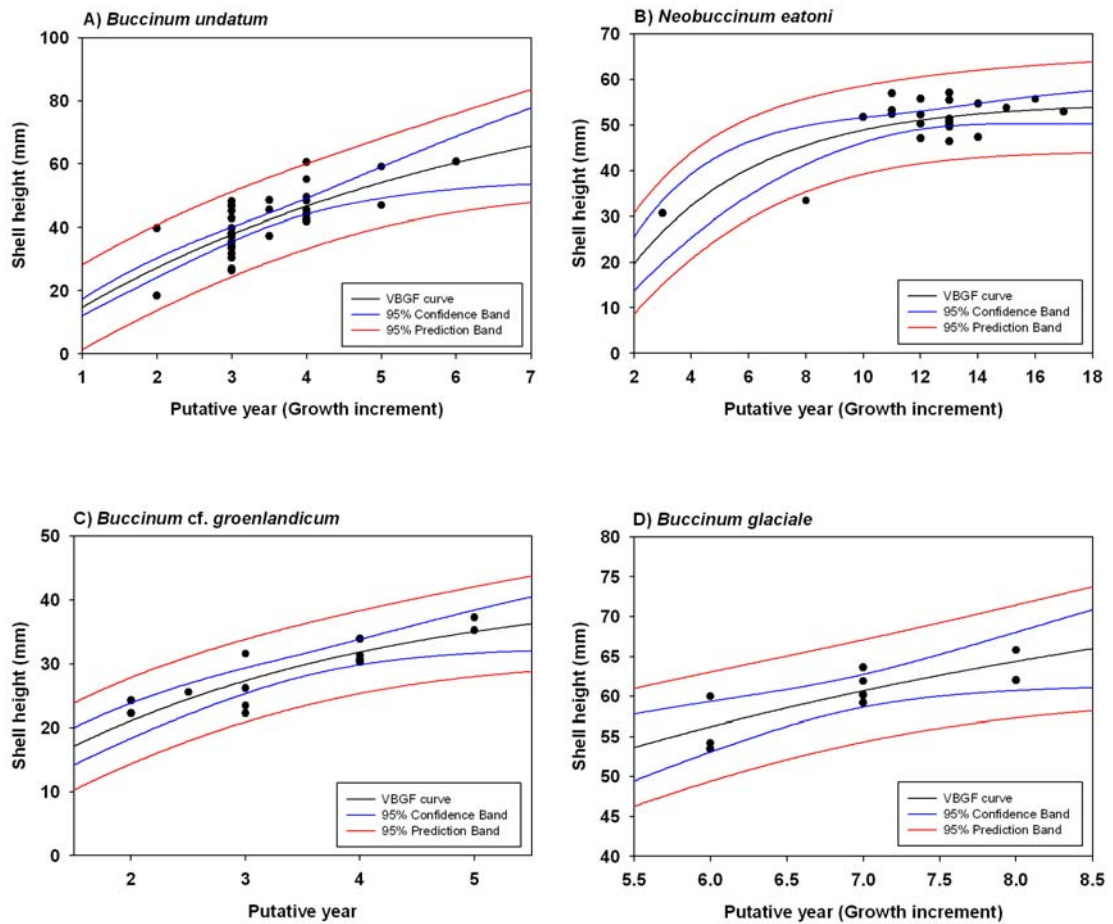


Figure 6.18 VBGF curves for A) *Buccinum undatum*, B) *Neobuccinum eatoni*, C) *Buccinum cf. groenlandicum* and D) *Buccinum glaciale*.

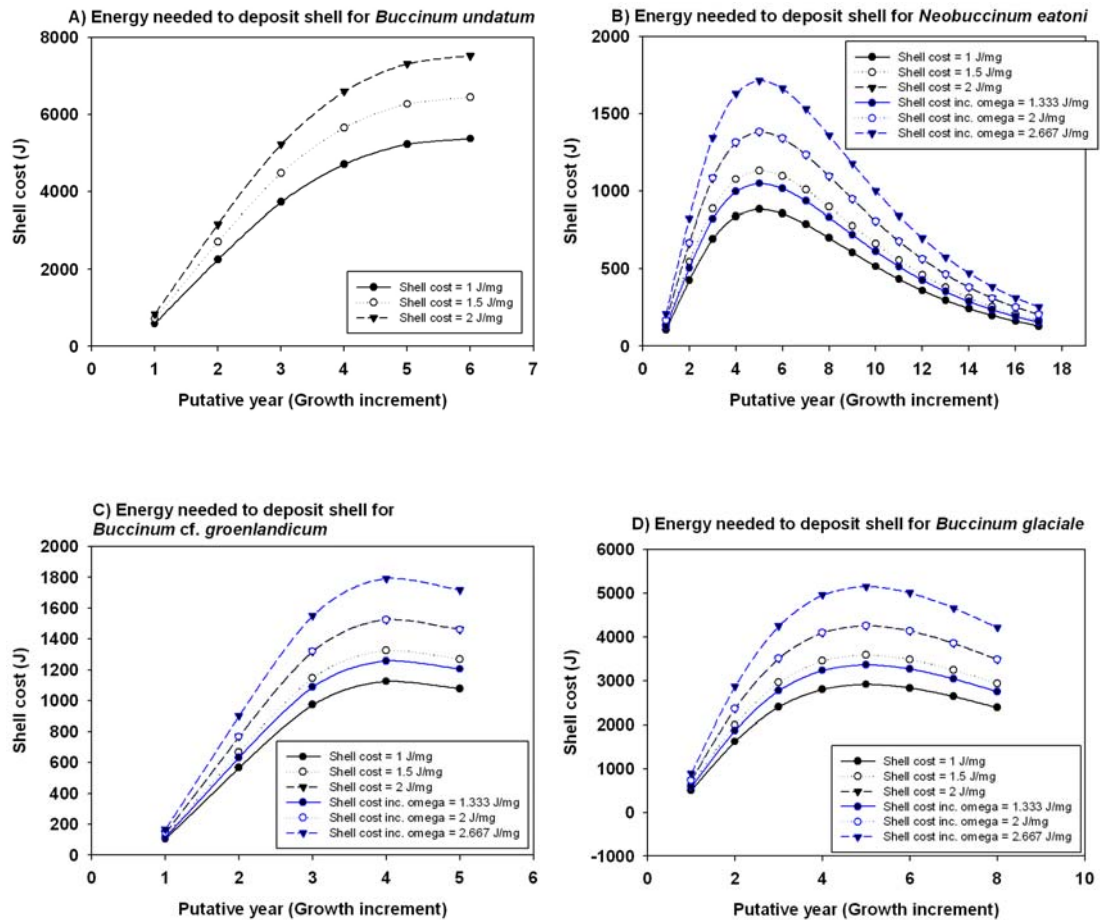


Figure 6.19 Energy required for shell deposition based on VBGF curves and CaCO_3 and organic matrix content of the shell for A) *Buccinum undatum*, B) *Neobuccinum eatoni*, C) *Buccinum cf. groenlandicum* and D) *Buccinum glaciale*. The theoretical extra cost of producing the shell based on differences in the saturation state of CaCO_3 in seawater, is shown as blue curves on the graphs. Note that the cost for the temperate species remains the same since Palmer's (1992) cost calculations were done at temperate conditions.

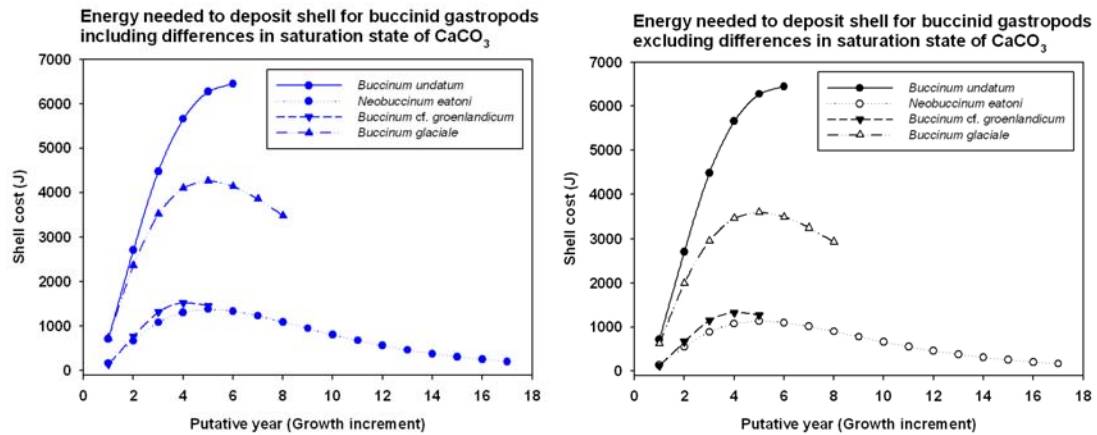


Figure 6.20 Energy required for shell deposition based on VBGF curves, CaCO_3 and organic matrix content of the shell for buccinid gastropods including differences in CaCO_3 saturation state (left) and excluding differences in CaCO_3 saturation state (right).

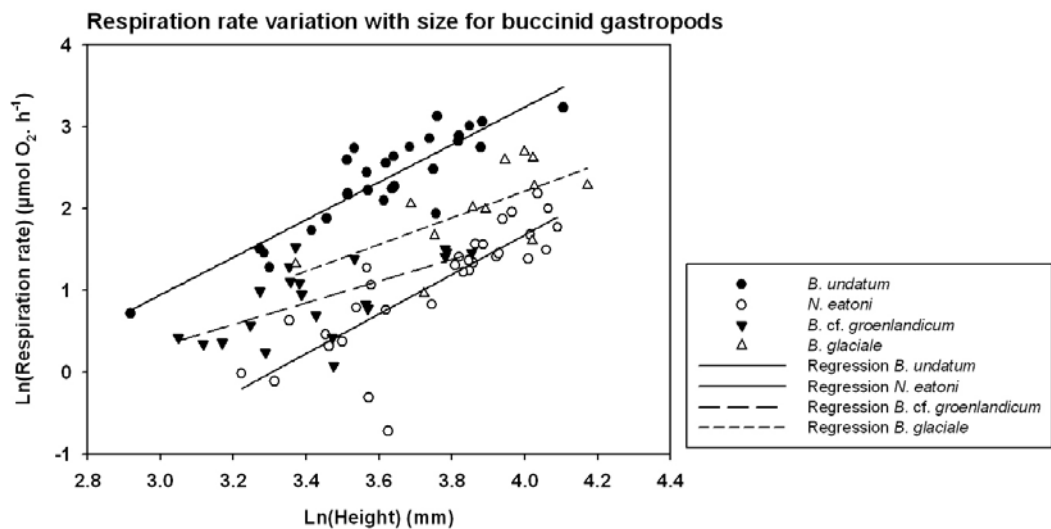


Figure 6.21 Variation in respiration rate with size for buccinid gastropods. All regressions were significant: *B. undatum* ($F = 103.8935$, $df = 1,26$, $p < 0.0001$), *N. eatoni* ($F = 60.6835$, $df = 1,29$, $p < 0.0001$), *B. cf. groenlandicum* ($F = 12.6214$, $df = 1,19$, $p = 0.0021$) and *B. glaciale* ($F = 7.1936$, $df = 1,10$, $p = 0.0230$).

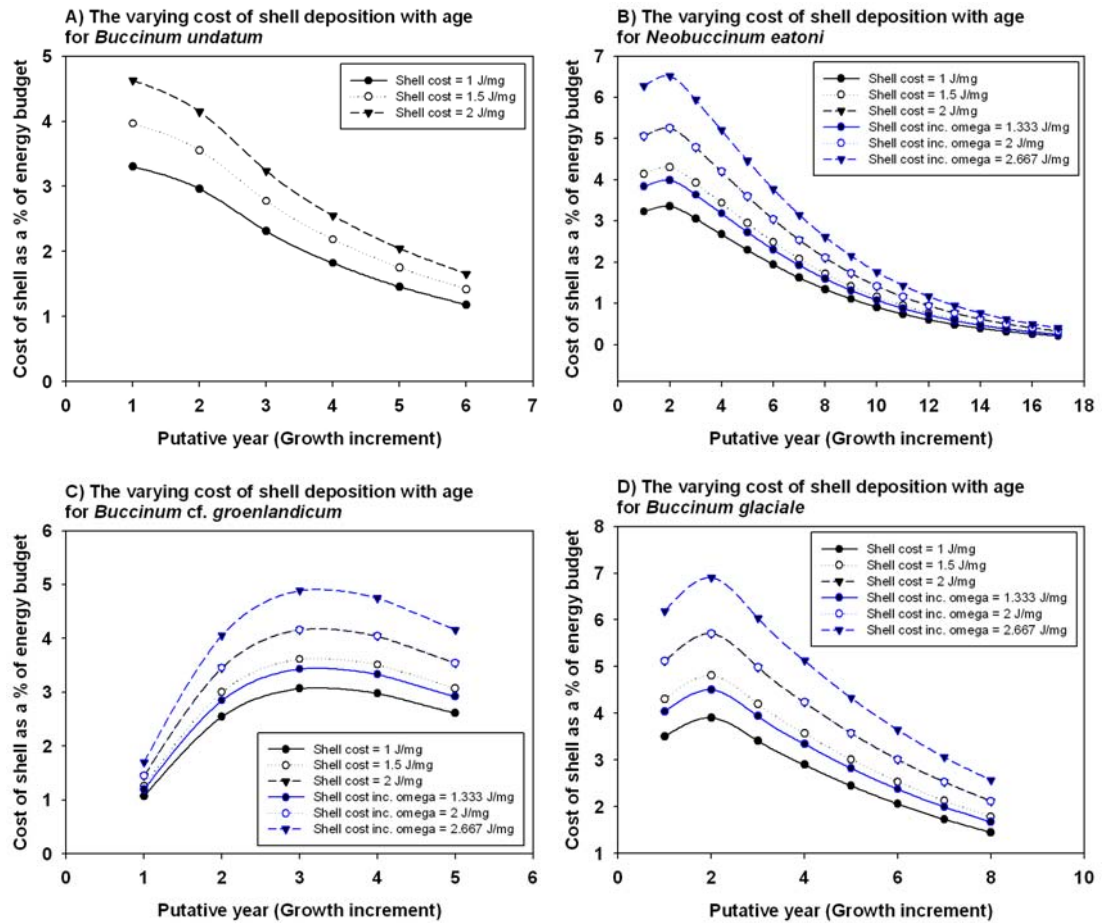


Figure 6.22 Variation in the cost of shell deposition with age for *Buccinum undatum*, *Neobuccinum eatoni*, *Buccinum cf. groenlandicum* and *Buccinum glaciale*.

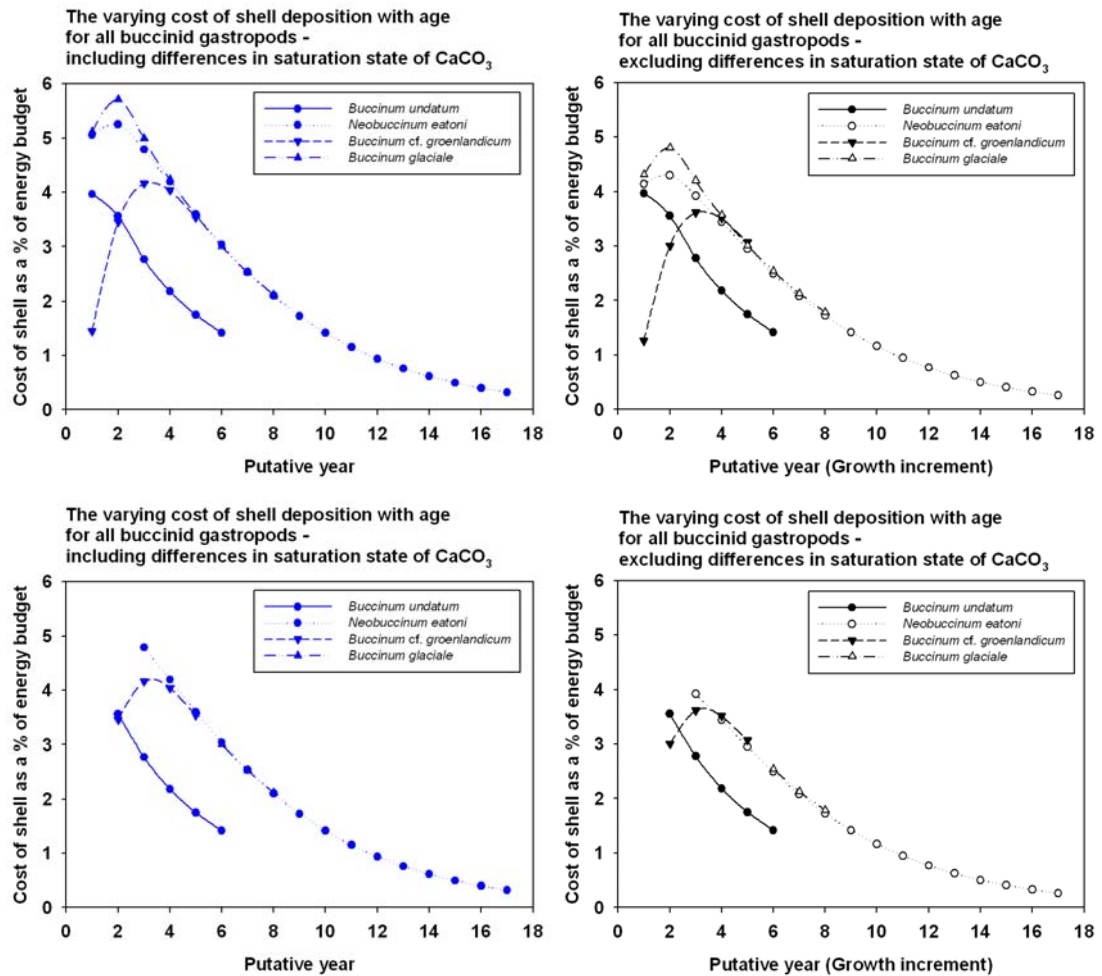


Figure 6.23 Variation in the cost of shell deposition as a percentage of the total energy budget (I) with age for all buccinid gastropods including differences in CaCO_3 saturation state (left) and excluding differences in CaCO_3 saturation state (right). The bottom graphs show data only for age ranges sampled.

6.4 Discussion

Growth

In general, polar species are characterised by slow, seasonal growth rates (Clarke, 1983; Peck, 2002). The polar clam had a low k value and so a slow rate of growth to maximum size. Tropical *Laternula* species had fast rates of growth to their maximum size (higher k values). However, tropical clams were smaller than the polar clam, and rate of absolute growth showed the polar species *Laternula elliptica* grew faster than all the other *Laternula* species studied (Figure 6.5). Everson (1977) found the Antarctic bivalves *Laternula elliptica* and *Adamussium colbecki* were relatively fast growing when compared to the temperate bivalve *Venus striatula* and Sato-Okoshi and Okoshi (2002) found no evidence that the growth rate of *Laternula elliptica* was low compared with temperate and tropical species. Clarke (1983) observes that the Antarctic *Laternula* grows faster than some temperate water species, but that when comparing species of similar ecology and maximum size, the polar species is always the slowest growing (e.g. Everson, 1977; Ralph & Maxwell, 1977; Clarke, 1980). *Laternula* clams studied had similar ecology (being infaunal congeners), but different maximum size. The observation from this chapter that it is not always appropriate to solely compare the k values for very different sized animals to determine relative growth rate is supported by the statement from Clarke (1983). The fast growth rates in *Laternula elliptica* shown in this chapter and in Everson (1977) could reflect the ecological need to deposit more shell (see Chapter 7).

Peck (1997a) showed that absolute annual growth in the Antarctic brachiopod *Liothyrella uva* was slower than that of temperate brachiopods reported by Collins (1991) and Doherty (1979). This chapter showed that the temperate brachiopod *Liothyrella neozelanica* grew approximately twice as fast as *Liothyrella uva*. *Liothyrella neozelanica* had a higher k value and absolute growth than *Liothyrella uva* showing that it is appropriate to compare k values to interpret absolute growth for species with a similar maximum size. These data agree with Clarke's (1983) observation that the polar species is the slowest growing when comparing species of similar ecology and maximum size. Thus comparisons of these two congeneric brachiopods agree with the general trend that polar animals have slow growth

(Clarke, 1983; Peck, 2002). For further work, it would be interesting to determine if *Liothyrella neozelanica* growth bands are deposited on an annual basis as there is evidence that bands are not formed annually in *Liothyrella uva* (Peck & Brey, 1996); however, as mentioned above this is currently under debate.

Like the *Laternula* bivalves, the smaller buccinid gastropods had the fastest rates of growth to maximum size (k values). These were both polar species. However, in terms of absolute growth, e.g. sized reached at a common age of 5 or 6 years, the temperate species *Buccinum undatum* reached the largest size at this age and, therefore, had a faster absolute growth rate. Another temperate buccinid *Buccinum isaotakii* reached a similar size to *B. undatum* at an age of 5 to 6 years (Ilano *et al.*, 2004) also growing faster than the polar buccinids studied here. Polar buccinids had slower absolute growth rates supporting the generalisation that polar species are slow growing (Clarke, 1983; Peck, 2002).

The pattern of fast absolute growth in the polar bivalve is in contrast to results for the polar gastropods and brachiopod, which had slow growth. There is evidence that growth rates during the brief polar summer may be comparable with temperate species (Nolan & Clarke, 1993; Peck & Bullough, 1993) and it has been argued that seasonal food availability rather than temperature *per se* limits growth in polar species (Clarke, 1983; Arntz *et al.*, 1994). Where growth is predominantly limited to the brief polar summer (Clarke & Lakhani, 1979; Richardson, 1979) or associated with food resources gained during the polar summer⁵ (Peck *et al.*, 1997a), then overall annual growth rates are limited by long periods of low resource availability. Perhaps then the polar soft-bottom filter-feeding clam can grow faster because this ecotype may not be as food limited as the scavenging gastropod or the hard-bottom filter-feeding brachiopod. However, it is unlikely that a scavenger will be more limited than a filter feeder (L. Peck, pers. comm.). Alternatively, perhaps the polar bivalve has such an efficient seasonal activity reduction (Morley *et al.*, 2007a) that it is more efficient than the other polar species.

⁵ Growth in *Liothyrella uva* is 2 times faster in winter than in summer but is decoupled from food availability.

Conclusion 1

Hypothesis 1: Warmer water species will have faster growth rates than cooler water species.

Accepted for buccinid gastropods and *Liothyrella* brachiopods in terms of absolute growth.

Rejected for *Laternula* bivalves in terms of absolute growth.

Energy required (J) to deposit shell

Unsurprisingly the largest animals within each taxon required more energy (in J) to deposit their shell e.g. *Laternula elliptica* (Figure 6.7), *Liothyrella neozelanica* (Figure 6.15), *Buccinum undatum* and *B. glaciale* (Figure 6.20). Since this absolute energy cost of the shell included organic matrix, it accounted for differences in cost due to variation in shell organic content among species. The percentage of shell organic content was generally similar enough within a taxon or low enough that it made little difference to shell cost among species.

Factoring in an approximate linear decrease in the saturation state of CaCO_3 with temperature, the shells of polar species cost proportionally more than the shells of temperate species per unit of CaCO_3 deposited, which in turn cost more than the shells of tropical species. Such costs may have been outweighed by large differences in organic content of the shells but this was not observed.

For the polar brachiopod *Liothyrella uva*, the increase in energy required to produce the shell caused by the increase in solubility of CaCO_3 in cold water was greater than the energy required to produce the shell with organic content included at both 1 and 3.87 % (Figure 6.14). Therefore, although organic matrix is energetically expensive to make (Palmer, 1992), given the proportions of organic matrix with the brachiopod shell, the cost of changes in solubility of CaCO_3 are greater and arguably more important than changes in the organic matrix content of between 0 – 4 %. Organic matrix content greater than around 5 % would start to incur a greater cost than that caused by CaCO_3 solubility. This may be an evolutionary tipping point. In cold waters, shells may be expected to remain below a 5 % organic matrix content as there is no advantage to producing a shell with a greater

amount of organic matrix as it is more expensive than dealing with the cost of solubility. Indeed none of the shells in this chapter were greater than 6 % organic content and only 1 polar species *Buccinum* cf. *groenlandicum* had a ‘whole shell’ organic content greater than 5 %.

Proportional cost of shell production as a percentage of the total energy budget

Metabolic rate and soft tissue growth increments were used to estimate the total energy budget for each species and, subsequently, compare the absolute energy (in J) required to deposit the shell with the total energy budget. Metabolic rate increases as temperature increases from polar regions to the tropics (Chapter 5). Adjustments were made for seasonal changes in metabolic rate in temperate and polar species. There may have been some intra-annual variation in other factors in the tropics such as the monsoon or productivity from variation in upwelling, but these potential changes in metabolic rate were assumed to be small compared to differences among latitudes. Growth does vary with season, usually occurring during periods of feeding (Clarke & Lakhani, 1979; Richardson, 1979). In the brachiopod *Liothyrella uva*, Peck *et al.* (1997a) showed growth was decoupled from energy input with shell growth taking place in winter. There was no need to adjust calculations for seasonal changes in grow rate and timing of growth because the results in this chapter show the cost of the shell as a percentage of the annual total energy budget.

It is clear that this chapter relies heavily on Palmer’s (1992) data as this is the only record of a cost of CaCO_3 production available in published scientific literature. It is thus essential for this chapter. Palmer (1992) used separate laboratory and field experiments conducted on two species of the gastropod genus *Nucella* of naturally different shell thickness to ascertain the cost of producing a CaCO_3 skeleton. The differences in the number of barnacles ingested between thick and thin morphs were calculated by batch processing of barnacles eaten per cage of snails, rather than for each individual snail. Although experimental conditions produced large differences among cages, there were small residual differences remaining among replicates. It was assumed that these residual differences in food intake resulted from differences in shell growth compared to body growth in different

batches of snails and also from random differences among cages. The residual differences were used to estimate the cost of CaCO_3 production.

Unfortunately, Palmer (1992) does not state the temperatures at which the experiments upon which he bases his shell cost calculations were conducted nor the temperature or range of temperatures that the cost of CaCO_3 production was calculated for. In one of the original papers on which the work was based, the seawater temperatures were approximately 11 °C (Appleton & Palmer, 1988). Since all the experiments were conducted at temperate locations, it is reasonable to assume these costs of shell production are for temperate conditions and will hold for temperate comparisons, but that adjustments are required for tropical and polar comparisons.

The fast growing polar clam *Laternula elliptica*, with the largest shell and lowest metabolic rate consequently had the greatest cost among *Laternula* species of shell production as a proportion of its total energy budget (I), at approximately 3 – 4 % of the total energy budget from clams aged 2 years upwards (Figure 6.9 and Figure 6.24). The cost of shell production was least in the tropical *Laternula* species and mid-range in the temperate species. The effect of the increase in CaCO_3 solubility at low temperatures meant that when the cost of CaCO_3 solubility was included, the cost of shell production in *Laternula elliptica* was approximately 0.5 % greater than the cost of shell production without the theoretical increase in solubility (Figure 6.10). Cold water does not seem to prevent fast growth, or the formation of a large, albeit comparatively costly shell in *Laternula elliptica*. This may be because for *Laternula elliptica*, the increase in cost associated with CaCO_3 solubility was quite small.

The free energy of precipitation of CaCO_3 from seawater increases in an approximate linear fashion as temperature decreases from 30 to 0 °C (Clarke, 1983). Clarke (1990) states that if the cost of producing a shell is only 1 % of the total energy budget, then temperature dependence of the metabolic cost of calcification is of little importance. However, if the cost of producing a shell is 15 % of the total energy budget, then the temperature effect on CaCO_3 solubility is very important. For the polar clam, the values found in this chapter are towards the lower end of this scale at around 2 – 3.5 % without including CaCO_3 solubility.

Including a linear increase in cost from solubility puts this figure slightly higher at 2.5 – 4.5 % which may be enough to form a significant proportion of the total energy budget.

The polar brachiopod had the highest cost of shell production of all taxa studied peaking at around 6 to 10 % excluding CaCO₃ solubility and 7 to 13 % including CaCO₃ solubility (Figure 6.17). The cost diminished with age as growth rate slowed. The increase in CaCO₃ solubility at low temperatures caused a 1 – 2 % increase in the cost of shell production in *Liothyrella uva* based on a mid-range valve of 1.5 J.mg⁻¹ for calcification (Figure 6.17). For brachiopods, these data suggest the temperature dependence of calcification (Clarke, 1990) could be very important to the animal. Brachiopods have low energy lifestyles (Curry & Ansell, 1986; Peck, 1992; Peck *et al.*, 1997b) and low metabolic rates (Chapter 5 and Peck *et al.*, 1986a; Peck *et al.*, 1986b; Peck *et al.*, 1987b; Peck, 1989; 1996; Peck *et al.*, 1997a). However, polar brachiopods did not have thinner shells than temperate congeners (Chapter 3) and this is why the cost of shell as a proportion of the total energy budget is high. There is one caveat to this is that Palmer (1992) calculated the cost of calcification in marine molluscs. Brachiopods are physiologically different to the Mollusca (e.g. Peck *et al.*, 1997b) and the cost of calcification could be slightly different in the Brachiopoda. However, there could just be an ecological need for a thick shell (e.g. protection) or an evolutionary constraint in the polar brachiopod and that this cost of this thick shell is met by the high proportion of the energy budget portioned into shell production.

The thick-shelled Arctic buccinid *B. glaciale* and the thin-shelled low-metabolism Antarctic buccinid *N. eatoni* had the highest costs of shell production for buccinids. The cost of the shell in thin-shelled Arctic buccinid *Buccinum* cf. *groenlandicum* is likely to be very similar to *B. glaciale* and *N. eatoni* but the different shape of the growth curve gave lower cost values for the first 2 years in *Buccinum* cf. *groenlandicum*. The effect of the increase in CaCO₃ solubility at cold temperatures is clearly seen in the buccinid shell cost data (Figure 6.23). Without CaCO₃ solubility included the cost of the shell to the polar species tracks around 1 % higher than that of the temperate species. With CaCO₃ solubility included, the cost of the shell to the polar species tracks around 1.5 % higher. Shell cost is likely to be very significant to the polar buccinids in the early years of life.

Summary graphs (Figure 6.24) compared shell cost as a percentage of the total energy budget across a common age for each taxon: age 3 for *Laternula* clams and age 5 for buccinid gastropods. These comparisons show shell cost for bivalves and gastropods was significantly related to temperature and latitude for bivalves. The latitudinal trend in gastropods was possibly obscured by the heating of the Arctic site by the Gulf Stream resulting in warmer, sub-Arctic water temperatures than may be expected for its high latitude. From these estimates of proportional shell cost, temperature seems to explain most of the variation in shell cost with latitude and may be the most important control in the cost of shell production rather than other factors that vary with latitude such as primary production.

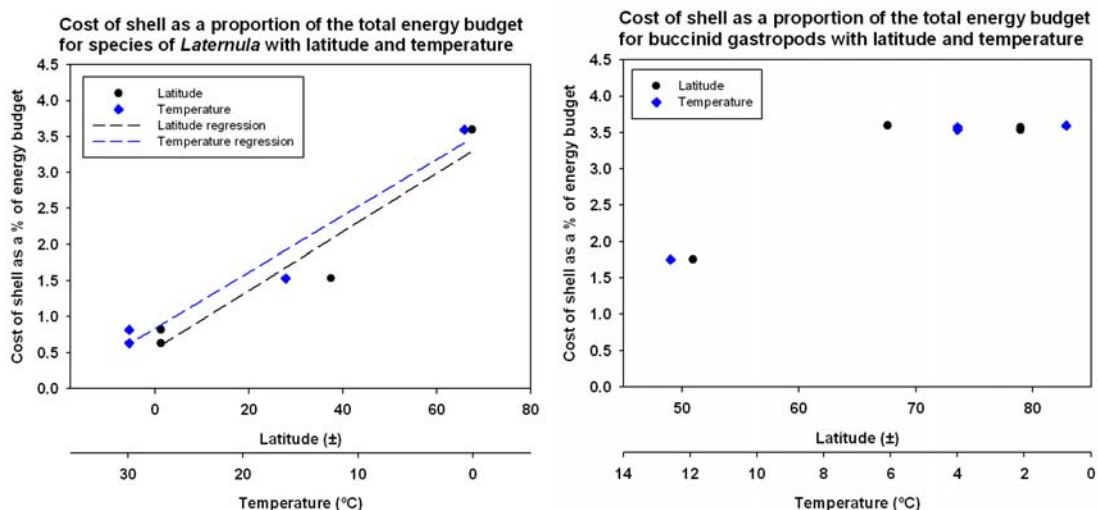


Figure 6.24 The cost of shell as a proportion of the total energy budget was significantly related to temperature for *Laternula* ($F = 47.4602$, $df = 1,2$, $p = 0.0204$) and for buccinid gastropods ($F = 22.6881$, $df = 1,2$, $p = 0.0414$). The cost of shell was significantly related to latitude in *Laternula* ($F = 23.7545$, $df = 1,2$, $p = 0.0396$) but not significantly related to latitude in the Buccinidae ($p = 0.0938$ NS). Cost values were taken at age 3 for *Laternula* and age 5 for buccinids because these ages overlapped measured individuals for most species within the taxa. These costs were based on mid-range data of 1.5 J.mg^{-1} of CaCO_3 from Palmer (1992).

Conclusion 2

Hypothesis 2: Colder water species have lower metabolic rates, so the cost of shell production as a proportion of the annual total energy budget (I) of each species will increase with increasing latitude or decreasing temperature.

Accepted for *Laternula* clams and buccinid gastropods.

Solubility of CaCO_3 , climate change and ocean acidification

Results from this chapter show that accounting for the effects of CaCO_3 saturation state can have an important effect on the energy required to deposit shell and shell cost in terms of the total energy budget. Anthropogenic carbon dioxide (CO_2) released into the atmosphere from fossil fuel combustion and deforestation is increasing at an unprecedented rate. Up to 40 % of this atmospheric CO_2 is absorbed by the oceans (Zeebe *et al.*, 2008) driving the equilibrium reactions (Equations 1-4) to produce more bicarbonate ions and hydrogen ions and thus lowering the saturation state (Ω) of CaCO_3 . This fall in Ω over the entire surface oceans is a phenomenon termed ocean acidification. Figure 6.25 shows the fall in Ω since pre-industrial times. On the plots, the rise in Ω for the higher northern latitudes exists because there are few or no data for that area; however, new research suggests that the Arctic will become undersaturated with respect to aragonite by 2050 (J. Orr, pers. comm.). Since Ω is already lowest in the polar regions and polar animals have some of the highest costs of shell production, ocean acidification is likely to have a dramatic impact on calcified marine animals in these regions. Using a value of $\Omega = 1$ for the year 2050 and an approximate 2.5 times increase in solubility from present-day conditions (i.e. a value of 2.5 for calcite from Figure 6.25 but also see Table 6.2), the theoretical increase in the proportional cost of shell production as a result of ocean acidification for Antarctic species is estimated to be 56 % for *Laternula elliptica*, for 68 % *Neobuccinum eatoni* and 79 % for *Liothyrella uva* in the year 2050. Chapter 8 provides more detail on ocean acidification and its effects on the early life stages of a mollusc.

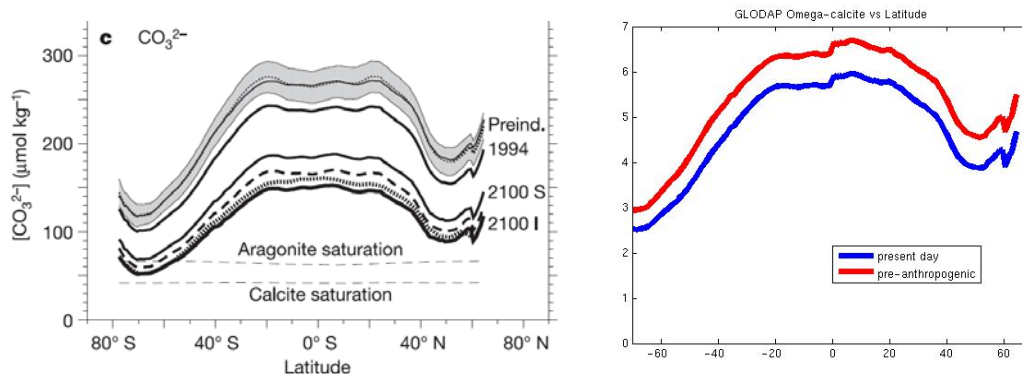


Figure 6.25 The decrease in carbonate ion concentration (Orr *et al.*, 2005) (left) and corresponding fall in saturation state (plot by T. Tyrrell from GLODAP data) (right) in the world's surface oceans since pre-industrial times.

Limitations

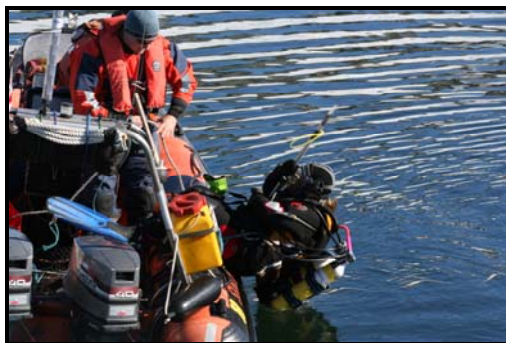
The same calculations were performed throughout on all species so there is reasonable confidence in the relative estimates of the cost of shell production among species. These costs are estimates and for some species there were no published seasonal respiration data available for comparison and also nitrogen excretion and faecal egestion were not included as measures in the energy budget. If available, the inclusion of these parameters is unlikely to affect the overall values by $> 50\%$ (L. Peck, pers. comm.). Some could argue that a limitation to this study is that it overestimates the cost of the organic matrix in the shell because it takes a 'whole shell' approach to the cost of production. If detailed data on organic matrix content of individual shell layers are available, it is of course possible to correct precisely for organic matrix content within individual shell layers if one so wishes. This was outside the scope of this thesis and such accuracy was not deemed suitable for these estimates of shell cost. In doing so it is likely that the costs as a percentage of the total energy budget will be fractionally lower.

Summary

The cost of shell production was greatest in the polar species compared to non-polar species. The proportional cost of shell in polar clams was 2 – 4.5 %. In polar buccinids the cost peaked at around 3 – 7 % of the total energy budget in the first few years of life and subsequently diminished. The cost in the polar brachiopod was very high, at 6 – 13 % of

the energy budget, decreasing to 3 – 8 % with age. Climate change has already reduced the saturation state of CaCO_3 in surface ocean waters across the globe. Further change will make shell production more difficult for calcareous animals.

Chapter 7: Predation pressure – latitudinal patterns in shell repair and defence morphology



Chapter 7: Predation pressure

– latitudinal patterns in shell repair and defence morphology

7.1 Introduction

The function of the shell in defence

Shells and exoskeletons provide protection from abiotic and biotic factors. In the process of protecting the inhabitant, injuries to shells can be caused by: 1) a shell-breaking predator; 2) grinding by rocks; 3) competition with rivals; and 4) prey attempting to break the predator's shell (Vermeij, 1987). Shells may also be eroded and weakened by shell-boring commensals such as sponges and polychaetes. According to Vermeij (1987), “predation is the most important cause of nonlethal injuries in most [gastropod] species”. Thus the integrity of the shell as a defence is vitally important in ensuring the survival of the organism and the requirement of particular shell morphologies to function in defence may be the alternative explanation of more massive, thicker shells at low latitudes and smaller, thinner shells at polar latitudes. This chapter questions whether a lack of shell drilling and crushing predators in high latitude shallow-shelf habitats (< 100 m depth) (Aronson & Blake, 2001; Clarke *et al.*, 2004; Aronson *et al.*, 2007) results in the patterns in shell morphology described in Chapter 3, and for some groups, a smaller or thinner shell.

As described in Chapter 1, extant predators of shelled animals include durophages (shell-crushing) and shell-boring (drilling) predators. Predators of armoured animals use 5 methods of subjugation:

- 1) whole-animal ingestion – where the victim is swallowed whole without damage to the skeleton,
- 2) insertion and extraction – where the predator penetrates between the shell valves or openings but without damage to the skeleton,
- 3) transport – the movement of the prey to an environment where continued survival is not possible,

- 4) pre-ingestive breakage – the mechanical destruction of the skeleton which causes breakage and death to the animal, and
- 5) drilling – a small hole is made through the prey's skeleton to the soft tissues below either mechanically or chemically, without other damage to the skeleton (Vermeij, 1987).

The exoskeleton functions in 1) predator avoidance, by minimising predator detection of the animal, and in 2) protection, during the subjugation phase of a predator attack. In gastropods, large size, thick shells and low spires provide resistance to predation (Vermeij, 1974; 1987). Additionally the presence of sculpture on the shell such as ribs, tubercles, spines and flanges increases resistance to attack. Sculpture increases shell strength and concentrates forces of crushing predators to small but thickened areas (Palmer, 1979). Sculpture also increases the size of the victim thus thwarting some whole-animal ingesting- and crushing-predators (Vermeij, 1987).

Shell surface relief encourages the settlement of sessile organisms such as encrusting animals and coralline algae on the shell surface. A covering of such organisms may make the animal harder to detect either by camouflage or smell. Most tropical reef snails are encrusted with coralline algae (including one of the tropical study species in this thesis *Cantharus fumosus*) providing an inconspicuous cover and protecting the shell from boring sponges and other bioeroders (Vermeij, 1987).

In coiled gastropods, the snail can often withdraw soft tissues completely into the shell avoiding detection and attacks via the aperture. For this reason narrow apertures confer greater resistance to predation (Palmer, 1979). Such occluded apertures are employed by marine benthic gastropods to thwart shell-breaking and shell-entering predators (Vermeij, 1974). Many tropical snails have narrow apertures. In most tropical marine assemblages from shallow-water sand bottoms, 50 – 60 % of marine snails have apertures defined as narrow; that is those with length:width ratios of 2.5 or higher (Vermeij, 1993).

The shells of bivalves are generally weaker than gastropods and the most important method of protection in bivalved animals is the tight seal (Vermeij, 1987). However, many

bivalves, especially deep burrowing groups, have permanent gapes between the two shells (Stanley, 1970; Runnegar, 1974). For bivalved animals with permanent gapes, complete protection by the shell is not as important against predation either because the animal lives in a relatively safe environment, for example below the sediment surface, or because the animal relies on defences other than armour, such as rapid escape (Vermeij, 1987) or chemical defences (McClintock *et al.*, 1993).

Traces of predation

Predation rate in natural ecosystems is often difficult to measure and lab experiments are not always able to mimic *in situ* conditions. For living and fossilised shelled animals, predation intensity can be inferred by analysis of repaired shell damage (e.g. Vermeij, 1982b; Alexander & Dietl, 2000; Alexander & Dietl, 2001; 2003; Harper *et al.*, submitted). Pre-ingestive breakage and drilling is not 100% successful and failed predation attempts of these types leave traces of damage in the form of scars and repair marks on the shells of living animals. The shape of the repair yields information such as the mode of attack on shelled animals, for example as repaired peeling injuries or incomplete drill holes. Thus analysis of repaired shell damage is a measure of unsuccessful, or failed, predator attacks on individuals in the population.

7.1.1 Aims

To test the hypothesis that at higher latitudes shelled marine invertebrates experience less predation by analysis of shell repair marks and shell defence morphology.

Hypothesis 1: There is a change in the frequency of shell repairs with latitude and, specifically, shell repairs decrease with increasing latitude.

H₀: There is no change in the frequency of shell repairs with latitude.

Hypothesis 2: There is a change in shell defence morphology with latitude and, specifically, shell defensive traits decrease with increasing latitude.

H₀: There is no change in shell defence morphology with latitude.

7.2 Methods

7.2.1 Observations of shell repairs on living specimens

Data on shell repair marks were collected from species across latitudes as described in Chapter 2. Morphological measurements were recorded as described in Chapter 3. The number of repaired injuries (damage) on each shell was counted. Generally bivalves are not very effective at repair after a predation attack because their body fluids can leak out and their mantle is often damaged. In contrast, gastropods are much better at surviving a predator attack because the mantle can retract into the shell. In gastropods, if the shape of the repair indicated that it was likely a predator caused the original shell breakage, then this was noted separately. Examples of gastropod repair marks that were characteristic of a predation attack are shown in Figure 7.5. These repaired injuries from predator attacks are a conservative measure of sub-lethal predation intensity. Repair marks were analysed according to Alexander and Dietl (2001). The shape of the repair mark and location on the shell provide a good indication of whether the original shell damage was caused by a predator or a different cause (see review by Alexander and Dietl (2003)).

Repair frequencies

Commonly used repair frequencies include:

- **Proportion of damaged individuals (N_d)** = number of individuals bearing 1 or more injuries / total number of individuals (e.g. Raffaelli, 1978; Cadée *et al.*, 1997)
- **Total number of injuries (N_i)** = number of injuries sustained within a sample / total number of individuals (e.g. Vermeij *et al.*, 1981; Dietl *et al.*, 2000)

In addition, further analyses were done on gastropods and predation-specific data on repair frequencies were obtained by:

- **Proportion of individuals damaged by predation (P_d)** = number of individuals bearing 1 or more injuries from predator attacks / total number of individuals

- **Total number of injuries from predation (P_i)** = number of injuries sustained from predator attacks within a sample / total number of individuals
- **Proportion of individuals with damage that was caused by a predator attack ($\propto P_d$)** = No. of individuals with predation injuries / No. of individuals with injuries
- **Proportion of all injuries that were caused by predator attacks ($\propto P_i$)** = No. of injuries from predation / No. of injuries in total

7.2.2 Observations of shell repairs on empty or ‘dead’ shells

Shell repairs on empty or ‘dead’ shells from shell assemblages were also counted.

However, in almost all sample locations it was difficult to find ‘dead’ shell assemblages, if indeed any empty shells at all. In fact, the only species for which empty shells could be found in abundance was *Laternula elliptica*.

7.2.3 Shell defence morphology: predator resistance

Additional shell morphology data were recorded from all species across latitudes to determine if characteristic shell defence structures differed with latitude. The size of gastropod aperture length and width (Chapter 3) and *Laternula* minimum and maximum shell inflation⁶ at the posterior gape and hinge, respectively, (Figure 7.1) were measured and related to overall body size for each species. These measurements are an indication of how well the animal can resist a predator attack by relying on the shell as a defence. In bivalves that have a permanent gape (such as the Laternulidae) the size of the gape is a likely indication of how well an individual can resist predation from above by withdrawing into its shell.

⁶ Bivalve shell inflation is sometimes referred to as shell width.

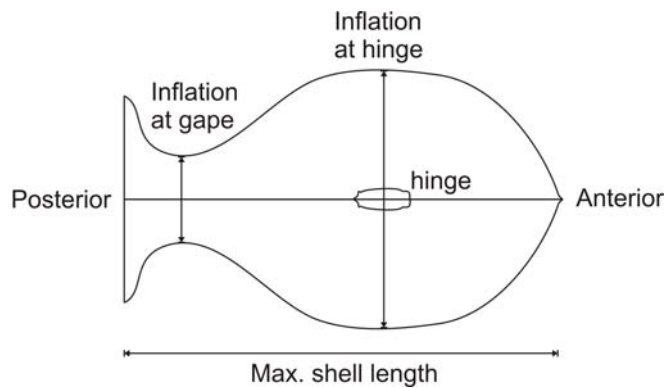


Figure 7.1 Diagram showing position of measurements of shell inflation in *Laternula* clams. The inflation at gape is the minimum inflation at the gape of the shell.

For gastropods, the size of the aperture relative to the total size of the shell (shell height) was calculated by Equation 1 as a measure of aperture resistance to predation. For bivalves, the inflation at the shell gape relative to the total size of the shell (maximum shell length) was calculated by Equation 2. These equations control for differences in shell size among species.

$$\text{Aperture relative size} = \text{aperture width} / \text{shell height} * 100 \% \quad \text{Equation 1}$$

$$\text{Gape relative size} = \text{min. inflation at gape} / \text{max. shell length} * 100 \% \quad \text{Equation 2}$$

Echinoid spine length was calculated by measuring the test diameter without spines and subtracting this from the total animal diameter (including spines) and then dividing by two.

7.2.4 Statistical analysis

Data were compiled on spreadsheets using MS Excel 2003. Statistical analyses were performed in SPSS 16.0 and SigmaPlot 10.0. Tests of normality and homogeneity of variance were conducted where appropriate and data were analysed using regression analysis, analysis of variance (ANOVA), analysis of covariance (ANCOVA) and post hoc tests. Where data did not have equal variances Welch's F test was used (Welch, 1951). Graphs were produced with SigmaPlot 10.0.

7.3 Results

Results are presented in relation to habitat type: firstly, the epifaunal groups (gastropods of the family Buccinidae and brachiopods of the genus *Liothyrella*), followed by the infaunal bivalves of the genus *Laternula*. As expected for counts close to zero, the distribution of repair marks on shells followed a Poisson distribution.

7.3.1 Observations of shell repairs on living animals

7.3.1.1 EPIFAUNA Gastropoda: family Buccinidae (superfamily Buccinoidea)

All shell repairs

Figure 7.2 and Table 7.1 show data for all shell repairs including those that were characteristic in shape of a predation attack. Figure 7.3 shows the Antarctic buccinid *Neobuccinum eatoni* has the lowest incidence of shell repairs. Shell repairs increase with increasing temperature for subtidal and immersed intertidal gastropods (Figure 7.4). N.B. the tropical gastropod are periodically emersed intertidal species.

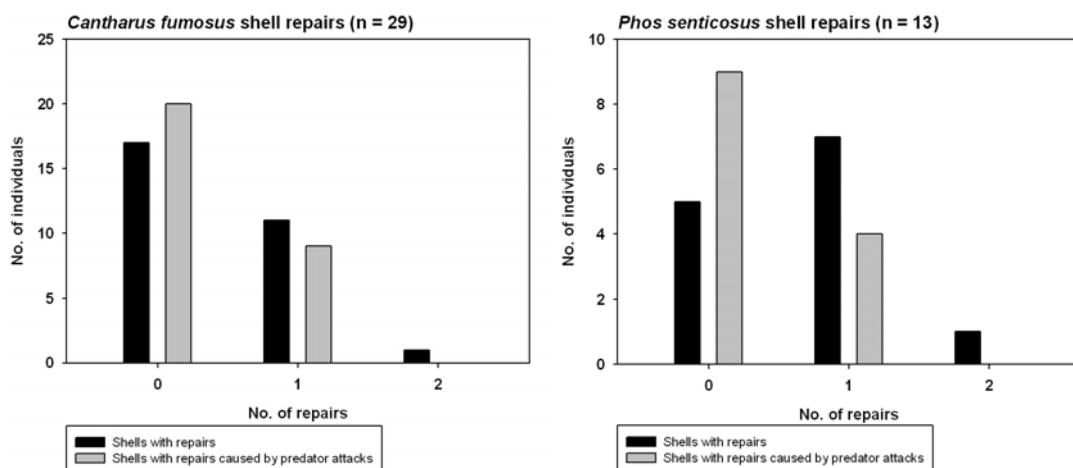


Figure 7.2 continues overleaf.

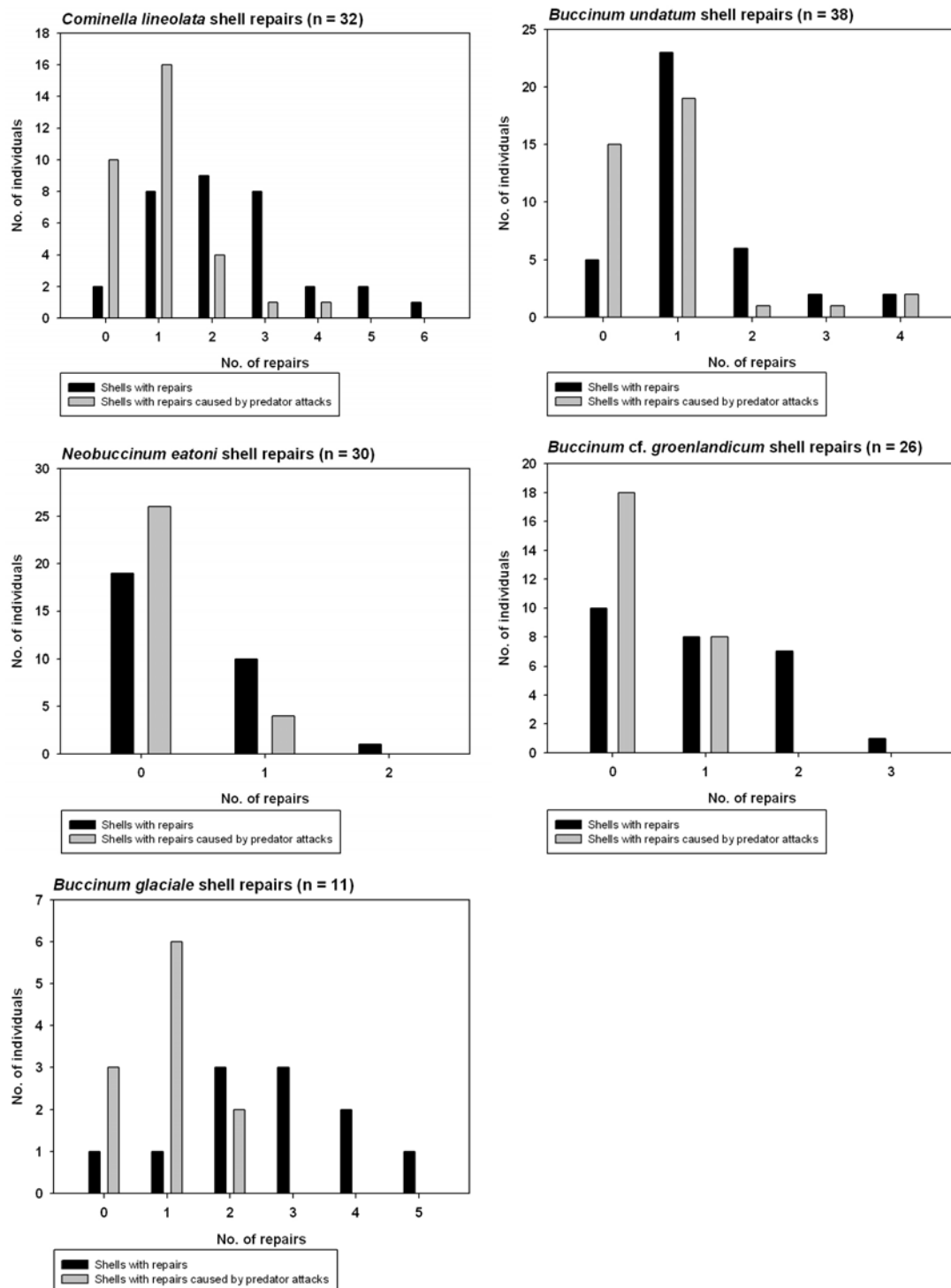


Figure 7.2 Histograms of number of repairs per shell in buccinid gastropods. All shell repairs are shown as black bars and shell repairs characteristic of predation damage are shown as grey bars. There were fewer repairs indicative of predation damage so the histograms for repairs caused by predator attacks are shifted to the left.

Table 7.1 Buccinid gastropod shell repair data.

Species	No. of inds.	No. of inds. with repairs	No. of repairs in total	No. of inds. with predation attack repairs	No. of predation attack repairs in total	N_d	N_i	P_d	P_i	αP_d	αP_i
<i>Cantharus fumosus</i>	29	12	13	9	9	0.414	0.448	0.310	0.310	0.750	0.692
<i>Phos senticosus</i>	13	8	9	4	4	0.615	0.692	0.308	0.308	0.500	0.444
<i>Cominella lineolata</i>	32	30	74	22	31	0.938	2.313	0.688	0.969	0.733	0.419
<i>Buccinum undatum</i>	38	33	49	23	32	0.868	1.289	0.605	0.842	0.697	0.653
<i>Neobuccinum eatoni</i>	30	11	12	4	4	0.367	0.400	0.133	0.133	0.364	0.333
<i>Buccinum</i> cf. <i>groenlandicum</i>	26	16	25	8	8	0.615	0.962	0.308	0.308	0.500	0.320
<i>Buccinum glaciale</i>	11	10	29	8	10	0.909	2.636	0.727	0.909	0.800	0.345

N_d : Proportion of damaged individuals

N_i : Total number of injuries

P_d : Proportion of individuals damaged by predation

P_i : Total number of injuries from predation

αP_d : Proportion of individuals with damage from predators

αP_i : Proportion of all repairs that were from predation attacks

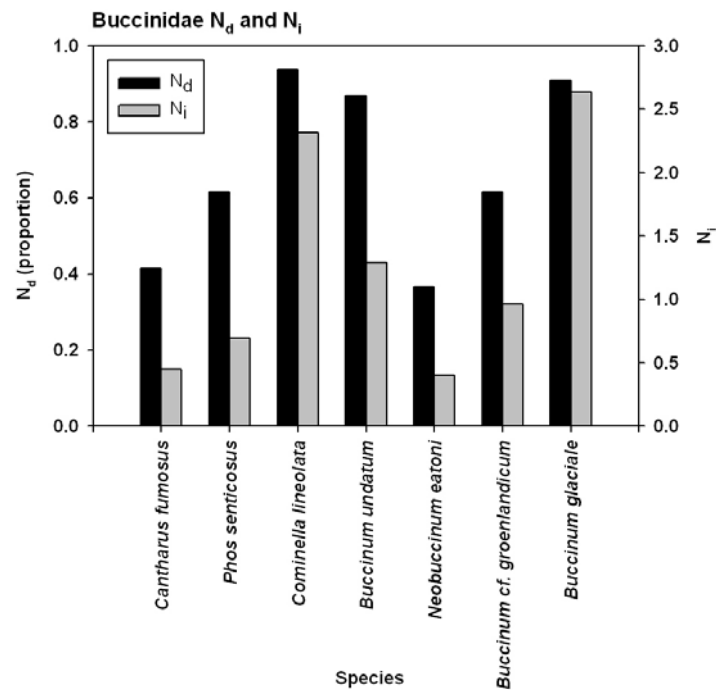


Figure 7.3 Shell damage data across the Buccinidae by species. N_d is the proportion of individuals with repairs and N_i is the total number of injuries (i.e. the number of repairs per shell).

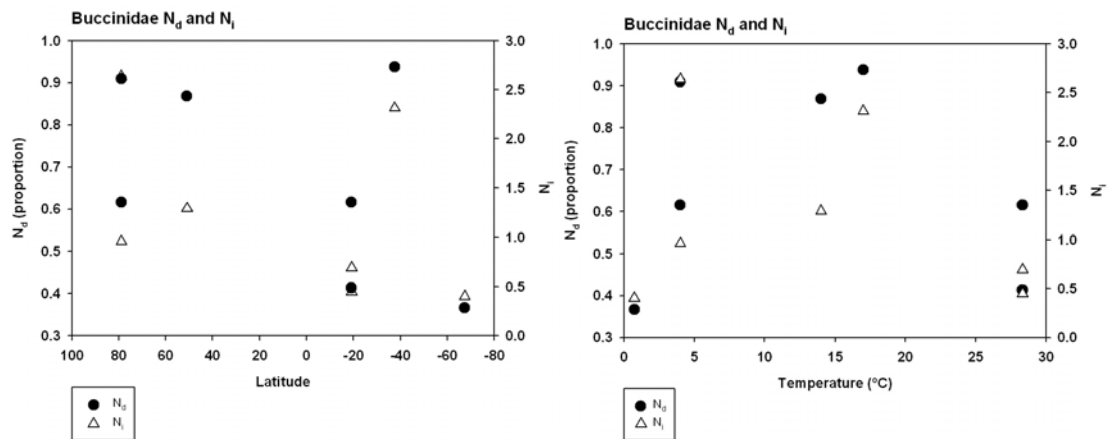


Figure 7.4 Shell repair data across the Buccinidae by latitude (left) and temperature (right). There were no statistically significant trends with latitude or temperature for N_d or N_i .

Shell repairs from predation damage

Repairs from predation (Figure 7.5) were also analysed separately from all repairs in gastropods. Figure 7.6 shows the Antarctic buccinid has low P_d and P_i . αP_i decreases from low to high latitudes in both hemispheres (Figure 7.7).

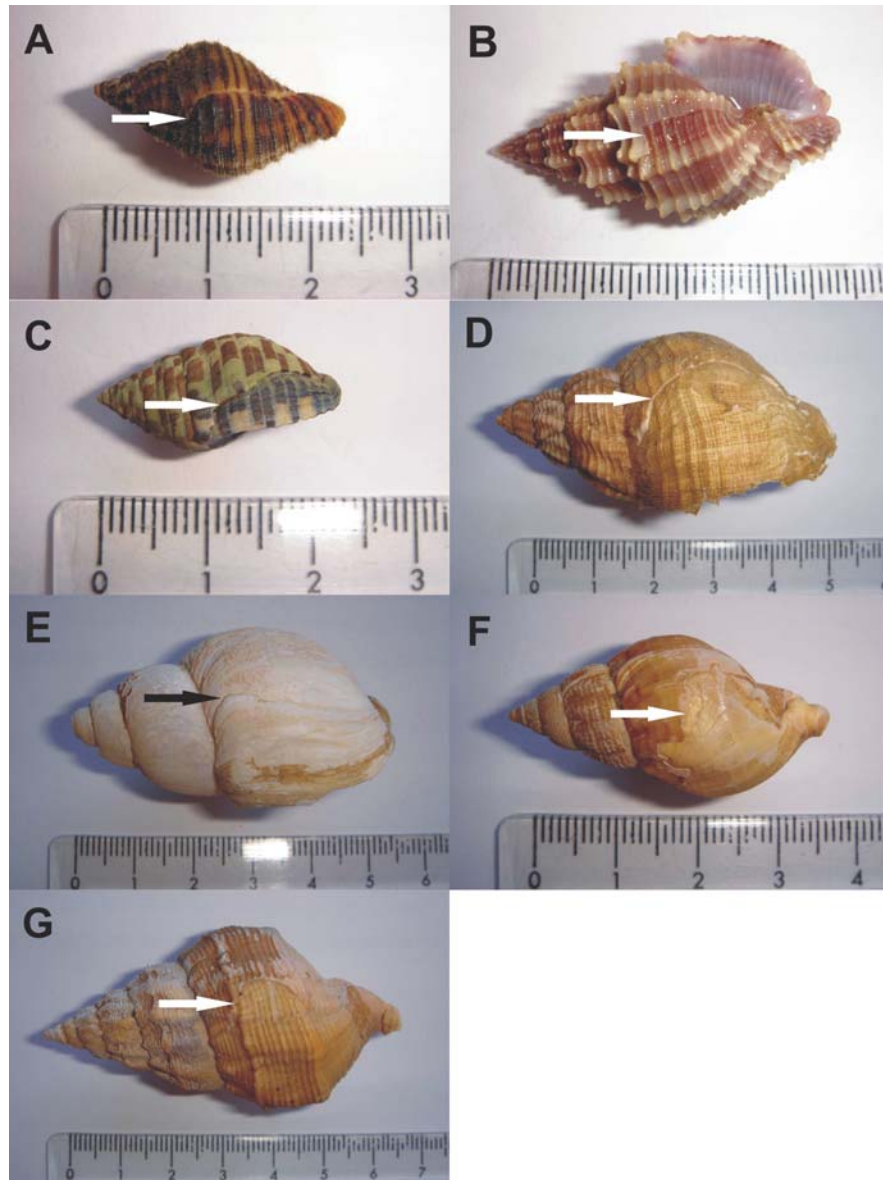


Figure 7.5 Repairs from shell damage likely to have been caused by a predator attack in A) *Cantharus fumosus*, B) *Phos senticosus*, C) *Cominella lineolata*, D) *Buccinum undatum*, E) *Neobuccinum eatoni*, F) *Buccinum cf. groenlandicum* and G) *Buccinum glaciale*.

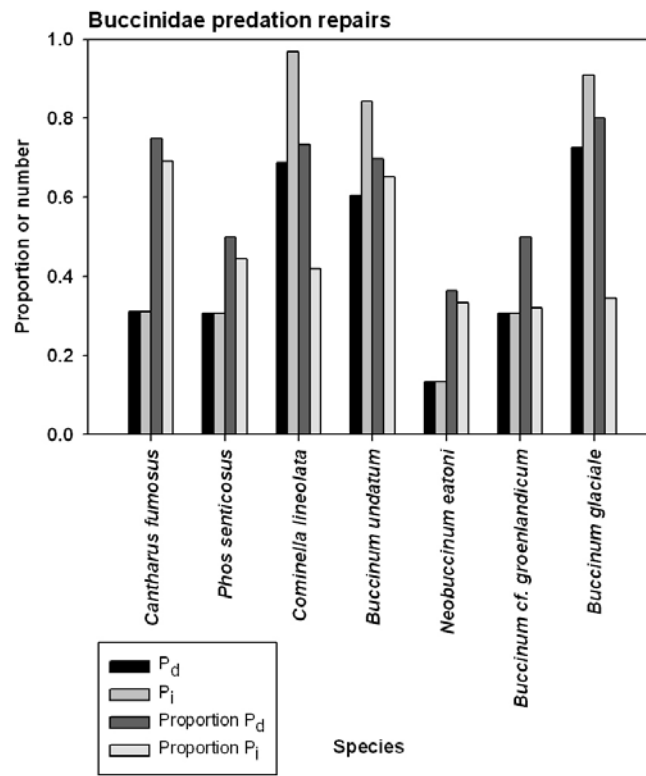


Figure 7.6 Shell damage characteristic of predation attacks across the Buccinidae by species. P_d is the proportion of individuals damaged by predation, P_i is the total number of injuries from predation, αP_d is the proportion of individuals with damage that was caused by a predator attack, and αP_i is the proportion of all injuries that were caused by a predator attack.

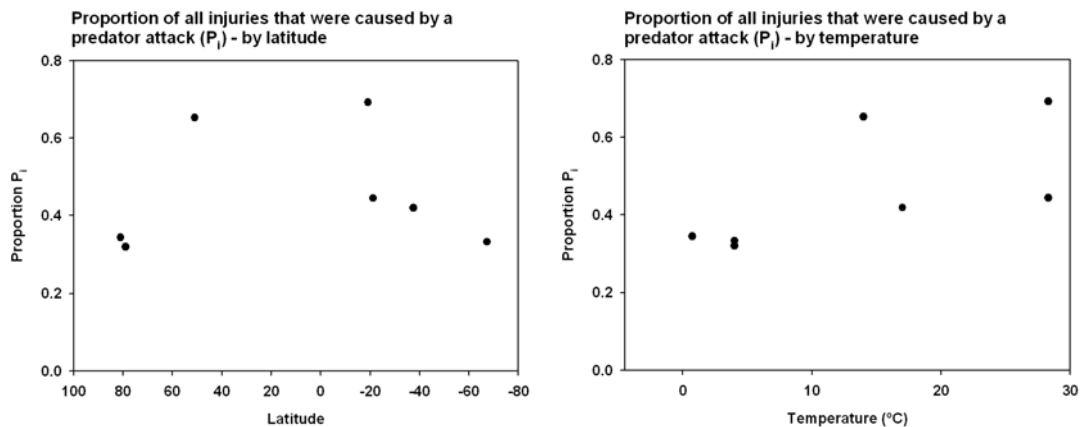


Figure 7.7 The proportion of all injuries that were caused by a predator attack (αP_i) across the Buccinidae by latitude (left) and temperature (right). αP_i decreases with increasing latitude in both hemispheres, although there was no statistically significant regression of αP_i on temperature ($p = 0.0961$ NS).

7.3.1.2 EPIFAUNA Brachiopoda

Examples of shell repairs found in brachiopods are shown in Figure 7.8. N_d and N_i were the same for each species of brachiopod as each individual had no more than one repair (Table 7.2). The two temperate species *Liothyrella neozelanica* and *Magellania venosa* had very similar repair frequencies (Figure 7.9). Both populations of the Antarctic brachiopod *L. uva* had repair frequencies which were half that of the temperate brachiopods.



Figure 7.8 Examples of brachiopod repaired shell damage in the form of a cleft in A) *Liothyrella neozelanica* and B) *L. uva*.

Table 7.2 Brachiopod shell repair data.

Species	No. of individuals	No. of individuals with repairs	No. of repairs in total	N_d	N_i
<i>Liothyrella neozelanica</i>	43	17	17	0.395	0.395
<i>Magellania venosa</i>	5	2	2	0.4	0.4
<i>L. uva</i> (from Signy)	10	2	2	0.2	0.2
<i>L. uva</i> (from Rothera)	29	6	6	0.207	0.207
<i>L. uva</i> (total)	39	8	8	0.205	0.205

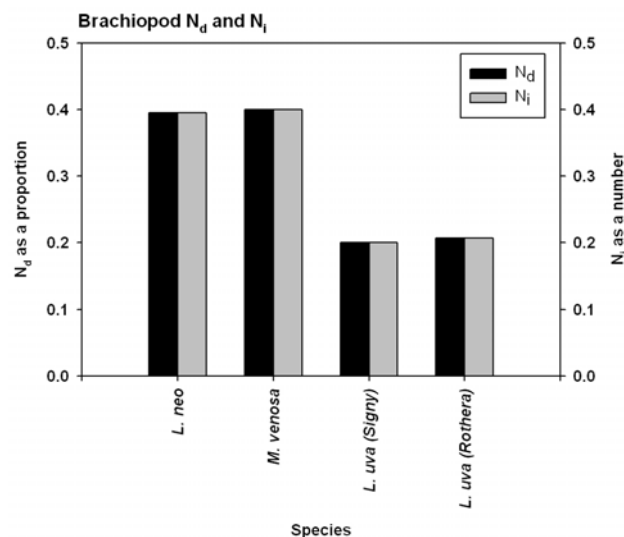


Figure 7.9 Repaired shell damage data in brachiopods studied. N_d is the proportion of individuals with repairs and N_i is the total number of injuries (i.e. the number of repairs per shell).

7.3.1.3 EPIFAUNA Echinoidea

Spine length of echinoids studied varied among species from different geographical locations. *Heliocidaris erythrogramma* had the longest spines, but was also the largest species. Of the confamilial echinoids, *Sterechinus neumayeri* had longer spines than *Psammechinus miliaris* (Figure 7.10). To control for difference in test size among species, spine length as a percentage of test diameter was calculated. This metric also varied among species from different geographical locations, but showed a striking relationship with

temperature (Figure 7.11). However, spine width was much thinner in the polar echinoid *S. neumayeri* than in its temperate relative *P. miliaris* (S. Watson, pers. obs.).

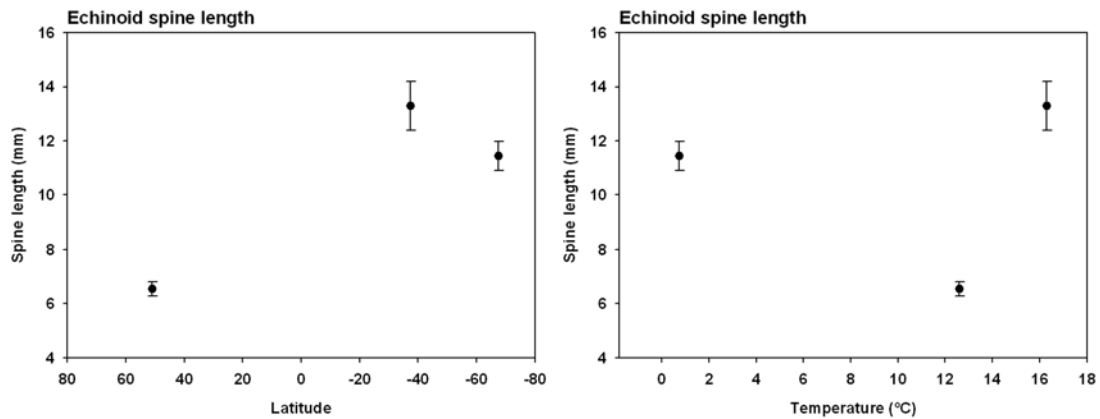


Figure 7.10 Echinoid spine length with latitude (left) and temperature (right).

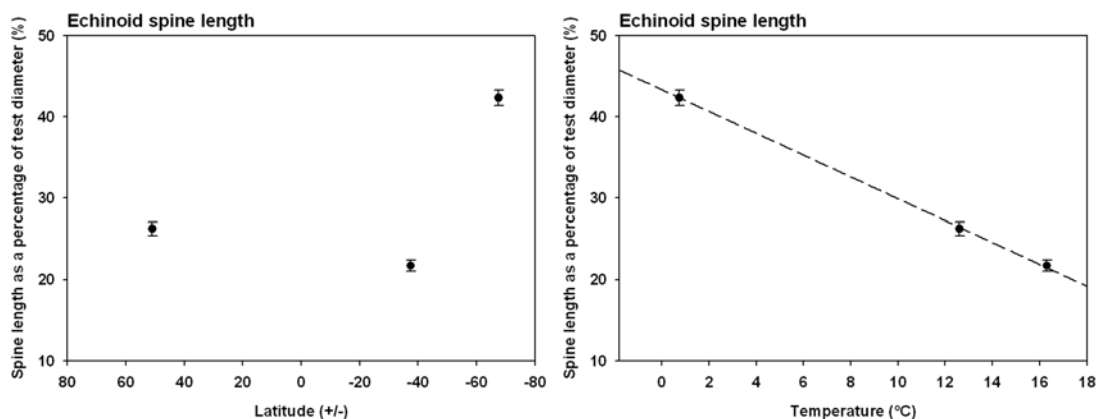


Figure 7.11 Echinoid spine length as a percentage of test diameter by latitude (left) and temperature (right). There was a significant regression of spine length as a percentage of test diameter on temperature ($F = 234.7335$, $df = 1,71$, $P < 0.0001$, $r^2 = 0.7645$).

7.3.1.4 INFAUNA Bivalvia: genus *Laternula*

None of the shell repairs analysed on any species of *Laternula* clam could be attributed to a predation attack, with the exception of 3 specimens of *L. recta* that had repairs indicative of bird predation (Figure 7.12). For all other species, damage to the shells was likely to have been caused by deep burrowing and deformities to the shell appeared indicative of growing around obstructions in the sediment. As the shell of *L. boschasina* is small, thin and

therefore fragile, it is likely that this species cannot survive to repair multiple shell breakages. Consequently, in this species, the numbers of repairs found on the shell were either 0 or 1, representing a binomial distribution (Figure 7.13). *L. elliptica* had many more shell repairs than the tropical and temperate species of *Laternula* (Figure 7.14). The mean number of repairs per shell (N_i) was 1.787 (Table 7.3) and the shell repair count data approached a normal distribution. *L. elliptica* is larger and buries more deeply than the tropical *Laternula* species studied with a mean maximum depth below the surface of 90.1 (± 20.8 , 1 s.d.) mm compared to 45.2 (± 8.7 , 1 s.d.) mm for *L. truncata* and 18.6 (± 2.0 , 1 s.d.) mm for *L. boschasina* based on approximations from animal total length (shell and siphon length) after extraction from the sediment.



Figure 7.12 Shell repair in *Laternula recta*. The original damage may have been caused by bird predation (E. Harper, pers. comm.).

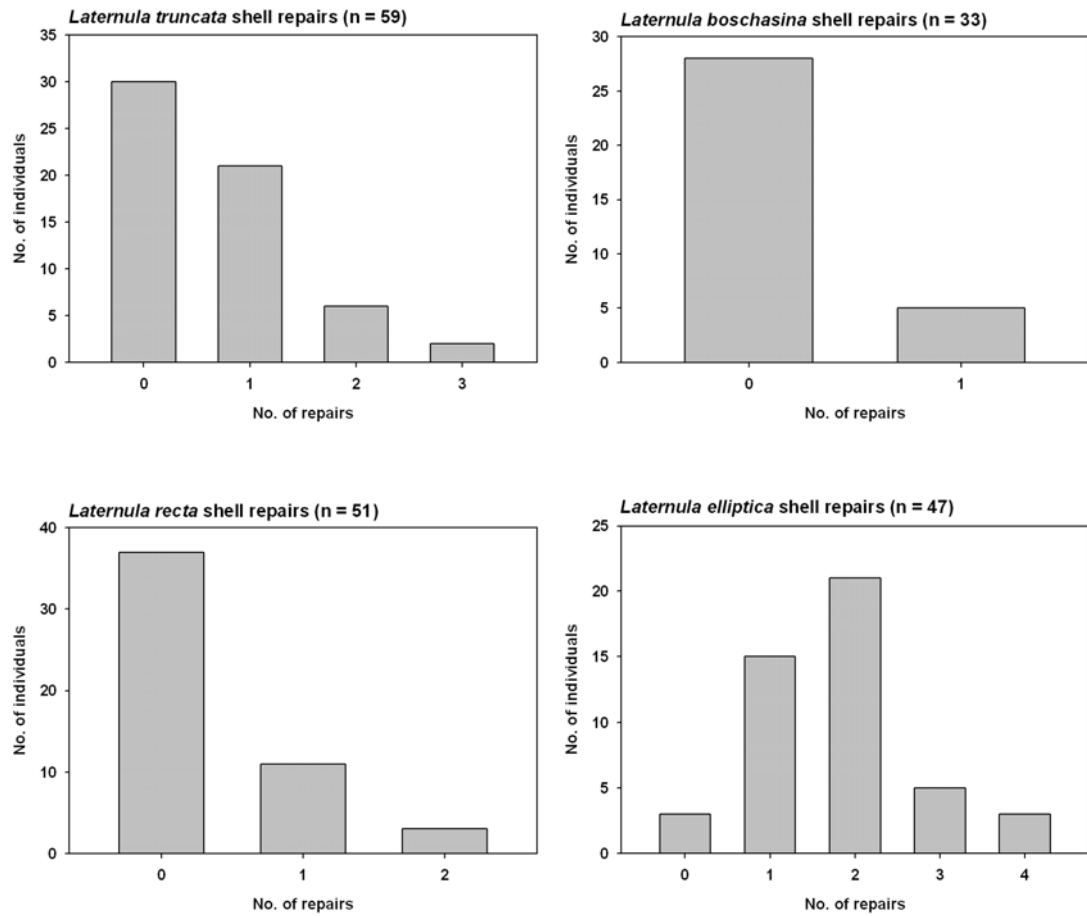


Figure 7.13 Histograms of incidence of shell repairs in species of *Laternula* from tropical to polar latitudes. Data show numbers of individuals in relation to the number of repairs identified on their shells.

Table 7.3 *Laternula* shell repair data.

Species	No. of individuals	No. of individuals with repairs	No. of repairs in total	N_d	N_i
<i>L. truncata</i>	59	29	39	0.491	0.661
<i>L. boschasina</i>	33	5	5	0.152	0.152
<i>L. recta</i>	51	15	18	0.294	0.353
<i>L. elliptica</i>	47	44	84	0.936	1.787

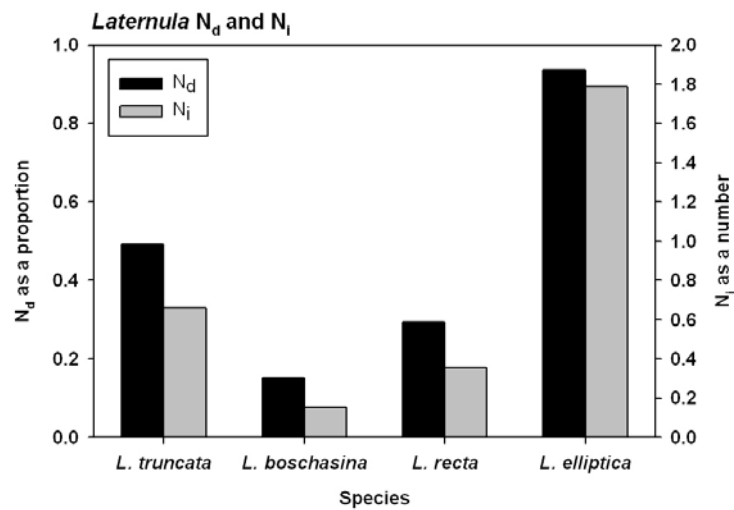


Figure 7.14 Graph showing two measures of shell damage repair in *Laternula* clams: the proportion of damaged individuals (N_d) and total number of injuries (N_i).

7.3.2 Observations of shell repairs on *Laternula* empty or ‘dead’ shell assemblages

In almost all environments studied, few empty shells from dead animals were present indicating that they had been rapidly washed away or destroyed by physical processes. The infaunal Antarctic bivalve *Laternula elliptica* was the one exception. Empty shells of *L. elliptica* occurred frequently on the surface of the substratum and were easily collected whilst SCUBA diving. The shells often occurred in clumps and this was probably due to iceberg activity as they are regularly seen in the bottom of new scours in clumps (L. Peck, pers. comm.). Fifty empty *L. elliptica* shells were collected from the sediment surface at Hangar Cove, Rothera. Of all the empty shells collected, only one drill hole was observed in an empty *L. elliptica* shell in Hangar Cove (Figure 7.15). The drill hole was 2.42 mm in diameter and the length of the *L. elliptica* shell was 43.9 mm. The drill hole could have been made by a muricid or naticid gastropod.



Figure 7.15 Shell from a dead *Laternula elliptica* with a drill hole found on the sediment surface whilst diving in Hangar Cove, Rothera, Antarctica (left). Close up of the drill hole in the *Laternula elliptica* shell from Hangar Cove (right).

7.3.3 Shell predator defence morphology

Gastropoda

There were significant regressions of aperture width on shell height for each gastropod species with $p < 0.0001$ for all species except *Buccinum glaciale* where $p = 0.0017$.

Among all species, the covariate shell height was significantly related to aperture width (ANCOVA: $F = 2606.635$, $df = 1,325$, $p < 0.001$). There was also a significant effect of species on aperture width after controlling for the effects of shell height ($F = 137.144$, $df = 7,325$, $p < 0.001$). The tropical Buccinidae had the greatest aperture resistance to predation (narrowest apertures compared to shell height) and the polar species had the least aperture resistance to predation (widest apertures compared to shell height). Species with larger aperture widths compared to their overall size are less predator resistant and have regression trendlines which become increasingly steep (e.g. *Neobuccinum eatoni*) (Figure 7.16).

Data on gastropod aperture width as a percentage of shell height did not have equal variances so Welch's F test (Welch, 1951) was used to test for differences among species. There was a significant difference in gastropod aperture width as a percentage of shell height among all species studied (Welch's $F = 302.271$, $df1 = 7$, $df2 = 88.669$, $p < 0.001$, $n = 333$) (Figure 7.17). There was also a significant difference in gastropod aperture width as a percentage of shell height among all buccinids studied (i.e. not including *Thais orbita*)

(Welch's $F = 315.001$, $df_1 = 6$, $df_2 = 75.148$, $p < 0.001$, $n = 291$). When plotted against latitude and temperature there were significant trends of increasing aperture width as a percentage of shell height with increasing latitude and decreasing temperature across the Buccinidae (Figure 7.18).

Data on gastropod aperture length:width ratios did not have equal variances. There was a significant difference in gastropod aperture length:width ratios among all species studied (Welch's $F = 176.600$, $df_1 = 7$, $df_2 = 94.337$, $p < 0.001$, $n = 335$). Post hoc comparisons using the Games-Howell procedure (appropriate for groups with unequal variances) showed the tropical buccinids, *Cantharus fumosus* and *Phos senticosus*, had aperture length:width ratios that were significantly different from each other and all other gastropod species studied ($p < 0.001$). The two tropical buccinids, *Cantharus fumosus* and *Phos senticosus*, had narrow apertures with aperture length:width ratios of more than 2.5 (Figure 7.19). Aperture length:width values decreased with increasing latitude (Figure 7.20).

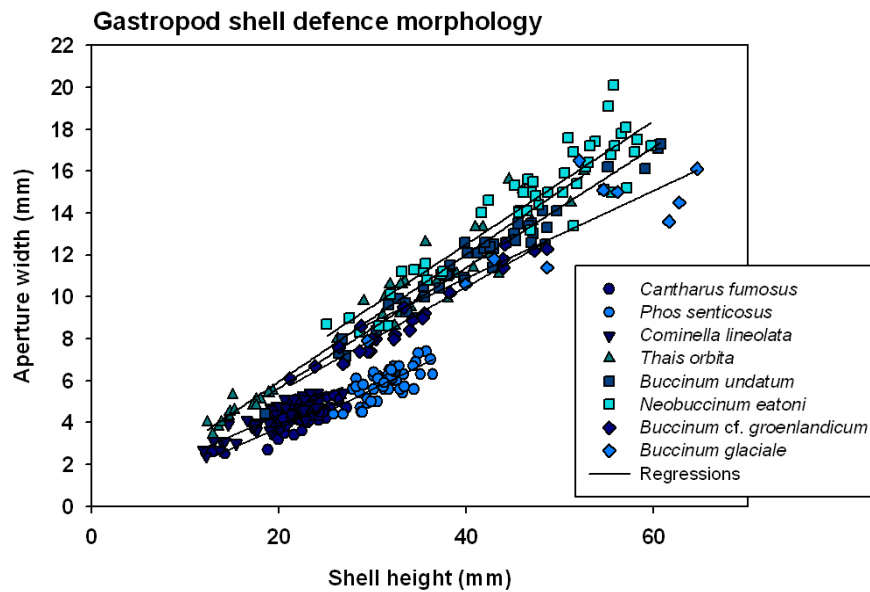


Figure 7.16 Relationships of shell height and aperture width in gastropods studied.

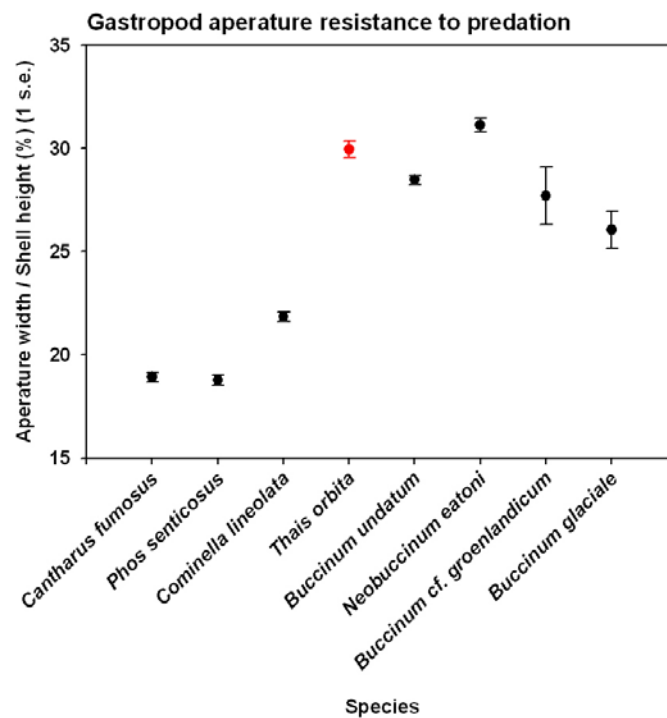


Figure 7.17 Gastropod aperture resistance to predation for each species studied in the form of aperture width as a percentage of shell height. The red point indicates a non-buccinid species.

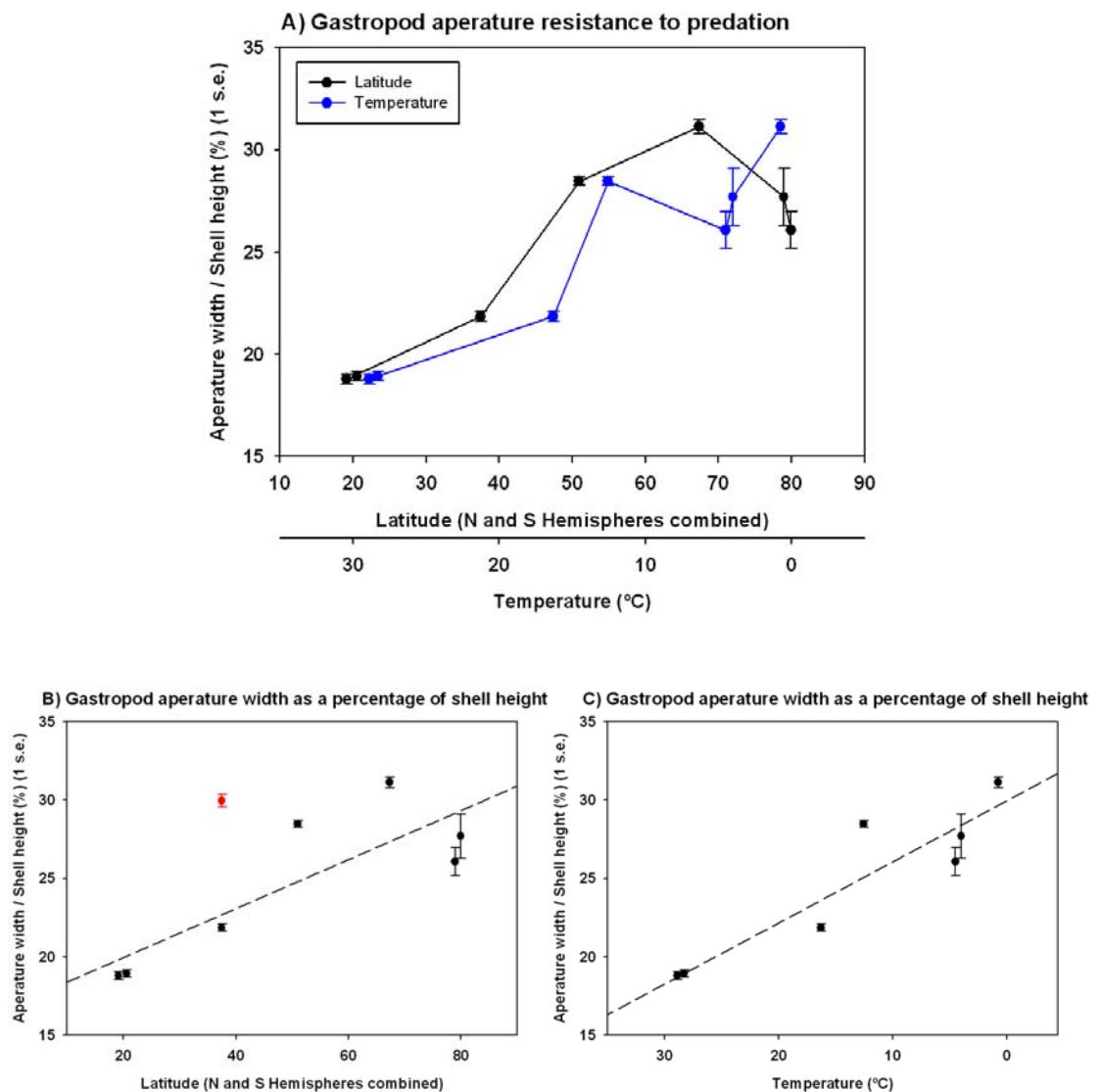


Figure 7.18 Variation in gastropod aperture resistance to predation with A) latitude and temperature, B) latitude regression and C) temperature regression. The red data point on plot B denotes a non-buccinid species and the trendlines are for buccinid species only. There were significant regressions in the ratio of aperture width to shell height with both latitude ($F = 11.7564$, $df = 1,5$, $P = 0.0187$, $r^2 = 0.6419$) and temperature ($F = 26.3014$, $df = 1,5$, $P = 0.0037$, $r^2 = 0.8083$).

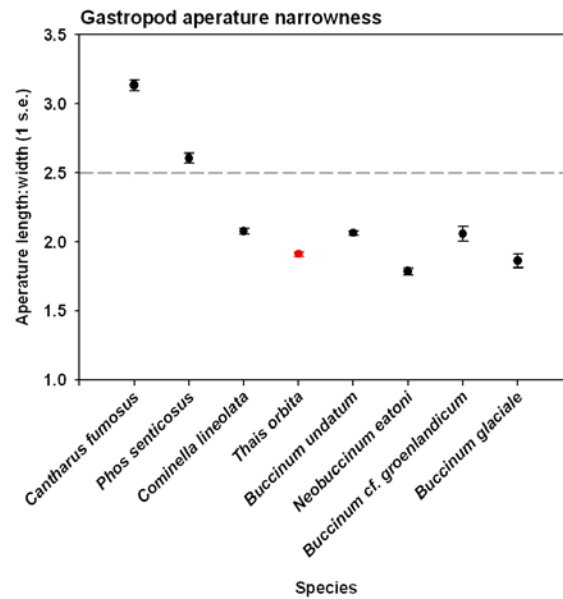


Figure 7.19 Variation in gastropod aperture narrowness (length/width ratio) by species. The two tropical species have narrow apertures with aperture length:width ≥ 2.5 . The red point indicates a non-buccinid species.

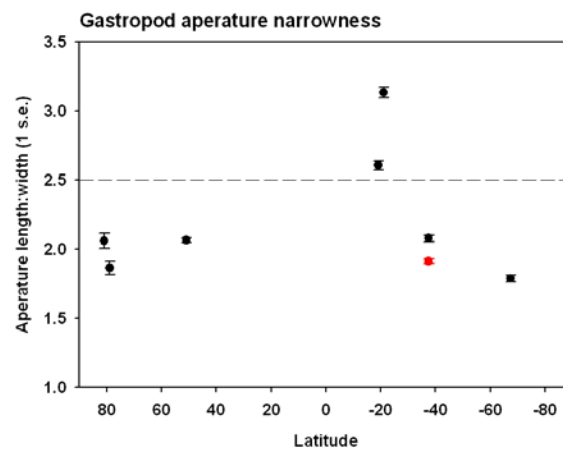


Figure 7.20 Variation in gastropod aperture narrowness across latitudes. The red point indicates a non-buccinid species.

Bivalvia: genus *Laternula*

For species of *Laternula*, the minimum shell inflation at the gape was compared to the shell inflation at the hinge as a measure of the predator resistance of the shell. Species with similar size openings to the shell height at the hinge are less resistant to predation from above the surface and have regression trendlines approaching 45 ° (i.e. a slope of 1) (Figure 7.21). There were significant regressions of shell inflation at gape on shell inflation at hinge for each *Laternula* species studied ($p < 0.001$). Among all species, the covariate shell inflation at hinge was significantly related to shell inflation at gape (ANCOVA: $F = 1057.543$, $df = 1,142$, $p < 0.001$). There was also a significant effect of species on shell inflation at gape after controlling for the effects of shell inflation at hinge ($F = 179.032$, $df = 3,142$, $p < 0.001$). Tropical species, especially *L. valenciennesii*, had smaller gapes. These morphological differences are possibly adaptations for decreasing the risk of predation from above.

Laternula shell inflation at the posterior gape was expressed as a percentage of shell length. Shells with wide openings for their size had high percentages and shells with small openings for their size had low percentages. There was a significant difference in shell inflation at gape as a percentage of shell length among all species studied ($F = 348.624$, $df = 3,143$, $p < 0.001$). The tropical *Laternula* species had smaller shell openings for their size than the Antarctic species *L. elliptica* (Figure 7.22). These shell inflation data suggest that *Laternula* shells are more predator resistant in the tropics than in polar waters.

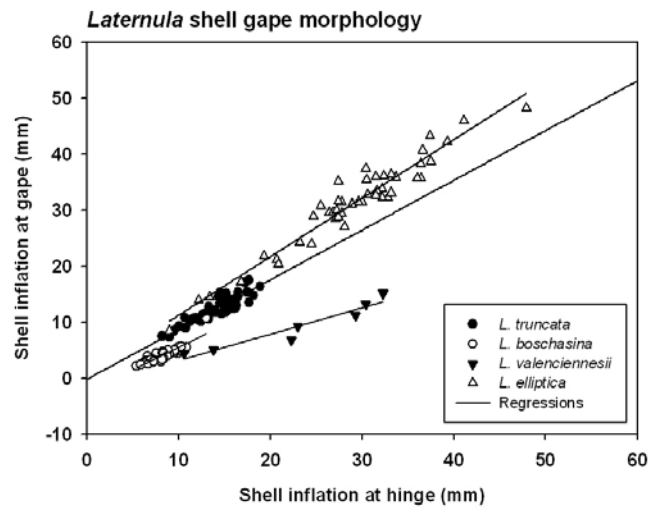


Figure 7.21 Relationships between *Laternula* shell inflation at hinge and inflation at gape.

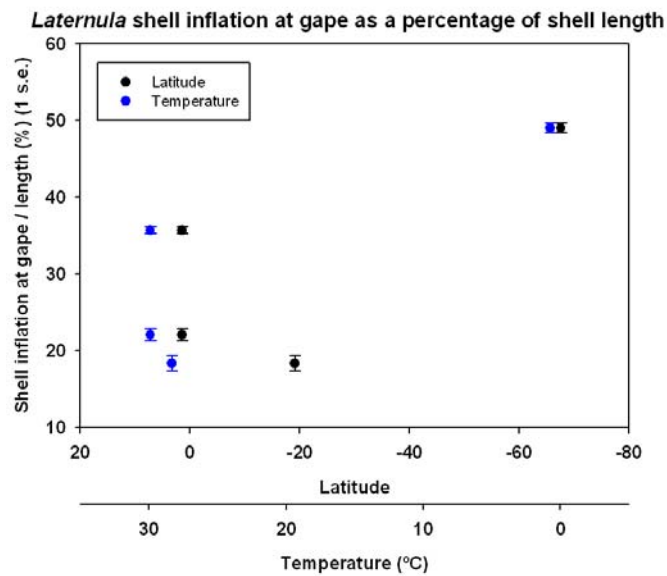


Figure 7.22 Variation in *Laternula* gape with latitude and temperature.

7.4 Discussion

Across latitudinal gradients, predation pressure is generally considered to decrease towards the poles (Paine, 1966; MacArthur, 1972). Shell repair in gastropods decreases from low to high latitudes (Vermeij, 1978; 1980; 1982a; Miller, 1983) and, in present-day oceans, durophagous predators are rare or absent from shallow-shelf habitats (< 100 m depth) in Antarctica (Aronson & Blake, 2001; Clarke *et al.*, 2004; Aronson *et al.*, 2007).

Shell damage and repair – evidence from living specimens

Damage repair marks on the shells of living marine invertebrates were studied for epifaunal gastropods and brachiopods, and infaunal bivalves. The frequency of repair is a conservative indicator of the failure of predators to break shells since subtle breakages may not be discernible from normal wear and tear (Vermeij, 1993). In buccinid gastropod shells, it was also possible to separate conservatively repairs caused by predation from other damage.

The Antarctic buccinid *Neobuccinum eatoni* had the lowest incidence of repaired shell damage (Figure 7.3). The tropical rocky reef buccinid *Cantharus fumosus* had the second lowest incidence of repaired shell damage. Most tropical reef snails are encrusted with coralline algae (Vermeij, 1987) and the tropical reef gastropod *C. fumosus* was no exception. This biotic cover may have afforded the shell of this species additional protection from physical damage and/or provided camouflage from predators resulting in fewer incidences of repaired shell damage than was expected given its low latitude. *Phos senticosus* and *Buccinum* cf. *groenlandicum* had intermediate levels of total shell repairs. *Cominella lineolata*, *B. undatum* and *B. glaciale* had the highest numbers of total shell repairs. *C. lineolata* is a temperate rocky reef gastropod and had one of the highest numbers of total repairs and predation repairs. Shells of this species were not covered by epiphytes (or epibionts), which suggests rocky reef buccinids without a coralline algae covering may be more susceptible to shell breakage.

For both the Northern and the Southern Hemisphere, temperate buccinids had more repairs than polar buccinid species, with the exception of the Arctic species *Buccinum glaciale*

(Figure 7.4). Excluding the tropical buccinids, shell repairs increased with increasing temperature once again with the exception of *B. glaciale*. *B. glaciale* is a large species whose shell may be more likely to encounter injury, especially from abiotic factors, because of its size.

In the buccinids, there was a clear latitudinal trend in the proportion of all injuries that were caused by a predator attack (αP_i) (Figure 7.7). αP_i decreased with increasing latitude in both hemispheres. Findings from this chapter for αP_i agree with the findings of Vermeij (1978; 1980; 1982a) and Miller (1983) of a decrease in shell repairs in gastropods from low to high latitudes, but data for total shell repairs (N_d and N_i) from this chapter did not show a latitudinal gradient.

In the brachiopods, temperate species had a higher incidence of repaired shell damage than the Antarctic brachiopod *Liothyrella uva*. Two populations of *L. uva* from Signy and Rothera had similar incidences of shell repair, which were half that of temperate brachiopods. These data agree with Harper *et al.* (submitted) who analysed much larger sample sizes and found that temperate brachiopods have higher repair rates than the Antarctic brachiopod *L. uva* (Figure 7.23).

Echinoid spines protect the test from impact by spreading the load of a force or breaking under impact (Strathmann, 1981). Spines are thus likely to have a function in defence against predators (Guidetti & Mori, 2005). Guidetti and Mori (2005) found spines were related to test size in two species of echinoid and concluded that longer spines in addition to a more robust test provided better defence against crushing predators such as fish. Spines of the polar echinoid *Stereochinus neumayeri* were longer than those of its temperate relative *Psammechinus miliaris* (Figure 7.10 and Figure 7.11) and among the three echinoid species studied, spine length decreased with increasing temperature. However, spine width was observed to be much thinner in the polar echinoid *S. neumayeri* than in its temperate relative *P. miliaris* and spines of the polar echinoid were fragile and easily broken. For these echinoids, spine length alone is not a good indicator of resistance to breakage by predators and test thickness (Chapter 3) is considered with these data in Chapter 9. Since predation pressure generally decreases with increasing latitude, the trend in spine length

suggests a non-predatory adaptation of spines. Régis (1986) found spine lengthening in echinoids was an adaptation to capture more seston from seawater. The polar echinoid, subject to a limited, highly seasonal food supply may have long but thin, and therefore energetically cheap, spines to facilitate the capture and ingestion of more food particles from seawater.

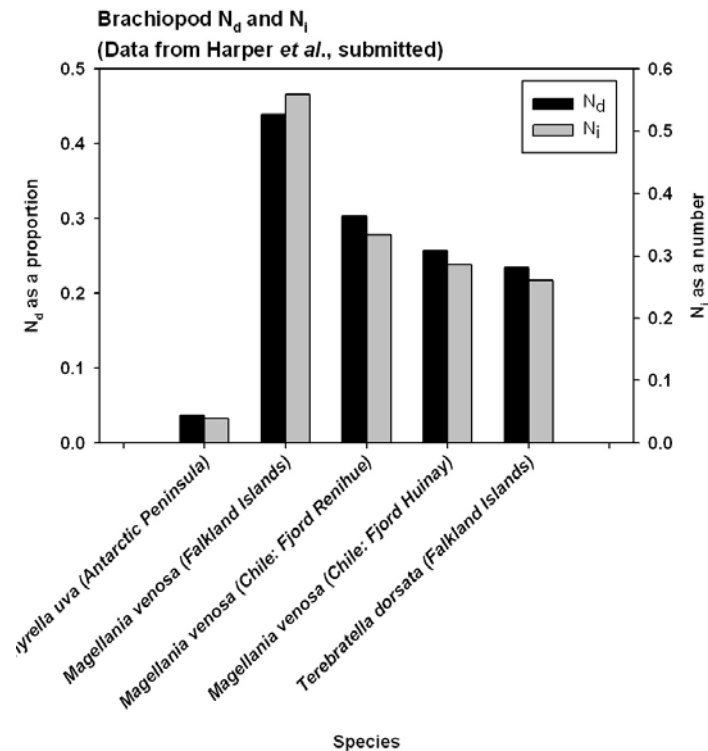


Figure 7.23 Data plotted from a table in Harper *et al.* (submitted) on repaired shell damage data in brachiopods. N_d is the proportion of individuals with repairs and N_i is the number of repairs per shell.

Of the two similar-sized *Laternula* clams, the tropical species *L. truncata* had more shell repairs than the temperate species *L. recta*. Tropical *L. boschasina* had the lowest incidence of shell repairs, perhaps because of its small size or an increased rate of mortality from shell damage in this species. *L. elliptica* had many more shell repairs than the tropical and temperate *Laternula* clams. An infaunal lifestyle provides a refuge from predation, because few shell-crushing predators can excavate prey living deep within the sediment (Alexander & Dietl, 2005), and was an adaptation to predation in the Late Mesozoic (Vermeij, 1977). Thus the high frequency of repairs on *L. elliptica* was most likely due to

abiotic factors such as the coarse, rocky nature of the heterogeneous substratum and incidence of ice scour at Rothera, rather than biotic factors such as predation. The chances of abiotic breakage to the shell of *L. elliptica* were high compared with the tropical and temperate clams, which were collected in fine to coarse grain homogenous sediment. Alexander and Dietl (2005) note that deep-burrowing bivalves often display high frequencies of shell repair caused by burrowing into the sediment. *L. elliptica* is larger and thus buries more deeply than the tropical *Laternula* species studied. *L. elliptica* is also longer lived, with more time to accumulate shell repairs and in addition, is subject to ice scour. Although a direct impact by a grounded iceberg is likely to be lethal, icebergs furrowing the sediment can exhume a buried *L. elliptica* which can then rebury (Zamorano *et al.*, 1986; Peck *et al.*, 2004). Disturbance and reburying are likely to be a cause of shell damage in this long-lived species. Interestingly the rate of burrowing in *Laternula* clams is the same for tropical and polar species and among the slowest of any bivalve studied (Morley *et al.*, 2007b).

Shell damage and repair – evidence from empty ‘dead’ shells

When investigating different types of drilling attack by predators across latitudes, Vermeij (1993) found that the only type of drilling that followed a latitudinal pattern was edge-drilling, which is common in clams in the tropics, but rare in cold-temperate species. Since no incomplete drill holes were noted on any living shells, latitudinal trends in drilling predation could not be tested. Although the lack of incomplete drill holes found could mean that drilling predation was 100 % successful, the scarcity of empty ‘dead’ drilled shells in areas where study species were found suggests this is unlikely.

Field observations did not note any predators removing *L. elliptica* individuals from burrows. Siphon nipping may have occurred, but was not observed, and damaged siphons have not been reported in previous extensive collections of this species at Rothera station (L. Peck, pers. comm.). It is likely that empty shells on the sediment surface were from animals that were removed from the substratum by a grounded iceberg scouring the seabed (Zamorano *et al.*, 1986). The ability to rebury is important (Peck *et al.*, 2004) because *L. elliptica* clams that remain unburied on the sediment surface are consumed by *Odontaster*

validus, *Cryptasterias turqueti*, *Parborlasia corrugatus*, *Neobuccinum eatoni* and amphipods (Zamorano *et al.*, 1986). These predators do not damage the shell.

One drill hole made by a muricid or naticid gastropod was found in an empty *L. elliptica* shell on the sediment surface in Hangar Cove, Rothera. As this shell was found with a group of other empty *L. elliptica* shells, it is likely that this individual was drilled by a gastropod as it lay exposed on the sediment surface (E. Harper, pers. comm.) after abiotic removal from the sediment. The Antarctic muricid gastropod *Trophon longstaffi* will drill *Laternula elliptica* and *Liothyrella uva* shells in a sediment-free aquarium environment (Harper & Peck, 2003). No predation attack repairs were observed on live *L. elliptica* individuals collected from their burrows by divers. Therefore, there was no evidence of any durophagous or drilling predation on *L. elliptica* individuals that remain buried in the sediment.

Hypothesis 1: There is a change in the frequency of shell repairs with latitude and, specifically, shell repairs decrease with increasing latitude.

Conclusion 1: Hypothesis 1 was 1) accepted for predation repairs in buccinid gastropods, but not for total repairs, 2) accepted for all repairs in brachiopods, and 3) rejected for all repairs in *Laternula* bivalves because, although there was a change in repairs among latitudes, there was no clear latitudinal trend and conversely, the polar *Laternula* species had more repairs.

Shell defence morphology

Analysis of shell defence morphology provided evidence of a poleward decrease in predation pressure. Narrow apertures confer greater resistance to predation (Palmer, 1979; Vermeij, 1993). Apertures of gastropods studied became narrower relative to shell height with decreasing latitude and increasing temperature supporting statements by Vermeij (1993) and indicating that predation pressure follows negative latitudinal and positive temperature gradients.

The Laternulidae are one of the few clam groups that cannot close their shell completely and have a permanent gape. *Laternula* clams are susceptible to siphon-nipping predators

and being able to withdraw the siphon into the shell and having a narrow gape improves resistance to these predators. Risk of predation via the gape is so important that no clams inhabiting firm bottom substrata have permanent gapes, although deep-burrowing clams often do (Vermeij, 1993). The minimum inflation of shell at the permanently open posterior end is a likely indicator of how resistant the shell is to predation attacks from above and, therefore, an indicator of predation pressure. Tropical species had smaller gapes than the polar species. These morphological differences are likely to be adaptations for decreasing the risk of predation from above. For the temperate species *L. recta*, there was some evidence from shell repairs at the posterior end of shells that this clam may be preyed upon by birds (Figure 7.12). The tropical clams *L. truncata* and *L. boschasina* are preyed upon by gastropod snails (Tan & Oh, 2002). Bivalves with permanent gapes comprise 16 % of tropical burrowing faunas, compared to 22 – 31 % of cool-temperature assemblages (Vermeij, 1993). These data suggest a latitudinal trend in predation even among the burrowing bivalves.

Hypothesis 2: There is a change in shell defence morphology with latitude and, specifically, shell defensive traits decrease with increasing latitude.

Conclusion 2: Shell defensive traits decreased with increasing latitude in *Laternula* bivalves and buccinid gastropods. Data on spine length suggest shell defence morphology did not decrease with increasing latitude in echinoids; however, spine length alone was not a good measure of predator resistance.

Summary

Data from this chapter on shell repairs in brachiopods, predator-related shell repairs in gastropods and data on shell defensive architecture in bivalve and gastropod molluscs show predation pressure decreased with increasing latitude agreeing with previous findings of a reduction in predation pressure with increasing latitude (Paine, 1966; MacArthur, 1972; Vermeij, 1978; 1980; 1982a; Miller, 1983; Aronson & Blake, 2001; Clarke *et al.*, 2004; Aronson *et al.*, 2007). The planetary temperature gradient is likely to be the primary control on predation pressure at high latitudes. Durophagous predators experience narcosis from a combination of cold temperatures and high haemolymph Mg^{2+} concentration (Frederich *et al.*, 2000; Frederich *et al.*, 2001). Additionally, since power output from fish

muscle drops by approximately 90 % from 25 °C to 0 °C (Wakeling & Johnston, 1998), a durophagous fish would require up to 10 times the muscle mass to crush a given shell in polar regions compared to the tropics (Aronson *et al.*, 2007).

The degree of predation pressure on shelled animals is important to understand because predation pressure provides an alternative explanation to the energetic cost of shell production to explain why shell morphology differs with latitude. It is likely that, predation intensity and shell damage are a function of habitat type, and shell repair data are discussed in relation to shell thickness, shell cost and defence morphology with latitude in Chapter 9.

**Chapter 8: The effects of ocean acidification
on early larval development of the Sydney
rock oyster *Saccostrea glomerata***



Chapter 8: The effects of ocean acidification on early larval development of the Sydney rock oyster *Saccostrea glomerata*

Preamble

This chapter is a reproduction of the Watson *et al.* (in press) manuscript:

Watson, S., Southgate, P. C., Tyler, P. A. & Peck, L. S. (in press). Early larval development of the Sydney rock oyster *Saccostrea glomerata* under near-future predictions of CO₂-driven ocean acidification. *Journal of Shellfish Research*. (Appendix 7).

Sue-Ann Watson designed and conducted the experiments and analysed the data for this publication. The manuscript was written by Sue-Ann Watson with only minor textual edits from the co-authors.

8.1 Introduction

Over the last 23 million years, atmospheric carbon dioxide (CO₂) concentrations have remained relatively stable between 140 to 340 ppm and surface ocean pH has remained constant between 8.0 to 8.3 pH units (Pearson & Palmer, 2000). Anthropogenic CO₂ emitted from fossil fuel combustion and deforestation since the onset of the Industrial Revolution has increased atmospheric concentrations of CO₂ from 280 to 380 ppmv in the last 200 years (Tans, NOAA/ESRL records). This rapid increase in CO₂ of 35 % is an order of magnitude faster than any change in CO₂ concentration that has occurred for millions of years (Doney & Schimel, 2007). The increase in this greenhouse gas is not only causing the planet to warm, but is also causing the oceans to acidify. This acidification is the result of increased CO₂ dissolving in seawater decreasing carbonate ion (CO₃²⁻) concentration and increasing bicarbonate ion (HCO₃⁻) concentration in a series of equilibrium reactions that release hydrogen ions (H⁺).

Over the past 200 years, the oceans have taken up ~ 40 % of the anthropogenic CO₂ emissions from the atmosphere (Zeebe *et al.*, 2008). This uptake of CO₂ has caused a 0.1 unit drop in the pH of the surface oceans (Caldeira & Wickett, 2003) which is equivalent to a 30 % increase in H⁺ concentration (Blackford & Gilbert, 2007). During the 1980s, ocean pH fell at a rate of 0.015 pH units per decade (Haugan & Drange, 1996) and present day average global surface ocean pH is 8.07 compared to the pre-industrial value of 8.17 (Cao *et al.*, 2007).

Models predict a further reduction in ocean pH by 0.3 to 0.5 units by 2100 (Haugan & Drange, 1996; Caldeira & Wickett, 2005; Orr *et al.*, 2005) which is equivalent to at least a 100-150% increase in H⁺ concentration (Orr *et al.*, 2005). Some reports suggest that increasing global temperatures caused by climate change will partially alleviate the effects of ocean acidification; however, Cao *et al.* (2007) show that ocean acidification is largely independent of temperature change. The predicted changes in ocean pH are not only greater but far more rapid than any experienced in the last 24 million years (see Blackford & Gilbert, 2007) and possibly the last 300 million years (Caldeira & Wickett, 2003).

Ocean acidification is likely to affect marine animals either by direct acidification of their environment or through hypercapnia. The decreasing pH of the oceans will lower the saturation state of calcium carbonate and therefore increase the solubility of calcareous structures. Consequently, calcifying species such as corals, foraminifera, coccolithophores, molluscs, brachiopods and echinoderms are thought to be particularly at risk. Kleypas *et al.* (2006) suggest that calcification rates could decrease by 60 % this century. Under conditions of the predicted atmospheric pCO₂ (~740 ppmv) in 2100 from the IPCC IS92a scenario, calcification was reduced by 25 % in the edible mussel *Mytilus edulis* and 10 % in the Pacific oyster *Crassostrea gigas* (Gazeau *et al.*, 2007).

Other negative effects of ocean acidification have been demonstrated in a variety of species, including decreased growth in the sea urchins *Hemicentrotus pulcherrimus* and *Echinometra mathaei* and the gastropod *Strombus luhuanus* (Shirayama & Thornton, 2005), and reduced fertilisation success in the sea urchin *Heliocidaris erythrogramma* (Havenhand *et al.*, 2008). Experiments investigating the effects of seawater acidification at

very low pH (under scenarios of leakage from geological CO₂ sequestration stores) have demonstrated increased mortality in the sea urchin *Psammechinus miliaris* (Miles *et al.*, 2007) and complex indirect effects on the induced defences in the gastropod *Littorina littorea* (Bibby *et al.*, 2007).

Lowered seawater pH reduces calcification in coral reefs (Langdon *et al.*, 2003) and the combination of stresses of climate change and ocean acidification is expected to reduce coral reef system diversity, with corals becoming increasingly rare (Hoegh-Guldberg *et al.*, 2007). Naturally occurring gradients of reduced pH around CO₂ vents in the Mediterranean Sea, have demonstrated ecosystem shifts and changes in species composition with a dramatic decrease in calcifying fauna in low pH areas (Hall-Spencer *et al.*, 2008).

Understanding the effects of acidification in commercially important species is of prime importance. The Sydney rock oyster *Saccostrea glomerata* (Gould, 1850) was chosen as a model species for this preliminary study. It is an important commercial species supporting an industry that currently generates \$34.5 million (AUD) annually in sales (O'Sullivan *et al.*, 2008). *S. glomerata* is a warm temperate bivalve mollusc endemic to Australia and New Zealand. Dove and Sammut (2007) showed that acidification of estuarine waters from terrestrial acid sulphate soil runoff increased mortality in *S. glomerata*. Small oysters showed the greatest mortality because their thinner shells were perforated by acid erosion.

Early life-history stages are generally thought to be vulnerable to stress and change (Peck, 2005). Studies have already shown that the early developmental stages of the oyster *Crassostrea gigas* (Kurihara *et al.*, 2007), copepod *Calanus finmarchicus* (Mayor *et al.*, 2007) and brittlestar *Ophiothrix fragilis* (Dupont *et al.*, 2008) are negatively affected by acidified conditions. We aimed to identify the effects of near-future CO₂-driven ocean acidification scenarios on the larval development of *S. glomerata*, and determine if this life-history stage is particularly susceptible to the stress of altered pH.

8.2 Methods

8.2.1 Experimental set-up and pH control

Experiments were conducted at the Aquarium Complex of the Marine and Aquaculture Research Facilities Unit (MARFU) at the James Cook University, Australia. Seawater obtained from the Australian Institute for Marine Science (AIMS) was filtered to 1 μm and sterilised by ultra-violet radiation. Seawater was held in a 3000 l reservoir tank in the laboratory and allowed to equilibrate to ambient temperature (26 °C). Seawater was pumped from the reservoir into three 500 l header tanks which filled on-demand via float valves (Figure 8.1).

The pH of seawater was controlled by manipulation of the partial pressure of CO_2 (pCO_2) reproducing the means by which atmospheric CO_2 will reduce the pH of the oceans. Seawater pH was regulated by a computerised control system (AquaMedic AT-Control) that introduced gaseous CO_2 into the header tanks as required via a solenoid valve. pH probes were calibrated with NBS buffer solutions and the pH values reported in this study are on the NBS scale. Values of pH were nominally set at 8.1 (control), 7.8 and 7.6. These treatments represent present-day pH, upper year 2100 pH predictions ($\Delta \text{pH} \approx -0.3$) and lower year 2100 pH predictions ($\Delta \text{pH} \approx -0.5$) of seawater, respectively. Seawater from the header tanks was gravity-fed (2.5 l.h^{-1}) to individual 60 l treatment tanks within 3000 l water-bath tanks. The actual pH values measured in the treatment tanks were 8.11, 7.81 and 7.64 (Table 1). Seawater samples were analysed for total alkalinity by titration. Other parameters of the carbonate system were calculated using the program CO2SYS (Lewis & Wallace, 1998).

Seawater temperature was maintained at 26 °C (to 2 significant figures) based on optimum temperatures reported for growth, development and survival of embryos and larvae of *S. glomerata* (Dove & O'Connor, 2007). Salinity was maintained at 32 parts per thousand (ppt) and seawater within the treatment tanks was mixed by aeration through a fine glass tube. Larvae were retained in the treatment tank by a fine mesh which covered the outflow pipe (Southgate & Beer, 1997). Used seawater was not re-circulated into the experimental

system. Treatment tanks were covered with transparent lids to minimise loss of CO₂ from the seawater to the atmosphere and were held under a 13 hL:11 hD lighting regime.

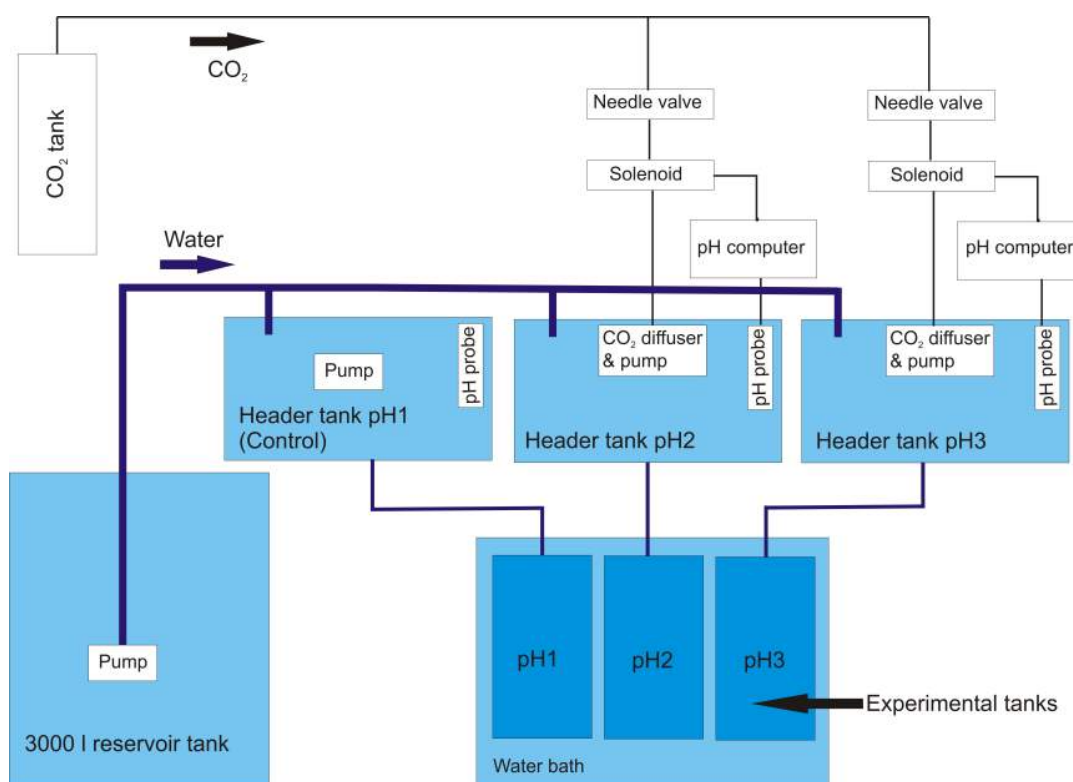


Figure 8.1 Set-up of experimental CO₂ system with 3 pH levels. Treatments labelled pH1, pH2 and pH3 were set to nominal pH values of 8.1, 7.8 and 7.6 respectively.

8.2.2 Spawning procedure and larval culture

Sydney rock oysters were obtained from a commercial oyster farm in central New South Wales, Australia and strip-spawned. Embryos were incubated in a 500 l tank filled with 1 μ m filtered sea water containing the antibiotic streptomycin sulphate at a concentration of 10 mg.l⁻¹. At 24 hours old, the larvae had reached D-veliger stage. Larvae were retained on a 25 μ m mesh screen, washed with 1 μ m filtered seawater and 90,000 larvae were transferred into each 60 l treatment tank creating a stocking density of 1.5 larvae.ml⁻¹ in each. In the treatment tanks, larvae were pulse fed daily with live cultured micro-algae composed of a 1:1 mixture of *Pavlova salina* and *Isochrysis* (clone T-Iso) fed at increasing concentrations of 5,000 to 20,000 cells.ml⁻¹ from days 1 to 8. Feeding rate was based on

previously published data for the larvae of *S. glomerata* (Nell & O'Connor, 1991) and sufficient concentrations of algal cells were fed to ensure food supply was not a limiting factor in survival, growth and development.

8.2.3 Processing of larvae

Larvae were removed from the treatment tanks when they were 8 days old by passing the contents of each treatment tank through a 37 µm mesh screen. Larvae were counted on a Sedgewick rafter counter using a light microscope. The antero-posterior measurement (APM) and dorso-ventral measurement (DVM) of 30 larvae per treatment were recorded. Further samples of larvae were frozen, freeze-dried and then weighed, or fixed in a 2 % gluteraldehyde solution in seawater for 2 hours. Fixed larvae were dehydrated through graded ethanol solutions, air-dried and transferred onto stainless steel stubs. The stubs and larvae were gold coated and imaged on a JEOL JSM-5410LV scanning electron microscope (SEM) using secondary electrons.

8.2.4 Empty shell counts

Shells of both living and dead calcareous animals experience dissolution in the marine environment (see Harper, 2000), so it was expected that some empty, or 'dead', larval shells would dissolve at each pH. To determine differences in shell dissolution between treatments, the percentage of empty shells remaining from larvae that had died during the experiment in each treatment tank was calculated. The number of larvae that had died, and therefore the number of empty shells that should have been present, was determined by subtraction of counts of surviving larvae at the end of an experiment from original stocking numbers. The actual numbers of empty shells remaining were counted on a Sedgewick rafter counter using a light microscope. The percentage of empty shells remaining was then calculated by dividing the number of empty shells counted by the number of dead larvae per treatment tank (Equation 1), thus correcting for differences in larval mortality between treatments.

Equation 1

Percent empty shells remaining = empty shells counted / number of dead larvae * 100%

8.2.5 Statistical analysis

Data were compiled on spreadsheets using MS Excel 2003. Statistical analyses were performed in SPSS 16.0 and SigmaPlot 10.0. Data were tested for normality where appropriate using the Shapiro-Wilk normality test. Relevant parametric (e.g. ANOVA, Pearson correlation) or non-parametric (e.g. Kruskal Wallis) statistical analyses were performed using SPSS 16.0. Graphs were produced with SigmaPlot 10.0.

8.3 Results

In the following sections, nominal pH values are used to refer to the treatment pH conditions (i.e. pH 8.1, 7.8 and 7.6). For actual pH values measured in the treatments and further water chemistry data, see Table 8.1.

Table 8.1 Water chemistry data for treatment tanks (mean \pm 1 s.d.).

Nominal pH	8.1	7.8	7.6
Measured pH _{NBS}	8.11 (\pm 0.02)	7.81 (\pm 0.03)	7.64 (\pm 0.04)
pH _{NBS} range (min. – max)	8.10 – 8.14	7.78 – 7.84	7.59 – 7.67
Alkalinity (mg/L as CaCO ₃)	101.1 (\pm 1.18)	102.27 (\pm 1.42)	101.23 (\pm 0.91)
Temperature (°C)	25.7 (\pm 0.2)	25.6 (\pm 0.2)	25.6 (\pm 0.1)
pCO ₂ (μ atm)	220.3 (\pm 16.1)	508.8 (\pm 45.7)	775.6 (\pm 75.7)
Ω_{cal}	1.67 (\pm 0.06)	0.93 (\pm 0.05)	0.65 (\pm 0.06)
Ω_{arag}	1.15 (\pm 0.04)	0.64 (\pm 0.03)	0.45 (\pm 0.05)

8.3.1 Larval survival

One-day old D-veliger larvae were introduced to the treatment tanks. By 8-days old, the majority had developed into umbonate larvae. The experiment was thus run between these two key developmental stages. Percentage larval survival decreases with decreasing pH (Figure 8.2A). There is a significant positive correlation between pH and mean larval survival ($r = 1.000$, $p = 0.004$, $N = 3$ for nominal pH; $r = 1.000$, $p = 0.032$, $N = 3$ for measured pH). Compared to the control treatment (pH 8.1), survival decreased by 43 % at pH 7.8 and by 72 % at pH 7.6.

8.3.2 Larval growth and morphology

Decreased pH had an effect on the morphology and growth of the larvae. There was a significant difference between the antero-posterior measurement (APM) of larvae at different pH (Chi-square = 13.697, $df = 2$, $p = 0.001$) and between the dorso-ventral

measurement (DVM) of larvae at different pH (Chi-square = 12.276, df = 2, p = 0.002). Larval APM was reduced by 6.3 % at pH 7.8 and 8.7 % at pH 7.6 (Figure 8.2B). Larval DVM was reduced by 5.1 % at pH 7.8 and 7.5 % at pH 7.6 (Figure 8.2C). It was expected that pH would affect larval dry mass (Figure 8.2D). However, preliminary mass data were limited and statistical tests showed no significant difference in mass between pH treatments.

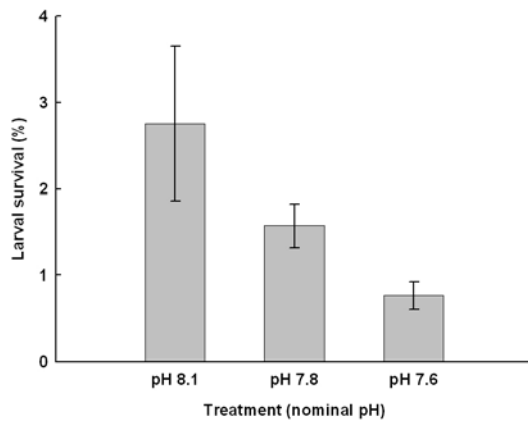
8.3.3 Empty shells recovered

There was a significant difference in the percentage of empty shells remaining between pH treatments ($F = 50.129$, $df = 2,7$, $p = 0.000$). At pH 7.8 and 7.6, the saturation state with respect to calcite and aragonite fell below $\Omega = 1$ (Table 8.1). The percentage of empty shells remaining decreased with decreasing pH by 16 % in pH 7.8 and 90 % in pH 7.6 (Figure 8.2E).

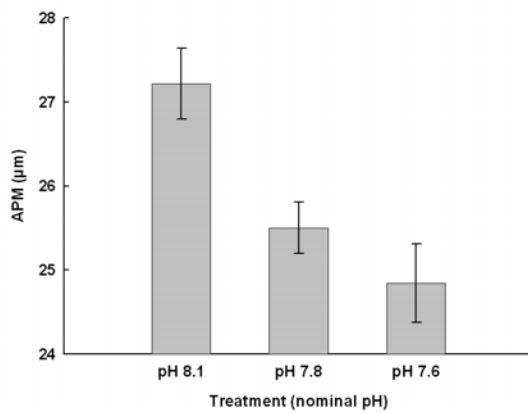
8.3.4 Shell surface structure

Shell surface characteristics were markedly affected by pH (Figure 8.3). In normal larval shell development (control treatment pH 8.1) the shell is smooth and rounded with even growth (Figure 8.3A). At pH 7.8 and pH 7.6, growth checks can be seen on the surface of the larval shell (marked by 'X' arrows) and are likely to be the result of physiological stress after the transfer to low pH conditions (Figure 8.3B and Figure 8.3C). Larval shell deposition under low pH (indicated by 'Y'), was no longer smooth, but appeared pitted and deformed particularly around the valve edge. These abnormalities in new shell growth indicate potential problems with shell deposition and/or periostracum formation. At low pH, areas in the middle of the shell surface, which were deposited before transfer to low pH conditions, showed surface pitting and were rough in appearance indicating dissolution of the larval shell after transfer to low pH conditions.

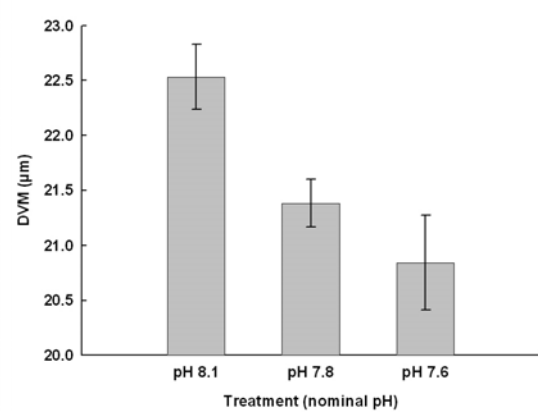
A



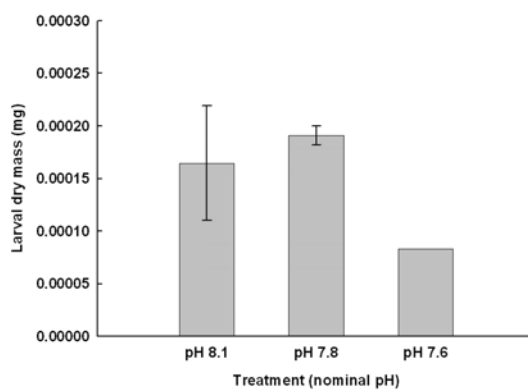
B



C



D



E

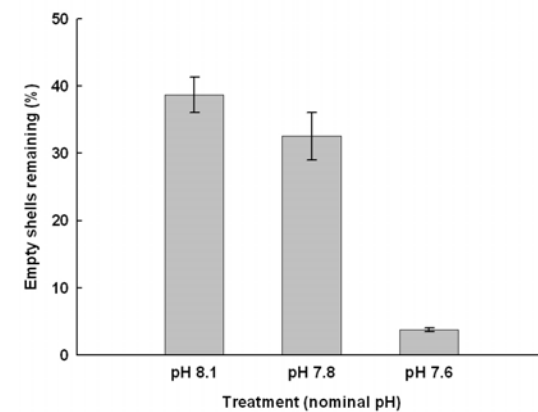


Figure 8.2 Qualitative and quantitative measurements of larval success at different pH: A, Larval survival ; B, APM of larvae; C, DVM of larvae; D, Percentage of empty shells remaining from dead larvae; E, Larval dry mass. Error bars are 1 s.e.

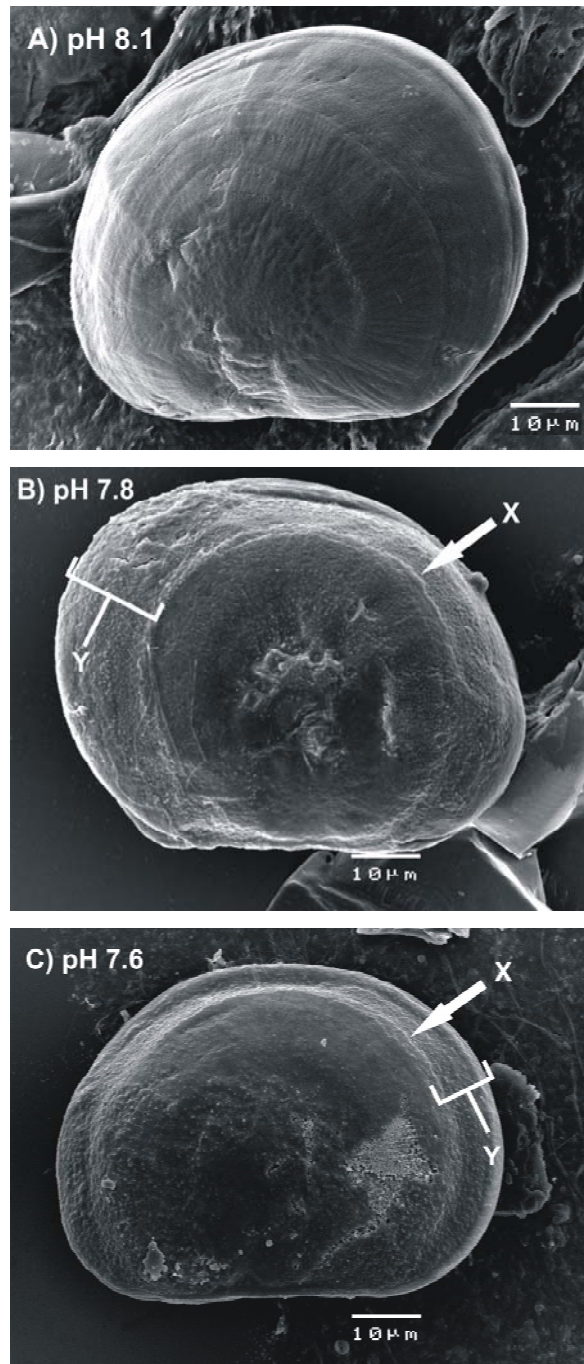


Figure 8.3 Scanning electron microscope (SEM) images of representative *Saccostrea glomerata* larvae at 8 days old from pH treatments: A) pH 8.1; B) pH 7.8; C) pH 7.6. All images were taken at the same magnification. ‘X’ arrows show a growth check and point of change in the surface of the shell to a pitted surface. ‘Y’ denotes areas of new shell growth during exposure to acidified seawater.

8.4 Discussion

Increasing anthropogenic emissions of CO₂ have already caused a decrease in ocean pH of 0.1 units (Caldeira & Wickett, 2003). Since the chemistry of seawater and the carbonate system is well known, we can be moderately confident about model predictions for future ocean pH scenarios of Δ pH -0.3 to -0.5 units by 2100 (Haugan & Drange, 1996; Caldeira & Wickett, 2005; Orr *et al.*, 2005) and -0.7 units by 2300 (Caldeira & Wickett, 2003).

Experiments were run with *S. glomerata* from 1 to 8 days old between key developmental stages: D-veliger to umbonate larvae. Compared to the control treatment (pH 8.1), survival decreased by 43 % in pH 7.8 (Δ pH -0.3 upper 2100 prediction) and 72 % in pH 7.6 (Δ pH -0.5 lower 2100 prediction). Although mortality during larval culture in the experiment was high across all treatments, commercial scale hatcheries also experience mass mortalities (i.e. > 80 %) of *S. glomerata* larvae. For example, half of all hatchery runs with this species over a five year period failed within the first 8 days (Heasman *et al.*, 2000; Dove & O'Connor, 2007). Furthermore, strip spawning of oysters is generally acknowledged to result in fewer viable larvae compared to natural or induced spawning methods (Gosling, 2003).

Larval growth (APM and DVM) was retarded with decreasing pH suggesting that larval development could take longer under ocean acidification, or that larvae will be smaller at each developmental stage. SEM images revealed growth abnormalities in the surface of the larval shell at low pH. Larval shells were pitted and deformed, particularly where shell was deposited during exposure to low pH. These shell surface abnormalities indicate larvae may have been experiencing: 1) problems with shell deposition, 2) retarded periostracum formation, and/or 3) increased shell dissolution, at low pH.

Initially oyster larvae deposit a predominantly amorphous calcium carbonate (ACC) shell, which later partially transforms into aragonite (Weiss *et al.*, 2002). This differs from the adult oyster shell which is composed predominantly of calcite (Stenzel, 1964). ACC is more soluble than aragonite (Brečević & Nielsen, 1989) which in turn is more soluble than calcite (Vermeij, 1993). Therefore the larval shell, particularly during the ACC phase, is the

most susceptible shelled life-history stage of the oyster to dissolution caused by ocean acidification.

Empty shell count data show that the percentage of empty shells, left by larvae which had died during the experiment, decreased considerably at pH 7.6. These data suggest the empty shells dissolved rapidly (within 7 days) at pH 7.6. In this experiment, calcite and aragonite were undersaturated ($\Omega < 1$) at pH 7.8 and 7.6 putting these minerals into a dissolution state. However, calculations of saturation state are based on non-biogenic minerals in artificial seawater. Biogenic calcium carbonate shell contains organic matrix and is often covered by a periostracum. Therefore the tipping point for dissolution of biological CaCO_3 may not occur at exactly $\Omega = 1$ for pure calcite or aragonite. In the experiment, there seemed to be a threshold between pH 7.8 and 7.6 at which rapid shell dissolution occurred and the parsimonious explanation is that the saturation state of the larval shell itself was $\Omega < 1$, and markedly so in the pH 7.6 treatment.

Larval dry mass was lowest in the most acidic treatment. This probably indicates a marked fall in larval soft tissue mass at pH 7.6 as dry mass in this treatment was approximately half that of the higher pH treatments and shell pitting clearly did not produce that level of decrease in shell mass (Figure 8.3). This suggests a marked effect on energy balance at low pH either through enhanced costs or reduced feeding abilities. Greatest larval mass was recorded at pH 7.8. This may be because the larvae that were able to survive in this treatment were the healthiest and thus heaviest; however, further studies are required to confirm this.

The results of this study demonstrate negative effects on larval survival and size, and increased shell abnormalities of *S. glomerata* in a high- CO_2 environment. Similar effects on early life-history stages of other marine invertebrates have been demonstrated. At low pH (7.4), reduced larval development and shell mineralisation was shown in the oyster *Crassostrea gigas* (Kurihara *et al.*, 2007). Other negative effects caused by low pH include reduced hatching rate and nauplius development in copepods (Kurihara *et al.*, 2004) and decreased fertilisation and larval size in sea urchins (Kurihara & Shirayama, 2004). Dupont *et al.* (2008) showed a reduction in larval survival and size, as well as increased larval

abnormalities in the brittlestar *Ophiothrix fragilis* at pH 7.9 and 7.7. Havenhand *et al.* (2008) found decreased sperm speed and motility and reduced developmental success in embryos and larvae of the sea urchin *Heliocidaris erythrogramma* at pH 7.7. Negative effects of ocean acidification on the early developmental stages of any species are likely to threaten its long-term viability by a reduction in recruitment of viable juveniles to the population.

Early reports assessing the effects of CO₂ on marine organisms have considered results of experiments that used mineral acid addition to lower the pH of seawater (see Auerbach *et al.*, 1997). However, reducing pH by CO₂ addition compared to acid addition can have greater negative effects on marine organisms for a given pH (Kikkawa *et al.*, 2004; Kurihara & Shirayama, 2004). In recent years, there has been a move to manipulate pH by the addition of CO₂ (e.g. Kurihara *et al.*, 2004; Gazeau *et al.*, 2007; Dupont *et al.*, 2008; Havenhand *et al.*, 2008), thus creating more realistic conditions in terms of the overall carbonate chemistry of seawater. This experiment aimed to create realistic near-future conditions of ocean acidification scenarios predicted to occur before the end of the century by the addition of CO₂ to seawater.

The through-flow system of elevated CO₂ seawater was a major advantage in this study, avoiding the need to use small containers in closed systems and providing the ability to rear larvae in acidified seawater for an extended period during their development. Using a closed system introduces organisms to chemical stress from changes in water quality, by the depletion of major nutrients and ions (such as Ca²⁺), and by the build up of waste products. Closed systems also induce physical stress during water changes. Our experiments allowed the continuous change of well-mixed seawater which removed the need to handle larvae until the experiment was finished. One µm filtered pristine seawater was used continuously, avoiding potential water quality issues with re-circulated water from the experiment. An additional advantage included the use of header tanks, avoiding the potential creation of pH gradients and/or considerable pH fluctuations in the experimental tanks. Manipulation of pH within the large (500 l) header tanks meant any fluctuations in pH caused by the CO₂ solenoid valves switching on and off, were not passed

onto the treatment tanks. Large treatment tanks (60 l) also minimised any variation in physical and chemical parameters throughout the experiment.

This study demonstrates that exposure to predicted upper and lower ocean pH levels for the end of the century has a dramatic negative effect on the survival, growth and shell formation of the early larval stages of the Sydney rock oyster, *S. glomerata*. Targeting a potentially vulnerable stage in a species' life-history is useful, but it is also important to research the effects of ocean acidification on all developmental stages, as organisms may differ in their 'ocean acidification tolerance windows' during different stages in their life-history. Such ocean acidification experiments in the laboratory and field, in addition to long-term ocean monitoring programmes, are urgently needed to generate data on which to base policies to mitigate the effects of climate change.

Chapter 9: Synthesis and conclusions - Latitudinal gradients in shell morphology and the controls of shell cost and predation pressure



Chapter 9: Synthesis and conclusions - Latitudinal gradients in shell morphology and the controls of shell cost and predation pressure

9.1 Introduction

Latitudinal gradients occur in both terrestrial and marine environments. Although latitude has no environmental meaning by itself, the total amount and seasonality of solar irradiation varies across latitudes. Solar energy input chiefly governs ambient temperature and primary production. In this thesis, the apparent trend in decreasing shell thickness with latitude reported by Nicol (1955; 1965) and Graus (1974) has been explored and reasons for trends in shell morphology have been investigated. Four taxa were compared across latitudinal gradients so that within- and among-taxon comparisons could be made. To reduce taxon-related variability in the parameters under investigation, species from the same genus or family were used in the comparisons. At higher latitudes the saturation state of seawater with respect to calcium carbonate (CaCO_3) is lower and so CaCO_3 is more soluble (Revelle & Fairbridge, 1957; Zeebe & Wolf-Gladrow, 2001; Sarmiento & Gruber, 2006). In these conditions, the energetic cost of producing a shell should be greater because shell-building ions (Ca^{2+} and CO_3^{2-}) are more soluble and hence more energetically expensive to remove from seawater (Graus, 1974; Vermeij, 1978; Clarke, 1983; 1990; 1993). Additionally, predation pressure is generally considered to decrease towards the poles (Paine, 1966; MacArthur, 1972) and modern durophagous predators are rare or absent in Antarctic shallow-shelf waters (< 100 m depth) (Aronson & Blake, 2001; Clarke et al., 2004; Aronson et al., 2007). The relative importance of each of these factors was tested to determine which, if any, proved the major control on shell morphology.

The chapters in this thesis show calcareous megabenthic marine invertebrates exhibit various latitudinal gradients in physiology and ecology. Trends with latitude in shell thickness, mass, inorganic content, elemental content, metabolic rate, growth, shell cost, shell repairs and shell defence morphology were all included. In addition, the effects of ocean acidification were demonstrated for an important commercial bivalve species. How can these trends help us to interpret the controls on shell morphology and importantly what controls shell thickness and shape: cost or predation? And what might the future hold for calcareous marine life? How each piece of research links together within this thesis is shown in Figure 9.1. This chapter will explore the interactions between the potential controls of shell production cost and predation pressure on the latitudinal patterns in shell morphology.

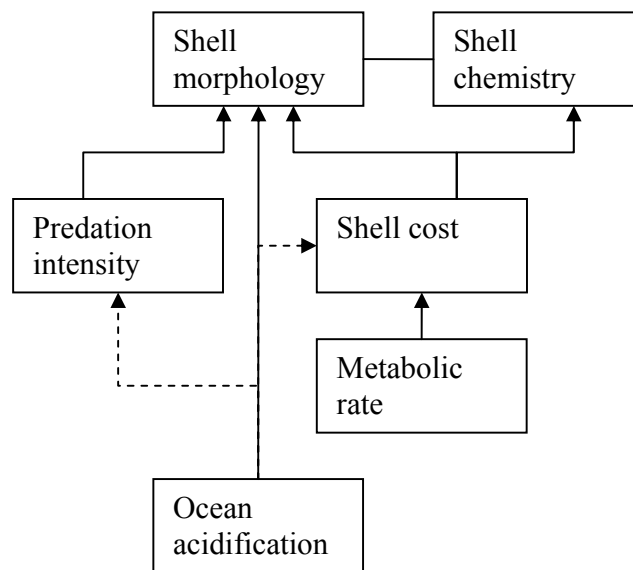


Figure 9.1 Flow chart showing how data chapters in this thesis were inter-linked.

9.1.1 Aims

The purpose of this thesis was:

- 1) To explore the latitudinal variation in shell thickness and skeletal composition in calcareous marine megabenthic invertebrates using molluscs, brachiopods and echinoderms as model taxa.
- 2) To determine if any variation or trend may be explained by energetic cost.
- 3) To determine if any variation or trend may be explained by predation pressure.

9.1.2 Data and statistical analysis

Data were compiled on spreadsheets using MS Excel 2003. Statistical analyses were performed in SPSS 16.0 and SigmaPlot 10.0 and included regression analyses and t-tests. Graphs were produced with SigmaPlot 10.0.

9.2 Key findings in shell morphology, chemistry, cost and predation

9.2.1 Shell morphology

Conclusion: Inorganic content decreased with increasing latitude as a function of temperature. Trends in shell thickness varied by taxon, and did not vary consistently with latitude.

Inorganic content decreased with increasing latitude across all taxa studied. The mismatch of the trend for the Arctic buccinids shows that this trend was related to temperature (Figure 9.2). Shell thickness decreased with latitude in buccinid gastropods and echinoids of the family Echinidea (Figure 9.3). Shell mass also decreased with increasing latitude in the buccinids. There was no evidence of a latitudinal trend in brachiopod shell thickness. Within the genus *Laternula*, the polar clam had the thickest shell.

Graus (1974) showed that marine gastropods decrease in their efficiency of calcium carbonate usage, measured as the amount of internal living space per unit shell deposited, with increasing latitude in the Northern Hemisphere. Calcification efficiency (expressed as a calcification index) also increased in variability towards the tropics. Both the most and least efficient calcifying gastropods were found in the tropics, although the mean trend was for calcium efficiency to decrease towards low latitudes. Latitudinal gradients from this thesis in shell morphology for buccinid gastropods and echinoids agree with the findings of Graus (1974).

Trussell (2000) found that shells of the intertidal gastropod *Littorina obtusata* from the Gulf of Maine weighed less, were thinner and weaker at higher latitudes than lower latitudes, although soft body tissue mass increased with increasing latitude. When transplanted to a different latitude, snails adopted the traits found at the new latitude demonstrating that phenotypic plasticity produces geographic variation within a species. The latitudinal gradients for buccinid gastropods and echinoids agree with the finding that shells are thinner at higher latitudes, but results here show inter- rather than intra-specific trends. Shell mass as a percentage of total animal dry mass decreased with increasing latitude in buccinid gastropods suggesting that the polar species had a relatively greater soft body tissue mass than their tropical and temperate counterparts, agreeing with Trussell (2000).

Overall there were clear trends of a decrease in total, or whole, animal inorganic content with latitude relative to total animal dry mass (Figure 9.2). These trends fitted well with the environmental temperature gradient. Shell thickness patterns, however, did not show consistent trends across taxa with latitude or temperature (Figure 9.3).

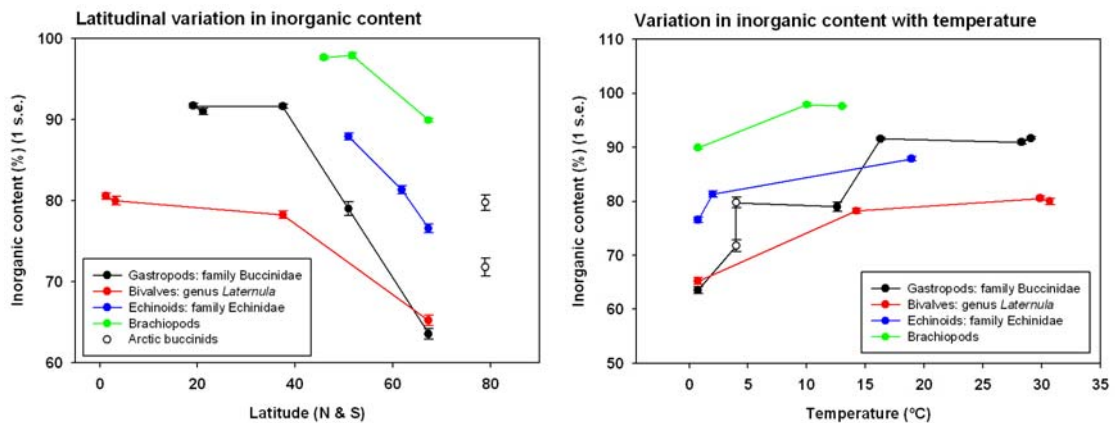


Figure 9.2 Variation in total animal inorganic content (ash as % dry mass) with latitude (left) and temperature (right). This metric is used because it is a good measure of the amount of skeleton and it is comparable among groups. Standard errors are mostly smaller than the points used to mark the mean. Black open circles denote Arctic buccinids.

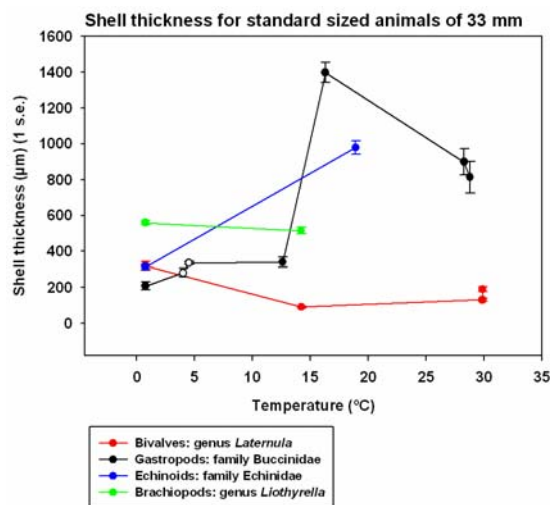


Figure 9.3 Variation in shell thickness with temperature for standard sized animals. Black open circles denote Arctic buccinids.

9.2.2 Shell chemistry

Using scanning electron microscope (SEM) energy dispersive spectroscopy (EDS) and wavelength dispersive spectroscopy (WDS), chemical variation in shell composition was analysed in biogenic carbonates in Chapter 4. However, there were no clear patterns in the shell composition of major and minor elements with latitude across all taxa. Ca was low in Antarctic gastropod and bivalve molluscs, but not low in Arctic gastropods. Na generally increased with increasing latitude in molluscs and brachiopods. Sr:Ca appeared to increase with latitude in the bi-valved groups studied (i.e. bivalves and brachiopods), but decreased with latitude in the coiled gastropods (Figure 9.4). Within the bi-valved groups, the exception to the Sr:Ca trend was species of *Laternula* bivalve that inhabit brackish water in the Straits of Johor between Singapore and Malaysia. Mg content decreased with latitude in the buccinids and between tropical and temperate *Laternula* bivalves but showed no latitudinal trend in the brachiopods. It seems the control of substitution of minor elements differs among each of the three model taxa (bivalve and gastropod molluscs and brachiopods) with latitude.

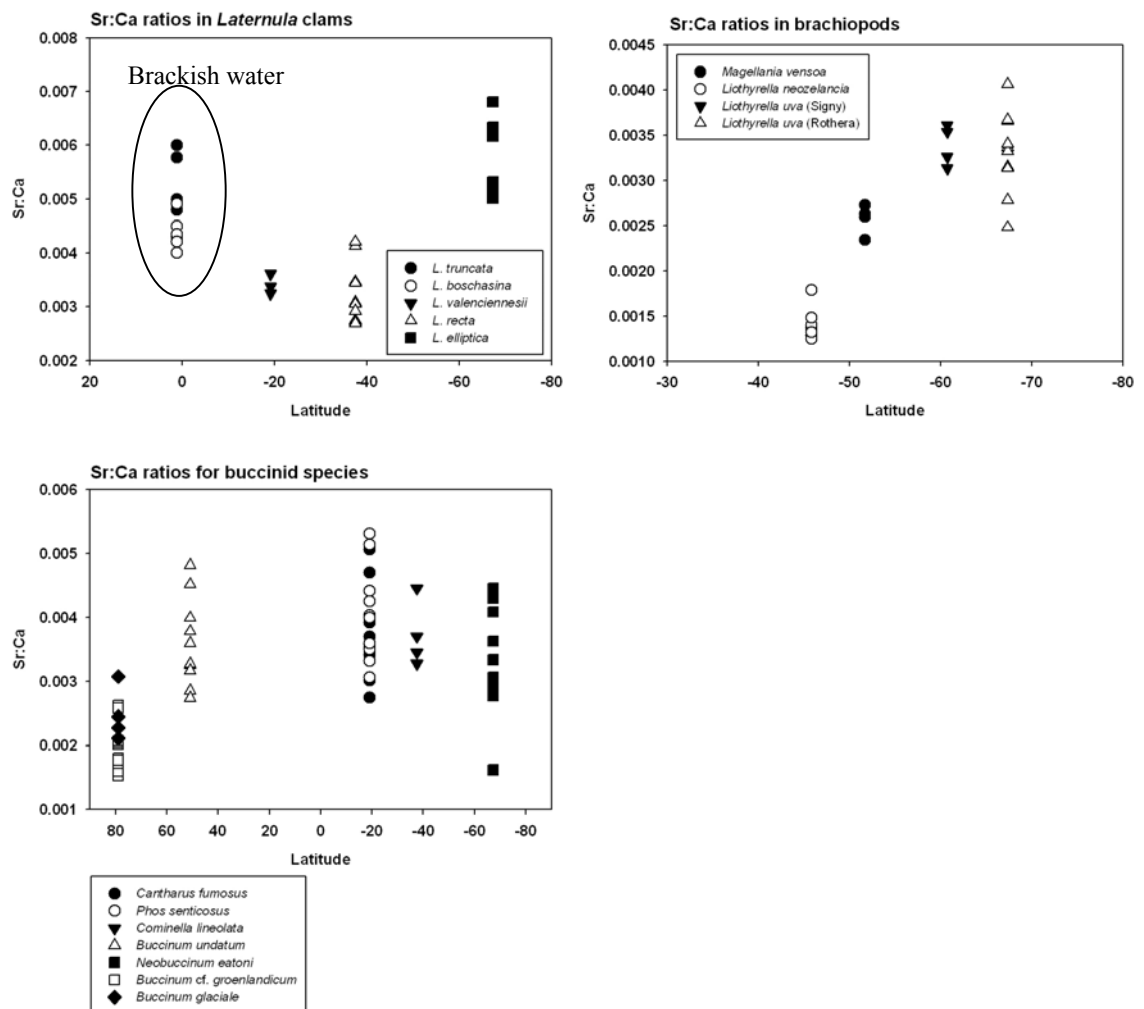


Figure 9.4 Latitudinal gradients in Sr:Ca ratios in *Laternula*, brachiopods and buccinids.

9.2.3 Shell cost

Conclusion: The proportional cost of calcification as a percentage of the total energy budget was greatest in polar species even though some polar species had slow growth rates.

Evolutionary costs of producing a calcium carbonate skeleton include: 1) a depositional cost (energetic) including production of the organic matrix and mineralization; 2) a

locomotory cost (energetic, post-deposition) for mobile organisms that must transport their skeleton; and 3) a cost (non-energetic) in terms of growth rate limitation set by the maximum rate at which skeleton can be produced (Palmer, 1981). There is also a cost of shell dissolution. Harper (2000) showed the loss in shell thickness due to dissolution was small at only $3 \pm 40 \mu\text{m.y}^{-1}$ in bivalves. The cost of replacing shell lost to dissolution is likely to be small. However, shell erosion in limpets may carry significant long-term costs (Day *et al.*, 2000).

In this thesis, estimates of the depositional cost of the shell are described in terms of the total energy budget. This depositional cost includes the cost of mineralisation (calcification) and the cost of producing the organic matrix. The cost of calcification is important in the understanding of skeletal evolution in marine invertebrates. Although this cost is difficult to measure because CaCO_3 is an inorganic material and the cost derives from metabolic costs of CaCO_3 production (accumulating, transporting and precipitating) that are hard to separate from other metabolic costs, Palmer (1992) calculated the cost of calcification to be $1\text{--}2 \text{ J.mg}^{-1}$ of CaCO_3 . From these calculations, Palmer (1992) suggested the cost of calcification compared to other metabolic costs is low in low- and mid-latitudes in marine surface waters.

Metabolic rate decreased with latitude as a function of temperature across all taxa studied (Chapter 5 and Figure 9.5). This meant that generally total energy budgets decreased with increasing latitude. The exception to this trend was the tropical emersed intertidal buccinid gastropods, which had lower metabolic rates than their subtidal or intertidal rock-pool dwelling temperate con-familial species.

Growth rate is reported to be slowest in polar species for species of similar size and ecology (Everson, 1977; Clarke, 1983) and the results of Chapter 6 agreed with these findings. However, absolute growth depends on animal size and the large polar clam had fast absolute growth compared to tropical and temperate congeners.

In the molluscs studied, shell production costs approximately 0.5 – 4 % of the total energy budget based on mid-range data of 1.5 J.mg^{-1} of CaCO_3 from Palmer (1992) (Figure 9.6).

The higher costs of 3 – 4 % are found in the polar species and are a result of lower metabolic rate (and subsequent lower total energy budget) and lower saturation states of seawater with respect to CaCO_3 (i.e. increased solubility of CaCO_3) at lower temperatures. In tropical and temperate locations, shells cost from 0.5 – 2 % of the energy budget to produce. Despite temperate buccinid shells being thicker and more heavy-set than shells of polar species (and having a faster growth rate), their cost as a proportion of the total energy budget (i.e. proportional cost) is less because of a higher metabolic rate (and subsequent higher total energy budget) and the higher saturation states of seawater with respect to CaCO_3 in temperate waters. So within the temperate and tropical species, shell cost is a small proportion of the total energy budget of the organism. Although the polar species of *Laternula* had the thickest shell, the proportional cost of the shell was almost identical to the cost in the polar buccinids. This similar cost between the polar molluscs may represent an upper or maximum cost of shell demonstrated in this environment, although data are limited. Estimates of proportional shell cost for the temperate species of *Laternula* and buccinid are also very similar. The Antarctic brachiopod *Liothyrella uva* had the highest estimated cost of shell production of up to 6 – 13 % of the total energy budget.

Thick-shelled morphs of the prosobranch gastropod *Thais* (= *Nucella*) *lamellosa* exhibit significantly slower rates of body growth than thin-shelled morphs, suggesting that there is an evolutionary cost of slower body growth in having thicker shells, i.e. the cost of growth rate limitation (Palmer, 1981). In Antarctica, where growth on an average annual basis is slow because food availability is limited to the short summer season (Clarke & Lakhani, 1979; Richardson, 1979; Clarke, 1983; Arntz *et al.*, 1994), shell thickness may be reduced if there is little to defend against so that the already limited rate of growth will not be further reduced by the cost of growth rate limitation.

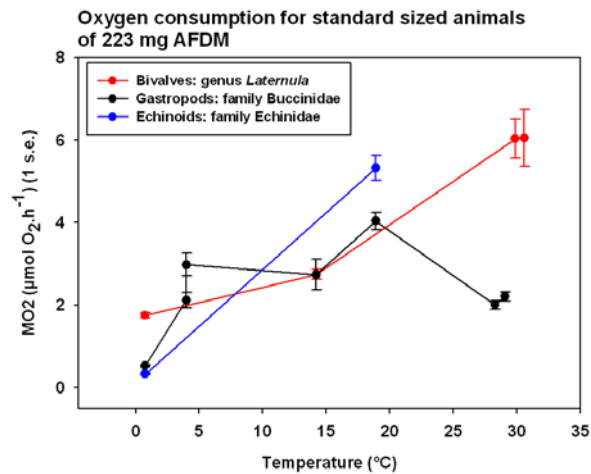


Figure 9.5 Summary of trends in standard animal (AFDM = 223 mg) mean respiration rate for each group with temperature.

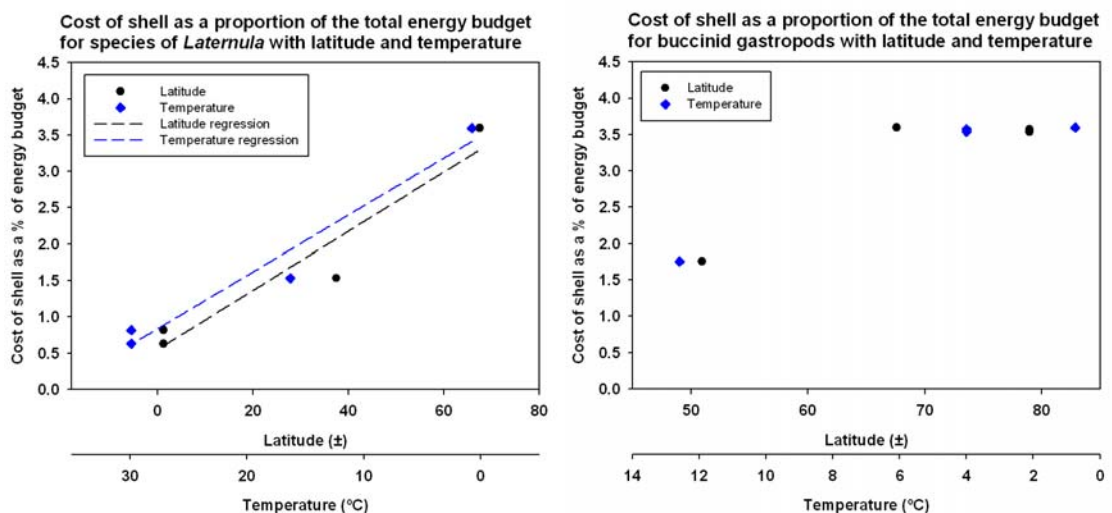


Figure 9.6 The cost of shell as a proportion of the total energy budget was significantly related to temperature for *Laternula* ($F = 47.4602$, $df = 1,2$, $p = 0.0204$) and for buccinid gastropods ($F = 22.6881$, $df = 1,2$, $p = 0.0414$). The cost of shell was significantly related to latitude in *Laternula* ($F = 23.7545$, $df = 1,2$, $p = 0.0396$) but not significantly related to latitude in the Buccinidae ($p = 0.0938$ NS). Cost values were taken at age 3 for *Laternula* and age 5 for buccinids because these ages overlapped measured individuals for most species within the taxa. These costs were based on mid-range data of 1.5 J.mg^{-1} of CaCO_3 from Palmer (1992).

9.2.4 Predation pressure: shell damage and defence morphology

Conclusion: The number of shell repairs decreased across latitudes as a function of temperature in buccinid gastropods and brachiopods, but not for bivalves of the genus *Laternula*.

One of the primary functions of the shell, or exoskeleton, is protecting the occupant. This protection provides a defence against abiotic factors, such as saltating rocks or ice scour, and biotic factors, such as overcrowding or predation. Predation pressure varies with latitude (Paine, 1966; MacArthur, 1972; Vermeij, 1993), and more specifically with the planetary temperature gradient in shallow water marine environments because cold temperatures are limiting factors to durophagous predators (Frederich *et al.*, 2000; Frederich *et al.*, 2001). Shell drilling and crushing predators are rare or absent in shallow-shelf Antarctic waters (< 100 m depth) (Aronson & Blake, 2001; Clarke *et al.*, 2004; Aronson *et al.*, 2007). Other factors which may cause shell damage may also vary with latitude and temperature, and one of these in particular, ice scour, will be discussed later.

Shells that were capable of resisting an attack will have scars from repaired breaks. Data here showed shell repairs decreased with increasing latitude and increased with seawater temperature (Chapter 7). Shell defences measured by defence morphology in molluscs also decreased with latitude and increased with seawater temperature. Shell repairs increased with increasing temperature between 0 to 20 °C for the epifaunal groups studied: brachiopods and buccinid gastropods (Figure 9.7). In the infaunal bivalve genus studied, shell repairs were greater in the Antarctic species compared to temperate and tropical congeners. These two contrasting patterns in shell repair with temperature between epifaunal groups exposed to predation and infaunal groups with some refuge from predation (Vermeij, 1977; Alexander & Dietl, 2005), provided some evidence that predation pressure drives the ecological need for increased shell thickness in epifaunal groups and that predation pressure controls shell defence morphology such as shell gape and aperture narrowness in both epi- and infaunal groups.

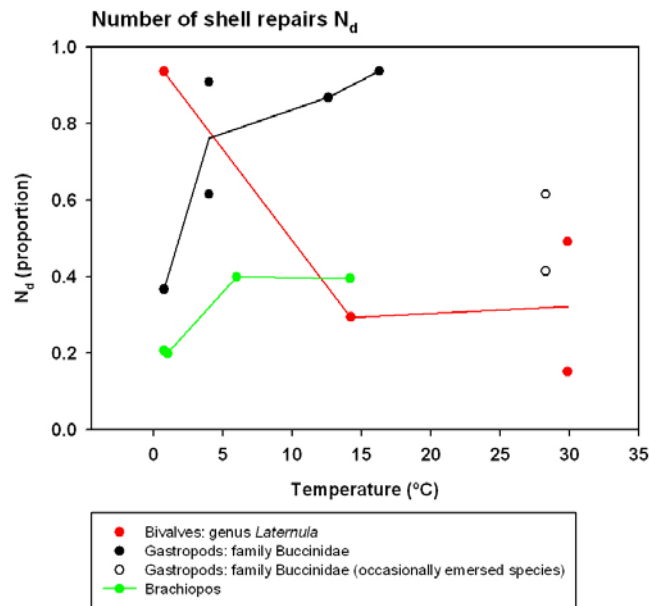


Figure 9.7 Shell repairs in relation to temperature.

9.3 Protection or production costs: the controls on shell morphology

Conclusion: Shell ecological function (i.e. protection) exerts a greater control on shell morphology than the proportional cost of shell production.

Shell morphology such as thickness and shape is likely to be controlled to different extents by physiological costs and ecological necessity for a shell. There are likely to be trade-offs in energetic cost and protection, for example, from predation. Evidence from this thesis suggests that the ecological function of the shell in protection is a more important control than the proportional cost of synthesising a shell. Although shells may be reasonably costly to produce (0.5 – 5 % of the energy budget in molluscs and higher in brachiopods), death is the ultimate cost to the shell producing organism for failed defences and protection is evolutionarily of utmost importance.

9.3.1 Why cost is not likely to be the primary control

Shell thickness alone was not significantly related to proportional shell cost among species in the gastropod and bivalve molluscs studied (Figure 9.8). However, the Antarctic species of *Laternula* clearly had a more costly and thicker shell than the temperate and tropical species. Proportional shell synthesis costs in this thesis are estimates based on the total energy budget calculations. However, since all species have been analysed in the same way we can be reasonably confident that the relationships of cost among species are representative. In the temperate and tropical molluscs studied, shell cost was a small proportion of the total energy budget of the organism (0.5 – 2 %). Polar species show shell cost can be up to 3 – 4 %, which is 1.33 to 8 times greater (Figure 9.6). This shows that the cost of the shell production in the temperate and tropical species is well within the possible range of shell cost given the higher values exhibited by polar species. For example, temperate buccinids are capable of producing a thicker shell at a lower proportional cost to the animal than the thinner shells of polar buccinids. Since molluscs are capable of exhibiting induced defences (Trussell, 1996; Trussell & Smith, 2000; Trussell & Nicklin, 2002; Dalziel & Boulding, 2005), given these proportional shell costs tropical and temperate molluscs would have the capability to double the cost of their shell production and still remain within the shell cost experienced by polar relatives. So proportional shell cost in temperate and tropical species does not seem to be a limiting factor and shell synthesis cost is unlikely to be the primary control on shell morphology, such as shell thickness.

The proportional cost of calcification was greatest in the polar molluscs despite the Antarctic buccinid and *Laternula* clam having less inorganic mass (CaCO_3) as a percentage of their total dry mass. However, the difference between the Antarctic buccinid and clam is that despite the elevated shell cost at polar latitudes, the clam *Laternula elliptica* still produces a thicker shell than congeners from lower latitudes. If cost was the primary control on shell morphology, one might expect the Antarctic clam to have a thinner shell.

Snails in calcium-poor habitats such as the deep-sea, freshwater and terrestrial habitats have thin shells and it is rare for sculpture or narrow apertures to be found (Vermeij & Covich,

1978). The author has observed deep-sea molluscs to lack coloration and have thin, fragile shells. Since animals in extremely calcium-poor environments such as terrestrial and freshwater habitats can still make CaCO_3 shells, albeit often thin ones, and since the cost of the shell is likely to be markedly higher in these environments because calcium is much more soluble or scarce, the cost of making shells is unlikely to be the main factor controlling shell thickness. Among different groups, evolutionary constraints could cause the continuation of shell production in environments where calcium is scarce. However, differences in shell morphology compared to cost among closely-related species suggest that the ecological need for a shell outweighs the energetic cost of shell production and is more likely to be a greater control on shell thickness. After all successful predation and death to the shell occupant is the ultimate cost, and a very strong fitness factor.

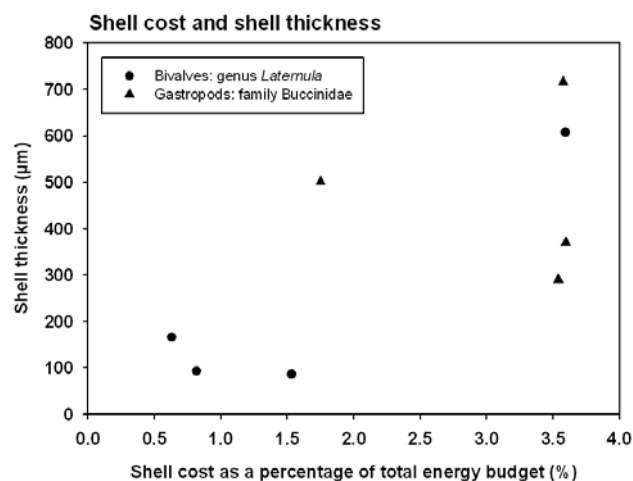


Figure 9.8 Shell cost and shell thickness for molluscs analysed. Regressions of shell thickness on shell cost were not significant for *Laternula* bivalves ($p = 0.0821$ NS) or buccinid gastropods ($p = 0.8946$ NS).

9.3.2 Why predation is likely to be the primary control

Prey species can reduce their risk of predation by morphological changes, avoidance behaviours or chemical defences (Trussell, 1996). Investigations in this thesis have considered the architectural morphology of shells across latitudinal gradients. Predator-inducible morphological defences are brought about when the predator or a cue (often

chemical) associated with the predator create shell structures in the prey which deter predators (Trussell, 1996). Predator cues induce bigger, more massive (Dalziel & Boulding, 2005) and thicker (Trussell & Nicklin, 2002) shells in some gastropods. Damaged conspecifics can induce thicker shells in marine snails that are additive to thickness changes caused by predator cues (Trussell & Nicklin, 2002). Thicker shells are more difficult for durophagous predators, such as crabs, to crush (Kitching *et al.*, 1966; Bertness & Cunningham, 1981; Palmer, 1985; Seeley, 1986). The crabs *Cancer productus* and *Rhacochilus vacca* exhibited higher rates of predation in thin-shelled *Littorina* species than thicker-shelled species (Boulding *et al.*, 1999). If the predation risk is defensible than defence structures can be modified accordingly.

Phenotypic plasticity in shell thickness may have evolved as a result of the threat of predation (Trussell, 1996), but if predation risk is low or cost of shell production high, the optimal adaptation is to not grow shell (i.e. shell-less growth) or to have no shell (Irie & Iwasa, 2005). The existence of inducible defences in modifying shell thickness proves that thicker shells are selected for by predation within populations of calcareous marine invertebrates. Such studies of variation in shell thickness and resistance to predation within populations imply that the latitudinal gradients in shell thickness and defence morphology are also likely to be affected by variation in predation pressure, albeit on an evolutionary timescale. It is worth noting too that inducible defensive traits in snails can be constrained by calcium availability in the environment (Rundle *et al.*, 2004). Data from different chapters of the thesis on latitudinal gradients in shell thickness, and shell repair and defence morphology, are considered here first by epifaunal groups then by the infaunal group.

Epifauna - Gastropoda: family Buccinidae

The Antarctic buccinid had the lowest proportion of individuals with repairs (N_d), lowest number of repairs per shell (N_i), lowest proportion of individuals damaged by predation (P_d) and the lowest total number of injuries from predation (P_i). These results agree with previous reports that durophagy (skeleton-crushing predation) is currently limited in Antarctica (Dell, 1972; Dayton *et al.*, 1974; Arntz *et al.*, 1994; McClintock & Baker, 1997). Considering shell thickness and shell repairs, there were no significant relationships of shell thickness on all shell repairs or shell repairs caused by predation damage (Figure 9.9). This

is not surprising as one might expect this relationship to be a horizontal line over time, with shell damage being compensated for by thicker, more damage resistant shells (L. Peck, pers. comm.). Since there are no significant relationships, it may well be the case that evolution and escalation and the predator-prey arms race (e.g. Vermeij, 1987) have cancelled out any trend in shell thickness and shell repairs over time.

Additionally, two measures were used as an indication of predator resistance in coiled gastropods: 1) aperture width/shell height and 2) the metric of aperture narrowness described by Vermeij (1993). Aperture width as a percentage of shell height increased with increasing latitude and decreasing temperature (Chapter 7). Apertures tended to become slightly narrower with increasing shell thickness across the buccinids studied (Figure 9.10). The Antarctic gastropod *Neobuccinum eatoni* had the second thinnest shell compared to other buccinids and, along with the Arctic gastropod *Buccinum glaciale*, the largest aperture width compared to shell height (Figure 9.10). By these criteria of shell defence morphology, *N. eatoni* had low resistance to predators. So shell damage and defence morphology decreased with increasing latitude in the buccinid gastropods. As narrow apertures confer greater resistance to predation (Palmer, 1979; Vermeij, 1993) and narrow apertures are related to shell thickness, this provides evidence that shell thickness in buccinids may function primarily in predator defence, rather than as a defence against other types of damage, such as abiotic damage.

Graus (1974) does not mention predation as a possible cause for the trends in calcification efficiency, but does say that the trends cannot be explained by temperature alone. However, Graus (1974) found that aperture shape did not change along a latitudinal gradient, which is in contrast to Vermeij (1993) who states that the incidence of narrow apertures is lower from low to high latitudes, and in contrast to the findings from this study that show aperture shape did change with latitude among closely related species, and that there was a latitudinal cline in aperture narrowness. The difference between the findings from this thesis and Graus (1974) is most likely because of the wider taxonomic range that Graus analysed. Confamilial trends found here may not hold for broader taxonomic comparisons.

Generally predation pressure decreases towards the poles (Paine, 1966; MacArthur, 1972; Aronson & Blake, 2001; Clarke *et al.*, 2004; Aronson *et al.*, 2007). Patterns in buccinid shell repairs and defence morphology support this. In this epifaunal group the shell is a key defence mechanism and predation, therefore, seems to be driving patterns in shell thickness in buccinid gastropods.

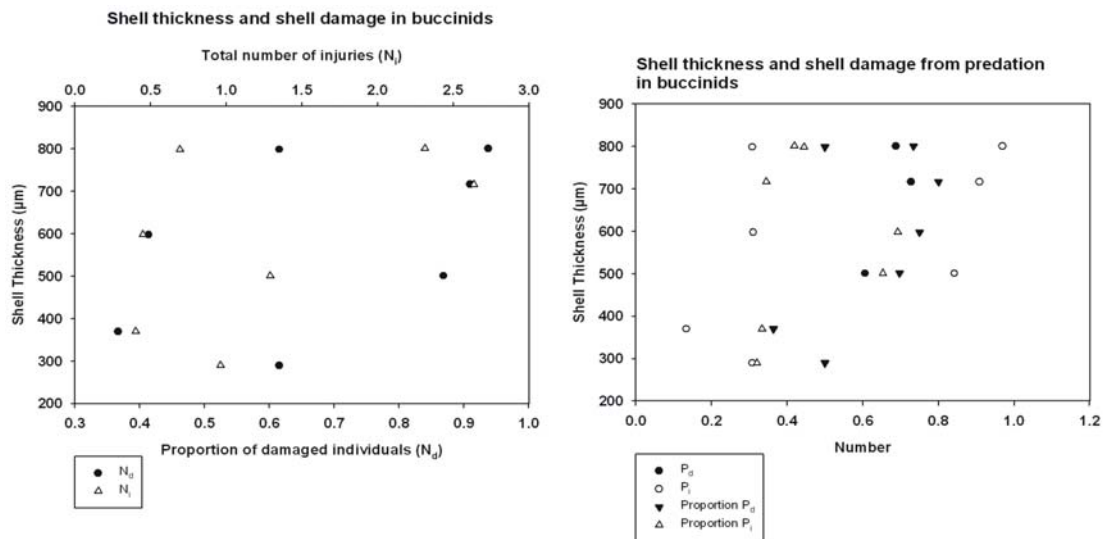


Figure 9.9 Plots of shell thickness and repaired shell damage in buccinid gastropods for all shell repairs (left) and repaired shell damage from predation (right). There were no significant relationships between shell thickness and the proportion of damaged individuals (N_d) ($p = 0.2728$ NS) and the total number of injuries (N_i) ($p = 0.2552$ NS) or for the proportion of individuals damaged by predation (P_d) ($p = 0.2098$ NS), the total number of injuries from predation (P_i) ($p = 0.2421$ NS), the proportion of individuals with damage that was caused by a predator attack ($\propto P_d$) ($p = 0.2140$ NS), and the proportion of all injuries that were caused by predator attack ($\propto P_i$) ($p = 0.7502$ NS).

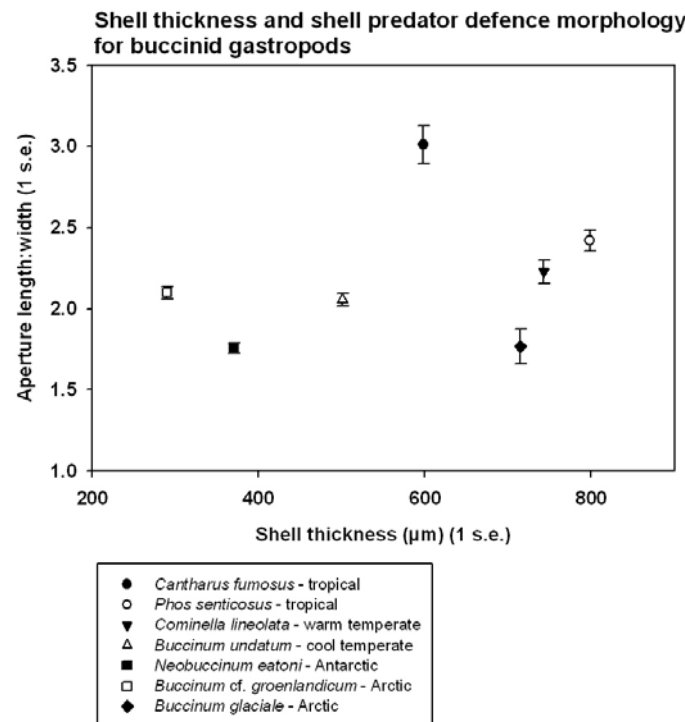


Figure 9.10 Buccinid gastropod shell thickness and aperture narrowness metric (aperture length/aperture width).

Epifauna - Brachiopods

Temperate brachiopods had twice as many repairs as polar brachiopods, but there was no difference in shell thickness between temperate and polar brachiopods. There were no significant regressions among brachiopod species of 1) shell thickness on length or 2) shell thickness on repairs (Figure 9.11). The reduced frequency of repairs in Antarctic brachiopods could be due to lower predation intensity, although this is not supported by a corresponding reduction in shell thickness.

Temperate brachiopods are repellent to predators (Thayer, 1985) and chemical defences with the tissues of the Antarctic brachiopod *Liothyrella uva* mean it too is unpalatable to predators (McClintock *et al.*, 1993). These chemical deterrents within the soft tissues of brachiopods are an alternative method of reducing the risk of predation compared to morphological changes and avoidance behaviours (Trussell, 1996). These chemical defences may be why latitudinal gradients in shell thickness were not apparent in the brachiopods studied. Brachiopods may be using chemical deterrents rather than

morphological structures as their primary defence to predation. As other shelled marine invertebrates are not distasteful to predators (Thayer, 1985), latitudinal gradients in shell thickness were seen, for example in gastropods of the family Buccinidae and echinoids of the family Echinidae.

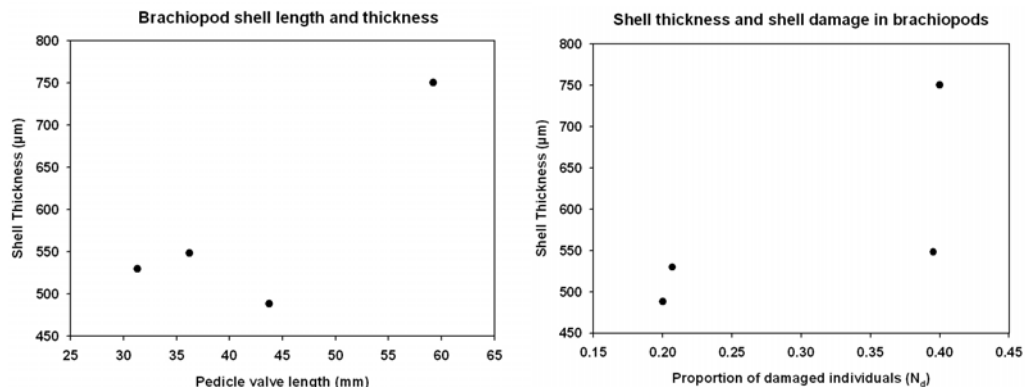


Figure 9.11 There were no significant inter-specific relationships between shell length and thickness ($p = 0.1824$ NS) (left) and shell repairs and thickness ($p = 0.2912$ NS) (right).

Epifauna - Echinoids

Although samples were limited and comparisons require more species for confirmation, within the family Echinidae, test thickness decreased with latitude suggesting a potential response to decreases in predation pressure. However, spine length as a percentage of test diameter increased. Thus the polar species had a thinner test but longer spines than the temperate species, which had a thicker test but shorter spines (Figure 9.12). Spine length in echinoids is usually associated with defence from predators as is test thickness (Guidetti & Mori, 2005). However, the author observed spine thickness and robustness to decrease markedly with latitude, so spine length alone may not be the best measure of spine resilience against predators. Spine lengthening in echinoids can be an adaptation to capture more food from seawater (Régis, 1986) and the longer spines of *Sterechinus neumayeri* may be an adaptation to the seasonally food-limited Antarctic environment, rather than a predator defence. Thus latitudinal gradients in test thickness in echinoids may be determined by predation pressure, although trends in spine length may be affected by resource availability as well as predation intensity.

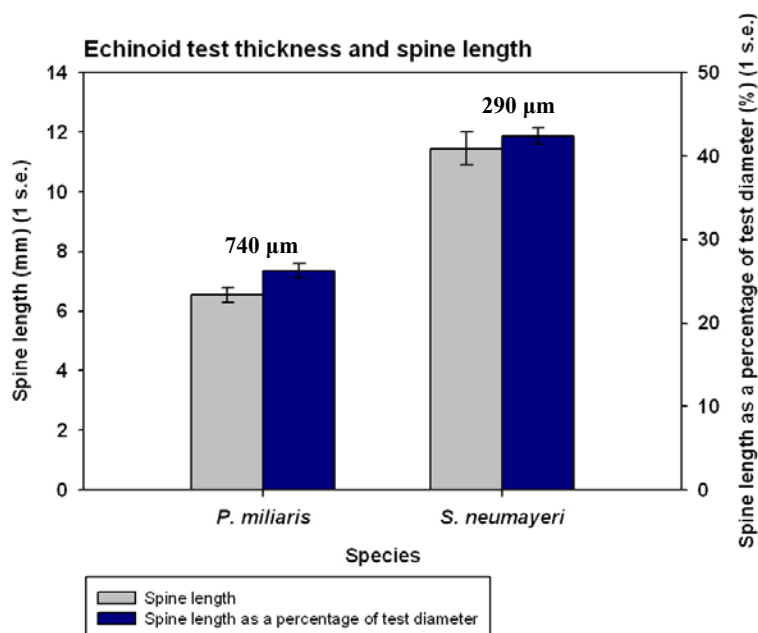


Figure 9.12 Echinoid spine length with test thickness written above the bar charts. There was a significant difference between test thickness and spine length ($t = -8.207$, $df = 52.256$, $p < 0.001$) and test thickness and spine length as a percentage of test diameter ($t = -12.640$, $df = 57.876$, $p = 0.024$).

Infauna - Bivalvia: genus *Laternula*

Laternula data show significant relationships between shell repairs and shell thickness, particularly for the polar species compared to the tropical and temperate species. Shell thickness was predicted by the proportion of damaged individuals (N_d) and the total number of injuries (N_i) (Figure 9.13). Either thicker shells are capable of protecting the occupant inside and repairing from more injuries, or shells have adapted becoming thicker in environments where they are needed to protect the occupant from injury. Where shell damage is caused by predation, one might expect this relationship to be a horizontal line over time, with shell damage being compensated for by thicker more damage resistant shells, as seems to be the case for the buccinid gastropods. However, an infaunal lifestyle provides a refuge from predation (Vermeij, 1977; Alexander & Dietl, 2005). Therefore, the control on shell thickness may not be from biotic damage, such as predation, which is subject to predator-prey driven evolution, but from an abiotic form of shell damage to which a maximum evolutionary response may be expected.

Across the genus *Laternula*, the shape of the Antarctic species' shell indicated least resistance to predation supporting findings that there is less predation pressure in Antarctic waters than in tropical and temperate waters (Chapter 7) (Aronson & Blake, 2001; Clarke *et al.*, 2004; Aronson *et al.*, 2007). The size of the gape (shell inflation at gape/length) was positively related to shell thickness; wider gapes were found on thicker shells within the genus *Laternula* (Figure 9.14). This means the thicker shells of the Antarctic species have other characteristics which are less predator resistant suggesting that increased shell thickness is not linked to increased predator defence characteristics of the shell, such as gape size. Buried *L. elliptica* are safe from natural predators which attack only when individuals have been exhumed by ice scour (Urban & Mercuri, 1998). This is further evidence that the thick shell in the Antarctic clam is not a protection against predation from above.

Irie and Iwasa (2003) suggest, from mathematical models, that latitudinal clines in body-size for marine ectotherms are controlled by the latitudinal gradient in predation pressure, and that the latitudinal clines in shell thickness are either controlled by predation pressure or another environmental factor such as seawater temperature. The conclusion from this thesis is that shells could be thinner at high latitudes because of the lack of drilling and crushing predators and latitudinal variation in selection by predation for thicker shells and exoskeletons may be the controlling factor in skeleton thickness. So why does the Antarctic burrowing bivalve *Laternula elliptica* have a thick shell?

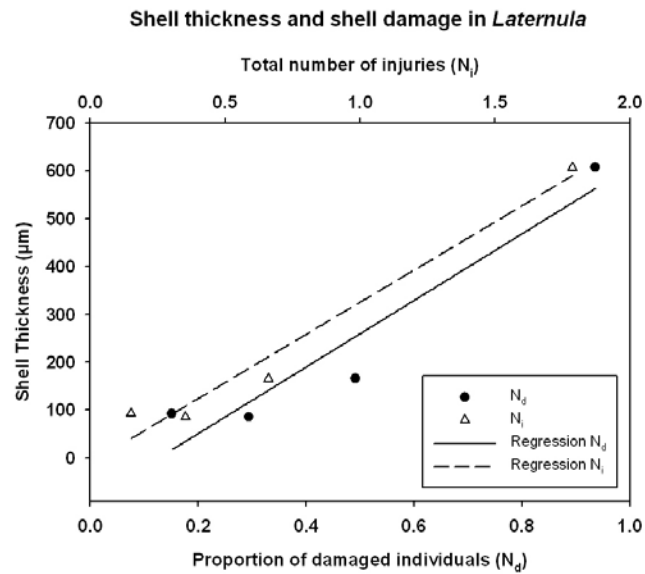


Figure 9.13 Relationship between shell thickness and repaired shell damage in species of *Laternula*. Shell thickness was predicted by the proportion of damaged individuals (N_d) ($F = 20.8045$, $df = 1,2$, $p = 0.0449$) and the total number of injuries (N_i) ($F = 64.2231$, $df = 1,2$, $p = 0.0152$).

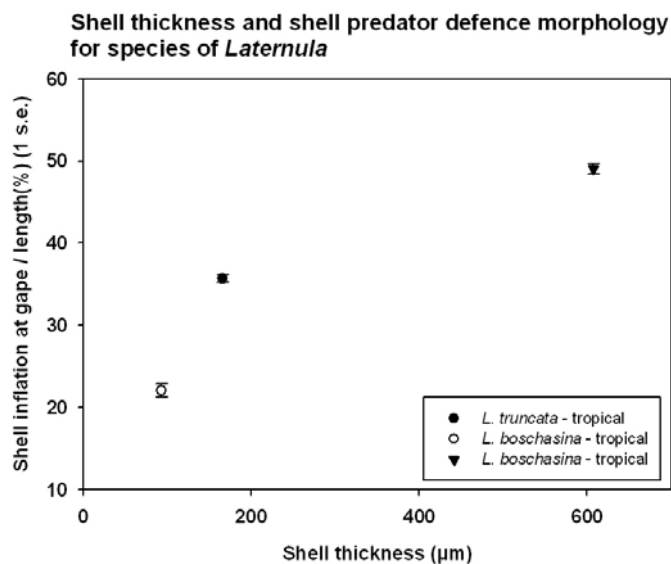


Figure 9.14 Relationship between shell thickness and shell predator defence morphology.

Latitudinal gradients in abiotic damage: the potential effects of ice scour

An abiotic factor that changes with latitude, and specifically temperature, is the presence of icebergs at high latitudes. If the keel depth of the ice exceeds the water depth, then floating ice collides with the seabed in a process termed ice scour (Conlan *et al.*, 1998; Barnes & Conlan, 2007). Ice scour is a major influence to the community structure of polar shallow-water benthic communities (Peck *et al.*, 1999; Smale, 2007; Smale *et al.*, 2007) and by clearing sites for settlement can lead to patchily or binomially distributed size cohorts (Peck & Bullough, 1993; Urban & Mercuri, 1998).

Ice can scour the seabed at depths of up to 500 m on the Antarctic shelf (Lien *et al.*, 1989; Gutt *et al.*, 1996). Around Rothera, observations of the distribution of benthic fauna suggest that ice regularly scours the benthos between 0 and 15 m deep (Brown *et al.*, 2004). At < 15 m depth the fauna is rather impoverished and dominated by motile species such as echinoderms and limpets. At > 15 m depth a range of long-lived sessile fauna appear such as brachiopods and giant sponges. On summer dives, icebergs were seen grounded in Hangar Cove at depths *c.* < 15 m, becoming more frequent at shallower depths. The Antarctic bivalve clam *Laternula elliptica* can be found in waters from 1 to 500 m deep in sheltered coastal sites (Dell, 1990) although it is more common from 15 to 45 m (Nonato *et al.*, 2000). *L. elliptica* has been reported to bury > 50 cm deep (Zamorano *et al.*, 1986) which would accordingly provide some protection from ice scour and predation (Rodrigues *et al.*, 2007). However, it seems unlikely that *L. elliptica* would have a siphon > 50 cm long needed to reach the surface to feed. Individuals of *L. elliptica* in this study were all collected buried < 50 cm deep in the sediment.

During summer SCUBA diving, on each dive at Hangar Cove groups of empty *Laternula elliptica* shells were observed lying on the sediment surface. Icebergs furrowing the sediment can exhume buried *L. elliptica* (Zamorano *et al.*, 1986; Peck *et al.*, 2004) and the groups of shells observed were almost certainly from clams that had been exhumed from the sediment by ice scour (L. Peck, pers. comm.). Brown *et al.* (2004) found that ice could scour a particular area between 9-17 m deep from 0 to 1.5 times per year around Adelaide Island and that North Cove, which is adjacent to and of the same aspect as Hangar Cove, was hit by icebergs twice as much as South Cove.

Iceberg scours produce long furrows in the sediment with berms at either side and troughs in the middle. *L. elliptica* exhumed from the sediment by an iceberg can be left exposed at the tops of berms but by jetting water from its siphon the clam can propel itself down into the bottoms of the troughs into a location more suitable for reburial whilst simultaneously avoiding scavenging predators (Ansell & Rhodes, 1997; Peck *et al.*, 2004). Shell defence structures suggest that the thicker shell of the Antarctic clam was not linked to an increased predation risk from above whilst the clam remains buried in the sediment (Figure 9.14). Predators of unburied *L. elliptica* include the asteroid *Odontaster validus* (Zamorano *et al.*, 1986; Urban & Mercuri, 1998), the nemertean *Parborlasia corrugatus* and the gastropod *Neobuccinum eatoni* (Urban & Mercuri, 1998). None of these predators are durophagous. If a thick shell is not a defence from shell-breaking and shell-crushing predators it may in fact be a defence against abiotic damage from ice scour and saltating rocks. The sediment in Hangar Cove is rocky and heterogeneous and in the process of being exhumed from the sediment, the shell of *L. elliptica* may be damaged by one of these rocks. In this case a thicker shell would increase the chances of survival.

Thus in infaunal *Laternula* bivalves it may be ecologically necessary for the polar clam to have a thick shell given its infaunal, deep-burrowing lifestyle in heterogeneous sediment and the risk of ice scour. Therefore, even though the cost of shell production is high in the polar clam, the ecological requirement for a shell is again likely to be the primary driving control on shell thickness.

Conflicting shell types of the Antarctic molluscs: the thick-shelled bivalve and thin-shelled gastropod

One question that arises is that if the Antarctic *Laternula* species has a thicker shell because of the potential of ice scour then why does not the Antarctic buccinid *Neobuccinum eatoni* have a thicker shell? *N. eatoni* is found in a similar location to *Laternula elliptica* in Hangar Cove, Rothera. However firstly, *L. elliptica* and *N. eatoni* are found at different depths and secondly, *L. elliptica* is infaunal and inhabits a fixed location, whereas *N. eatoni* remains largely above the sediment surface and is motile. Ice scour creates the potential

removal of infaunal organisms from the sediment and the potential collision with saltating rocks within and above the sediment.

In Hangar Cove, Adelaide Island, *L. elliptica* is found in waters as shallow as 3 m, although mostly only juvenile cohorts < 4 years old are found in these shallows, presumably because of the high incidence of ice scour. *L. elliptica* collected for this study were from 13-18 m deep, with the majority collected at approximately 15 m. *N. eatoni* is most commonly found below 18 m and individuals in this study were collected from 18-25 m, with the majority collected at 21-25 m. Thus individuals of *N. eatoni* in this study were found at depths that are below regular ice scour. Additionally, motile animals, such as *N. eatoni*, may be able to avoid scours (Brown *et al.*, 2004). It would be interesting for future work to determine if the number of repairs on shells of *L. elliptica* below the range of frequent ice scour were less than those of individuals from ≤ 15 m and so to determine the proportion of the shell damage caused by removal from the sediment by ice scour. Although digging for *L. elliptica* whilst SCUBA diving at more than 20 m would result in few animals per dive because of the time limitations on SCUBA at depth. Urban and Mercuri (1998) suggest mortality in *L. elliptica* from iceberg activity was greater at a site < 10 m in water depth because of increased ice scour than at a site > 10 m in water depth.

The second hypothesis is that differences in shell thickness occur between epi- and infaunal groups because there are ecological differences between these two lifestyles. The gastropods, echinoids and brachiopods studied are epifaunal, whereas the bivalves studied are infaunal. In this thesis data on the cost of synthesising a shell were presented. Other key costs associated with a shell include 1) a post-depositional locomotory cost of transporting the shell and 2) growth rate limitation (Palmer, 1981). The locomotory cost is limited to organisms that must transport their shell and may help to explain the differences in shell thickness. The gastropods and echinoids studied are motile and thus have an ongoing cost of transporting the shell. *Laternula* clams are non-motile, with the exception of 'jetting' (Ansell & Rhodes, 1997), which can be considered infrequent locomotion compared to the gastropods and echinoids, because it only occurs when individuals are removed from sediment. This additional cost of locomotion in gastropods and echinoids could be why the polar species have thinner shells than temperate and tropical confamilials.

Although brachiopods are epifaunal, they remain attached to the substratum and so incur no cost of shell transportation. The thickness of polar brachiopod shells was no different to that of temperate brachiopods including congeners. As they do not endure a cost of locomotion, the shell may be relatively thicker than that for motile epifauna. If this hypothesis is true, the additional locomotory cost of transporting the shell could be significant to polar animals and is a potential additional selective force leading to thinner shells in some Antarctic species. Activity is markedly reduced in Antarctic species, generally by factors of x2 to x5 compared to temperate species (Peck *et al.*, 2006), suggesting locomotory costs may be minimised.

9.4 The implications of climate change

Since the Industrial Revolution carbon dioxide (CO₂) from anthropogenic emissions such as fossil fuel burning and deforestation have increased the concentration of atmospheric CO₂ from 280 to 387 ppmv in the last 200 years (Tans, NOAA/ESRL). This increase in CO₂ as well as other greenhouse gases is causing global climate destabilisation, known as climate change. Global warming and ocean acidification, dubbed the silent climate change issue, are two of the main effects of climate change that are causing and will continue to cause problems for marine animals. In the Southern Ocean, many marine species are stenothermal and limited to life within a narrow temperature range of a just a few degrees centigrade (Peck, 2005). However, climate predictions suggest the Southern Ocean will experience some of the most rapid water temperature (Meredith & King, 2005) and pH changes (Orr *et al.*, 2005) on the planet.

9.4.1 Global warming

Conclusion: Increasing seawater temperatures resulting in increased ice scour in the short- to mid-term and the possible of invasion of durophagous predators could cause major problems for the Antarctic near-shore benthic communities whose exoskeletons have evolved in the absence of durophagy.

Seawater temperatures in the Western Antarctic Peninsula (WAP) have already risen by 1 °C during the second half of the twentieth century (Meredith & King, 2005). Climate warming in the short to medium term is likely to increase the iceloading of polar near-shore communities and therefore the frequency of ice scouring (Brown *et al.*, 2004; Smale & Barnes, 2008). In addition to increased disturbance, increasing water temperatures may also bring another problem – predation.

Modern durophagous predators are rare or absent in Antarctic shallow waters (Aronson & Blake, 2001; Clarke *et al.*, 2004; Aronson *et al.*, 2007) and crabs went extinct from Antarctic waters approximately 15 million years ago in the Miocene (Feldmann, 1998). Reptant decapod crustaceans (sub-order Reptantia) are poor regulators of magnesium in their haemolymph and are narcotised by the combination of low temperatures and high Mg^{2+} concentration in the haemolymph (Frederich *et al.*, 2001). The result is an exclusion of Reptantia from areas with temperatures below 0 °C (Frederich *et al.*, 2000). Reptant decapods appear unable to inhabit the permanently cold waters of Antarctica and are largely absent in waters < 200 m in depth south of the Antarctic Convergence (Frederich *et al.*, 2001).

Recently records of large populations of lithodid crabs in deeper waters of the Antarctic continental slope at temperatures > 1 °C have been published (Klages *et al.*, 1995; Arana & Retamal, 1999) and consequently the return of crabs to Antarctic waters has been suggested (Thatje *et al.*, 2005; Aronson *et al.*, 2007). If water temperatures rise to above 0 °C year-round with climate warming, then Reptantia could prey upon the shallow water marine benthos around Antarctica causing significant alteration of the ancient community structure (Aronson *et al.*, 2007).

9.4.2 Ocean acidification

Conclusion: Ocean acidification negatively affects calcareous marine invertebrates and seawater pH levels predicted for the year 2100 significantly reduced survival, growth and development of early larval stages of the commercially important edible Sydney rock oyster *Saccostrea glomerata*.

The oceans have taken up ~ 40 % of the anthropogenic CO₂ emissions from the atmosphere (Zeebe *et al.*, 2008) and are already 0.1 pH units more acidic than 200 years ago (Caldeira & Wickett, 2003) with a present day average global surface ocean pH of 8.07 compared to a pre-industrial pH of 8.17 (Cao *et al.*, 2007). This acidification is lowering the saturation state of seawater with respect to calcium carbonate and is making life more difficult for animals with calcium skeletons.

Chapter 8 and Watson *et al.* (in press) (Appendix 7) showed that survival, growth and development of larvae of the commercially important edible temperate Sydney rock oyster *Saccostrea glomerata* was negatively affected by levels of ocean acidification predicted for the year 2100. These data show that despite the reasonably small cost of shell production, estimated as a percentage of the total energy budget for juvenile and adult life stages of < 4 % in molluscs and < 1.5 % in the temperate bivalve, the larvae of calcareous bivalves are vulnerable to ocean acidification. The additional cost of producing a shell in acidified seawater may be too much to tolerate for larvae of the edible oyster *Saccostrea glomerata*, which showed a marked reduction in survival of 43 and 72 % under upper and lower seawater pH conditions predicted for the year 2100.

The calcium carbonate compensation depth (CCD) is relatively shallow at high latitudes and ocean acidification will cause the shoaling of the CCD to even shallower waters. The Southern Ocean surface waters around Antarctica will begin to become undersaturated with respect to aragonite by the year 2050 (Orr *et al.*, 2005). Once undersaturated, aragonite minerals will begin to dissolve. The cost of dissolution, which currently may be small (Harper, 2000), is expected to become higher with ocean acidification. There is likely to be

an increased energetic cost associated with the maintenance of skeletons in waters less saturated and undersaturated with respect to CaCO_3 . It is therefore likely that ocean acidification will change community structures, with the differential survival of species. Ocean acidification may affect predation intensity. Shell boring predators use acid of pH 4 to bore holes in the shell (Carriker & Williams, 1978) and seawater acidification could increase boring predation success, although this effect may only be small since the change in seawater pH from acidification is relatively small compared to the strength of the acid used to bore shells. More likely, ocean acidification could increase predation success by making prey shells thinner and could affect the optimum size of prey attacked by predators.

9.4.3 Summary of the potential effects of climate change

Conclusion: The combination of warming seas and ocean acidification could be particularly problematic for shallow-water Antarctic calcareous benthic invertebrates.

Climate change processes including global warming and cooling, acidification of the oceans and carbonate compensation feedback will have effects on organisms whose physiological processes are affected by temperature and pH. It is important to understand the controls on calcification and the effects of seawater temperature and pH on calcifying marine organisms. Temperature change and ocean acidification will make life more difficult for calcareous marine invertebrates and the combination of warming seas bringing increased ice scour (in the short- to mid-term) and potentially increased predation, as well as the increased solubility of CaCO_3 could be particularly problematic for shallow-water Antarctic benthic invertebrates, especially those whose calcareous shells have evolved in the absence of predators. Ocean acidification, however, is likely to be problematic too for calcified crustacean predators and mounting evidence shows ocean acidification will affect both calcareous and non-calcareous organisms. Carbon dioxide emissions are already tracking higher than worst case CO_2 emission scenarios predicted by IPCC reports in the 1990s and rapid reductions of CO_2 emissions of 40 % by 2020 and 80 % by 2050 are needed to avert the worst effects of climate change on oceanic pH (C. Veron, pers. comm.).

Stenothermal organisms are found in tropical and polar regions. Constrained to life within a narrow temperature range, these organisms are likely to be the first to suffer the effects of global temperature change. Understanding the effect of temperature and seawater pH on marine invertebrate skeletons is important in predicting the effects of climate change.

9.5 Limitations and suggestions for further work

This Ph.D. covered a wide range of research using multidisciplinary techniques and international collaborative effort. As this was a 3-year study, consequently some research was beyond the scope of this thesis. Limitations of the study included the fact that species were occasionally collected or measured in a different season to others within the taxon (e.g. temperate Australian species were measured in the austral winter). Whilst this was corrected for where possible, it is appreciated that there may have been some seasonal differences in measures such as soft body tissue composition. Another limitation was that in some areas numbers evaluated were low. If there was more time or the opportunity to undertake future projects, the following areas may warrant further research.

Enhancing the data set

- More species from related and unrelated groups could be analysed to form a broader dataset. Where data were limited to the size cohorts of a population found within an area, additional samples over a greater size range would enhance the dataset for certain species, e.g. *Laternula boschasina*.
- During the study it was not possible to measure metabolic rates for the New Zealand brachiopod *Liothyrella neozelanica*. Obtaining these data would enable the comparison of the cost of shell as a percentage of the total energy budget between *L. neozelanica* and the polar congeneric *L. uva*.
- It is appreciated that using energy budgets to calculate proportional shell cost provides an estimate of shell cost and that there are errors associated with calculations of energy budgets. Every attempt was made to minimise any errors. When further published data on energy budgets becomes available, then these data can be included in the proportional shell cost calculations to strengthen the

estimates. For example, to determine the importance of shell synthesis costs in echinoderms.

Other techniques

- This study has focused primarily on shallow water marine benthos. It would be interesting to continue the investigation of shell morphology, shell cost and predation pressure into deep-sea abyssal and chemosynthetic environments, pelagic environments, freshwater environments and those affected by naturally high pCO₂ such as vent sites.
- Determining the intra- and inter-specific effects of ocean acidification on different life-stages and the variation in response to ocean acidification across latitudes will be important in generating data on which to base policies to mitigate the effects of climate change.
- Scanning electron microscope (SEM) energy dispersive spectrometry (EDS) and wavelength dispersive spectrometry (WDS) are useful techniques for analysing major and minor elements. Laser ablation inductively coupled plasma mass spectrometry (LA-ICP-MS) is an appropriate technique for analysing minor and trace elements and further work could involve the use of LA-ICP-MS to analyse trace elements in shells in combination with SEM EDS/WDS to calibrate the major elements.
- One may wish to focus on a particular species or taxa and utilise improved methods of ageing shells such as acetate peel techniques and use markers or mark-recapture techniques to enhance growth analyses.
- Given the importance of the control of predation on shell morphology, determining predation rates in the field or in laboratory experiments across latitudes would be interesting. Across latitudes one could also run predation experiments on individuals with shells of different thickness both intra- and inter-specifically to determine whether thinner shells are more susceptible to predation across latitudes.

9.6 Summary of the major findings of this study

- In the calcareous marine megabenthic invertebrates studied, total inorganic content as a proxy for the amount of skeletal calcium carbonate decreased with latitude as a function of temperature. Latitudinal trends in shell thickness varied by taxon. Shells of gastropods of the family Buccinidae and echinoids of the family Echinidae decreased in thickness with increasing latitude. Shells within the bivalve genus *Laternula* and brachiopod genus *Liothyrella* did not follow this trend. *Liothyrella* shell thickness was no different between temperate and polar latitudes and of species studied within the bivalve genus *Laternula* the polar species *Laternula elliptica* had the thickest shell.
- Using SEM EDS and WDS there was no clear pattern in the shell composition of major and minor elements with latitude. Sr:Ca appeared to increase with latitude in the bi-valved groups studied, but decreased with latitude in the coiled gastropods. It seems the control of substitution of minor elements differs among each of the four groups with latitude.
- Metabolic rate generally increased with temperature across latitudes in all four invertebrate taxa. Analysis of Q_{10} values provided no evidence of metabolic cold adaptation (MCA), i.e. elevated physiological rates for polar organisms.
- Growth was slowest in the polar species for buccinid gastropods and *Liothyrella* brachiopods, but was fastest in the polar species within the bivalve genus *Laternula*.
- A method was devised to estimate absolute cost of shell production as a proportion of the total energy budget. The proportional cost of shell production was greatest in polar congeneric bivalves and confamilial gastropods even though the polar gastropods had slow growth rates. The proportional cost of shell production increased with decreasing temperature in the Mollusca.
- The number of shell repairs decreased across latitudes as a function of temperature in buccinid gastropods and brachiopods, but not for bivalves of the genus *Laternula*. Shell defence morphology in the Mollusca decreased with latitude suggesting that predation pressure decreased with latitude. However, the requirement of the shell to protect from abiotic damage may lead to exceptions in the general trends of decreasing shell thickness with increasing latitude.

- Of the two controls on shell morphology tested, the ecological function of the shell in defence (against factors such as predation) proved to be more important than the proportional synthesis cost of the shell. Thus it seems shell ecological function (i.e. protection) exerts a greater control on shell morphology than the cost of shell production.
- Increasing seawater temperatures predicted to result in increased ice scour and the possible invasion of durophagous predators, could cause major problems for the Antarctic near-shore benthic communities whose exoskeletons have evolved in the absence of durophagy, although the chelae of durophagous predators are also likely to be affected by ocean acidification.
- Ocean acidification negatively affects calcareous marine invertebrates and reduced survival, growth and development of early larval stages of the commercially important edible Sydney rock oyster *Saccostrea glomerata*. Despite the small cost of shell production, many calcareous forms are vulnerable to climate change and in particular to ocean acidification. The additional cost of producing a shell in acidified seawater may be too much to tolerate for larvae of *S. glomerata*, which showed a marked reduction in survival of 43 and 72 % under two seawater pH conditions predicted for the year 2100.
- The combination of warming seas and ocean acidification could be particularly problematic for Antarctic shallow-water calcareous benthic invertebrates.

References

- Ahn IY, Shim JH (1998) Summer metabolism of the Antarctic clam, *Laternula elliptica* (King and Broderip) in Maxwell Bay, King George Island and its implications. *Journal of Experimental Marine Biology and Ecology* **224**: 253-264
- Ahn IY, Surh J, Park YG, Kwon H, Choi KS, Kang SH, Choi HJ, Kim KW, Chung H (2003) Growth and seasonal energetics of the Antarctic bivalve *Laternula elliptica* from King George Island, Antarctica. *Marine Ecology Progress Series* **257**: 99-110
- AIMS, Centre CRR, GBRMPA (2009) Sea temperature data from the Australian Institute of Marine Sciences (AIMS) <http://www.aims.gov.au/docs/data-centre/seatemperatures.html>
- Akaike H (1974) A new look at the statistical model identification. *IEEE Transactions on Automatic Control* **19**: 716-723
- Alexander RR, Dietl G (2000) Frequency of shell repairs in common clams from New Jersey. *Journal of Shellfish Research* **19**: 658-659
- Alexander RR, Dietl GP (2001) Shell repair frequencies in New Jersey bivalves: a recent baseline for tests of escalation with Tertiary, mid-Atlantic congeners. *Palaios* **16**(4), August 2001:354-371.
- Alexander RR, Dietl GP (2003) The fossil record of shell-breaking predation on marine bivalves and gastropods. *Topics in Geobiology* **20**: 141-176
- Alexander RR, Dietl GP (2005) Non-predatory shell damage in Neogene Western Atlantic deep-burrowing bivalves. *Palaios* **20**: 280-295
- Ansell AD, Rhodes MC (1997) Unusual capabilities for surface movement in a normally deep-burrowed Antarctic bivalve. *Journal of Molluscan Studies* **63**: 109-111
- Appleton RD, Palmer AR (1988) Water-borne stimuli released by predatory crabs and damaged prey induce more predator-resistant shells in a marine gastropod. *Proceedings of the National Academy of Sciences, USA* **85**: 4387-4391
- Arana PM, Retamal MA (1999) Nueva distribución de *Paralomis birsteini* Macpherson 1988 en aguas antárticas (Anomura, Lithodidae, Lithodinae). *Investigaciones Marinas (Valparaíso)* **27**: 101-110
- Arnaud PM (1974) Contribution a la bionomie marine benthique des régions antarctiques et subantarctiques. *Tethys* **6**: 465-656
- Arntz WE, Brey T, Gallardo VA (1994) Antarctic zoobenthos. *Oceanography and Marine Biology: An Annual Review* **32**: 241-304
- Aronson RB, Blake DB (2001) Global climate change and the origin of modern benthic communities in Antarctica. *American Zoologist* **41**: 27-39
- Aronson RB, Thatje S, Clarke A, Peck LS, Blake DB, Wilga CD, Seibel BA (2007) Climate change and invasibility of the Antarctic benthos. *Annual Review of Ecology Evolution and Systematics* **38**: 129-154
- Auerbach DI, Caulfield JA, Adams EE, Herzog HJ (1997) Impacts of ocean CO₂ disposal on marine life: I. A toxicological assessment integrating constant-concentration laboratory assay data with variable-concentration field exposure. *Environmental Modeling and Assessment* **2**: 333-343
- Barnes DKA, Conlan KE (2007) Disturbance, colonization and development of Antarctic benthic communities. *Royal Society Philosophical Transactions Biological Sciences* **362**(1477), January 29 2007: 11-38.

- Barnes RSK, Calow P, Olive PJW, Golding DW, Spicer JJ (1993) The invertebrates: a synthesis. 2nd edition. Blackwell Science, U.K. 576 pp.
- Berner RA (1975) The role of magnesium in the crystal growth of calcite and aragonite from sea water. *Geochimica et Cosmochimica Acta* **39**: 489-504
- Bertness MD, Cunningham C (1981) Crab shell-crushing predation and gastropod architectural defense. *J. Exp. Mar. Biol. Ecol.* **50**: 213-230
- Bertness MD, Garrity SD, Levings SC (1981) Predation Pressure and Gastropod Foraging: A Tropical-Temperate Comparison. *Evolution* **35**: 995-1007
- Bibby R, Cleall-Harding P, Rundle S, Widdicombe S, Spicer J (2007) Ocean acidification disrupts induced defences in the intertidal gastropod *Littorina littorea*. *Biology Letters* **3**: 699-701
- Bischoff WD, Mackenzie FT, Bishop FC (1987) Stabilities of synthetic magnesian calcites in aqueous solution: comparison with biogenic materials. *Geochimica et Cosmochimica Acta* **51**: 1413-1423
- Blackford JC, Gilbert FJ (2007) pH variability and CO₂ induced acidification in the North Sea. *Journal of Marine Systems* **64**: 229-241
- Boulding EG, Holst M, Pilon V (1999) Changes in selection on gastropod shell size and thickness with wave-exposure on Northeastern Pacific shores. *Journal of Experimental Marine Biology and Ecology* **232**: 217-239
- Brečević L, Nielsen AE (1989) Solubility of amorphous calcium carbonate. *Journal of Crystal Growth* **98**: 504-510
- Brey T (1999) Growth performance and mortality in aquatic macrobenthic invertebrates. *Advances in Marine Biology* **35**: 153-223
- Brey T, Mackensen A (1997) Stable isotopes prove shell growth bands in the Antarctic bivalve *Laternula elliptica* to be formed annually. *Polar Biology* **17**: 465-468
- Brey T, Pearse J, Basch L, McClintock J, Slattery M (1995) Growth and production of *Sterechinus neumayeri* (Echinoidea: Echinodermata) in McMurdo Sound, Antarctica. *Marine Biology* **124**: 279-292
- Brey T, Rumohr H, Ankar S (1988) Energy content of macrobenthic invertebrates: general conversion factors from weight to energy. *Journal of Experimental Marine Biology and Ecology* **117**: 271-278
- Brockington S (2001) The seasonal energetics of the Antarctic bivalve *Laternula elliptica* (King and Broderip) at Rothera Point, Adelaide Island. *Polar Biology* **24**: 523-530
- Brockington S, Peck LS (2001) Seasonality of respiration and ammonium excretion in the Antarctic echinoid *Sterechinus neumayeri*. *Marine Ecology Progress Series* **219**: 159-168
- Bromley RG (1981) Concepts in ichnotaxonomy illustrated by small round holes in shells. *Acta Geol. Hisp.* **16**: 55-64
- Brown KM, Fraser KPP, Barnes DKA, Peck LS (2004) Links between the structure of an Antarctic shallow-water community and ice-scour frequency. *Oecologia* **141**: 121-129
- Brusca RC, Brusca GJ (2003) Invertebrates. Sinauer Associates, 2nd ed. 936 pp.
- Cadée GC (1999) Shell damage and shell repair in the Antarctic limpet *Nacella concinna* from King George Island. *Journal of Sea Research* **41**: 149-161
- Cadée GC, Walker SE, Flessa KW (1997) Gastropod shell repair in the intertidal of Bahía la Choya (N. Gulf of California). *Palaeogeography Palaeoclimatology Palaeoecology* **136**: 67-78
- Caldeira K, Wickett ME (2003) Anthropogenic carbon and ocean pH. *Nature* **425**: 365

- Caldeira K, Wickett ME (2005) Ocean model predictions of chemistry changes from carbon dioxide emissions to the atmosphere and ocean. *Journal of Geophysical Research* **110**: 12 pp
- Cao L, Caldeira K, Jain AK (2007) Effects of carbon dioxide and climate change on ocean acidification and carbonate mineral saturation. *Geophysical Research Letters* **34**: 5 pp.
- Carre M, Bentaleb I, Bruguier O, Ordinola E, Barrett NT, Fontugne M (2006) Calcification rate influence on trace element concentrations in aragonitic bivalve shells: evidences and mechanisms. *Geochimica et Cosmochimica Acta* **70**: 4906-4920
- Carter JG (1980a) Appendix 2 Part B: Guide to bivalve shell microstructures. In Rhoads, D. C. and Lutz, R. A. *Skeletal growth of aquatic organisms: biological records of environmental change*, pp. 645-673. Plenum Press, New York.
- Carter JG (1980b) Environmental and biological controls of bivalve shell mineralogy and microstructure. In Rhoads, D. C. and Lutz, R. A. *Skeletal growth of aquatic organisms: biological records of environmental change*, pp. 69-113. Plenum Press, New York.
- Castro P, Huber ME (2005) *Marine biology*. 6th edition. WCB/McGraw-Hill, U.S.A. 460 pp.
- Chapelle G, Peck LS (1995) The influence of acclimation and substratum on the metabolism of the Antarctic amphipods *Waldeckia obesa* (Chevreux 1905) and *Bovallia gigantea* (Pfeffer 1888). *Polar Biology* **15**: 225
- Chave KE (1954) Aspects of the biogeochemistry of magnesium. 1. Calcareous marine organisms. *J. Geol.* **62**: 266-283
- Chen M-H, Soong K (2002) Estimation of age in the sex-changing, coral-inhabiting snail *Coralliophila violacea* from the growth striae on opercula and a mark-recapture experiment. *Marine Biology* **140**: 337-342
- Clarke A (1980) A reappraisal of the concept of metabolic cold adaptation in polar marine invertebrates. *Biological Journal of Linnean Society* **14**: 77-92
- Clarke A (1983) Life in cold water: the physiological ecology of polar marine ectotherms. *Oceanography and Marine Biology: Annual Reviews* **21**: 341-453
- Clarke A (1990) Temperature and Evolution: Southern Ocean Cooling and the Antarctic Marine Fauna, p 9-22. In Kerry, K. R. & Hempel G. (eds) *Antarctic Ecosystems: Ecological Change and Conservation*. Springer-Verlag Berlin Heidelberg.
- Clarke A (1991) What is cold adaptation and how should we measure it? *American Zoologist* **31**: 81-92
- Clarke A (1993) Temperature and extinction in the sea: A physiologist's view. *Paleobiology* **19**: 499-518
- Clarke A, Aronson RB, Alistair Crame J, Gili JM, Blake DB (2004) Evolution and diversity of the benthic fauna of the Southern Ocean continental shelf. *Antarctic Science* **16**: 559-568
- Clarke A, Johnston NM (1999) Scaling of metabolic rate with body mass and temperature in teleost fish. *Journal of Animal Ecology* **68**: 893-905
- Clarke A, Lakhani KH (1979) Measures of biomass, moulting behaviour and the pattern of early growth in *Chorismus antarcticus* (Pfeffer). *British Antarctic Survey Bulletin* **47**: 61-88
- Clarke FW, Wheeler WC (1922) The inorganic constituents of marine invertebrates. U.S. Geol. Surv. Prof. Pap. **124**: 1-62

- Collins MJ (1991) Growth rate and substrate-related mortality of a benthic brachiopod population. *Lethaia* **24**: 1-11
- Conlan KE, Lenihan HS, Kvitek RG, Oliver JS (1998) Ice scour disturbance to benthic communities in the Canadian High Arctic. *Marine Ecology Progress Series* **166**: 1-16
- Cottier F, Tverberg V, Inall M, Svendsen H, Nilsen F, Griffiths C (2005) Water mass modification in an Arctic fjord through cross-shelf exchange: The seasonal hydrography of Kongsfjorden, Svalbard. *Journal of Geophysical Research* **110**: C12005, doi:10.1029/12004JC002757
- Cox LR (1960) Gastropoda - General Characteristics of Gastropoda. In Moore R. C. (eds). *Treatise on Invertebrate Paleontology, Part I, Brookes Knight, J. et al. (eds) Part 1 Mollusca 1. Geological Society of America and University of Kansas*, pp. 184-1169.
- Cox LR, Nuttall CP, Trueman ER (1969) General features of bivalvia. In Moore R. C. (eds). *Treatise on Invertebrate Paleontology, Part N, Cox L. R. et al. (eds) Volume 1 (of 3) Mollusca 6: Bivalvia. Geological Society of America and University of Kansas*, pp. N2-N129.
- Crenshaw MA (1980) Mechanisms of shell formation and dissolution. In Rhoads, D. C. & Lutz, R. A. *Skeletal growth of aquatic organisms; biological records of environmental change*. Plenum Press, New York. Pp. 115-132
- Crisp DJ (1984) Energy flow measurements. In *Methods for the Study of Marine Benthos*. International Biological Programme Handbook No. 16, 2nd Edition. (eds. Holme, N.A & McIntyre, A.D.) pp. 285-367. Blackwell Scientific Publications, Oxford.
- Crisp M, Davenport J, Shumway SE (1978) Effects of feeding and of chemical stimulation on the oxygen uptake of *Nassarius reticulatus* (Gastropoda: Prosobranchia). *Journal of the Marine Biological Association, UK* **58**: 387-399
- Curry GB, Ansell AD (1986) Tissue mass in living brachiopods. In *Les Brachiopodes Fossiles et actuels. Proc. 1st Int. Cong. on Brachiopods* (ed. P. R. Racheboeuf & C. C. Emig). *Biostratigraphie du Paleozoique*. **4**: 231-241
- Dahm C, Brey T (1998) Determination of growth and age of slow growing brittle stars (Echinodermata: Ophiuroidea) from natural growth bands. *Journal of the Marine Biological Association of the United Kingdom* **78**: 941-951
- Dalziel B, Boulding EG (2005) Water-borne cues from a shell-crushing predator induce a more massive shell in experimental populations of an intertidal snail. *Journal of Experimental Marine Biology and Ecology* **317**: 25-35
- Dauphin Y, Marin F, Gautret P, Cuif JP (1990) The substitution index of minor elements in the carbonate lattice: a criteria for discrimination of aragonitic fibrous biomineralizations in sponges, cnidaria and molluscs. [Discrimination des biomineralisations aragonitiques fibreuses des Spongiaires, Cnidaires et Mollusques, par l'indice de substitution des elements mineurs dans le reseau carbonate]. *Comptes Rendus - Academie des Sciences, Serie II* **311**: 1111-1116
- Day EG, Branch GM, Viljoen C (2000) How costly is molluscan shell erosion? A comparison of two patellid limpets with contrasting shell structures. *Journal of Experimental Marine Biology and Ecology* **243**: 185-208
- Dayton PK, Robilliard GA, Paine RT, Dayton LB (1974) Biological accommodation in the benthic community at McMurdo Sound, Antarctica. *Ecol. Monogr.* **44**: 105-128
- del Rio CM (2008) Metabolic theory or metabolic models? *Trends in Ecology & Evolution* **23**: 256-260
- Dell RK (1972) Antarctic benthos. *Advances in Marine Biology* **10**: 1-216

- Dell RK (1990) Antarctic Mollusca with special reference to the fauna of Ross Sea. *Bulletin of Royal Society of New Zealand* **27**: 1-311
- Dietl GP, Alexander RR, Bien WF (2000) Escalation in Late Cretaceous-Early Paleocene Oysters (Gryphaeidae) from the Atlantic Coastal Plain. *Paleobiology* **26**: 215-237
- Dodd JR (1965) Environmental control of strontium and magnesium in *Mytilus*. *Geochimica et Cosmochimica Acta* **29**: 385-398
- Dodd JR (1966) Diagenetic stability of temperature-sensitive skeletal properties in *Mytilus* from the Pleistocene of California. *Geol. Soc. Am. Bull.* **77**: 1213-1224
- Dodd JR (1967) Magnesium and strontium in calcareous skeletons: a review. *Journal of Paleontology* **41**: 1313-1329
- Doherty PJ (1979) A demographic study of a subtidal population of the New Zealand articulate brachiopod *Terebratella inconspicua*. *Marine Biology* **52**: 331-342
- Doney SC, Schimel DS (2007) Carbon and climate system coupling on timescales from the Precambrian to the Anthropocene. *Annual Review of Environment and Resources* **32**: 31-66
- Dove MC, O'Connor WA (2007) Salinity and temperature tolerance of Sydney rock oysters *Saccostrea glomerata* during early ontogeny. *Journal of Shellfish Research* **26**: 939-947
- Dove MC, Sammut J (2007) Histological and feeding response of Sydney rock oysters, *Saccostrea glomerata*, to acid sulfate soil outflows. *Journal of Shellfish Research* **26**: 509-518
- Dupont S, Havenhand J, Thorndyke W, Peck L, Thorndyke M (2008) Near-future level of CO₂-driven ocean acidification radically affects larval survival and development in the brittlestar *Ophiothrix fragilis*. *Marine Ecology Progress Series* **373**: 285-294
- Elliott JM, Davison W (1975) Energy equivalents of oxygen consumption in animal energetics. *Oecologia* **19**: 195-201
- Everson I (1977) Antarctic marine secondary production and the phenomenon of cold adaptation. *Philosophical Transactions - Royal Society of London, B* **279**: 55-66
- Feldmann RM (1998) *Paralomis debodeorum*, a new species of decapod crustacean from the Miocene of New Zealand: first notice of the Lithodidae in the fossil record. *New Zealand Journal of Geology and Geophysics* **41**: 35-38
- Field A (2009) *Discovering statistics using SPSS*. 3rd ed. Sage Publications, UK. 822 pp.
- Frederich M, Sartoris FJ, Arntz WE, Pörtner HO (2000) Haemolymph Mg²⁺ regulation in decapod crustaceans: physiological correlates and ecological consequences in polar areas. *The Journal of Experimental Biology* **203**: 1383-1393
- Frederich M, Sartoris FJ, Portner HO (2001) Distribution patterns of decapod crustaceans in polar areas: a result of magnesium regulation? *Polar Biology* **24**: 719-723
- Freitas P, Clarke LJ, Kennedy H, Richardson C, Abrantes F (2005) Mg/Ca, Sr/Ca, and stable-isotope ($\delta^{18}\text{O}$ and $\delta^{13}\text{C}$) ratio profiles from the fan mussel *Pinna nobilis*; seasonal records and temperature relationships. *Geochemistry Geophysics Geosystems* **6**: Q04D14, doi:10.1029/2004GC000872
- Freitas P, Clarke LJ, Kennedy H, Richardson C, Abrantes F (2006) Environmental and biological controls on elemental (Mg/Ca, Sr/Ca and Mn/Ca) ratios in shells of the king scallop *Pecten maximus*. *Geochimica et Cosmochimica Acta* **70**: 5119-5133
- Freitas PS, Clarke LJ, Kennedy H, Richardson CA (2009) Ion microprobe assessment of the heterogeneity of Mg/Ca, Sr/Ca and Mn/Ca ratios in *Pecten maximus* and *Mytilus edulis* (Bivalvia) shell calcite precipitated at constant temperature. *Biogeosciences Discuss* **6**: 1267-1316

- Füchtbauer H, Hardie LA (1976) Experimentally determined homogeneous distribution coefficients for precipitated magnesium calcites. *Geol. Soc. Am. Abstr.* **8**: 877
- Gabriel JM (1981) Differing Resistance of Various Mollusc Shell Materials to Simulated Whelk Attack. *Journal of Zoology* **194**: 363-369
- Gage JD (1992) Natural growth bands and growth variability in the sea urchin *Echinus esculentus*: results from tetracycline tagging. *Marine Biology* **114**: 607-616
- Gage JD, Tyler PA (1985) Growth and recruitment of the deep-sea urchin *Echinus affinis*. *Marine Biology* **90**: 41-53
- Garamszegi LZ (2006) Comparing effect sizes across variables: generalization without the need for Bonferroni correction. *Behavioural Ecology* **17**: 682-687
- Garcia LV (2004) Escaping the Bonferroni iron claw in ecological studies. *Oikos* **105**: 657-663
- Gazeau F, Quiblier C, Jansen JM, Gattuso J-P, Middelburg JJ, Heip CHR (2007) Impact of elevated CO₂ on shellfish calcification. *Geophysical Research Letters* **34**: [np]
- Gibbs MT, Bowman MJ, Dietrich DE (2000) Maintenance of near-surface stratification in Doubtful Sound, a New Zealand fjord. *Estuarine, Coastal and Shelf Science* **51**: 683-704
- Gillooly JF, Brown JH, West GB, Savage VM, Charnov EL (2001) Effects of size and temperature on metabolic rate. *Science* **293**: 2248-2251
- Goldberg ED (1957) The biogeochemistry of trace metals, in: *Treatise on Marine Ecology and Paleoecology* (J. W. Hedgpeth, ed.). *Geol. Soc. Amer. Mem.* **67**: 345-358
- Goldstein JI, Newbury DE, Echlin P, Joy DC, Lyman CE, Lifshin E, Sawyer L, Michael JR (2003) Scanning electron microscopy and x-ray microanalysis. 3rd edition. Kluwer Academic/Plenum Publishers, New York, 689 pp.
- Gosling E (2003) Bivalve Molluscs; Biology, Ecology and Culture. Blackwell Science, Oxford. 456 pp.
- Graus RR (1974) Latitudinal trends in the shell characteristics of marine gastropods. *Lethaia* **7**: 303-314
- Guidetti P, Mori M (2005) Morpho-functional defences of Mediterranean sea urchins, *Paracentrotus lividus* and *Arbacia lixula*, against fish predators. *Marine Biology* **147**: 797-802
- Gunatilaka A (1975) The chemical composition of some carbonate secreting marine organisms from Connemara. *Proc. R. Ir. Acad. Sect. B* **75**: 543-556
- Gutt J, Starmans A, Dieckmann G (1996) Impact of iceberg scouring on polar benthic habitats. *Marine Ecology Progress Series* **137**: 311-316
- Hall-Spencer JM, Rodolfo-Metalpa R, Martin S, Ransome E, Fine M, Turner SM, Rowley SJ, Tedesco D, Buia MC (2008) Volcanic carbon dioxide vents show ecosystem effects of ocean acidification. *Nature* **454**: 96-99
- Harper EM (2000) Are calcitic layers an effective adaptation against shell dissolution in the Bivalvia? *Journal of Zoology* **251**: 179-186
- Harper EM, Checa AG, Rodríguez-Navarro AB (2009) Organization and mode of secretion of the granular prismatic microstructure of *Entodesma navicula* (Bivalvia: Mollusca). *Acta Zoologica* **90**: 132-141
- Harper EM, Peck L (2003) Predatory behaviour and metabolic costs in the Antarctic muricid gastropod *Trophon longstaffi*. *Polar Biology* **26**: 208-217
- Harper EM, Peck LS, Hendry KR (submitted) Patterns of shell repair indicates size forms a refuge from predation in articulate brachiopods. *Marine Biology*

- Harriss RC (1965) Trace element distribution in molluscan skeletal material. I. Magnesium, iron, manganese, and strontium. *Bulletin of Marine Science* **15**: 265-273
- Haugan PM, Drange H (1996) Effects of CO₂ on the ocean environment. *Energy Conversion and Management* **37**: 1019-1022
- Havenhand JN, Buttler FR, Thorndyke MC, Williamson JE (2008) Near-future levels of ocean acidification reduce fertilization success in a sea urchin. *Current Biology* **18**: R651
- Hawkins BA, Albuquerque FS, Araújo MB, Beck J, Bini LM, Cabrero-Sañudo FJ, I. Castro-Parga, Diniz-Filho JAF, Ferrer-Castán D, Field R, Gómez JF, Hortal J, Kerr JT, Kitching IJ, León-Cortés JL, Lobo JM, Montoya D, Moreno JC, Olalla-Tárraga MÁ, Pausas JG, Qian H, Rahbek C, Rodríguez MÁ, Sanders NJ, Williams P (2007) A global evaluation of metabolic theory as an explanation for terrestrial species richness gradients. *Ecology* **88**: 1877–1888
- Heasman MP, Goard L, Diemar J, Callinan RB (2000) Improved Early Survival of Molluscs: Sydney Rock Oyster (*Saccostrea glomerata*). Aquaculture CRC Project A.2.1, NSW Fisheries Final Report Series No. 29, Nelson Bay, Australia
- Hoegh-Guldberg O, Mumby PJ, Hooten AJ, Steneck RS, Greenfield P, Gomez E, Harvell CD, Sale PF, Edwards AJ, Caldeira K, Knowlton N, Eakin CM, Iglesias-Prieto R, Muthiga N, Bradbury RH, Dubi A, Hatziaelos ME (2007) Coral reefs under rapid climate change and ocean acidification. *Science* **318**: 1737-1742
- Hoff GR, Fuiman LA (1995) Environmentally induced variation in elemental composition of red drum (*Sciaenops ocellatus*) otoliths. *Bulletin of Marine Science* **56**: 578-591
- Ilano AS, Ito A, Fujinaga K, Nakao S (2004) Age determination of *Buccinum isaotakii* (Gastropoda: Buccinidae) from the growth striae on operculum and growth under laboratory conditions. *Aquaculture* **242**: 181-195
- Ireland MP (1991) The effect of dietary calcium on growth, shell thickness and tissue calcium distribution in the snail *Achatina fulica*. *Comparative Biochemistry and Physiology, A* **98A**: 111-116
- Irie T (2006) Geographical variation of shell morphology in *Cypraea annulus* (Gastropoda: Cypraeidae). *Journal of Molluscan Studies* **72**: 31-38
- Irie T, Iwasa Y (2003) Optimal growth model for the latitudinal cline of shell morphology in cowries (genus *Cypraea*). *Evolutionary Ecology Research* **5**: 1133-1149
- Irie T, Iwasa Y (2005) Optimal growth pattern of defensive organs: the diversity of shell growth among mollusks. *The American Naturalist* **165**: 238-249
- James MA, Ansell AD, Collins MJ, Curry GB, Peck LS, Rhodes MC (1992) Biology of living brachiopods. *Advances in Marine Biology* **28**: 175-388
- John GT, Klimant I, Wittmann C, Heinzle E (2003) Integrated optical sensing of dissolved oxygen in microtiter plates: A novel tool for microbial cultivation. *Biotechnology and Bioengineering* **81**: 829-836
- Jones DS, Arnold B, Quitmyer I, Schöne BR, Surge D (2007) 1st International Sclerochronology Conference. <http://conference.ifas.ufl.edu/sclerochronology>.
- Jubb MR, Wilkin TA, Gosler AG (2006) Eggshell-pigmentation, soil calcium and the local abundance, distribution and diversity of woodland snails (Mollusca). *Ardea* **94**: 59-70
- Kabat AR (1990) Predatory ecology of naticid gastropods with a review of shell boring. *Malacologia* **32**: 155-193
- Kideys AE (1998) Physiological energetics of *Buccinum undatum* L. (Gastropoda) off Douglas, Isle of Man (the Irish Sea). *Turkish Journal of Zoology* **22**: 49-61

- Kikkawa T, Kita J, Ishimatsu A (2004) Comparison of the lethal effect of CO₂ and acidification on red sea bream (*Pagrus major*) during the early developmental stages. *Marine Pollution Bulletin* **48**: 108-110
- Kinsman DJJ (1969) Interpretation of Sr²⁺ concentrations in carbonate minerals and rocks. *J. Sed. Petrol.* **39**: 486-508
- Kinsman DJJ, Holland HD (1969) The co-precipitation of cations with CaCO₃ - IV. The coprecipitation of Sr²⁺ with aragonite between 16° and 96°C. *Geochimica et Cosmochimica Acta* **33**: 1017
- Kitching JA, Muntz L, Ebling FJ (1966) The ecology of Lough Ine. XV. The ecological significance of shell and body forms in *Nucella*. *J. Anim. Ecol.* **35**: 113-126
- Klages M, Gutt J, Starmans A, Bruns T (1995) Stone crabs close to the Antarctic continent: *Lithodes murrayi* Henderson, 1888 (Crustacea; Decapoda; Anomura) off Peter I Island (68°51'S, 90°51'W). *Polar Biology* **15**: 73-75
- Klein RT, Lohmann KC, Thayer CW (1996a) Bivalve skeletons record sea-surface temperature and delta ¹⁸O via Mg/Ca and ¹⁸O/¹⁶O ratios. *Geology* **24**: 415-418
- Klein RT, Lohmann KC, Thayer CW (1996b) Sr/Ca and ¹³C/¹²C ratios in skeletal calcite of *Mytilus trossulus*: Covariation with metabolic rate, salinity, and carbon isotopic composition of seawater. *Geochimica et Cosmochimica Acta* **60**: 4207-4221
- Kleypas JA, Feely RA, Fabry C, Langdon C, Sabine C, Robbins LL (2006) Impacts of ocean acidification on coral reefs and other marine calcifiers: a guide for future research. A report of a workshop held 18-20 April 2005, St. Petersburg, FL, sponsored by NSF, NOAA, and the U.S. Geological Survey, 88 pp.
- Krogh A (1916) *Respiratory Exchange of Animals and Man*. Longmans, Green, London.
- Kurihara H, Kato S, Ishimatsu A (2007) Effects of increased seawater pCO₂ on early development of the oyster *Crassostrea gigas*. *Aquatic Biology* **1**: 91-98
- Kurihara H, Shimode S, Shirayama Y (2004) Effects of raised CO₂ concentration on the egg production rate and early development of two marine copepods (*Acartia steueri* and *Acartia erythraea*). *Marine Pollution Bulletin* **49**: 721-727
- Kurihara H, Shirayama Y (2004) Effects of increased atmospheric CO₂ on sea urchin early development. *Marine Ecology Progress Series* **274**: 161-169
- Lamare MD, Channon T, Cornelisen C, Clarke M (2009) Archival electronic tagging of a predatory sea star - Testing a new technique to study movement at the individual level. *Journal of Experimental Marine Biology and Ecology* **373**: 1-10
- Langdon C (1997) Effect of calcium carbonate saturation state on the rate of calcification of an experimental coral reef. *American Zoologist* **37**: 72A
- Langdon C, Broecker WS, Hammond DE, Glenn E, Fitzsimmons K, Nelson SG, Peng TH, Hajdas I, Bonani G (2003) Effect of elevated CO₂ on the community metabolism of an experimental coral reef. *Global Biogeochemical Cycles* **17**: 1011, doi:10.1029/2002GB001941
- Lea DW, Mashiotto TA, Spero HJ (1999) Controls on magnesium and strontium uptake in planktonic foraminifera determined by live culturing. *Geochimica et Cosmochimica Acta* **63**: 2369-2379
- Lewis E, Wallace DWR (1998) Program Developed for CO₂ System Calculations. ORNL/CDIAC-105. Carbon Dioxide Information Analysis Center, Oak Ridge National Laboratory, U.S. Department of Energy, Oak Ridge, Tennessee.
- Libes SM (1992) *An Introduction to Marine Biogeochemistry*. John Wiley and Sons, Inc. U.S.A 734 pp.

- Lien R, Solheim A, Elverhoi A, Rokoengen K (1989) Iceberg scouring and sea bed morphology on the eastern Weddell Sea shelf, Antarctica. *Polar Research* **7**: 43-57
- Lorens RB, Bender ML (1980) The impact of solution chemistry on *Mytilus edulis* calcite and aragonite. *Geochimica et Cosmochimica Acta* **44**: 1265-1278
- Lorrain A, Gillikin DP, Paulet Y-M, Chauvaud L, Le Mercier A, Navez J, Andre L (2005) Strong kinetic effects on Sr/Ca ratios in the calcitic bivalve *Pecten maximus*. *Geology* **33**: 965-968
- Lowenstam HA (1963) Biologic problems relating to the composition and diagenesis of sediments, in: *The Earth Sciences* (T. W. Donnelly, ed.), pp. 137-195, Rice University, Houston
- Lowenstam HA (1964a) Coexisting calcites and aragonites from skeletal carbonates of marine organisms and their strontium and magnesium contents. In *Recent Researches in the Fields of Hydrosphere, Atmosphere and Nuclear Geochemistry* (eds. Y. Miyake and T. Koyama), pp. 373-404. Maruzen Co. Ltd., Tokyo.
- Lowenstam HA (1964b) Strontium-calcium ratio of skeletal aragonites from the recent marine biota at Palau and from fossil gastropods, in: *Isotopic and Cosmic Chemistry* (H. Craig, S. L. Miller, and G. J. Wasserburg, eds.), pp. 114-132, North Holland, Amsterdam.
- Lowenstam HA, Weiner S (1989) On Biomineralization. OUP, New York, U.S.A. 324 pp.
- Lutz RA, Rhoads DC (1980) Growth patterns within the molluscan shell. In Rhoads, D. C. and Lutz, R. A. *Skeletal growth of aquatic organisms: biological records of environmental change*, pp. 203- 254. Plenum Press, New York.
- MacArthur RH (1972) *Geographical ecology: patterns in the distribution of species*. New York: Harper and Row. 269 pp.
- Mann S (2001) *Biomineralization: principles and concepts in bioinorganic materials chemistry*. Oxford Chemistry Masters, 5. OUP, UK. 198 pp.
- Martin GB, Thorrold SR (2005) Temperature and salinity effects on magnesium, manganese, and barium incorporation in otoliths of larval and early juvenile spot *Leiostomus xanthurus*. *Marine Ecology Progress Series* **293**: 223-232
- Mayor DJ, Matthews C, Cook K, Zuur AF, Hay S (2007) CO₂-induced acidification affects hatching success in *Calanus finmarchicus*. *Marine Ecology Progress Series* **350**: 91-97
- McClintock JB, Baker BJ (1997) A review of the chemical ecology of Antarctic marine invertebrates. *American Zoologist* **37**: 329-342
- McClintock JB, Slattery M, Thayer CW (1993) Energy content and chemical defense of the articulate brachiopod *Liothyrella uva* (Jackson, 1912) from the Antarctic Peninsula. *Journal of Experimental Marine Biology and Ecology* **169**: 103-116
- Meredith MP, King JC (2005) Rapid climate change in the ocean west of the Antarctic Peninsula during the second half of the 20th century. *Geophysical Research Letters* **32**: L19604, doi:10.1029/2005GL024042
- Miles H, Widdicombe S, Spicer JJ, Hall-Spencer J (2007) Effects of anthropogenic seawater acidification on acid-base balance in the sea urchin *Psammechinus miliaris*. *Marine Pollution Bulletin* **54**: 89-96
- Miller WI (1983) Biogenic shell damage in the small gastropod *Odostomia impressa* (Say). *Tulane Studies in Geology and Paleontology* **17**: 105-116
- Morley SA, Peck LS, Miller AJ, Pörtner HO (2007a) Hypoxia tolerance associated with activity reduction is a key adaptation for *Laternula elliptica* seasonal energetics. *Oecologia* **153**: 29-36

- Morley SA, Peck LS, Tan KS, Martin SM, Pörtner HO (2007b) Slowest of the slow: latitudinal insensitivity of burrowing capacity in the bivalve *Laternula*. *Marine Biology* **151**: 1823-1830
- Nakagawa S (2004) A farewell to Bonferroni: the problems of low statistical power and publication bias. *Behavioural Ecology* **15**: 1044-1045
- Nell JA, O'Connor WA (1991) The evaluation of fresh algae and stored algal concentrates as a food source for Sydney rock oyster *Saccostrea commercialis* (Iredale & Roghley) larvae. *Aquaculture* **99**: 277-284
- Nicol D (1955) An analysis of the Arctic marine pelecypod fauna. *Nautilus* **68**: 115-122
- Nicol D (1964a) An essay on size of marine pelecypods. *Journal of Paleontology* **38**: 968-974
- Nicol D (1964b) Lack of shell-attached pelecypods in Arctic and Antarctic waters. *Nautilus* **77**: 92-93
- Nicol D (1965) Ecological implications of living pelecypods with calcareous spines. *Nautilus* **78**: 109-116
- Nicol D (1966) Size of pelecypods in Recent marine faunae. *Nautilus* **79**: 109-113
- Nicol D (1967) Some characteristics of cold-water marine pelecypods. *Journal of Paleontology* **41**: 1330-1340
- Nicol D (1970) Antarctic pelecypod faunal peculiarities. *Science* **168**: 1248-1249
- Nolan CP, Clarke A (1993) Growth in the bivalve *Yoldia eightsi* at Signy Island, Antarctica, determined from internal shell increments and calcium-45 incorporation. *Marine Biology* **117**: 243-250
- Nonato EF, Brito TAS, Paiva PC, Petti MAV, Corbisier T (2000) Benthic megafauna of the nearshore zone of Martel Inlet (King George Island, South Shetland Islands, Antarctica): depth zonation and underwater observations. *Polar Biology* **23**: 580-588
- Nürnberg D, Bijma J, Hemleben C (1996) Assessing the reliability of magnesium in foraminiferal calcite as a proxy for water mass temperatures. *Geochimica et Cosmochimica Acta* **60**: 803-814
- O'Sullivan D, Savage J, Fay A (2008) Status of Australian Aquaculture in 2005/2006. *Austasia Aquaculture Trade Directory 2008*, Turtle Press, Hobart, Tasmania, pp. 6-24.
- Orr JC, Fabry VJ, Aumont O, Bopp L, Doney SC, Feely RA, Gnanadesikan A, Gruber N, Ishida A, Joos F, Key RM, Lindsay K, Maier-Reimer E, Matear R, Monfray P, Mouchet A, Najjar RG, Plattner GK, Rodgers KB, Sabine CL, Sarmiento JL, Schlitzer R, Slater RD, Totterdell IJ, Weirig MF, Yamanaka Y, Yool A (2005) Anthropogenic ocean acidification over the twenty-first century and its impact on calcifying organisms. *Nature* **437**: 681-686
- Otero-Villanueva MM, Kelly MS, Burnell G (2004) How diet influences energy partitioning in the regular echinoid *Psammechinus miliaris*; constructing an energy budget. *Journal of Experimental Marine Biology and Ecology* **304**: 159-181
- Ozgo M, Bogucki Z (2006) Shell predation and cannibalism in land snails living on acid and calcium-deficient soils. *Folia Malacologica* **14**: 217-220
- Padin XA, Vázquez-Rodríguez M, Ríos AF, Pérez FF (2007) Surface CO₂ measurements in the English Channel and Southern Bight of North Sea using voluntary observing ships. *Journal of Marine Systems* **66**: 297-308
- Paine RT (1966) Food web complexity and species diversity. *The American Naturalist* **100**: 65-75

- Paine RT (1995) A Conversation on Refining the Concept of Keystone Species. *Conservation Biology* **9**: 962-964
- Palmer AR (1979) Fish Predation and the Evolution of Gastropod Shell Sculpture - Experimental and Geographic Evidence. *Evolution* **33**: 697-713
- Palmer AR (1981) Do carbonate skeletons limit the rate of body growth? *Nature* **292**: 150-152
- Palmer AR (1985) Adaptive value of shell variation in *Thais lamellosa*: effect of thick shells on vulnerability to and preference by crabs. *Veliger* **27**: 349-356
- Palmer AR (1992) Calcification in marine molluscs: How costly is it? *Proceedings of the National Academy of Sciences, USA* **89**: 1379-1382
- Pearson PN, Palmer MR (2000) Atmospheric carbon dioxide concentrations over the past 60 million years. *Nature* **406**: 695-699
- Peck LS (1989) Temperature and basal metabolism in two Antarctic marine herbivores. *Journal of Experimental Marine Biology and Ecology* **127**: 1-12
- Peck LS (1992) Body volumes and internal space constraints in articulate brachiopods. *Lethaia* **25**: 383-390
- Peck LS (1993) The tissues of articulate brachiopods and their value to predators. *Philosophical Transactions - Royal Society of London, B* **339**: 17-32
- Peck LS (1996) Metabolism and feeding in the Antarctic brachiopod *Liothyrella uva*: A low energy lifestyle species with restricted metabolic scope. *Proceedings of the Royal Society - Biological Sciences (Series B)* **263**: 223-228
- Peck LS (1998) Feeding, metabolism and metabolic scope in Antarctic marine ectotherms. In Pörtner, H. O. and Playle, R. C. (eds.) *Cold Ocean Physiology*. pp. 365-390. Society of Experimental Biology Seminar Series, no. 66.
- Peck LS (2002) Ecophysiology of Antarctic marine ectotherms: Limits to life. *Polar Biology* **25**: 31-40
- Peck LS (2005) Prospects for survival in the Southern Ocean: Vulnerability of benthic species to temperature change. *Antarctic Science* **17**: 497-507
- Peck LS, Ansell AD, Webb KE, Hepburn L, Burrows M (2004) Movements and burrowing activity in the Antarctic bivalve molluscs *Laternula elliptica* and *Yoldia eightsi*. *Polar Biology* **27**: 357-367
- Peck LS, Brey T (1996) Bomb signals in old Antarctic brachiopods. *Nature* **380**: 207-208
- Peck LS, Brockington S, Brey T (1997a) Growth and metabolism in the Antarctic brachiopod *Liothyrella uva*. *Philosophical Transactions of the Royal Society of London Series B Biological Sciences* **352**: 851-858
- Peck LS, Brockington S, Vanhove S, Beghyn M (1999) Community recovery following catastrophic iceberg impacts in a soft-sediment shallow-water site at Signy Island, Antarctica. *Marine Ecology Progress Series* **186**: 1-8
- Peck LS, Bullough LW (1993) Growth and population structure in the infaunal bivalve *Yoldia eightsi* in relation to iceberg activity at Signy Island, Antarctica. *Marine Biology* **117**: 235-242
- Peck LS, Clarke A, Holmes LJ (1987a) Size, shape and the distribution of organic matter in the Recent Antarctic brachiopod *Liothyrella uva*. *Lethaia* **20**: 33-40
- Peck LS, Clarke A, Holmes LJ (1987b) Summer metabolism and seasonal changes in biochemical composition of the Antarctic brachiopod *Liothyrella uva* (Broderip, 1833). *Journal of Experimental Marine Biology and Ecology* **114**: 85-97

- Peck LS, Convey P, Barnes DKA (2006) Environmental constraints on life histories in Antarctic ecosystems: Tempos, timings and predictability. *Biological Reviews of the Cambridge Philosophical Society* **81**: 75-109
- Peck LS, Conway LZ (2000) The myth of metabolic cold adaptation: oxygen consumption in stenothermal Antarctic bivalves. In: Harper EM, Taylor JD, Crame JA (eds) *The evolutionary biology of the Bivalvia*. *Geol Soc Lond Spec Publ* **177**: 441-450
- Peck LS, Culley MB, Helm MM (1987c) A laboratory energy budget for the ormer *Haliotis tuberculata* L. *Journal of Experimental Marine Biology and Ecology* **106**: 103-123
- Peck LS, Edwards TM (1996) Organic contents and elemental composition of brachiopod shell and mantle tissues. In Cooper, P. & Jin, J., ed. *Brachiopods. Proceedings of the Third International Brachiopod Congress*, Sudbury, Ontario, Canada, September 1995. Rotterdam, Balkema, pp. 203-207.
- Peck LS, Holmes LJ (1989) Seasonal and ontogenetic changes in tissue size in the Antarctic brachiopod *Liothyrella uva* (Broderip, 1833). *Journal of Experimental Marine Biology and Ecology* **134**: 25-36
- Peck LS, Morris DJ, Clarke A (1986a) Oxygen consumption and the role of caeca in the Recent Antarctic brachiopod *Liothyrella uva notorcadensis* (Jackson, 1912). In Racheboeuf, P. R. and Emig, C. C. (eds.) *Les Brachiopodes fossiles et actuels. Biostratigraphie du Paléozoïque*, 4, 500 pp.
- Peck LS, Morris DJ, Clarke A, Holmes LJ (1986b) Oxygen-consumption and nitrogen-excretion in the Antarctic brachiopod *Liothyrella uva* (Jackson, 1912) under simulated winter conditions. *Journal of Experimental Marine Biology and Ecology* **104**: 203-213
- Peck LS, Rhodes MC, Curry GB, Ansell AD (1997b) Physiology and metabolism. In *Treatise on invertebrate palaeontology, H: Brachiopoda* (ed. A. Williams). Lawrence, KS: Geological Society of America and the University of Kansas. pp. 213 - 242.
- Peck LS, Uglow RF (1990) Two methods for the assessment of the oxygen content of small volumes of seawater. *Journal of Experimental Marine Biology and Ecology* **141**: 53-62
- Peck LS, Veal R (2001) Feeding, metabolism and growth in the Antarctic limpet, *Nacella concinna* (Strebel 1908). *Marine Biology* **138**: 553-560
- Perneger TV (1998) What's wrong with Bonferroni adjustments. *British Medical Journal* **316**: 1236-1238
- Pilkey OH, Goodell HG (1963) Trace elements in recent mollusk shells. *Limnology and Oceanography* **8**: 137-148
- Purton LMA, Shields GA, Brasier MD, Grime GW (1999) Metabolism controls Sr/Ca ratios in fossil aragonitic mollusks. *Geology* **27**: 1083-1086
- Putten EV, Dehairs F, Keppens E, Baeyens W (2000) High resolution distribution of trace elements in the calcite shell layer of modern *Mytilus edulis*: environmental and biological controls. *Geochimica et Cosmochimica Acta* **64**: 997-1011
- Raffaelli DG (1978) The relationship between shell injuries, shell thickness and habitat characteristics of the intertidal snail *Littorina rudis* Maton. *Journal of Molluscan Studies* **44**: 166-170
- Ralph R, Maxwell JGH (1977) Growth of two Antarctic Lamellibranchs: *Adamussium colbecki* and *Laternula elliptica*. *Marine Biology* **42**: 171-175
- Randall D, Burggren W, French K (1997) *Animal Physiology*. 4th Edition. W.H. Freeman and Company, New York. 727 pp.

- Régis MB (1986) Adaptive microstructure of the spines of *Paracentrotus lividus* (Echinodermata: Echinoidea) in an area polluted by domestic effluents. *Marine Biology* **90**: 271-277
- Revelle R, Fairbridge R (1957) Carbonates and carbon dioxide. *Memoirs of the Geological Society of America* **67**: 239-296
- Richardson CA, Peharda M, Kennedy H, Kennedy P, Onofri V (2004) Age, growth rate and season of recruitment of *Pinna nobilis* (L) in the Croatian Adriatic determined from Mg:Ca and Sr:Ca shell profiles. *Journal of Experimental Marine Biology and Ecology* **299**: 1-16
- Richardson CA, Saurel C, Barroso CM, Thain J (2005) Evaluation of the age of the red whelk *Neptunea antiqua* using statoliths, opercula and element ratios in the shell. *Journal of Experimental Marine Biology and Ecology* **325**: 55-64
- Richardson MG (1979) The ecology and reproduction of the brooding Antarctic bivalve *Lissarca miliaris*. *British Antarctic Survey Bulletin* **49**: 91-115
- Rodrigues E, Vani GS, Lavrado HP (2007) Nitrogen metabolism of the Antarctic bivalve *Laternula elliptica* (King and Broderip) and its potential use as biomarker. *Oecol. Bras.* **11**: 37-49
- Rosenberg GD (1980) An ontogenetic approach to the environmental significance of bivalve shell chemistry. In Rhoads, D. C. & Lutz, R. A. (eds.) *Skeletal growth of aquatic organisms: biological records of environmental change*. Plenum Press, New York. pp. 133-168.
- Rosenthal Y, Boyle EA, Slowey NC (1997) Temperature control on the incorporation of magnesium, strontium, fluorine, and cadmium into benthic foraminiferal shells from Little Bahama Bank: prospects for thermocline paleoceanography. *Geochimica et Cosmochimica Acta* **61**: 3633-3643
- Rundle SD, Spicer JI, Coleman RA, Vosper J, Soane J (2004) Environmental calcium modifies induced defences in snails. *Proceedings of the Royal Society of London - Biological Sciences* **271**: S67-S70
- Runnegar B (1974) Evolutionary history of the bivalve subclass Anomalodesmata. *Journal of Paleontology* **48**: 904-940
- Santarelli L, Gros P (1985) Age and growth of the whelk *Buccinum undatum* L. (Gastropoda: Prosobranchia) using stable isotopes of the shell and operculum striae. *Oceanologica acta* **8**: 221-229
- Sarmiento JL, Gruber N (2006) *Ocean Biogeochemical Dynamics*. Princeton University Press, USA. 503 pp.
- Sato-Okoshi W, Okoshi K (2002) Application of fluorescent substance to the analysis of growth performance in Antarctic bivalve, *Laternula elliptica*. *Polar Bioscience* **15**: 66-74
- Savage VM, Gillooly JF, Woodruff WH, West GB, Allen AP, Enquist BJ, Brown JH (2004) The predominance of quarter-power scaling in biology. *Functional Ecology* **18**: 257-282
- Schifano G (1982) Temperature-magnesium relations in the shell carbonate of some modern marine gastropods. *Chem. Geol.* **35**: 321-332
- Schmidt-Nielsen K (1990) *Animal physiology: adaptation and environment*. 4th edition. Cambridge University Press, UK. 602 pp.
- Scholander PF, Flagg W, Walters V, Irving L (1953) Climatic adaptation in Arctic and tropical poikilotherms. *Physiological Zoology* **26**: 67-92

- Schone BR (2008) The curse of physiology - challenges and opportunities in the interpretation of geochemical data from mollusk shells. *Geo-Mar Lett* **28**: 269-285
- Seeley RH (1986) Intense natural selection caused a rapid morphological transition in a living marine snail. *Proc. Natl. Acad. Sci. USA* **83**: 6897-6901
- Shawl A, Davis M (2006) Effects of Dietary Calcium and Substrate on Growth and Survival of Juvenile Queen Conch (*Strombus gigas*) Cultured for Stock Enhancement. *Proceedings of the Gulf and Caribbean Fisheries Institute* **57**: 955-962
- Shirayama Y, Thornton H (2005) Effect of increased atmospheric CO₂ on shallow water marine benthos. *Journal of Geophysical Research* **110**: C09S08, doi:10.1029/2004JC002618
- SigmaPlot *SigmaPlot 10.0: Userguide*. 900 pp.
- Smale DA (2007) Ice disturbance intensity structures benthic communities in nearshore Antarctic waters. *Marine Ecology Progress Series* **349**: 89-102
- Smale DA, Barnes DKA (2008) Likely responses of the Antarctic benthos to climate-related changes in physical disturbance during the 21st century, based primarily on evidence from the West Antarctic Peninsula region. *Ecography* **31**: 289-305
- Smale DA, Barnes DKA, Fraser KPP (2007) The influence of depth, site exposure and season on the intensity of iceberg scouring in nearshore Antarctic waters. *Polar Biology* **30**: 769-779
- Sokolova IM, Pörtner HO (2001) Physiological adaptations to high intertidal life involve improved water conservation abilities and metabolic rate depression in *Littorina saxatilis*. *Marine Ecology Progress Series* **224**: 171-186
- Southgate PC, Beer AC (1997) Hatchery and early nursery culture of the blacklip pearl oyster *Pinctada margaritifera* (L.). *Journal of Shellfish Research* **16**: 561-568
- Stanley SM (1970) Relation of shell form to life habits of the Bivalvia (Mollusca). *Geol. Soc. Amer. Mem.* **125**
- Stecher HA, III, Krantz DE, Lord CJ, III, Luther GW, III, Bock KW (1996) Profiles of strontium and barium in *Mercenaria mercenaria* and *Spisula solidissima* shells. *Geochimica et Cosmochimica Acta* **60**: 3445-3456
- Stenzel HB (1964) Oysters: Composition of the Larval Shell. *Science* **145**: 155-156
- Stenzel HB (1971) Oysters. In Moore R. C. (eds). *Treatise on Invertebrate Paleontology*, Part N, Cox L. R. *et al.* (eds) Volume 3 (of 3) Mollusca 6: Bivalvia. Geological Society of America and University of Kansas, 1224 pp.
- Strathmann RR (1981) The role of spines in preventing structural damage to echinoid tests. *Paleobiology* **7**: 400-406
- Stringer IAN, Bassett SM, McLean MJ, McCartney J, Parrish GR (2003) Biology and conservation of the rare New Zealand land snail *Paryphanta busbyi wattii* (Mollusca, Pulmonata). *Invertebrate Biology* **122**: 241-251
- Svendsen H, Beszczynska-Møller A, Hagen JO, Lefauconnier B, Tverberg V, Gerland S, Ørbæk JB, Bischof K, Papucci C, Zajaczkowski M, Azzolini R, Bruland O, Wiencke C, Winther J, Dallmann W (2002) The physical environment of Kongsfjorden-Krossfjorden, and Arctic fjord system in Svalbard. *Polar Research* **21**: 133-166
- Takesue RK, Bacon CR, Thompson JK (2008) Influences of organic matter and calcification rate on trace elements in aragonitic estuarine bivalve shells. *Geochimica et Cosmochimica Acta* **72**: 5431-5445

- Tan KS, Oh TM (2002) Feeding habits of *Chicoreus capucinus* (Neogastropoda: Muricidae) in a Singapore mangrove. *Bollettino Malacologico* **38**: 43-50
- Tans P NOAA/ESRL (www.esrl.noaa.gov/gmd/ccgg/trends)
- Taylor JD, Reid DG (1990) Shell microstructure and mineralogy of the Littorinidae: ecological and evolutionary significance. *Hydrobiologia* **193**: 199-215
- Thatje S, Anger K, Calcagno JA, Lovrich GA, Pörtner HO, Arntz WE (2005) Challenging the cold: Crabs reconquer the Antarctic. *Ecology* **86**: 619-625
- Thayer CW (1985) Brachiopods versus Mussels: Competition, Predation, and Palatability. *Science* **228**: 1527-1528
- Thompson RJ, Bayne BL (1972) Active metabolism associated with feeding in the mussel *Mytilus edulis* L. *Journal of Experimental Marine Biology and Ecology* **9**: 111-124
- Thompson TG, Chow TJ (1955) The strontium-calcium atom ratio in carbonate secreting marine organisms, in *Pap. Mar. Biol. Oceanogr., Suppl.* to. *Deep Sea Res* **3**: 20-39
- Townsend DW, Radtke RL, Malone DP, Wallinga JP (1995) Use of otolith strontium:calcium ratios for hindcasting larval cod *Gadus morhua* distributions relative to water masses on Georges Bank. *Marine Ecology Progress Series* **119**: 37-44
- Trussell GC (1996) Phenotypic plasticity in an intertidal snail: The role of a common crab predator. *Evolution* **50**: 448-454
- Trussell GC (2000) Phenotypic clines, plasticity, and morphological trade-offs in an intertidal snail. *Evolution* **54**: 151-166
- Trussell GC, Nicklin MO (2002) Cue sensitivity, inducible defense, and trade-offs in a marine snail. *Ecology* **83**: 1635-1647
- Trussell GC, Smith LD (2000) Induced defenses in response to an invading crab predator: An explanation of historical and geographic phenotypic change. *Proceedings of the National Academy of Sciences of the United States of America* **97**: 2123-2127
- Tsipursky SJ, Buseck PR (1993) Structure of magnesian calcite from sea urchins. *American Mineralogist* **78**: 775-781
- Ueda T, Suzuki Y, Nakamura R (1973) Accumulation of strontium in marine organisms. I. Strontium and calcium contents, CF and OR values in marine organisms. *Bull. Jpn. Soc. Sci. Fish.* **39**: 1253-1262
- Urban HJ, Mercuri G (1998) Population dynamics of the bivalve *Laternula elliptica* from Potter Cove, King George Island, South Shetland Islands. *Antarctic Science* **10**: 153-160
- Vermeij GJ (1973) Morphological patterns in high-intertidal gastropods: Adaptive strategies and their limitations. *Marine Biology* **20**: 319-346
- Vermeij GJ (1974) Marine faunal dominance and molluscan shell form. *Evolution* **28**: 656-664
- Vermeij GJ (1977) The Mesozoic marine revolution: evidence from snails, predators and grazers. *Paleobiology*. **3**: 245-258
- Vermeij GJ (1978) *Biogeography and adaptation: patterns of marine life*. Harvard University Press, Cambridge, Massachusetts, U.S.A. 332 pp.
- Vermeij GJ (1980) Predation in time and space: peeling and drilling in Terebrid gastropods. *Paleobiology* **6**: 352-364
- Vermeij GJ (1982a) Environmental change and the evolutionary history of the periwinkle (*Littorina littorea*) in North America. *Evolution* **36**: 561-580
- Vermeij GJ (1982b) Gastropod shell form, breakage, and repair in relation to predation by the crab *Calappa*. *Malacologia* **23**: 1-12

- Vermeij GJ (1987) *Evolution and escalation: an ecological history of life*. Princeton University Press, New Jersey. 527pp.
- Vermeij GJ (1993) *A Natural History of Shells*. Princeton University Press, Princeton, New Jersey. 207 pp.
- Vermeij GJ, Covich AP (1978) Coevolution of freshwater gastropods and their predators. *Am. Nat.* **112**: 833-843
- Vermeij GJ, Schindel DE, Zipser E (1981) Predation Through Geological Time: Evidence from Gastropod Shell Repair. *Science* **214**: 1024-1026
- Wakeling JW, Johnston IA (1998) Muscle power output limits fast-start performance in fish. *Journal of Experimental Biology* **201**: 1505-1526
- Walter LM, Morse JW (1984) Magnesian calcite stabilities: a reevaluation. *Geochimica et Cosmochimica Acta* **48**: 1059-1069
- Wasylenki LE, Dove PM, De Yoreo JJ (2005) Effects of temperature and transport conditions on calcite growth in the presence of Mg^{2+} : implications for paleothermometry. *Geochimica et Cosmochimica Acta* **69**: 4227-4236
- Watson S, Southgate PC, Tyler PA, Peck LS (in press) Early larval development of the Sydney rock oyster *Saccostrea glomerata* under near-future predictions of CO_2 -driven ocean acidification. *Journal of Shellfish Research*
- Weber JN (1969) The incorporation of magnesium into the skeletal calcite of echinoderms. *American Journal of Science* **267**: 537-566
- Weibel ER, Bacigalupe LD, Schmitt B, Hoppeler H (2004) Allometric scaling of maximal metabolic rate in mammals: muscle aerobic capacity as determinant factor. *Respiratory Physiology & Neurobiology* **140**: 115-132
- Weibel ER, Hoppeler H (2005) Exercise-induced maximal metabolic rate scales with muscle aerobic capacity. *Journal of Experimental Biology* **208**: 1635-1644
- Weiss IM, Tuross N, Addadi L, Weiner S (2002) Mollusc larval shell formation: Amorphous calcium carbonate is a precursor phase for aragonite. *Journal of Experimental Zoology* **293**: 478-491
- Welch BL (1951) On the comparison of several mean values: An alternative approach. *Biometrika* **38**: 330-336
- West GB, Brown JH (2005) The origin of allometric scaling laws in biology from genomes to ecosystems: towards a quantitative unifying theory of biological structure and organization. *The Journal of Experimental Biology* **208**: 1575-1592
- West GB, Savage VM, Gillooly J, Enquist BJ, Woodruff WH, Brown JH (2003) Why does metabolic rate scale with body size? *Nature* **421**: 713
- Wheeler AP, Sikes CS (1989) Matrix-crystal interactions in $CaCO_3$ biomineralisation. In Mann, S., Webb, J. and Williams, R. J. P. (eds.) *Biomineralization: chemical and biochemical perspectives*. VCH, New York, U.S.A. pp 95-131.
- Wilbur KM, Jodrey LH (1955) Studies on shell formation. V. The inhibition of shell formation by carbonic anhydrase inhibitors. *Biological Bulletin* **108**: 359-365
- Wilbur KM, Manyak DM (1984) Biochemical aspects of molluscan shell mineralization. In: J.D. Costlow and R.C. Tipper (Eds.), *Marine Biodeterioration: An Interdisciplinary Study*, Naval Institute Press, Annapolis, pp. 30-37.
- Williams A, Brunton CHC, MacKinnon DI (1997a) Morphology. In Williams, A., Brunton, C. H. C., Carlson, S. J. *et al.* *Treatise on Invertebrate Paleontology, Part H, Brachiopoda: Revised*. Volume 1: Introduction. Geological Society of America and University of Kansas, Boulder, Colorado, and Lawrence, Kansas. pp. 321-422.

- Williams A, James MA, Emig CG, Mackay S, Rhodes MC (1997b) Anatomy. In Williams, A., Brunton, C. H. C., Carlson, S. J. *et al. Treatise on Invertebrate Paleontology, Part H, Brachiopoda: Revised*. Volume 1: Introduction. Geological Society of America and University of Kansas, Boulder, Colorado, and Lawrence, Kansas. pp. 8-188.
- Willmer P, Stone G, Johnston I (2005) *Environmental physiology of animals*. 2nd edition. Blackwell Publishing, Oxford, U.K. 754 pp.
- Wohlschlag DE (1964) Respiratory metabolism and ecological characteristics of some fishes in McMurdo Sound, Antarctica. Antarctic Research Series of the American Geophysical Union **1**: 33-62
- Wolf KH, Chilingar GV, Beals FW (1967) Elemental composition of carbonate skeletons, minerals and sediments, in: *Carbonate Rocks, Developments in Sedimentology*, Vol 9B (G. V. Chilingar, H. J. Bissel, and R. W. Fairbridge, eds.), pp. 23-150, Elsevier, Amsterdam
- Wyckoff RWG (1972) *The Biochemistry of Animal Fossils*, Scientichnica, Bristol, 127 pp.
- Zamorano JH, Duarte WE, Moreno CA (1986) Predation upon *Laternula elliptica* (Bivalvia, Anatinidae): A field manipulation in South Bay, Antarctica. Polar Biology **6**: 139-143
- Zeebe RE, Wolf-Gladrow D (2001) *CO₂ in seawater: equilibrium, kinetics, isotopes*. Elsevier Oceanography Series, 65. Amsterdam, The Netherlands. 346 pp.
- Zeebe RE, Zachos JC, Caldeira K, Tyrrell T (2008) Oceans - Carbon emissions and acidification. Science **321**: 51-52
- Zhuang S (2005) The influence of body size and water temperature on metabolism and energy budget in *Laternula marilina* Reeve. Aquaculture Research **36**: 768-775

Appendices

Appendix 1 WDS data: Pearson product moment correlation statistics for elements for individual species. Cell contents are correlation coefficient (r), probability value (p) and number of samples (n). *Denotes p values that are significant at the $p < 0.0125$ level.

Bivalve: <i>Laternula truncata</i> including pallial data						
		Sr	S	Mg	Si	Na
Ca	r	-0.0066	-0.0027	0.376	0.000	-0.475
	p	0.965	0.985	0.0091*	--	0.0007*
	n	47	47	47	1	47
Sr	r		0.252	0.306	0.000	-0.0183
	p		0.0874	0.0364	--	0.903
	n		47	47	1	47
S	r			0.294	0.000	-0.267
	p			0.0447	--	0.0698
	n			47	1	47
Mg	r				0.000	-0.541
	p				--	0.0001*
	n				1	47
Si	r					0.000
	p					--
	n					1

Bivalve: *Laternula truncata* excluding pallial data. Pallial data drive the positive correlation with Mg and negative correlation with Na in the table above. These relationships were based on only a few pallial data points, so data were also analysed without pallial data.

		Sr	S	Mg	Si	Na
Ca	r	-0.109	-0.161	0.0498	0.000	0.0814
	p	0.482	0.297	0.748	--	0.599
	n	44	44	44	1	44
Sr	r		0.206	0.307	0.000	0.0569
	p		0.180	0.0429	--	0.714
	n		44	44	1	44
S	r			0.272	0.000	-0.239
	p			0.0739	--	0.119
	n			44	1	44

Mg	r				0.000	-0.308
	p				--	0.0422
	n				1	44
Si	r					0.000
	p					--
	n					1

Bivalve: <i>Laternula boschasina</i> (no pallial data were available for comparison)						
		Sr	S	Mg	Si	Na
Ca	r	-0.223	0.296	--	0.250	-0.0576
	p	0.359	0.219	--	0.303	0.815
	n	19	19	0	19	19
Sr	r		0.225	--	0.561	-0.0632
	p		0.355	--	0.0124*	0.797
	n		19	0	19	19
S	r			--	0.400	-0.526
	p			--	0.0893	0.0207
	n			0	19	19
Mg	r				--	--
	p				--	--
	n				0	0
Si	r					-0.318
	p					0.184
	n					19

Bivalve: <i>Laternula valenciennesii</i> (empty shells)						
		Sr	S	Mg	Si	Na
Ca	r	-0.219	0.182	--	-0.463	-0.736
	p	0.572	0.640	--	0.209	0.0237
	n	9	9	0	9	9
Sr	r		0.680	--	-0.0992	-0.149
	p		0.0438	--	0.800	0.703
	n		9	0	9	9
S	r			--	0.000794	-0.341
	p			--	0.998	0.370
	n			0	9	9
Mg	r				--	--

	p				--	--
	n				0	0
Si	r					0.176
	p					0.650
	n					9

Bivalve: <i>Laternula recta</i> including pallial data						
		Sr	S	Mg	Si	Na
Ca	r	0.385	0.354	0.314	-0.384	-0.571
	p	0.0063*	0.0125	0.0299	0.616	<0.0001*
	n	49	49	48	4	49
Sr	r		0.885	0.404	-0.317	-0.691
	p		<0.0001*	0.0045*	0.683	<0.0001*
	n		49	48	4	49
S	r			0.446	0.350	-0.738
	p			0.0015*	0.650	<0.0001*
	n			48	4	49
Mg	r				0.194	-0.610
	p				0.806	<0.0001*
	n				4	48
Si	r					-0.464
	p					0.536
	n					4

Bivalve: <i>Laternula recta</i> excluding pallial data						
		Sr	S	Mg	Si	Na
Ca	r	0.0843	-0.0065	-0.144	-0.410	-0.0792
	p	0.591	0.967	0.363	0.493	0.614
	n	43	43	42	5	43
Sr	r		0.829	0.452	-0.352	-0.553
	p		<0.0001*	0.0027*	0.562	0.0001*
	n		43	42	5	43
S	r			0.585	0.0720	-0.602
	p			<0.0001*	0.908	<0.0001*
	n			42	5	43
Mg	r				-0.0571	-0.373
	p				0.927	0.0150

	n				5	42
Si	r					-0.471
	p					0.424
	n					5

Bivalve: <i>Laternula elliptica</i> (trends were no different with or without pallial data)						
		Sr	S	Mg	Si	Na
Ca	r	-0.0292	-0.0247	-0.630	0.117	0.151
	p	0.847	0.871	0.0378	0.511	0.315
	n	46	46	11	34	46
Sr	r		0.754	0.0496	-0.0616	-0.299
	p		<0.0001*	0.885	0.729	0.0434
	n		46	11	34	46
S	r			-0.105	0.0101	-0.168
	p			0.760	0.955	0.265
	n			11	34	46
Mg	r				-1.000	0.107
	p				--	0.755
	n				2	11
Si	r					0.250
	p					0.154
	n					34

Gastropod: <i>Cantharus fumosus</i>						
		Sr	S	Mg	Si	Na
Ca	r	-0.391	0.107	0.293	0.142	-0.152
	p	0.0588	0.619	0.209	0.909	0.480
	n	24	24	20	3	24
Sr	r		-0.478	0.130	0.951	0.350
	p		0.0183	0.585	0.200	0.0935
	n		24	20	3	24
S	r			-0.255	-0.0524	0.121
	p			0.277	0.967	0.572
	n			20	3	24
Mg	r				--	-0.622
	p				--	0.0034*
	n				0	20

Si	r					0.189
	p					0.879
	n					3

Gastropod: <i>Phos senticosus</i>						
		Sr	S	Mg	Si	Na
Ca	r	0.353	0.0228	-0.283	--	-0.101
	p	0.0440	0.903	0.110	--	0.577
	n	33	31	33	0	33
Sr	r		-0.435	-0.289	--	-0.654
	p		0.0145	0.102	--	<0.0001*
	n		31	33	0	33
S	r			0.166	--	0.412
	p			0.372	--	0.0213
	n			31	0	31
Mg	r				--	-0.111
	p				--	0.538
	n				0	33
Si	r					--
	p					--
	n					0

Gastropod: <i>Cominella lineolata</i>						
		Sr	S	Mg	Si	Na
Ca	r	-0.221	-0.0979	0.726	-0.218	-0.0696
	p	0.411	0.718	0.165	0.497	0.798
	n	16	16	5	12	16
Sr	r		-0.500	-0.372	0.397	-0.156
	p		0.0483	0.537	0.201	0.563
	n		16	5	12	16
S	r			0.787	-0.220	-0.0126
	p			0.114	0.492	0.963
	n			5	12	16
Mg	r				0.000	0.788
	p				--	0.114
	n				1	5
Si	r					0.216
	p					0.500

	n					12
--	----------	--	--	--	--	----

Gastropod: <i>Buccinum undatum</i>						
		Sr	S	Mg	Si	Na
Ca	r	-0.467	0.0760	-0.332	--	0.413
	p	0.0031*	0.650	0.0630	--	0.0100*
	n	38	38	32	0	38
Sr	r		-0.0915	0.659	--	-0.469
	p		0.585	<0.0001*	--	0.0030*
	n		38	32	0	38
S	r			-0.194	--	0.457
	p			0.287	--	0.0039*
	n			32	0	38
Mg	r				--	-0.514
	p				--	0.0026*
	n				0	32
Si	r					--
	p					--
	n					0

Gastropod: <i>Neobuccium eatoni</i>						
		Sr	S	Mg	Si	Na
Ca	r	0.0191	-0.233	0.341	0.0330	0.181
	p	0.901	0.123	0.0951	0.928	0.233
	n	45	45	25	10	45
Sr	r		0.712	0.0860	-0.631	-0.527
	p		<0.0001*	0.683	0.0506	0.0001*
	n		45	25	10	45
S	r			-0.107	-0.407	-0.303
	p			0.611	0.244	0.0431
	n			25	10	45
Mg	r				0.000	0.154
	p				--	0.462
	n				1	25
Si	r					0.230
	p					0.522
	n					10

Gastropod: <i>Buccinum cf. groenlandicum</i>						
		Sr	S	Mg	Si	Na
Ca	r	-0.0998	0.360	0.401	0.568	0.447
	p	0.557	0.0284	0.251	0.0271	0.0055*
	n	37	37	10	15	37
Sr	r		0.310	0.551	-0.0734	-0.256
	p		0.0618	0.0986	0.795	0.127
	n		37	10	15	37
S	r			0.141	0.616	0.0005
	p			0.698	0.0145	0.997
	n			10	15	37
Mg	r				--	0.256
	p				--	0.475
	n				0	10
Si	r					0.485
	p					0.0666
	n					15

Gastropod: <i>Buccinum glaciale</i>						
		Sr	S	Mg	Si	Na
Ca	r	0.00866	0.514	--	-0.135	0.481
	p	0.977	0.0599	--	0.691	0.0818
	n	14	14	0	11	14
Sr	r		0.0941	--	-0.328	-0.175
	p		0.749	--	0.325	0.549
	n		14	0	11	14
S	r			--	-0.112	0.219
	p			--	0.743	0.451
	n			0	11	14
Mg	r				--	--
	p				--	--
	n				0	0
Si	r					0.232
	p					0.493
	n					11

Brachiopod: <i>Liothyrella neozelanica</i>						
		Sr	S	Mg	Si	Na

Ca	r	0.188	0.0931	--	0.0558	0.222
	p	0.271	0.589	--	0.746	0.193
	n	36	36	0	36	36
Sr	r		0.811	--	0.720	0.908
	p		<0.0001*	--	<0.0001*	<0.0001*
	n		36	0	36	36
S	r			--	0.821	0.879
	p			--	<0.0001*	<0.0001*
	n			0	36	36
Mg	r				--	--
	p				--	--
	n				0	0
Si	r					0.810
	p					<0.0001*
	n					36

Brachiopod: <i>Liothyrella uva</i> from Signy						
		Sr	S	Mg	Si	Na
Ca	r	-0.626	-0.325	--	-0.0980	-0.125
	p	0.0294	0.303	--	0.762	0.699
	n	12	12	12	12	12
Sr	r		0.0628	--	0.164	0.442
	p		0.846	--	0.611	0.151
	n		12	12	12	12
S	r			--	0.657	-0.0581
	p			--	0.0203	0.858
	n			12	12	12
Mg	r				--	--
	p				--	--
	n				12	12
Si	r					0.174
	p					0.588
	n					12

Brachiopod: <i>Liothyrella uva</i> from Rothera						
		Sr	S	Mg	Si	Na
Ca	r	-0.312	-0.268	-0.774	-0.787	-0.409
	p	0.0102*	0.0286	0.0004*	<0.0001*	0.0006*

	n	67	67	16	51	67
Sr	r		0.498	0.763	0.419	0.666
	p		<0.0001*	0.0006*	0.0022*	<0.0001*
	n		67	16	51	67
S	r			0.692	0.668	0.506
	p			0.0030*	<0.0001*	<0.0001*
	n			16	51	67
Mg	r				--	0.599
	p				--	0.0141
	n				0	16
Si	r					0.457
	p					0.0007*
	n					51

Brachiopod: <i>Magellania venosa</i>						
		Sr	S	Mg	Si	Na
Ca	r	0.121	0.170	0.0309	--	0.391
	p	0.694	0.578	0.920	--	0.187
	n	13	13	13	0	13
Sr	r		0.302	0.223	--	0.516
	p		0.316	0.464	--	0.0709
	n		13	13	0	13
S	r			0.879	--	0.665
	p			0.0001*	--	0.0131
	n			13	0	13
Mg	r				--	0.371
	p				--	0.212
	n				0	13
Si	r					--
	p					--
	n					0

Appendix 2 EDS data: Pearson product moment correlation statistics for elements for individual species. Cell contents are correlation coefficient (r), probability value (p) and number of samples (n). *Denotes p values that are significant at the $p < 0.0125$ level.

Bivalve: <i>Laternula elliptica</i>				
		S	Mg	Na
Ca	r	-0.121	0.226	-0.0614
	p	0.563	0.590	0.771
	n	25	8	25
S	r		0.681	-0.131
	p		0.0630	0.532
	n		8	25
Mg	r			-0.116
	p			0.784
	n			8

Bivalve: <i>Yolida eightsi</i>				
		S	Mg	Na
Ca	r	0.256	0.158	0.0288
	p	0.250	0.685	0.899
	n	22	9	22
S	r		-0.457	0.174
	p		0.216	0.438
	n		9	22
Mg	r			-0.821
	p			0.0067*
	n			9

Gastropod: <i>Buccinum undatum</i>				
		S	Mg	Na
Ca	r	0.0317	0.0073	-0.132
	p	0.861	0.986	0.465
	n	33	8	33
S	r		0.150	-0.151
	p		0.723	0.400
	n		8	33
Mg	r			0.0379

	p			0.929
	n			8

Brachiopod: <i>Liothyrella neozelanica</i>				
		S	Mg	Na
Ca	r	-0.619	-0.525	-0.176
	p	0.0013*	0.0085*	0.409
	n	24	24	24
S	r		0.795	-0.0697
	p		<0.0001*	0.746
	n		24	24
Mg	r			-0.124
	p			0.565
	n			24

Brachiopod: <i>Liothyrella uva</i>				
		S	Mg	Na
Ca	r	-0.467	-0.457	-0.378
	p	0.0092*	0.0111*	0.0396
	n	30	30	30
S	r		0.852	0.217
	p		<0.0001*	0.249
	n		30	30
Mg	r			0.227
	p			0.228
	n			30

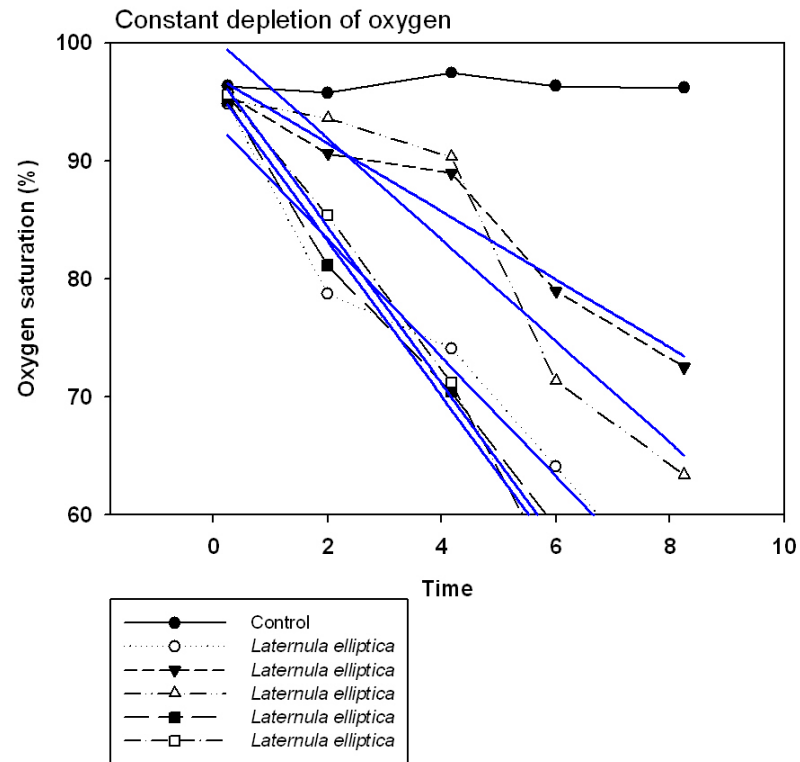
Brachiopod: <i>Magellania fragilis</i>				
		S	Mg	Na
Ca	r	-0.855	-0.821	0.695
	p	<0.0001*	<0.0001*	<0.0001*
	n	42	38	42
S	r		0.802	-0.634
	p		<0.0001*	<0.0001*
	n		38	42
Mg	r			-0.552
	p			0.0003*
	n			38

Brachiopod: <i>Terebratulina retusa</i>				
--	--	--	--	--

		S	Mg	Na
Ca	r	-0.274	-0.362	-0.135
	p	0.123	0.0386	0.453
	n	33	33	33
S	r		0.120	0.159
	p		0.505	0.377
	n		33	33
Mg	r			0.401
	p			0.0209
	n			33

Echinoid: <i>Sterechinus neumayeri</i>				
		S	Mg	Na
Ca	r	0.0309	-0.547	-0.447
	p	0.909	0.0282	0.0825
	n	16	16	16
S	r		0.129	0.0675
	p		0.633	0.804
	n		16	16
Mg	r			0.256
	p			0.338
	n			16

Appendix 3 An of example of trials showing the constant depletion of oxygen down from 100 to < 70 % saturation. Regression lines are all significant ($p < 0.05$).



Appendix 4 Gompertz growth curve parameters, fitted using $y=a*\exp(-\exp(-(x-x_0)/b))$.

Species	a	b	c (x ₀)	r ²	s.e.	F	df	p
<i>Laternula truncata</i>	28.0895	3.7814	2.9053	0.9619	1.0293	820.9532	2,63	<0.0001
<i>Laternula boschasina</i>	12.6964	2.2252	1.3129	0.9489	0.5520	437.7275	2,45	<0.0001
<i>Laternula recta</i>	26.7382	5.0806	4.2727	0.9710	0.7139	1188.3350	2,69	<0.0001
<i>Laternula elliptica</i>	56.0257	4.5000	4.8389	0.9539	2.7556	1304.6328	2,124	<0.0001
<i>Liothyrella neozelanica</i>	51.6013	4.9557	4.9640	0.9689	1.9618	1634.1392	2,103	<0.0001
<i>Liothyrella uva</i>	40.9032	8.7911	8.5485	0.9726	1.4031	2678.8835	2,149	<0.0001
<i>Buccinum undatum</i>	78.0973	2.8910	2.0752	0.4650	6.5977	19.2517	2,40	<0.0001
<i>Neobuccinum eatoni</i>	56.9763	5.0989	0.9537	0.5402	4.4672	13.9239	2,20	0.0002
<i>Buccinum cf. groenlandicum</i>	did not converge							
<i>Buccinum glaciale</i>	did not converge							

Appendix 5 VBGF parameters, fitted using $y=a*(1-\exp(-b*(x-x_0)))$, however infinity is rather high, and values for small individuals are also high (because the curve does not pass close enough to the origin).

Species	L _∞ (a)	K (b)	t ₀ (x ₀)	r ²	s.e.	F	df	p
<i>Laternula truncata</i>	51.2467	0.0647	-0.6374	0.9632	1.0117	850.8921	2,63	<0.0001
<i>Laternula boschasina</i>	14.8196	0.2279	-0.3697	0.9486	0.5540	434.3664	2,45	<0.0001
<i>Laternula recta</i>	104.7184	0.0193	-0.8782	0.9719	0.7027	1227.5173	2,69	<0.0001
<i>Laternula elliptica</i>	160.7785	0.0294	0.0788	0.9526	2.7929	1268.4120	2,124	<0.0001
<i>Liothyrella neozelanica</i>	113.4204	0.0370	-0.1032	0.9682	1.9817	1600.4287	2,103	<0.0001
<i>Liothyrella uva</i>	111.9357	0.0161	-0.6061	0.9729	1.3951	2710.6391	2,149	<0.0001
<i>Buccinum undatum</i>	91.7635	0.1779	0.0097	0.4637	6.6054	19.1594	2,40	<0.0001
<i>Neobuccinum eatoni</i>	58.4427	0.1475	-1.7493	0.5343	4.4956	13.6226	2,20	0.0002
<i>Buccinum cf. groenlandicum</i>	133.9191	0.0425	-2.2752	0.7239	2.6719	16.7326	2,10	0.0006
<i>Buccinum glaciale</i>	66.6022	0.6882	3.3435	0.5521	2.7058	5.9303	2,6	0.0379

Appendix 6 Mean shell cost, respiration and tissue energy costs for each species taken from an example mid-valve of $1.5 \text{ J.mg}^{-1} \text{ CaCO}_3$ and including differences in CaCO_3 saturation state.

	Cost of shell deposited (J.y^{-1})	Energy from routine metabolic rate (J.y^{-1})	Caloric content of soft tissue gained (J.y^{-1})	Estimate of total energy budget (I) (J.y^{-1})	Cost of shell as a % of I
Bivalves					
<i>Laternula truncata</i>	320	34331	897	55917	0.545
<i>Laternula boschasina</i>	62	7263	134	11740	0.751
<i>Laternula recta</i>	130	11581	897	19806	1.016
<i>Laternula elliptica</i>	4551	74248	17546	145705	3.074
Brachiopod					
<i>Liothyrella uva</i>	311	2907	199	4930	7.474
Gastropods					
<i>Buccinum undatum</i>	4380	102676	12392	221284	2.608
<i>Neobuccinum eatoni</i>	758	20478	3859	46801	2.258
<i>Buccinum</i> cf. <i>groenlandicum</i>	1043	12202	2646	28553	3.329
<i>Buccinum glaciale</i>	3304	43775	7972	99514	3.909

Appendix 7 Watson, S., Southgate, P. C., Tyler, P. A. & Peck, L. S. (in press). Early larval development of the Sydney rock oyster *Saccostrea glomerata* under near-future predictions of CO₂-driven ocean acidification. Journal of Shellfish Research. (Proof from publishers. Expected publication date August 2009.)

Journal of Shellfish Research, Vol. 28, No. 3, 431–437, 2009.

EARLY LARVAL DEVELOPMENT OF THE SYDNEY ROCK OYSTER *SACCOSTREA GLOMERATA* UNDER NEAR-FUTURE PREDICTIONS OF CO₂-DRIVEN OCEAN ACIDIFICATION

SUE-ANN WATSON,^{1*} PAUL C. SOUTHGATE,² PAUL A. TYLER¹ AND AND LLOYD S. PECK³

¹National Oceanography Centre, Southampton, School of Ocean and Earth Science, University of Southampton, European Way, Southampton, SO14 3ZH, United Kingdom; ²AIMS at JCU and School of Marine and Tropical Biology, James Cook University, Townsville, Qld, 4811, Australia; ³British Antarctic Survey, Natural Environment Research Council, High Cross, Madingley Road, Cambridge, CB3 0ET, United Kingdom

ABSTRACT Anthropogenic emissions of carbon dioxide (CO₂) from fossil fuel combustion and deforestation are rapidly increasing the atmospheric concentration of CO₂ and reducing the pH of the oceans. This study shows that predicted near-future levels of ocean acidification have significant negative effects on early larval development of the Sydney rock oyster *Saccostrea glomerata* (Gould, 1850). CO₂ was added to seawater to produce pH levels set at 8.1 (control), 7.8, and 7.6 (actual pH values were 8.11, 7.81, and 7.64, respectively). These treatments represent present-day surface ocean pH, as well as upper (Δ pH \approx -0.3) and lower (Δ pH \approx -0.5) pH predictions for the surface oceans in 2100. With decreasing pH, survival of *S. glomerata* larvae decreased, and growth and development were retarded. Larval survival decreased by 43% at pH 7.8 and by 72% at pH 7.6. Antero-posterior measurement (APM) was reduced by 6.3% at pH 7.8 and 8.7% at pH 7.6, and dorso-ventral measurement (DVM) was reduced by 5.1% at pH 7.8 and 7.5% at pH 7.6. The percentage of empty shells remaining from dead larvae decreased by 16% at pH 7.8 and by 90% at pH 7.6 indicating that the majority of empty shells dissolved within 7 days at pH 7.6. Scanning electron microscope images of 8-day-old larvae show abnormalities on the shell surface at low pH suggesting (1) problems with shell deposition, (2) retarded periostracum formation, and/or (3) increased shell dissolution. Larval life-history stages are considered particularly susceptible to climate change, and this study shows that *S. glomerata* larvae are sensitive to a high-CO₂ world and are, specifically, negatively affected by exposure to pH conditions predicted for the world's oceans for the year 2100.

KEY WORDS: climate change, ocean acidification, carbon dioxide, oyster, survival, larval development

INTRODUCTION

Over the last 23 million years, atmospheric carbon dioxide (CO₂) concentrations have remained stable between 140 to 340 ppm and surface ocean pH has remained constant between 8.0 to 8.3 pH units (Pearson & Palmer 2000). Anthropogenic CO₂ emitted from fossil fuel combustion and deforestation since the onset of the Industrial Revolution has increased atmospheric concentrations of CO₂ from 280 to 380 ppmv in the last 200 y (Tans NOAA/ESRL records). This rapid increase in CO₂ of 35% is an order of magnitude faster than any change in CO₂ concentration that has occurred for millions of years (Doney & Schimel 2007). The increase in this greenhouse gas is not only causing the planet to warm but is also causing the oceans to acidify. This acidification is the result of increased CO₂ dissolving in seawater decreasing carbonate ion (CO₃²⁻) concentration and increasing bicarbonate ion (HCO₃⁻) concentration in a series of equilibrium reactions that release hydrogen ions (H⁺).

Over the past 200 y, the oceans have taken up ~40% of the anthropogenic CO₂ emissions from the atmosphere (Zeebe et al. 2008). This uptake of CO₂ has caused a 0.1 unit drop in the pH of the surface oceans (Caldeira & Wickett 2003) which is equivalent to a 30% increase in H⁺ concentration (Blackford & Gilbert 2007). By the 1980s, ocean pH was falling at a rate of 0.015 pH units per decade (Haugan & Drange 1996) and present day average global surface ocean pH is 8.07 compared with the preindustrial value of 8.17 (Cao et al. 2007).

Models predict a further reduction in ocean pH by 0.3 to 0.5 units by 2100 (Haugan & Drange 1996, Caldeira & Wickett 2005, Orr et al. 2005), which is equivalent to at least a 100–150% increase

in H⁺ concentration (Orr et al. 2005). Some reports suggest that increasing global temperatures caused by climate change will partially alleviate the effects of ocean acidification; however, Cao et al. (2007) show that ocean acidification is largely independent of temperature change. The predicted changes in ocean pH are not only greater but far more rapid than any experienced in the last 24 million years (see Blackford & Gilbert 2007) and possibly the last 300 million years (Caldeira & Wickett 2003).

Ocean acidification is likely to affect marine animals either by direct acidification of their environment or through hypercapnia. The decreasing pH of the oceans will lower the saturation state of seawater with respect to calcium carbonate and therefore increase the solubility of calcareous structures. Consequently, calcifying species such as corals, foraminifera, coccolithophores, molluscs, brachiopods, and echinoderms are thought to be particularly at risk. Kleypas et al. (2006) suggest that calcification rates could decrease by 60% this century. Under experimental conditions of the predicted atmospheric pCO₂ (~740 ppmv) in 2100 from the IPCC IS92a scenario, calcification was reduced by 25% in the edible mussel *Mytilus edulis* and 10% in the Pacific oyster *Crassostrea gigas* (Gazeau et al. 2007).

Other negative effects of ocean acidification have been demonstrated in various species, including decreased growth in the sea urchins *Hemicentrotus pulcherrimus* and *Echinometra mathaei* and the gastropod *Strombus luhuanus* (Shirayama & Thornton 2005), and reduced fertilization success in the sea urchin *Heliocidaris erythrogramma* (Havenhand et al. 2008). Experiments investigating the effects of seawater acidification at low pH (under scenarios of leakage from geological CO₂ sequestration stores) have demonstrated increased mortality in the sea urchin *Psammechinus miliaris* (Miles et al. 2007) and

*Corresponding author. E-mail: suwa@noc.soton.ac.uk

complex indirect effects on the induced defenses in the gastropod *Littorina littorea* (Bibby et al. 2007).

Lowered seawater pH reduces calcification in coral reefs (Langdon et al. 2003) and the combination of stresses of climate change and ocean acidification is expected to reduce coral reef system diversity, with corals becoming increasingly rare (Hoegh-Guldberg et al. 2007). Naturally occurring gradients of reduced pH around CO₂ vents in the Mediterranean Sea, have demonstrated ecosystem shifts and changes in species composition with a dramatic decrease in calcifying fauna in low pH areas (Hall-Spencer et al. 2008).

Understanding the effects of acidification in commercially important species is of prime importance. The Sydney rock oyster *Saccostrea glomerata* (Gould, 1850) was chosen as a model species for this preliminary study. It is an important commercial species supporting an industry that currently generates \$34.5 million (AUD) annually in sales (O'Sullivan et al. 2008). *S. glomerata* is a warm temperate bivalve mollusc endemic to Australia and New Zealand. Dove and Sammut (2007) showed that acidification of estuarine waters from terrestrial acid sulphate soil runoff increased mortality in *S. glomerata*. Small oysters showed the greatest mortality because their thinner shells were perforated by acid erosion.

Early life-history stages are generally believed to be vulnerable to stress and change (Peck 2005). Studies have already shown that the early developmental stages of the oyster *Crassostrea gigas* (Kurihara et al. 2007), copepod *Calanus finmarchicus* (Mayor et al. 2007) and brittlestar *Ophiothrix fragilis* (Dupont et al. 2008) are negatively affected by acidified conditions. We aimed to identify the effects of near-future CO₂-driven ocean acidification scenarios on the larval development of *S. glomerata*, and determine if this life-history stage is particularly susceptible to the stress of altered pH.

MATERIALS AND METHODS

Experimental Set-up and pH Control

Experiments were conducted at the Aquarium Complex of the Marine and Aquaculture Research Facilities Unit (MARFU) at James Cook University, Australia. Seawater obtained from the Australian Institute for Marine Science (AIMS) was filtered to 1 µm and sterilized by ultra-violet radiation. Seawater was held in a 3,000-L reservoir tank in the laboratory and allowed to equilibrate to ambient temperature (26°C). Seawater was pumped from the reservoir into three 500-L header tanks, which filled on-demand via float valves (Fig. 1).

The pH of seawater was controlled by manipulation of the partial pressure of CO₂ (pCO₂) reproducing the means by which atmospheric CO₂ will reduce the pH of the oceans. Seawater pH was regulated by a computerized control system (AquaMedic AT-Control) that introduced gaseous CO₂ into the header tanks as required via a solenoid valve. pH probes were calibrated with NBS buffer solutions and the pH values reported in this study are on the NBS scale. Values of pH were nominally set at 8.1 (control), 7.8, and 7.6. These treatments represent present-day pH, upper year 2100 pH predictions ($\Delta \text{pH} \approx 0.3$) and lower year 2100 pH predictions ($\Delta \text{pH} \approx 0.5$) of seawater, respectively. Seawater from the header tanks was gravity-fed (2.5 l.h⁻¹) to individual 60-L treatment tanks within 3,000-L water-bath tanks. The actual pH values measured in the treatment tanks were 8.11, 7.81, and 7.64 (Table 1). Seawater samples were analyzed for total alkalinity by titration. Other parameters of the carbonate system were calculated using the program CO2SYS (Lewis & Wallace 1998).

Seawater temperature was maintained at 26°C (to 2 significant figures) based on optimum temperatures reported for

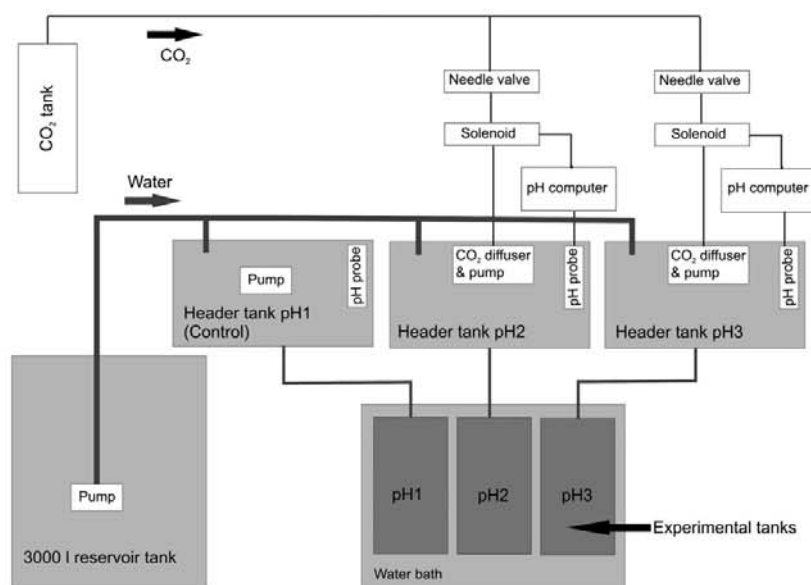


Figure 1. Set-up of experimental CO₂ system with 3 pH levels. Treatments labeled pH 1, pH 2, and pH 3 were set to nominal pH values of 8.1, 7.8, and 7.6 respectively.

TABLE 1.
Water chemistry data for treatment tanks (mean \pm 1 S.D.).

Nominal pH	8.1	7.8	7.6
Measured pH _{NBS}	8.11 (\pm 0.02)	7.81 (\pm 0.03)	7.64 (\pm 0.04)
pH _{NBS} range (min. – max.)	8.10–8.14	7.78–7.84	7.59–7.67
Alkalinity (mg/L as CaCO ₃)	101.1 (\pm 1.18)	102.27 (\pm 1.42)	101.23 (\pm 0.91)
Temperature (°C)	25.7 (\pm 0.2)	25.6 (\pm 0.2)	25.6 (\pm 0.1)
pCO ₂ (μ atm)	220.3 (\pm 16.1)	508.8 (\pm 45.7)	775.6 (\pm 75.7)
Ω_{cal}	1.67 (\pm 0.06)	0.93 (\pm 0.05)	0.65 (\pm 0.06)
Ω_{arag}	1.15 (\pm 0.04)	0.64 (\pm 0.03)	0.45 (\pm 0.05)

growth, development, and survival of embryos and larvae of *S. glomerata* (Dove & O'Connor 2007). Salinity was maintained at 32 and seawater within the treatment tanks was mixed by aeration through a fine glass tube. Larvae were retained in the treatment tank by a fine mesh, which covered the outflow pipe (Southgate & Beer 1997). Used seawater was not recirculated into the experimental system. Treatment tanks were covered with transparent lids to minimize loss of CO₂ from the seawater to the atmosphere and were held under a 13 hL:11 hD lighting regime.

Spawning Procedure and Larval Culture

Sydney rock oysters were obtained from a commercial oyster farm in central New South Wales, Australia and strip-spawned. Embryos were incubated in a 500-L tank filled with 1- μ m filtered seawater containing the antibiotic streptomycin sulphate at a concentration of 10 mg.L⁻¹. At 24 h old, the larvae had reached D-veliger stage. Larvae were retained on a 25- μ m mesh screen, washed with 1- μ m filtered seawater and 90,000 larvae were transferred into each 60-L treatment tank creating a stocking density of 1.5 larvae.mL⁻¹ in each. In the treatment tanks, larvae were pulse fed daily with live cultured microalgae composed of a 1:1 mixture of *Pavlova salina* and *Isochrysis* (clone T-Iso) fed at increasing concentrations of 5,000–20,000 cells.mL⁻¹ from days 1–8. Feeding rate was based on previously published data for the larvae of *S. glomerata* (Nell & O'Connor 1991) and sufficient concentrations of algal cells were fed to ensure food supply was not a limiting factor in survival, growth and development.

Processing of Larvae

Larvae were removed from the treatment tanks when they were 8 days old by passing the contents of each treatment tank through a 37- μ m mesh screen. Larvae were counted on a Sedgewick rafter counter using a light microscope. The antero-posterior measurement (APM) and dorso-ventral measurement (DVM) of 30 larvae per treatment were recorded. Further samples of larvae were frozen, freeze-dried, and then weighed or fixed in a 2% glutaraldehyde solution in seawater for 2 h. Fixed larvae were dehydrated through graded ethanol solutions, air-dried and transferred onto stainless steel stubs. The stubs and larvae were gold coated and imaged on a JEOL JSM-5410LV scanning electron microscope (SEM) using secondary electrons.

Empty Shell Counts

Shells of both living and dead calcareous animals experience dissolution in the marine environment (see Harper 2000), so it

was expected that some empty, or 'dead', larval shells would dissolve at each pH. To determine differences in shell dissolution between treatments, the percentage of empty shells remaining from larvae that had died during the experiment in each treatment tank was calculated. The number of larvae that had died, and therefore the number of empty shells that should have been present, was determined by subtraction of counts of surviving larvae at the end of an experiment from original stocking numbers. The actual numbers of empty shells remaining were counted on a Sedgewick rafter counter using a light microscope. The percentage of empty shells remaining was then calculated by dividing the number of empty shells counted by the number of dead larvae per treatment tank (Eq. 1), thus correcting for differences in larval mortality between treatments.

$$\text{Percent empty shells remaining} = \frac{\text{empty shells counted}}{\text{number of dead larvae}} \times 100\% \quad (1)$$

Statistical Analysis

Data were tested for normality where appropriate using the Shapiro-Wilk normality test. Relevant parametric (e.g., ANOVA, Pearson correlation) or nonparametric (e.g., Kruskal Wallis) statistical analyses were performed using SPSS 16.0.

RESULTS

In the following sections, nominal pH values are used to refer to the treatment pH conditions (i.e., pH 8.1, 7.8, and 7.6). For actual pH values measured in the treatments and further water chemistry data, see Table 1.

Larval Survival

One-day-old D-veliger larvae were introduced to the treatment tanks. By 8-days-old, the majority had developed into umbonate larvae. The experiment was thus run between these two key developmental stages. Percentage larval survival decreases with decreasing pH (Fig. 2A). There is a significant positive correlation between pH and mean larval survival ($r = 1.000$, $P = 0.004$, $n = 3$ for nominal pH; $r = 1.000$, $P = 0.032$, $n = 3$ for measured pH). Compared with the control treatment (pH 8.1), survival decreased by 43% at pH 7.8 and by 72% at pH 7.6.

Larval Growth and Morphology

Decreased pH had an effect on the morphology and growth of the larvae. There was a significant difference between the

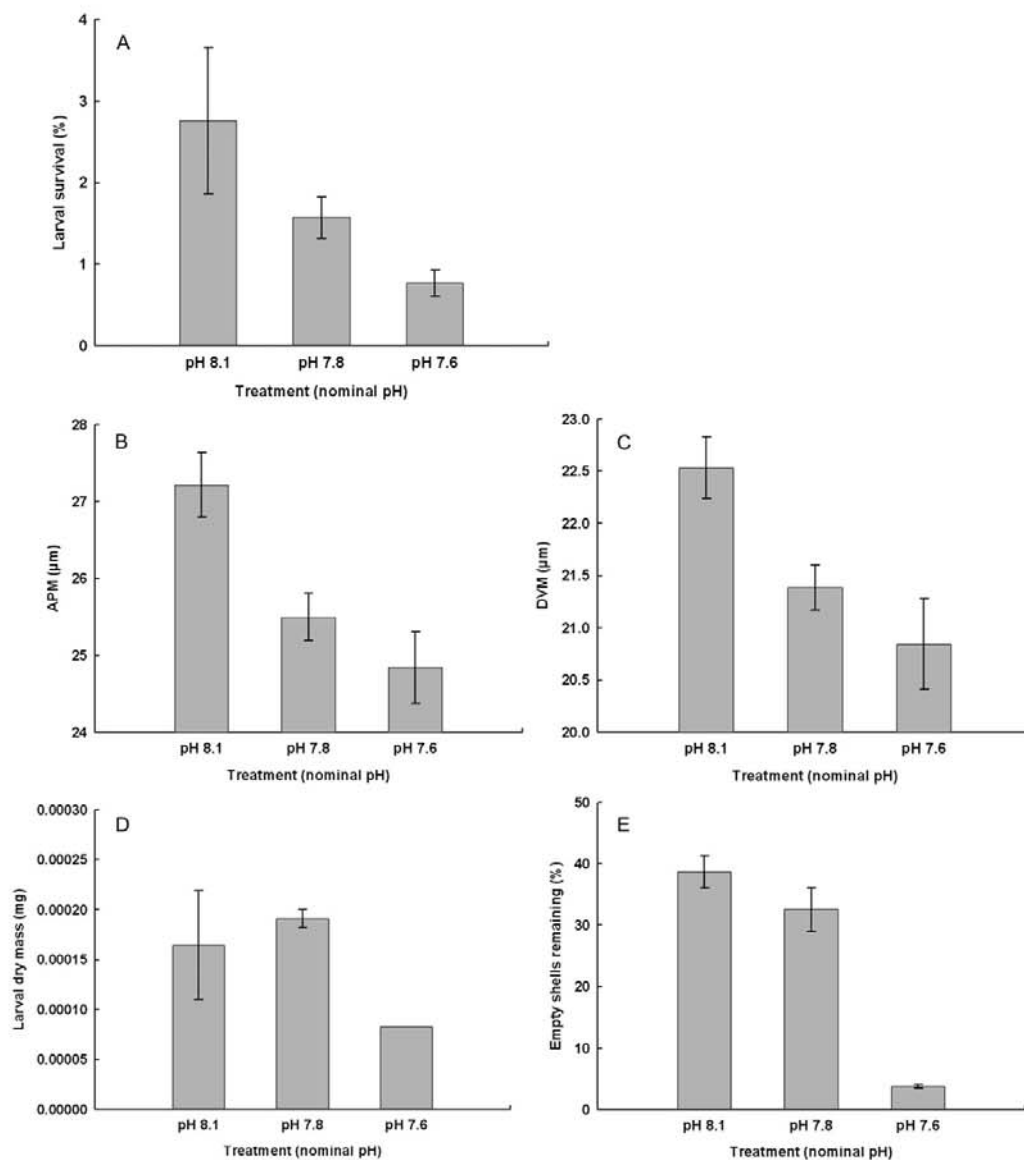


Figure 2. Qualitative and quantitative measurements of larval success at different pH: A, Larval survival; B, APM of larvae; C, DVM of larvae; D, Percentage of empty shells remaining from dead larvae; E, Larval dry mass. Error bars are 1 S.E.

antero-posterior measurement (APM) of larvae at different pH ($\chi^2 = 13.697$, $df = 2$, $P = 0.001$) and between the dorso-ventral measurement (DVM) of larvae at different pH ($\chi^2 = 12.276$, $df = 2$, $P = 0.002$). Larval APM was reduced by 6.3% at pH 7.8 and 8.7% at pH 7.6 (Fig. 2B). Larval DVM was reduced by 5.1% at pH 7.8 and 7.5% at pH 7.6 (Fig. 2C). It was expected that pH would affect larval dry mass (Fig. 2D). However, preliminary mass data were limited and statis-

tical tests showed no significant difference in mass among pH treatments.

Empty Shells Recovered

There was a significant difference in the percentage of empty shells remaining between pH treatments ($F = 50.129$, $df = 2,7$, $P < 0.001$). At pH 7.8 and 7.6, the saturation state of seawater

with respect to calcite and aragonite fell below $\Omega = 1$ (Table 1). The percentage of empty shells remaining decreased with decreasing pH by 16% in pH 7.8 and 90% in pH 7.6 (Fig. 2E).

Shell Surface Structure

Shell surface characteristics were markedly affected by pH (Fig. 3). In normal larval shell development (control treatment pH 8.1) the shell is smooth and rounded with even growth (Fig. 3A). At pH 7.8 and pH 7.6, growth checks can be seen on the surface of the larval shell (marked by "X" arrows) and are likely to be the result of physiological stress after the transfer to low pH conditions (Figs. 3B and 3C). Larval shell deposition under low pH (indicated by "Y"), was no longer smooth, but appeared pitted and deformed particularly around the valve edge. These abnormalities in new shell growth indicate potential problems with shell deposition and/or periostracum formation. At low pH, areas in the middle of the shell surface, which were deposited before transfer to low pH conditions, showed surface pitting and were rough in appearance indicating dissolution of the larval shell after transfer to low pH conditions.

DISCUSSION

Increasing anthropogenic emissions of CO_2 have already caused a decrease in ocean pH of 0.1 units (Caldeira & Wickett 2003). Since the chemistry of seawater and the carbonate system is well known, we can be moderately confident about model predictions for future ocean pH scenarios of ΔpH 0.3 to 0.5 units by 2100 (Haugan & Drange 1996, Caldeira & Wickett 2005, Orr et al. 2005) and 0.7 units by 2300 (Caldeira & Wickett 2003).

Experiments were run with *S. glomerata* from 1 to 8 days old between key developmental stages: D-veliger to unbonate larvae. Compared to the control treatment (pH 8.1), survival decreased by 43% in pH 7.8 (ΔpH 0.3 upper 2100 prediction) and 72% in pH 7.6 (ΔpH 0.5 lower 2100 prediction). Although mortality during larval culture in the experiment was high across all treatments, commercial scale hatcheries also experience mass mortalities (i.e. >80%) of *S. glomerata* larvae. For example, half of all hatchery runs with this species over a five-year period failed within the first 8 days (Heasman et al. 2000, Dove & O'Connor 2007). Furthermore, strip spawning of oysters is generally acknowledged to result in fewer viable larvae compared with natural or induced spawning methods (Gosling 2003).

Larval growth (APM and DVM) was retarded with decreasing pH suggesting that larval development could take longer under ocean acidification, or that larvae will be smaller at each developmental stage. SEM images revealed growth abnormalities in the surface of the larval shell at low pH. Larval shells were pitted and deformed, particularly where shell was deposited during exposure to low pH. These shell surface abnormalities indicate larvae may have been experiencing: (1) problems with shell deposition, (2) retarded periostracum formation, and/or (3) increased shell dissolution, at low pH.

Initially oyster larvae deposit a predominantly amorphous calcium carbonate (ACC) shell, which later partially transforms into aragonite (Weiss et al. 2002). This differs from the adult oyster shell, which is composed predominantly of calcite (Stenzel 1964). ACC is more soluble than aragonite (Brečević

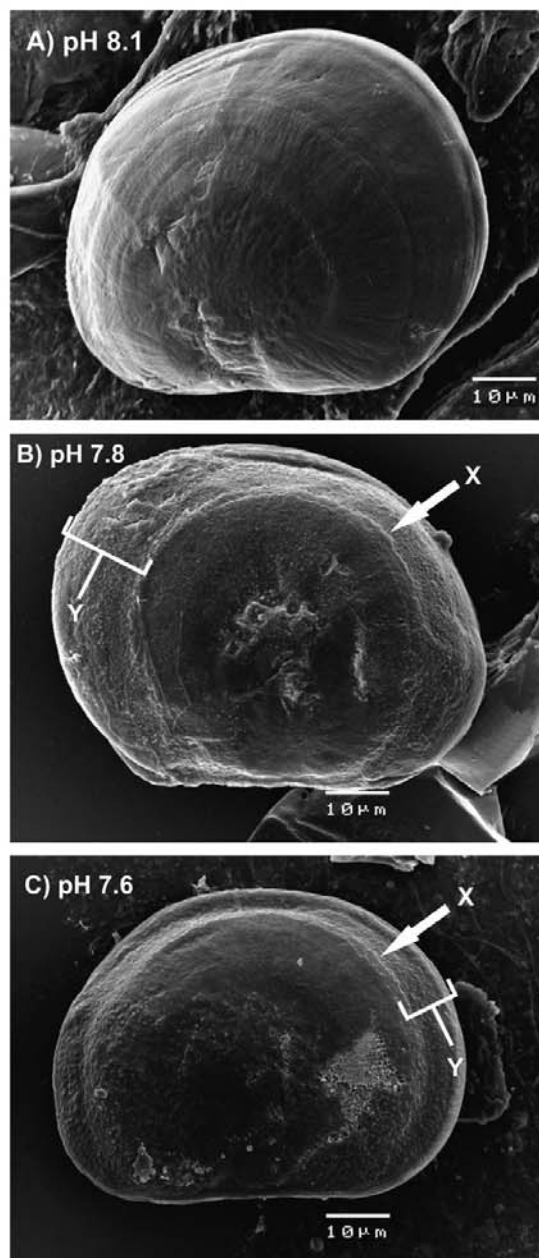


Figure 3. Scanning electron microscope (SEM) images of representative *Saccostrea glomerata* larvae at 8 days old from pH treatments: (A) pH 8.1; (B) pH 7.8; (C) pH 7.6. All images were taken at the same magnification. 'X' arrows show a growth check and point of change in the surface of the shell to a pitted surface. 'Y' denotes areas of new shell growth during exposure to acidified seawater.

& Nielsen 1989), which in turn is more soluble than calcite (Vermeij 1993). Therefore the larval shell, particularly during the ACC phase, is the most susceptible shelled life-history stage of the oyster to dissolution caused by ocean acidification.

Empty shell count data show that the percentage of empty shells, left by larvae, which had died during the experiment, decreased considerably at pH 7.6. These data suggest the empty shells dissolved rapidly (within 7 days) at pH 7.6. In this experiment, calcite and aragonite were undersaturated ($\Omega < 1$) at pH 7.8 and 7.6 putting these minerals into a dissolution state. However, calculations of saturation state are based on non-biogenic minerals in artificial seawater. Biogenic calcium carbonate shell contains an organic matrix and is often covered by a periostracum. Therefore the tipping point for dissolution of biological CaCO_3 may not occur at exactly $\Omega = 1$ for pure calcite or aragonite. In the experiment, there seemed to be a threshold between pH 7.8 and 7.6 at which rapid shell dissolution occurred and the parsimonious explanation is that the saturation state of seawater with respect to the larval shell itself was $\Omega < 1$, and markedly so in the pH 7.6 treatment.

Larval dry mass was lowest in the most acidic treatment. This probably indicates a marked fall in larval soft tissue mass at pH 7.6 because dry mass in this treatment was approximately half that of the higher pH treatments and shell pitting clearly did not produce that level of decrease in shell mass (Fig. 3); this suggests a marked effect on energy balance at low pH either through enhanced costs or reduced feeding abilities. Greatest larval mass was recorded at pH 7.8. This may be because the larvae that were able to survive in this treatment were the healthiest and thus heaviest; however, further studies are required to confirm this.

The results of this study demonstrate negative effects on larval survival and size and increased shell abnormalities of *S. glomerata* in a high- CO_2 environment. Similar effects on early life-history stages of other marine invertebrates have been demonstrated. At low pH (7.4), reduced larval development and shell mineralization was shown in the oyster *Crassostrea gigas* (Kurihara et al. 2007). Other negative effects caused by low pH include reduced hatching rate and nauplius development in copepods (Kurihara et al. 2004) and decreased fertilization and larval size in sea urchins (Kurihara & Shirayama 2004). Dupont et al. (2008) showed a reduction in larval survival and size, as well as increased larval abnormalities in the brittlestar *Ophiothrix fragilis* at pH 7.9 and 7.7. Havenhand et al. (2008) found decreased sperm speed and motility and reduced developmental success in embryos and larvae of the sea urchin *Heliocidaris erythrogramma* at pH 7.7. Negative effects of ocean acidification on the early developmental stages of any species are likely to threaten its long-term viability by a reduction in recruitment of viable juveniles to the population.

Early reports assessing the effects of CO_2 on marine organisms have considered results of experiments that used mineral acid addition to lower the pH of seawater (see Auerbach et al. 1997). However, reducing pH by CO_2 addition

compared with acid addition can have greater negative effects on marine organisms for a given pH (Kikkawa et al. 2004, Kurihara & Shirayama 2004). In recent years, there has been a move to manipulate pH by the addition of CO_2 (e.g., Kurihara et al. 2004, Gazeau et al. 2007; Havenhand et al. 2008, Dupont et al. 2008), thus creating slightly more realistic conditions in terms of the overall carbonate chemistry of seawater. This experiment aimed to create realistic near-future conditions of ocean acidification scenarios predicted to occur before the end of the century by the addition of CO_2 to seawater.

The through-flow system of elevated CO_2 seawater was a major advantage in this study, avoiding the need to use small containers in closed systems and providing the ability to rear larvae in acidified seawater for an extended period during their development. Using a closed system introduces organisms to chemical stress from changes in water quality, by the depletion of major nutrients and ions (such as Ca^{2+}) and by the build up of waste products. Closed systems also induce physical stress during water changes. Our experiments allowed the continuous change of well-mixed seawater, which removed the need to handle larvae until the experiment was finished. One- μm filtered pristine seawater was used continuously, avoiding potential water quality issues with recirculated water from the experiment. An additional advantage included the use of header tanks, avoiding the potential creation of pH gradients and/or considerable pH fluctuations in the experimental tanks. Manipulation of pH within the large (500 L) header tanks meant any fluctuations in pH caused by the CO_2 solenoid valves switching on and off, were not passed onto the treatment tanks. Large treatment tanks (60 L) also minimized any variation in physical and chemical parameters throughout the experiment.

This study demonstrates that exposure to predicted upper and lower ocean pH levels for the end of the century has a dramatic negative effect on the survival, growth, and shell formation of the early larval stages of the Sydney rock oyster, *S. glomerata*. Targeting a potentially vulnerable stage in a species' life-history is useful, but it is also important to research the effects of ocean acidification on all developmental stages, because organisms may differ in their "ocean acidification tolerance windows" during different stages in their life-history. Such ocean acidification experiments in the laboratory and field, in addition to long-term ocean monitoring programs, are urgently needed to generate data on which to base policies to mitigate the effects of climate change.

ACKNOWLEDGMENTS

The authors thank John Morrison, Simon Wever, Matthew Wassnig and Michael Milione for technical assistance with this study. This study was funded by AIMS@JCU. The first author was funded by a studentship from the Natural Environment Research Council (NER/S/A/2005/13476) and a Co-operative Award in Science and Engineering studentship from the British Antarctic Survey.

LITERATURE CITED

- Auerbach, D. I., J. A. Caulfield, E. E. Adams & H. J. Herzog. 1997. Impacts of ocean CO_2 disposal on marine life: I. A toxicological assessment integrating constant-concentration laboratory assay data with variable-concentration field exposure. *Environ. Model. Assess.* 2:333–343.

- Bibby, R., P. Cleall-Harding, S. Rundle, S. Widdicombe & J. Spicer. 2007. Ocean acidification disrupts induced defences in the intertidal gastropod *Littorina littorea*. *Biol. Lett.* 3:699–701.
- Blackford, J. C. & F. J. Gilbert. 2007. pH variability and CO₂ induced acidification in the North Sea. *J. Mar. Syst.* 64:229–241.
- Brešević, L. & A. E. Nielsen. 1989. Solubility of amorphous calcium carbonate. *J. Cryst. Growth* 98:504–510.
- Caldeira, K. & M. E. Wickett. 2003. Anthropogenic carbon and ocean pH. *Nature* 425:365.
- Caldeira, K. & M. E. Wickett. 2005. Ocean model predictions of chemistry changes from carbon dioxide emissions to the atmosphere and ocean. *J. Geophys. Res.* 110:12.
- Cao, L., K. Caldeira & A. K. Jain. 2007. Effects of carbon dioxide and climate change on ocean acidification and carbonate mineral saturation. *Geophys. Res. Lett.* 34:5.
- Doney, S. C. & D. S. Schimel. 2007. Carbon and climate system coupling on timescales from the Precambrian to the Anthropocene. *Annu. Rev. Environ. Resour.* 32:31–66.
- Dove, M. C. & W. A. O'Connor. 2007. Salinity and temperature tolerance of Sydney rock oysters *Saccostrea glomerata* during early ontogeny. *J. Shellfish Res.* 26:939–947.
- Dove, M. C. & J. Sammut. 2007. Histological and feeding response of Sydney rock oysters, *Saccostrea glomerata*, to acid sulfate soil outflows. *J. Shellfish Res.* 26:509–518.
- Dupont, S., J. Havenhand, W. Thorndyke, L. Peck & M. Thorndyke. 2008. Near-future level of CO₂-driven ocean acidification radically affects larval survival and development in the brittlestar *Ophiothrix fragilis*. *Mar. Ecol. Prog. Ser.* 373:285–294.
- Gazeau, F., C. Quiblier, J. M. Jansen, J.-P. Gattuso, J. J. Middelburg & C. H. R. Heip. 2007. Impact of elevated CO₂ on shellfish calcification. *Geophys. Res. Lett.* 34: L07603. DOI: 10.1029/2006GL028554.
- Gosling, E. 2003. Bivalve Molluscs; biology, ecology and culture. Oxford: Blackwell Science. 456 pp.
- Hall-Spencer, J. M., R. Rodolfo-Metalpa, S. Martin, E. Ransome, M. Fine, S. M. Turner, S. J. Rowley, D. Tedesco & M. C. Buia. 2008. Volcanic carbon dioxide vents show ecosystem effects of ocean acidification. *Nature* 454:96–99.
- Harper, E. M. 2000. Are calcitic layers an effective adaptation against shell dissolution in the Bivalvia? *J. Zool.* 251:179–186.
- Haugan, P. M. & H. Drange. 1996. Effects of CO₂ on the ocean environment. *Energy Convers. Manage.* 37:1019–1022.
- Havenhand, J. N., F. R. Buttler, M. C. Thorndyke & J. E. Williamson. 2008. Near-future levels of ocean acidification reduce fertilization success in a sea urchin. *Curr. Biol.* 18:R651.
- Heasman, M. P., L. Goard, J. Diemar & R. B. Callinan. 2000. Improved Early Survival of Molluscs: Sydney Rock Oyster (*Saccostrea glomerata*). Aquaculture CRC Project A.2.1, NSW Fisheries Final Report Series No. 29, Nelson Bay, Australia.
- Hoegh-Guldberg, O., P. J. Mumby, A. J. Hooten, R. S. Steneck, P. Greenfield, E. Gomez, C. D. Harvell, P. F. Sale, A. J. Edwards, K. Caldeira, N. Knowlton, C. M. Eakin, R. Iglesias-Prieto, N. Muthiga, R. H. Bradbury, A. Dubi & M. E. Hatzioiols. 2007. Coral reefs under rapid climate change and ocean acidification. *Science* 318:1737–1742.
- Kikkawa, T., J. Kita & A. Ishimatsu. 2004. Comparison of the lethal effect of CO₂ and acidification on red sea bream (*Pagrus major*) during the early developmental stages. *Mar. Pollut. Bull.* 48:108–110.
- Kleypas, J. A., R. A. Feely, C. Fabry, C. Langdon, C. Sabine & L. L. Robbins. 2006. Impacts of ocean acidification on coral reefs and other marine calcifiers: a guide for future research. A report of a workshop held April 18–20, 2005, St. Petersburg, Florida, sponsored by NSF, NOAA, and the US Geological Survey. 88 pp.
- Kurihara, H., S. Kato & A. Ishimatsu. 2007. Effects of increased seawater pCO₂ on early development of the oyster *Crassostrea gigas*. *Aquat. Biol.* 1:91–98.
- Kurihara, H., S. Shimode & Y. Shirayama. 2004. Effects of raised CO₂ concentration on the egg production rate and early development of two marine copepods (*Acartia steueri* and *Acartia erythraea*). *Mar. Pollut. Bull.* 49:721–727.
- Kurihara, H. & Y. Shirayama. 2004. Effects of increased atmospheric CO₂ on sea urchin early development. *Mar. Ecol. Prog. Ser.* 274:161–169.
- Langdon, C., W. S. Broecker, D. E. Hammond, E. Glenn, K. Fitzsimmons, S. G. Nelson, T. H. Peng, I. Hajdas & G. Bonani. 2003. Effect of elevated CO₂ on the community metabolism of an experimental coral reef. *Global Biogeochem. Cycles* 17:1011. DOI: 10.1029/2002GB001941, 2003.
- Lewis, E. & D. W. R. Wallace. 1998. Program Developed for CO₂ System Calculations. ORNL/CDIAC-105. Carbon Dioxide Information Analysis Center, Oak Ridge National Laboratory, US Department of Energy, Oak Ridge, Tennessee.
- Mayor, D. J., C. Matthews, K. Cook, A. F. Zuur & S. Hay. 2007. CO₂-induced acidification affects hatching success in *Calanus finmarchicus*. *Mar. Ecol. Prog. Ser.* 350:91–97.
- Miles, H., S. Widdicombe, J. I. Spicer & J. Hall-Spencer. 2007. Effects of anthropogenic seawater acidification on acid-base balance in the sea urchin *Psammechinus miliaris*. *Mar. Pollut. Bull.* 54:89–96.
- Nell, J. A. & W. A. O'Connor. 1991. The evaluation of fresh algae and stored algal concentrates as a food source for Sydney rock oyster *Saccostrea commercialis* (Iredale & Roghley) larvae. *Aquaculture* 99:277–284.
- O'Sullivan, D., J. Savage & A. Fay. 2008. Status of Australian aquaculture in 2005/2006. Austasia Aquaculture Trade Directory 2008, Turtle Press, Hobart, Tasmania. pp. 6–24.
- Orr, J. C., V. J. Fabry, O. Aumont, L. Bopp, S. C. Doney, R. A. Feely, A. Gnanadesikan, N. Gruber, A. Ishida, F. Joos, R. M. Key, K. Lindsay, E. Maier-Reimer, R. Matear, P. Monfray, A. Mouchet, R. G. Najjar, G. K. Plattner, K. B. Rodgers, C. L. Sabine, J. L. Sarmiento, R. Schlitzer, R. D. Slater, I. J. Totterdell, M. F. Weirig, Y. Yamanaka & A. Yool. 2005. Anthropogenic ocean acidification over the twenty-first century and its impact on calcifying organisms. *Nature* 437:681–686.
- Pearson, P. N. & M. R. Palmer. 2000. Atmospheric carbon dioxide concentrations over the past 60 million years. *Nature* 406:695–699.
- Peck, L. S. 2005. Prospects for survival in the Southern Ocean: Vulnerability of benthic species to temperature change. *Antarct. Sci.* 17:497–507.
- Shirayama, Y. & H. Thornton. 2005. Effect of increased atmospheric CO₂ on shallow water marine benthos. *J. Geophys. Res.* 110:C09S09. DOI: 10.1029/2004JC002618.
- Southgate, P. C. & A. C. Beer. 1997. Hatchery and early nursery culture of the blacklip pearl oyster *Pinctada margaritifera* (L.). *J. Shellfish Res.* 16:561–568.
- Stenzel, H. B. 1964. Oysters: Composition of the Larval Shell. *Science* 145:155–156.
- Tans, P. NOAA/ESRL (www.esrl.noaa.gov/gmd/ccgg/trends).
- Vermeij, G. J. 1993. A Natural History of Shells. Princeton University Press, Princeton, New Jersey. 207 pp.
- Weiss, I. M., N. Tuross, L. Addadi & S. Weiner. 2002. Mollusc larval shell formation: Amorphous calcium carbonate is a precursor phase for aragonite. *J. Exp. Zool.* 293:478–491.
- Zeebe, R. E., J. C. Zachos, K. Caldeira & T. Tyrrell. 2008. Oceans—Carbon emissions and acidification. *Science* 321:51–52.